NASA/CR—2000-210039 R98AEB152

# AST Critical Propulsion and Noise Reduction Technologies for Future Commercial Subsonic Engines

## Separate-Flow Exhaust System Noise Reduction Concept Evaluation

B.A. Janardan, G.E. Hoff, J.W. Barter, S. Martens, and P.R. Gliebe
General Electric Aircraft Engines, Cincinnati, Ohio

V. Mengle and W.N. Dalton
Allison Engine Company, Indianapolis, Indiana

December 2000

The NASA STI Program Office . . . in Profile

Since its founding, NASA has been dedicated to the advancement of aeronautics and space science. The NASA Scientific and Technical Information (STI) Program Office plays a key part in helping NASA maintain this important role.

The NASA STI Program Office is operated by Langley Research Center, the Lead Center for NASA's scientific and technical information. The NASA STI Program Office provides access to the NASA STI Database, the largest collection of aeronautical and space science STI in the world. The Program Office is also NASA's institutional mechanism for disseminating the results of its research and development activities. These results are published by NASA in the NASA STI Report Series, which includes the following report types:

- TECHNICAL PUBLICATION. Reports of completed research or a major significant phase of research that present the results of NASA programs and include extensive data or theoretical analysis. Includes compilations of significant scientific and technical data and information deemed to be of continuing reference value. NASA's counterpart of peer-reviewed formal professional papers but has less stringent limitations on manuscript length and extent of graphic presentations.

- TECHNICAL MEMORANDUM. Scientific and technical findings that are preliminary or of specialized interest, e.g., quick release reports, working papers, and bibliographies that contain minimal annotation. Does not contain extensive analysis.

- CONTRACTOR REPORT. Scientific and technical findings by NASA-sponsored contractors and grantees.

- CONFERENCE PUBLICATION. Collected papers from scientific and technical conferences, symposia, seminars, or other meetings sponsored or cosponsored by NASA.

- SPECIAL PUBLICATION. Scientific, technical, or historical information from NASA programs, projects, and missions, often concerned with subjects having substantial public interest.

- TECHNICAL TRANSLATION. English-language translations of foreign scientific and technical material pertinent to NASA's mission.

Specialized services that complement the STI Program Office's diverse offerings include creating custom thesauri, building customized data bases, organizing and publishing research results . . . even providing videos.

For more information about the NASA STI Program Office, see the following:

- Access the NASA STI Program Home Page at ***http://www.sti.nasa.gov***

- E-mail your question via the Internet to help@sti.nasa.gov

- Fax your question to the NASA Access Help Desk at 301–621–0134

- Telephone the NASA Access Help Desk at 301–621–0390

- Write to:
  NASA Access Help Desk
  NASA Center for AeroSpace Information
  7121 Standard Drive
  Hanover, MD 21076

NASA/CR—2000-210039 R98AEB152

# AST Critical Propulsion and Noise Reduction Technologies for Future Commercial Subsonic Engines

## Separate-Flow Exhaust System Noise Reduction Concept Evaluation

B.A. Janardan, G.E. Hoff, J.W. Barter, S. Martens, and P.R. Gliebe
General Electric Aircraft Engines, Cincinnati, Ohio

V. Mengle and W.N. Dalton
Allison Engine Company, Indianapolis, Indiana

Prepared under Contract NAS3–27720, Area of Interest 14.3

National Aeronautics and
Space Administration

Glenn Research Center

December 2000

## Acknowledgments

The authors thank Dr. N. Saiyed and Dr. J. Bridges of NASA Lewis (now NASA Glenn) for their significant efforts in program coordination, test planning, test conduct, and data processing. The authors also acknowledge J.F. Brausch, R.S. Coffin, and B.R. Delaney of GE Aircraft Engines and F. Smith and Dr. B.R. Vittal of Allison Engine Company for technical support and unique contributions to this program effort.

Note that at the time of research, the NASA Lewis Research Center was undergoing a name change to the NASA John H. Glenn Research Center at Lewis Field. Both names may appear in this report.

Available from

NASA Center for Aerospace Information
7121 Standard Drive
Hanover, MD 21076
Price Code: A13

National Technical Information Service
5285 Port Royal Road
Springfield, VA 22100
Price Code: A13

Available electronically at http://gltrs.grc.nasa.gov/GLTRS

# PREFACE

In 1995, NASA GRC initiated efforts to meet the US industry's rising need to develop jet noise technology for separate flow nozzle exhaust systems. Such technology would be applicable to long-range aircraft using medium to high by-pass ratio engines. With support from the Advanced Subsonic Technology Noise Reduction program, these efforts resulted in the formulation of an experimental study, the Separate Flow Nozzle Test (SFNT). SFNT's objectives were to develop a data base on various by-pass ratio nozzles, screen quietest configurations and acquire pertinent data for predicting the plume behavior and ultimately its corresponding jet noise. The SFNT was a team effort between NASA GRC's various divisions, NASA Langley, General Electric, Pratt&Whitney, United Technologies Research Corporation, Allison Engine Company, Boeing, ASE FluiDyne, MicroCraft, Eagle Aeronautics and Combustion Research and Flow Technology Incorporated.

SFNT found several exhaust systems providing over 2.5 EPNdB reduction at take-off with less than 0.5% thrust loss at cruise with simulated flight speed of 0.8 Mach. Please see the following SFNT related reports: Saiyed, et al. (NASA/TM—2000-209948), Saiyed, et al. (NASA/CP—2000-210524), Low, et al. (NASA/CR—2000-210040), Janardan et al. (NASA/CR—2000-210039), Bobbitt, et al. (NASA/CR—201-210706) and Kenzakowski et al. (NASA/CR—2001-210611.).

I wish to thank the entire SFNT team of nearly 50 scientists, engineers, technicians and programmers involved in this project. SFNT would have fallen well short of its goals without their untiring support, dedication to developing the jet noise technology.

Naseem Saiyed
SFNT Research Engineer

# Table of Contents

# Table of Contents (Continued)

# Table of Contents (Continued)

# Table of Contents (Concluded)

Page

# List of Illustrations

# List of Illustrations (Continued)

| Figure | Title | Page |
|---|---|---|

# List of Illustrations (Continued)

# List of Illustrations (Continued)

## List of Illustrations (Continued)

# List of Illustrations (Concluded)

| Figure | Title | Page |
|---|---|---|

# List of Tables

# 1.0 Summary

This report describes the work performed by GEAE (GE Aircraft Engines) and AEC (Allison Engine Company) on NASA Contract NAS3–27720 AoI 14.3.

The objectives of this contract were to:

1. generate a high-quality jet noise acoustic database for separate-flow nozzle models and
2. design and verify new jet noise reduction concepts over a range of simulated engine cycles and flight conditions.

Five baseline axisymmetric separate-flow nozzle models having bypass ratios of 5 and 8 (with internal and external plugs) and eleven different GEAE/AEC supplied mixing-enhancer model nozzles (including chevrons, vortex-generator doublets, and a "tongue" mixer) were designed and tested in model scale. Additionally, Pratt and Whitney (P&W) provided nine mixing-enhancer model nozzles representing five jet noise reduction devices (offset-centerline fan nozzle, flipper-tabbed fan and core nozzles, scarfed fan nozzle, core full mixer, and core half mixer) into the overall NASA program effort. The full and half mixer for the core nozzle were NASA concepts. Using available core and fan nozzle hardware in various combinations, 28 GEAE/AEC separate-flow nozzle/mixing-enhancer configurations and an additional 24 P&W configurations were acoustically evaluated in the NASA Lewis Research Center Aeroacoustic and Propulsion Laboratory Nozzle Acoustic Test Rig facility during the March through June 1997 time period.

The acoustic design and measured acoustic characteristics of GEAE/AEC exhaust systems are discussed in this report. In addition to acoustic results, this report describes GEAE/AEC model nozzle features, facility and test instrumentation, test procedures, test matrix summary, and the data acquisition/reduction/analysis methodology.

# 2.0 Introduction

During the 1960's, significant attention was directed toward the prediction and reduction of jet mixing noise. The turbojet and low-bypass turbofans used for aircraft propulsion during that era had acoustic signatures dominated by jet mixing noise produced by the high-speed, high-temperature exhaust.

Although increasing bypass ratio (BPR) tends to lower the contribution of the jet as a noise source relative to the turbomachinery, modern higher BPR engines continue to generate significant farfield jet noise at high-thrust takeoff conditions. Also, for growth applications (increased takeoff gross weight) of existing aircraft such as the Boeing 747, 757, 767, and 777, high-BPR engines that provide increased thrust are needed. New large engines and derivatives of existing large engines capable of producing the needed higher thrust generally operate with higher fan pressure ratios and consequently higher fan and core exhaust jet velocities.

For these reasons, jet mixing noise will continue to be a significant contribution to engine acoustic signatures at takeoff power. However, development of mixing-enhancement devices would enable airplane/engine growth without need for costly major engine/nacelle redesigns.

In the AST program, NASA has addressed the need to reduce jet mixing noise through research into the noise-reduction potential of new exhaust nozzle designs. An effort was identified to develop (1) a subsonic separate-flow nozzle system jet noise database and (2) concepts for reducing separate-flow jet noise. NASA Lewis awarded GEAE a contract (NAS3–27720, AoI 14.3) to design, build, and test separate-flow exhaust system scale models, in the BPR range of 5 to 8, that employ various potential jet noise reduction features in the form of mixing-enhancement devices.

This NASA test program involved efforts from NASA Lewis Research Center, GEAE, and P&W with technical assistance from AEC (subcontractor to GEAE) and the Boeing Commercial Aircraft Company (subcontractor to P&W).

GEAE/AEC provided 5 baseline axisymmetric separate-flow nozzle models (BPR = 5 and 8) with internal and external plugs and 11 mixing-enhancer designs consisting of various chevrons, vortex-generator doublets, and a "tongue" mixer.

P&W, under contract NAS3–27727 (Task Order 14.2), supplied nine enhanced-mixing nozzle models representing five jet noise reduction designs (offset-centerline fan nozzle, flipper-tabbed fan and core nozzles, scarfed fan nozzle, core full-mixer nozzle, and core half-mixer nozzle). All P&W hardware was adaptable only to the GEAE-provided, BPR = 5, external-plug, separate-flow, baseline exhaust system model.

The model test program was conducted in the NASA Lewis Aeroacoustic and Propulsion Laboratory (AAPL) Nozzle Acoustic Test Rig (NATR) facility in the March through June 1997 time frame. Farfield noise measurements were acquired in this test program. The NATR was not configured for nozzle thrust measurements for this test program.

This report describes the model test program that evaluated selected GEAE and AEC jet noise reduction concepts potentially applicable to current and future, separate-flow, high-BPR engine/nacelle exhaust systems. The specific objectives of this NASA test program are summarized below:

1. Generate a high-quality jet noise acoustic database for baseline separate-flow nozzle models for a range of simulated operating/flight conditions.

2. Evaluate and validate (relative to baseline configurations) noise-reduction concepts for high-bypass, separate-flow exhaust systems that could reduce noise in the range of 3 EPNdB for the exhaust jet noise component of modern, high-bypass turbofans.

3. Perform limited nearfield noise testing of selected promising noise-reduction concepts using a Boeing provided phased-array microphone system in an attempt to locate major sources of jet noise radiation.

4. Conduct jet plume survey (pressure and temperature) testing on selected promising noise-reduction concepts to correlate with jet noise farfield measurements to further understand jet noise signatures.

GEAE contracted effort focused on Objectives 1 and 2.

# 3.0 Selection of Baseline Nozzles and Mixing-Enhancer Concepts

Brief descriptions of the selected baseline nozzles are provided in Section 3.1. Section 3.2 contains a listing of potential mixing-enhancer concepts that were initially selected by GEAE/AEC for screening, details of the conducted computational fluid dynamics (CFD) analysis, and brief descriptions of the concepts finally selected for fabrication. Details of the baseline nozzle and mixing-enhancer hardware are described in Section 4.

## 3.1 Selected Baseline Nozzles

McDonnell Douglas, under NASA Langley Contract NAS1–20103 (Task Order 6 "Subsonic Dual Stream Jet Noise Database") has designed a series of high-bypass-ratio, separate-flow, scale-model nozzles representing typical geometry variations of current and advanced engine exhaust systems. It was decided to use the aerodynamic flow lines of some of these generic designs for the baseline nozzles of this program, and the following separate-flow exhaust systems were selected:

- BPR = 5.0 with Coplanar Exit
- BPR = 5.0 with Internal Plug
- BPR = 5.0 with External Plug
- BPR = 8.0 with Internal Plug
- BPR = 8.0 with External Plug
- BPR = 5.0 with External Plug and Short Fan Nozzle (this one was later deleted from the program)

Bypass ratios of 5 and 8 were selected because they represent BPR's of current and growth product-engine applications The selected geometry details address key nozzle variables, and the measured results from this program will provide a parametric database including dependency on BPR and internal versus external core plugs. The coplanar-exit nozzle represents a reference baseline geometry.

The model hardware fabricated under the Langley/Douglas program for testing in the Langley JNL facility could not be used directly in the NASA Lewis AAPL facility because the flange mountings and the structure of the AAPL system were not compatible (scale factor difference of 1.0224).

## 3.2 Mixing-Enhancer Candidates

At the outset of this program, GEAE/AEC decided to consider mainly those mixing-enhancer concepts that had the potential to provide significant jet noise reduction with minimal nozzle performance (thrust) loss and minimal nozzle weight increase. The potential candidates were also mostly limited to those that were somewhat easily adaptable to engine applications.

The initial candidate concepts were selected based on anticipated ability to enhance mixing of the higher velocity core jet with the lower velocity fan stream relative to that of a separate-flow baseline nozzle. Although, in principle, enhanced mixing should reduce noise metrics such as perceived noise level (PNL), it has not always been so in practical applications. Increased mixing, in general, has decreased jet sound pressure level (SPL) at lower frequencies but has also increased SPL at higher frequencies (References 1–4). The increase in higher frequency sound levels exacerbates annoyance (Noy factor) and thus offsets some of the reduction at frequencies where jet mixing noise produces peak SPL.

The increase in higher frequency noise has sometimes been attributed to increased turbulence due to enhanced mixing. To minimize or avoid the increase in SPL at higher frequencies, mixing of the two streams should take place without significant increase in flow turbulence intensity. Therefore, most of the mixing candidates that were considered under this program were concepts that would provide a "gentler" mixing of the two streams outside and downstream of the respective nozzle exits rather than a "forced" mixing inside the exhaust duct. By this approach, it was anticipated that the candidate concept, if successful in enhancing mixing and thus providing significant noise benefit, would also impose a minimal associated performance thrust loss.

GEAE and AEC collaborated to come up with 38 potential concepts for jet mixing enhancement. They are summarized in Table 1. The concepts included chevrons, flipper chevrons, chevrons with tabs, tabs, flipper tabs/paddles, vortex generators, a scarfed nozzle, an elliptic nozzle, and a "tongue" mixer for core nozzle application. Chevrons, flipper chevrons, tabs, vortex generators, a scarfed nozzle, and an elliptic nozzle were the potential concepts for fan nozzle application.

Descriptions of the mixing mechanisms provided by some of these concepts can be found in References 5–15. Chevrons, tabs, paddles, scarfed nozzles, and elliptic nozzles provide additional shear perimeter relative to a separate-flow baseline nozzle and thus increase interfacial mixing area. Chevrons, tabs, paddles, and vortex generators generate large-scale, streamwise, counterrotating vortices that enhance mixing. The idea behind the "tongue" mixer is to have contoured chutes penetrate the core flow for forced mixing of core and fan streams.

To keep the overall test program within scope and avoid duplication of concepts that NASA Langley and P&W were considering (flipper tabs/paddles and scarfed nozzles) in their respective separate-flow jet noise programs, the initial GEAE/AEC selection matrix was trimmed to 30 candidates (see Table 1). Of these 30 concepts, only chevron and inward flipper chevron designs were identified for screening by computational fluid dynamics (CFD) analysis by GEAE, and the tongue mixer was identified for CFD analysis by AEC. The results of CFD analyses of the chevrons, flipper chevrons, and the tongue mixer are summarized in Sections 3.3 and 3.4 of this report.

## 3.3 GEAE CFD Analysis of Chevron Concepts

The primary consideration in the design of the chevrons was to maintain a continuous flowpath with no slope discontinuities. The chevrons were designed on stringers using a cubic or quadratic fit between the trailing edge of the nozzle and the end of the chevron. The end of the chevron was selected based on the desired penetration into the core or fan stream. For the concept analysis, penetration depth was selected to be one boundary layer thickness.

GEAE performed the CFD analyses of the selected chevron concepts. All of the analyses were conducted on the BPR = 5, external plug exhaust system. A typical takeoff operating point was selected for the analyses. The pressure ratio and total temperature for the core and fan streams, respectively were: 1.65/1650°R and 1.80/665°R. The free-stream Mach number was 0.29. The following discussions detail the analysis procedure and summarize the results.

### 3.3.1 Analysis Procedure

To analyze the potential benefit of the proposed chevron configurations, a 3D, viscous CFD analysis of the chevrons was conducted. To analyze each configuration, PAB3D (developed and maintained by NASA Langley) was used. PAB3D solves the 3D thin-layer Navier–Stokes equations on a multiblock grid using a variety of turbulence models. It has been calibrated for and widely used on exhaust system flows. Details of this code are described in References 16–18.

**Table 1. Separate-Flow Nozzle Mixing-Enhancer Concept Selection Matrix**

Arrows Indicate Revisions

| Concept Description | | Model 2 BPR = 5 Internal Plug | Model 3 BPR = 5 External Plug | Model 4 BPR = 8 Internal Plug | Model 5 BPR = 8 External Plug | Model 6 BPR = 5 Ext. Plug Short Fan | Total Concepts | Possible Mixing Mechanisms |
|---|---|---|---|---|---|---|---|---|
| Chevrons (N= 8, 12, 24) | Core | 2 | 2** | | 1 | 1 | 6 | Increase Shear Perimeter<br>Generate Vorticity |
| | Fan* | 1 | 1** | 1 | 1 | | 1 | |
| Flipper Chevrons (N= 12 or 24) | Core | 2 | 2** | | | | 4 | Increase Shear Perimeter<br>Generate Vorticity<br>Forced Mixing |
| | Fan* | 1 | 1** | 1 | 1 | | 1 | |
| Chevrons with Tabs (N= ?) | Core | 1 | 1 | | | | 2 | Increase Shear Perimeter<br>Generate Vorticity |
| | Fan* | | | | | | | |
| Tabs (N= ?) | Core | 2 ➧ 1 | 2 ➧ 1 | | 1 | | 5 ➧ 3 | Increase Shear Perimeter<br>Generate Vorticity |
| | Fan* | 1 | 1 | 1 | 1 | | 1 | |
| Flipper Tabs / Paddles*** | Core | 2 ➧ 0 | 2 ➧ 0 | | | | 4 ➧ 0 | Increase Shear Perimeter<br>Generate Vorticity<br>Forced Mixing |
| | Fan* | | | | | | | |
| Vortex Generators Singlet, Doublet (N=?) | Core | 2 | 3 | | | 2 | 7 | Generate Vorticity |
| | Fan* | 2 | 2 | 2 | 2 | | 2 | |
| Scarfed Nozzle*** | Core | 1** ➧ 0 | | | | | 1 ➧ 0 | Increase Shear Perimeter<br>Alter Noise Directivity |
| | Fan* | 1 ➧ 0 | | | | | 1 ➧ 0 | |
| Tongue Mixer | Core | 1** | | | | | 1 | Forced Mixing of Core and Fan Streams |
| | Fan* | | | | | | | |
| Elliptic Nozzle | Core | 1 | | | | | 1 | Increase Shear Perimeter<br>Alter Noise Directivity |
| | Fan* | 1 | | | | | 1 | |
| | | | | | **Total Concept Hardware** | | **38 ➧ 30** | |

* Fan nozzle hardware is common for Models 2 through 5.
** Identified for initial CFD assessment.
*** Deleted from consideration to avoid duplication of possible P&W hardware.

To analyze the chevron configurations, a three-block grid was used with one block each for the core stream, fan stream, and free stream. Figure 1 is a meridional view of a typical grid in the vicinity of the exhaust system. The grid extended 9 fan diameters radially into the free stream and 30 fan diameters axially downstream of the nozzle exhaust. The grid extended circumferentially over half of one chevron, so symmetry boundary conditions were used to account for the circumferential periodicity of the geometry and flowfield.

As stated earlier, PAB3D solved the thin-layer Navier–Stokes equations. For analysis of the chevrons, the option that couples the j and k directions (radial and circumferential, respectively) was selected. The Jones and Launder turbulence model was selected, and the flowfield was gridded to $y+ \simeq 1$. Third-order accurate spatial discretization was used with the *minmod* limiter.

### 3.3.2 Postprocessing

Effectiveness of various chevron configurations was evaluated by examining the PAB3D solutions in several ways. The circumferentially averaged velocity and turbulent kinetic energy (TKE) profiles were used to evaluate the decay of the plume and the transfer of energy from low frequencies (large-scale plume structure) to high frequencies (turbulence). Typical profiles for a 12-chevron core nozzle, separate-flow configuration are illustrated in Figure 2. The velocity profiles indicate the mixing of the core and fan stream and decay of the plume. The TKE profiles indicate all of the TKE, initially, is confined to the shear layers that develop between the core and fan streams and between the fan stream and the free stream. As the plume develops, the shear layers become thicker and grow together. It is interesting to note that TKE is higher in the fan/free-stream shear layer than in the core/fan shear layer. This is consistent with the fact that the velocity difference between the fan stream and free stream is greater than that between the core and fan streams.

Cross-stream cuts through the flowfield were used to examine mixing effectiveness and to understand the physical effect of the chevrons on the flowfield. Typical cross-stream cuts obtained with the 12-straight-chevron core nozzle configuration and a 12-flipped-chevron (into core flow) core nozzle configuration are shown in Figure 3. The total temperature contours at the plug trailing edge for the two configurations are compared in this figure. Note that for a baseline configuration, with no

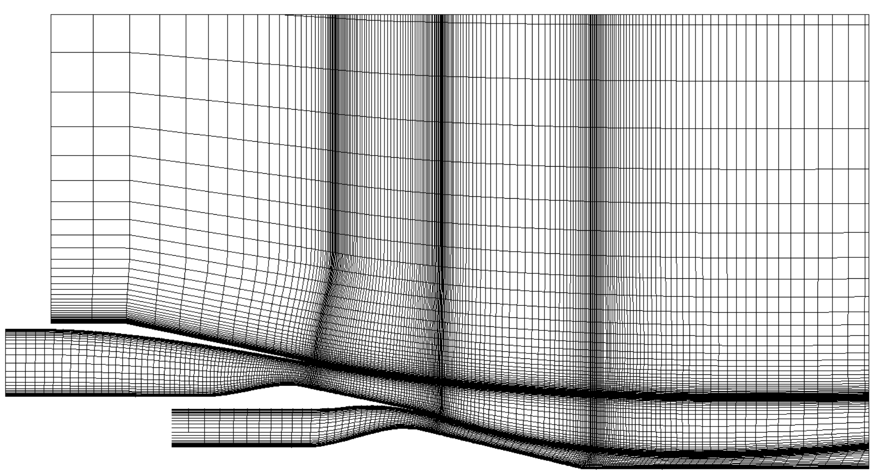

**Figure 1. Typical Grid Used to Analyze a Chevron Configuration**

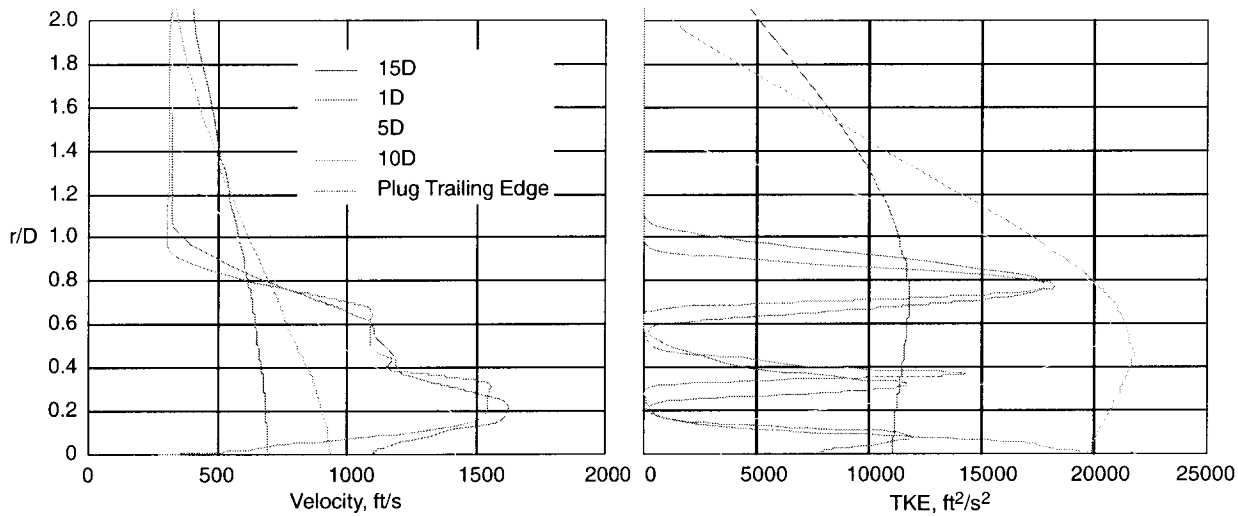


**Figure 2.** **Example of Circumferentially Averaged Velocity and TKE Plume Profiles for 12 Chevrons on the Core Nozzle**

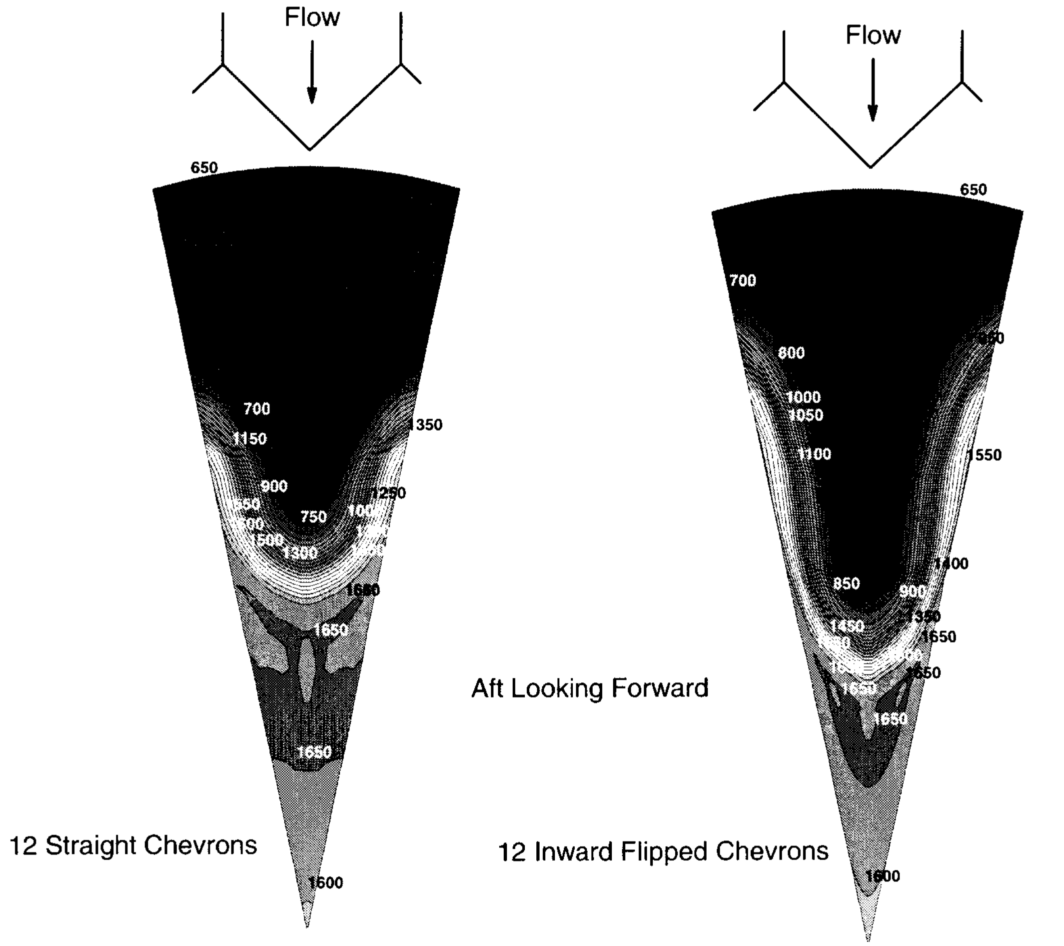


**Figure 3.** **Total Temperature Contours at the Plug Trailing Edge for Two Configurations of Core Chevrons: 12 Straight and 12 Inward Flipped**

chevrons on the core nozzle, the temperature contours would be circular arcs. The temperature profiles indicate cross flow of the hot core and cooler fan streams with core nozzle chevrons. The depth of penetration of the streams appears to be greater with the flipper-chevron configuration than with the straight-chevron configuration.

A great difficulty with postprocessing the CFD results was interpreting the acoustic benefit of the chevrons. More rapid plume decay should reduce the strength of noise sources located far downstream and thus reduce low-frequency noise. However, higher turbulence near the nozzle exit could increase high-frequency noise. If the effect of the chevrons on turbulence was not considered, one would be driven to designs that maximize plume decay regardless of the effect on turbulence and associated high-frequency noise. Therefore, it is necessary to consider the effect of the chevrons on TKE production. Since the TKE profile trends qualitatively appear reasonable, they were considered in the final comparative analysis of the various chevron designs. It is recognized that this introduced some uncertainty into the quantitative results as the magnitude of TKE is not a parameter which, to the authors' knowledge, has been validated against test data for separate-flow exhaust system plumes.

#### 3.3.3 Analysis Results

Seven chevron configurations were analyzed in addition to the baseline BPR = 5 external plug exhaust system. The chevron configurations analyzed were 8, 12, and 18 straight chevrons on the core nozzle; 12, 24, and 36 straight chevrons on the fan nozzle; and 12 flipped (into core stream) chevrons on the core nozzle. The chevrons were all placed at equal angular intervals. All of the chevron configurations analyzed appeared to have some mixing benefit relative to the baseline nozzle.

For all configurations, the chevrons had the same qualitative effect on the flowfield. Each chevron generated a pair of counterrotating streamwise vortices. This is shown in Figure 4 for the 12-chevron core nozzle configuration. These vortices enhanced the transverse convective transport of mass, momentum, and energy between the adjacent streams and thus resulted in more rapid mixing of the plume and faster decay of the higher speed core jet. An added benefit of the chevrons is that they reduce, in an average sense, the gradient between the adjacent streams. Since TKE is a strong function of gradients in the flow, reduced gradients produce less TKE in the shear layers and therefore could result in less high-frequency noise.

Based on these analyses, the most promising configurations were found to be 8 and 12 chevrons on the core nozzle and 12 and 24 chevrons on the fan nozzle. The 8 chevrons on the core appeared to be better than 12 chevrons on the core, and the 24 chevrons on the fan appeared to be slightly better than 12 chevrons on the fan. The results for the 12 chevrons flipped into the core stream were inconclusive; a tremendous plume velocity reduction was effected, but the configuration also appeared to generate substantially more TKE. From the above described CFD results, it was not possible to definitely determine whether the noise due to the increased TKE would outweigh the benefit due to the reduced plume velocities.

### 3.4 AEC CFD Analysis of Tongue Mixer

The AEC concept focused on aggressive mixing strategies. The mixer concept, referred to as a tongue mixer, was modeled using CFD by AEC.

#### 3.4.1 Numerical Modeling

A 3D, viscous CFD analysis was conducted on the proposed tongue mixer configuration using the NPARC analysis code. The NPARC code (Reference 19), Version 3.0, solves the full,

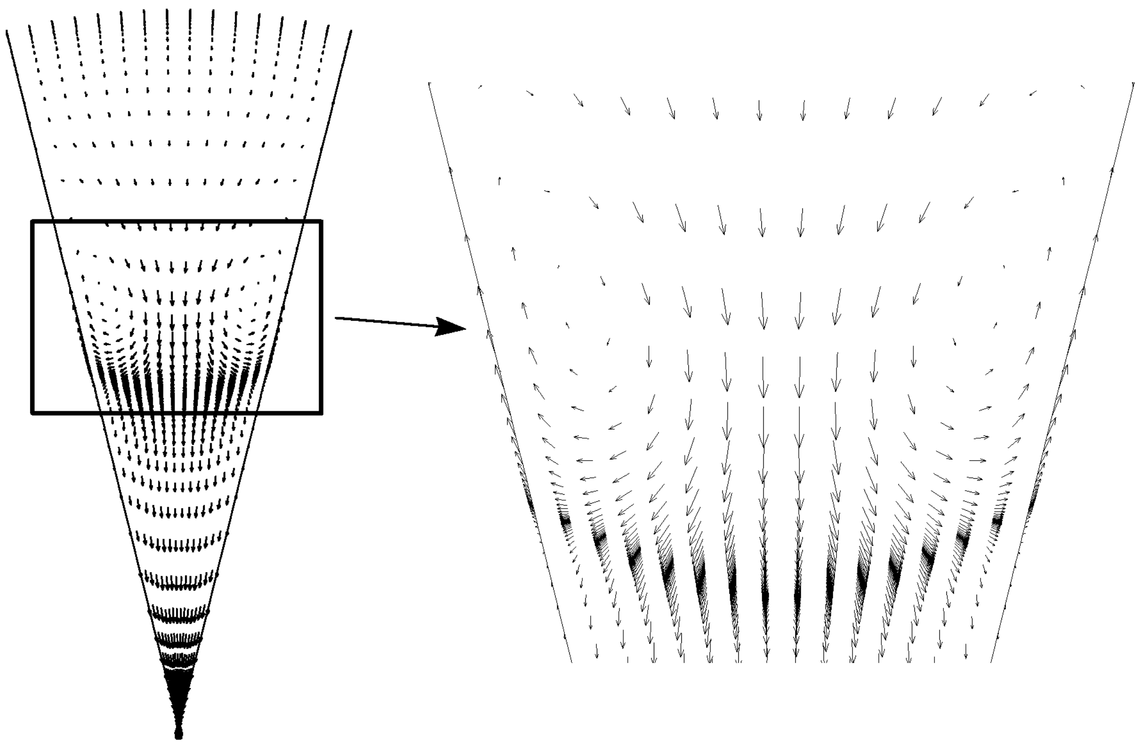

**Figure 4. Velocity Vectors at the Plug Trailing Edge for 12 Chevrons on the Core Nozzle**

three-dimensional, Reynolds-averaged, Navier–Stokes equations in strong conservation form using the Beam and Warming approximate factorization scheme to obtain a block tridiagonal system of equations. Pulliam's scalar pentadiagonal transformation provides an efficient solver. The code has several turbulence models available. The calculations presented in this study used the Chien low Reynolds number k–ε model. The scheme uses a central difference approximation. Artificial dissipation is introduced to eliminate oscillations associated with the differencing scheme. The code uses structured, multiple grid blocks. Information is transferred across grid block interfaces using trilinear interpolation. The NPARC code has been used extensively at AEC to predict both internal and external flows associated with mixer/nozzle exhaust systems.

### 3.4.2 Grid generation

The tongue mixer is composed of 12 identical pairs of chutes or tongues spaced at equal angular intervals along the circumference. In each pair, one chute is deflected into the core nozzle, and the other is aligned with the undisturbed bypass flow streamlines. This periodic geometry was exploited to reduce the computational requirements — resulting in a grid extending circumferentially between the centerline and one tongue pair, as shown in Figure 5. The GRIDGEN code (Reference 20) was used to generate the computational grid. The grid consisted of 8 blocks with a total of 1.8 million grid points. Both contiguous and noncontiguous block interfaces were used. Grid density near boundaries was sufficient to resolve boundary and shear layers. The down-

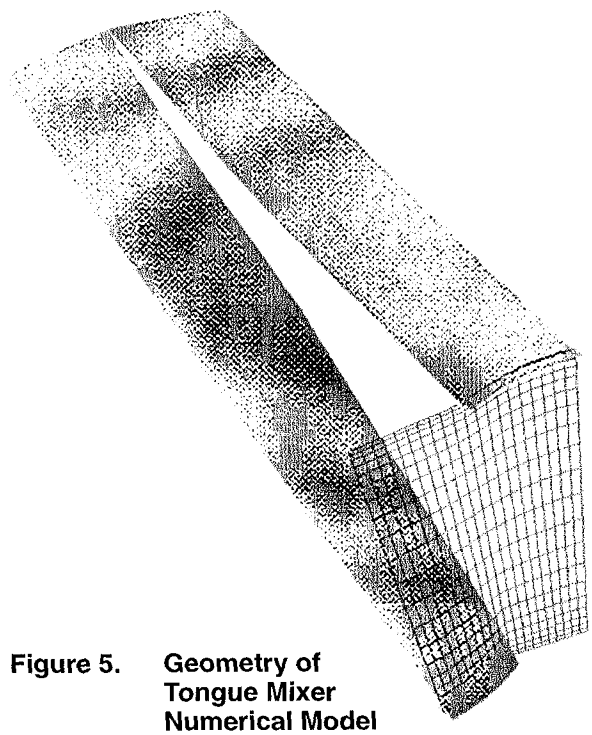

**Figure 5. Geometry of Tongue Mixer Numerical Model**

stream boundary was established 30 diameters aft of the nozzle exit in order to capture a significant portion of the plume development. The outer radial boundary is approximately 22 diameters from the nozzle centerline. Figure 1 shows a meridonal view of the grid.

### 3.4.3 Boundary Conditions

Fan and core total pressures and temperatures were specified on upstream boundaries internal to the nozzle. Solid walls were modeled as adiabatic, no-slip surfaces. For the external flow, upstream total pressure and temperature were specified and set consistent with the desired free-stream Mach number. Symmetry conditions were applied at the centerline and across the edge boundaries in the radial/axial plane, while the outer radial boundary in the free stream was modeled as a slip surface.

### 3.4.4 Results

The results presented in this section correspond to a fan total pressure ratio of 1.6 and a core total pressure ratio of 1.35. The internal total temperatures were set to 1.19 and 2.59 times ambient for the fan and core streams, respectively. All results are for a free-stream Mach number of 0.28. Initial geometric definition of the tongue mixer was based on previous internal mixer experience. The intent was to vary key geometric parameters to optimize the configuration. Acoustic performance was to be qualitatively assessed based on the production of TKE. However, the numerical solution in the plume proved extremely slow to converge. As a result, it was not feasible to explore alternate configurations such as different numbers of chutes, chute deflection angle, or tongue shape.

The numerical results confirm that the selected configuration is aerodynamically acceptable, producing no regions of separated flow and acceptable losses. As can be seen in Figure 6, the core centerline temperature begins to decay at approximately six diameters downstream of the mixer exit; this is similar to single-stream jet flows. It should be noted that full convergence has not been achieved in the region downstream of 20 diameters. In addition, the lack of monotonic decay of the centerline total temperature from three to 20 diameters (including spikes in Figure 6) is due to either lack of convergence or numerical issues related to how NPARC treats the coordinate transformation Jacobian at the centerline. The centerline axial velocity decay is shown in Figure 7. This trend is similar to total temperature decay.

As a check on the results, the numerical results were compared with ideal core velocity and total temperature. The maximum numerical value of axial velocity occurs on the centerline and is very close to the ideal levels. The ideal mixed total temperature was reached approximately 10 diameters downstream of the mixer exit, similar to the behavior measured on other mixer/nozzle configurations. Displaying the centerline velocity and temperature evolution on a log/linear scale showed decay behavior

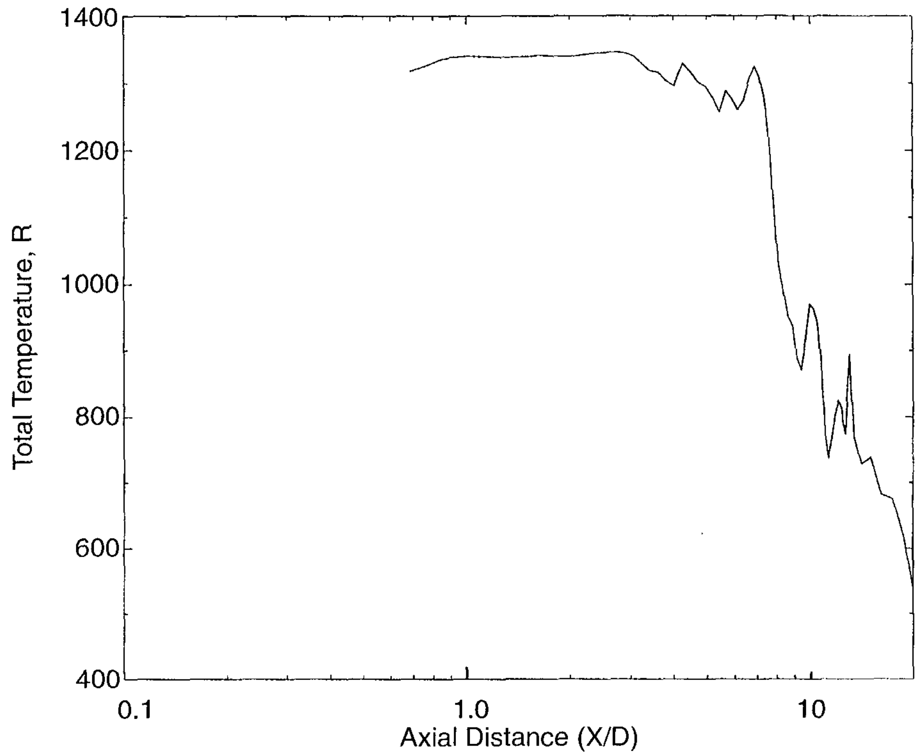


**Figure 6. Total Centerline Temperature Decay**

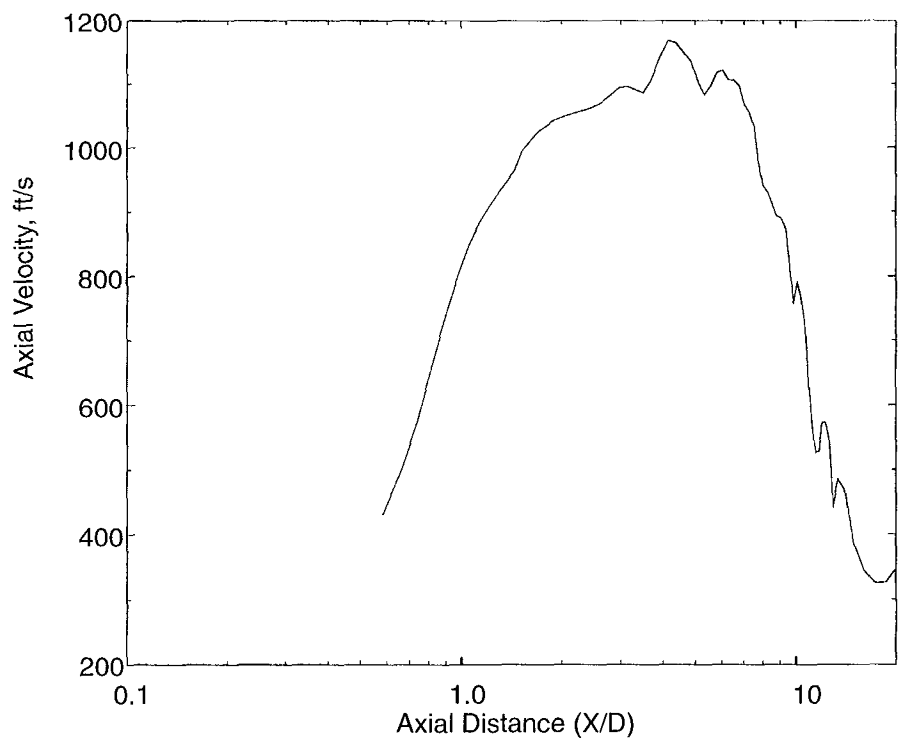


**Figure 7. Axial Centerline Velocity Decay**

very similar to that observed in single-stream jets, except in the region between the nozzle exit and two diameters downstream. In this region, the velocity field is controlled by the wake from the core nozzle plug.

Contour plots of total temperature and TKE are presented in Figures 8 and 9. These figures demonstrate the qualitative effect of the tongue mixer on the mixing of the core and fan streams. The predicted contours show the formation of a strong axial vortex. In contrast to more traditional mixed-flow configurations, this vortex forms in a region of relatively high axial velocity and is not constrained by the presence of duct walls. Interactions between the vortex and the primary-to-secondary shear layer in the vortex formation region appear weak. The strength of the vortex has decayed an order of magnitude by five diameters downstream of the core nozzle exit.

Referring to Figure 9, the annular concentration of TKE in the core cowl shear layer is initially generated by the roll-up of the axial vortex and its interaction with the tongue boundary layers. As the plume evolves, the TKE continues to increase. A maximum is reached approximately one-half diameter downstream of the core nozzle exit and persists well downstream. This is accompanied by a general dispersion of turbulence across the

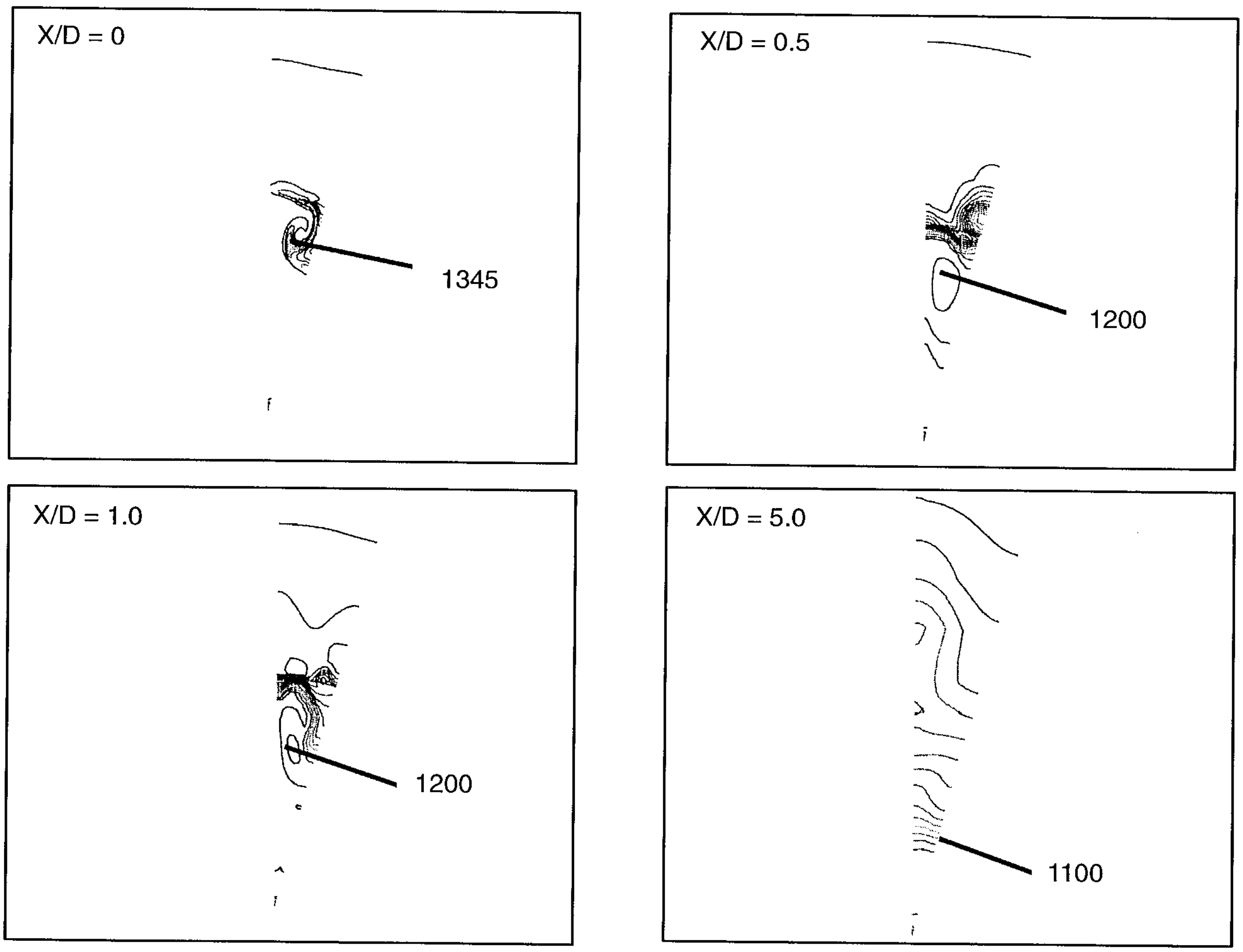


Temperatures are in °R; contours are in 50° increments.

**Figure 8. Total Temperature Contours**

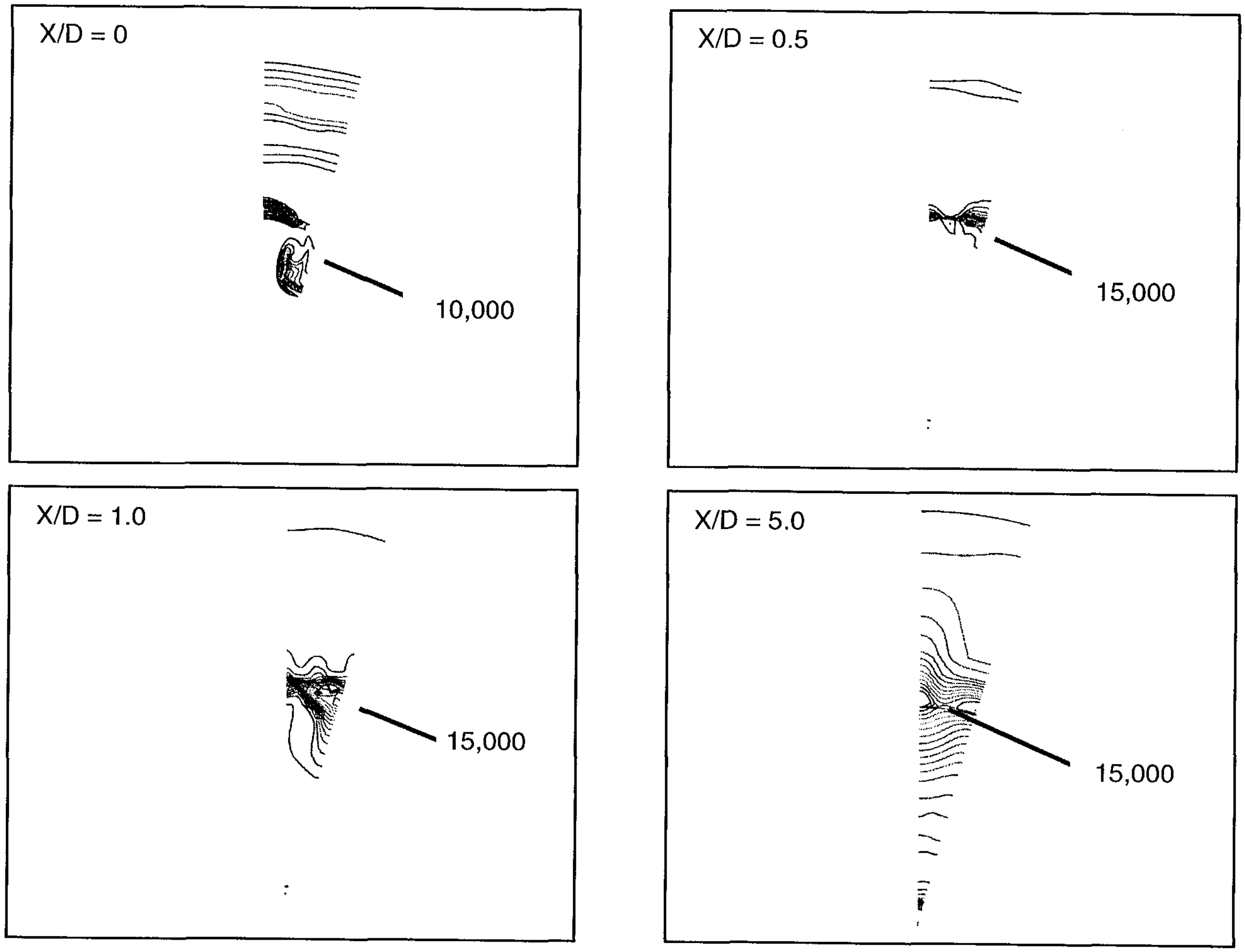


TKE in $ft^2/s^2$, contours in 1200-$ft^2/s^2$ increments.

**Figure 9. Kinetic Energy Contours**

plume, until at five diameters downstream of the core nozzle exit, turbulence is found across the entire radial extent of the plume. Not surprisingly, this corresponds to the end of the primary jet potential core. Evolution of the turbulence properties in this annular region is likely to be strongly influenced by numerical modeling approximations. The grid blocking scheme employed in this region produced a noncontiguous, overlapping grid interface. As previously mentioned, information is transferred across such boundaries by interpolation. The interpolation process may well be the reason for the TKE tending to the constant maximum value mentioned earlier. Due to extremely slow convergence of the numerical results, it was not possible to investigate the sensitivity of turbulence to changes in grid structure or interpolation scheme.

Interpretation of the CFD results in terms of acoustic impact was difficult. It was initially intended to use TKE as a discriminator of acoustic performance. Since no calibration of numerical TKE predictions and measured noise levels was available for a reference configuration, qualitative rather than quantitative comparisons were intended. The formation of the region of fairly high TKE near the core nozzle exit, as shown in Figure 9, is physically consistent with the existence of a strong vortex in this region. Due to the relatively high velocities, noise produced in this region would be observed at higher frequencies than typically associated with jet mixing. However, persistence of the TKE maximum up to the end of the primary potential core does not appear to be a correct physical trend, making direct acoustic interpretation of CFD results impossible.

### 3.5 Doublet Design Review

The doublet concept was mainly based on the work by Barter and McCormick (References 13 and 15). Their studies showed that doublets generate strong streamwise vortices with little drag penalty. It was decided to select a doublet design identical to that used by Barter and McCormick but scaled for differences in boundary layer thickness (based on velocity).

### 3.6 Selected Mixing-Enhancer Concepts

Cost quotes were obtained for the 30 sets of mixing-enhancement candidate hardware listed in Table 2. Out of these 30, a total of 11 were selected for fabrication (denoted by * in Table 2). The selection was guided by CFD results for selected chevron designs, configuration considerations relative to what NASA Langley and P&W were planning for their test configurations, and budgetary limitations.

The selected devices, categorized in terms of the candidate mixing-enhancement concepts, for the different baseline separate-flow exhaust model applications are listed in Table 3. Table 4 is a condensed summary of the reasoning for eliminating concepts. Table 5 is a summary of the noise-reduction concepts finally selected for fabrication and acoustic evaluation.

#### 3.6.1 Selected Core Nozzle Concepts

For the BPR = 5 internal plug baseline nozzle (Model 2), a 12-chevron core nozzle and an AEC defined tongue mixer were chosen.

Because it is typical of many full-scale engine nozzles, the BPR = 5 external plug baseline nozzle (Model 3) was chosen as the exhaust system of most interest; consequently, most of the noise-reduction concepts were developed for application on this configuration. These included: an 8-chevron core nozzle, a 12-chevron core nozzle, a 12-chevron core nozzle with chevrons deflected into the core stream (inward flipper chevrons), a 12-chevron core nozzle with chevrons deflected alternately into the core and fan streams (alternating flipper chevrons), a core nozzle with 64 doublet vortex generators installed on the internal/core flow side, and a core nozzle with 20 doublet vortex generators installed on the external/fan flow side.

For the BPR = 8 external plug baseline nozzle (Model 5), a 12-chevron core nozzle was chosen.

No core nozzle mixing enhancer concepts were chosen for use on the BPR = 8 internal plug nozzle (Model 4) or the BPR = 5 coplanar baseline nozzle (Model 1) configurations.

#### 3.6.2 Selected Fan Nozzle Concepts

Separate-flow exhaust system fan nozzle hardware is the same for the BPR = 5 and 8 internal and external plug nozzle models. Therefore, any fan nozzle mixing-enhancer concept hardware chosen for one of these configurations can be employed on all of them. The types of devices selected for investigation on the fan nozzle include a 24-chevron arrangement and a nozzle with 96 doublet vortex generators installed on the internal/fan flow side near the fan nozzle exit plane.

The baseline BPR = 5 external plug with short fan nozzle model was deleted from the program. Hence, no noise-reduction devices were selected for study with this exhaust system design.

**Table 2. Mixing-Enhancer Candidate Concept List**

➧ Selected concepts indicated with an asterisk (*)

| Model | Item | Description |
|---|---|---|
| 2 | * 6a | Core Nozzle, 12 Chevron |
| | 6b | Core Nozzle, 24 Chevron |
| | 6c | Core Nozzle, Inward Flipper Chevron (12 or 24) |
| | 6d | Core Nozzle, Alternating Flipper Chevron (12 or 24) |
| | 6e | Core Nozzle, Chevron with Tabs (12 or 24) |
| | 6f | Core Nozzle with 18 Tabs |
| | 6g | Core Nozzle, 48 Internal Vortex-Generator Doublets |
| | 6h | Elliptic Core Nozzle |
| | * 6i | Core Nozzle, with Tongued Mixer |
| | 6j | Core Nozzle, 48 Internal Vortex-Generator Singlets |
| 2–5 | * 7a | Fan Nozzle, 24 Chevron |
| | 7b | Fan Nozzle, Flipper Chevron (12 or 24) |
| | 7c | Fan Nozzle, with 50 Tabs |
| | * 7d | Fan Nozzle, 96 Internal Vortex-Generator Doublets |
| | 7e | Elliptic Fan, Nozzle |
| | 7f | Fan Nozzle, 96 Internal Vortex-Generator Singlets |
| 3 | * 9a | Core Nozzle, 12 Chevron |
| | * 9b | Core Nozzle, 8 Chevron |
| | * 9c | Core Nozzle, Inward Flipper Chevron (12) |
| | * 9d | Core Nozzle, Alternating Flipper Chevron (12) |
| | 9e | Core Nozzle, Chevron with Tabs (12 or 24) |
| | 9f | Core Nozzle with 18 Tabs |
| | * 9g | Core Nozzle, 64 Internal Vortex-Generator Doublets |
| | 9h | Core Nozzle, 64 Internal Vortex-Generator Singlets |
| | * 9i | Core Nozzle, 20 External Vortex-Generator Doublets |
| 5 | * 13a | Core Nozzle, 12 Chevron |
| | 13b | Core Nozzle with 18 Tabs |
| Original 6 | 18a | Core Nozzle, 12 Chevron |
| | 18b | Core Nozzle, 64 Internal Vortex-Generator Doublets |
| | 18c | Core Nozzle, 64 Internal Vortex-Generator Singlets |

## Table 3. Mixing-Enhancer Concepts Selection

1. Comparison of Core Chevrons on Different Type Nozzles

| Model | BPR | Plug | Number of Chevrons | Item |
|---|---|---|---|---|
| 2 | 5.0 | Internal | 12 | 6a |
| 3 | 5.0 | External | 12 | 9a |
| 5 | 8.0 | External | 12 | 13a |

2. Comparison of Number of Chevrons on Core

| Model | BPR | Plug | Number of Chevrons | Item |
|---|---|---|---|---|
| 3 | 5.0 | External | 12 | 9a |
| 3 | 5.0 | External | 8 | 9b |

3. Comparison of Chevron Types on Core

| Model | BPR | Plug | Type of Chevrons | Item |
|---|---|---|---|---|
| 3 | 5.0 | External | Basic (12) | 9a |
| 3 | 5.0 | External | Inward Flipper (12) | 9c |
| 3 | 5.0 | External | Alternating Flipper (12) | 9d |

4. Comparison of Core Vortex Generators

| Model | BPR | Plug | Type of Vortex Generator | Item |
|---|---|---|---|---|
| 3 | 5.0 | External | Internal Doublet (64) | 9g |
| 3 | 5.0 | External | External Doublet (20) | 9i |

5. Comparison of Different Enhancer Devices on Core

| Model | BPR | Plug | Type of Enhancer | Item |
|---|---|---|---|---|
| 2 | 5.0 | Internal | 12 Chevrons | 6a |
| 2 | 5.0 | Internal | Tongue Mixer | 6i |

6. Fan Nozzle Enhancers

| Model | BPR | Plug | Type of Enhancer | Item |
|---|---|---|---|---|
| 2–5 | 5.0 – 8.0 | Internal and External | 24 Chevrons | 7a |
| 2–5 | 5.0 – 8.0 | Internal and External | Internal Doublet (96) | 7d |

Total Number of Concepts Selected: 11

Table 4. **Reasons for Elimination of Some of Mixing-Enhancer Concepts**

| Item | Reason |
|---|---|
| 6b | 12 Chevrons (6a) anticipated to be better |
| 6c | Effects on external plug nozzle (9c) more desirable |
| 6d | Effects on external plug nozzle (9d) more desirable |
| 6e | Anticipated effectiveness deemed not worth cost |
| 6f | 12 Chevrons (6a) anticipated to be better |
| 6g | Effects on external plug nozzle (9g) more desirable |
| 6h | Too expensive |
| 6j | Anticipated effectiveness deemed not worth cost |
| 7b | Anticipated effectiveness deemed not worth cost |
| 7c | NASA Langley and P&W concepts similar |
| 7e | Too expensive |
| 7f | Anticipated effectiveness deemed not worth cost |
| 9f | NASA Langley and P&W concepts similar |
| 9e | 12 Chevrons alone (9a) anticipated to be better |
| 9h | Doublets (9g) anticipated to be better |
| 13b | 12 Chevrons (13a) anticipated to be better |
| 18a | Original Model No. 6 deleted |
| 18b | Original Model No. 6 deleted |
| 18c | Original Model No. 6 deleted |

Table 5. **Noise-Reduction Concepts Selected for Evaluation**

| Core Nozzle | Model | | | | | Fan Nozzle * | Model | | | | |
|---|---|---|---|---|---|---|---|---|---|---|---|
| | 1 | 2 | 3 | 4 | 5 | | 1 | 2 | 3 | 4 | 5 |
| Chevron (8) | | | x | | | Chevron (24) | | x | x | x | x |
| Chevron (12) | | x | x | | x | | | | | | |
| Flipper Chevron (12) (Inward Flip) | | | x | | | | | | | | |
| Flipper Chevron (12) (Alternately Flip) | | | x | | | | | | | | |
| Vortex Generating Doublet (64) (Core Flow Side) | | | x | | | Vortex-Generating Doublet (96) (Fan Flow Side) | | x | x | x | x |
| Vortex Generating Doublet (20) (Fan Flow Side) | | | x | | | | | | | | |
| Tongue Mixer | | x | | | | | | | | | |

* Fan Nozzle Hardware Is Common For Models 2 Through 5

# 4.0 Separate-Flow Exhaust System Model Design, Fabrication, and Instrumentation

Five scale-model, separate-flow exhaust nozzles, representative of current and advanced high-BPR engines, were selected as baseline configurations for this program. Mixing-enhancement devices can be incorporated into the fan and core components of these nozzles. Twenty mixing-enhancement concepts (11 GEAE/AEC and 9 P&W) were chosen for the NASA testing, 7 for the fan nozzle and 13 for the core nozzle. The GEAE/AEC hardware is discussed in detail in the following paragraphs. Table 6 is a list of the contractor-fabricated model hardware for this program. Details of the separate-flow nozzle (SFN) model hardware are available in ASE series 2078 and 2087 drawings and in Reference 21.

## 4.1 Baseline Models

The baseline models consist of a BPR = 5 coplanar exhaust system and internal and external plug nozzle concepts of BPR = 5 and 8. These are scaled (scale factor = 1.0224) versions of concepts planned to be tested at NASA Langley. Estimated nozzle areas (at operating conditions) are presented in Table 7.

**Table 6. Separate-Flow Nozzle (SFN) Test Contractor Hardware List**

| ASE Dwg | Description | Contractor |
|---|---|---|
| 2078–001 | Model Nos. 2 – 5, fan nozzle | GEAE |
| 2078–002 | Model No. 1, fan nozzle | GEAE |
| 2078–003 | Model Nos. 2 – 5, 24-chevron fan nozzle | GEAE |
| 2078–004 | Model Nos. 2 – 5, 96 internal vortex generator doublet fan nozzle | GEAE |
| 2078–005 | Model No. 3, 20 external vortex generator doublet core nozzle | GEAE |
| 2078–402 | Model No. 3, tailcone forward section | GEAE |
| 2078–403 | Core nozzle adapter | GEAE |
| 2078–404 | Model No. 2/No. 3, core nozzle forward section | GEAE |
| 2078–405 | Model No. 3, core nozzle aft section | GEAE |
| 2078–406 | Model No. 5, tailcone forward section | GEAE |
| 2078–407 | Model No. 2, core nozzle aft section | GEAE |
| 2078–408 | Model No. 5, tailcone aft section | GEAE |
| 2078–409 | Model No. 4/No. 5, core nozzle forward section | GEAE |
| 2078–410 | Model No. 5, core nozzle aft section | GEAE |
| 2078–411 | Model No. 3, tailcone aft section | GEAE |
| 2078–412 | Model No. 4, core nozzle aft section | GEAE |
| 2078–413 | Model No. 1, core nozzle | GEAE |
| 2078–414 | Tongue mixer core nozzle forward ring | GEAE |
| 2078–416 | Tongue mixer core nozzle forward section | GEAE |

Table 6. Separate-Flow Nozzle (SFN) Test Contractor Hardware List (Concluded)

| ASE Dwg | Description | Contractor |
|---|---|---|
| 2078–422 | Model No. 3, 12-chevron core nozzle aft section | GEAE |
| 2078–423 | Model No. 3, 8-chevron core nozzle aft section | GEAE |
| 2078–424 | Model No. 5, 12-chevron core nozzle aft section | GEAE |
| 2078–425 | Model No. 2, 12-chevron core nozzle aft section | GEAE |
| 2078–426 | Model No. 3, 64 internal vortex generator doublet core nozzle aft section | GEAE |
| 2078–427 | Model No. 3, 12 inward flipper chevron core nozzle aft section | GEAE |
| 2078–428 | Core nozzle adapter strut body | GEAE |
| 2078–429 | Model No. 3, 12 alternating flipper chevron core nozzle aft section | GEAE |
| 2078–601 | Forward plug adapter | GEAE |
| 2078–602 | Model No. 1, tailcone | GEAE |
| 2078–603 | Model No. 2/No. 4, tailcone | GEAE |
| 2078–603A | Model No. 2/No. 4, extended tailcone | AEC |
| 2078–604 | Forward plug closeout | GEAE |
| 2078–605 | Model No. 2/No. 3, core nozzle cover ring | GEAE |
| 2078–606 | Core nozzle split ring cover | GEAE |
| 2078–607 | Model No. 4/No. 5, core nozzle cover ring | GEAE |
| 2078–608 | Tongue mixer core nozzle cover ring | GEAE |
| 2078–609 | Centerbody sliding sleeve | GEAE |
| 2078–611 | Tongue mixer fan lobe | GEAE |
| 2078–612 | Tongue mixer core lobe | GEAE |
| 2078–801 | Core ID sleeve | GEAE |
| 2078–802 | Core nozzle adapter strut body plug nose | GEAE |
| 2087–001 | Model No. 3, 48 flipper tab fan nozzle | P&W |
| 2087–002 | Model No. 3, 24 flipper tab fan nozzle | P&W |
| 2087–003 | Model No. 3, medium offset fan nozzle | P&W |
| 2087–004 | Model No. 3, max offset fan nozzle | P&W |
| 2087–006 | Model No. 3, scarf fan nozzle | P&W |
| 2087–401 | Model No. 3, 48 flipper tab core nozzle aft section | P&W |
| 2087–402 | Model No. 3, 24 flipper tab core nozzle aft section | P&W |
| 2087–404 | Model No. 3, half-mixer core nozzle aft section | P&W |
| 2087–407 | Model No. 3, full-mixer core nozzle aft section | P&W |
|  | Seals | GEAE |
|  | Fasteners | GEAE |

Table 7. Estimated Nozzle Areas at Simulated Takeoff Operating Conditions

| Model | Description | Estimated Area, $in^2$ | |
|---|---|---|---|
| | | Core | Fan |
| 1 | BPR = 5.0, Coplanar | 11.30 | 29.58 |
| 2 | BPR = 5.0, Internal Plug | 11.19 | 28.94 |
| 3 | BPR = 5.0, External Plug | 10.53 | 28.94 |
| 4 | BPR = 8.0, Internal Plug | 7.96 | 32.72 |
| 5 | BPR = 8.0, External Plug | 8.64 | 32.72 |

### 4.1.1 Model No. 1, Coplanar (BPR = 5.0)

Model No. 1 (Figure 10) is a BPR = 5 system with coplanar exit stations; it includes a tailcone aft section (ASE drawing 2078–602) and (ASE 2078–413) core nozzle (3.753-in cold exit diameter) and (ASE 2078–002) fan nozzle (7.246-in cold exit diameter). Based on previous scale-model nozzle experience, a fan nozzle external boattail angle of approximately 14° was selected. No mixing-enhancer devices were tested on this configuration. The purpose of this model was to provide a common concept for comparing acoustic data from NASA Lewis (AAPL) and NASA Langley (JNL).

### 4.1.2 Model No. 2, Internal Plug (BPR = 5.0)

Model No. 2 (Figure 11) is a BPR = 5 system with an internal plug. Components include a fan nozzle (ASE 2078–001), a tailcone (ASE 2078–603), core nozzle forward and aft sections (ASE 2078–404, 407), and a core nozzle cover ring (ASE 2078–605). The fan nozzle (9.629-in cold exit diameter) is common to model Nos. 2 through No. 5 and has an external boattail angle of approximately 14°. For testing, the fan nozzle exit plane was situated 24.39 inches aft — jet exit rig (JER) station 156.49 — of the facility free-jet nozzle exit plane at JER station 132.10. The tailcone is also used on Model No. 4 (BPR = 8, internal plug). Because of the flow lines, the core nozzle forward section is also common with Model No. 3 (BPR = 5, external plug), but the core nozzle aft section is unique to Model No. 2 and has an external boattail angle of approximately 14°. The core nozzle exit plane was designed to be 7.081 inches downstream of the fan nozzle exit plane at cold static conditions and has a cold exit diameter of 3.753 in. The core nozzle cover ring is also used on Model No. 3 (BPR = 5, external plug). Mixing-enhancer devices were tested on both the core and fan nozzles of Model No. 2.

### 4.1.3 Model No. 3, External Plug (BPR = 5.0)

Model No. 3 (Figure 12) is a BPR = 5 system with an external plug. Model No. 3 hardware includes the fan nozzle common to Model Nos. 2 through No. 5 as well as the core nozzle forward section and nozzle cover ring that are common with Model No. 2. The (ASE 2078–405) core nozzle aft section and (ASE 2078–402, 411) tailcone (external plug) are unique to Model No. 3. The plug angle is approximately 16°. The core cowl exit diameter is 5.156 inches (cold) and the core cowl external boattail angle is approximately 14°. Also, at cold conditions, the core cowl exit plane is 4.267 inches downstream of the fan nozzle exit plane. Model No. 3 was the workhorse for testing mixing-enhancer devices on both the core and fan nozzles.

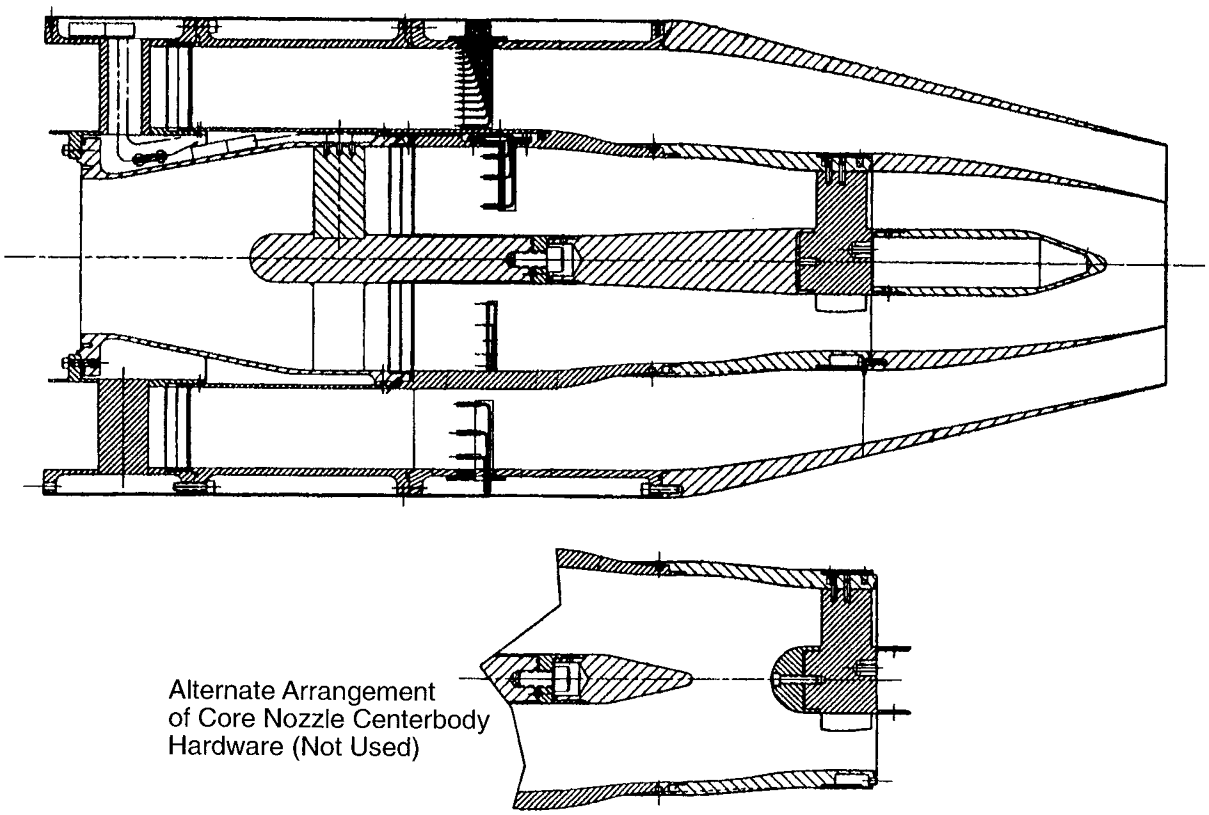


**Figure 10. Model System No. 1, BPR = 5.0, Coplanar**

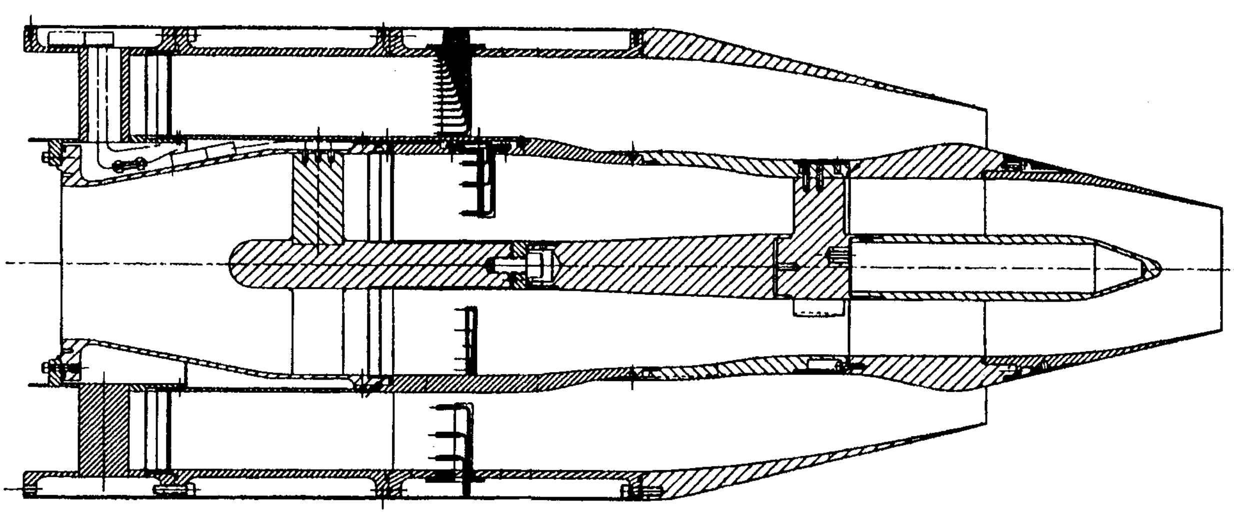

**Figure 11. Model System No. 2, BPR = 5.0, Internal Plug**

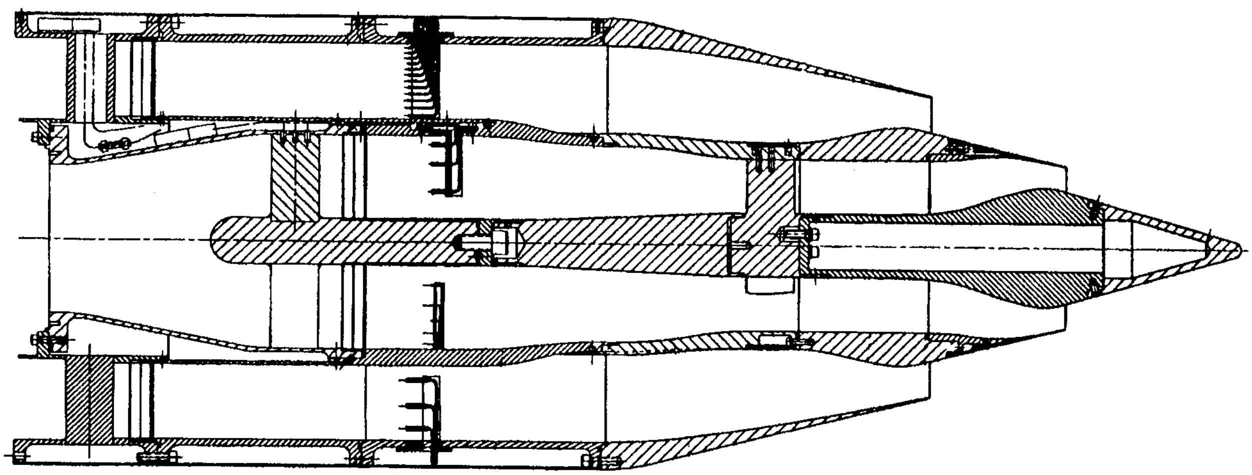

Figure 12. Model System No. 3, BPR = 5.0, External Plug

### 4.1.4 Model No. 4, Internal Plug (BPR = 8.0)

Model No. 4 (Figure 13) is a BPR = 8 system with an internal plug. Hardware components consist of the Model Nos. 2 through No. 5 common fan nozzle, the tailcone that is common with Model No. 2, a core nozzle forward and a core nozzle aft section (ASE 2078–409, 412) and a core nozzle cover ring (ASE 2078–607). The core nozzle forward section and cover ring are also used in Model No. 5 (BPR = 8, external plug). The Model No. 4 core nozzle aft section has a cold exit diameter of 3.165 inches, and the exit plane extends downstream from the fan nozzle exit plane by approximately 7.6 inches (cold). The external boattail angle of the core nozzle for Model No. 4 is approximately 14°. Mixing-enhancer concepts were available for the fan nozzle of Model No. 4, but none were tested.

### 4.1.5 Model No. 5, External Plug (BPR = 8.0)

Model No. 5 (Figure 14) is a BPR = 8 system with an external plug. It uses the Model Nos. 2 through No. 5 fan nozzle and the Model No. 4 core nozzle forward section and cover ring. However, the Model No. 5 core nozzle aft section (ASE 2078–410) has a cold exit diameter of 4.827 inches, and the exit plane extends downstream of the fan nozzle exit plane by 4.265 inches (cold). The core cowl external boattail angle is approximately 14°. The Model No. 5 tailcone (ASE 2078–406, 408) has a plug angle of approximately 16°. Mixing-enhancer devices were tested on both the core and the fan nozzles of Model No. 5.

### 4.1.6 Adapter Hardware

Baseline separate-flow exhaust system hardware interfaced with facility hardware in three areas. At the facility core centerbody (a 1.38-in diameter cylinder), an adapter (ASE 2078–601) attached to and encompassed the facility hardware, and a sleeve (ASE 2078–801) extended forward to act as the inner retainer for the core-flow screen assembly. The facility centerbody was then extended to the centerbody/plug of the core nozzle adapter piece with struts (ASE 2078–428) via a sliding sleeve (ASE 2078–609).

The interface at the core nozzle was designed to occur at JER station 146.1185. Here the core nozzle adapter piece (ASE 2078–403) provided the transition between the facility core hardware (ASE 2043–007) and the baseline

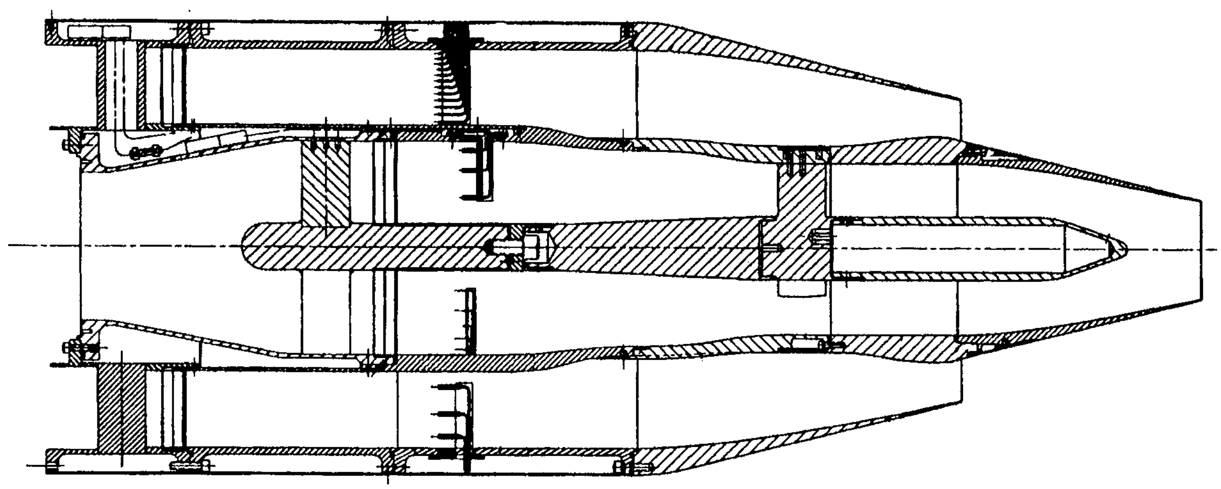

**Figure 13. Model System No. 4, Internal Plug, BPR = 8.0**

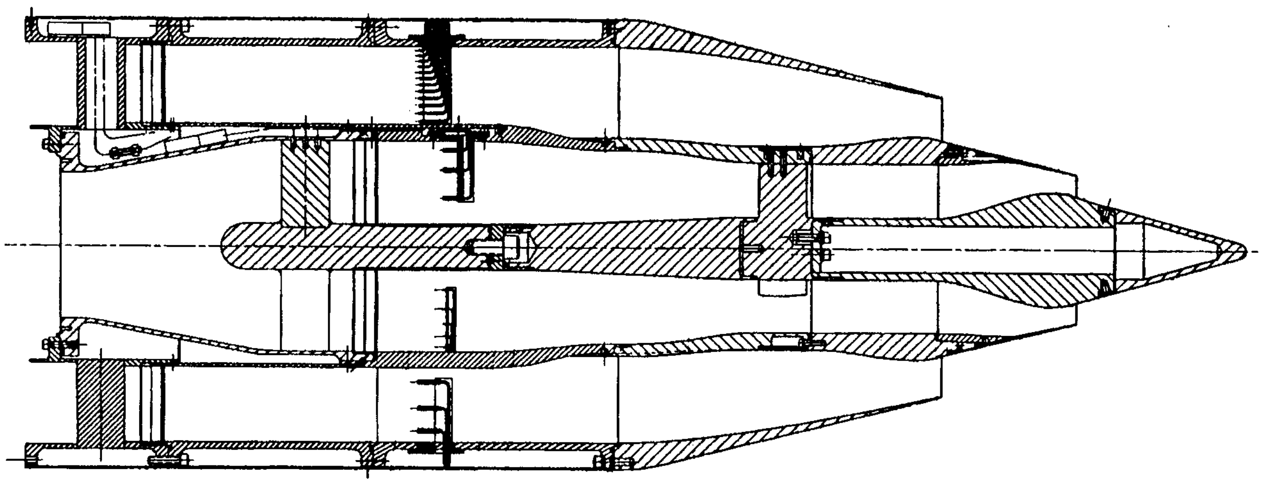

**Figure 14. Model System No. 5, External Plug, BPR = 8.0**

core nozzle forward sections. Struts (three) extending inward at the aft end of this adapter piece were part of a centerbody/plug (ASE 2078–428) to which the baseline hardware plugs attached.

As a precaution, in the event of differential thermal expansion complications associated with the sliding sleeve, an alternate configuration for the core nozzle centerbody hardware was available. In this alternate configuration, the facility centerbody is closed out by replacing the sliding sleeve with a 13° tailcone piece (ASE 2078–604). The resulting exposed front end of the core nozzle adapter piece with struts, including the sliding surface for the sliding sleeve, would be covered with a bulletnose (ASE 2078–802). This alternate arrangement, illustrated in Figure 10, was not used.

NASA provided a 12.739-in ID fan nozzle spool piece (NASA drawing 28529M42A001) that contained fan flow charging station instrumentation. SFN baseline and mixing-enhancer fan nozzle hardware attached to the aft flange of the spool piece at JER station 146.1185.

## 4.2 GEAE/AEC Mixing-Enhancer Concepts

The GEAE/AEC mixing-enhancement devices chosen for this program include chevrons, vortex-generator doublets, and a "tongue" mixer. These devices (included on new nozzle hardware) replaced the core nozzle aft sections and the fan nozzles of specified baseline separated-flow exhaust nozzle scale-model configurations (Model Nos. 2 through 5). Two GEAE mixing enhancer devices were fabricated for the baseline fan nozzles, and nine GEAE/AEC mixing enhancer devices were built for application on the baseline core nozzles. These are summarized in Table 8.

**Table 8. GEAE/AEC Mixing-Enhancer Devices**

| | |
|---|---|
| Fan | 24 Chevrons |
| | 96 Internal Vortex-Generator Doublets |
| Core | Tongue Mixer (Model No. 2) |
| | 12 Chevrons (Model No. 2) |
| | 8 Chevrons (Model No. 3) |
| | 12 Chevrons (Model No. 3) |
| | 12 Inward Flipper Chevrons (Model No. 3) |
| | 12 Alternating Flipper Chevrons (Model No. 3) |
| | 64 Internal Vortex-Generator Doublets (Model No. 3) |
| | 20 External Vortex-Generator Doublets (Model No. 3) |
| | 12 Chevrons (Model No. 5) |

### 4.2.1 Chevrons

Chevrons are a serrated continuation of a nozzle trailing edge. They were either straight extensions to the existing baseline nozzle, or they were directed inward; alternately, they were directed inward and outward at the nozzle exit to effect a flipper chevron geometry. For this test program, a 24-chevron fan nozzle and a 12-chevron core nozzle were tested on Model Nos. 2, 3, and 5. An 8-chevron core nozzle was tested on Model No. 3 as were 12-chevron inward and 12-chevron alternating flipper chevron configurations. Figure 15 illustrates the chevron geometry/nomenclature with respect to a baseline nozzle exit plane, and Table 9 lists the basic design parameters for the chevrons associated with this program.

The overall design philosophy of the chevron was to generate mixing between the core and fan streams and between the fan stream and the free stream, with minimum thrust loss. To minimize thrust loss, relatively minor flowpath changes were considered. Further design considerations allowed no surface discontinuities, and the chevrons blended smoothly to the baseline exhaust system. Surface discontinuities could lead to flow separation, thrust loss, and (potentially) increased noise.

To define the surface shape of the chevrons, second-order curves were used to generate a set of stringers. The boundary conditions that defined the shape of the curve were the location and slope of the upstream end of the chevron and the location of the downstream end of the chevron.

### 4.2.2 Vortex-Generator Doublets

The vortex-generator doublets selected by GEAE for testing consisted of tandem wedges located internally near the exit of a fan and a core nozzle and externally near the exit of a core nozzle. Reference 15 indicates that these generators can produce strong, streamwise vortices in transonic and supersonic wall-bounded flows.

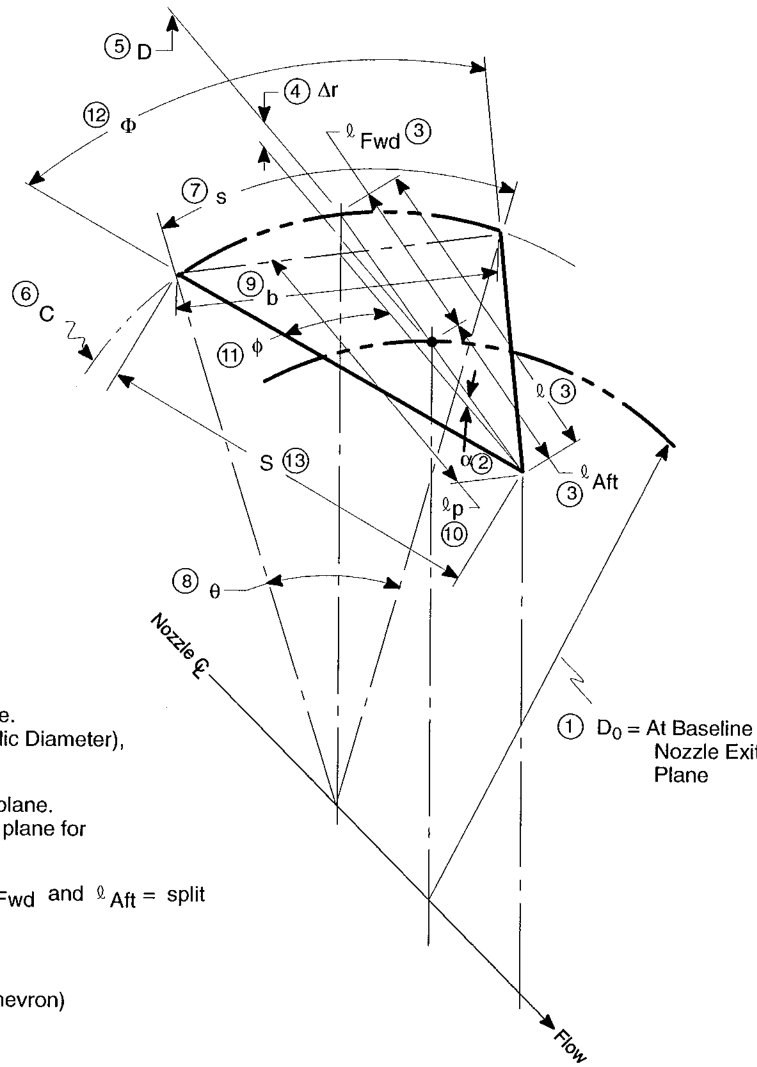


(1) $D_0$ = Nozzle ID at baseline nozzle throat plane. Also defined as PHD (Perimeter Hydraulic Diameter), for normalization

(2) $\alpha$ = Nozzle internal flowpath angle at throat plane. Used to project forward and aft of throat plane for definition of chevron parameters

(3) $\ell$ = Chevron length along inner flowpath; $\ell_{Fwd}$ and $\ell_{Aft}$ = split of length forward and aft of throat plane

(4) $\Delta r$ = $\ell_{Fwd} \times \sin\alpha$

(5) D = Do + $2\Delta r$ (Internal diameter at base of chevron)

(6) C = $\pi D$ (Circumference at base of chevron)

(7) s = C/N (Arc length at base of chevron where N = number of chevrons)

(8) $\theta$ = 360°/N degrees or $2\pi/N$ radians

(9) b = $D\sin(\theta/2)$, Chord length at base of chevron, $\theta$ in radians

(10) $\ell p$ = $\ell\cos\alpha$, projected (planform) length of chevron

(11) $\phi$ = $\arctan[(b/2)/(\ell p)]$, half angle of chevron tip

(12) $\Phi$ = $2\phi$ (included angle of chevron tip)

(13) S = $\sqrt{(b/2)^2 + (\ell p)^2}$, length of chevron side

(14) P = N x 2S (perimeter of all chevrons)

(15) $\ell$/PHD = Normalized chevron length

(16) P/PHD = Normalized chevron perimeter

**Figure 15. Chevron Nomenclature and Geometry with Respect to Baseline Nozzle Exit Plane**

**Table 9. Basic Chevron Design Parameters** *All dimension in inches unless otherwise specified.*

| Parameter | | Model No. | | | | |
|---|---|---|---|---|---|---|
| | | 3 | 3 | 5 | 2 | 2 – 5 |
| BPR | | 5.0 | 5.0 | 8.0 | 5.0 | 5.0 and 8.0 |
| Plug | | External | External | External | Internal | Internal and External |
| Nozzle Application | | Core | Core | Core | Core | Fan |
| Mixing Enhancer Item | | 9a | 9b | 13a | 6a | 7a |
| N | | 12 | 8 | 12 | 12 | 24 |
| 1 | $D_0$ (PHD) | 5.156 | 5.156 | 4.827 | 3.753 | 9.629 |
| 2 | $\alpha$ (degrees) | 11.92 | 11.92 | 12.02 | 11.02 | 11.99 |
| 3 | $\ell$ | 1.0 | 1.0 | 1.0 | 1.0 | 1.0 |
| 3 | $\ell_{fwd}$ | 0.5 | 0.5 | 0.5 | 0.5 | 0.5 |
| 3 | $\ell_{aft}$ | 0.5 | 0.5 | 0.5 | 0.5 | 0.5 |
| 4 | $\Delta r$ | 0.1033 | 0.1033 | 0.1041 | 0.0956 | 0.1039 |
| 5 | D | 5.3626 | 5.3626 | 5.0352 | 3.9442 | 9.8368 |
| 6 | C | 16.847 | 16.847 | 15.819 | 12.391 | 30.903 |
| 7 | s | 1.4039 | 2.1059 | 1.3182 | 1.0326 | 1.2876 |
| 8 | $\theta$ (degrees) | 30 | 45 | 30 | 30 | 15 |
| 8 | $\theta$ (radians) | 0.5236 | 0.7854 | 0.5236 | 0.5236 | 0.2618 |
| 9 | b | 1.3879 | 2.0522 | 1.3032 | 1.0208 | 1.2840 |
| 10 | $\ell_p$ | 0.9784 | 0.9784 | 0.9781 | 0.9816 | 0.9782 |
| 11 | $\phi$ (degrees) | 35.35 | 46.36 | 33.67 | 27.47 | 33.28 |
| 12 | $\Phi$ (degrees) | 70.69 | 92.73 | 67.34 | 54.95 | 66.55 |
| 13 | S | 1.1995 | 1.4178 | 1.1753 | 1.1064 | 1.1701 |
| 14 | P | 28.79 | 22.68 | 28.21 | 26.55 | 56.16 |
| 15 | $\ell$/PHD | 0.194 | 0.194 | 0.207 | 0.266 | 0.104 |
| 16 | P/PHD | 5.58 | 4.40 | 5.84 | 7.08 | 5.83 |

The fan nozzle internal doublet configuration (ASE 2078–004) was tested on Model No. 2 and contained 96 doublets. The core nozzle internal doublet scheme (ASE 2078–426) had 64 doublets and was tested on Model No. 3, as was the core nozzle external doublet design (ASE 2078–005) with 20 doublets. Doublet descriptions are summarized in Figure 16.

### 4.2.3 Tongue Mixer

The AEC-defined tongue mixer, Figures 17 (ASE 2078–415) and 18 (ASE 2078–417), consisted of 12 equally spaced, specially contoured chutes within the circumference of a core nozzle that partially penetrates into the core flow. This mixing-enhancer device was

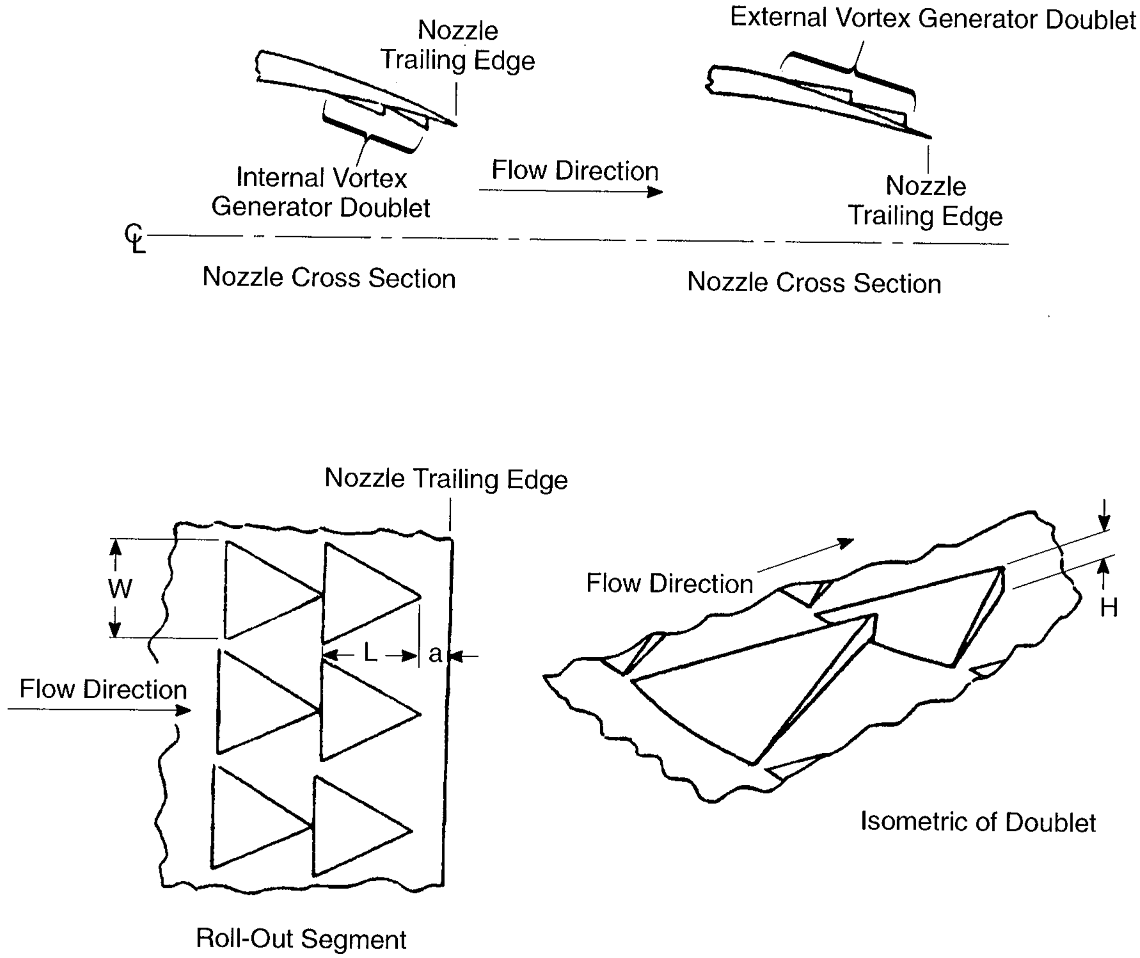


| Description | Number of Doublets | H (in) | a (in) | L (in) | W (in) (Arc Length) |
|---|---|---|---|---|---|
| Internal Placement on the BPR = 5 External Plug Core Nozzle | 64 | 0.05 | 0.50 | 0.35 | 0.25 |
| External Placement on the BPR= 5 External Plug Core Nozzle | 20 | 0.15 | 0.50 | 1.05 | 0.75 |
| Internal Placement on the Fan Nozzle Common to Models 2-5 | 96 | 0.06 | 0.60 | 0.42 | 0.30 |

**Figure 16. Vortex Generator Doublet Description**

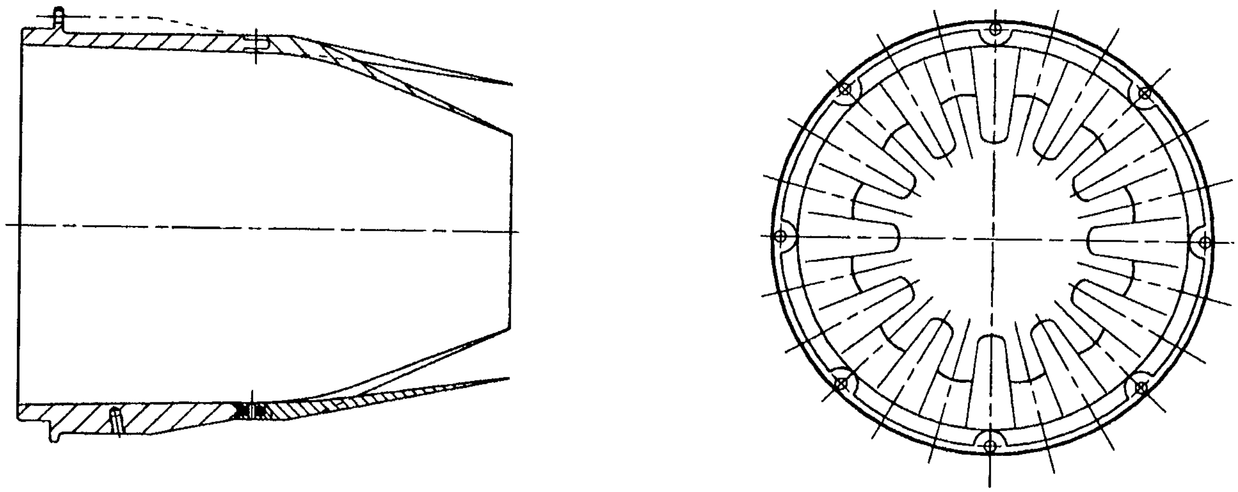

**Figure 17. Tongue Mixer Concept**

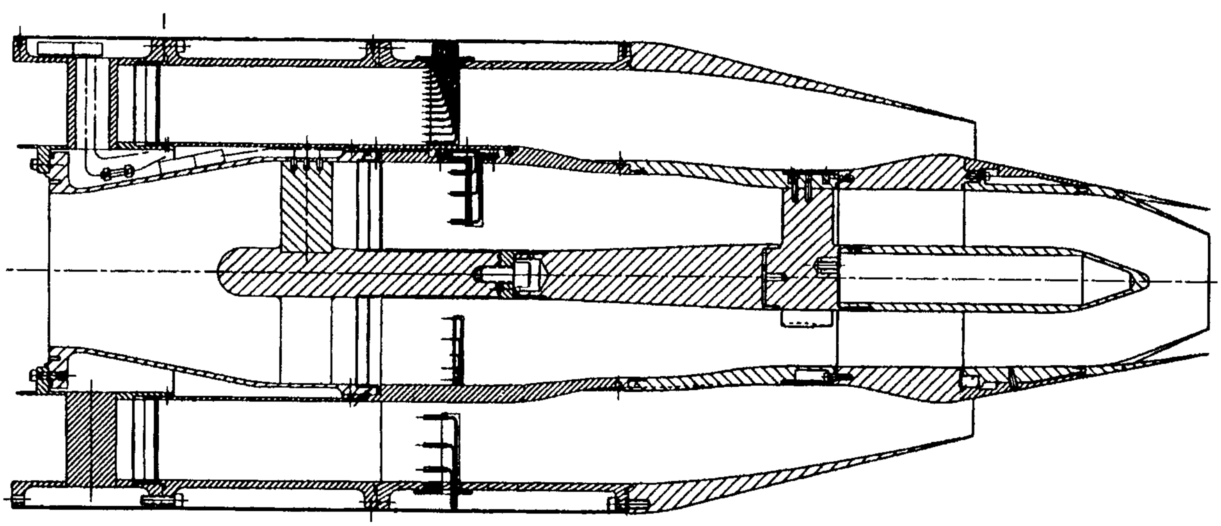

**Figure 18. Tongue Mixer Configuration Assembly**

evaluated on Model No. 2. Because of the complicated flow lines, this mixing-enhancer device required a dedicated core nozzle forward section (ASE 2078–416).

AEC developed the tongue mixer concept from earlier, NASA-sponsored, internal-mixer testing. The idea is to let the core and fan flows mix together downstream of the core cowl so that jet-mixing noise is reduced. The design consists of 24 periodically spaced, contoured chutes, called "tongues" herein, within the circumference of a core nozzle. The 12 alternate tongues, of equal width at the root, penetrate the core flow. The penetration depth and tongue length are selected such that the fan flow over the tongues will not separate. Since these tongues create a blockage of the core flow, the remaining 12 tongues are radially opened up such that the axially projected core-flow area at the core nozzle exit plane is kept equal to that of the baseline coaxial nozzle. However, to avoid creation of a concave corner on the outer surface of the core cowl (from the viewpoint of shockless supersonic fan flow at cruise conditions), that surface is kept smooth and conical with less deflection of the fan flow downstream of the fan throat than that in the baseline nozzle. The concept is depicted in Figure 17 (ASE 2078–415) and 18 (ASE 2078–417). To maintain the original length between fan and core nozzle exit planes, provide sufficient attachment area, and maintain smooth flow lines into the mixing section, a dedicated, unique, core nozzle forward section was required (ASE 2078–416).

Initial testing of the tongue mixer configuration produced core mass flow rates significantly higher than design intent (about 42% higher), resulting in bypass ratios below the desired range (about 3.64 instead of 5.2). Since program constraints made modification of the tongue geometry impractical, a new core plug was defined (ASE 2078–603A) that extended into the core nozzle exit plane to provide additional flow blockage. The outer diameter of the cylindrical portion of the extended plug was identical to the original short plug, and the length was established such that the cylindrical section extended to the core nozzle exit plane. The reduction in core flow area achieved due to this extended plug turns out to be the same percent as the reduction in core flow rate obtained with the baseline nozzle compared to the unmodified plug at all core nozzle pressure ratios tested. Figure 19 shows the tongue mixer with the extended plug.

## 4.3 Instrumentation

No instrumentation was installed on the contractor-supplied model hardware.

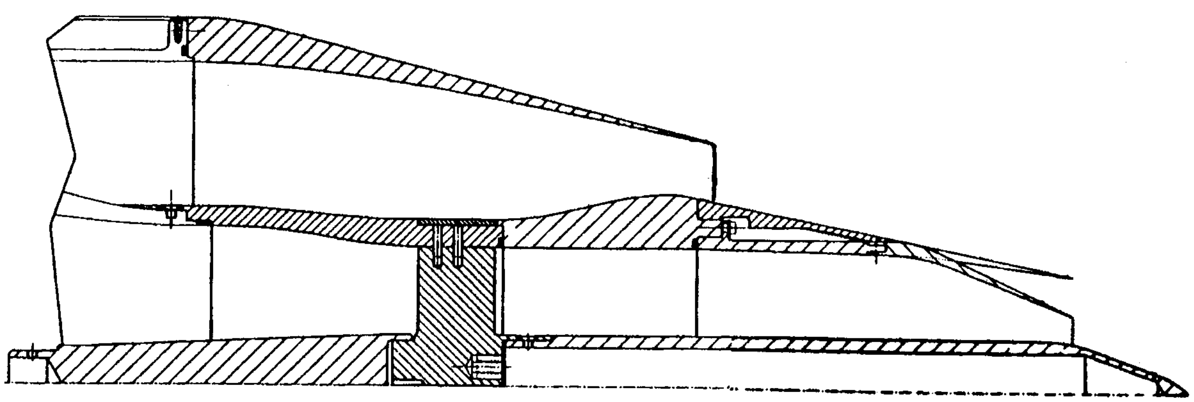

**Figure 19. Tongue Mixer With Extended Plug (Model 6)**

# 5.0 Acoustic Test Facility and Test Scope

Testing of the SFN exhaust system baseline and mixing enhancer hardware was conducted in the NASA Lewis Research Center Aeroacoustic and Propulsion Laboratory (AAPL). A 7½-week installation and checkout time frame was followed by 5 weeks of acoustic testing, 2 weeks of Boeing phased-array installation and testing, another week to revert back to and conduct more acoustic testing, and then 2 additional weeks for plume survey rake installation and testing. During acoustic testing, NASA periodically acquired their own phased-array data and took infrared camera shots of selected exhaust nozzle configuration jet plumes. Test variables included free-jet Mach number, fan nozzle pressure ratio, core nozzle pressure ratio, fan flow temperature, and core flow temperature. A test plan report (Reference 22) was jointly prepared for this test program by GEAE and P&W with contributions from NASA Lewis facilities personnel, AEC, and the Boeing Commercial Aircraft Company.

## 5.1 Facility Description and Instrumentation

The AAPL at NASA Lewis is a 65-ft radius, anechoic, geodesic-dome, hemispherical housing (Figures 20 and 21). The walls of the dome and approximately half of the floor area are treated with acoustic wedges. Within the confines of the dome is the Nozzle Acoustic Test Rig (NATR). The NATR (Figure 22) is a free-jet, forward-flight-simulation test rig. The duct work is acoustically lined and extends from an annular air ejector system to a plenum and transition (bellmouth) section that is an ASME long-radius, low-β-ratio nozzle followed by a free-jet nozzle duct having an exit inner diameter of 53 inches and a nozzle centerline approximately 10 feet above the

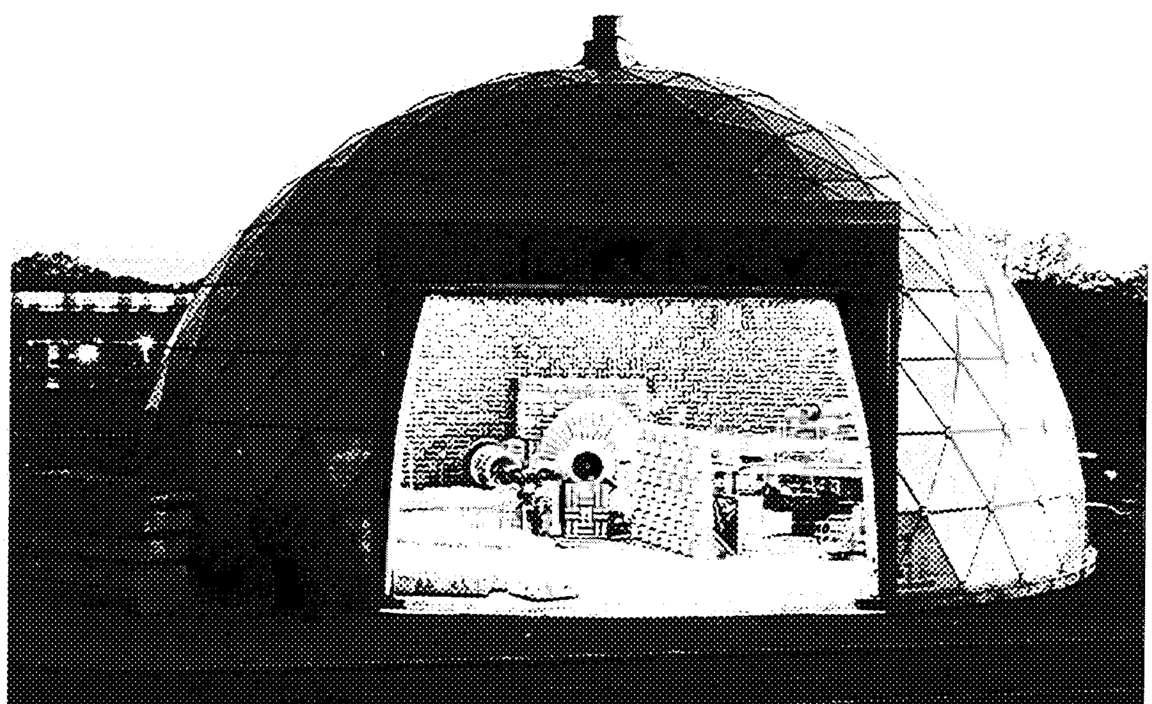

**Figure 20. Photo of NASA Lewis AAPL Facility**

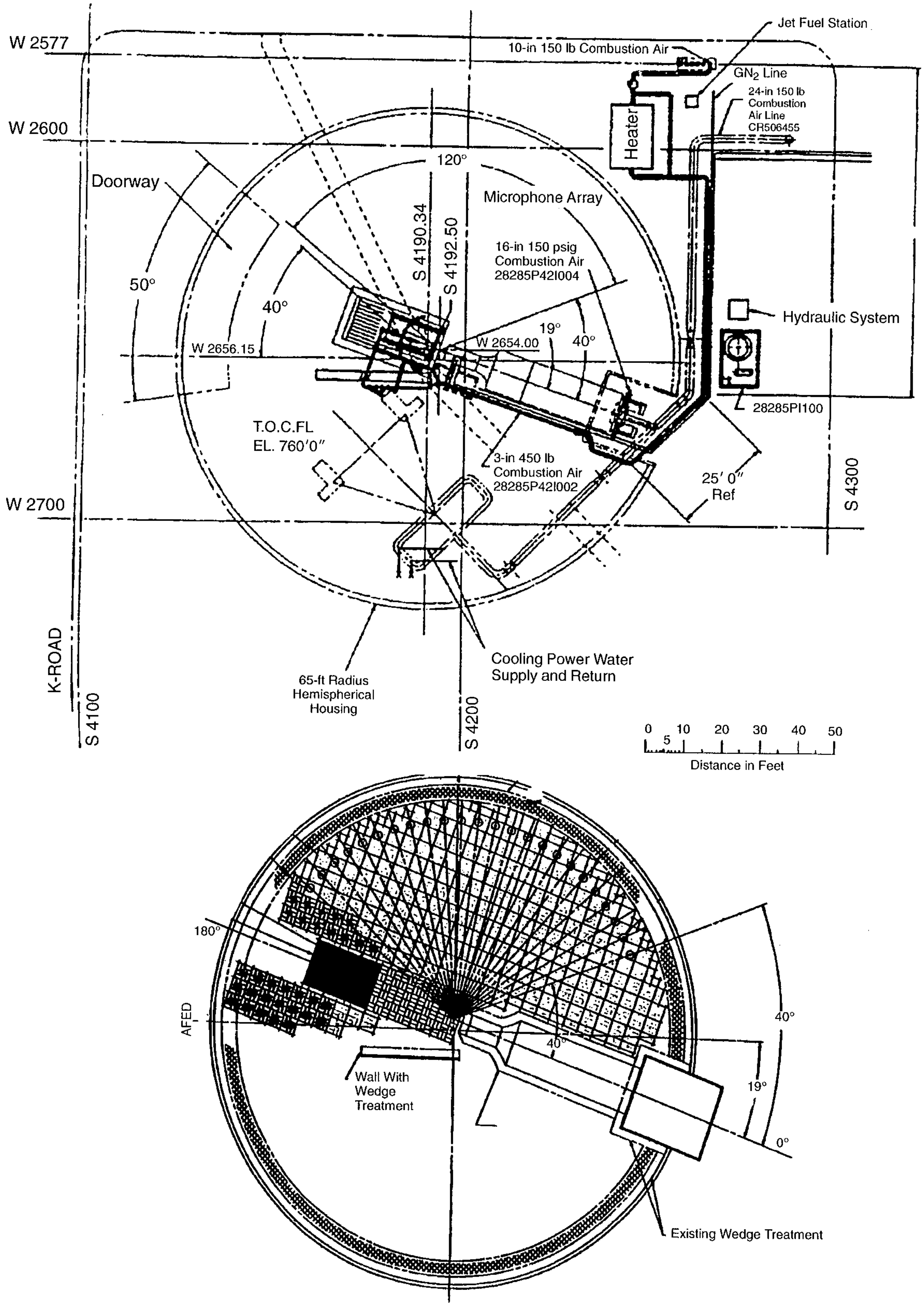


**Figure 21. NASA Lewis Aeroacoustic Propulsion Laboratory Facility**

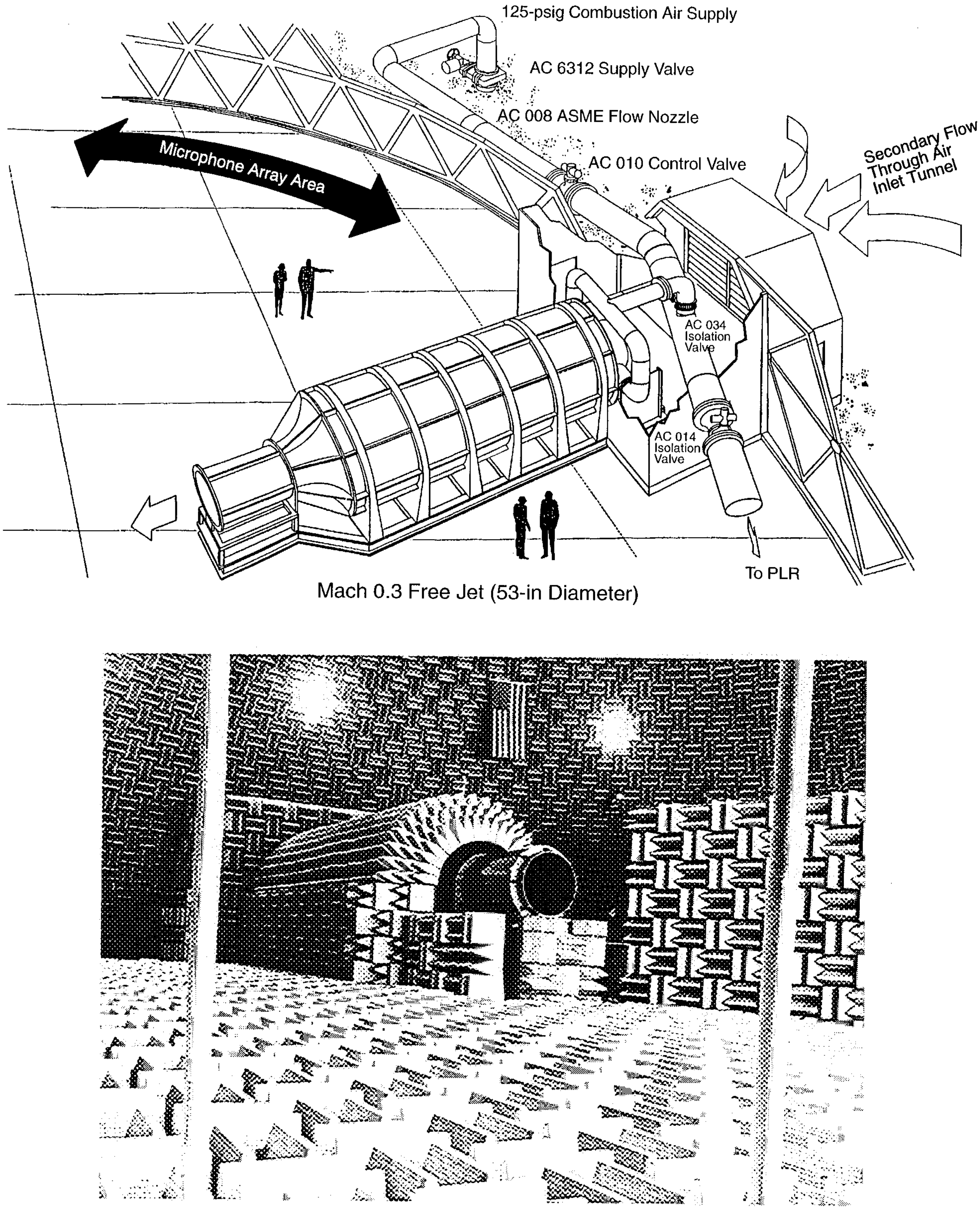


**Figure 22. Nozzle Acoustic Test Rig**

floor. This arrangement allows free-jet Mach number capability up to 0.3. An acoustically treated wall installed in the AAPL near the NATR exit plane and extending aft along the jet exit rig shields the test article noise source from being reflected off powered lift rig (PLR) test equipment toward the facility farfield microphones.

Downstream of the NATR is the jet exit rig. Test models are installed on the aft end of the JER, and the movable JER is positioned axially relative to the NATR free-jet nozzle exit plane at the desired location (generally a distance that aligns the test model nozzle exit approximately 24 inches downstream of the NATR exit plane) to appropriately use the 48-ft arc microphone array of the AAPL. The JER is the structure through which airflow is delivered to the test article via connections to facility compressed air supplies. For this program, the JER was a tandem-strut arrangement (NASA drawing 28529M42A000). This JER setup and arrangement relative to the NATR are shown in Figures 23 and 24. Exhaust gases from the JER/NATR are expelled through the 43-ft high by 55-ft wide AAPL exhaust door. A 60-in exhaust fan in the top of the dome provides air circulation. More detailed information relative to the AAPL facility, test rigs, and support systems is available in Reference 23.

Nozzle airflows, pressures, and temperatures are monitored using JER/NATR instrumentation. Choked-flow venturi locations in the facility compressed air system and associated instrumentation are illustrated in Figures 25 and 26, respectively. Four total pressure/temperature rakes (with five $P_T$ and five $T_T$ elements each) are installed at the charging station of the fan and of the core ducts of the JER. The fan rakes are installed at circumferential angle positions of 0°, 90°, 180°, and 270° (aft looking forward). Core nozzle rakes are located at circumferential angles of 60°, 150°, 240°, and 330° (aft looking forward). The $P_T/T_T$ measurement plane for the fan flow is JER station 140.025, and the radial locations of the $P_T$ and $T_T$ sensors on the fan rakes are given in NASA drawing 28529M42A002. The $P_T/T_T$ measurement plane for the core flow is JER station 140.741, and the radial locations of the $P_T$ and $T_T$ sensors on the core rakes are detailed in NASA drawing 28529M42A003.

Acoustic instrumentation in the AAPL consists of twenty-six ¼-in B&K microphones on a 48-ft radius arc. These microphones are mounted in the dome on 10-ft pole stands bolted to the floor. For this test program, the angle range for the microphones was from 40° in the front quadrant to 165° in the aft quadrant and in 5° intervals. This microphone array is illustrated in Figure 21 and shown in a photo in Figure 27. Microphone checks were conducted daily to assess the need for recalibration or replacement.

## 5.2 Model Interface

Separate-flow exhaust system model fan nozzle hardware was designed to attach to the NASA-supplied fan spool piece (NASA drawing 28529M42A001) at cold JER station 146.1185. Model core cowl/nozzle hardware was designed to attach to the facility core duct (ASE 2043–007) at cold JER station 146.1185. Model centerbody/plug hardware was designed to attach to the facility core/tailcone extension weldment (ASE 2043–406) at cold JER station 142.1925. When assembled and positioned, the separate-flow exhaust system fan nozzle exit plane of Models Nos. 2 through 5 was designed to be positioned at cold JER station 156.49, and the NATR exit plane was to be located at cold JER station 132.10. The nozzle model centerline was elevated 10 feet above the facility floor.

Because of the different length, the Model 1 fan nozzle exit plane was designed to be positioned at cold JER station 161.221 (4.731 inches further downstream than Models 2 through 5).

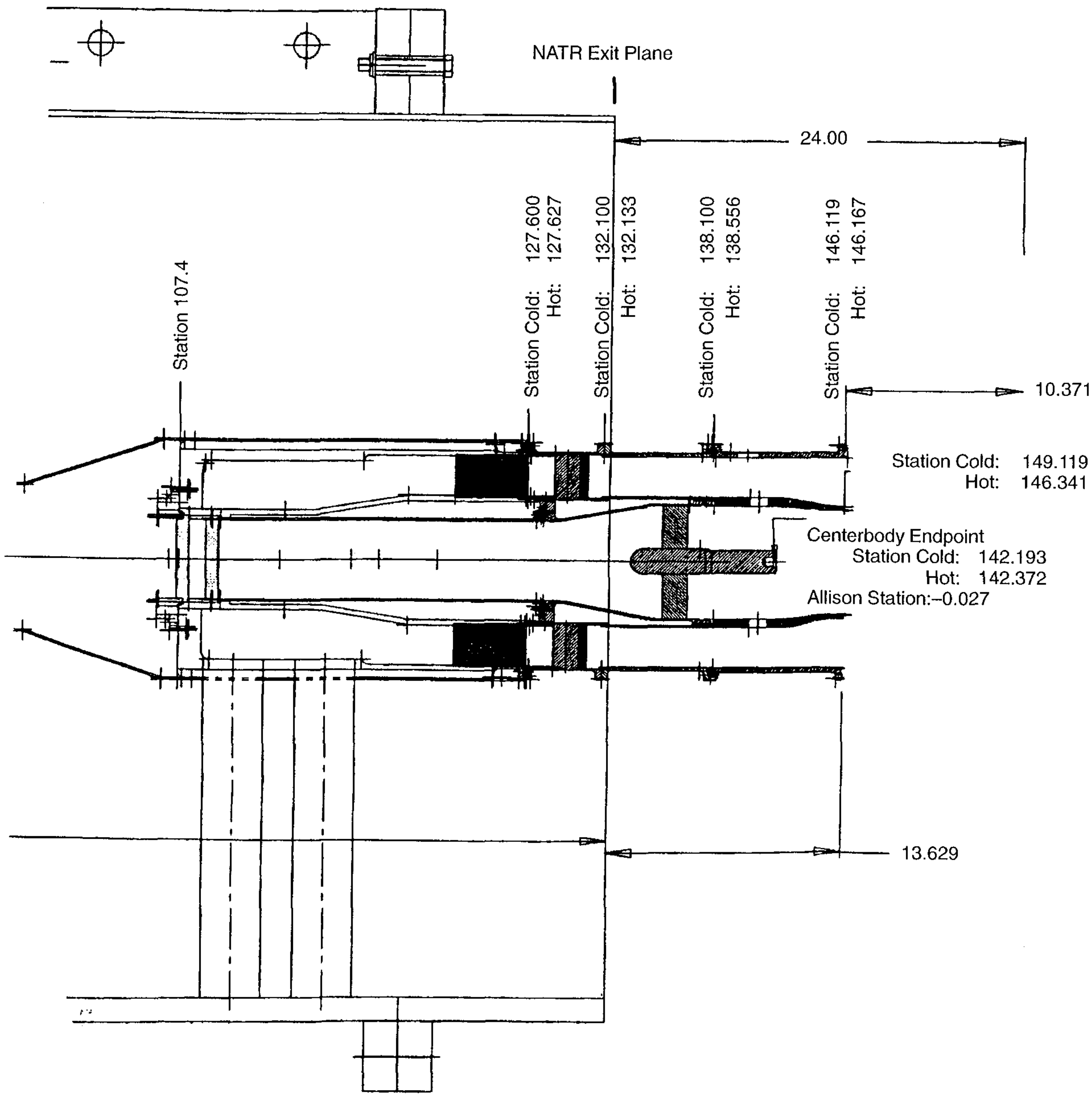


**Figure 23. NATR/JER Dispostion for SFN Test**

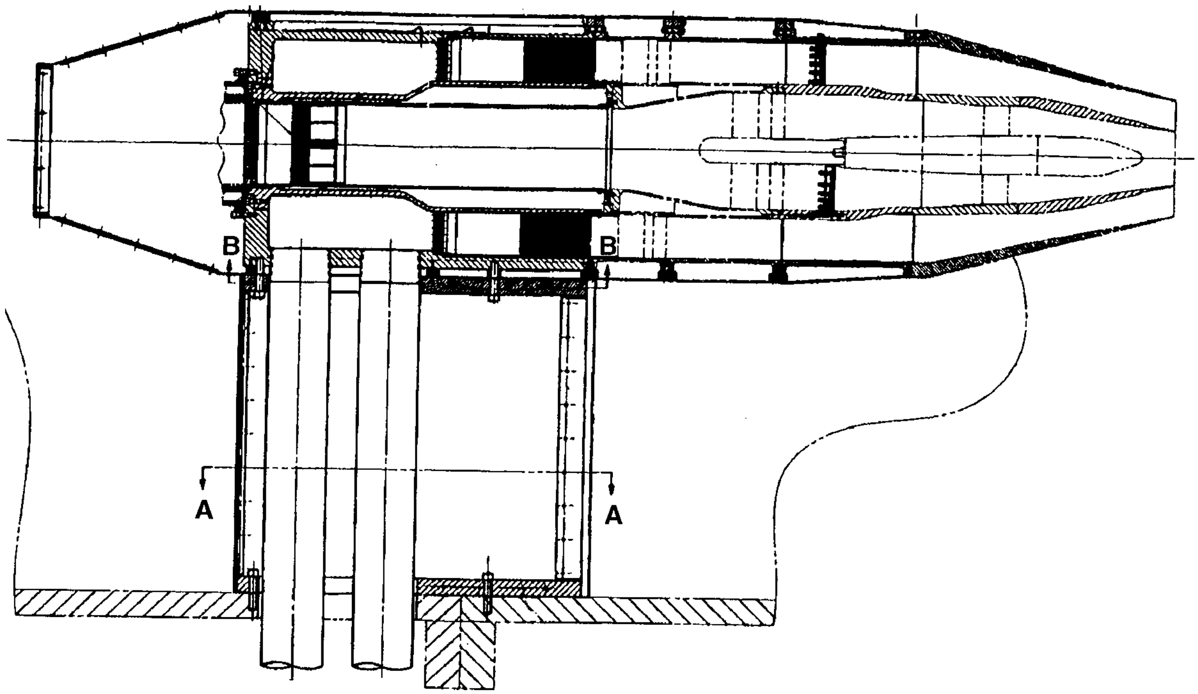


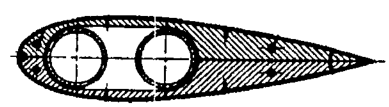

Section B–B

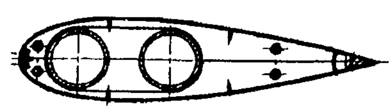

Section A–A

**Figure 24. Jet Exit Rig Configuration for SFN Test**

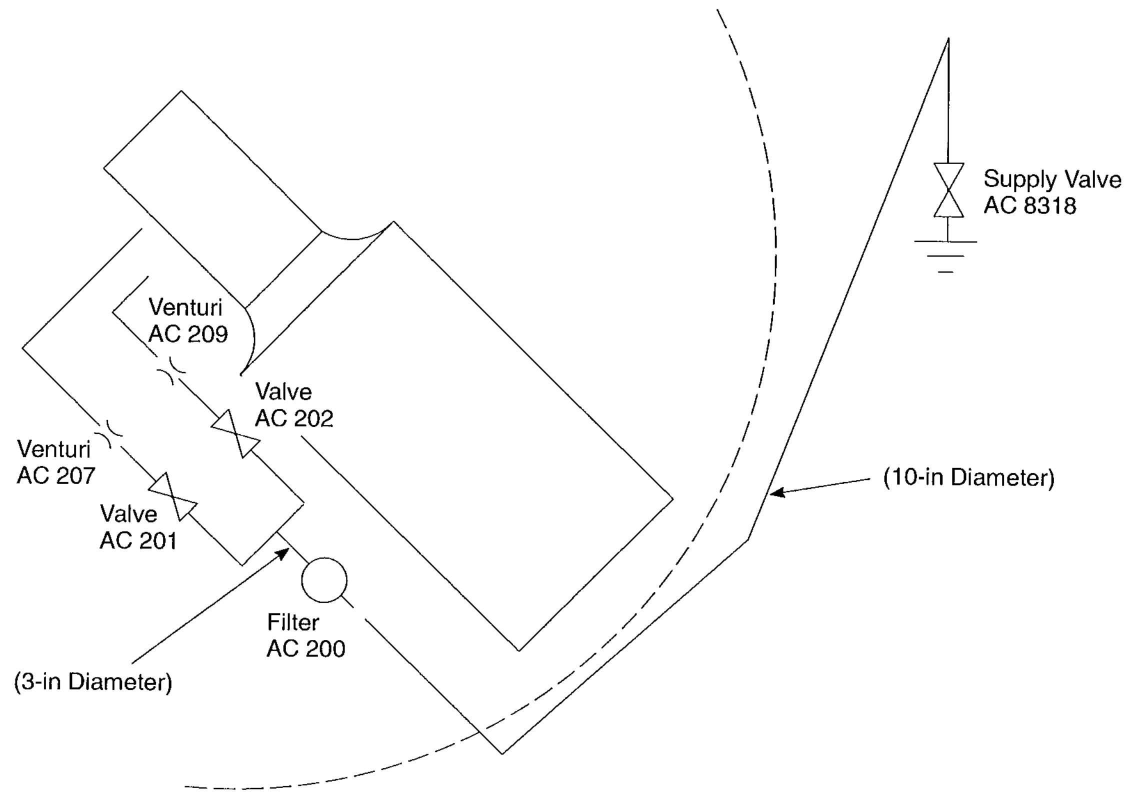


**Figure 25. AAPL Flow Measurement Venturi Locations**

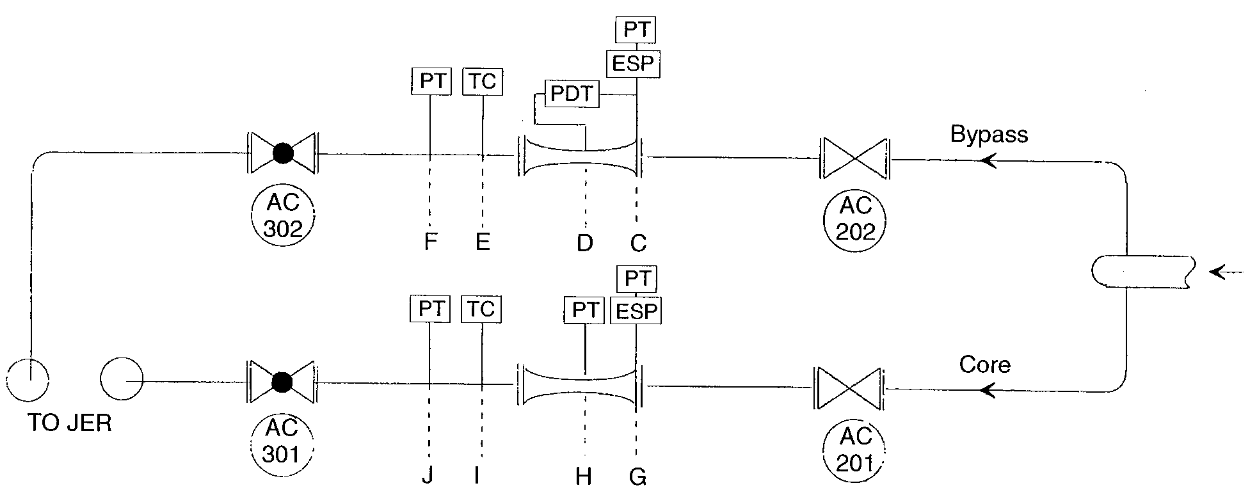


**Figure 26. AAPL 450 psig Compressed Air System Instrumentation**

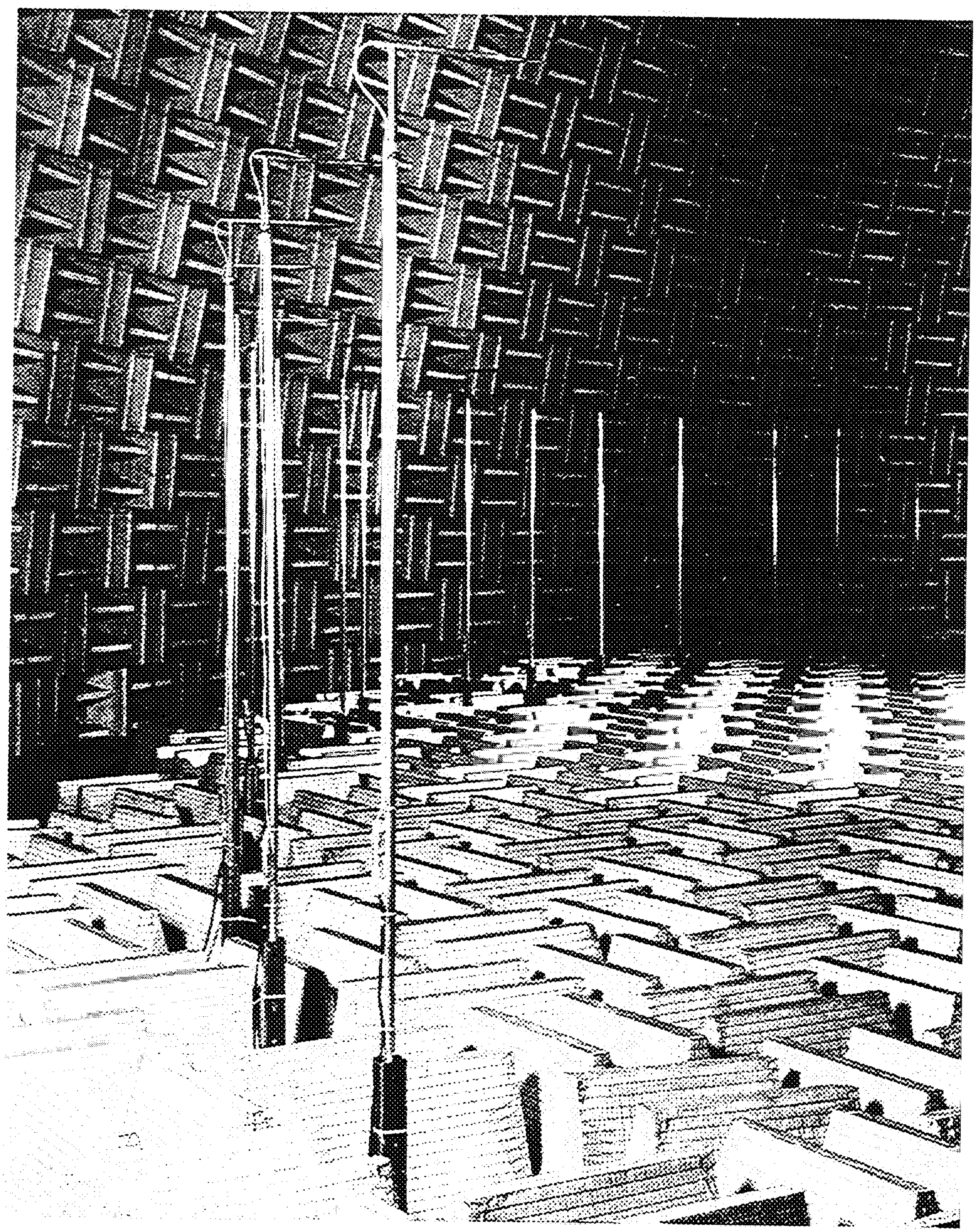

Figure 27. AAPL Microphone Array

Figure 28 shows the intended JER/separate-flow exhaust system model hardware interface. However, a cold measurement taken during the test program (3/24/97) indicated that the core nozzle interface station was approximately 0.06 inch further aft than desired — causing the core nozzle hardware to be built-up slightly farther aft relative to the fan nozzle hardware than originally intended. This could mean that the actual fan nozzle throat areas during testing were slightly different than anticipated, due to the altered fan inner and outer flowpath alignment caused by the hardware stackup resulting from the core interface station anomaly. This situation, however, existed for all nozzle configurations. The influence of the interface alignment anomaly, if any, on acoustic measurements would be the same for all configurations when comparisons are made to evaluate noise-reduction concepts. For this reason, the interface alignment issue is considered a moot point and only mentioned for documentation.

### 5.3 Acoustic Test Conditions

The AAPL SFN test was mostly devoted to acoustics. Noise data were measured for the baseline separate-flow configurations at Mach numbers of 0.0, 0.20, and 0.28. Power settings, as defined by Cycles 1 and 3 (see Table 10), were used to duplicate those planned to be tested at the NASA Langley JNL facility.

Baseline noise data at power settings defined by Cycles 2 and 4 (Table 10) were acquired to establish a benchmark for assessing the noise-reduction effectiveness of subsequently tested mixing-enhancement devices.

Cycle 5 test conditions (Table 10) with elevated core flow temperature were set to determine the impact of this parameter on noise for baseline configurations 1 and 2BB (Model Nos. 1 and 2 baseline configurations).

Cycle 2 power settings (see Table 10) at Mach numbers of 0.0, 0.20, and 0.28 were used for acoustic data point settings associated with mixing enhancer configurations of Model Nos. 2 and 3. Similarly, Cycle 4 (see Table 10) was used with Model Nos. 4 and 5 mixing-enhancer configurations for acoustic data point settings.

The desired fan and core nozzle pressure ratio ranges for acoustic testing were dependent on the design bypass ratio of the test configuration. For BPR 5 models, the fan nozzle pressure ratio range was 1.27 to 1.89 and the core nozzle pressure ratio range was 1.12 to 1.79. With the BPR 8 models, the fan pressure ratio range was 1.17 to 1.62 and the core pressure ratio range was 1.05 to 1.60.

Fan and core flow temperature ranges were similar for the two bypass ratios and were 560° to 662°R for the fan flow and 1185° to 1580°R for the core flow. The core flow temperature setting ranged to 1640°R for Cycle 5. This condition was only experienced during Model Nos. 1 and 2 baseline hardware configurations at limited Mach/power setting situations (Table 10). Tested power setting conditions of Cycles 2 and 4 are plotted in Figure 29.

To investigate the feasibility of noise reduction for different engine operating cycles, configuration 3BB (Model No. 3 baseline) and the best mixing-enhancer configuration (3IC) were tested at set-point parameters representative of an engine cycle with a more open core nozzle area than the original Cycles 1 and 2. Cycle 6 power setting parameters are listed in Table 11.

Model 4 hardware was altered for the acoustic test by substituting the new core plug (fabricated to modify the tongue mixer configuration) to create a BPR 14 test nozzle. The power setting parameters of Cycle 7 (listed in Table 12) were used for acoustic data point settings.

Acoustic testing was conducted by setting a specified free-jet Mach number and acquiring acoustic data during power setting sweeps in accordance with set-point conditions outlined in Tables 10, 11, and 12.

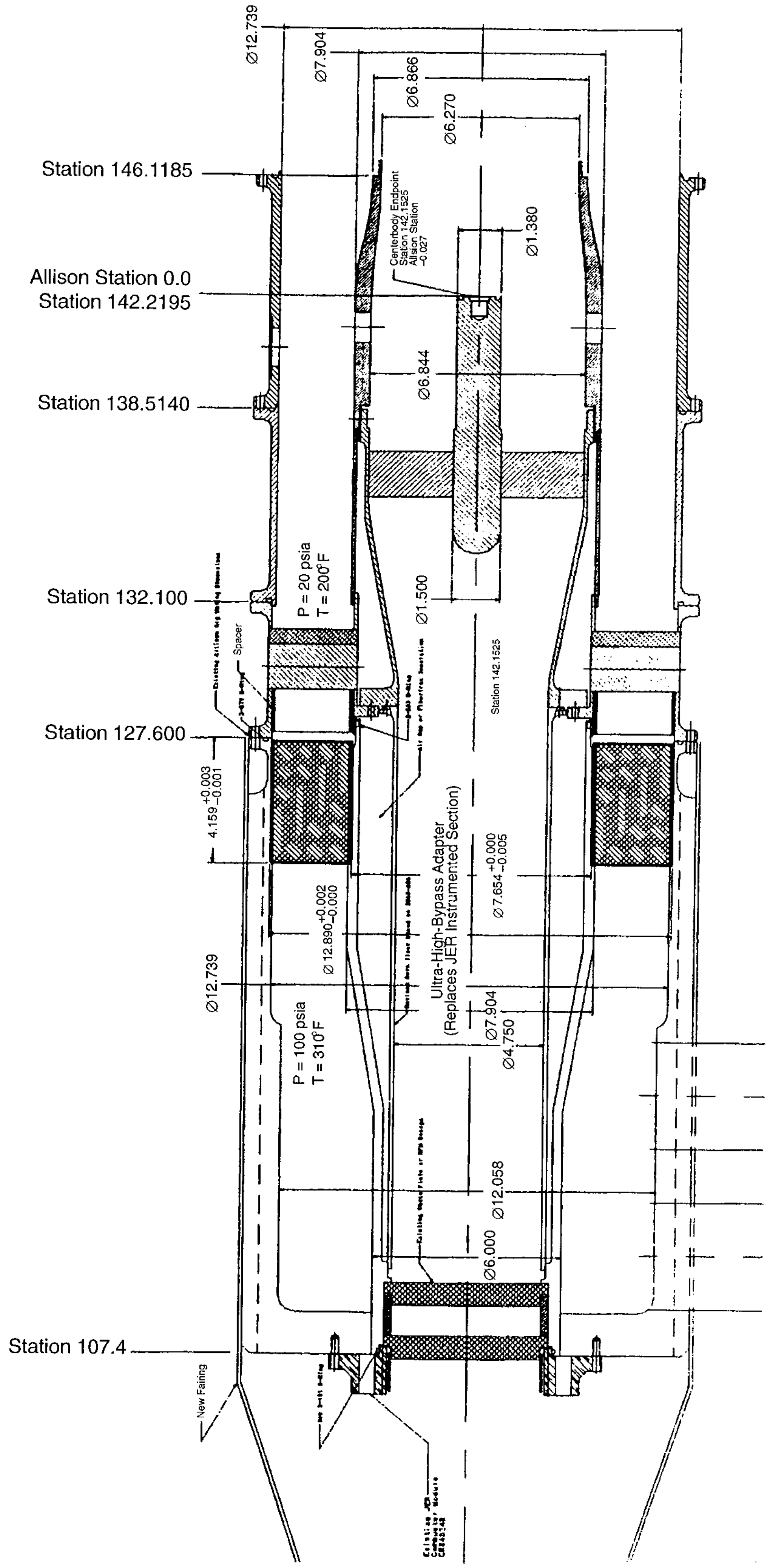


**Figure 28. JER/Separate-Flow Exhaust System Interfaces**

Table 10. Power Setting Parameters for AAPL Test

| Cycle | Test Point | Fan Nozzle | | Core Nozzle | | Free-Jet Mach No. | | | Langley Number |
|---|---|---|---|---|---|---|---|---|---|
| | | PR(f) | $T_T$(f), °R | PR(c) | $T_T$(c), °R | 0 | 0.2 | 0.28 | |
| Cycle 1 Langley BPR 5 | 10 | 1.750 | 647 | 1.560 | 1491 | X | X | X | 15.05 |
| | 11 | 1.630 | 629 | 1.445 | 1390 | X | X | X | 12.05 |
| | 12 | 1.510 | 612 | 1.330 | 1300 | X | X | X | 5.05 |
| | 13 | 1.390 | 596 | 1.240 | 1240 | X | X | X | 2.05 |
| | 14 | 1.270 | 582 | 1.150 | 1190 | X | X | | 1.05 |
| Cycle 2 Lewis BPR 5 | 20 | 1.890 | 662 | 1.790 | 1540 | X | | X | |
| | 21 | 1.830 | 655 | 1.680 | 1500 | X | X | X | |
| | 22 | 1.730 | 640 | 1.510 | 1420 | X | | X | |
| | 23 | 1.600 | 620 | 1.350 | 1345 | X | | X | |
| | 24 | 1.510 | 612 | 1.270 | 1300 | X | X | X | |
| | 25 | 1.420 | 600 | 1.200 | 1260 | | X | | |
| | 26 | 1.280 | 580 | 1.120 | 1200 | X | X | | |
| Cycle 3 Langley BPR 8 | 30 | 1.560 | 608 | 1.350 | 1385 | X | X | X | 15.08 |
| | 31 | 1.460 | 593 | 1.260 | 1339 | X | X | X | 12.08 |
| | 32 | 1.360 | 580 | 1.170 | 1280 | X | X | X | 5.08 |
| | 33 | 1.265 | 570 | 1.110 | 1235 | X | X | X | 2.08 |
| | 34 | 1.170 | 563 | 1.050 | 1185 | X | X | | 1.08 |
| Cycle 4 Lewis BPR 8 | 40 | 1.620 | 630 | 1.600 | 1580 | X | | X | |
| | 41 | 1.570 | 625 | 1.520 | 1520 | X | | X | |
| | 42 | 1.520 | 620 | 1.440 | 1460 | X | | X | |
| | 43 | 1.440 | 600 | 1.330 | 1400 | X | | X | |
| | 44 | 1.340 | 590 | 1.220 | 1320 | X | X | X | |
| | 45 | 1.250 | 580 | 1.150 | 1270 | | X | X | |
| | 46 | 1.180 | 560 | 1.090 | 1220 | X | X | | |
| Cycle 5 P&W BPR 5 | 50 | 1.830 | 655 | 1.680 | 1640 | X | | X | |
| | 51 | 1.600 | 620 | 1.350 | 1450 | X | | X | |
| | 52 | 1.420 | 600 | 1.200 | 1300 | X | | X | |

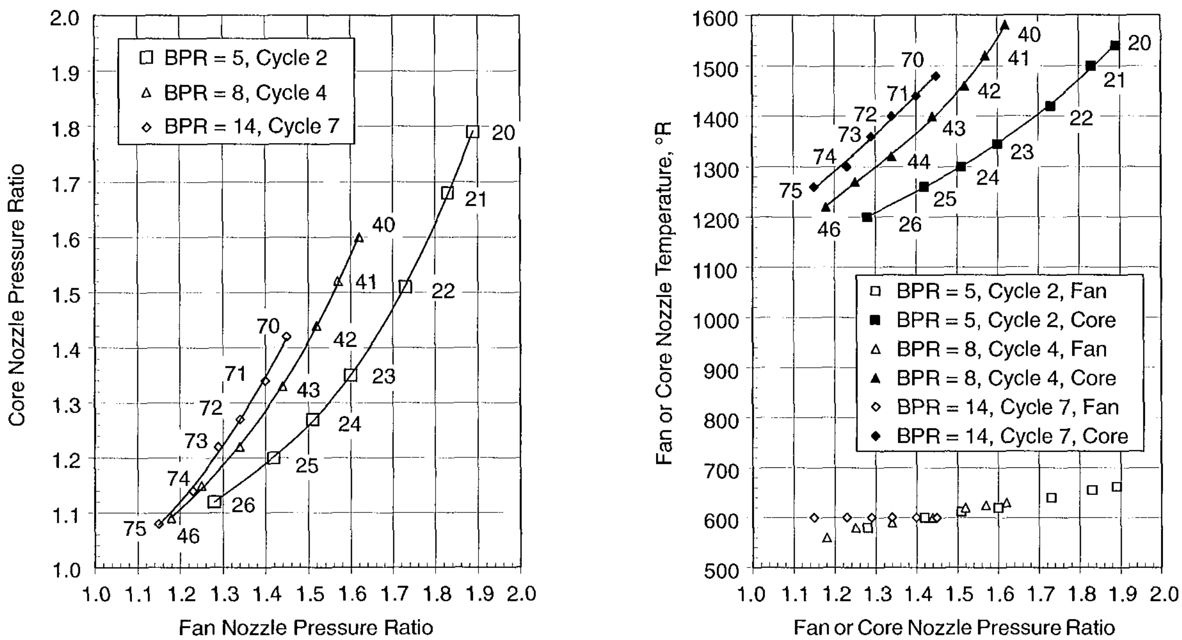


**Figure 29. BPR = 5 and 8 Power Setting Conditions**

**Table 11. Simulated Open $A_8$ Power Setting Parameters for AAPL Test: BPR = 5**

| Test Point | Fan Nozzle | | Core Nozzle | | Free-Jet Mach No. | | | Langley Number |
|---|---|---|---|---|---|---|---|---|
| | PR(f) | $T_T$(f), °R | PR(c) | $T_T$(c), °R | 0 | 0.2 | 0.28 | |
| 60 | 1.92 | 600 | 1.62 | 1470 | | | X | |
| 61 | 1.86 | 600 | 1.54 | 1440 | X | | X | |
| 62 | 1.76 | 600 | 1.43 | 1380 | | | X | |
| 63 | 1.62 | 600 | 1.28 | 1300 | X | | X | |
| 64 | 1.52 | 600 | 1.22 | 1270 | | | X | |

Table 12. Power Setting Parameters for AAPL Test: BPR = 14

| Test Point | Fan Nozzle | | Core Nozzle | | Free-Jet Mach No. | | |
|---|---|---|---|---|---|---|---|
| | PR(f) | $T_T$(f), °R | PR(c) | $T_T$(c), °R | 0 | 0.2 | 0.28 |
| 70 | 1.45 | 600 | 1.42 | 1480 | X | X | |
| 71 | 1.4 | 600 | 1.34 | 1440 | X | X | X |
| 72 | 1.34 | 600 | 1.27 | 1400 | X | X | |
| 73 | 1.29 | 600 | 1.22 | 1360 | X | X | |
| 74 | 1.23 | 600 | 1.14 | 1300 | X | X | |
| 75 | 1.15 | 600 | 1.08 | 1260 | X | X | |

## 5.4 Acoustic Test Configuration Summary

A summary of the AAPL acoustic testing is presented in Tables 13 and 14. These tables list the test sequence, test configuration identifications and codes, model hardware designations and descriptions, and test variables. They also show the number of data points acquired for each test configuration.

To accomplish the goal of developing a separate-flow nozzle system jet noise database, five baseline nozzle configurations were tested. The models were:

- A BPR 5 coplanar system (No. 1)
- A BPR 5 internal plug system (No. 2)
- A BPR 5 external plug system (No. 3)
- A BPR 8 internal plug system (No. 4)
- A BPR 8 external plug system (No. 5)

Model No. 1 was tested at several Mach/power setting combinations. These are summarized in Table 13; additional test variable details are listed in Table 10. No mixing enhancer configurations were tested on Model No. 1. Data from this configuration were acquired to be compared to acoustic data from NASA Langley (JNL) on a somewhat smaller version of the nozzle design.

Model No. 2 was tested in the baseline configuration and with combinations of two different fan nozzle mixing enhancers (24 chevrons and 96 vortex-generator internal doublets) and two different core nozzle mixing enhancers (12 chevrons and a "tongue" mixer). In all, seven GEAE/AEC Model No. 2 hardware configurations were acoustically evaluated on Model No. 2 (see Tables 13 and 14 for specifics).

An additional NASA configuration involving an external boundary layer trip device on the 24-chevron fan nozzle (2CC*) was also tested. Test variables associated with Tables 13 and 14 Mach numbers/power settings for Model No. 2 test configurations are given in Table 10.

Model No. 3 bore the brunt of the testing for this program. In addition to the baseline configuration, 6 fan nozzle (24 chevrons, 96 vortex-generator internal doublets, a scarfed nozzle, a maximum offset nozzle, 24 flipper tabs, and 48 flipper tabs) and 10 core nozzle (24 flipper tabs, 48 flipper tabs, a core full mixer, a core half mixer, 12 chevrons, 8 chevrons, 12 inward flipper chevrons, 12 alternating flipper chevrons, 64 vortex-generator internal doublets, and 20 vortex-generator external doublets) mixing-enhancer devices were tested in several combinations.

## Table 13. AAPL Separate-Flow Nozzle Acoustic Test Summary

| Test Configuration | Configuration Code | Model No. | BPR | Plug | Core Mixing Enhancer | Fan Mixing Enhancer | Mixing Concept Orig. | Clock Pos. (°) | Mach Nos. | Power Setting Cycle(s) | Total Data Points | Date Tested |
|---|---|---|---|---|---|---|---|---|---|---|---|---|
| 1 | 100000 | 1 | 5 | Int. | Base | Base | GEAE | 0 | 0, 0.2, 0.28 | 1, 2, 5 | 42 | 3/20/97 |
| 2BB | 200000 | 2 | 5 | Int. | Base | Base | GEAE | 0 | 0, 0.2, 0.28 | 1, 2, 5 | 38 | 3/25/97 |
| 2BB(r) | 2000000 | 2 | 5 | Int. | Base | Base | GEAE | 0 | 0, 0.2, 0.28 | 1, 2 | 16 | 4/21/97 |
| 2BD | 200200 | 2 | 5 | Int. | Base | 96 Int. Doublet | GEAE | 0 | 0,.28 | 2 | 10 | 3/25/97 |
| 2BC | 200100 | 2 | 5 | Int. | Base | 24 Chevron | GEAE | 0 | 0, 0.2, 0.28 | 2 | 18 | 3/28/97 |
| 2BC(r) | 2000100 | 2 | 5 | Int. | Base | 24 Chevron | GEAE | 0 | 0, 0.2, 0.28 | 2 | 7 | 4/21/97 |
| 2CC | 201100 | 2 | 5 | Int. | 12 Chevron | 24 Chevron | GEAE | 0 | 0, 0.2, 0.28 | 2 | 17 | 3/27/97 |
| 2CC(r) | 2010100 | 2 | 5 | Int. | 12 Chevron | 24 Chevron | GEAE | 0 | 0, 0.2, 0.28 | 2 | 7 | 4/21/97 |
| 2CC* | 201800 | 2 | 5 | Int. | 12 Chevron | 24 Chevron (blt) | GEAE/NASA | 0 | 0.28 | 2 | 6 | 3/27/97 |
| 2CB | 201000 | 2 | 5 | Int. | 12 Chevron | Base | GEAE | 0 | 0, 0.2, 0.28 | 2 | 18 | 3/27/97 |
| 2TmB | 210000 | 2 | 5 | Int. | Tongue Mixer | Base | GEAE/AEC | 0 | 0, 0.2, 0.28 | 2 | 21 | 3/26/97 |
| 2TmC | 210100 | 2 | 5 | Int. | Tongue Mixer | 24 Chevron | GEAE/AEC | 0 | 0, 0.2, 0.28 | 2 | 21 | 3/26/97 |
| 3BB | 300000 | 3 | 5 | Ext. | Base | Base | GEAE | 0 | 0, 0.2, 0.28 | 1, 2 | 38 | 4/1/97 |
| 3BC* | 300900 | 3 | 5 | Ext. | Base | 24 Chevron (vg) | GEAE/NASA | 0 | 0.28 | 2 | 6 | 4/1/97 |
| 3BC | 300100 | 3 | 5 | Ext. | Base | 24 Chevron | GEAE | 0 | 0, 0.2, 0.28 | 2 | 23 | 4/2/97 |
| 3BS(0) | 300700 | 3 | 5 | Ext. | Base | Scarf Nozzle | P&W | 0 | 0, 0.2, 0.28 | 2 | 18 | 4/2/97 |
| 3BS(90) | 300709 | 3 | 5 | Ext. | Base | Scarf Nozzle | P&W | 90 | 0, 0.2, 0.28 | 2 | 7 | 4/2/97 |
| 3BS(180) | 300718 | 3 | 5 | Ext. | Base | Scarf Nozzle | P&W | 180 | 0, 0.2, 0.28 | 2 | 7 | 4/2/97 |
| 3BOmax(0) | 3000500 | 3 | 5 | Ext. | Base | Max. Offset Nozzle | P&W | 0 | 0, 0.2, 0.28 | 2 | 8 | 4/9/97 |
| 3BOmax(0)(r) | 3000500 | 3 | 5 | Ext. | Base | Max. Offset Nozzle | P&W | 0 | 0.28 | 2 | 5 | 4/10/97 |
| 3BOmax(90) | 3000509 | 3 | 5 | Ext. | Base | Max. Offset Nozzle | P&W | 90 | 0, 0.2, 0.28 | 2 | 7 | 4/10/97 |
| 3BOmax(180) | 3000518 | 3 | 5 | Ext. | Base | Max. Offset Nozzle | P&W | 180 | 0, 0.2, 0.28 | 2 | 7 | 4/10/97 |
| $3BT_{24}$ | 3000300 | 3 | 5 | Ext. | Base | 24 Flip Tabs | P&W | 0 | 0, 0.2, 0.28 | 2 | 7 | 4/11/97 |
| $3BT_{48}$ | 3000400 | 3 | 5 | Ext. | Base | 48 Flip Tabs | P&W | 0 | 0, 0.2, 0.28 | 2 | 8 | 4/10/97 |
| $3T_{24}T_{24}$ | 3070300 | 3 | 5 | Ext. | 24 Flip Tabs | 24 Flip Tabs | P&W | 0 | 0, 0.2, 0.28 | 2 | 8 | 4/23/97 |
| $3T_{24}B$ | 3070000 | 3 | 5 | Ext. | 24 Flip Tabs | Base | P&W | 0 | 0, 0.2, 0.28 | 2 | 8 | 4/23/97 |
| $3T_{48}B$ | 3080000 | 3 | 5 | Ext. | 48 Flip Tabs | Base | P&W | 0 | 0, 0.2, 0.28 | 2 | 8 | 4/23/97 |
| $3T_{48}T_{48}$ | 3080400 | 3 | 5 | Ext. | 48 Flip Tabs | 48 Flip Tabs | P&W | 0 | 0, 0.2, 0.28 | 2 | 7 | 4/23/97 |
| $3T_{48}C$ | 3080100 | 3 | 5 | Ext. | 48 Flip Tabs | 24 Chevron | GEAE/P&W | 0 | 0.28 | 2 | 5 | 4/23/97 |
| 3HmB(0) | 3090000 | 3 | 5 | Ext. | Half Mixer | Base | P&W | 0 | 0, 0.2, 0.28 | 2 | 18 | 4/3/97 |
| 3HmB(0)(r) | 3090000 | 3 | 5 | Ext. | Half Mixer | Base | P&W | 0 | 0, 0.2, 0.28 | 2 | 9 | 4/8/97 |
| | | | | | | | | | 0.28 | 2 | 5 | 4/17/97 |

## Table 13. AAPL Separate-Flow Nozzle Acoustic Test Summary (Continued)

| Test Configuration | Configuration Code | Model No. | BPR | Plug | Core Mixing Enhancer | Fan Mixing Enhancer | Mixing Concept Orig. | Clock Pos. (°) | Mach Nos. | Power Setting Cycle(s) | Total Data Points | Date Tested |
|---|---|---|---|---|---|---|---|---|---|---|---|---|
| 3HmB(90) | 3090009 | 3 | 5 | Ext. | Half Mixer | Base | P&W | 90 | 0, 0.2, 0.28 | 2 | 7 | 4/3/97 |
| 3HmB(180) | 3090018 | 3 | 5 | Ext. | Half Mixer | Base | P&W | 180 | 0, 0.2, 0.28 | 2 | 7 | 4/3/97 |
| 3HmB(45) | 3090045 | 3 | 5 | Ext. | Half Mixer | Base | P&W | 45 | 0, 0.2, 0.28 | 2 | 9 | 4/17/97 |
| 3HmS(0) | 3090700 | 3 | 5 | Ext. | Half Mixer | Scarf Nozzle | P&W | 0 | 0, 0.2, 0.28 | 2 | 13 | 4/3/97 |
| 3HmC(0) | 3090100 | 3 | 5 | Ext. | Half Mixer | 24 Chevron | GEAE/P&W | 0 | 0, 0.2, 0.28 | 2 | 18 | 4/4/97 |
| 3HmC(0)(r) | 3090100 | 3 | 5 | Ext. | Half Mixer | 24 Chevron | GEAE/P&W | 0 | 0, 0.2, 0.28 | 2 | 11 | 4/8/97 |
| 3HmC(45) | 3090145 | 3 | 5 | Ext. | Half Mixer | Base | GEAE/P&W | 45 | 0, 0.2, 0.28 | 2 | 15 | 4/8/97 |
| 3HmOmax(0) | 3090500 | 3 | 5 | Ext. | Half Mixer | Max. Offset Nozzle | P&W | 0 | 0, 0.2, 0.28 | 2 | 12 | 4/9/97 |
| $3C_{12}B$ | 3010000 | 3 | 5 | Ext. | 12 Chevron | Base | GEAE | 0 | 0, 0.2, 0.28 | 2 | 10 | 4/11/97 |
| $3C_{12}C$ | 3010100 | 3 | 5 | Ext. | 12 Chevron | 24 Chevron | GEAE | 0 | 0, 0.2, 0.28 | 2 | 8 | 4/15/97 |
| $3C_8C$ | 3020100 | 3 | 5 | Ext. | 8 Chevron | 24 Chevron | GEAE | 0 | 0, 0.2, 0.28 | 2 | 7 | 4/16/97 |
| $3C_8B$ | 3020000 | 3 | 5 | Ext. | 8 Chevron | Base | GEAE | 0 | 0, 0.2, 0.28 | 2 | 7 | 4/14/97 |
| 3IB | 3030000 | 3 | 5 | Ext. | 12 In–Flip Chevrons | Base | GEAE | 0 | 0, 0.2, 0.28 | 2 | 7 | 4/14/97 |
| 3IB(r) | 3030000 | 3 | 5 | Ext. | 12 In–Flip Chevrons | Base | GEAE | 0 | 0, 0.2, 0.28 | 2 | 7 | 4/15/97 |
| 3IC | 3030100 | 3 | 5 | Ext. | 12 In–Flip Chevrons | 24 Chevron | GEAE | 0 | 0, 0.2, 0.28 | 2, 6 | 7 | 4/15/97 |
| 3IC(r) | 3030100 | 3 | 5 | Ext. | 12 In–Flip Chevrons | 24 Chevron | GEAE | 0 | 0, 0.2, 0.28 | 2 | 27 | 4/18/97 |
| 3AC | 3040100 | 3 | 5 | Ext. | 12 Alt–Flip Chevrons | 24 Chevron | GEAE | 0 | 0, 0.2, 0.28 | 2 | 7 | 4/16/97 |
| 3AB | 3040000 | 3 | 5 | Ext. | 12 Alt–Flip Chevrons | Base | GEAE | 0 | 0, 0.2, 0.28 | 2 | 7 | 4/14/97 |
| 3DiB | 3050000 | 3 | 5 | Ext. | 64 Int. Doub. | Base | GEAE | 0 | 0, 0.2, 0.28 | 2 | 9 | 4/15/97 |
| 3DxB | 3060000 | 3 | 5 | Ext. | 20 Ext. Doub. | Base | GEAE | 0 | 0, 0.2, 0.28 | 2 | 7 | 4/17/97 |
| 5BB | 5000000 | 5 | 8 | Ext. | Base | Base | GEAE | 0 | 0, 0.2, 0.28 | 3, 4 | 24 | 4/22/97 |
| 5BC | 5000100 | 5 | 8 | Ext. | Base | 24 Chevron | GEAE | 0 | 0, 0.2, 0.28 | 4 | 8 | 4/22/97 |
| 5CC | 5010100 | 5 | 8 | Ext. | 12 Chevron | 24 Chevron | GEAE | 0 | 0, 0.2, 0.28 | 4 | 8 | 4/22/97 |
| 5CB | 5010000 | 5 | 8 | Ext. | 12 Chevron | Base | GEAE | 0 | 0, 0.2, 0.28 | 4 | 8 | 4/22/97 |
| 4BB | 4000000 | 4 | 8 | Int. | Base | Base | GEAE | 0 | 0, 0.2, 0.28 | 3, 4 | 24 | 4/21/97 |
| 3BB(r) | 3000000 | 3 | 5 | Ext. | Base | Base | GEAE | 0 | 0, 0.2, 0.28 | 2 | 20 | 4/4/97 |
| | | | | | | | | | 0 | 2 | 21 | 4/7/97 |
| | | | | | | | | | 0, 0.2, 0.28 | 2 | 10 | 4/8/97 |
| | | | | | | | | | 0, 0.2, 0.28 | 2 | 11 | 4/9/97 |
| | | | | | | | | | 0, 0.2, 0.28 | 2 | 10 | 4/10/97 |
| | | | | | | | | | 0, 0.2, 0.28 | 2 | 7 | 4/11/97 |
| | | | | | | | | | 0, 0.2, 0.28 | 2 | 8 | 4/14/97 |

## Table 13. AAPL Separate-Flow Nozzle Acoustic Test Summary (Concluded)

| Test Configuration | Configuration Code | Model No. | BPR | Plug | Core Mixing Enhancer | Fan Mixing Enhancer | Mixing Concept Orig. | Clock Pos. (°) | Mach Nos. | Power Setting Cycle(s) | Total Data Points | Date Tested |
|---|---|---|---|---|---|---|---|---|---|---|---|---|
| 3BB(r) | 3000000 | 3 | 5 | Ext. | Base | Base | GEAE | 0 | 0, 0.2, 0.28 | 2 | 12 | 4/15/97 |
| | | | | | | | | | | 2 | 8 | 4/16/97 |
| | | | | | | | | | | 2 | 8 | 4/17/97 |
| | | | | | | | | | | 1, 2, 6 | 20 | 4/18/97 |
| | | | | | | | | | | 2 | 7 | 4/23/97 |

Notes: (blt) = boundary layer trip
(vg) = vortex generators
Total # of Data Points includes background noise conditions

## Table 14. Additional AAPL Separate-Flow Nozzle Acoustic Testing

| Test Configuration | Configuration Code | Model No. | BPR | Plug | Core Mixing Enhancer | Fan Mixing Enhancer | Mixing Concept Orig. | Clock Pos. (°) | Mach Nos. | Power Setting Cycle(s) | Total Data Points | Date Tested |
|---|---|---|---|---|---|---|---|---|---|---|---|---|
| 2BB(r) | 2000000 | 2 | 5 | Int. | Base | Base | GEAE | 0 | 0, 0.2, 0.28 | 2 | 10 | 5/12/97 |
| 6TmB | 6100000 | 2 | 5 | New | Tongue Mixer | Base | GEAE/AEC | 0 | 0, 0.2, 0.28 | 2 | 7 | 5/12/97 |
| 6TmC | 6100100 | 2 | 5 | New | Tongue Mixer | 24 Chevron | GEAE/AEC | 0 | 0, 0.2, 0.28 | 2 | 7 | 5/12/97 |
| 7BB | 7000000 | 4 | 14 | New | Base | Base | NASA | 0 | 0, 0.2, 0.28 | 7 | 7 | 5/12/97 |
| 3BB(r) | 3000000 | 3 | 5 | Ext. | Base | Base | GEAE | 0 | 0, 0.2, 0.28 | 2 | 10 | 5/13/97 |
| 3FB | 3110000 | 3 | 5 | Ext. | Full Mixer | Base | NASA | 0 | 0,.28 | 2 | 6 | 5/13/97 |
| 3HmB(0)r | 3090000 | 3 | 5 | Ext. | Half Mixer | Base | P&W | 0 | 0,.28 | 2 | 6 | 5/13/97 |
| 3FC | 3110100 | 3 | 5 | Ext. | Full Mixer | 24 Chevron | GEAE/NASA | 0 | 0,.28 | 2 | 6 | 5/13/97 |
| $3T_{24}T_{48}$ | 3070400 | 3 | 5 | Ext. | 24 Flip Tabs | 48 Flip Tabs | P&W | 0 | 0,.28 | 2 | 6 | 5/13/97 |
| 3BB(r) | 3000000 | 3 | 5 | Ext. | Base | Base | GEAE | 0 | 0, 0.2, 0.28 | 2 | 10 | 6/17/97 |
| $3T_{24}C$ | 3070100 | 3 | 5 | Ext. | 24 Flip Tabs | 24 Chevron | GEAE/P&W | 0 | 0, 0.2, 0.28 | 2 | 8 | 6/17/97 |
| 3BB(r) | 3000000 | 3 | 5 | Ext. | Base | Base | GEAE | 0 | 0.28 | 2 | 5 | 6/18/97 |
| $3T_{24}B(r)$ | 3070000 | 3 | 5 | Ext. | 24 Flip Tabs | Base | P&W | 0 | 0.28 | 2 | 6 | 6/18/97 |

Note: Matrix does not include flexible wire (attached to centerbody plug trailing edge) configurations testing conducted on 6/18/97.

GEAE provided two of the fan nozzle mixing-enhancer devices (24 chevrons, 96 vortex-generator internal doublets) and six of the core nozzle mixing enhancer concepts (12 chevrons, 8 chevrons, 12 inward flipper chevrons, 12 alternating flipper chevrons, 64 vortex-generator internal doublets, and 20 vortex-generator external doublets). A fan medium-offset nozzle was also built but was not tested.

In all, 36 Model 3 configurations (12 of which involved only GEAE hardware) were acoustically assessed in this program (Tables 13 and 14). In addition, a NASA-defined configuration using vortex generators on the external surface of the 24-chevron fan nozzle was tested. Model 3 test variables are listed in Tables 13 and 14. Related power-setting parameters are listed in Tables 10 and 11.

Model No. 5 was tested after Model No. 3. In addition to the baseline configuration, mixing enhancers for the core nozzle (one device, 12 chevrons) and fan nozzle (one device, 24 chevrons) were evaluated in various combinations. In all, four configurations underwent acoustic testing using Model No. 5 hardware. Table 13 lists the test variables, and Table 10 details associated power setting parameters.

Model No. 4 succeeded Model No. 5 in the acoustic test sequence. Although two fan nozzle mixing enhancer devices (24 chevrons and 96 vortex-generator internal doublets) were available for testing on Model No. 4, only the baseline configuration was run. Again, Table 13 lists pertinent test variables, and Table 10 specifies power setting details.

The new extended core plug paired with the existing tongue mixer was designated Model No. 6. It was tested with the baseline and 24-chevron fan nozzles (see Table 14). Tables 10 and 14 again provide pertinent test variables and power setting parameters.

To simulate a BPR = 14 separate-flow exhaust system, the new extended core plug was matched with Model No. 4 hardware. This assembly resulted in a core nozzle with reduced core area (compared to Model No. 4) due to the protrusion of the core plug past the core nozzle exit plane. Test variables and power setting parameters for this configuration are defined in Tables 12 and 14.

All configurations of baseline and mixing-enhancer hardware (except 2CC* and 3BC*) assembled for this test program are identified by the "Test Configuration" designations in Tables 13 and 14. They are also tabulated and pictorially represented in Appendix A herein.

During acoustic testing, NASA conducted (on a noninterference basis) phased-array testing on selected configurations at selected power settings using a NASA-defined linear microphone array located at the 90° azimuthal position slightly beyond the farfield microphone radius. Table 15 is the NASA phased-array test matrix.

Boeing also conducted phased-array testing as a separate segment of this program. Table 16 is a summary of the testing.

In addition, and again on a noninterference basis, NASA took infrared camera shots of the exhaust jet plume of selected test configurations at specified power settings. Table 17 is the IR camera test summary.

## 5.5 Plume Survey Testing

Following the acoustic and Boeing phased-array testing, the NASA plume-survey apparatus was installed in the AAPL. Model configurations for plume surveys were chosen based on results from acoustic testing. The specified condition for the plume surveys coincided with test point 21 of Cycle 2 at a free-jet Mach number of 0.28 (see Table 10).

Table 15. AAPL Separate-Flow Nozzle Phased Array (NASA) Test Summary

| Seq. | Test Configuration | Model No. | BPR | Plug | Core Nozzle | Fan Nozzle | Clock Position | Mach No. | Cycle/P.S. | Escort Readings | Date Tested |
|---|---|---|---|---|---|---|---|---|---|---|---|
| 1 | 2BB | 2 | 5 | Int. | Base | Base | N/A | ? | ? | ? | 3/25/97 |
| 2 | 2BD | 2 | 5 | Int. | Base | 96 Int. Doublet | N/A | ? | ? | ? | 3/25/97 |
| 3 | 2CC | 2 | 5 | Int. | 12 Chevrons | 24 Chevrons | N/A | 0, 0.28 | 2/20 | 339, 340 | 3/27/97 |
| 4 | 2BC | 2 | 5 | Int. | Base | 24 Chevrons | N/A | 0, 0.28 | 2/20 | 352, 353 | 3/28/97 |
| 5 | 3HmB(90) | 3 | 5 | Ext. | Half Mixer | Base | 90° | 0, 0.28 | 2/21 | 497, 500 | 4/3/97 |
| 6 | 3HmB(180) | 3 | 5 | Ext. | Half Mixer | Base | 180° | 0, 0.28 | 2/21 | 505, 507 | 4/3/97 |
| 7 | 3BB | 3 | 5 | Ext. | Base | Base | N/A | 0, 0.28 | 2/20, 21 | 549, 561 | 4/4/97 |
| 8 | 3BB | 3 | 5 | Ext. | Base | Base | N/A | 0 | 2/Special | 576–585 | 4/7/97 |
| 9 | 3HmB(0) | 3 | 5 | Ext. | Half Mixer | Base | 0° | 0, 0.28 | 2/21 | 603, 606 | 4/8/97 |
| 10 | 3BOmax(0) | 3 | 5 | Ext. | Base | Max. Offset Nozzle | 0° | 0.28 | 2/21 | 655 or 657 | 4/9/97 |
| 11 | 3HmOmax(0) | 3 | 5 | Ext. | Half Mixer | Max. Offset Nozzle | 0° | 0, 0.28 | 2/20, 21 | 668, 670 | 4/9/97 |
| 12 | 3BOmax(90) | 3 | 5 | Ext. | Base | Max. Offset Nozzle | 90° | 0.28 | 2/20 | 690 | 4/10/97 |
| 13 | 3BOmax(180) | 3 | 5 | Ext. | Base | Max. Offset Nozzle | 180° | 0.28 | 2/20 | 697 | 4/10/97 |
| 14 | 3BT48 | 3 | 5 | Ext. | Base | 48 Flip Tabs | N/A | 0.28 | 2/20 | 709 | 4/10/97 |
| 15 | 3BT24 | 3 | 5 | Ext. | Base | 24 Flip Tabs | N/A | 0.28 | 2/20 | 727 | 4/11/97 |
| 16 | 3C12B | 3 | 5 | Ext. | 12 Chevrons | Base | N/A | 0.28 | 2/20 | 741 | 4/11/97 |
| 17 | 3IB | 3 | 5 | Ext. | 12 In-Flip Chevs. | Base | N/A | 0.28 | 2/20 | 771 | 4/14/97 |
| 18 | 3AB | 3 | 5 | Ext. | 12 Alt-Flip Chevs. | Base | N/A | 0.28 | 2/20 | 778 | 4/14/97 |
| 19 | 3DiB | 3 | 5 | Ext. | 64 Int. Doublet | Base | N/A | 0.28 | 2/20 | 801 | 4/15/97 |
| 20 | 3IC | 3 | 5 | Ext. | 12 In-Flip Chevs. | 24 Chevrons | N/A | 0.28 | 2/20 | 816 | 4/15/97 |
| 21 | 3C12C | 3 | 5 | Ext. | 12 Chevrons | 24 Chevrons | N/A | 0.28 | 2/20 | 824 or 826 | 4/15/97 |
| 22 | 3C8C | 3 | 5 | Ext. | 8 Chevrons | 24 Chevrons | N/A | 0.28 | 2/20 | 843 | 4/16/97 |
| 23 | 3AC | 3 | 5 | Ext. | 12 Alt-Flip Chevs. | 24 Chevrons | N/A | 0.28 | 2/20 | 851 | 4/16/97 |
| 24 | 3HmB(45) | 3 | 5 | Ext. | Half Mixer | Base | 45° | 0.28 | 2/20 | 875 | 4/17/97 |
| 25 | 3DxB | 3 | 5 | Ext. | 20 Ext. Doublet | Base | N/A | 0.28 | 2/20 | 882 | 4/17/97 |
| 26 | 3IC | 3 | 5 | Ext. | 12 In-Flip Chevs. | 24 Chevrons | N/A | 0.28 | 2/20 | 892 | 4/18/97 |
| 27 | 3BB | 3 | 5 | Ext. | Base | Base | N/A | 0.28 | 2/20 | 918 | 4/18/97 |
| 28 | 2BC | 2 | 5 | Ext. | Base | Base | N/A | 0.28 | 2/20 | 958 | 4/21/97 |
| 29 | 4BB | 4 | 8 | Int. | Base | Base | N/A | 0.28 | 4/41 | 975 | 4/21/97 |

## Table 16. AAPL Separate-Flow Nozzle Phased Array (Boeing) Test Summary

| Seq. | Test Configuration | Model No. | BPR | Plug | Core Nozzle | Fan Nozzle | Clock Position | Array Angle | Mach No. | Cycle/P.S. | Escort Readings | Date Tested |
|---|---|---|---|---|---|---|---|---|---|---|---|---|
| 1 | 1 | 1 | 5 | Int. | Base | Base | N/A | 90° | 0, 0.2, 0.28 | 2/1–7,21–23 | 1088–1101 | 4/28/97 |
| 2 | 3IB | 3 | 5 | Ext. | 12 In–Flip Chevrons | Base | N/A | 90° | 0, 0.28 | 2/21–23 | 1102–1106 | 4/29/97 |
| 3 | 3IC | 3 | 5 | Ext. | 12 In–Flip Chevrons | 24 Chevrons | N/A | 90° | 0, 0.28 | 2/21–23 | 1107–1111 | 4/29/97 |
| 4 | 3BB | 3 | 5 | Ext. | Base | Base | N/A | 90° | 0, 0.2, 0.28 | 2/20–24 | 1112–1119 | 4/29/97 |
| 5 | 3AB | 3 | 5 | Ext. | 12 Alt–Flip Chevrons | Base | N/A | 90° | 0, 0.28 | 2/21–23 | 1120–1124 | 4/30/97 |
| 6 | 3T24T48 | 3 | 5 | Ext. | 24 Flip Tabs | 48 Flip Tabs | N/A | 90° | 0, 0.28 | 2/21–23 | 1125–1129 | 4/30/97 |
| 7 | 3T48T48 | 3 | 5 | Ext. | 48 Flip Tabs | 48 Flip Tabs | N/A | 90° | 0, 0.2, 0.28 | 2/20–24 | 1130–1138 | 4/30/97 |
| 8 | 3T48B | 3 | 5 | Ext. | 48 Flip Tabs | Base | N/A | 90° | 0, 0.28 | 2/21–23 | 1139–1143 | 4/30/97 |
| 9 | 3HmB(0) | 3 | 5 | Ext. | Half Mixer | Base | 0° | 90° | 0, 0.28 | 2/21–23 | 1144–1147 | 5/1/97 |
| 10 | 3HmB(90) | 3 | 5 | Ext. | Half Mixer | Base | 90° | 90° | 0, 0.28 | 2/21,23 | 1148–1150 | 5/1/97 |
| 11 | 3HmB(180) | 3 | 5 | Ext. | Half Mixer | Base | 180° | 90° | 0, 0.28 | 2/21,23 | 1151–1153 | 5/1/97 |
| 12 | 3T24B | 3 | 5 | Ext. | 24 Flip Tabs | Base | N/A | 90° | 0, 0.28 | 2/21–23 | 1154–1158 | 5/1/97 |
| 13 | 3T24T24 | 3 | 5 | Ext. | 24 Flip Tabs | 24 Flip Tabs | N/A | 90° | 0, 0.28 | 2/21–23 | 1159–1163 | 5/2/97 |
| 14 | 3BOmax(0) | 3 | 5 | Ext. | Base | Max. Offset | 0° | 90° | 0, 0.28 | 2/21,23 | 1164–1166 | 5/2/97 |
| 15 | 3BOmax(180) | 3 | 5 | Ext. | Base | Max. Offset | 180° | 90° | 0, 0.28 | 2/21,23 | 1167–1169 | 5/2/97 |
| 16 | 3C12B | 3 | 5 | Ext. | 12 Chevrons | Base | N/A | 90° | 0.28 | 2/21–23 | 1170–1172 | 5/2/97 |
| 17 | 2BB | 2 | 5 | Int. | Base | Base | N/A | 90° | 0, 0.28 | 2/21,23 | 1173–1175 | 5/2/97 |
| 18 | 2BB | 2 | 5 | Int. | Base | Base | N/A | 120° | 0, 0.28 | 2/21–23 | 1176–1180 | 5/5/97 |
| 19 | 3BB | 3 | 5 | Ext. | Base | Base | N/A | 120° | 0, 0.28 | 2/21–23 | 1181–1185 | 5/5/97 |
| 20 | 3T24B | 3 | 5 | Ext. | 24 Flip Tabs | Base | N/A | 120° | .28 | 2/21–23 | 1186–1188 | 5/5/97 |
| 21 | 3T24T24 | 3 | 5 | Ext. | 24 Flip Tabs | 24 Flip Tabs | N/A | 120° | .28 | 2/21–23 | 1189–1191 | 5/5/97 |
| 22 | 3IC | 3 | 5 | Ext. | 12 In–Flip Chevrons | 24 Chevrons | N/A | 120° | 0, 0.28 | 2/21–23 | 1192–1196 | 5/6/97 |
| 23 | 3HmB(0) | 3 | 5 | Ext. | Half Mixer | Base | 0° | 120° | 0, 0.28 | 2/21,23 | 1197–1199 | 5/6/97 |
| 24 | 3HmB(90) | 3 | 5 | Ext. | Half Mixer | Base | 90° | 120° | 0, 0.28 | 2/21,23 | 1200–1202 | 5/6/97 |
| 25 | 3HmB(180) | 3 | 5 | Ext. | Half Mixer | Base | 180° | 120° | 0, 0.28 | 2/21,23 | 1203–1205 | 5/6/97 |
| 26 | 3T24B | 3 | 5 | Ext. | 24 Flip Tabs | Base | N/A | 120° | 0 | 2/21,23 | 1206–1207 | 5/6/97 |
| 27 | 3T24T24 | 3 | 5 | Ext. | 24 Flip Tabs | 24 Flip Tabs | N/A | 120° | 0 | 2/21,23 | 1208–1209 | 5/6/97 |
| 28 | 3BOmax(0) | 3 | 5 | Ext. | Base | Max. Offset | 0° | 120° | 0, 0.28 | 2/21–23 | 1210–1214 | 5/7/97 |
| 29 | 3BOmax(180) | 3 | 5 | Ext. | Base | Max. Offset | 180° | 120° | 0, 0.28 | 2/21–23 | 1215–1219 | 5/7/97 |
| 30 | 3BS(0) | 3 | 5 | Ext. | Base | Scarf | 0° | 120° | 0, 0.28 | 2/21–23 | 1220–1224 | 5/7/97 |
| 31 | 3BS(180) | 3 | 5 | Ext. | Base | Scarf | 180° | 120° | 0, 0.28 | 2/21–23 | 1225–1229 | 5/7/97 |

Table 17. AAPL Separate-Flow Nozzle IR Camera Test Summary

| Configuration | Date | Mach No. | Cycle/Power Setting | Corresponding Escort Reading | IR Reading |
|---|---|---|---|---|---|
| 3HmB(0) | 4/8/97 | 0.28 | 2/20 | 603 | 4 |
| | | 0.0 | 2/21 | 606 | 5 |
| 3HmC(0) | 4/8/97 | 0.28 | 2/20 | 616 | 6 |
| 3HmC(45) | 4/8/97 | 0.28 | 2/21 | 626 | 7 |
| 3BB | 4/9/97 | 0.0 | 2/21 | 640 | 8 |
| | | 0.28 | 2/21 | 642 | 9 |
| 3BOmax(0) | 4/9/97 | 0.28 | 2/23 | 652 | 10 |
| | | | 2/22 | 653 | 11 |
| | | | 2/21 | 654 | 12 |
| | | | 2/20 | 655 | 13 |
| | | 0.0 | 2/21 | 659 | 14 |
| 3HmOmax(0) | 4/9/97 | 0.28 | 2/23 | 664 | 15 |
| | | | 2/21 | 665 | 16 |
| | | | 2/20 | 668 | 17 |
| | | 0.0 | 2/21 | 670 | 18 |
| | | | 2/20 | 671 | 19 |
| 3BOmax(90) | 4/10/97 | 0.28 | 2/21 | 689 | 20 |
| | | 0.0 | 2/21 | 692 | 21 |
| 3BOmax(180) | 4/10/97 | 0.28 | 2/21 | 696 | 22 |
| | | | 2/20 | 697 | 23 |
| | | 0.0 | 2/21 | 699 | 24 |
| $3BT_{24}$ | 4/11/97 | 0.28 | 2/20 | 727 | 25 |
| $3C_8B$ | 4/14/97 | 0.28 | 2/20 | 762 | 1 |
| 3IB | 4/14/97 | 0.28 | 2/20 | 771 | 2 |
| 3AB | 4/14/97 | 0.28 | 2/20 | 778 | 3 |
| 3DiB | 4/15/97 | 0.28 | 2/20 | 801 | 4 |
| 3IC | 4/15/97 | 0.28 | 2/20 | 816 | 5 |
| $3C_{12}C$ | 4/15/97 | 0.28 | 2/20 | 824 | 6 |
| $3C_{12}C$ | 4/15/97 | 0.28 | 2/20 | 826 | 7 |
| 3BB | 4/16/97 | 0.28 | 2/24 | 832 | 8 |
| | | | 2/23 | 834 | 9 |
| | | | 2/22 | 835 | 10 |
| | | | 2/21 | 836 | 11 |
| | | | 2/20 | 837 | 12 |
| 3C8C | 4/16/97 | 0.28 | 2/20 | 842 | 13 |

### Table 17. AAPL Separate-Flow Nozzle IR Camera Test Summary (Concluded)

| Configuration | Date | Mach No. | Cycle/Power Setting | Corresponding Escort Reading | IR Reading |
|---|---|---|---|---|---|
| 3AC | 4/16/97 | 0.28 | 2/22 | 849 | 14 |
| | | | 2/20 | 851 | 15 |
| | | 0.0 | 2/21 | 853 | 16 |
| 3HmB(45) | 4/17/97 | 0.28 | 2/20 | 875 | 17 |
| 3DxB | 4/17/97 | 0.28 | 2/20 | 882 | 18 |
| 3IC | 4/18/97 | 0.28 | 2/20 | 892 | 19 |
| 3BB | 4/18/97 | 0.28 | 2/20 | 918 | 20 |
| 4BB | 4/21/97 | 0.28 | 4/41 | 975 | 2 |
| 5CB | 4/22/97 | 0.28 | 4/41 | 1023 | 3 |
| $3T_{24}B$ | 2/23/97 | 0.28 | 2/20 | 1057 | 4 |
| 3BB | 4/23/97 | 0.28 | 2/20 | 1073 | 5 |
| $3T_{48}C$ | 4/23/97 | 0.28 | 2/20 | 1080 | 6 |
| $3T_{48}T_{48}$ | 4/23/97 | 0.28 | 2/20 | 1085 | 7 |
| 1BB | 4/28/97 | 0.28 | 2/23 | 1097 | 9 |
| | | | 2/22 | 1098 | 10 |
| | | | 2/21 | 1099 | 11 |
| 6TmB | 5/12/97 | 0.28 | 2/21 | 1251 | 2 |
| | | | 2/20 | 1252 | 3 |
| 6TmC | 5/12/97 | 0.28 | 2/21 | 1258 | 4 |
| | | | 2/20 | 1259 | 5 |
| 3BB | 5/13/97 | 0.28 | 2/21 | 1275 | 6 |
| 3FB | 5/13/97 | 0.28 | 2/21 | 1283 | 7 |
| 3HmB | 5/13/97 | 0.28 | 2/21 | 1290 | 9 |
| 3FC | 5/13/97 | 0.28 | 2/21 | 1296 | 10 |
| $3T_{24}T_{48}$ | 5/13/97 | 0.28 | 2/21 | 1302 | 11 |

A typical survey comprised six lateral traverses at axial locations downstream of the separate-flow nozzle, with the plume survey assembly total pressure rake starting out positioned at the nozzle centerline (see Figure 30). The surveys were performed in two modes: cross-sectional scans and axial scans. Also, because of the geometries of the coplanar, internal plug, and external plug models (Nos. 1, 2, and 3 respectively), the corresponding surveys were somewhat different.

For Model No. 1 (coplanar), cross-sectional scans were performed at axial distances 6, 12, 18, 30, 60, and 100 inches from the plane of the Model No. 3 (external plug) fan nozzle exit. At the 6 and 12-in axial positions, the survey rake traversed 8 inches laterally in 0.25-in intervals (a total of 33 individual positions). In order for the outboard static pressure rake to cover the same survey territory as the total pressure rake, however, another 36 lateral stops were required at 0.25-in increments.

At the 18-in axial location, data were acquired with the rake assembly over a 10-in lateral span in 0.5-in increments (21 positions). Here, the survey was extended to include an additional

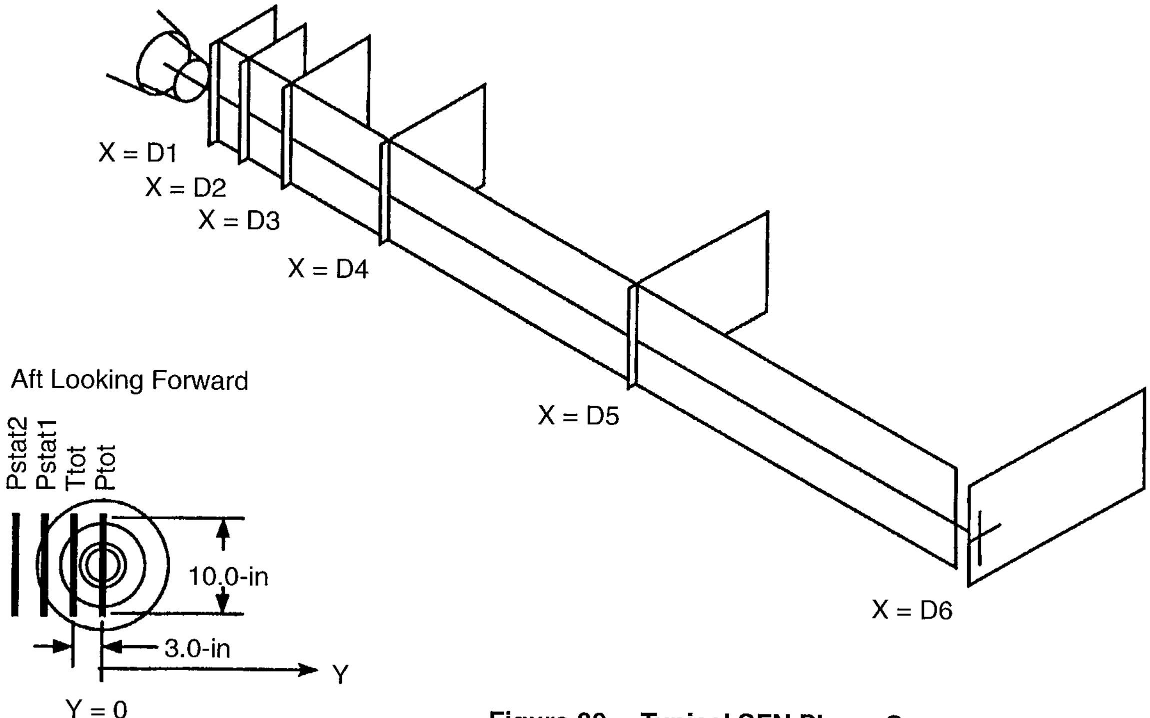


**Figure 30. Typical SFN Plume Survey**

six lateral positions to accommodate the needed travel for the outboard static pressure rake to encompass the same domain as the total pressure rake. The additional lateral positions, however, were minimized by assuming symmetry about the nozzle centerline and not duplicating static pressure rake positions whose mirror image was previously accounted for during the initial 10-in lateral traverse.

For the 30-in scan, the survey embodied a 12-in lateral traverse in 0.5-in intervals (25 positions) with an additional six spanwise locations for completion of the static pressure rake data acquisition. The 60-in axial position had a 16-in lateral traverse stopping every inch to acquire data for a total of 17 initial survey positions. Three more were added for static pressure rake data completeness.

Finally, the 100-in axial scan involved a 20-in lateral movement (21 individual positions) at 1-in intervals with an additional three stoppages beyond the 20-in travel to accommodate the needs of the static pressure rake. In all, 240 surveys were made for the cross-sectional scans with the Model No. 1 coplanar nozzle (see Figure 31).

For axial scans associated with Model No. 1, the plume-survey rake was positioned with the total pressure rake at the nozzle centerline (y = 0). The rake was then traversed axially along the nozzle centerline from 6 to 22 inches, taking data at 0.5-in intervals (33 positions). Following this, the rake traveled from 22 to 46 inches, stopping every inch to acquire data (total of 25 positions).

Finally, from 46 to 98 inches along the nozzle centerline, the rake took survey data at 4-in intervals (14 positions). When this was completed, the rake assembly was moved laterally to line up the total temperature rake with the model nozzle centerline (y = 3.0), and the entire process was repeated in reverse order (see Figure 31). When all were done, 144 axial scans had been conducted, and Model 1 combined cross-sectional and axial scans totaled 384.

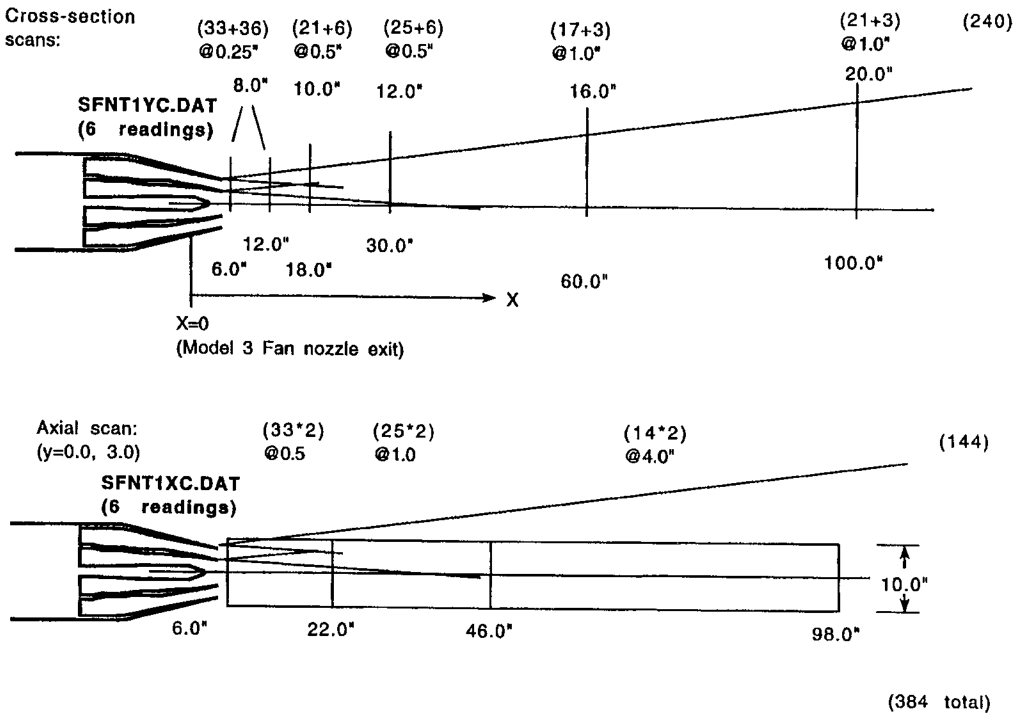


**Figure 31. Plume Surveys for Model No. 1**

For the BPR = 5 internal plug nozzle model (Model No. 2), the 332 plume surveys taken are pictorially defined in Figure 32.

Likewise, for Model No. 3 (external plug nozzle), 318 plume surveys acquired data according to the criteria outlined in Figure 33. In addition, to analyze flowfield properties in the region between the fan nozzle exit plane and the core plug trailing edge, some external plug nozzle/flow-enhancer configurations were chosen for further plume-survey investigation at the end of the test program. Here, near the nozzle at axial distances of 1.0, 2.5, 4.5, and 7.5 inches from the fan nozzle exit, traverses were made in 0.25-in increments from a point 6 inches away from the nozzle centerline inward until just before touching either the core cowl or plug hardware (see Figure 34).

For this type of survey, only 11 sensors (centerline, 5 above, and 5 below) on the total pressure rake of the plume survey assembly were used to acquire data.

The plume survey assembly contained four rakes in an envelope roughly the size of a standard 8½ by 11-in sheet of paper. Looking downstream, the left outboard rake contained 41 total pressure elements equally spaced at 0.25-in intervals and positioned 4.28 inches from the rake assembly centerline. At 1.28 inches to the left, forward looking aft (FLA), of the rake assembly centerline was a 41-element total temperature rake (left inboard rake) with sensors equally spaced at 0.25 in. The right inboard (FLA) rake was 1.28 inches from the rake assembly centerline and contained 21 static pressure sensors equally spaced at 0.50-in intervals. Finally, the right outboard (FLA) rake was also a static pressure sensor rake. This rake contained 20 $P_S$ measurement stations equally spaced at 0.5 inch at a distance from the rake assembly centerline of 4.28 in.

Figure 35 is a schematic of the plume survey rake sensor measurement arrangement, and Figure 36 is a photograph of a typical plume survey apparatus installation in the AAPL.

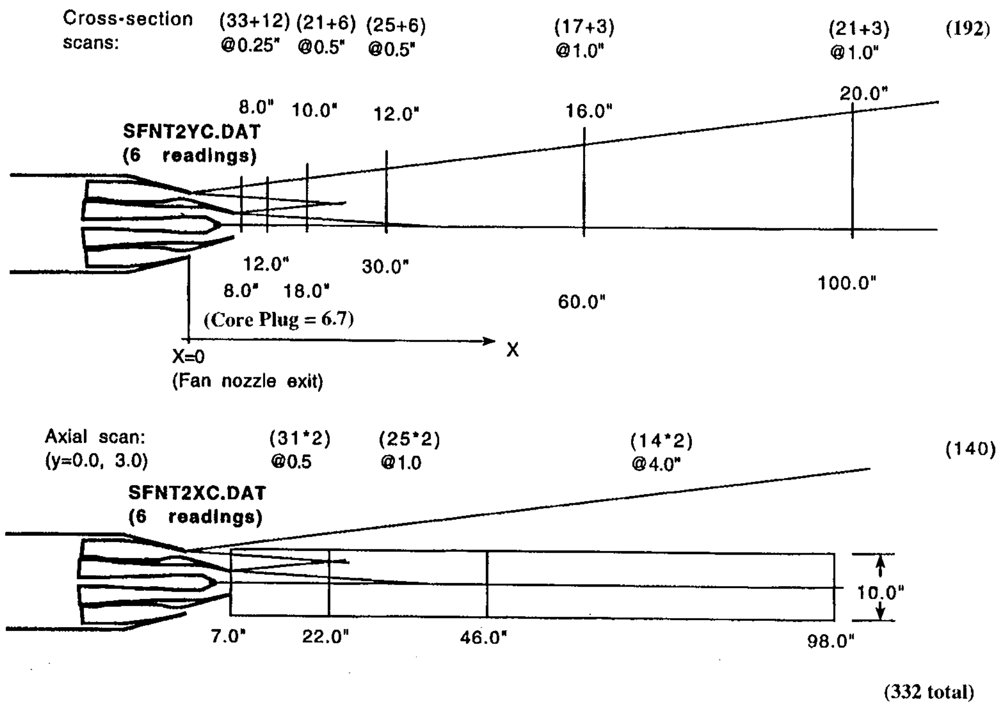


Figure 32. Plume Surveys for Model No. 2

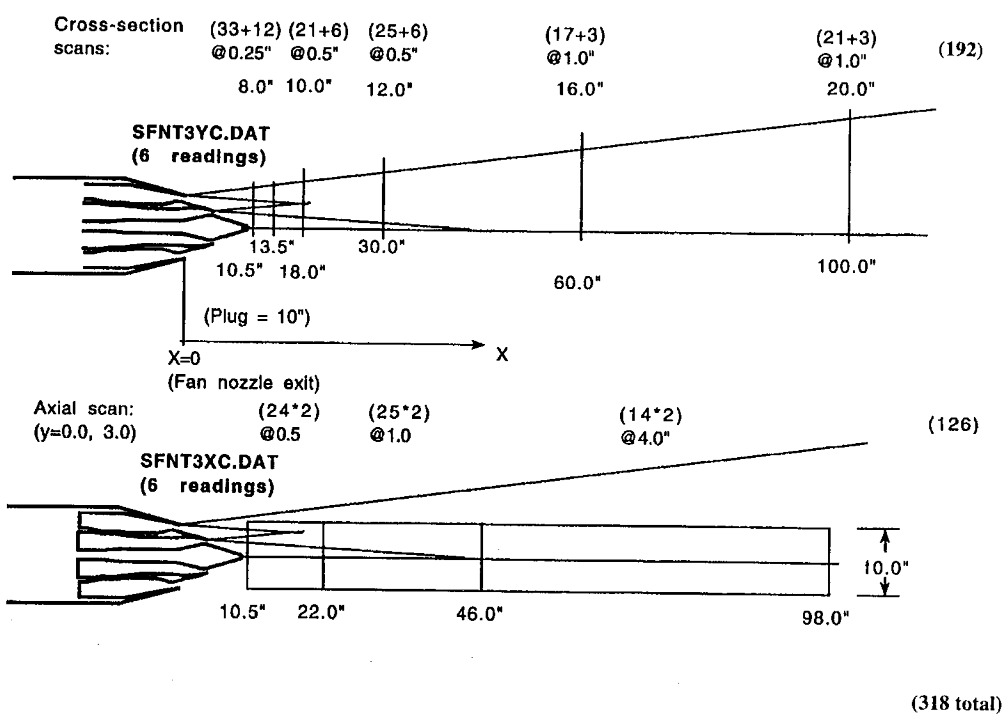


Figure 33. Plume Surveys for Model No. 3

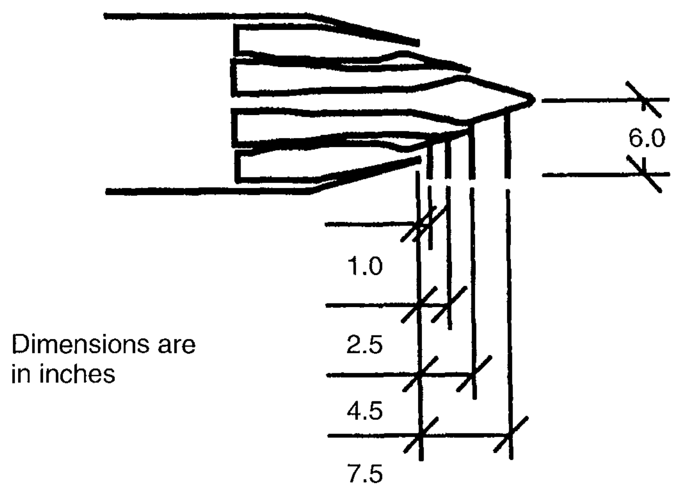


**Figure 34. Near-Nozzle Plume Surveys (for 3BB, 3BC, and 3BT24 Only)**

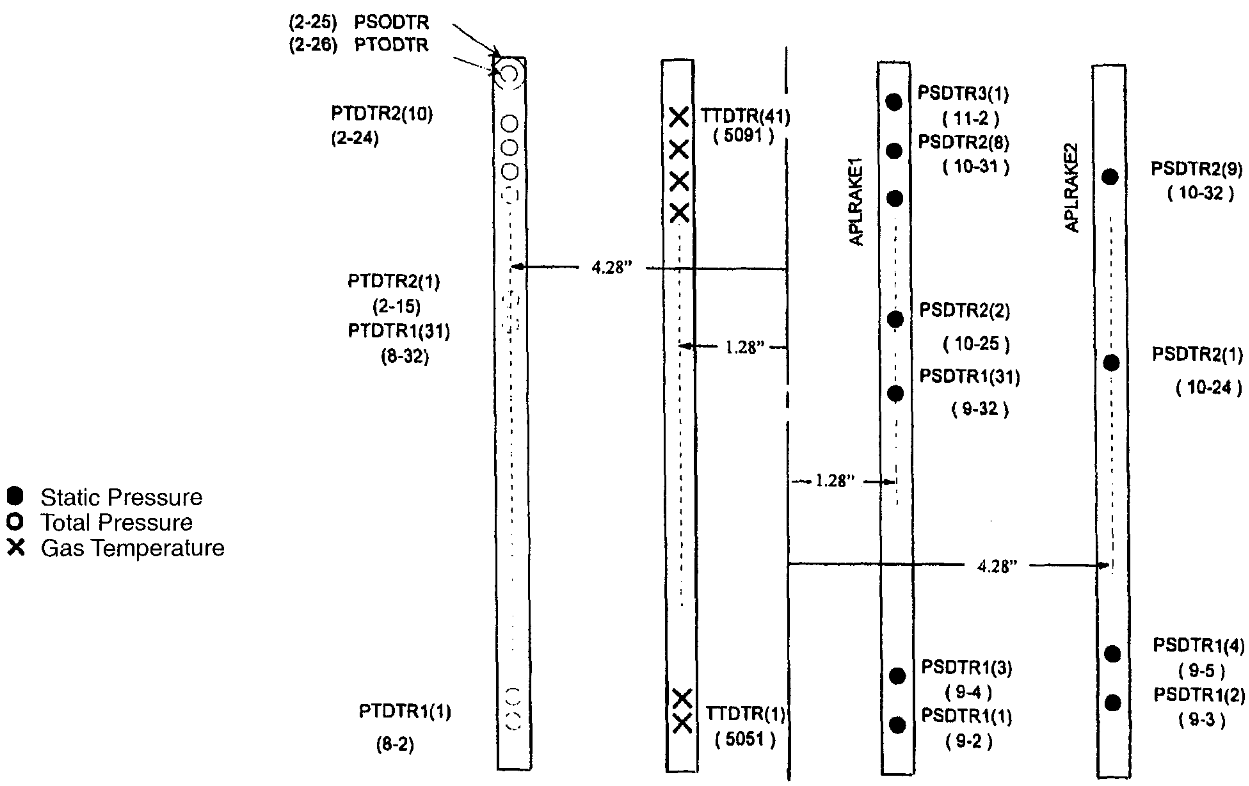


**Figure 35. Plume Traverse Survey Rake (Dense)** *Looking downstream (forward looking aft).*

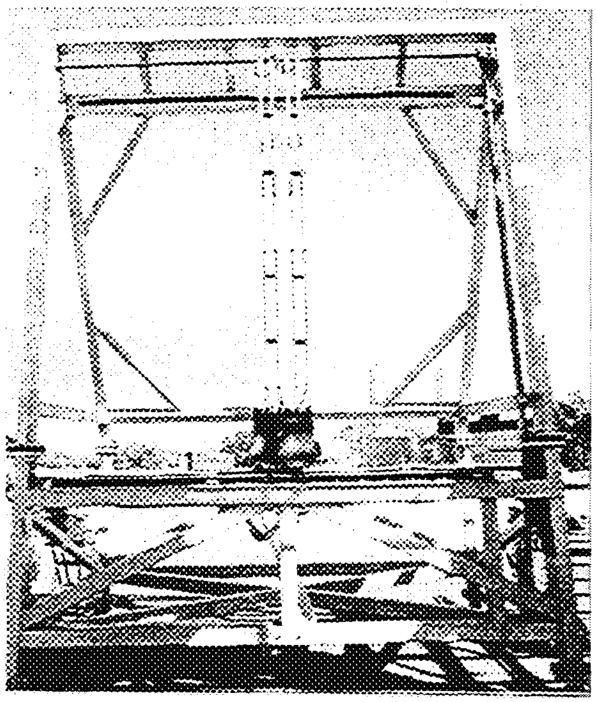

**Figure 36. Plume Survey Traversing Rake Apparatus**

Table 18 is a test-matrix summary for the AAPL/SFN plume surveys.

## 5.6 Test Procedures

Facility startup, shutdown, and emergency shutdown procedures are provided in the NATR Operations Manual along with associated mechanical check sheets.

Acoustic testing was conducted by establishing the initial desired free-jet Mach number in the NATR. Following this, generally, the lowest pressure ratio test point conditions were fixed by attaining the appropriate fan and core flows in the JER to give the desired fan and core flow total pressures and temperatures. When conditions stabilized, acoustic data were acquired. Fan and core flows were then adjusted to the pressure and temperature conditions corresponding to the power setting for the next higher pressure ratio test point. After conditions stabilized, acoustic data were again acquired. This procedure was repeated in the order of increasing pressure ratio until acoustic data were acquired for all power setting simulations at the first Mach number.

Once this was accomplished, the free-jet Mach number was changed, and the procedures described above were repeated in reverse order (decreasing pressure ratio) until acoustic data had been acquired at all desired power settings associated with the second Mach number.

For the third and final Mach number, those procedures for setting test conditions and acquiring acoustic test data outlined for the initial Mach number setting were repeated.

During this sequence of events, at selected test conditions, NASA phased-array and IR camera data were also acquired. Pertinent test variables are listed in Tables 10, 11, and 12.

## 5.7 Data Acquisition, Reduction, and Processing

The acoustic data and the test conditions of the program were provided by NASA Lewis to GEAE, AEC, and P&W in electronic database formats. The final posttest acoustic data were provided as follows.

First, NASA Lewis supplied as-measured, 1/3-octave-band, acoustic data with front-end instrumentation corrections only. Instrumentation corrections included all data-acquisition system and procedure corrections and data-amplification and analyzer system corrections. Second, NASA Lewis provided 1/3-octave data corrected for free-jet shear-layer effects. Third, NASA Lewis provided narrowband acoustic data corrected for shear-layer effects and at 1-ft and lossless conditions. Finally, NASA Lewis provided 1/3-octave data scaled to engine size (using a scale factor of 8 relative to model-scale hardware) and extrapolated to a 1500-ft sideline distance along with associated PNLT and EPNL output.

**Table 18. AAPL Separate-Flow Nozzle Plume Survey Test** *For all configurations, M = 0.28 and Cycle 2/Point 21 were test conditions.*

| Sequence | Test Configuration | Model | BPR | Plug | Core Nozzle | Fan Nozzle | Clock Position | Date Tested |
|---|---|---|---|---|---|---|---|---|
| 1 | 3BB | 3 | 5 | Ext. | Base | Base | N/A | 5/20/97 |
| 2 | 3C12B | 3 | 5 | Ext. | 12 Chevrons | Base | N/A | 5/20/97 |
| 3 | 3C12C | 3 | 5 | Ext. | 12 Chevrons | 24 Chevrons | N/A | 5/21/97 |
| 4 | 3BC | 3 | 5 | Ext. | Base | 24 Chevrons | N/A | 5/22/97 |
| 5 | 3IC | 3 | 5 | Ext. | 12 In-Flip Chevs. | 24 Chevrons | N/A | 5/22/97 |
| 6 | 3T24C | 3 | 5 | Ext. | 24 Flip Tabs | 24 Chevrons | N/A | 5/22/97 |
| 7 | 3C8B | 3 | 5 | Ext. | 8 Chevrons | Base | N/A | 5/23/97 |
| 8 | 3IB | 3 | 5 | Ext. | 12 In-Flip Chevrons | Base | N/A | 5/23/97 |
| 9 | 3AB | 3 | 5 | Ext. | 12 Alt–Flip Chevs. | Base | N/A | 5/23/97 |
| 10 | 3HmB(90) | 3 | 5 | Ext. | Half Mixer | Base | 90° | 5/23/97 |
| 11 | 3FB | 3 | 5 | Ext. | Full Mixer | Base | N/A | 5/27/97 |
| 12 | 3T48B | 3 | 5 | Ext. | 48 Flip Tabs | Base | N/A | 5/27/97 |
| 13 | 3T24B | 3 | 5 | Ext. | 24 Flip Tabs | Base | N/A | 5/27/97 |
| 14 | 3T24T24 | 3 | 5 | Ext. | 24 Flip Tabs | 24 Flip Tabs | N/A | 5/27/97 |
| 15 | 3BT24 | 3 | 5 | Ext. | Base | 24 Flip Tabs | N/A | 5/28/97 |
| 16 | 3BOmax(90) | 3 | 5 | Ext. | Base | Max. Offset Noz. | 90 | 5/28/97 |
| 17 | 3T24T48 | 3 | 5 | Ext. | 24 Flip Tabs | 48 Flip Tabs | N/A | 5/28/97 |
| 18 | 4BB | 4 | 8 | Int. | Base | Base | N/A | 5/29/97 |
| 19 | 1 | 1 | 5 | Int. | Base | Base | N/A | 5/30/97 |
| 20 | 6TmB | 2 | 5 | New | Tongue Mix. | Base | N/A | 5/30/97 |
| 21 | 7BB | 4 | 14 | New | Base | Base | N/A | 5/30/97 |
| 22 | 3BB | 3 | 5 | Ext. | Base | Base | N/A | 6/30/97 |
| 23 | 3BC | 3 | 5 | Ext. | Base | 24 Chev. | N/A | 6/30/97 |
| 24 | 3BT24 | 3 | 5 | Ext. | Base | 24 Flip Tabs | N/A | 6/30/97 |

These data formats correspond to blocks II, IV, III, and V respectively of the NASA Lewis acoustic data processing scheme outlined in Figure 37. Ambient static temperature, pressure, and relative humidity in the free-jet and inside the test chamber as well as test conditions (free-jet Mach number, total temperature, total pressure, etc.) were included with every final posttest acoustic data point provided by NASA Lewis. The test conditions included test point settings, meteorological conditions, model instrumentation parameters, nozzle performance parameters, and engineering units calculations.

For data reduction/correlation purposes, a test configuration code (Tables 13 and 14) was provided (see Figure 38) to identify, via manual input to the computer data-reduction program, the separate-flow exhaust system model hardware definition associated with data point printout.

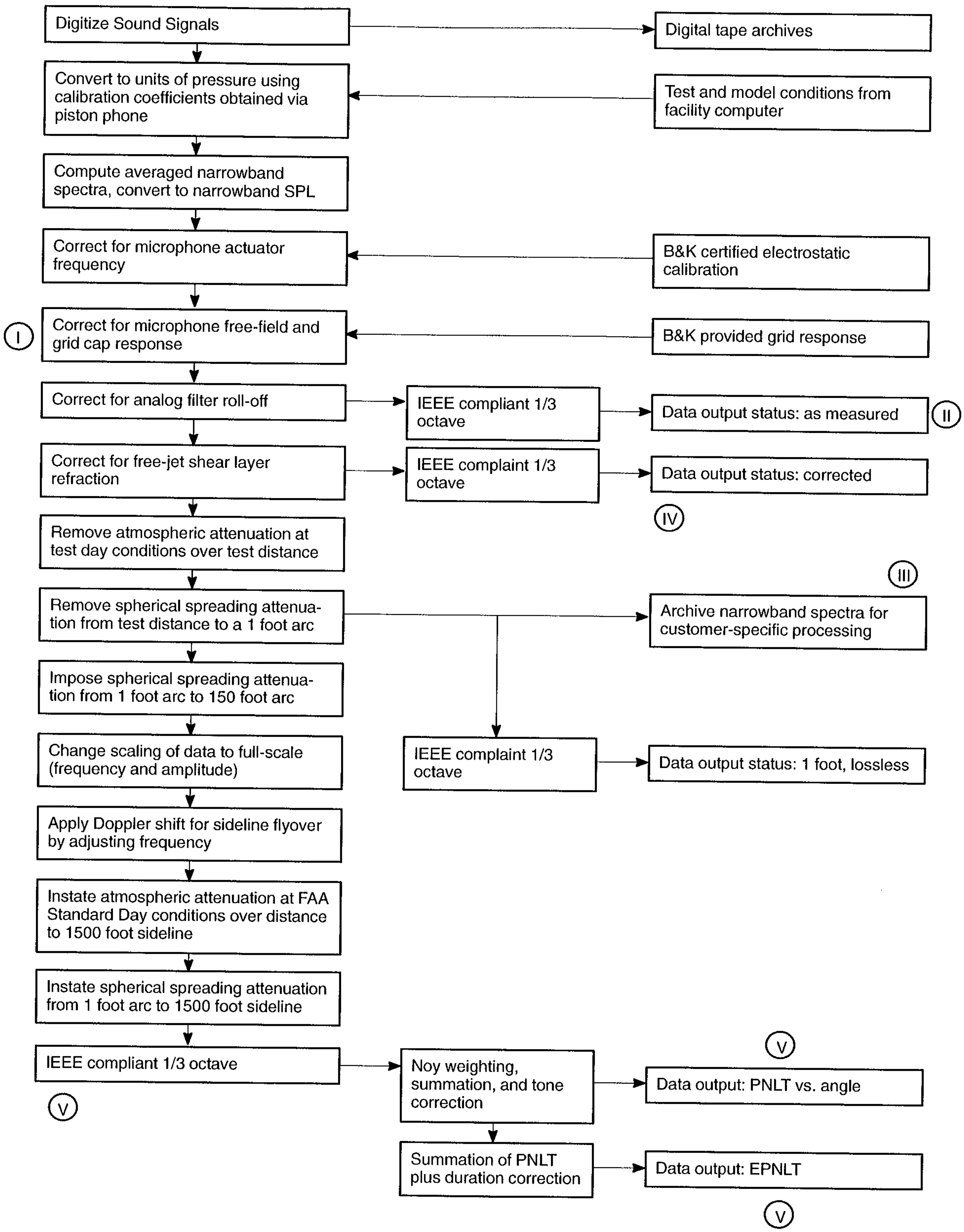


**Figure 37. NASA Lewis Acoustic-Data Processing Scheme**

Test Configuration Code: W XX YY ZZ

Model No. (W)

1 = Coplanar (BPR = 5)
2 = Internal Plug (BPR = 5)
3 = External Plug (BPR = 5)
4 = Internal Plug (BPR = 8)
5 = External Plug (BPR = 8)
6 = New Plug
7 = BPR = 14.0

Core Nozzle Mixing Enhancer (XX)

00 = Baseline (No mixing enhancer)
01 = 12 Chevrons
02 = 8 Chevrons
03 = 12 Inward Flipper Chevrons
04 = 12 Alternating Flipper Chevrons
05 = 64 Internal Doublet Vortex Generators
06 = 20 External Doublet Vortex Generators
07 = 24 Flipper Tabs (P&W)
08 = 48 Flipper Tabs (P&W)
09 = Half Mixer (P&W)
10 = Tongue Mixer
11 = Full Mixer

Fan Nozzle Mixing Enhancer (YY)

00 = Baseline (No mixing enhancer)
01 = 24 Chevrons
02 = 96 Internal Doublet Vortex Generators
03 = 24 Flipper Tabs (P&W)
04 = 48 Flipper Tabs (P&W)
05 = Maximum Offset Nozzle (P&W)
06 = Medium Offset Nozzle (P&W)
07 = Scarf Nozzle (P&W)
08 = 24 Chevrons with B. L. Trip
09 = 24 Chevrons with 24 V.G.

Nozzle Circumferential Position (ZZ)

00 = 0°
18 = 180°
09 = 90°
45 = 45°

**Figure 38. AAPL SFN Test "Configuration Codes"**

In Tables 13 and 14 the "Test Configuration" label is also used as an abbreviated name to identify model configurations. The nomenclature for the labels associated with the GEAE and AEC test configurations is as follows. The initial number in the label sequence corresponds to the model number of the Configuration Code presented in Figure 38. A "2," for example, signifies Model No. 2 (the BPR = 5 internal plug model). The upper case letter (sometimes accompanied by a lower case letter or number) following the initial number identifies the model core nozzle configuration. Here, "B" stands for Baseline, "C12" represents a 12-chevron nozzle. "Tm" designates the Tongue Mixer design, "I" the inward-flipper chevron nozzle, "A" the alternating flipper chevron core nozzle, "Di" the internal doublet mixing-enhancer concept, "Dx" the external doublet concept, and so forth. The next upper case letter in the Test Configuration sequence identifies the fan nozzle used in the model test configuration, for example: B for Baseline, C for Chevron, and D for Doublet. An "r" in parenthesis following the Test Configuration label indicated a "repeat" test configuration. Even though test results for the P&W configurations are not reported in this document, the Test Configuration nomenclature and Configuration Code are provided so the complete SFN test summary can be presented. For these configurations, "S" is a scarfed fan nozzle, "Omax" is an offset fan nozzle, "T24" and "T48" represent flipper tab nozzles with 24 and 48 flipper tabs respectively, "Hm" is a half-mixer core nozzle, and "F" is a full-mixer core nozzle. The numbers in parenthesis accompanying some of the P&W labels indicate the nozzle circumferential position.

The NASA Lewis acoustic data processing scheme outlined in Figure 37 takes into account microphone calibrations, actuator frequency, free-field and grid cap response, narrowband spectra conversions, analog filter roll-off corrections, free-jet shear-layer refraction, atmospheric and spherical spreading attenuation, data scaling, Doppler shift, standard day considerations, Noy weighting, summation and tone corrections, and duration corrections as well as test and model conditions supplied by the facility computer. The free-jet background noise was subtracted from the measured acoustic data for test points simulating flight conditions.

The method used to process the AAPL SFN test measured scale-model acoustic data included application of the Amiet point-source, shear-layer-correction model to the simulated-flight test data.

This set of scale-model data was also processed by GEAE using two shear-layer correction methods: the Amiet point-source model and the Mani distributed-source model. Comparison of the NASA and GEAE results indicated GEAE processed EPNL values, for a given test point, to be generally lower by 2 dB relative to NASA processed preliminary data. Upon review of their preliminary data-processing setup, NASA Lewis determined that there was a booking anomaly and subsequently reprocessed the results. The NASA reprocessed results agreed with GEAE processed data to within 0.5 EPNdB. This is further discussed in Subsection 6.1.1.2.

Also, NASA Lewis provided as-measured, 1/3-octave-band, scale-model data of selected test points of test configurations 3BB, 3IB, and 3IC.

# 6.0 Data Analysis and Discussion of Results

The acoustic test results from the GEAE/AEC nozzle configurations were analyzed to assess the noise-reduction characteristics of the concepts tested and evaluate how well the concepts worked relative to expectations.

As a preliminary step to evaluating the noise-reduction concepts, data scatter and uncertainty were first analyzed. Baseline Model 3 (BPR = 5, external plug) nozzle acoustic data were measured several times during the course of the test program, providing sufficient repeat data to assess uncertainty and repeatability.

As much as possible, an attempt was made to correlate either CFD analysis results or flow survey test results with the measured acoustic characteristics, as a way of relating the flow physics with the noise generation and noise reductions observed.

Acoustic test cycle conditions for each model configuration are summarized in Appendix B. Test conditions were established by setting a fixed total-to-ambient pressure ratio and total temperature for the core and fan streams.

With the exception of the tongue mixer, the noise-reduction concepts tested produced only minimal changes to the exhaust system overall aerodynamic characteristics.

## 6.1 Acoustic Results

Acoustic results for each configuration are generally discussed by examining peak noise (aft) angle perceived noise level ($PNL_{max}$) for static conditions (no forward-flight simulation, free jet not operating) and by examining effective perceived noise level (EPNL) for simulated flight cases. The data are typically plotted against ideal $V_{mix}$ and/or ideal net thrust. Selected PNL directivities, sound power level (PWL) spectra, sound pressure level (SPL) spectra, and Noy spectra are also presented at typical takeoff and cutback test conditions. These test conditions correspond to engine ideal thrust of 44,500 and 32,000 lbf under static conditions and engine ideal net thrust of 33,000 and 22,000 lbf for Mach 0.28 ($M_0$ = 0.28) simulated-flight conditions.

The model data have been scaled to projected engine size using a factor of 8. Due to the weighting attributes of some of the subjective noise metrics (in particular PNL), the benefits and conclusions presented in this section may change when other substantially different scale factors are considered. The calculation of EPNL was based on assuming a level flyover at 1500-ft altitude with the observer under the flight path, for one engine, and includes Doppler and atmospheric-absorption effects but neglects ground reflection, ground absorption, or aircraft shielding effects. The SPL's have been adjusted to reference atmospheric conditions of 77°F and 70% relative humidity.

### 6.1.1 Data Quality

Concerns arose regarding the repeatability of acoustic results from the early phase of the test. On a couple of occasions, differences in acoustic results were noted when the Model 3 baseline nozzle data were repeated. In addition, a 1 to 1.5 EPNdB difference was noted between Model 2 (BPR = 5, internal plug) and Model 3 (BPR = 5, external plug). This was in contrast to GEAE experience from similar scale-model tests. Hence, it was decided to repeat some configurations during the acoustic testing phase. For example, the Model 2 baseline test was repeated twice, and Model 3 baseline test was repeated 15 times during this test series.

This subsection includes a discussion on the repeatability of the measured acoustic data. It also includes typical comparisons of model data scaled to engine size using NASA and GEAE scaling and extrapolation procedures.

#### 6.1.1.1 Data Repeatability

Engine-size EPNL data for all Model 3 baseline tests, corresponding to different power settings along the Cycle 2 operating line (see Table 10), are summarized in Figure 39 as a function of $V_{mix}$. The parameter $V_{mix}$ is nozzle exit mass-averaged ideal velocity, defined as follows:

$$V_{mix} = \frac{(m_{core}V_{core,\, ideal} + m_{fan}V_{fan,\, ideal})}{(m_{core} + m_{fan})} \tag{1}$$

The ideal core and fan exit velocities are computed from the nozzle total pressures and temperatures and ambient pressure. This figure indicates that, for a given test condition, the EPNL data are scattered within a ±1-dB band. The data of Figure 39 are plotted as a function of net thrust in Figure 40. Figure 40 also indicates the variation in EPNL and net thrust for Cycle 2 test conditions. A similar observation is made with regard to the PNL directivity and SPL spectra in the vicinity of peak noise level, as shown in Figure 41, for test condition 21. Test condition 21 corresponds to a typical, full-power, takeoff-cycle operating condition.

During these repeat tests, it was noticed that ambient temperature had varied from 32° to 74°F. The EPNL data of Figure 39 were therefore replotted as a function of the ambient temperature, as shown in Figure 42. Each of the five rows of data in this figure correspond to different power settings along the Cycle 2 operating line. Figure 42 clearly indicates a sensitivity of the scaled acoustic results to the ambient temperature. It can be seen from Figures 39 and 41 that the measured variations for the same configuration were about the order of magnitude as the noise reductions expected from some of the noise-reduction concepts; therefore, the observed measurement variations were unacceptable from the standpoint of assessing noise reductions.

Over the years, scaled acoustic results from model nozzle tests in GEAE Cell 41 have traditionally been presented after normalizing EPNL data with respect to a reference density and thrust. This normalization was done to account for variations both in ambient conditions and in nozzle conditions of repeat test points. The normalization factor, *NF*, established from acoustic scaling laws, is defined as follows:

$$NF = -10 \log (F/F_{ref})(\varrho_j/\varrho_o)^{\omega-1} \tag{2}$$

In this equation, $\omega$ is a density exponent (as described and quantified in Reference 24), $\varrho_j$ is jet density, and $\varrho_o$ is ambient air density. Using a value of 1000 lbf for $F_{ref}$, the data of Figure 39 have been replotted in terms of normalized EPNL, defined as *EPNL* + *NF*, against a normalized $V_{mix}$, defined as $V_{mix}/c_{amb}$, where $c_{amb}$ is the ambient speed of sound. That plot is presented in Figure 43. The Model 3 external plug separate-flow nozzle results are now seen to be very repeatable with about ±0.5 EPNdB of data scatter.

Different versions of the above normalization procedure were investigated, and the results are summarized in Figures 44 and 45. In Figure 44, the EPNL data are normalized to a reference thrust only (1000 lbf), without the density correction, and are plotted against normalized $V_{mix}$. In Figure 45, the EPNL data without any normalization are plotted against normalized $V_{mix}$. The good correlation indicates that, for well-repeated nozzle flow conditions, normalization of $V_{mix}$ by $c_{amb}$ alone appears to reduce adequately data scatter due to different test day ambient temperatures.

Based on these results, the format with EPNL data normalized to reference thrust (1000 lbf) and plotted against normalized $V_{mix}$ was selected for most EPNL data comparisons in subsequent analyses, and discussions in the following subsections refer to such unless otherwise stated.

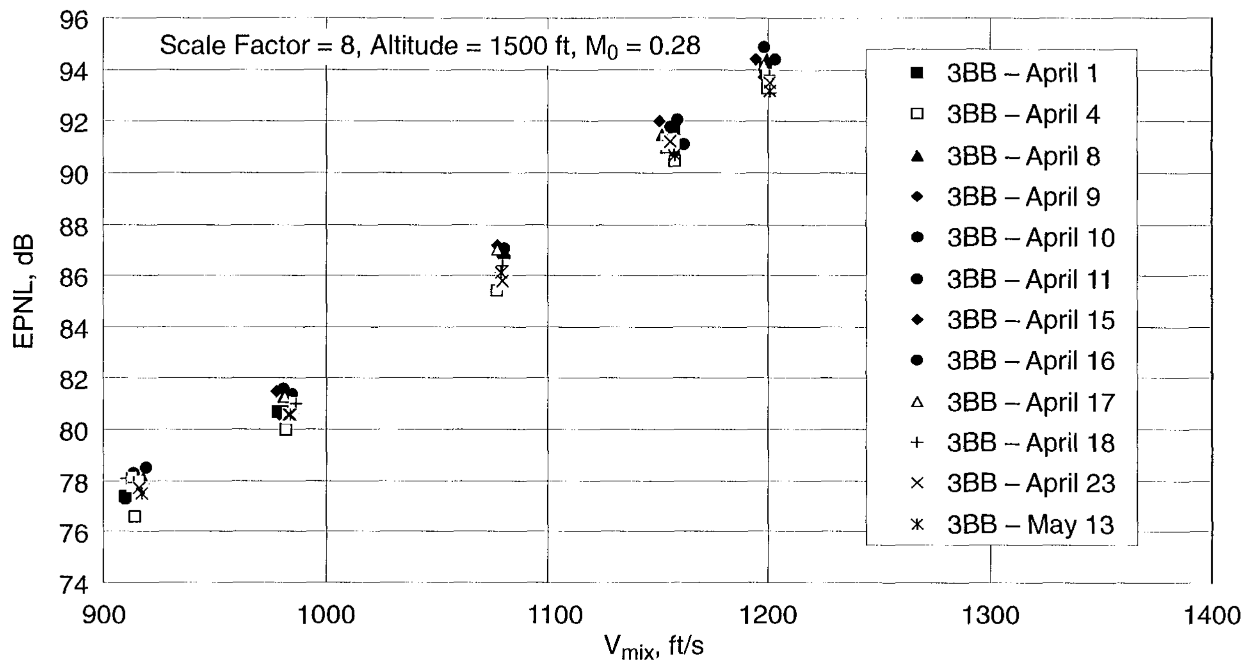


**Figure 39. EPNL as a Function of $V_{mix}$ for Baseline BPR = 5 Nozzle with External Plug (3BB)**

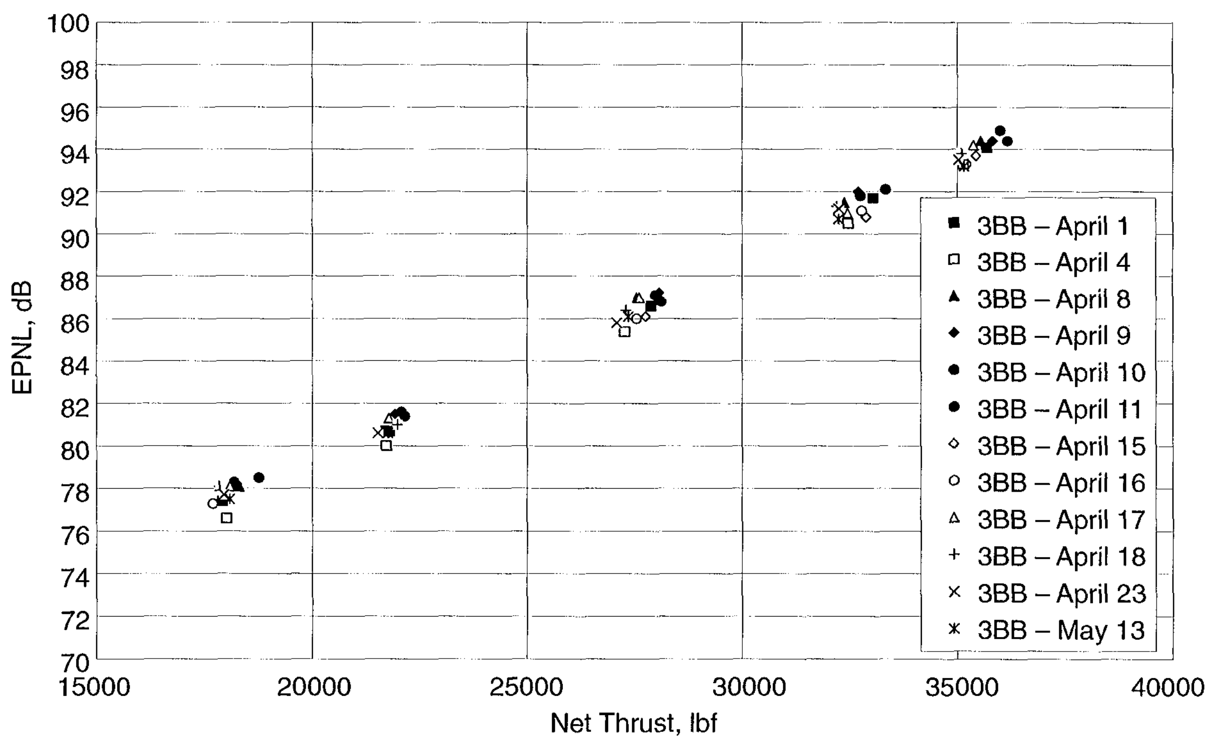


**Figure 40. EPNL as a Function of Net Thrust for Baseline BPR = 5 Nozzle with External Plug (3BB)**

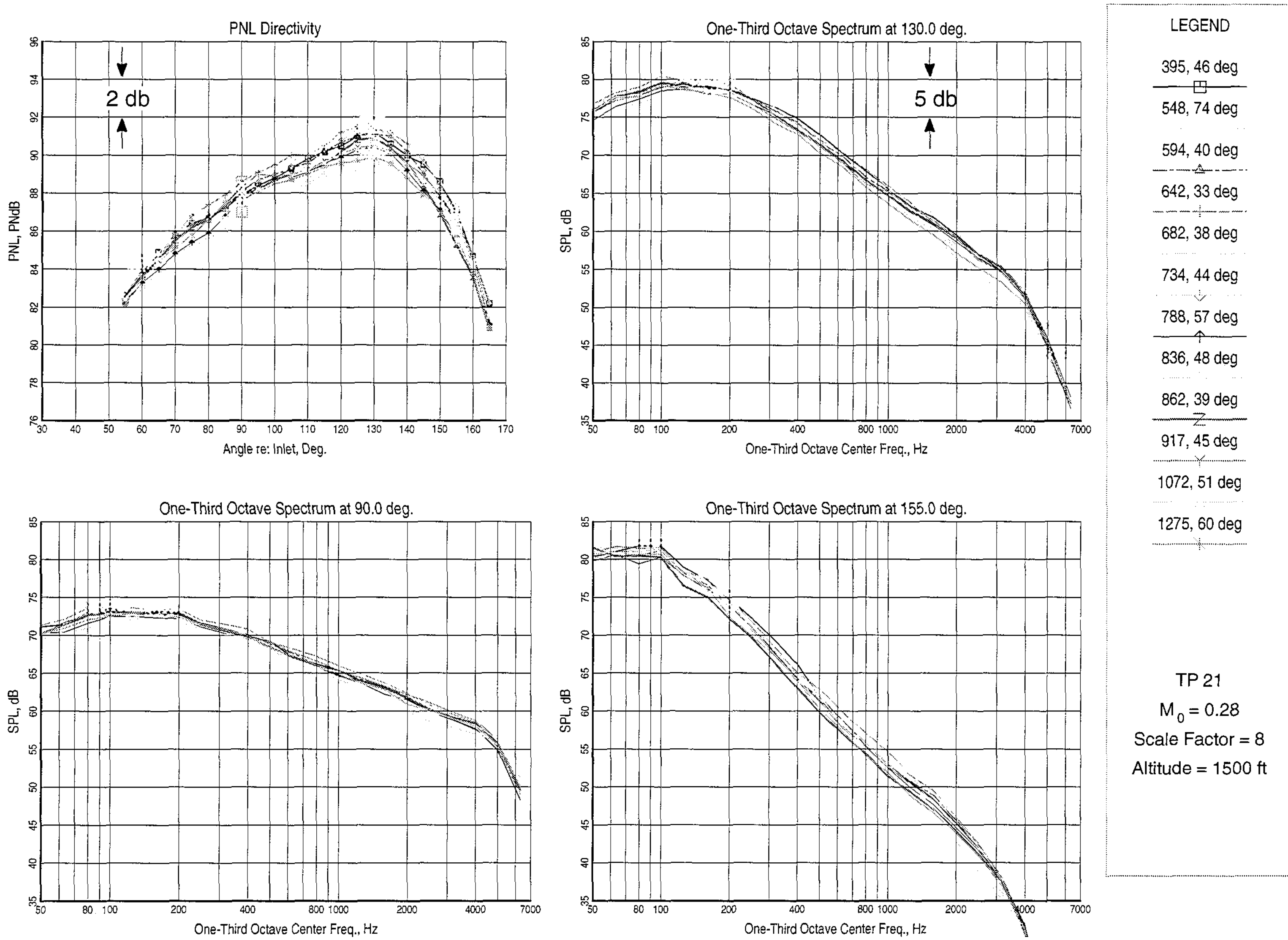


**Figure 41. Baseline BPR = 5 Nozzle (3BB) PNL Directivity and SPL Spectra Repeatability**

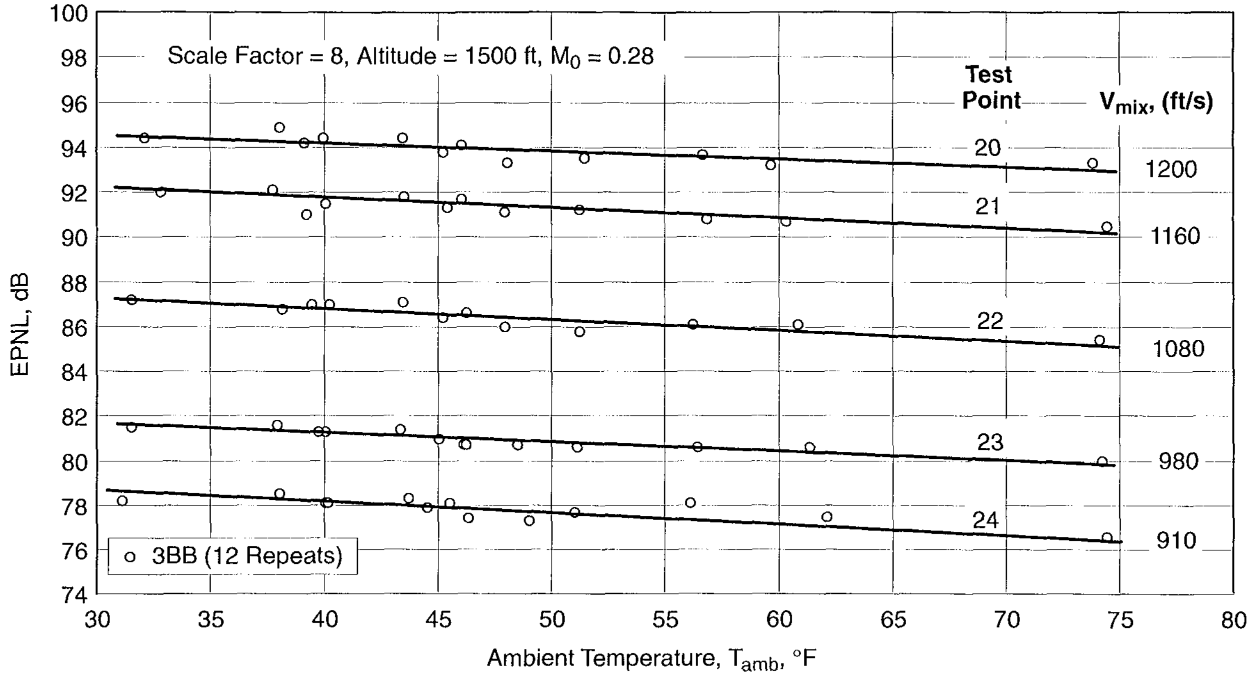


**Figure 42. EPNL as a Function of $T_{amb}$ for Baseline BPR = 5 Nozzle (3BB)**

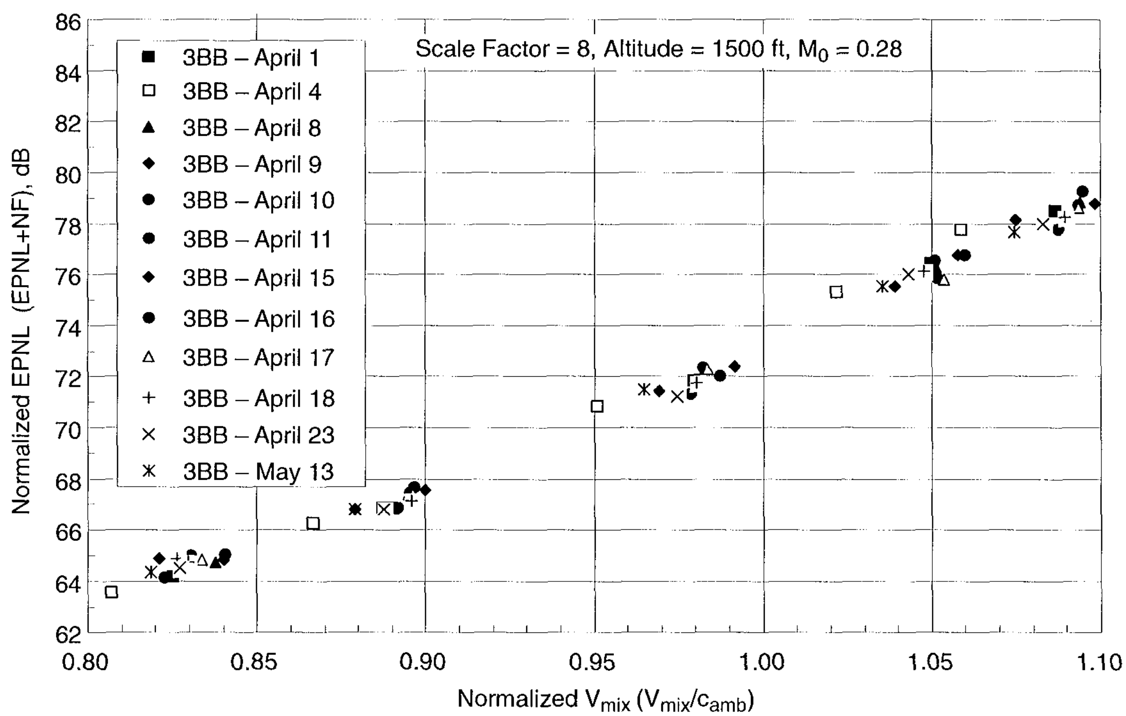


**Figure 43. Normalized EPNL as a Function of Normalized $V_{mix}$ for Baseline BPR = 5 Nozzle with External Plug (3BB)**

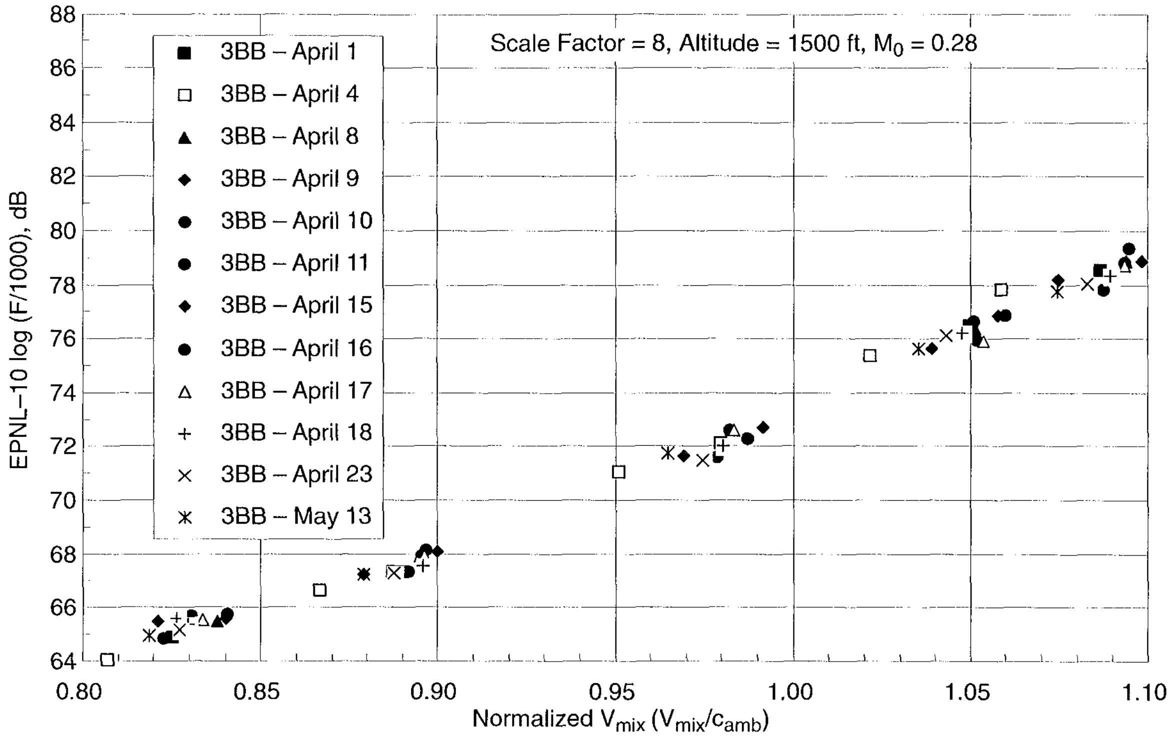


**Figure 44. Normalized EPNL (to Reference Thrust Only) as a Function of Normalized $V_{mix}$ for Baseline BPR = 5 Nozzle with External Plug (3BB)**

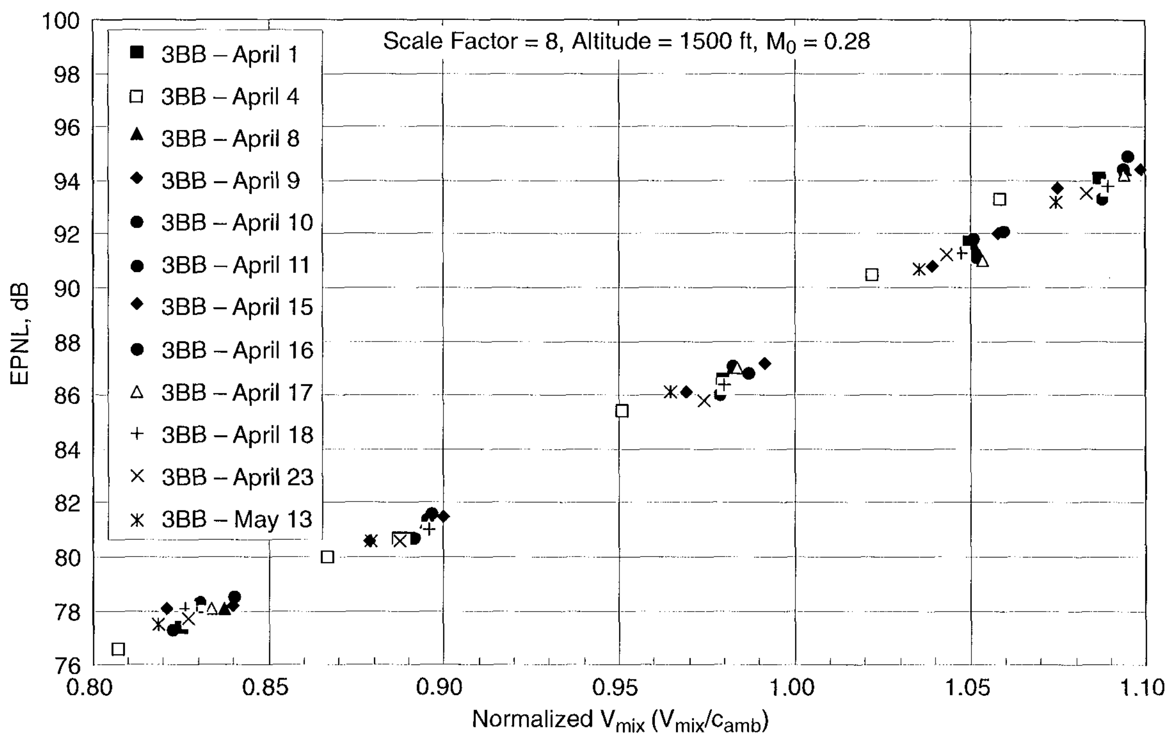


**Figure 45. EPNL as a Function of Normalized $V_{mix}$ for Baseline BPR = 5 Nozzle with External Plug (3BB)**

#### 6.1.1.2 Data Processing

The method used to process AAPL measured scale-model acoustic data is described in Section 5.7. It includes application of the Amiet point-source, shear-layer correction model (Reference 25) for adjusting measured flight-simulation test data, scaling the data to engine size, and extrapolating to a sideline distance. Selected scale-model AAPL data were also processed using two alternate methods: (1) the Amiet point-source, shear-layer correction model implemented in the GEAE PANDA scaling and extrapolation program and (2) the Mani distributed-source, shear-layer correction model (Reference 26) and GEAE in-house DATPROC scaling and extrapolation program.

Model 3 baseline configuration (3BB) data processed with the GEAE methods are compared with NASA-method-processed data in Figure 46 (normalized EPNL plotted against normalized $V_{mix}$). The three sets of results are within a ±0.5 EPNdB band. The GEAE/Amiet results are higher than those of NASA/Amiet by 0.5 EPNdB, and GEAE/Mani data are higher than those of GEAE/Amiet by another 0.5 EPNdB. The two GEAE methods approach each other at high values of normalized $V_{mix}$, and the NASA and GEAE/Amiet methods approach each other at low values of $V_{mix}$.

To further understand the differences in data-processing methods, typical PNL directivity comparisons are shown in Figure 47 and SPL spectrum comparisons at 60°, 90°, and 120° emission angles in Figures 48 through 50 for Test Point 20 (see Table 10). The three sets of results are comparable, but the NASA/Amiet and GEAE/Amiet results agree well with each other whereas the GEAE/Mani method seems to give different results away from 90°. The GEAE/Amiet EPNL values are higher than those of NASA/Amiet, as shown in Figure 46, due to the fact that NASA PNL directivity patterns are not extrapolated and ramped, as in the GEAE/Amiet method, on either side of the measured directivity to obtain 10-dB down points for the EPNL integration calculation.

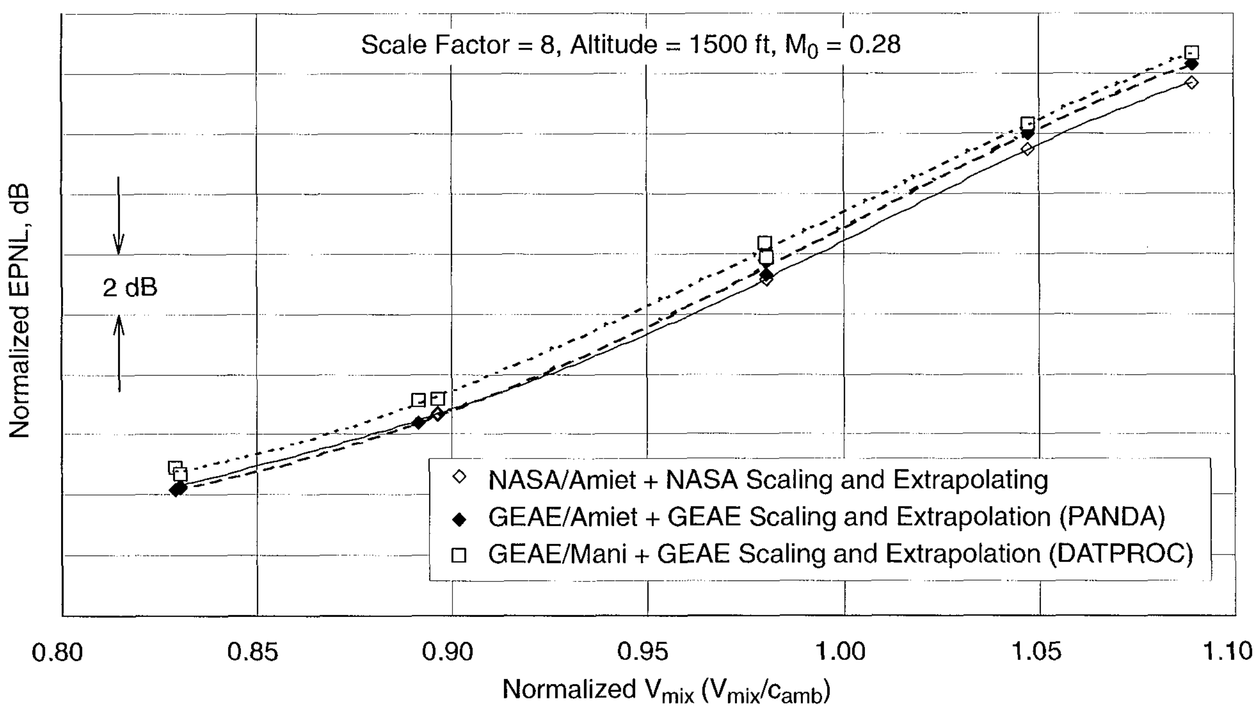


**Figure 46. Normalized EPNL as a Function of Normalized $V_{mix}$ for Baseline BPR =5 Nozzle with External Plug (3BB), NASA and GEAE Processed Data**

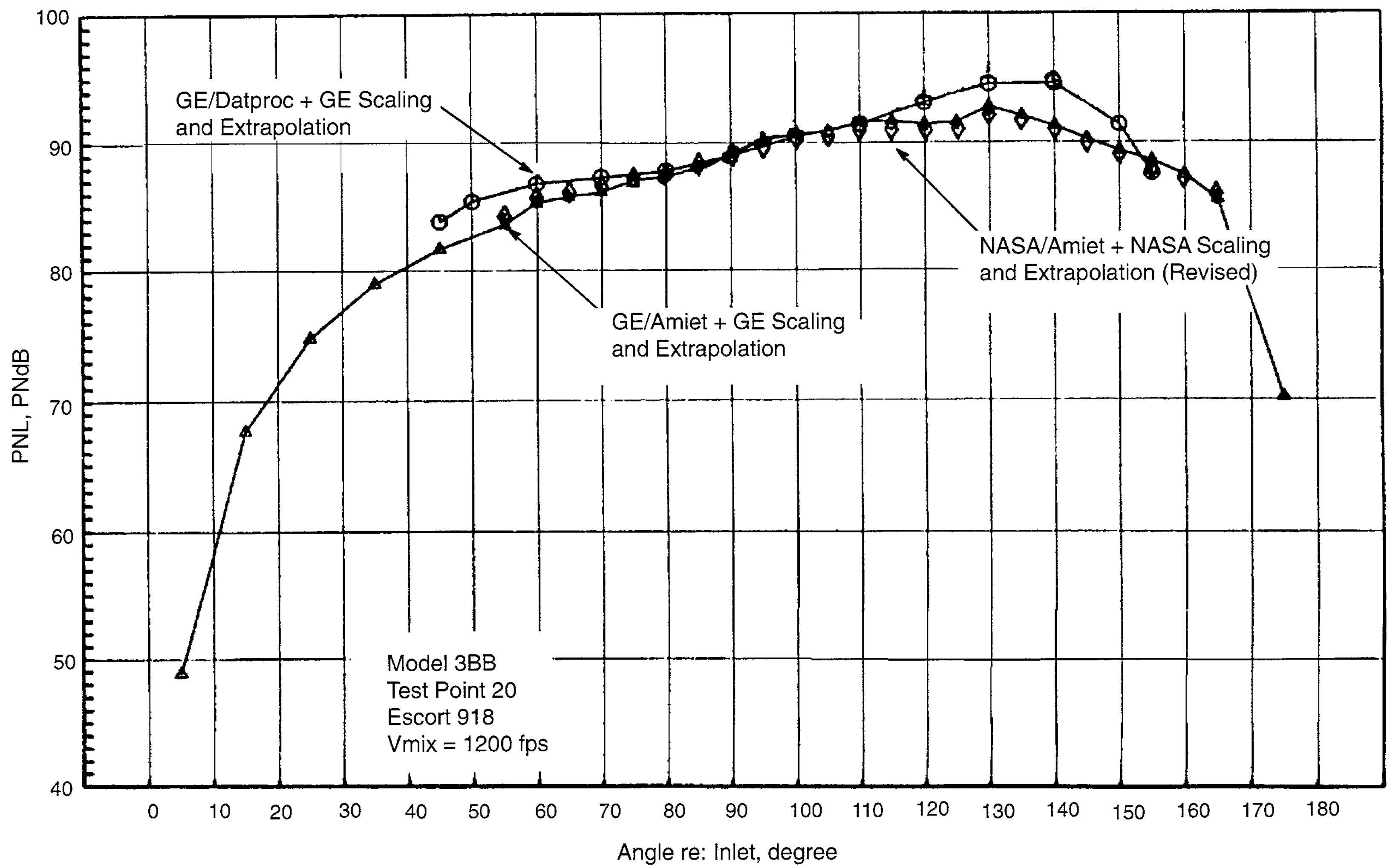


**Figure 47. PNL Directivity Comparison, NASA and GEAE Processed Data**

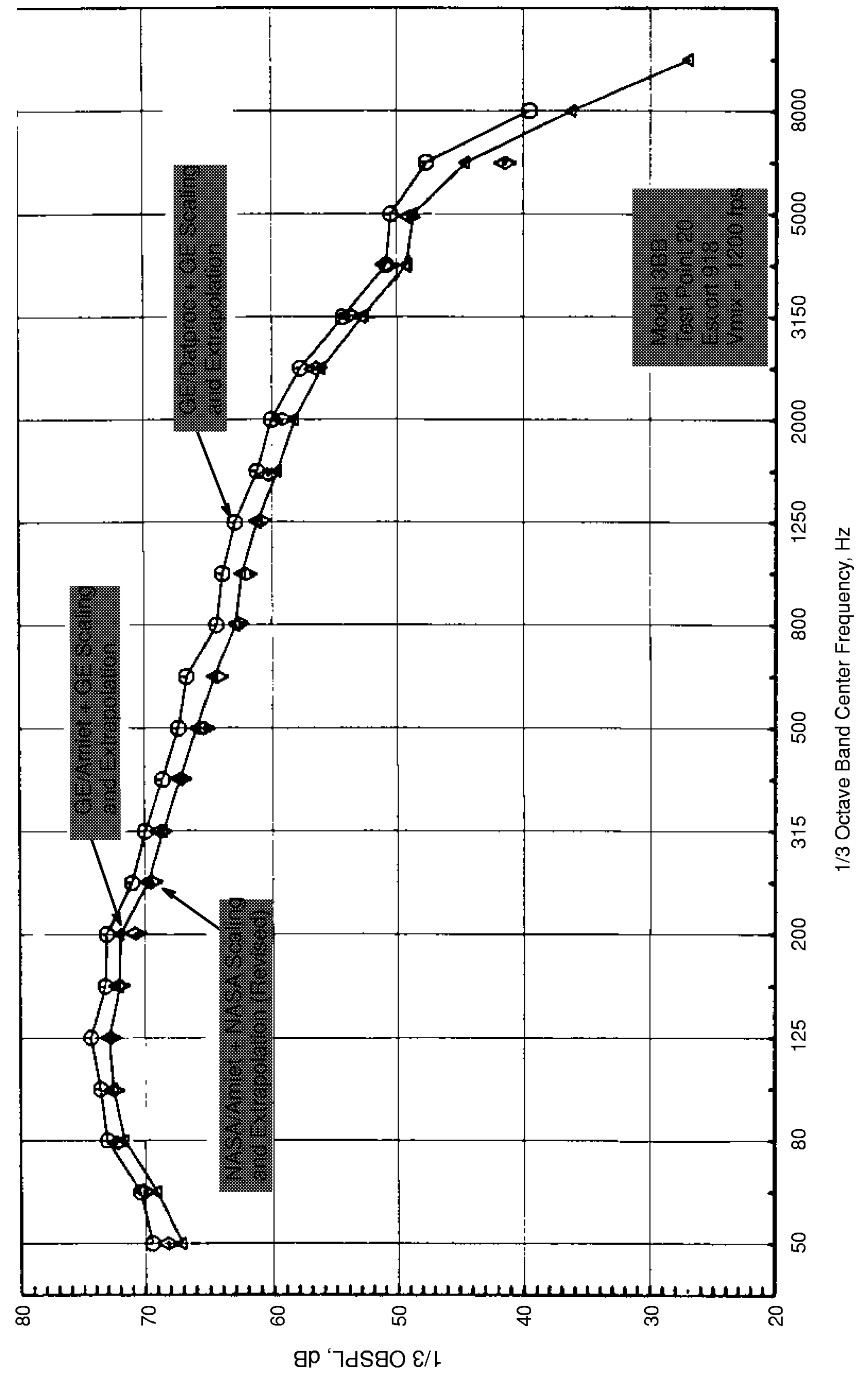


**Figure 48.** **Spectral Comparison at 60 Degrees, NASA and GEAE Processed Data**

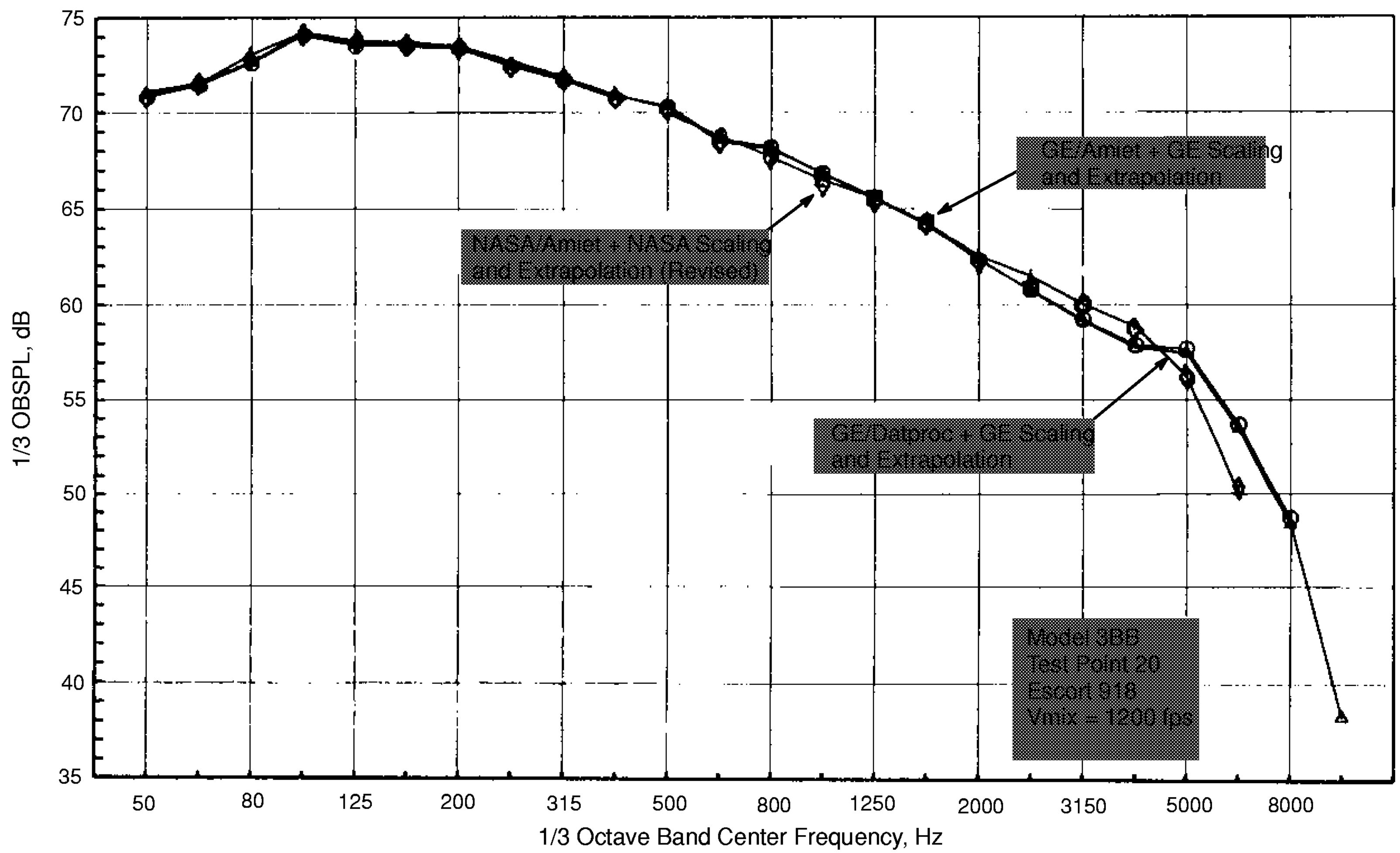


**Figure 49. Spectral Comparison at 90 Degrees, NASA and GEAE Processed Data**

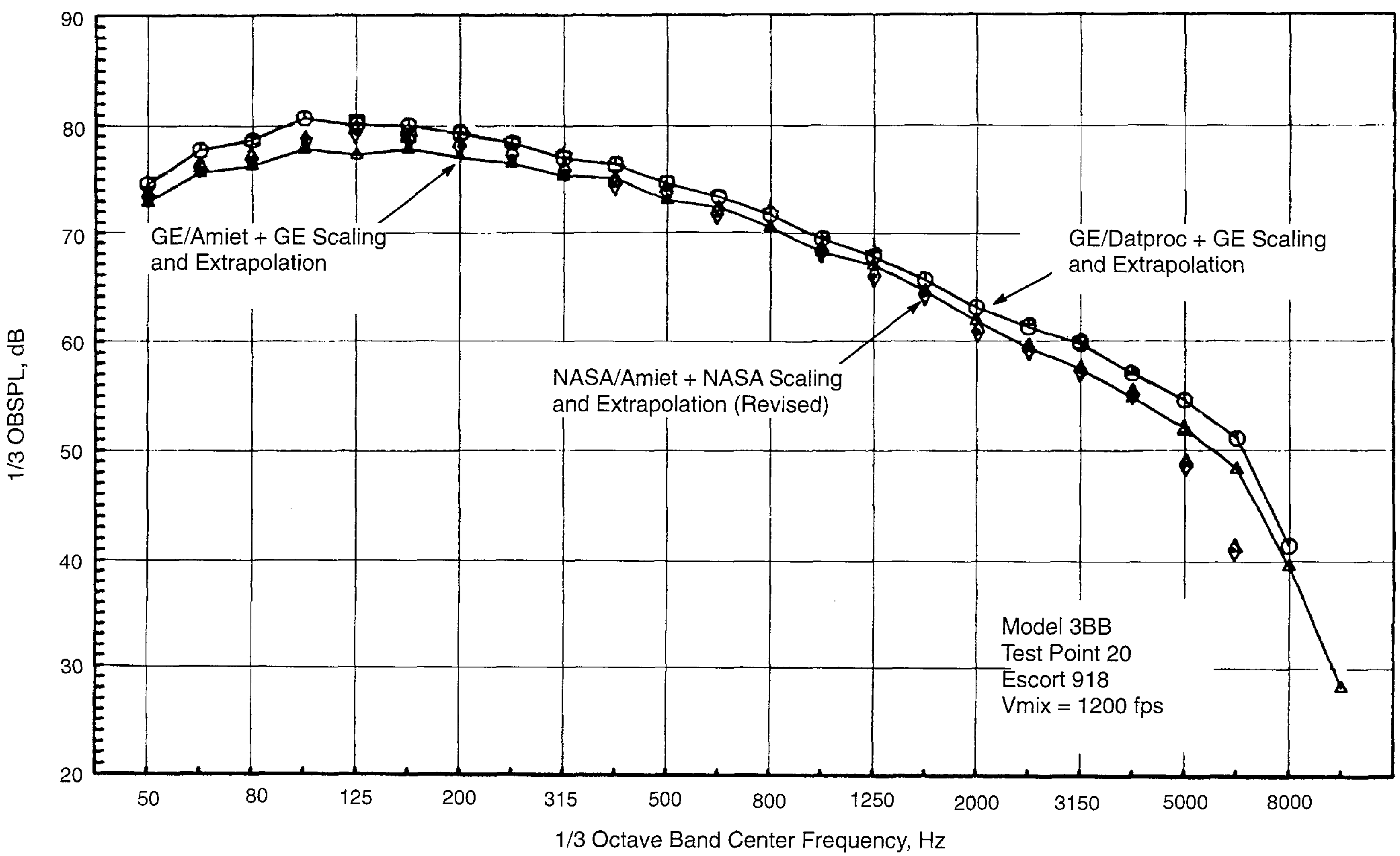


**Figure 50. Spectral Comparison at 120 Degrees, NASA and GEAE Processed Data**

The validity of either shear-layer correction method can only be assessed with true forward-flight or wind tunnel data. Such data are beyond the scope of this program. However, the above results suggest that, if the NASA processing were to incorporate directivity extrapolation and ramping, it would agree better with the GEAE/Amiet method at high jet velocities, and all the methods would be within about 0.5 EPNdB of each other.

Selected test points of configurations with noise-reduction features (3IB and 3IC) were also processed by GEAE and compared with NASA data. The comparisons show the same trends as observed with the baseline 3BB nozzle (Figures 46 through 50). The NASA method should probably include extrapolation to provide sufficient PNL directivity range to reach the 10-dB down points for a better estimate of EPNL; otherwise, the NASA process appears satisfactory. Acoustic data in the following sections were processed by NASA using the Amiet shear-layer correction model.

### 6.1.2 Baseline Nozzle Comparisons

Several baseline (no noise-reduction concepts installed) nozzles were tested in this program:

1. BPR = 5 coplanar-exit nozzle, Configuration 1BB (Figure 10)
2. BPR = 5 staggered exit nozzle with internal plug, Configuration 2BB (Figure 11)
3. BPR = 5 staggered exit nozzle with external plug, Configuration 3BB (Figure 12)
4. BPR = 8 staggered exit nozzle with internal plug, Configuration 4BB (Figure 13)
5. BPR = 8 staggered exit nozzle with external plug, Configuration 5BB (Figure 14)

It is of interest to know whether any of these baseline nozzles provide acoustic benefit relative to the others, so comparisons were made of the acoustic results of the coplanar, the internal plug, and the external plug BPR = 5 baseline nozzles. Similarly, comparisons were made of the internal plug and external plug BPR = 8 baseline nozzles. The effects of bypass ratio variation and forward flight Mach number variation on baseline nozzle acoustic characteristics were also investigated, and the results of these analyses are discussed below.

#### 6.1.2.1 Coplanar, Internal Plug, and External Plug BPR=5 Nozzle Comparisons

The engine-size EPNL data for the baseline nozzles (Models 1BB, 2BB, and 3BB), corresponding to different power settings along the Cycle 2 operating line, are summarized in Figure 51 as a function of ambient temperature. EPNL data points of 1BB and 2BB are seen to merge with the data and trend line of 3BB that was shown in Figure 42 and at each of the cycle conditions. The normalized EPNL data are presented in Figure 52 as function of normalized $V_{mix}$. Figures 51 and 52 both indicate no significant difference in EPNL values among the coplanar, internal, and external plug baseline nozzles for a given test cycle condition.

PNL directivity and 1/3-octave SPL spectra at three different angles for the coplanar and external plug nozzle are presented in Figure 53 for $V_{mix}$ = 1150 ft/s (cycle point 21). While the EPNL values are approximately the same, the coplanar nozzle PNL is slightly higher at the forward (< 90°) and extreme aft (> 140°) angles and slightly lower between 90° and 140°, compared to the external plug nozzle. In terms of the spectra, the external plug SPL's are slightly higher at the lower frequencies (< 1 kHz) and lower in the midrange frequencies (between 1 and 4 kHz).

The PNL directivity and 1/3-octave spectra for the internal and external plug nozzles are compared in Figure 54 for $V_{mix}$ = 1150 ft/s (cycle point 21). Again, although EPNL values are very similar, there are subtle differences in

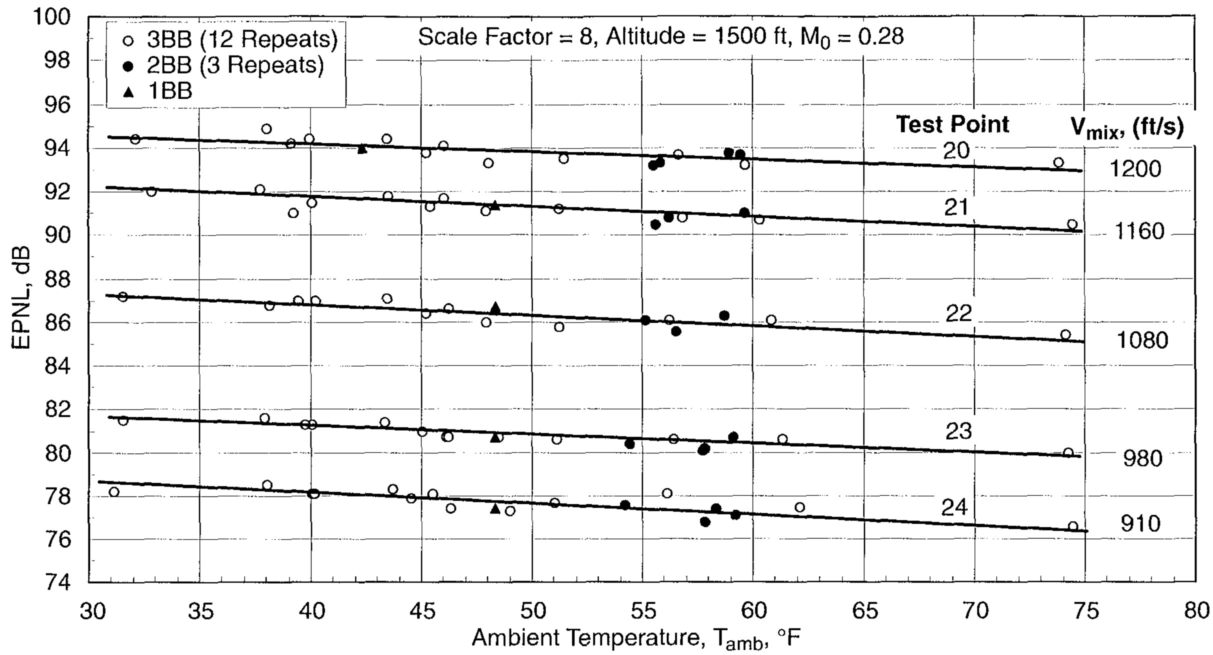


**Figure 51. EPNL as a Function of $T_{amb}$ for Baseline BPR = 5 Nozzles: Coplanar (1BB), Internal Plug (2BB), and External Plug (3BB)**

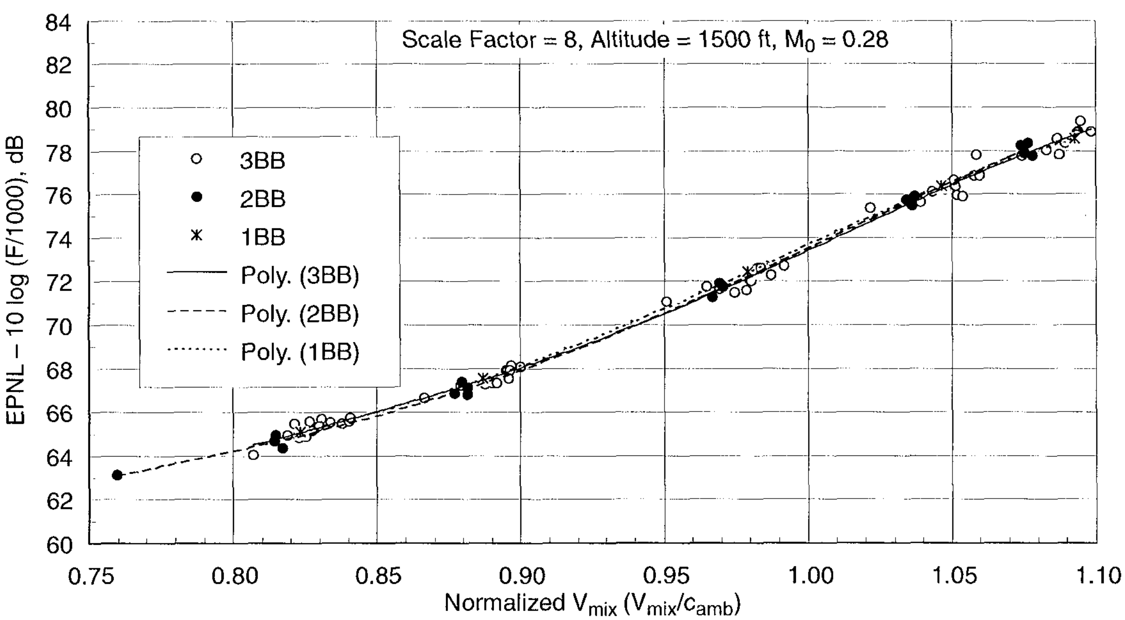


**Figure 52. Normalized EPNL as a Function of Normalized $V_{mix}$ for Baseline BPR =5 Nozzles: Coplanar (1BB), Internal Plug (2BB), and External Plug (3BB)**

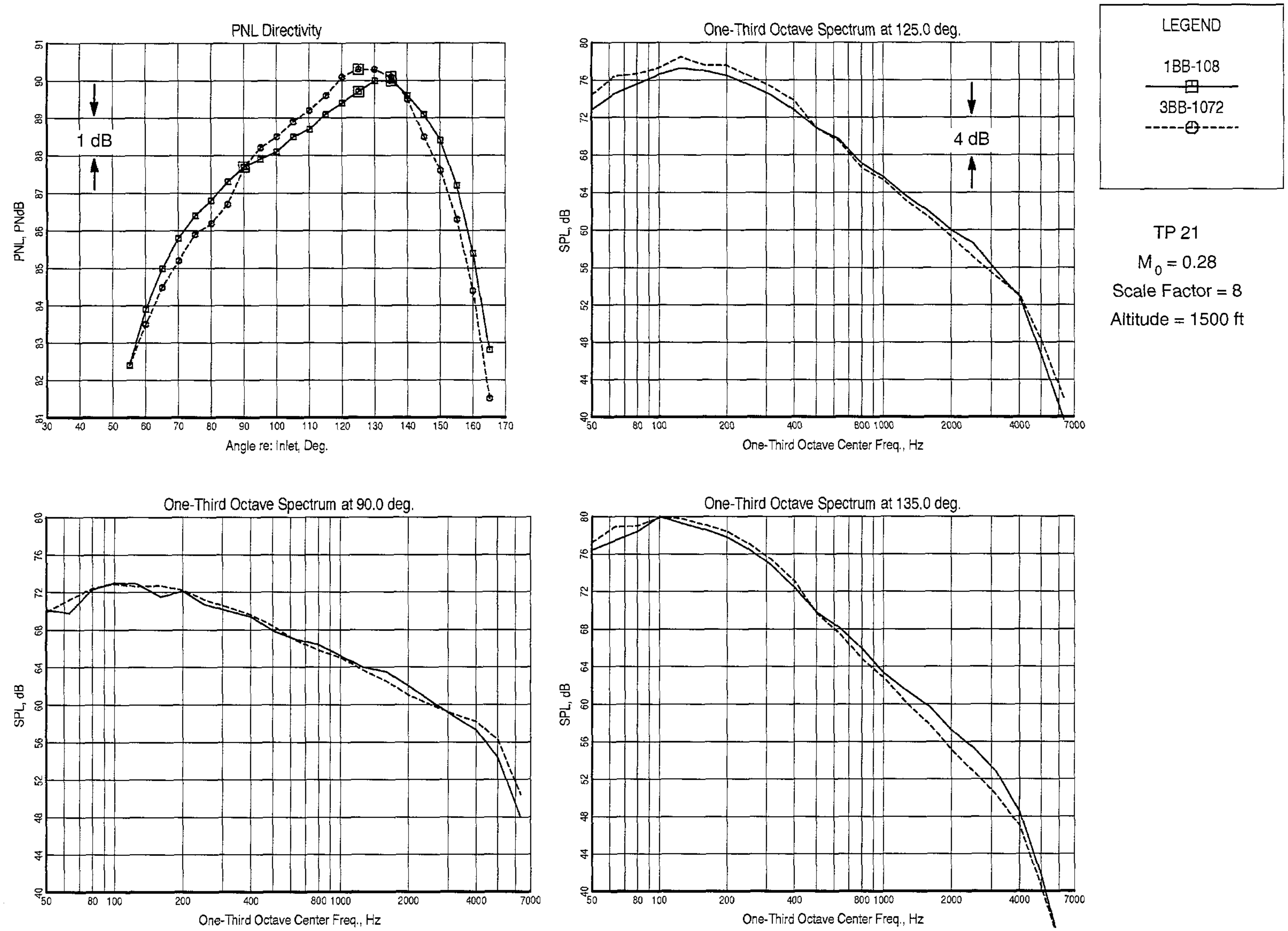


**Figure 53. PNL Directivity and SPL Spectra: Coplanar (1BB) Compared with External Plug (3BB) BPR = 5 Nozzles**

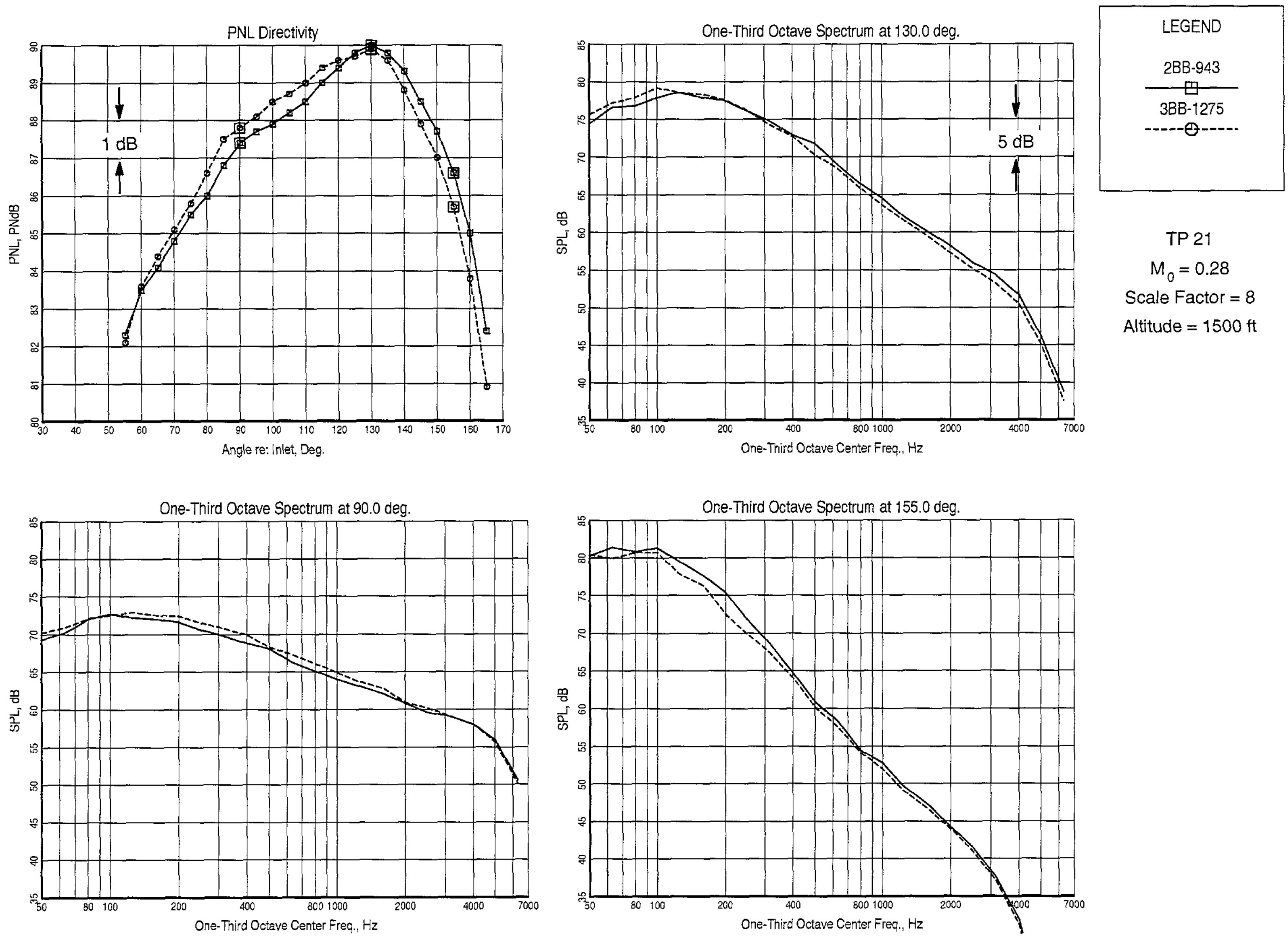


**Figure 54. PNL Directivity and SPL Spectra: Internal Plug (2BB) Compared with External Plug (3BB) BPR = 5 Nozzles**

the PNL directivity and SPL spectra. The internal plug nozzle has lower PNL relative to external plug nozzle up to the peak PNL angle, around 130°, and is higher at the extreme aft (> 140°) angles. Spectrally, the internal plug is generally lower at low frequencies (< 1 kHz). However, in general, there is very little significant difference or discernible trend in the acoustic data of the three baseline nozzle configurations.

The directivity and spectral differences shown in Figures 53 and 54 are mostly small, fractions of a decibel in the case of PNL and less than 2 dB in the case of spectra. It was expected that tested noise-reduction concepts would exhibit larger differences. This is not to say, however, that a given noise-reduction concept will not give significantly different results on one baseline versus another baseline nozzle design.

#### 6.1.2.2 Internal Plug and External Plug BPR=8 Nozzle Comparisons

Engine-scale EPNL data for the BPR = 8 baseline nozzles (Models 4BB and 5BB), along the Cycle 4 operating line, are presented in Figure 55 as function of normalized $V_{mix}$. Again, in terms of normalized data, no significant differences are noted between the internal and external plug baseline nozzle acoustic measurements. Also, looking at individual points (such as the cycle point labeled 41 on Figure 55, see Table 10), it can be seen that the same cycle point setting produced different values of normalized $V_{mix}$ for the internal and external configurations. This is due to different ambient temperatures (54°F for Model 4BB and 45°F for Model 5BB), when the test data were taken, and slightly different $V_{mix}$ values (992 ft/s for Model 4BB and 998 ft/s for Model 5BB).

PNL directivity and 1/3-octave spectral comparisons are presented in Figure 56. Although the internal plug noise data appear lower than the external plug noise levels, it should be remembered that the internal plug configuration is effectively at a smaller value of normalized $V_{mix}$, as indicated by the differences shown in Figure 55. For example, the cycle point 41 EPNL values are different by about 0.7 dB (5BB is higher), and this is consistent with

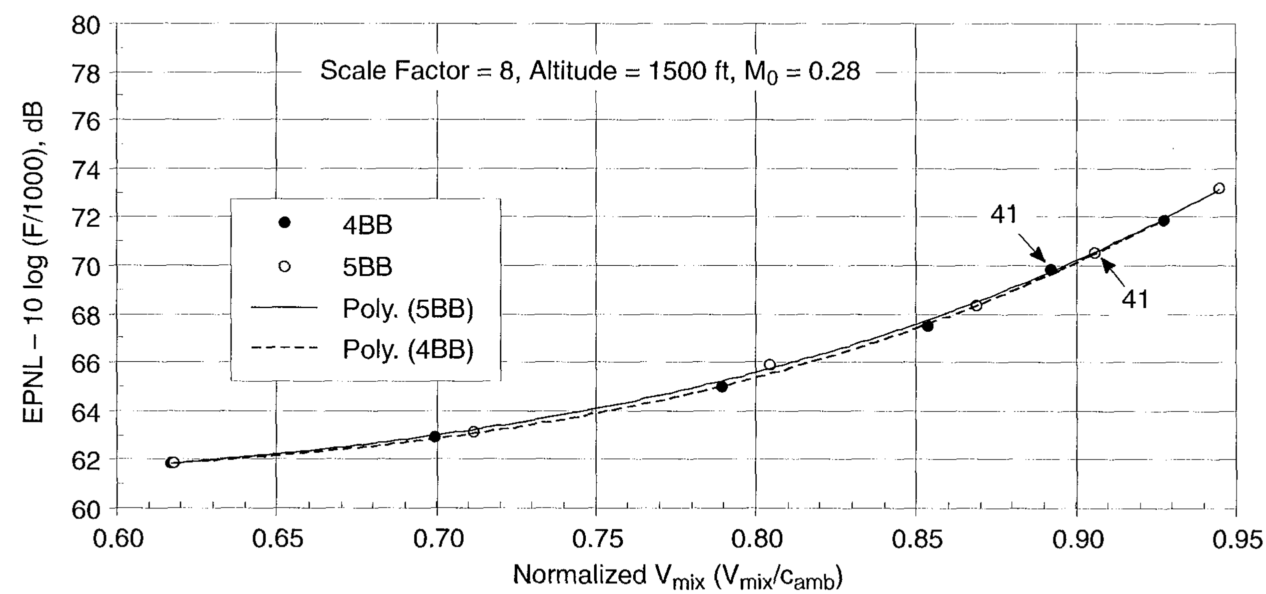


**Figure 55. Normalized EPNL as a Function of Normalized $V_{mix}$ for Baseline BPR =8 Nozzles with Internal (4BB) and External Plugs (5BB)**

the differences noted in directivity and spectra shown in Figure 56. Therefore, it was concluded that there is no significant difference between the acoustic results of internal and external plug BPR = 8 baseline configurations.

#### 6.1.2.3 BPR Variation

It was of interest to evaluate the jet noise reductions achievable through increasing bypass ratio. The models tested in this program provided an opportunity to evaluate this experimentally. In addition to the two baseline nozzles designed for BPR = 5 and BPR = 8, an additional test was run with an extended internal core plug, as a modification to Model 2BB. The extended core plug reduced the size of the core nozzle exit area and hence increased the bypass ratio from the nominal value of 8 to a nominal value of 14. Thus we were able to acquire data for three distinct bypass ratios. The modified Model 7BB, corresponding to BPR = 14, was run along an operating line corresponding to Cycle 7, listed in Table 12.

Test data for the different bypass ratios cannot be sized using the same scale factor because larger bypass ratios imply a larger engine for the same thrust. Also, they cannot be compared on a constant $V_{mix}$ basis, because larger BPR implies lower $V_{mix}$ for the same takeoff thrust. The proper procedure is to select a cycle point on the operating lines, given in Tables 10 and 12, that corresponds to the full-power takeoff condition for each cycle. This determines the model-scale ideal thrust for each configuration at the takeoff flight speed. These thrust levels will be different for different models; therefore, the scale factors must be selected such that the thrust of each scaled nozzle is the same.

If we select the BPR = 5 nozzle as the reference, which has a scale factor of 8:1, we then must scale the other two nozzles such that they give the same net corrected thrust at the designated full-power takeoff point. Table 19 lists the full-power takeoff cycle points selected for the three bypass ratios and the corresponding scale factors required to give the same takeoff thrust.

They do not have the same $V_{mix}$ at full-power takeoff; therefore, comparing EPNL as a function of $V_{mix}$ is not appropriate for this assessment. Instead, EPNL is plotted as a function of corrected thrust, realizing that the $V_{mix}$ variation is different for the different bypass ratios.

To illustrate, the original (all model data scaled using a factor of 8:1) $V_{mix}$ versus corrected thrust schedule for the three bypass ratios is shown in Figure 57. Note there is little difference in net thrust at a given mixed velocity for the three bypass ratios when the scale factor is the same for all nozzles; this is due to the fact that all nozzles have the same fan diameter and approximately the same total flow area. Also, note that for BPR = 14 there is only one data point at a simulated flight Mach number of 0.28 and five data points for Mach 0.20. The original (scale factor = 8) Mach 0.20 net-thrust data were first adjusted by calculating ram drag based on measured flow rates and test free-jet Mach number and then by computing gross thrust by adding ram drag. Then the ram drag corresponding to a flight Mach number of 0.28 was computed and subtracted from the calculated gross thrust to get corrected net thrust at a Mach number of 0.28. The net-thrust data of BPR = 8 and BPR = 14 (now all at Mach 0.28) were next calculated using the scale factors listed in Table 19. The modified data, shown in Figure 58, have a $V_{mix}$ versus net thrust characteristic that is much different than that shown in Figure 57.

The selected takeoff thrust sizing point is shown as a horizontal line in Figure 58, and the mixed velocity at this thrust varies from 726 to 1158 ft/s in going from a bypass ratio of 14 to 5, as given in Table 19. Also shown on Figure 58 are second-order curve fits of these characteristics, and they all yield zero net thrust at approximately the $V_{mix}$ corresponding to flight speed $V_{amb}$.

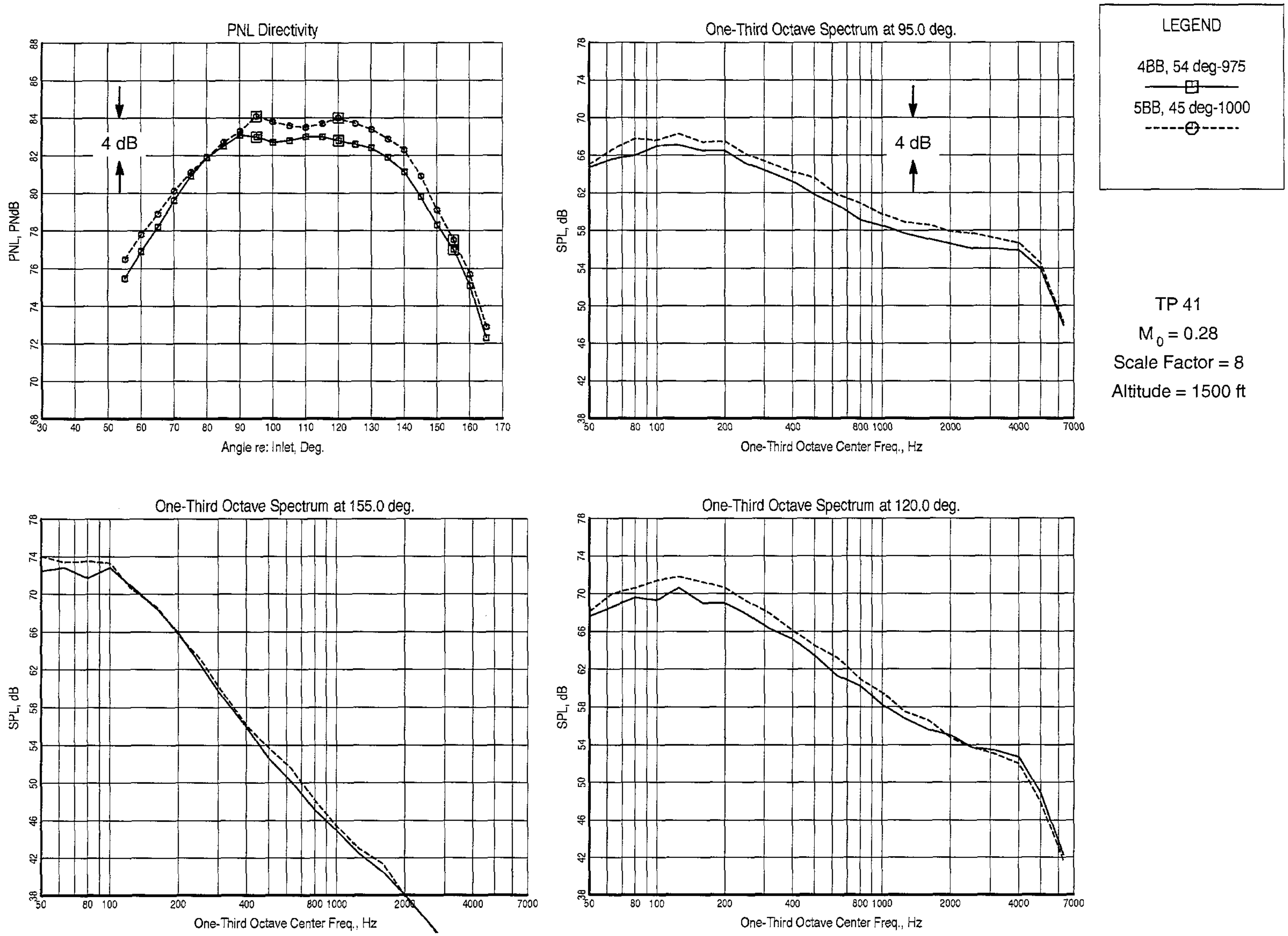


**Figure 56. PNL Directivity and SPL Spectra: Internal Plug (4BB) Compared with External Plug (5BB) BPR = 8 Nozzles**

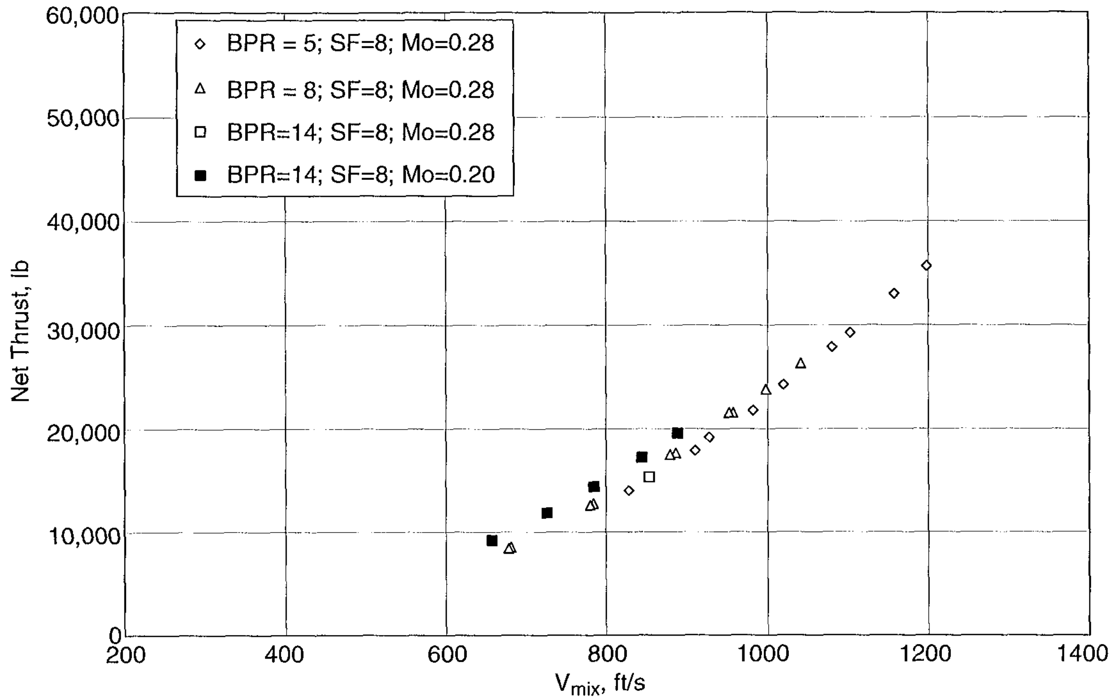


**Figure 57. Thrust as a Function of $V_{mix}$ for External Plug Nozzles: Constant Scale Factor (8)**

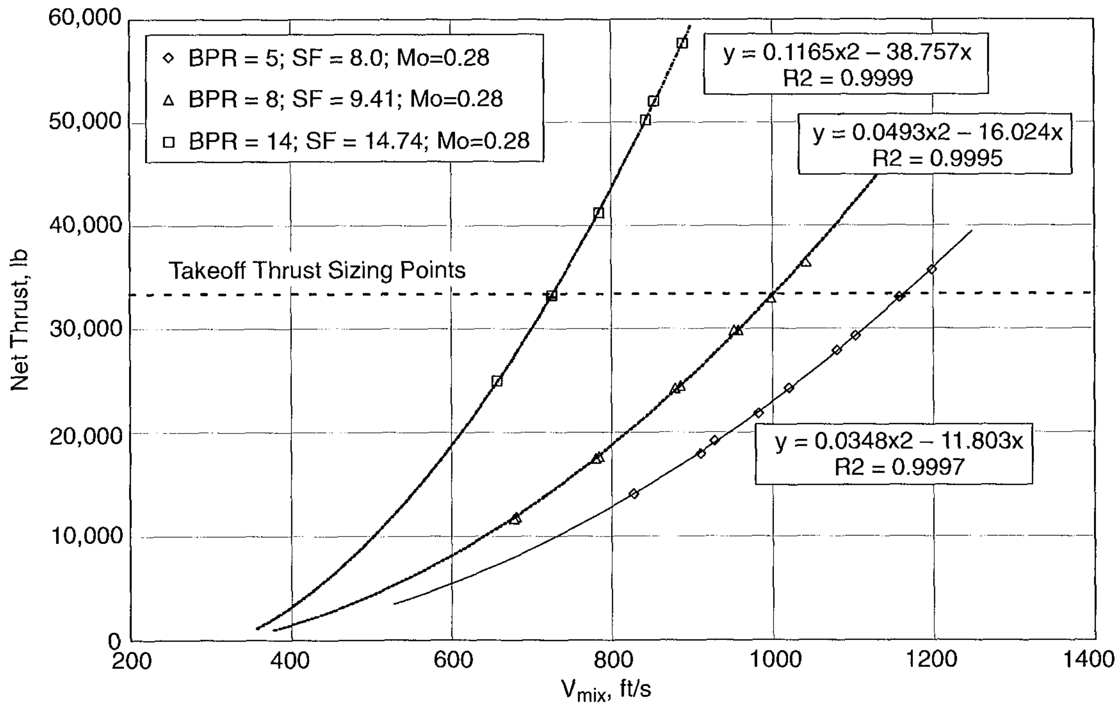


**Figure 58. Thrust as a Function of $V_{mix}$ for External Plug Nozzles: Scale Factor Varied with BPR**

**Table 19. Baseline Nozzle Full-Power Takeoff Conditions for Scaling to Constant Thrust**

| Configuration | BPR | Cycle | Point | Fan PR | Core PR | Fan $T_T$, °R | Core $T_T$, °R | $V_{mix}$, ft/s | SF |
|---|---|---|---|---|---|---|---|---|---|
| 3BB | 5 | 2 | 21 | 1.83 | 1.68 | 655 | 1500 | 1158 | 8.0 |
| 5BB | 8 | 4 | 41 | 1.57 | 1.52 | 625 | 1520 | 998 | 9.41 |
| 7BB | 14 | 7 | 73 | 1.29 | 1.22 | 600 | 1360 | 726 | 14.74 |

There is some approximation in the scale factors derived in Table 19, because the sizing points were selected based on experience, cycle studies and data from engine tests, in terms of selecting the fan nozzle pressure ratio which most appropriately represents the full-power condition for the bypass ratio being considered. The BPR = 5 nozzle fan pressure ratio selected is 1.83, typical of the CF6–80E1 engine at full-power takeoff. The BPR = 8 nozzle fan pressure ratio selected is 1.57, slightly higher than that of the GE90 engine at full-power takeoff, but the GE90 engine actually has a bypass ratio of about 9. Finally, the BPR = 14 nozzle fan pressure ratio selected is 1.29, similar to that of the ultra-high-bypass study engine designed by GEAE as part of a contract for NASA (Reference 27).

Another approximation that may be called into question is sizing at full-power takeoff for equal net thrust. Depending on the bypass ratio and corresponding engine cycle lapse rate, the limiting thrust may be at *top of climb*, not at sea level. For the purposes of this analysis, however, time and resources were insufficient to carry out the appropriate cycle and mission analyses to determine the limiting thrust requirements for each bypass ratio, so the approximation of sea level takeoff as the sizing point was assumed. Within the limitations that may be imposed by these assumptions, the sea level static or takeoff gross thrust ratings for the three engines turn out to be 45,000, 48,000, and 58,000 lbf for BPR = 5, 8, and 14, respectively.

The EPNL versus $V_{mix}$ characteristics for the three bypass ratio nozzles with the same scale factor (8) is shown in Figure 59. Figure 60 shows corresponding EPNL versus net thrust comparisons. These figures do not show the adjustments that should be made for cycle differences and scale factors.

Time and resources precluded rescaling and reflying the data for the BPR = 8 and 14 nozzles using the scale factors shown in Table 19, but an approximate trend can be extracted as follows. The EPNL for the BPR = 14 data can be first corrected from 0.2 to 0.28 Mach number by assuming that the EPNL varies as the 5$^{th}$ power of $(V_{mix} - V_{amb})$, sort of an average between high- and low-frequency relative velocity dependence. The EPNL correction for Mach number then becomes:

$$\Delta EPNL = 50 \cdot \log_{10}\left[\frac{V_{mix} - 0.28 \cdot c_{amb}}{V_{mix} - 0.20 \cdot c_{amb}}\right] \qquad (3)$$

where $c_{amb}$ = ambient speed of sound. The EPNL values at scale factor (8) can be adjusted for differences in scale factor as follows:

$$EPNL_{SF} = EPNL_{SF=8} + 20 \times \log_{10}[SF/8.0] \qquad (4)$$

where $SF$ = scale factor as listed in Table 19. Using this expression, the EPNL values were corrected by 1.4 EPNdB and 5.3 EPNdB for BPR = 8 and 14, respectively. The resulting EPNL versus $V_{mix}$ trends are shown in Figure 61. Also noted in the figure are the three sizing points that give equal net thrust. Thus, although the noise levels increase monotonically with bypass ratio for a given $V_{mix}$, noise drops significantly with increasing bypass ratio at a given net thrust. This is, of course, a significant reason to consider increasing bypass ratio when new engine designs are contemplated. The scale factors are significantly larger, but the

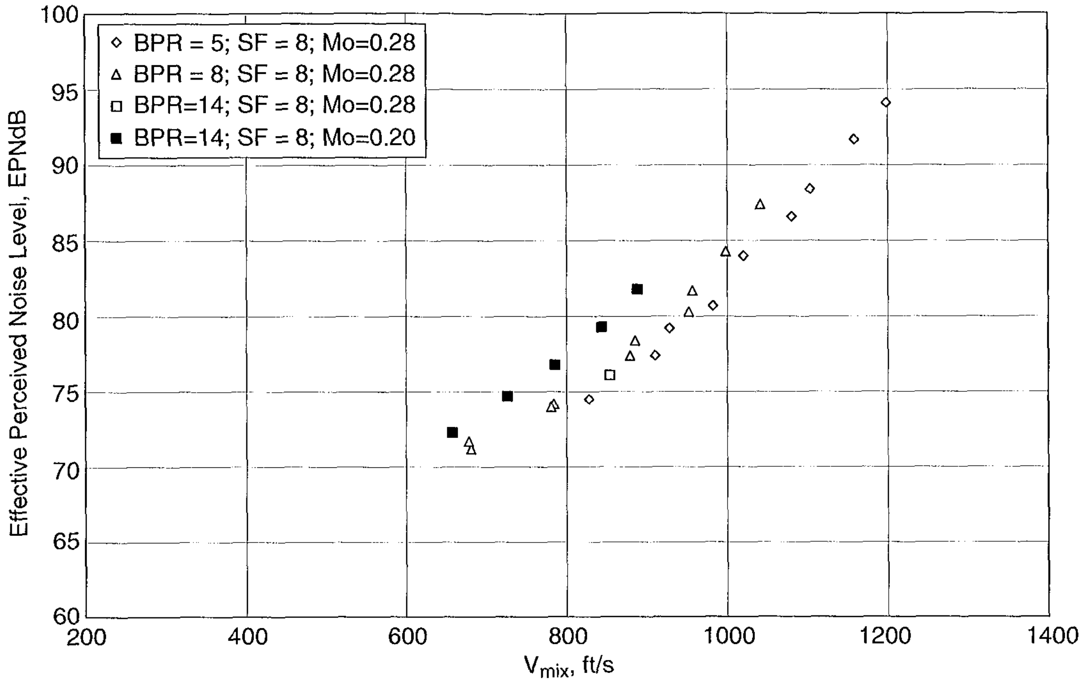


**Figure 59. EPNL as a Function of $V_{mix}$ for External Plug Nozzles: Constant Scale Factor (8)**

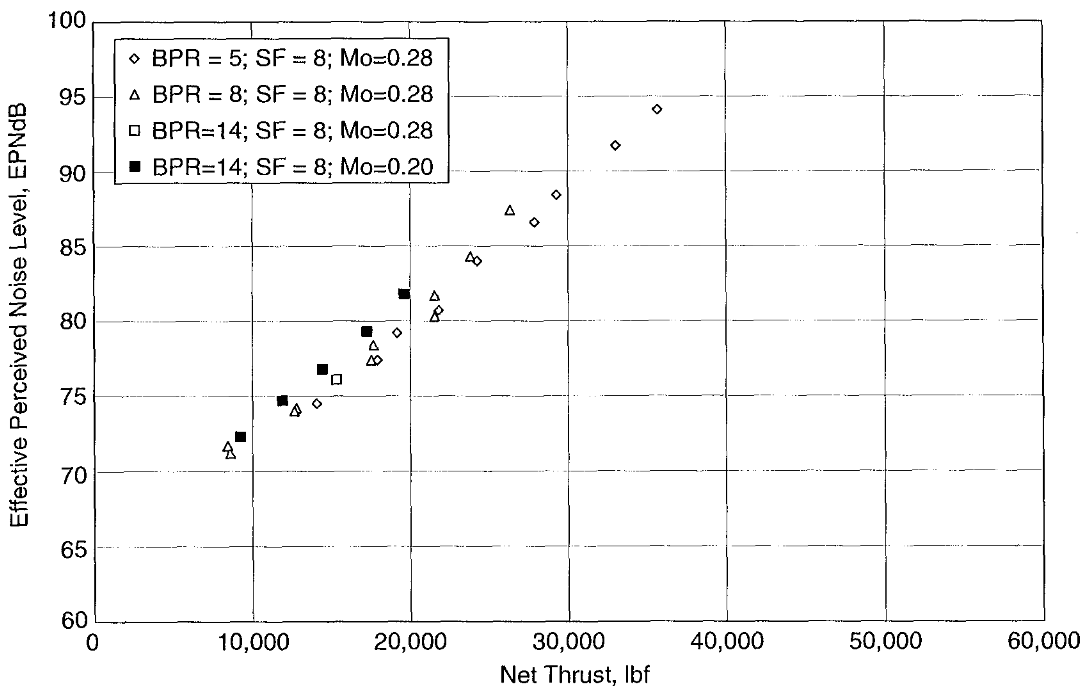


**Figure 60. EPNL as a Function of Net Thrust for External Plug Nozzles: Constant Scale Factor (8)**

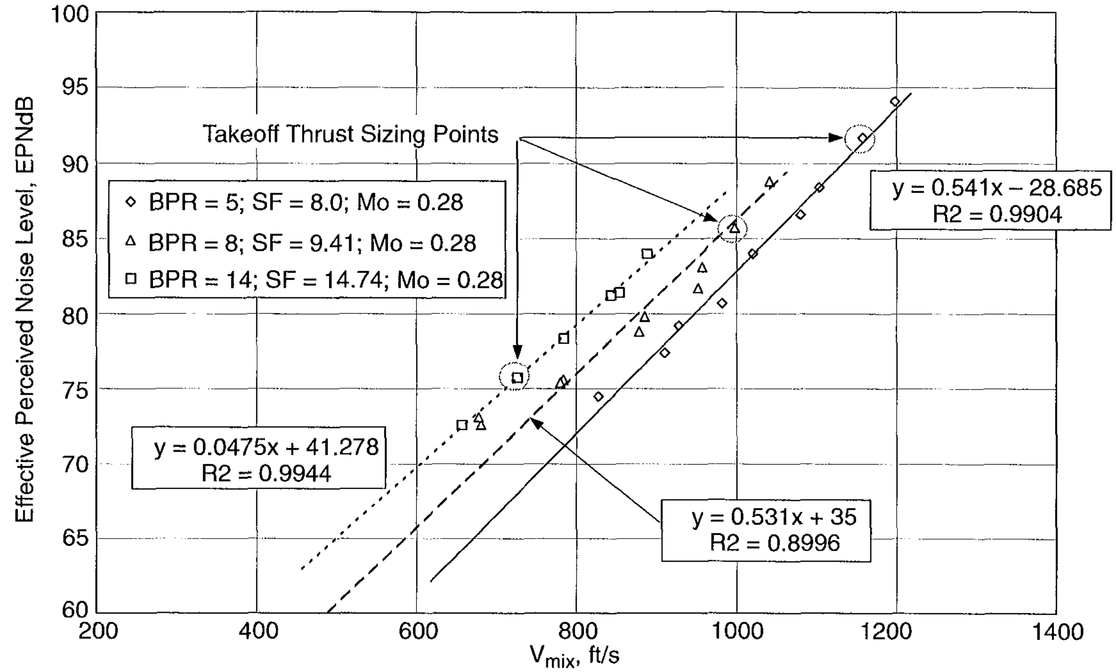


**Figure 61. EPNL as a Function of $V_{mix}$ for External Plug Nozzles: Scale Factor Varied with BPR**

equivalent thrust is achieved at lower values of $V_{mix}$, so jet noise at a given thrust is reduced as the "design" bypass ratio is increased.

Also shown in Figure 61 are linear curve fits of the data trends for the three bypass ratios plotted. The corresponding trends of EPNL versus net thrust are shown in Figure 62, where the dramatic impact of "design" bypass ratio on jet noise is clear. The plots correspond to a prediction based on the curve fits in Figures 58 and 61, and they fit the data trends quite well.

In conclusion, the data obtained in this test program were used to extract a systematic dependency of separate-flow jet noise on bypass ratio. This quantifies, perhaps for the first time, the benefits of increasing engine bypass ratio on jet noise for realistic simulations of engine exhaust systems.

#### 6.1.2.4 Mach Number Variation

It was of interest to evaluate the effect of flight Mach number variation on the noise characteristics of the various baseline nozzles. Some limited data were taken to evaluate this effect, and results of evaluating flight Mach number effects are summarized in Figure 63 for the BPR = 5 external plug baseline (3BB) nozzle. The figure shows variation of peak angle perceived noise level ($PNL_{max}$) for the 3BB nozzle, scaled to full size with a scale factor 8:1, as a function of normalized mixed velocity ($V_{mix}/c_{amb}$). It can be seen that peak jet noise is reduced as flight Mach number increases, on the order of 10 PNdB from static to $M_o = 0.28$, and the reduction is fairly constant over the range of $0.82 < V_{mix}/c_{amb} < 1.09$.

Corresponding PNL directivity trends and SPL spectrum comparisons are shown in Figure 64 for cycle point 21, which corresponds to $V_{mix}/c_{amb} \simeq 1.05$. This figure shows that the flight effect or noise reduction due to forward velocity occurs over the entire measured angle range, although it is greatest at the peak angle (130° to 140°) and becomes smaller at shallow angles, forward and aft. Reduction in SPL is fairly constant over most of the spectrum and doesn't seem to favor high or low frequencies.

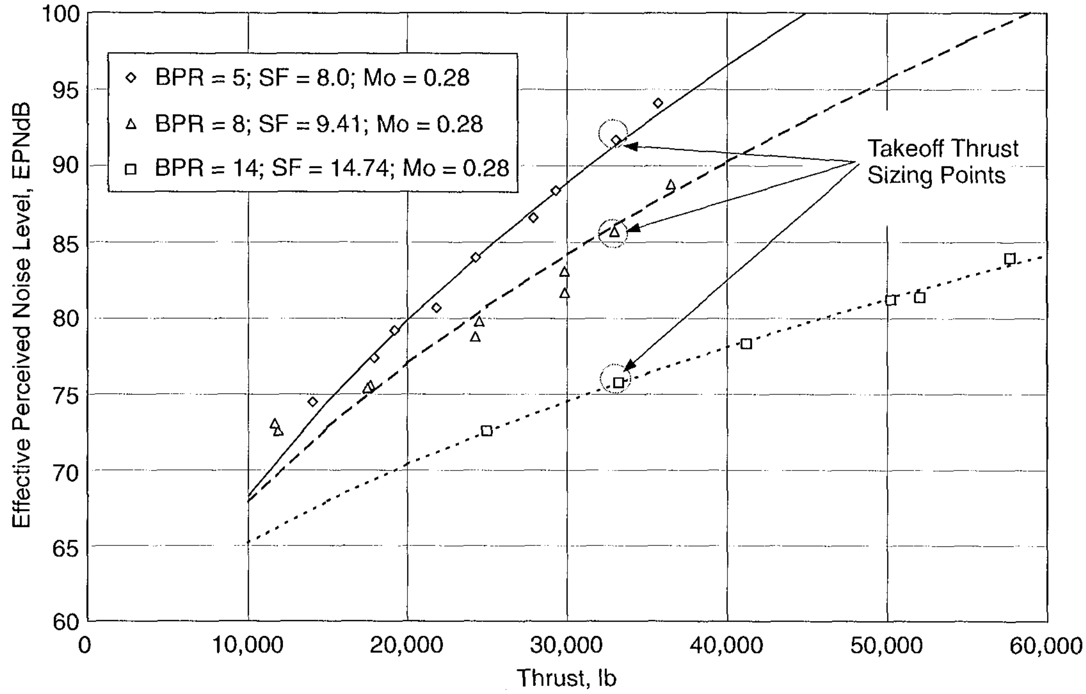


**Figure 62. EPNL as a Function of Net Thrust for External Plug Nozzles: Scale Factor Varied with BPR**

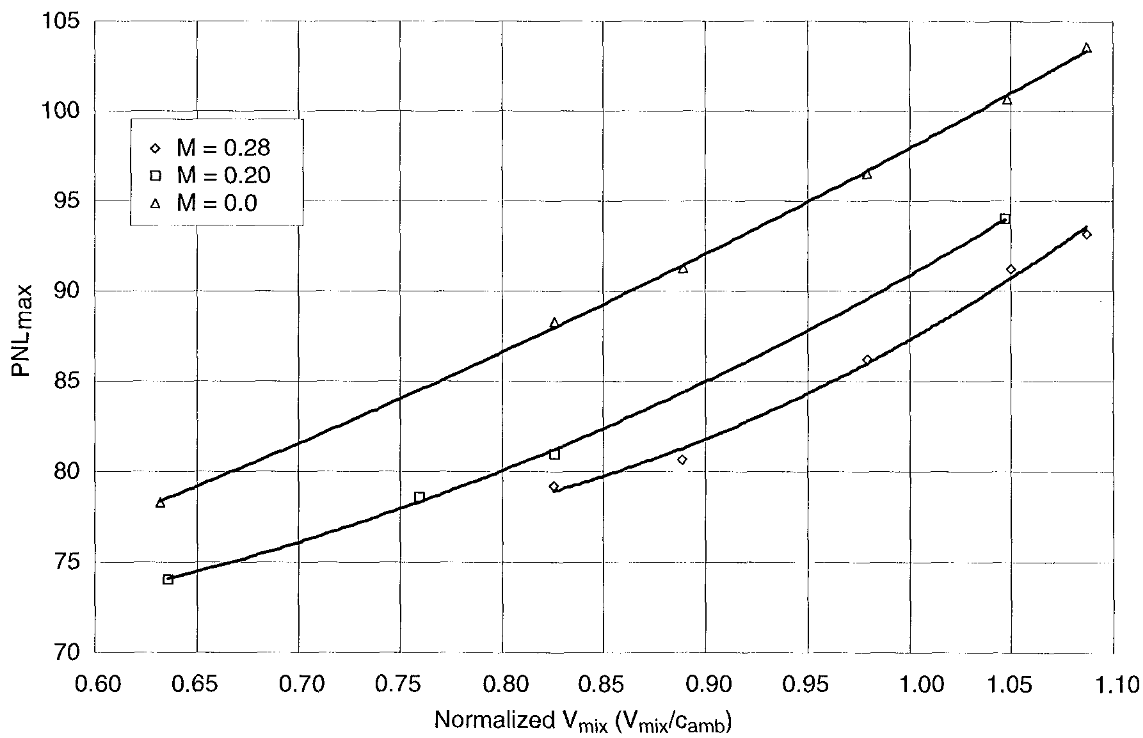


**Figure 63. Effect of Flight on Baseline BPR = 5 Nozzle (3BB), $PNL_{max}$ as a Function of Normalized $V_{mix}$**

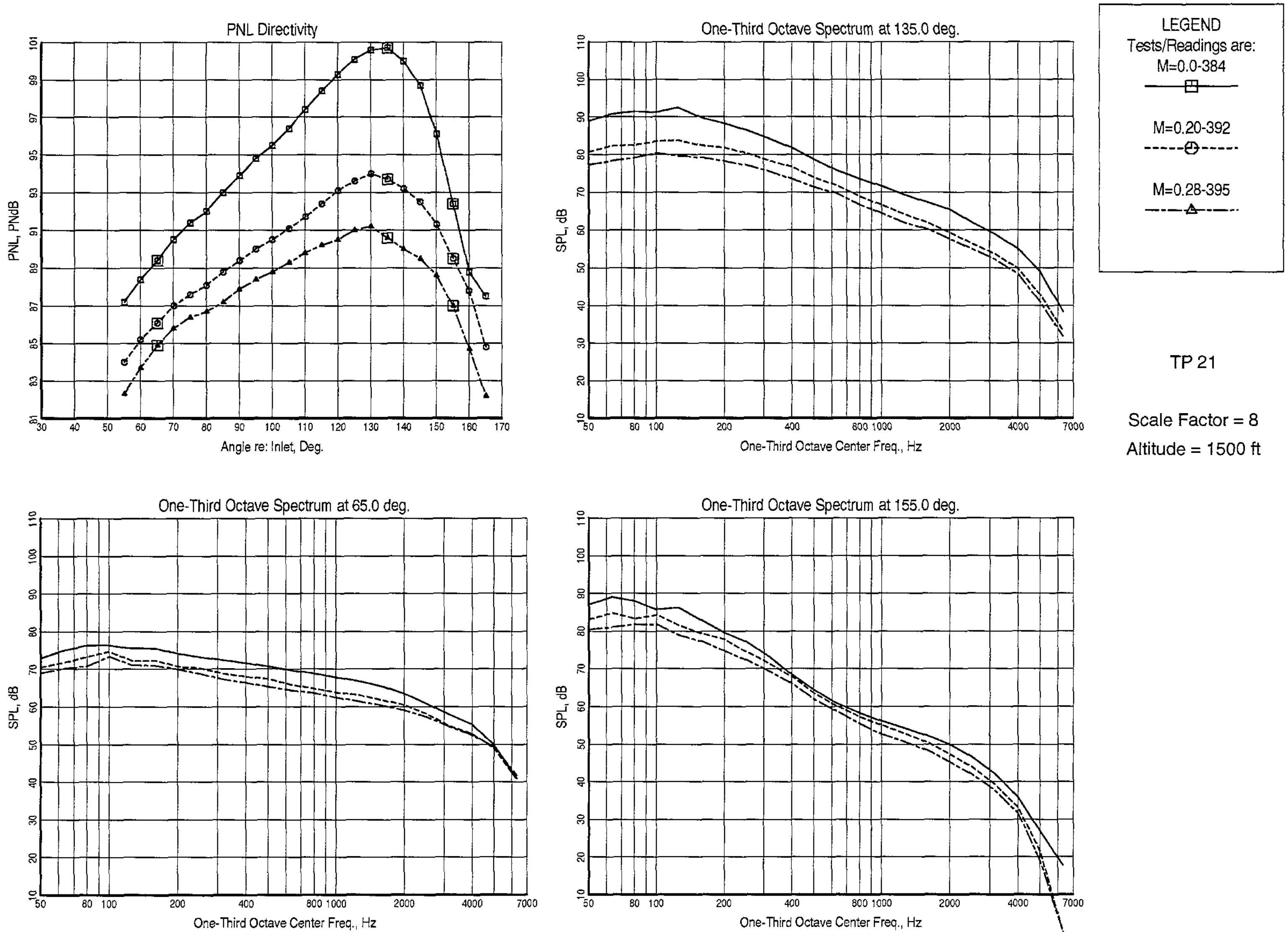


**Figure 64. Effect of Flight on PNL Directivity and SPL Spectra: Baseline BPR = 5 External Plug Nozzle (3BB)**

The corresponding Noy-weighted spectra are shown in Figure 65, and these results indicate the reduction at lower frequencies provide the greatest PNL benefit.

A comparison similar to that in Figure 64 was also done for the BPR = 8 external plug baseline (5BB) nozzle, and this is shown in Figure 66. The cycle data point (32) chosen corresponds to $V_{mix}/c_{amb} \simeq 0.709$. Again, it is observed that noise is substantially reduced over most of the directivity range, but in this case the peak angle changes because the "flight effect" is stronger at angles above 100° to 110° — on the order of 8 PNdB reduction. Also, there is a small but significant bias toward low frequencies; that is, the "flight effect" seems to become greater as frequency is reduced.

The Noy-weighted spectra corresponding to Figure 66 are shown in Figure 67. It can be seen that Noy weighting favors the higher frequencies for this nozzle, especially around the peak PNL angles, about 100° to 120°. For this case, the jet-to-free-stream velocity ratio ($V_{mix}/V_{amb}$) is much smaller (on the order of 2.53) compared with the BPR = 5 nozzle (which had a ratio of 3.75). This difference could be a cause for the better low-frequency noise benefit (compare Figure 64 with Figure 66).

If we assume low-frequency noise is roughly proportional to the relative mixed velocity to some power (say, for example, to the $7^{th}$ power if we assume Lighthill's $8^{th}$ power law but take out one power for equivalent mass flow), then we can postulate that the "flight effect" should reduce low-frequency noise on the order of:

$$\Delta SPL \propto 70 \cdot \log_{10}\left[\frac{V_{mix}-V_{amb}}{V_{mix}}\right] \qquad (5)$$

Substituting values of $V_{mix}/V_{amb}$ given above, the formula would suggest that the flight effect should be about 9.6 dB for the BPR = 5 case and about 15.5 dB for the BPR = 8 case. Examining Figures 64 and 66, we see that the average low-frequency noise reduction is about 10 and 13 dB for the BPR = 5 case and BPR = 8 cases, respectively. This is a reasonable estimate of absolute noise reduction and a good estimate of the difference in flight effects between the two cases. The outcome may be fortuitous, but it certainly indicates that the flight effects are not inconsistent with classical theories of jet noise.

As a final assessment of forward-flight effects, a comparison was made for the BPR = 5 external plug nozzle with the inward-flipped, 12-chevron (3IB), noise-reduction device on the core nozzle (the noise-reduction devices are discussed in Subsection 6.1.3). Figures 68 and 69 show PNL directivity and SPL and Noy-weighted spectra comparisons. Flight effects are again very substantial, about 7 PNdB at the peak angle, and again show more reduction at low frequencies than at high frequencies.

Another observation worth noting is that the noise reduction measured statically is also realized with simulated forward flight. Figure 64 shows a static peak PNL of 100.7 PNdB and a $M_o = 0.28$ flight peak PNL of 91.0 PNdB for the 3BB baseline configuration. The corresponding static and flight peak PNL values for the 3IB chevron configuration are 98.0 and 88.8 PNdB, respectively. Thus the static peak noise reductions are observed to be 2.7 PNdB statically and 2.2 PNdB in flight, suggesting that these mixing-enhancement devices retain much noise-reduction effectiveness in flight.

### 6.1.3 Noise-Reduction Concept Assessment

Acoustic assessments for the GEAE/AEC noise-reduction devices tested in this program were grouped into three categories. Concepts tested on the:

1. Internal plug BPR = 5 Model 2
2. External plug BPR = 5 Model 3
3. External plug BPR = 8 Model 5

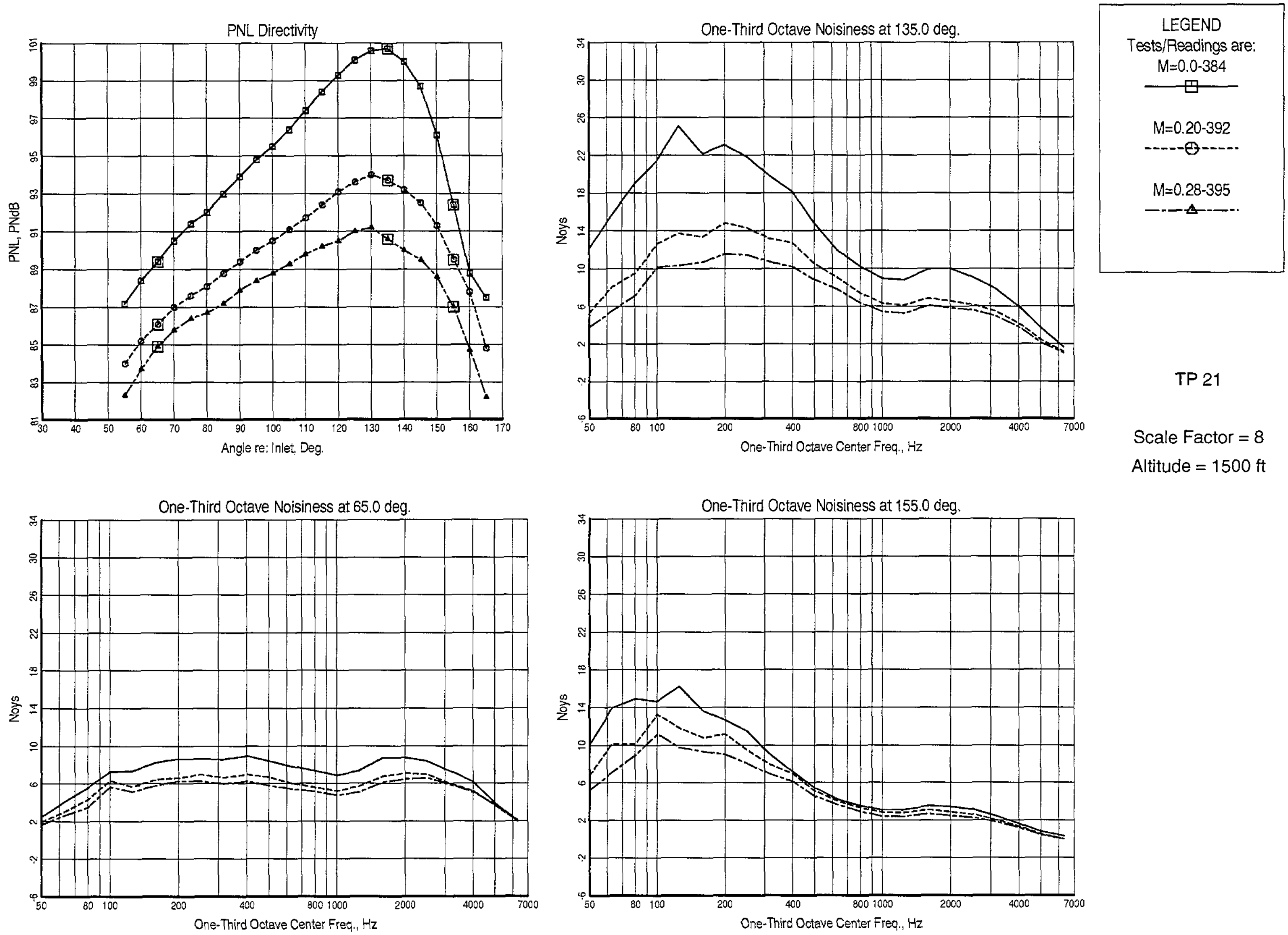


**Figure 65. Effect of Flight on PNL Directivity and Noy Spectra: Baseline BPR = 5 External Plug Nozzle (3BB)**

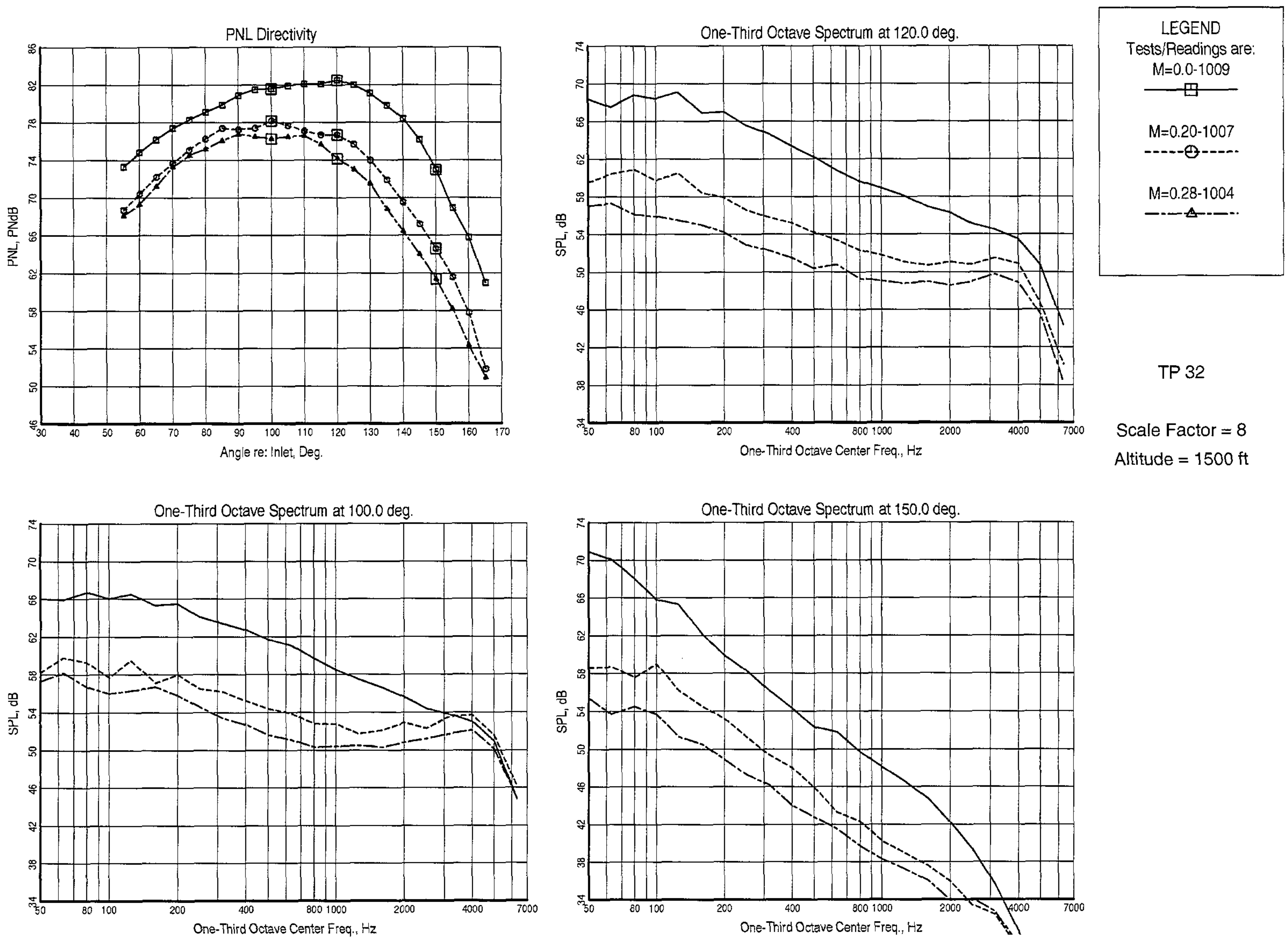


**Figure 66. Effect of Flight on PNL Directivity and SPL Spectra: Baseline BPR = 8 External Plug Nozzle (5BB)**

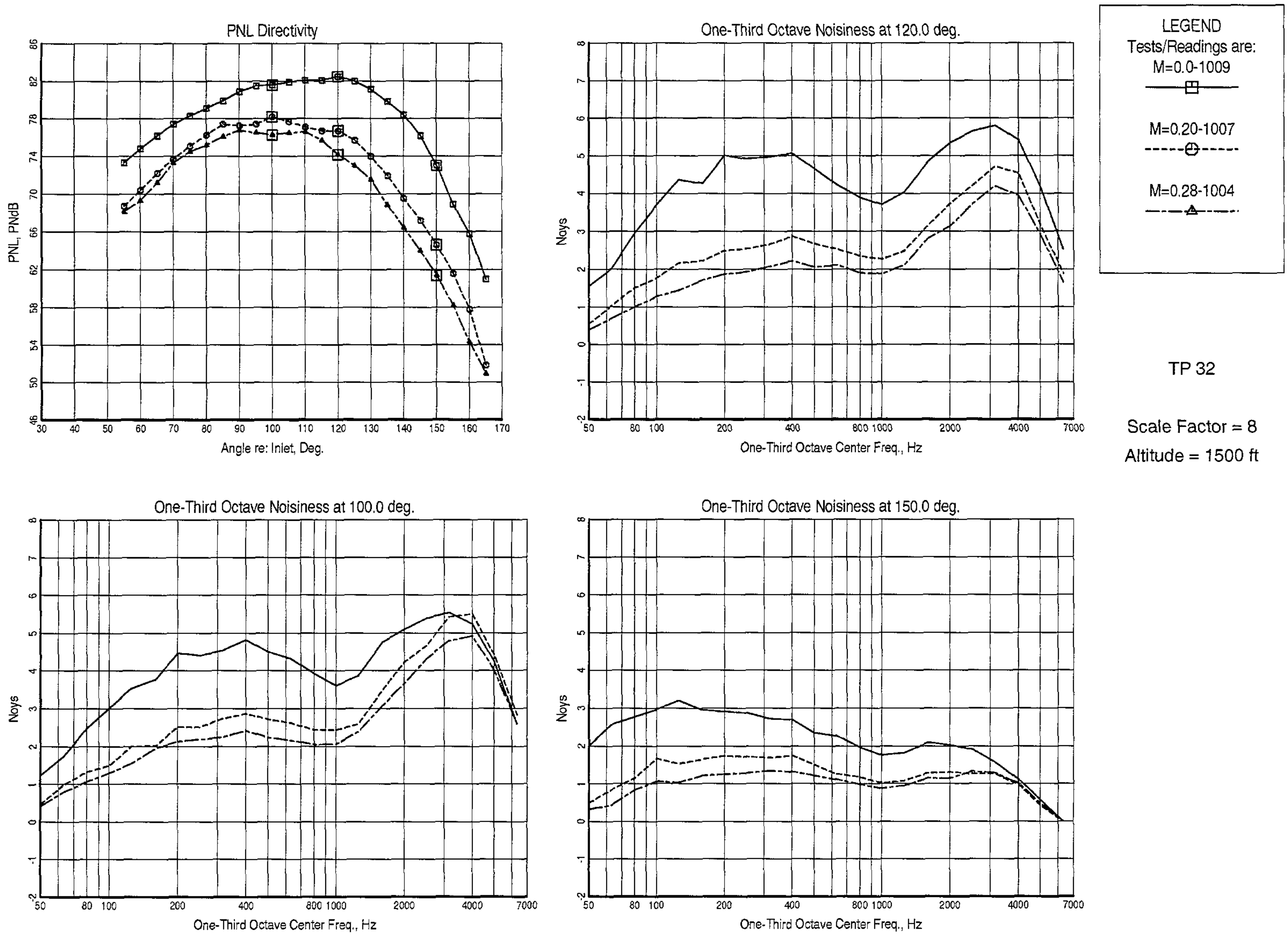


**Figure 67. Effect of Flight on PNL Directivity and Noy Spectra: Baseline BPR = 8 External Plug Nozzle (5BB)**

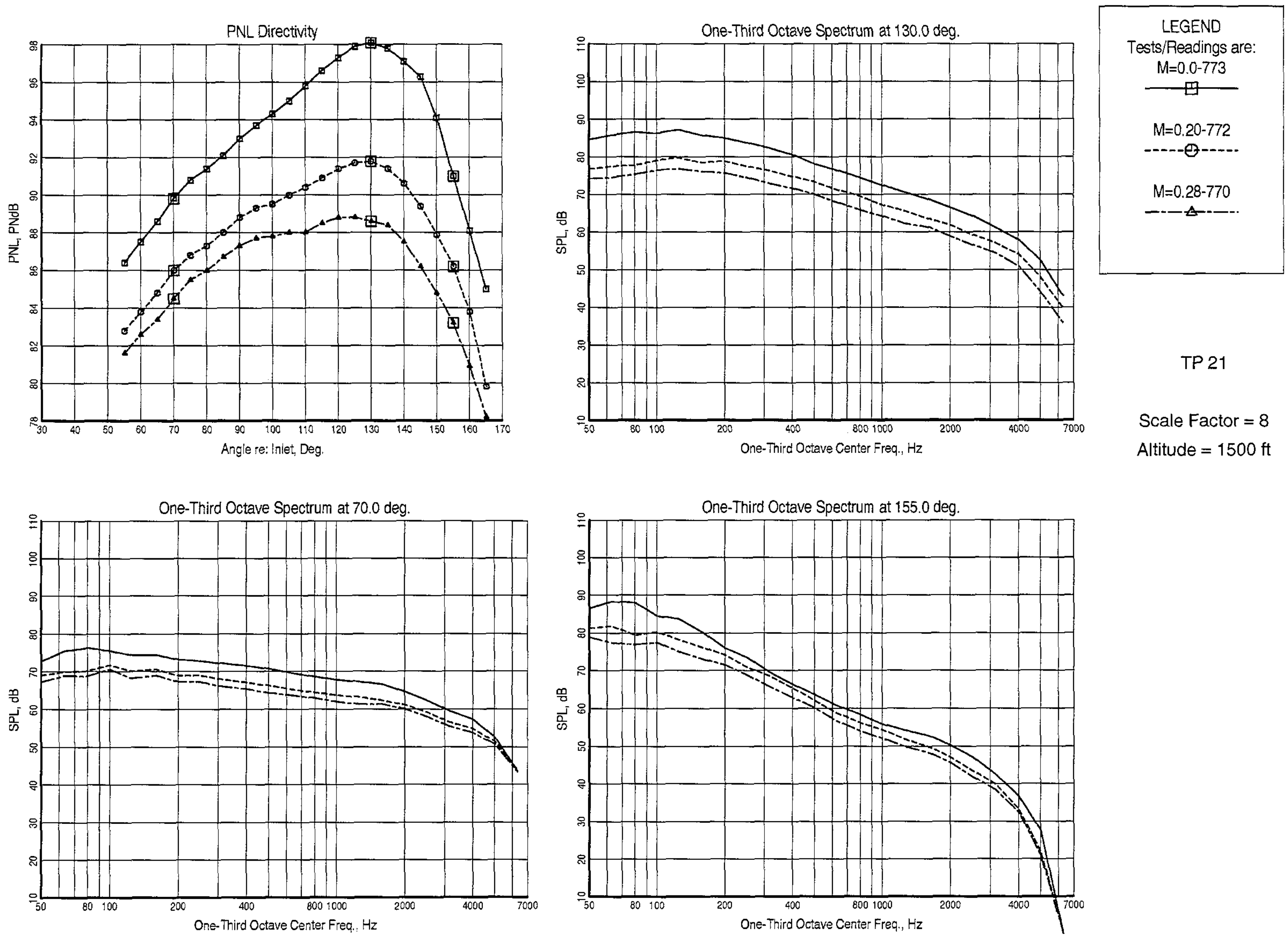


Figure 68. Effect of Flight on PNL Directivity and SPL Spectra: BPR = 5 External Plug Nozzle with Core Chevrons (3IB)

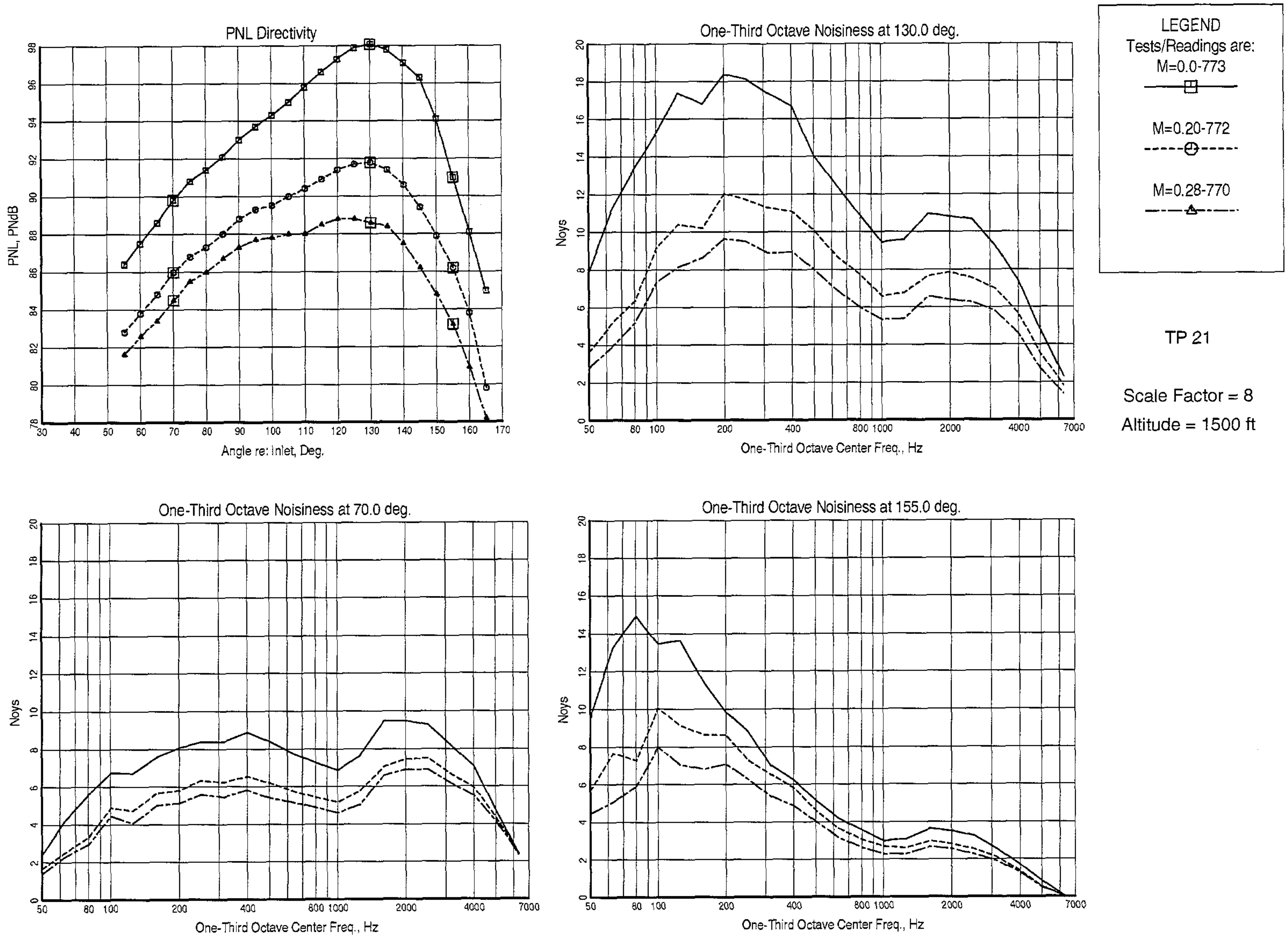


**Figure 69. Effect of Flight on PNL Directivity and Noy Spectra: BPR = 5 External Plug Nozzle with Core Chevrons (3IB)**

The results for the the three groupings are discussed in the following subsections.

#### 6.1.3.1 Internal Plug BPR=5 Configurations

The baseline internal plug BPR = 5 configuration (Model 2, shown in Figure 11) is composed of a fan nozzle with a nominal hot throat area of 28.94 $in^2$, a core nozzle of nominal hot throat area of 11.19 $in^2$, and an internal core plug. Acoustic farfield data were obtained on the Cycle 2 operating line (Table 10) for this baseline configuration at several simulated aircraft forward velocities. Four noise-reduction devices were selected for testing on this model: two fan nozzle concepts and two core nozzle concepts. The core nozzle concepts included chevrons and a unique variation on the traditional forced mixer referred to as the "tongue mixer." The fan nozzle concepts included chevrons and tandem triangular vortex generators referred to as "doublets." A physical description of each of these concepts is provided in Section 4.2. All acoustic data presented in this section have been scaled to represent a full-size engine with a fan stream throat area of 1852 $in^2$ and a core stream throat area of 716.2 $in^2$. This corresponds to a scale factor of 8 relative to the scale-model size.

For the test point representative of thrust levels at the sideline certification condition, the maximum variation in mass flow observed with the introduction of chevrons was 1.5% for the fan stream and 5% for the core stream, relative to the baseline nozzles. The doublet vortex generators produced virtually no change in operating conditions. For the tongue mixer as originally configured, core flow rate at each of the test conditions were substantially higher than for any of the other configurations. For example, for cycle point 21 it was 42% higher than the baseline nozzle, at a free-jet Mach number of 0.28. As a result, bypass ratio fell substantially below design intent — from 5.23 to 3.64 for the above condition. This also resulted in substantially higher thrust levels at a given operating point, 9.2% higher for the above condition.

In an attempt to move the operating characteristics of the tongue mixer concept closer to the baseline, a longer core plug was fabricated. The cylindrical section of this plug was the same diameter and maintained the same taper profile as the original. The length was increased such that the constant radius cylindrical section extended to the end of the tongue segments. This produced the maximum reduction in core flow area possible without changing the mixer chutes. The resulting configuration, designated Model 6, is shown in Figure 19. Test data show that the increased blockage due to the extended plug reduced the core mass flow rate but not quite to the extent desired. The final bypass ratio of Model 6 was 4.55 at the sideline condition, as compared to 5.15 for the baseline model at the same primary and secondary nozzle pressure ratios. This difference must be considered in interpreting the acoustic results.

##### 6.1.3.1.1 Core Nozzle Concepts

The following core nozzle noise-reduction devices were tested on the BPR = 5 internal plug nozzle:

1. Configuration 2C12B, 12-chevron core nozzle (see page 163 in Appendix A of this report)
2. Configuration 2TmB, tongue mixer core nozzle with short core plug (page 164)
3. Configuration 6TmB, tongue mixer core nozzle with extended core plug (page 196)

The normalized EPNL of 2C12B, 2TmB, 6TmB and the baseline 2BB configurations, as a function of normalized $V_{mix}$ for the $M_o = 0.28$ forward-flight-simulation condition, are presented in Figure 70. The results show a maximum noise benefit of 1 EPNdB, for any of the

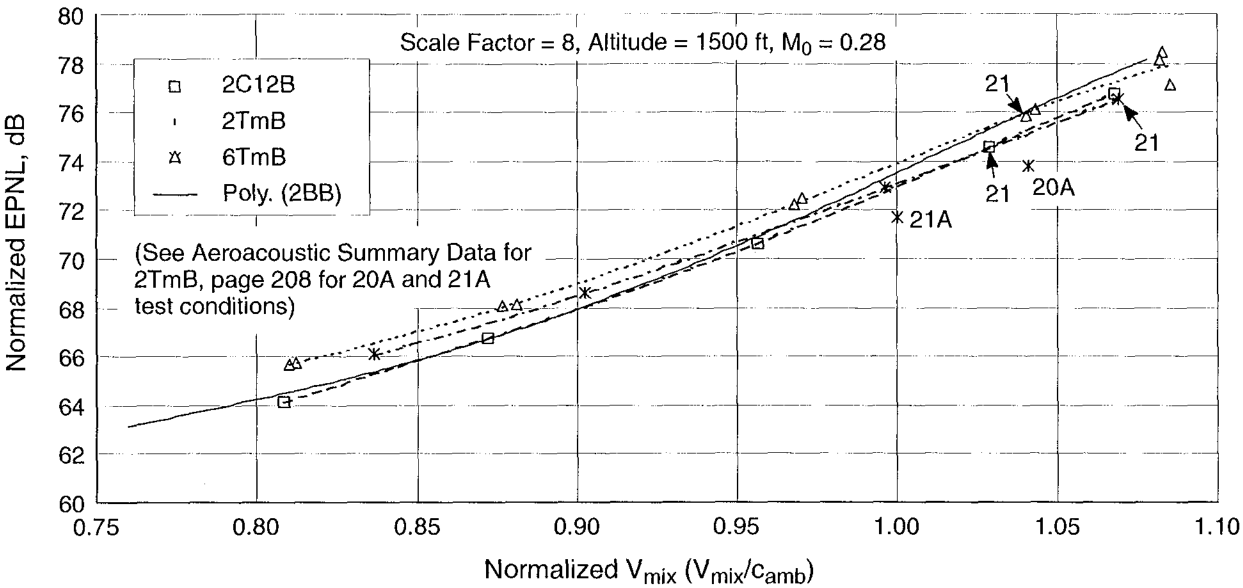


**Figure 70. Normalized EPNL Variation with Normalized $V_{mix}$: Baseline BPR = 5 Nozzle with Internal Plug (2BB); with Chevron and Tongue Mixer on Core Nozzle (2C12B, 2TmB, and 6TmB)**

core nozzle devices, relative to the baseline. The chevron concept was effective over the largest range of operating conditions ($V_{mix}$). For values of normalized $V_{mix}$ less than 0.95, the chevrons produced essentially the same farfield noise levels as the baseline nozzle. As normalized $V_{mix}$ increased beyond 0.95, the chevrons reduced noise compared to the baseline. The chevrons produced little or no noise reduction at typical approach or cutback conditions (cycle point 23, $V_{mix}/c_{amb} < 0.88$) and about 0.8 dB at a typical sideline condition (cycle point 21, $V_{mix}/c_{amb} = 1.034$).

Both the original tongue mixer configuration with the short internal plug (2TmB) and the modified tongue mixer configuration with the longer plug (6TmB) are significantly louder than the baseline nozzle at lower values of normalized $V_{mix}$. As normalized $V_{mix}$ is increased above 0.95, configuration 6TmB approaches the baseline results. However, configuration 2TmB shows noise reduction trends very similar to those of the chevron configuration. That result was unexpected because 2TmB produced a significantly lower bypass ratio than any of the other configurations. This behavior is related to the different operating conditions of the configuration, which are highlighted when $V_{mix}$ is referenced to the nozzle operating conditions that produced it. Figure 70 for cycle point 21 shows that, for fixed nozzle inlet conditions, configuration 2TmB is the loudest, but normalized mixed velocity is also highest for 2TmB.

The above observation is further demonstrated when EPNL is displayed as a function of ideal net thrust (defined as ideal gross separate-flow thrust minus the ram drag due to the total inlet mass flow at free-jet speed), as presented in Figure 71. In this figure, net thrust is also normalized to reference standard-day conditions by using the factor $\delta = P_{amb}/P_{ref}$ where $P_{amb}$ is the test-day condition and $P_{ref}$ is sea level standard pressure (14.696 psia).

It is noted that the increase in noise level with thrust is lower for tongue mixer configuration 2TmB than for any of the other configurations. This result can be traced back to the higher core-flow discharge coefficient, $C_{D8}$, of this configuration, which allows a required level of

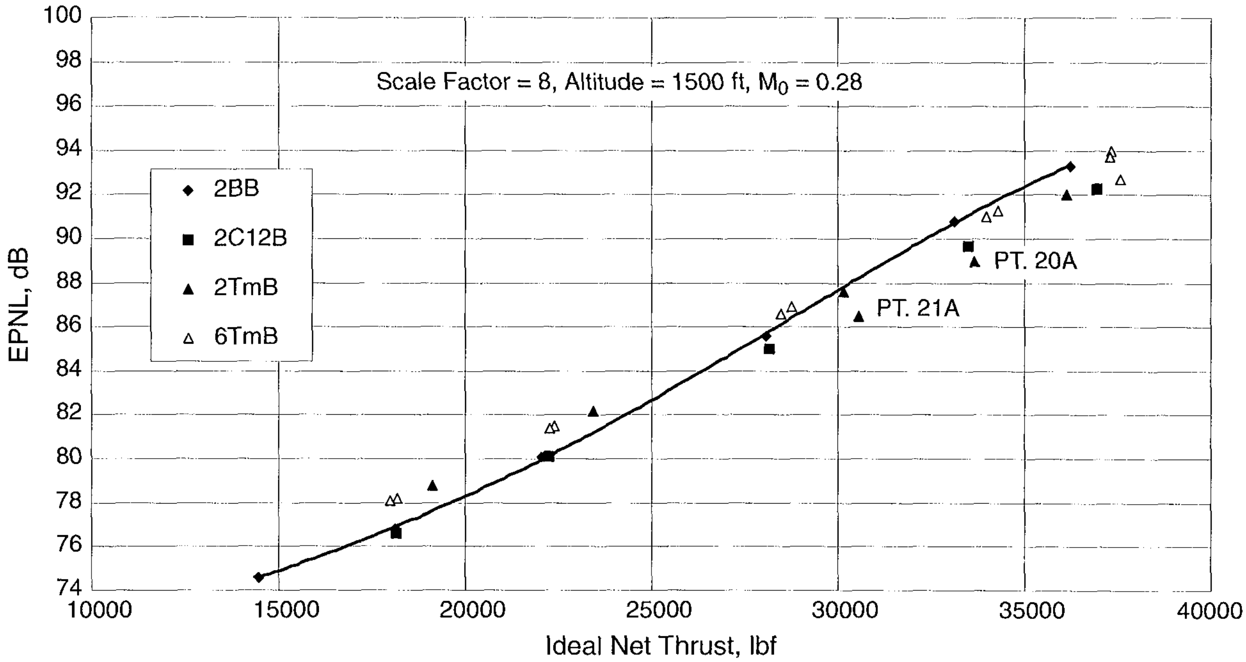


**Figure 71. EPNL Variation with Net Thrust: Baseline BPR = 5 Nozzle with Internal Plug (2BB); with Chevron and Tongue Mixer on Core Nozzle (2C12B, 2TmB, and 6TmB)**

thrust to be achieved at lower core nozzle pressure ratios (see summary tables in Appendix B for $C_{D8}$ values). However, the tongue mixer has significantly lower core jet velocity for the same thrust, so the noise reduction is due in major part to the reduced $V_{mix}$ at the same thrust.

For diagnostic purposes, two additional operating conditions, labeled cycle points 21A and 20A, were run only for this configuration. For these operating conditions, fan nozzle pressure ratio (NPR) was set to the values typical of cycle points 21 and 20, while core NPR was reduced at fixed temperature until the bypass ratio of the original cycle points was matched. The EPNL values associated with points 20A and 21A were below all the other data at the corresponding thrusts. The reduction in core nozzle pressure ratio required to generate a given thrust, resulting from the higher discharge coefficient of the tongue mixer, is controlling the noise signature. Configuration 6TmB, with the extended plug to reduce the core nozzle area, required a higher core NPR to reach a specified thrust, giving higher core velocity and hence higher noise levels than 2TmB.

EPNL is a complex, nonlinear function of the spectral content, level, and directivity of the radiated sound field. In particular, PNL is an overall metric calculated on a spectrally weighted basis. The sound power spectrum (PWL) is useful for comparing the overall source characteristics of different configurations. A comparison of the sound power spectrum of the four core nozzle configurations tested on Model 2 is presented in Figure 72 for cycle point 21, which corresponds to a typical sideline certification condition. For the chosen scale factor of 8:1, the baseline nozzle sound power level (PWL) spectrum data in Figure 72 have a broad peak in the 1/3-octave bands between 80 and 125 Hz. Away from the peak, the level drops off at approximately 1 dB per band up to 3.15 kHz. Above 3.15 kHz, there an increase is indicated, but this may be an artifact

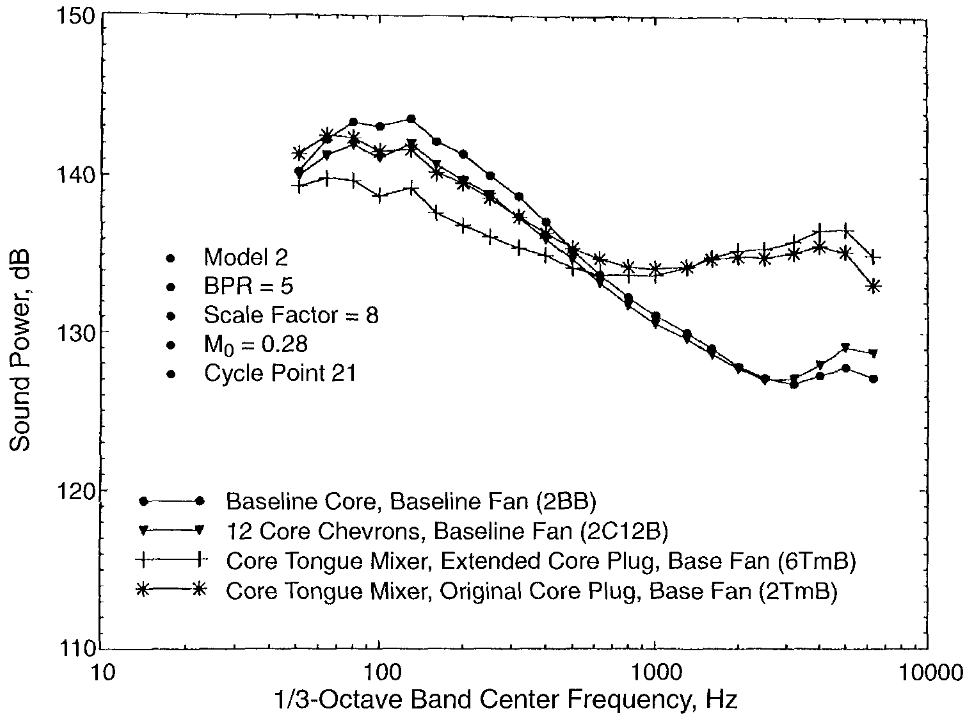


**Figure 72. Comparison of SPL for Core Nozzle Mixing Enhancers (2BB, 2C12B, 2TmB, and 6TmB)**

of the scaling process due to large atmospheric absorption corrections required at the corresponding very high model-scale frequencies (above 25 kHz).

Fisher, Preston, and Bryce (Reference 28) have shown that, for a secondary-to-primary velocity ratio less than 1.0, the jet-mixing noise levels of coplanar, coannular nozzles are controlled by that portion of the plume downstream of the end of the secondary flow potential core. Further, at the velocity ratio represented by the condition selected from the current test (0.7), the data in Reference 28 suggest that the peak levels are controlled by the fully mixed region of the plume, which lies downstream of the primary nozzle potential core. Although the noise-generation source strength per unit length of jet plume in this region is not as great as near the nozzle exit plane, an identifiable velocity profile persists many diameters downstream from the end of the primary potential core. Based on Strouhal number and "slice of jet" source location arguments, this region of the plume — with large turbulent-eddy length scales — will primarily contribute to the low-frequency portion of the resulting PWL spectrum.

It can be speculated that if the rate of decay of the downstream jet plume can be accelerated without significantly altering the source density, or if the jet exit velocity itself is reduced, then low-frequency noise should be reduced. In fact, introduction of the chevron core nozzle produces a modest reduction in sound power levels in the low-frequency spectrum (below 1 kHz), with virtually no change from the baseline at the higher frequencies. Plume survey data obtained with chevron configurations on Model 3 (to be discussed in a later subsection) showed indications of the formation of fairly weak vortices from each of the chevrons. Further downstream, the vortices can no longer be identified, but the measured velocity profile was observed to be more uniform than the baseline, as shown by a smaller diameter centerline hot streak. Acoustically, this mixing enhances the decay of the fully mixed region of the plume by reducing the "fully merged" velocity levels, thus reducing noise emission from this region.

Fisher et al. (Reference 28) demonstrated that a second important "interaction region" responsible for acoustic radiation in coannular nozzle systems is the region between the ends of secondary and primary potential core, where the two shear layers from the two nozzle edges interact and the turbulent-eddy length scales are smaller than they are further downstream. The strength and spectral characteristics of this region scale with the primary jet velocity, resulting in contributions to the higher frequency bands. If vortex-induced mixing increases turbulence in this interaction region, a shift in the spectral peak toward higher frequencies and an increase in level at this peak can be expected. This was not clearly observed with the chevron nozzle. From these observations it can be inferred that the vorticity introduced by the chevrons is strong enough to reduce the overall length of the jet plume but not strong enough to significantly increase turbulence in the interaction zone. Rather, it is speculated that the chevrons produce large-scale, longitudinal vortices that, as they roll up and convect downstream, entrain fan stream flow into the core stream and core stream flow into the fan stream, effectively increasing the mixing perimeter between the two streams.

For the tongue mixer configurations, a reduction in the low-frequency portion of the sound power spectrum relative to the baseline is shown in Figure 72. However, the extended plug (6TmB) produced the largest decrease. This trend was offset by a major increase in the spectral levels above 1 kHz. The effectiveness of the tongues in reducing the low-frequency noise is strongly influenced by free-jet Mach number, with maximum suppression observed at static (no free-jet velocity) conditions, compared to the baseline nozzle.

An example of the effect of free-jet speed on the acoustic power spectrum is given in Figure 73 for the 6TmB tongue mixer. Sensitivity to forward-flight speed is typical of noise generated in the fully mixed region of the flow, supporting the conclusion that the low-frequency suppression provided by the tongue mixer is a result of enhanced decay of the far-downstream plume. It can also be inferred that the tongue mixer produces higher turbulence near the nozzle exit, increasing high-frequency noise in the PWL spectra. It is also possible that there is unsteady lift on the tongue trailing edges, due to vortex shedding. If this does occur, it would explain why the high-frequency noise is relatively insensitive to free-jet Mach number. Such a nonconvecting source doesn't realize the benefit of reduced convective amplification with increasing flight speed.

It is hypothesized that low-frequency noise is reduced through more rapid mixing of the hot and cold streams, as a result of the formation of counterrotating streamwise-vortex pairs downstream of the tongues. Figure 72 shows that the extended-plug tongue mixer (6TmB) produces a larger suppression of the low-frequency spectrum compared to the original tongue mixer configuration (2TmB). One plausible explanation is that the extended plug in the 6TmB mixer forces core flow in the tongue region to be more axial and less radially converging towards the centerline relative to the 2TmB mixer. This could lead to stronger streamwise vorticity in 6TmB than in 2TmB, resulting in more rapid mixing and consequently more rapid decay of the plume in 6TmB. Also the percent of core flow that participates in mixing due to streamwise vorticity produced by the tongues will be larger in 6TmB than that in 2TmB due to the constraint of the extended plug, in spite of the reduced core-flow rate for

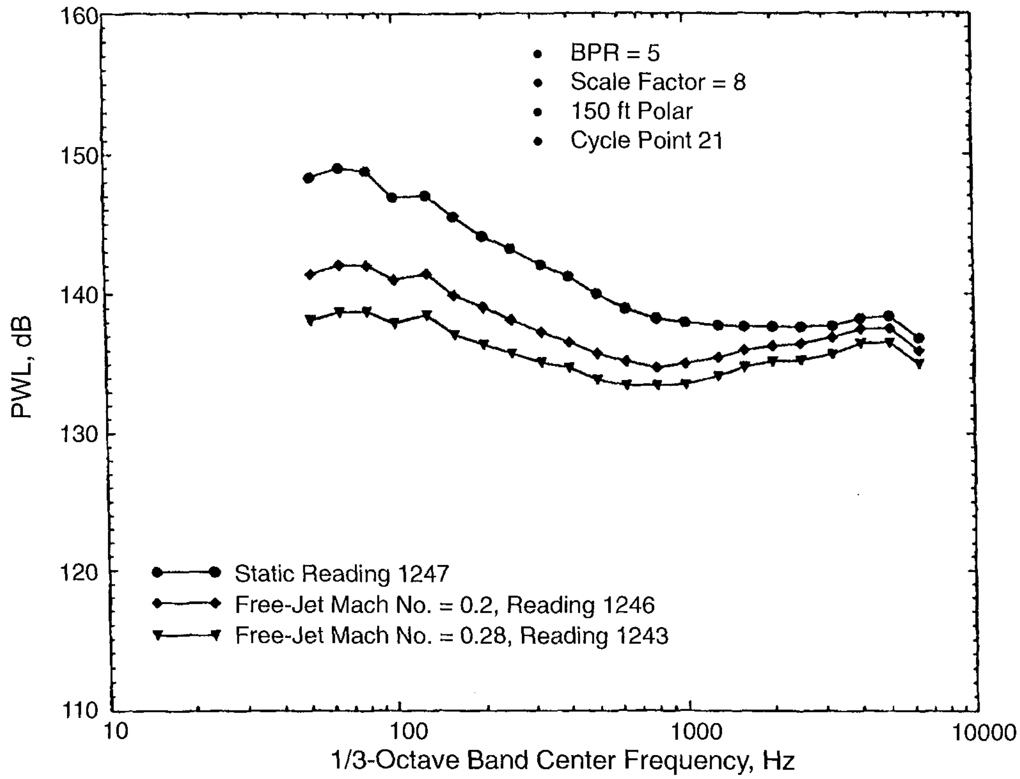


**Figure 73. Effect of Free-Jet Mach Number on Sound Power Spectrum of Core Tongue Mixer with Extended Plug (6TmB)**

6TmB mixer. This too can possibly lead to stronger streamwise vorticity and faster plume decay. Alternatively, the 6TmB mixer core flow, being smaller than for the 2TmB mixer, may cause the core velocity to decay more rapidly, since the tongue size is a larger portion of the core annulus height.

While the sound power spectrum gives a useful overall picture of the source characteristics of a sound field, the Noy-weighting of the sound pressure level spectra and the corresponding directivity determine the EPNL. The PNL variation with emission angle for a 1500-ft-altitude level flyover is presented in Figure 74. Note the SPL spectra at peak PNL emission angle and at 90°. The peak noise level of the baseline nozzle (2BB) occurs at an emission angle of 130° and is associated with a dominant frequency range of 100 to 200 Hz. The addition of chevrons to the core nozzle (2C12B) reduces peak PNL approximately 1.5 dB with no significant change in PNL directivity pattern compared to the baseline configuration.

Comparing the spectra of the baseline and core chevron nozzles at the peak PNL angle of 130°, the chevrons are observed to reduce SPL at frequencies below 400 Hz. At higher frequencies, the spectral change is minimal. These observations are consistent with the sound power results discussed earlier and support the conclusion that the chevrons produce a longitudinal vortex entrainment effect that enhances decay of the fully developed segment of the plume without generating the intense turbulence near the nozzle exit associated with elevated high-frequency content.

The two tongue mixers produced significantly higher high-frequency noise, as indicated in Figure 74, at 90° and 110°, resulting in a 3 dB higher peak PNL and a shift in peak PNL angle

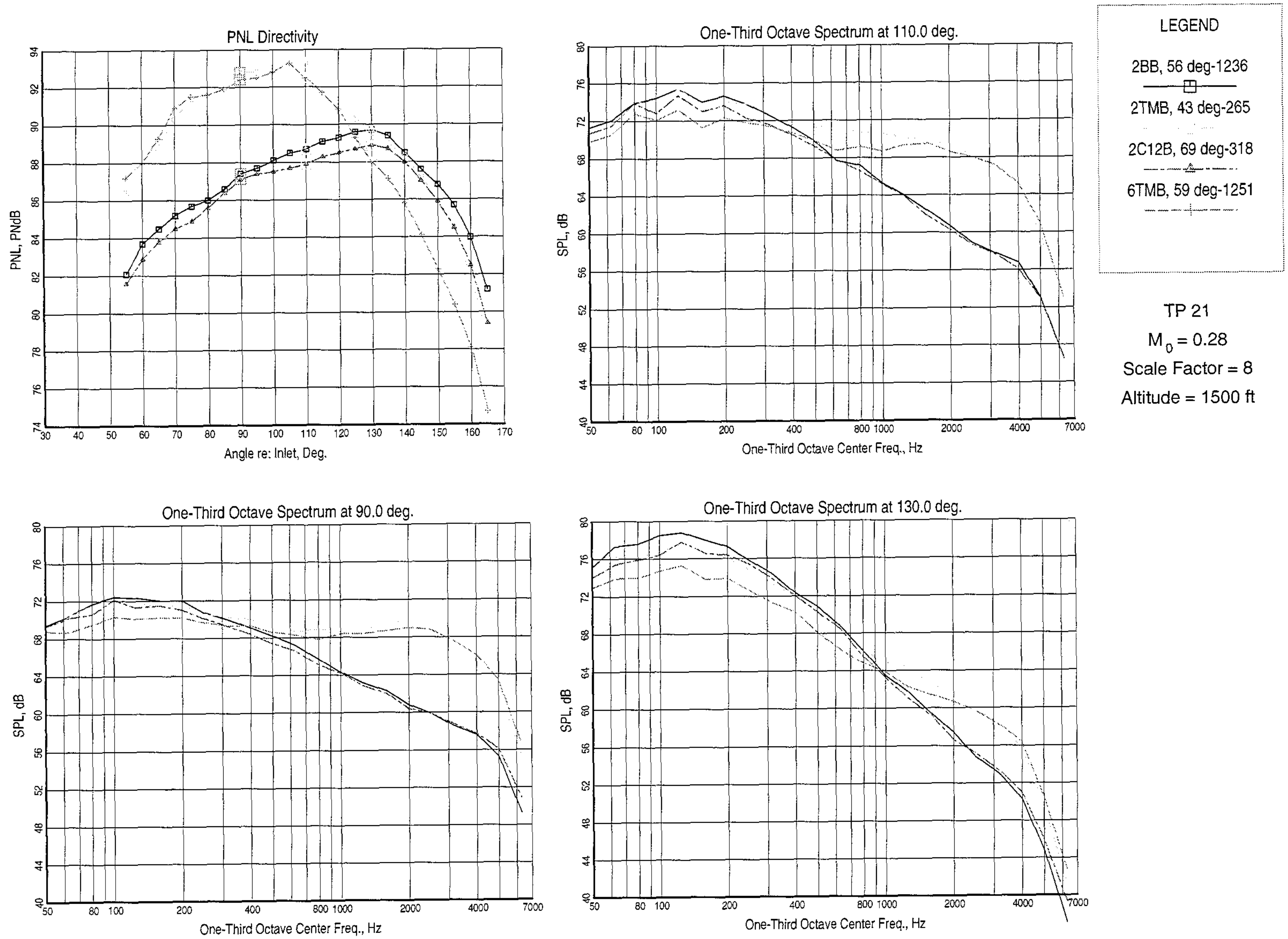


**Figure 74. PNL Directivity and SPL Spectra: Baseline BPR = 5 Nozzle with Internal Plug (2BB); with Chevrons and Tongue Mixer on Core Nozzle (2C12B, 2TmB, and 6TmB)**

from 130° to 105° – 110°. The configuration with the extended core plug (6TmB) is the most effective of all devices tested in reducing the classical low-frequency mixing noise, but it produced significant increases in spectral levels for higher frequencies. The 150-ft-arc overall sound pressure levels (OASPL) directivity of all four configurations are shown in Figure 75. The directivity patterns are very similar, suggesting that the directionality of the total acoustic energy is not materially altered by the mixing devices,but rather the frequency content (lower low-frequency noise and higher high-frequency noise) is the dominant change that impacts EPNL.

The corresponding Noy-weighted spectra are shown in Figure 76. At the 110° (peak noise) angle, the peak SPL for the mixer configurations (see Figure 74) is in the same frequency band, approximately 125 Hz, as the baseline nozzle, and the levels in the 2- to 3.15-kHz bands are 5 to 16 dB below the peak, depending on the mixing concept. However, the Noy-weighted spectra for these same configurations is dominated by the 2- to 3.15-kHz bands, and the tongue mixers apparently create the highest noise levels in the frequencies of highest Noy-weighting. Consequently, these results are sensitive to the chosen scale factor. For smaller scale factors, the SPL spectra will shift to higher frequency bands for all angles. The combination of: (a) moving the high-frequency noise increase out of the range of highest Noy weighting and (b) the additional atmospheric absorption at these higher frequencies reduces the noise increase caused by the tongue mixers and could even result in an EPNL reduction.

In summary, the mixing devices applied to the core nozzle for Model 2 produced a maximum EPNL reduction of 1 dB at operating conditions

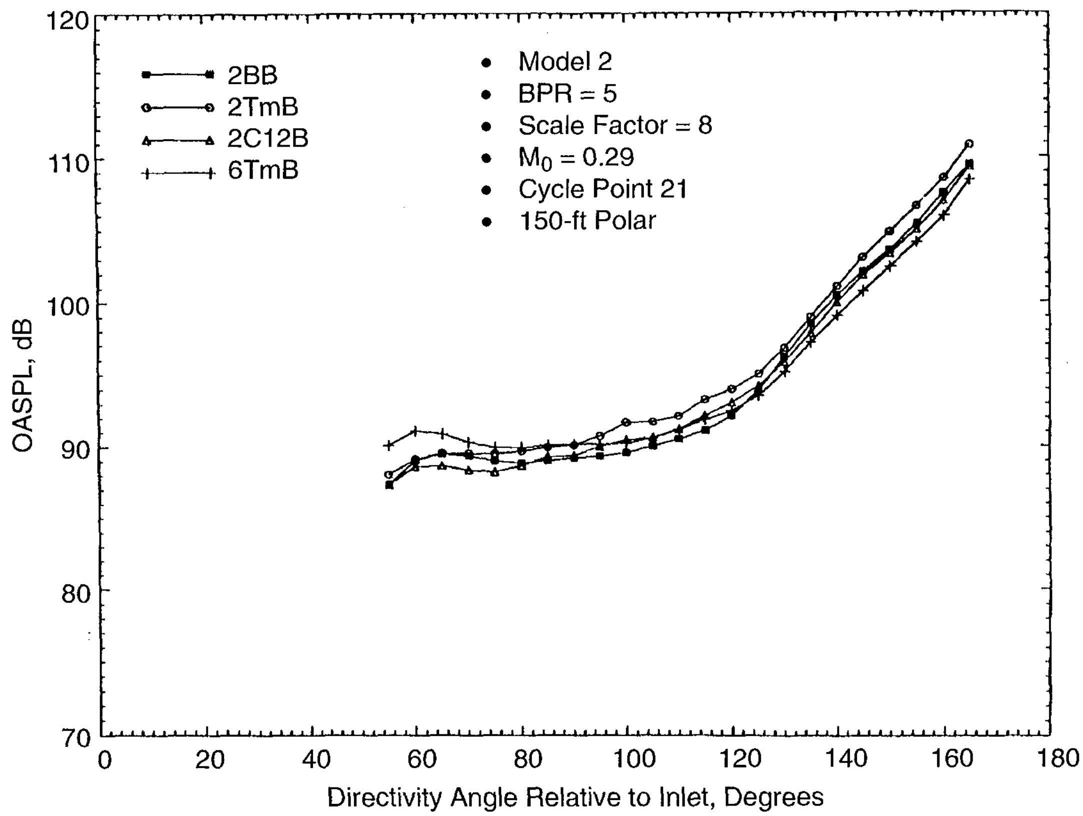


**Figure 75. Comparison of OASPL Directivity for Core Nozzle Mixing Enhancers (2BB, 2C12B, 2TmB, and 6TmB)**

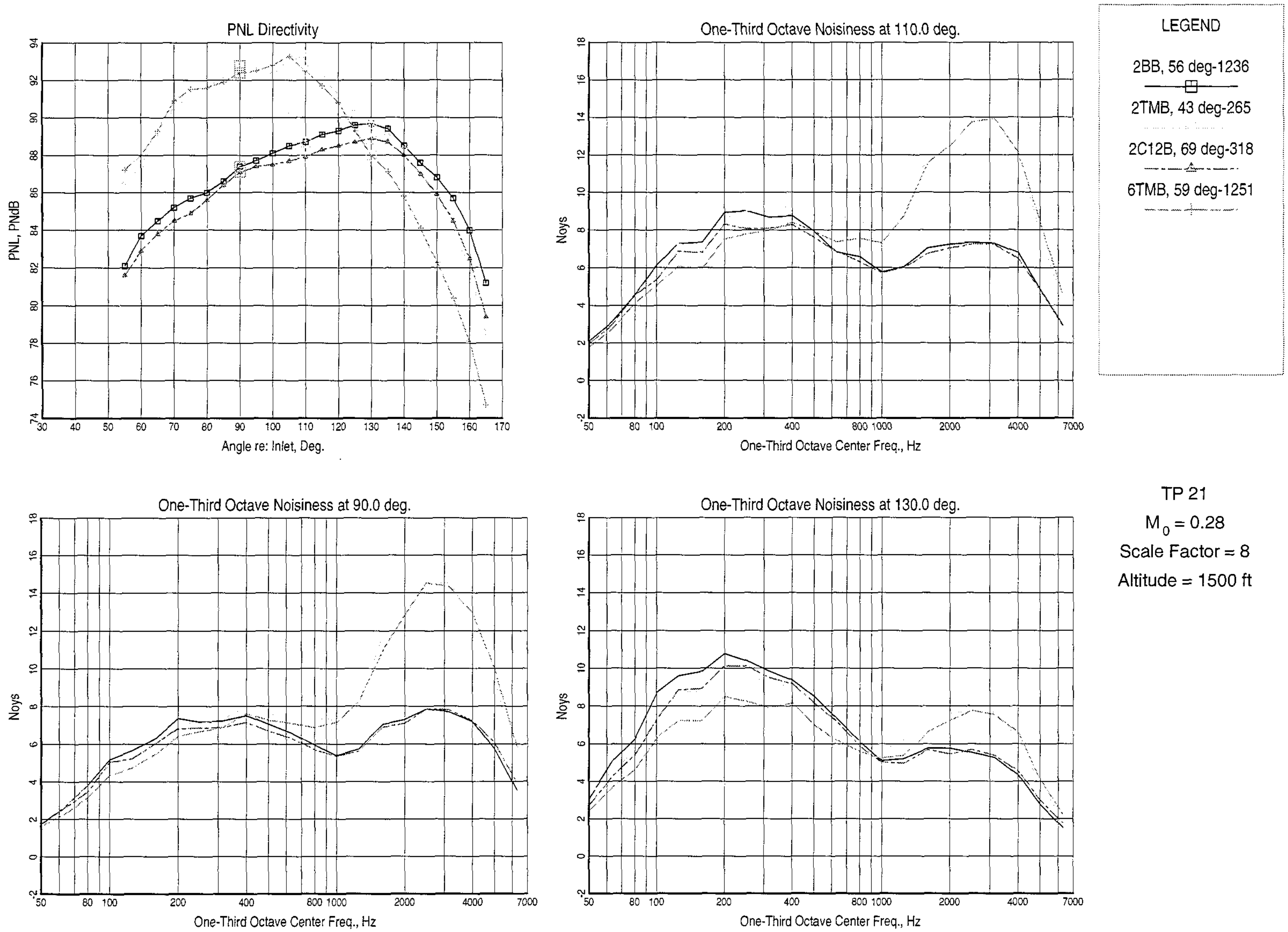


**Figure 76. PNL Directivity and Noy Spectra: Baseline BPR = 5 Nozzle with Internal Plug (2BB); with Chevrons and Tongue Mixer on Core Nozzle (2C12B, 2TmB, and 6TmB)**

representative of the sideline certification point. Little or no benefit was observed at lower thrust conditions. For the selected reference engine size, the chevron concept was more effective than the aggressive tongue mixer design at a given nozzle pressure ratio. Due to differences in the core mass flow characteristics of the chevron and tongue mixer concepts, the data trends are different when the comparison is made at a given thrust. In particular, at very high thrusts chevron and tongue mixer concepts produced similar EPNL reductions.

The chevron apparently introduces a weak, longitudinal vortex structure into the shear layer between the primary and secondary flow streams. This vortex enhances decay of the fully merged portion of the plume by enlarging the mixing perimeter, thus increasing mixing without producing significant additional turbulence near the nozzle exit plane.

The tongue mixer produces a stronger vortex system than chevrons and thus promotes more rapid decay of the fully merged plume. This is apparently accompanied by increased turbulence in the initial mixing region. Acoustically, this produces a significant reduction in low-frequency noise, accompanied by a corresponding large increase in the higher frequency noise that is heavily weighted in annoyance-based metrics such as EPNL. Because of the spectrum shape dependence on scale factor and atmospheric absorption, the noise-reduction effectiveness of the tongue mixer concept is only likely to be favorable for small engines.

#### 6.1.3.1.2 Fan Nozzle Concepts

Two mixing enhancement devices were tested on the internal plug BPR = 5 configuration:

1. Configuration 2BC24, 24-straight-chevron fan nozzle (see page 161)
2. Configuration 2BD, doublet or vortex-generator fan nozzle (94 doublets on inside of fan nozzle) (page 160).

A comparison of normalized EPNL for 2BC24, 2BD, and the baseline 2BB nozzle configurations as a function of normalized $V_{mix}$ for the Mach 0.28 flight simulation condition is presented in Figure 77. The data trends indicate an EPNL benefit of 0.5 to 1.0 dB relative to the baseline nozzle. Changes in normalized $V_{mix}$ at a fixed nozzle pressure ratio are indicated in Figure 77 by marking the cycle point 21 for the three test configurations. Performance data recorded during the acoustic test of these configurations showed no significant differences in the fan stream mass flow for given nozzle pressure ratio. Hence, differences in normalized $V_{mix}$ are due to differences in the ambient speed of sound resulting from variations in ambient temperature during the test.

The EPNL data of these test configurations are displayed as a function of ideal net thrust in Figure 78. In this figure, configuration 2BD is observed to be ineffective in reducing noise level relative to baseline 2BB. A 0.5 to 1.0 dB benefit in EPNL is noted for the chevron 2BC24 configuration. This indicates that, unless test conditions are exactly the same from configuration to configuration, determining a test concept effectiveness in reducing EPNL is sometimes difficult when noise benefits are small — of the order of 0.5 to 1.0 EPNdB. This is particularly so when the ambient temperature differences also result in a same order-of-magnitude change.

PWL spectra comparisons for the three fan nozzle configurations are presented in Figure 79. Data are presented for cycle point 21 (typical sideline condition) and a free-jet Mach number of 0.28. Results at other operating points were observed to be very similar. As on the core nozzle, chevrons produce a moderate reduction in the spectral peak compared to the baseline. The primary effect of the fan chevrons is to enhance mixing between the fan flow and the free jet. The reductions are observed for a wider range of frequencies away from the peak

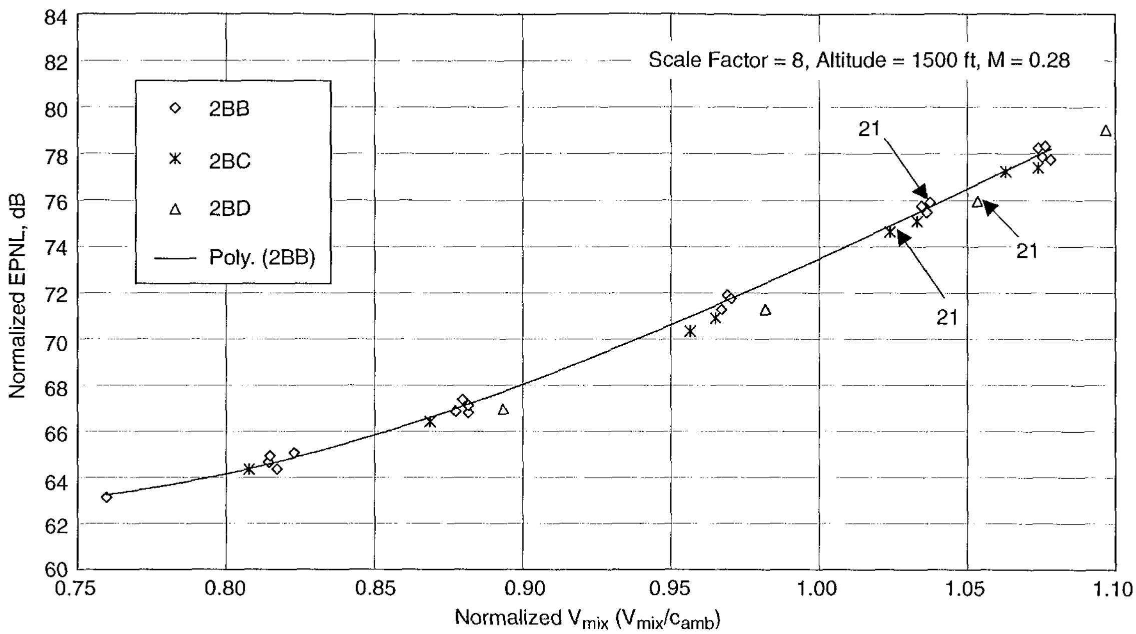


**Figure 77. Normalized EPNL Variation with Normalized $V_{mix}$: BPR = 5 Baseline Nozzles with Internal Plug (2BB); with Chevrons and Doublets on Fan Nozzle (2BC, 2BD)**

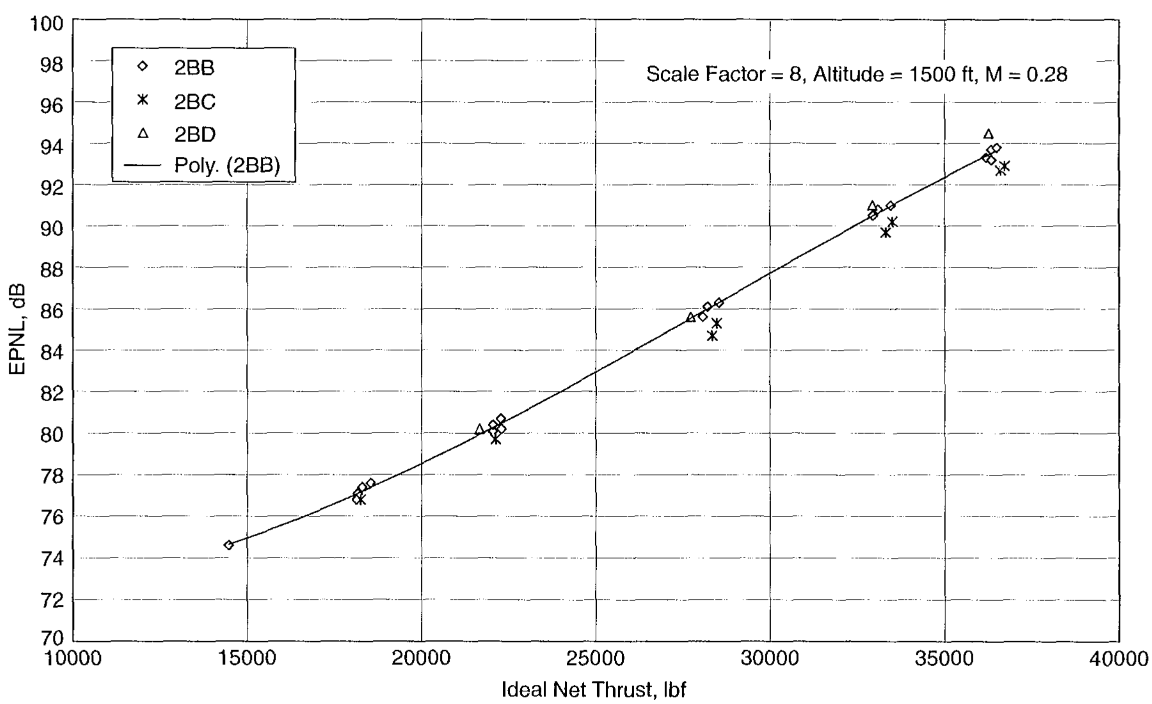


**Figure 78. EPNL Variation with Net Thrust: Baseline BPR = 5 Nozzles with Internal Plug (2BB); with Chevrons and Doublets on Fan Nozzle (2BC, 2BD)**

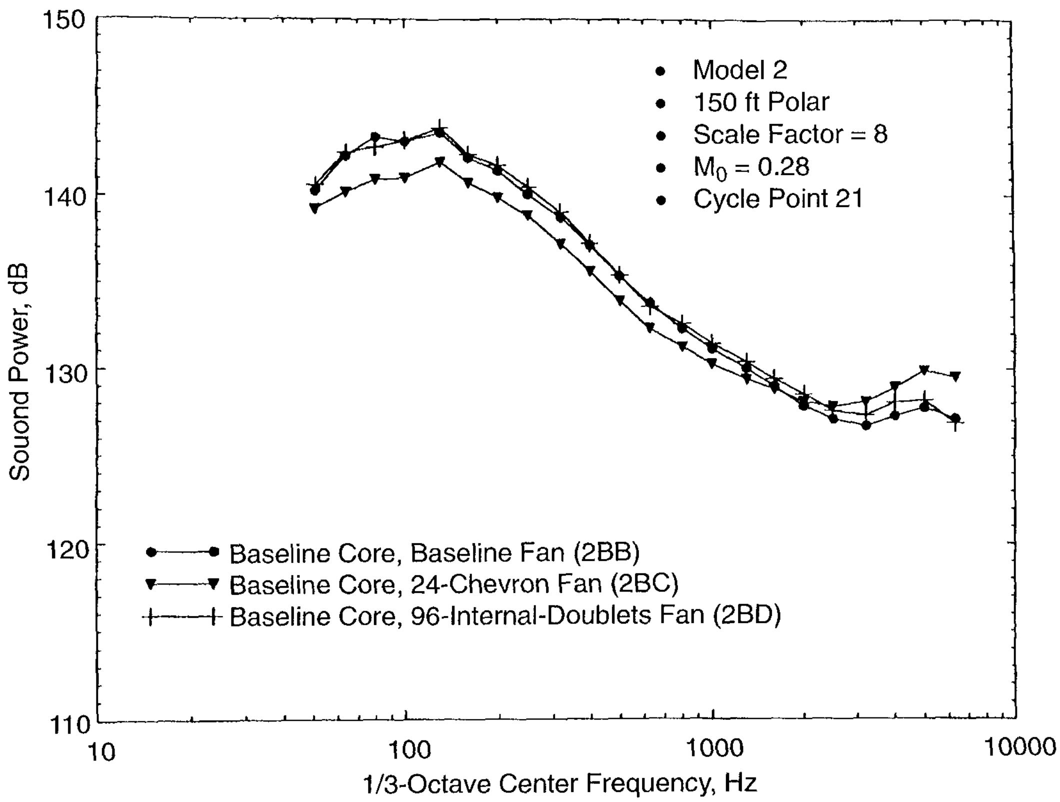


**Figure 79. Comparison of Sound Power for Fan Nozzle Mixing Enhancers (2BB, 2Bc, and 2BD)**

than was the case for core nozzle chevrons, up to 1.6 kHz. Between 1.6 and 3.15 kHz, the chevron spectra become essentially identical to those of the baseline nozzle. The doublets produced no significant spectral variations from the baseline on a sound power basis.

Comparisons of the PNL directivity, 1/3-octave and Noy spectra (at three angles) of 2BB, 2BD, and 2BC configurations at test point 21 (Cycle 2) and Mach 0.28 conditions are presented in Figures 80 and 81. For all configurations, peak PNL is at an emission angle of 130°. The fan chevrons reduce peak PNL 1.5 dB relative to baseline nozzle. A PNL benefit of 1 dB persists for angles between 95° and 160°. This follows trends previously observed for chevrons applied to the core nozzle. The doublet configuration actually produces a small increase in peak PNL (0.8 dB) compared to the baseline nozzle. Similar results are observed for angles between 120° and 150°, with the maximum difference between baseline and doublet configurations increasing to 1.5 dB at 140°.

The SPL spectral results for the various angles (Figure 80) indicate that the primary effect of the chevrons is to again reduce the levels in the low-frequency portion of the spectrum while having virtually no effect above 1.6 kHz. This observation is further supported by the Noy spectra (Figure 81). For the doublet configuration, the spectral levels associated with the peak PNL angle are approximately 1 dB higher than the baseline for the frequency bands between 200 and 1000 Hz, as more clearly shown in the Noy spectra (Figure 81). For angles approaching the jet axis, differences between the SPL spectra of the doublets and the baseline become negligible except in the bands centered at 160 and 200 Hz. The fan nozzle chevrons and doublets were both intended to promote mixing

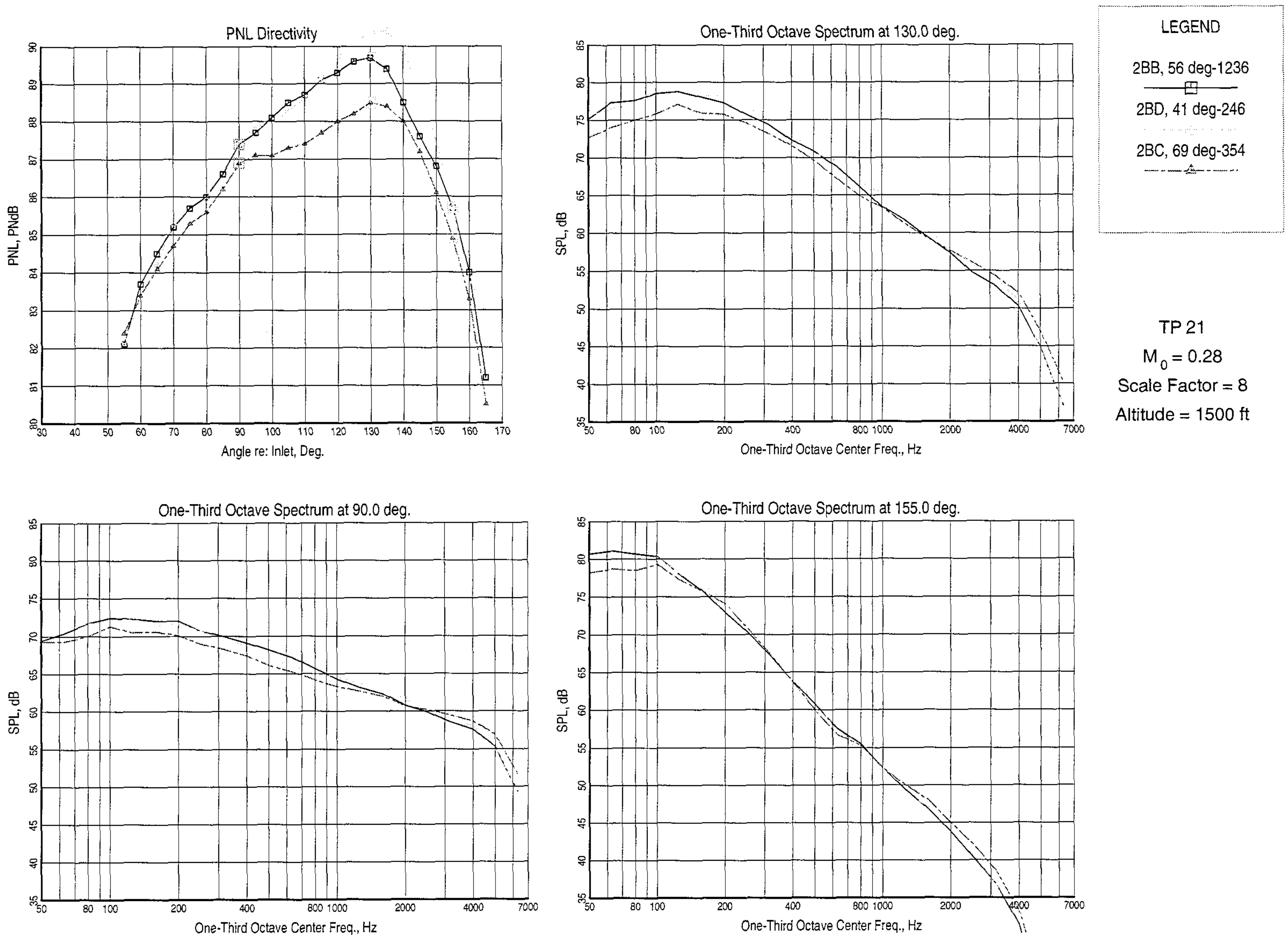


**Figure 80. PNL Directivity and SPL Spectra: Baseline BPR = 5 Nozzle with Internal Plug (2BB); with Chevrons and Doublets on Fan Nozzle (2BC and 2BD)**

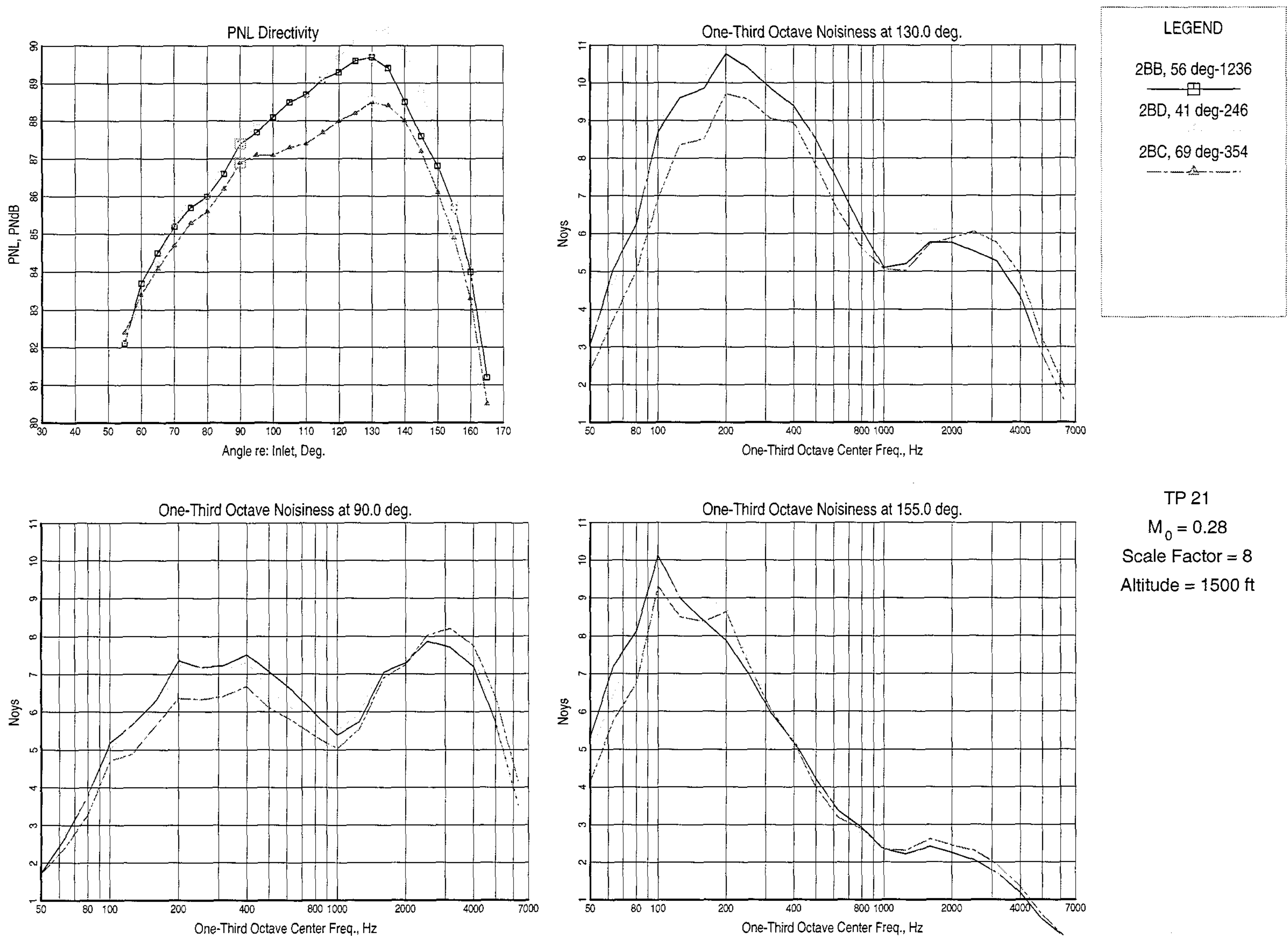


**Figure 81. PNL Directivity and Noy Spectra: Baseline BPR = 5 Nozzle with Internal Plug (2BB); with Chevrons and Doublets on Fan Nozzle (2BC and 2BD)**

between the fan and surrounding ambient flow streams to enhance the plume velocity decay and reduce the average velocity levels in the far-downstream region. The spectral results suggest that the chevron configuration performed somwhat as intended. However, the primary effect of the doublets was to shift the spectral peak at the angle corresponding to peak PNL from 100 to 200 Hz, without reducing the SPL. Hence, it appears that the thickness or the shape of the doublets selected was not conducive to improved fan flow/free-jet mixing for this configuration.

In summary, chevrons on the fan nozzle produced a maximum reduction in EPNL of 1 dB at the typical sideline certification point. The effect of the chevrons was to reduce the levels of the low frequency portion of the spectrum (below 400 Hz), with little or no change from the baseline at higher frequencies. On a directivity basis, the chevrons reduced PNL at the peak and higher angles but did not alter the angle at which the peak occurred. The paired, cascaded, triangular vortex generators (or doublets) were not effective in reducing noise, compared to the baseline nozzle. At the highest pressure ratios tested, an increase of 1 EPNdB relative to the baseline was observed. This was primarily the result of a shift in the spectral peak from 100 Hz in the baseline model to 200 Hz in the doublet configuration, without any reduction at the peak frequency. As with the chevrons, the doublets had no effect on the directivity angle corresponding to peak PNL.

#### 6.1.3.1.3 Combined Core and Fan Nozzle Concepts

Based on the results described in the previous two subsections, three configurations employing combinations of fan and core nozzle mixing concepts were tested:

1. Configuration 2C12C, 12-chevron core nozzle and 24-chevron fan nozzle (page 162)
2. Configuration 2TmC, tongue mixer core nozzle with short core plug and 24-chevron fan nozzle (page 165)
3. Configuration 6TmC, tongue mixer core nozzle with extended core plug and 24-chevron fan nozzle (page 197)

The EPNL results for these configurations are presented in Figures 82 and 83. EPNL normalized for thrust as a function of effective mixed-jet velocity normalized to the ambient speed of sound is presented in Figure 82. Unnormalized EPNL as a function of standard-day net thrust is presented in Figure 83. These figures show a maximum reduction of 2 dB. The maximum suppression occurred at an operating condition typical of the sideline certification point.

For configuration 2TmC, the tongue mixer with the short core plug, two additional conditions (labeled points 21A and 20A) are also presented in Figures 82 and 83. As previously explained, this configuration of the tongue mixer delivered a considerably higher core mass flow rate for a given core nozzle pressure ratio than any of the other configurations, due to incorrect design of the effective throat area. For cycle points 20A and 21A , the core nozzle pressure ratio was reduced until the core mass flow rates matched those observed in the other configurations at cycle points 20 and 21 respectively. For these altered cycle points, 3 EPNdB reduction relative to the baseline coaxial nozzle is indicated for the tongue mixer 2TmC on a "same thrust" basis. Of course, some of this same effect could be achieved by resizing the core nozzle to give the higher mass flow at a lower pressure ratio, hence lowering the core jet velocity and therefore reducing the noise.

The combination of chevrons on the fan and core nozzle was the most successful and demonstrated noise suppression over the largest range of operating conditions. At the lowest nozzle pressure ratios, noise levels for this

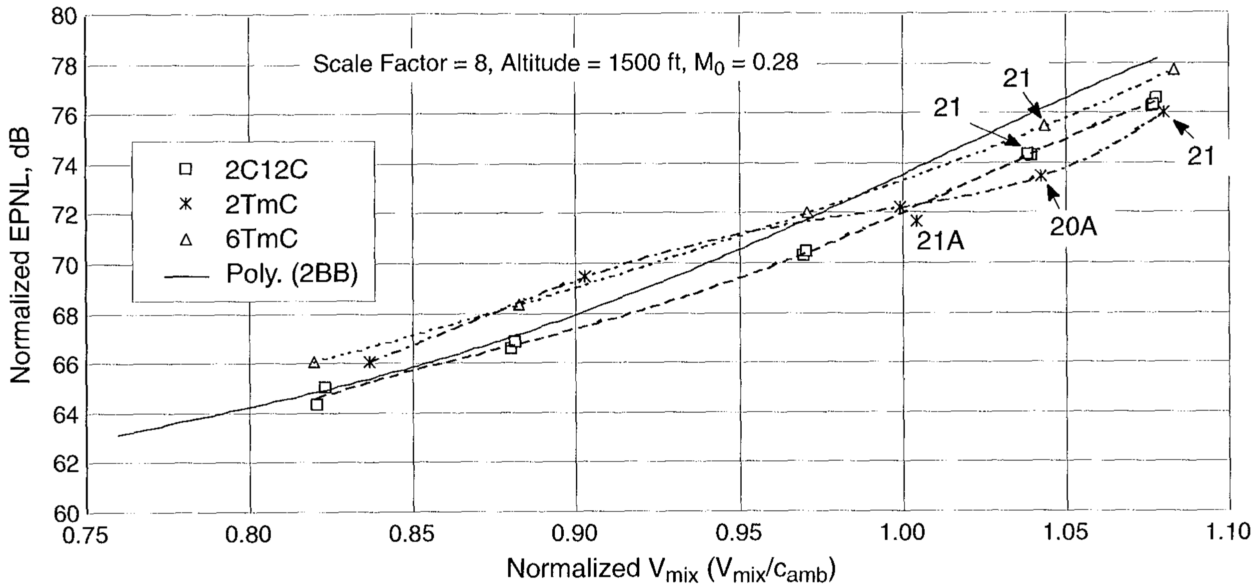


**Figure 82.** **Normalized EPNL Variation with Normalized $V_{mix}$: Baseline BPR = 5 Nozzle with Internal Plug (2BB); Combined Core/Fan Nozzle Concepts (2C12C, 2TmC, and 6TmC)**

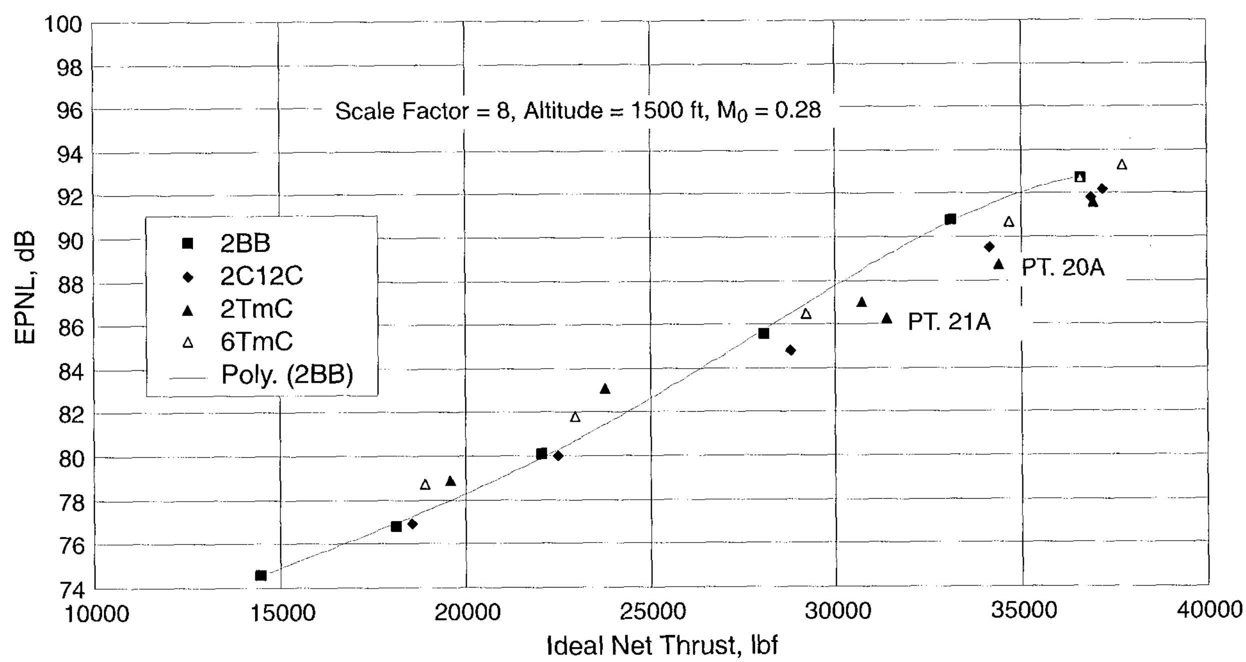


**Figure 83.** **EPNL Variation with Net Thrust: Baseline BPR = 5 Nozzle with Internal Plug (2BB); Combined Core/Fan Nozzle Concepts (2C12C, 2TmC, and 6TmC)**

configuration were virtually identical to those of the baseline arrangement. Reduced noise relative to the baseline was observed for values of normalized $V_{mix}$ greater than 0.88. This typically translates to reduced jet noise at both cutback and sideline certification conditions.

The tongue mixer configurations on the core nozzle, in combination with fan nozzle chevrons, also demonstrated significant low-frequency, peak-noise reductions compared to the baseline, at the higher nozzle pressure ratios, as shown in the PWL spectra comparisons in Figure 84 for cycle point 21. At lower nozzle pressure ratios, the tongue mixer combinations increased noise relative to the baseline, as can be seen in Figures 82 and 83. As the nozzle pressure ratio is reduced at fixed free-jet Mach number, the difference in velocity between adjacent streams starts decreasing, the shear layers grow faster, and the extent of the plume is reduced. Thus mixing enhancement will have less effect at lower pressure ratios.

As with the baseline fan nozzle, the tongue mixer configurations with fan chevrons at fixed cycle conditions show the mixer to be always noisier. Most of the noise suppression observed with the tongue mixer at fixed thrust (lower core pressure ratio to match thrust) is the result of reduced primary jet velocity compared to other configurations. In the combined case with fan chevrons, the enhanced mixing of the fan flow and free jet continues (just as in the fan-chevrons-only case), but it also further alters the flow characteristics due to the core chevrons or tongues with the net effect being even more beneficial to noise than the fan-chevrons-only case. The combination of the tongue mixer on the core nozzle with chevrons on the fan nozzle almost doubled the peak noise decibel reduction compared to the mixer by

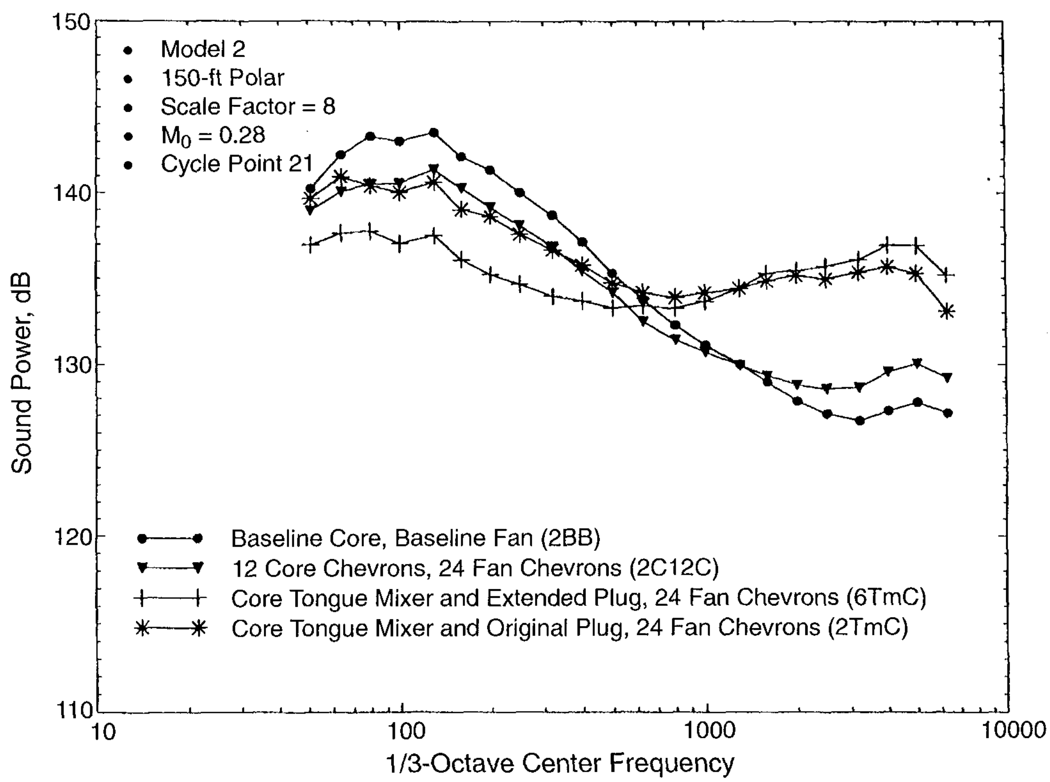


**Figure 84. Comparison of Sound Power for Combined Nozzle Mixing Enhancers (2BB, 2C12C, 2TmC, and 6TmC)**

itself, but the high-frequency noise increase due to the tongue mixer was not changed with the addition of the fan chevrons. However, the combination of chevrons on both fan and core nozzles doubled the peak noise level reduction with no appreciable increase in high frequency noise, resulting in a much greater EPNL reduction.

The sound power spectrum for the combination of fan and core nozzle devices at cycle point 21 is presented in Figure 84. The general characteristics in this figure are similar to those presented in Figure 72 for the core nozzle devices alone. All configurations reduced the low-frequency noise that dominates the baseline nozzle spectrum. Similarly, both configurations employing the core tongue mixer produced large increases in sound power level at frequencies above 1 kHz. The combination of fan nozzle chevrons with the core nozzle devices significantly improves low-frequency suppression compared to the core devices alone. This is particularly true for the configuration employing the tongue mixer with extended plug (6TmC), where an additional 2 dB reduction was observed over the frequency range of 50 to 400 Hz. For the other two configurations, addition of the fan nozzle chevrons produced another 1 dB in noise reduction over the frequency range 50 to 1000 Hz, compared to the results with only the core nozzle devices. However, the tongue mixer combinations still exhibited significantly higher high-frequency noise. No significant changes in the spectral level were observed above 1 kHz for any of the core configurations as a result of adding chevrons to the fan nozzle.

Comparing the PNL data of Figure 85 with those of Figure 74 indicates that inclusion of the chevrons on the fan nozzle did not significantly affect the shape of the PNL directivity patterns for the various core nozzle configurations. However, reductions in the peak PNL of 1–2 PNdB were measured. As observed without the fan nozzle chevrons, the PNL for the tongue mixer configurations peaked at a much lower angle (100°) than either the baseline or the chevron configurations. In addition, the tongue mixer configurations continue to produce much higher levels in the forward arc than do the other configurations, in spite of the addition of chevrons to the fan nozzle.

Comparing sound pressure spectra at several angles (Figures 85 and 74), it can be seen that all the devices tested reduced noise in the low-frequency portion of the spectrum, and the reductions were observed over a wide range of angles. Addition of the fan nozzle chevrons produced the maximum impact at aft angles, closer to the jet axis, almost doubling the decibel reduction at 130° compared to the configurations without chevrons on the fan nozzle. The high-frequency increases observed in the PWL for the core nozzle mixer configurations are primarily associated with angles near 90°. The Noy curves of Figure 86 further substantiate these observations, showing the total dominance of the high-frequency portion of the spectrum at the 100° angle for the two tongue mixer configurations and the substantial reduction in annoyance for all configurations in the lower frequencies.

In summary, the combination of fan nozzle chevrons with the previously described core nozzle concepts produced a significant additional decrease in farfield noise levels. Maximum reductions in EPNL of 2 dB relative to the baseline nozzle were observed. This is approximately double the decibel reduction observed when only the core nozzle devices were used. Combining the core nozzle concepts with chevrons on the fan nozzle did not significantly alter the shape of the directivity curves but did reduce noise levels. Configuration 2C12C was the best in terms of noise reduction for the internal plug BPR = 5 nozzle.

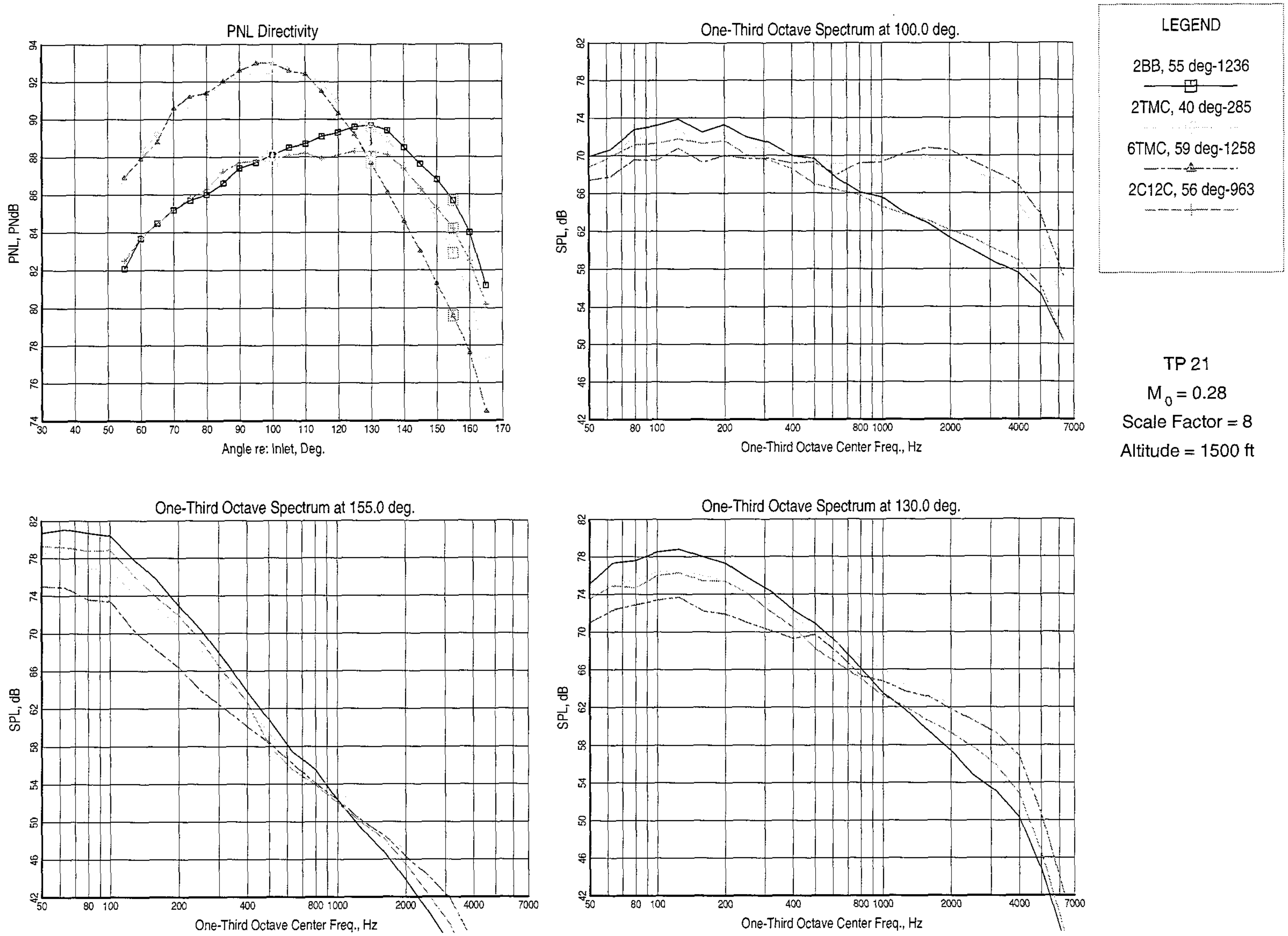


**Figure 85. PNL Directivity and SPL Spectra: Baseline BPR = 5 Nozzle with Internal Plug (2BB); Combined Fan and Core Nozzle Concepts (2C12C, 2TmC, and 6TmC)**

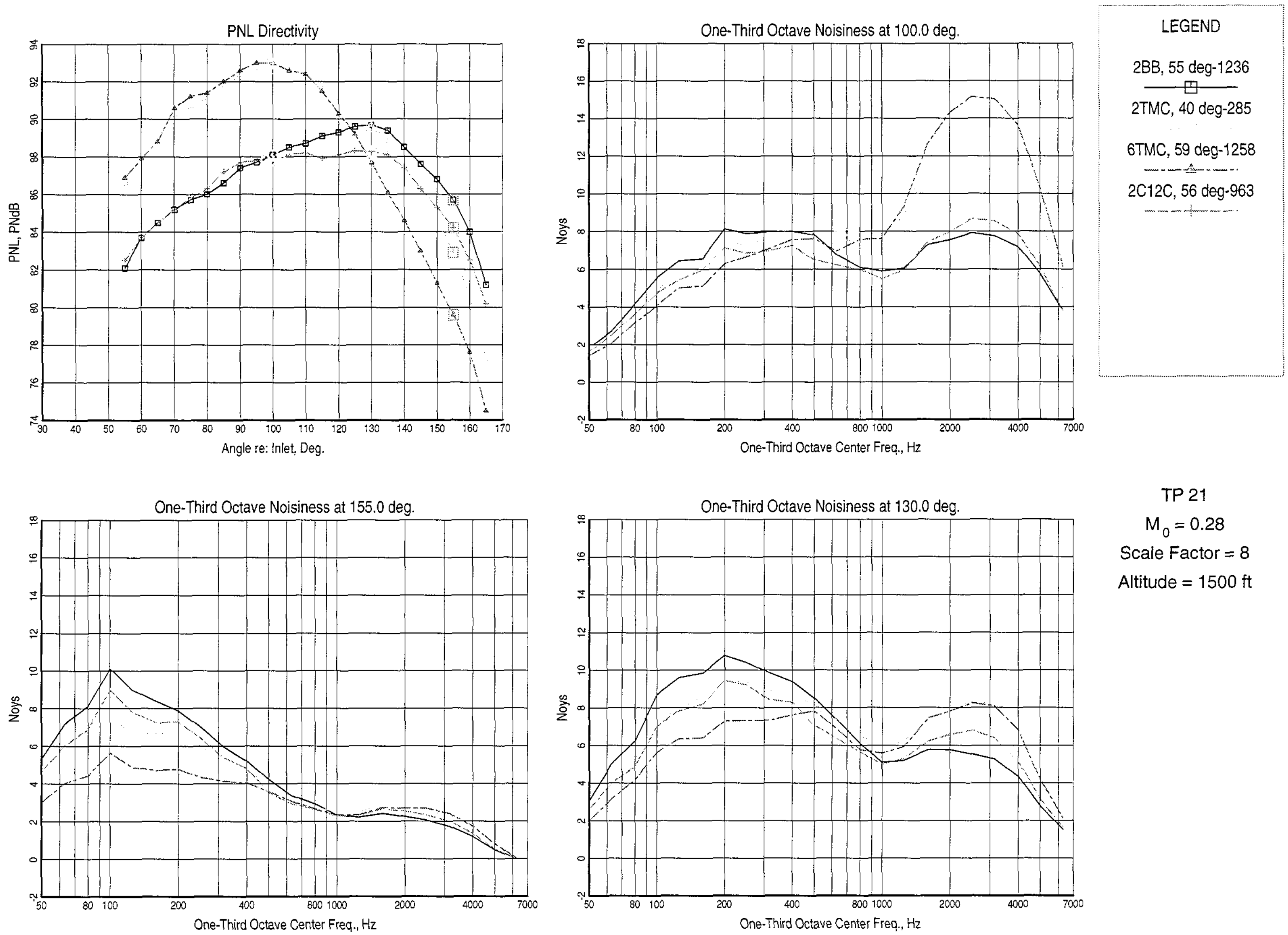


**Figure 86. PNL Directivity and Noy Spectra: Baseline BPR = 5 Nozzle with Internal Plug (2BB); Combined Fan and Core Nozzle Concepts (2C12C, 2TmC, and 6TmC)**

The EPNL benefits of all mixing-enhancer devices tested with Model 2 BPR = 5 internal plug nozzle are summarized in Figure 87.

### 6.1.3.2 External Plug BPR=5 Configurations

In this section, acoustic results measured with mixing-enhancement concepts tested on the external plug BPR = 5 nozzle (Model 3) are discussed. The baseline nozzle configuration is shown in Figure 12. This section is further divided into three subsections corresponding to mixing-enhancement devices used on the core only, fan only, and core and fan combinations.

#### 6.1.3.2.1 Core Nozzle Concepts

This subsection discusses results of having mixing-enhancement devices on the core nozzle of the external plug BPR = 5 configuration. The tested core nozzle devices include:

1. Configuration 3C8B, 8-straight-chevron core nozzle (page 184)
2. Configuration 3C12B, 12-straight-chevron core nozzle (page 181)
3. Configuration 3IB, 12-inward-bent-chevron core nozzle (page 185)
4. Configuration 3AB, 12-alternating-bent-chevron core nozzle (page 188)
5. Configuration 3DiB, internal doublet core nozzle (64 in the core flow side) (page 189)
6. Configuration 3DxB, external-doublet core nozzle (20 in the fan flow side) (page 190)

A comparison of normalized EPNL for 3C8B, 3C12B, 3IB, 3AB, and the baseline 3BB configurations as a function of normalized $V_{mix}$ for the Mach 0.28 flight-simulation condition is presented in Figure 88. The trends

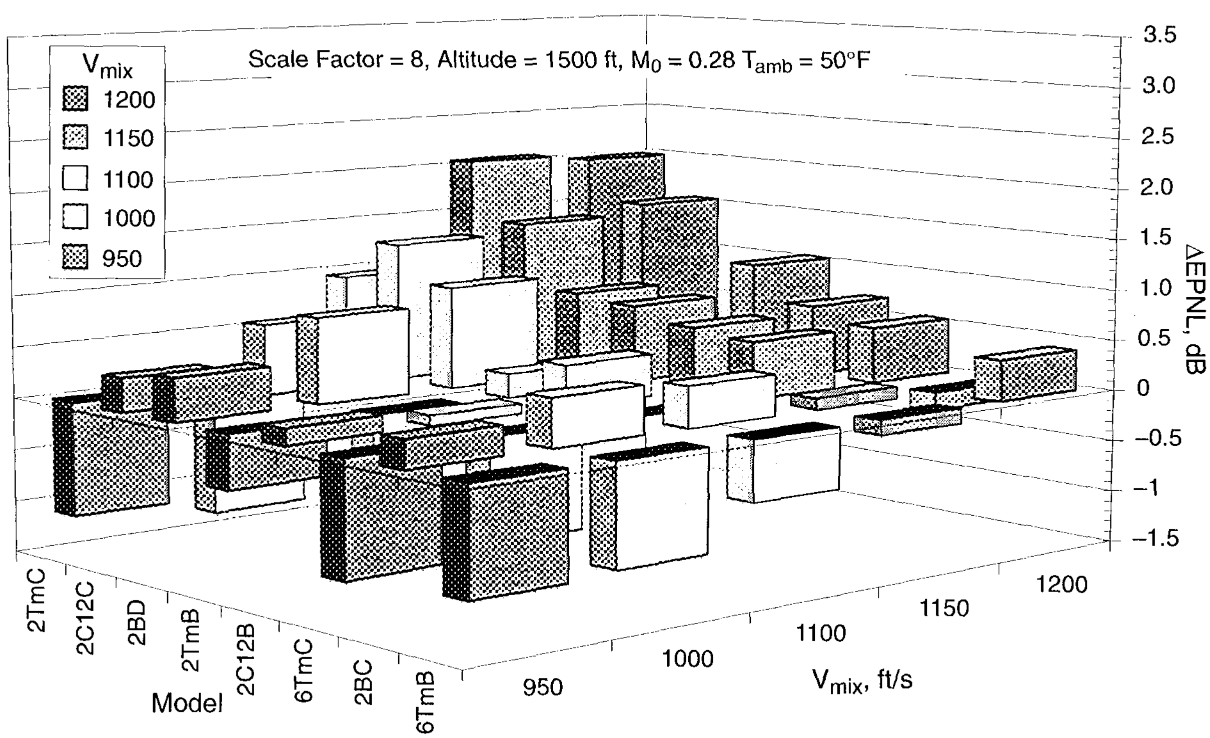


**Figure 87. Mixing-Enhancer Noise Benefits Relative to Baseline BPR = 5 Internal Plug Nozzle (Model 2)**

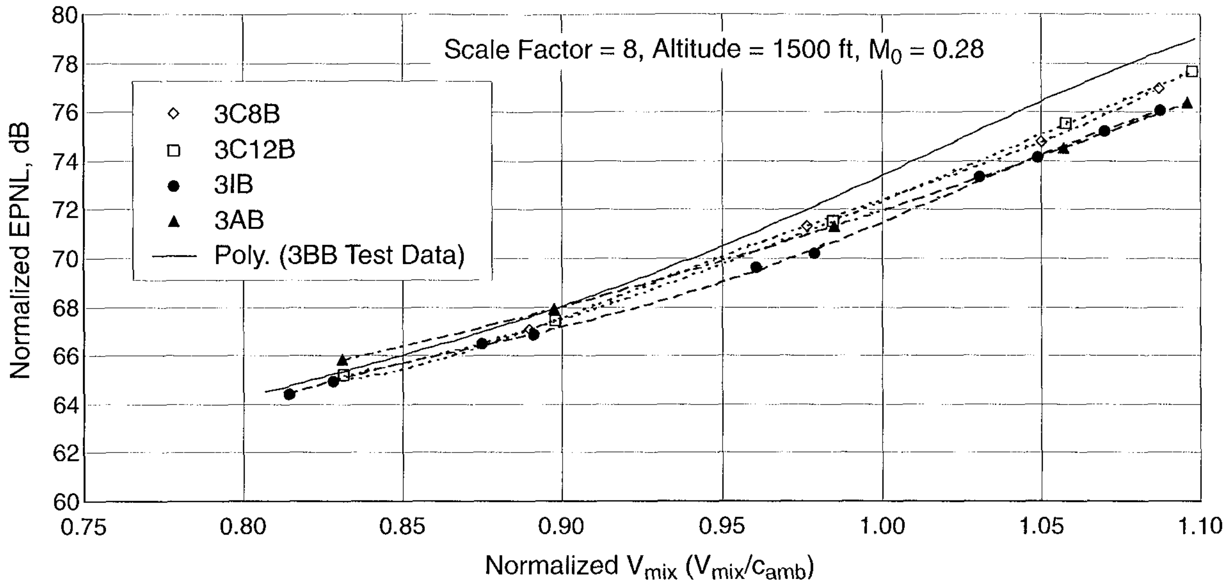


**Figure 88. Normalized EPNL Variation with Normalized $V_{mix}$: Baseline BPR = 5 Nozzle with External Plug (3BB); Four Different Chevron Core Nozzles (3C8B, 3C12B, 3IA, and 3AB)**

of 3C8B and 3C12B are very similar and show EPNL reduction relative to the baseline, with the fewer number of chevrons (3C8B) providing a slightly increased benefit over the higher number of chevrons (3C12B) at higher normalized $V_{mix}$ values. The inward and alternating flip chevrons are very similar at the higher values of $V_{mix}$ and provide a significant noise benefit relative to the baseline. However, at lower velocities, the noise benefit with 3AB decreases, and it produces even higher values of EPNL relative to the baseline at the lowest jet velocities tested. The 3IB configuration gives the best noise benefit among the four test core chevron devices at all velocities.

Comparisons of the PNL directivity, 1/3-octave and Noy spectra (at three angles) of 3BB, 3C8B, 3C12B, 3IB, and 3AB configurations at the test point 21 (Cycle 2 operating line) and Mach 0.28 simulated-flight speed condition are presented in Figures 89 and 90 (see Appendix C for comparisons at all angles). PNL directivity shows that the core chevrons significantly decrease peak PNL relative to baseline and cause peak PNL to occur at different angles. The peak PNL of configuration 3IB is reduced by more than 2 dB, and the peak PNL angle of Configuration 3AB is shifted from 130° to 120°. The spectra show that the alternating flip chevron offers the most low-frequency suppression but is highest at the medium to high frequencies. The other chevron designs provide different degrees of low-frequency suppression with high-frequency levels at or below those of the baseline. Similar trends are also noted from the sound power spectral comparisons presented in Figure 91.

A comparison of the normalized EPNL of 3DiB, 3DxB, and baseline 3BB configurations as a function of normalized $V_{mix}$ for the Mach 0.28 flight-simulation condition is presented in Figure 92. Overall, the doublets were rather disappointing in noise benefits. The internal doublets were louder than the baseline at high velocities, and the external doublets were louder than the baseline at lower velocities.

Comparisons of the PNL directivity and 1/3-octave spectra (at three angles) of 3BB, 3DiB and 3DxB configurations at the test point 21 (Cycle 2) and Mach 0.28 condition are presented in Figures 93 and 94. The PNL directivities of 3BB and 3DiB are very similar,

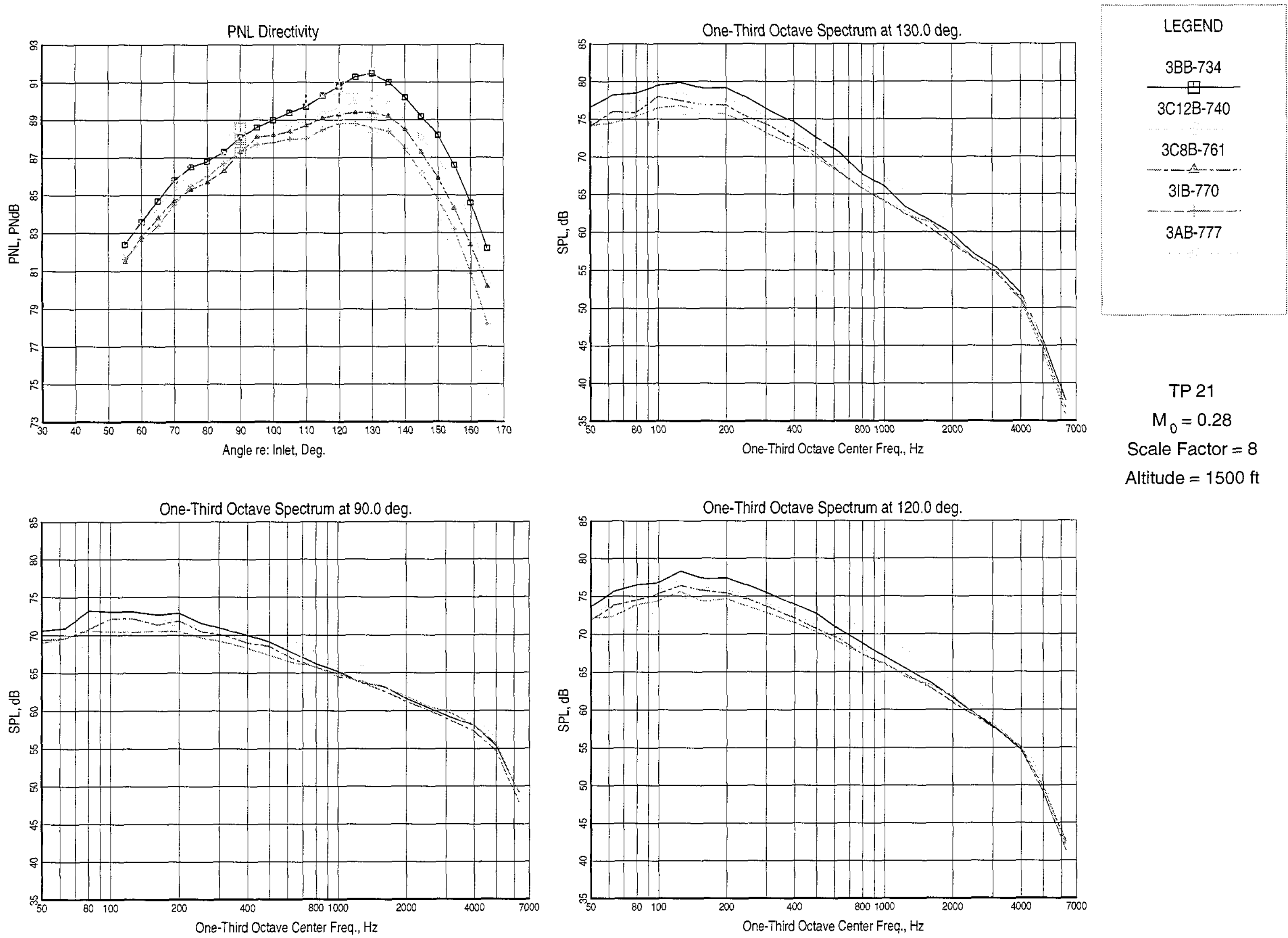


**Figure 89. PNL Directivity and SPL Spectra: Baseline BPR = 5 External Plug Nozzle (3BB); Four Different Chevron Core Nozzles (3C8B, 3C12B, 3IB, and 3AB)**

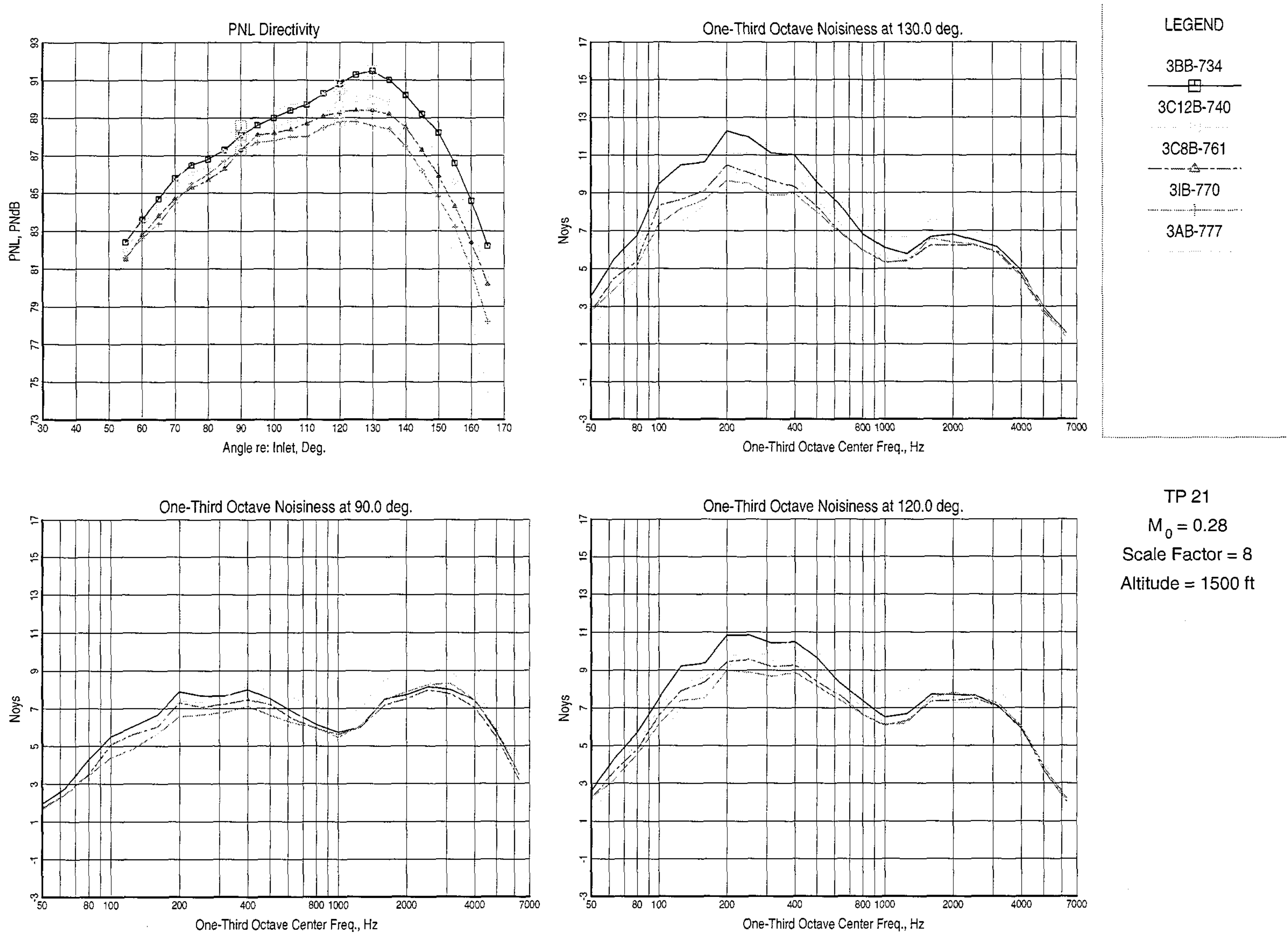


**Figure 90. PNL Directivity and Noy Spectra: Baseline BPR = 5 External Plug Nozzle (3BB); Four Different Chevron Core Nozzles (3C8B, 3C12B, 3IB, and 3AB)**

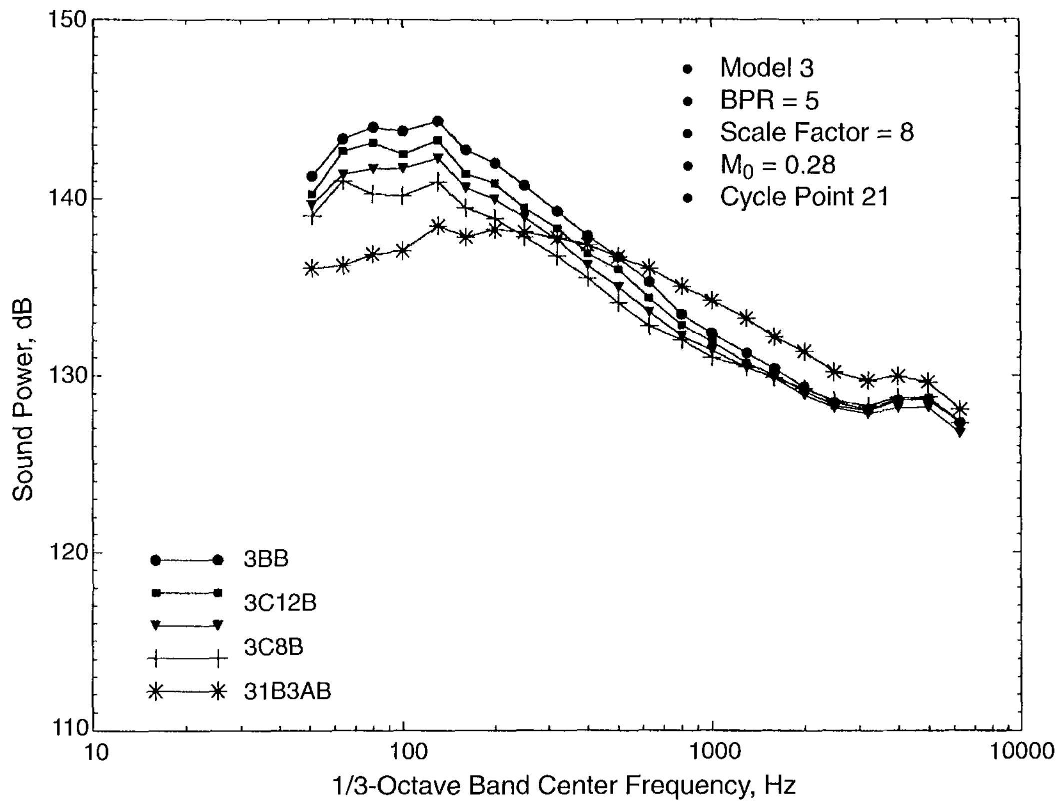


**Figure 91. Comparison of Sound Power for Core Nozzle Mixing Enhancers (3BB, 3C8B, 3C12B, and 3AB)**

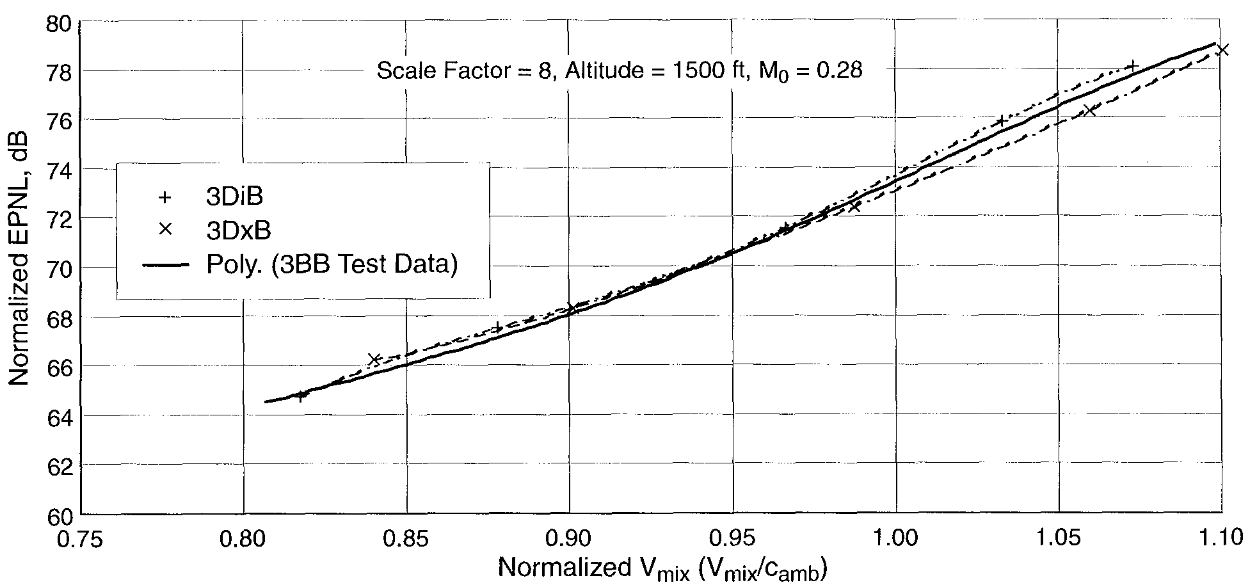


**Figure 92. Normalized EPNL Variation with Normalized $V_{mix}$: Baseline BPR = 5 Nozzle with External Plug (3BB); Doublet Core Nozzles (3DiB and 3DxB)**

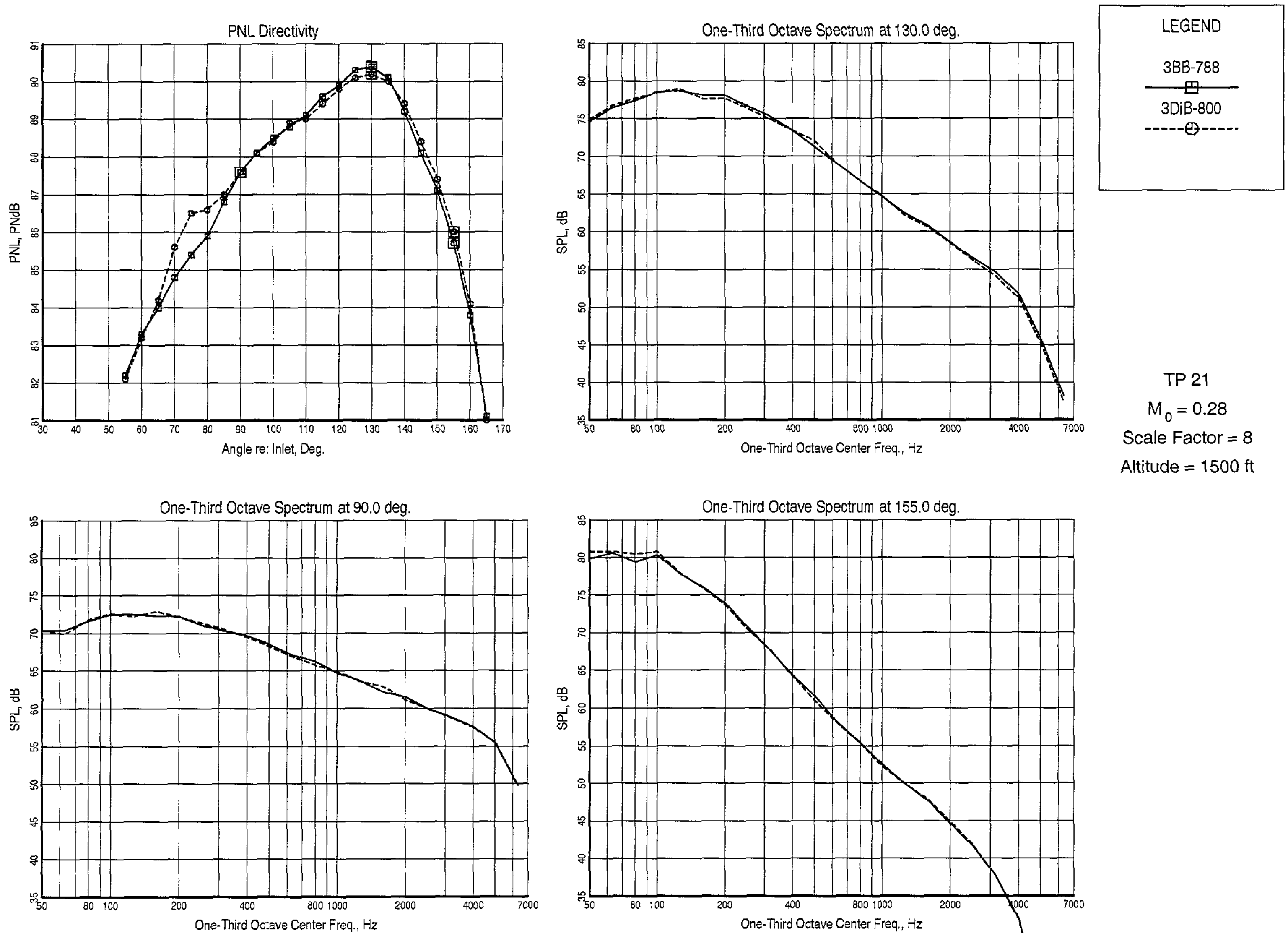


**Figure 93. PNL Directivity and SPL Spectra: Baseline BPR = 5 External Plug Nozzle (3BB); 64 Internal Doublets on Core Nozzle (3DiB)**

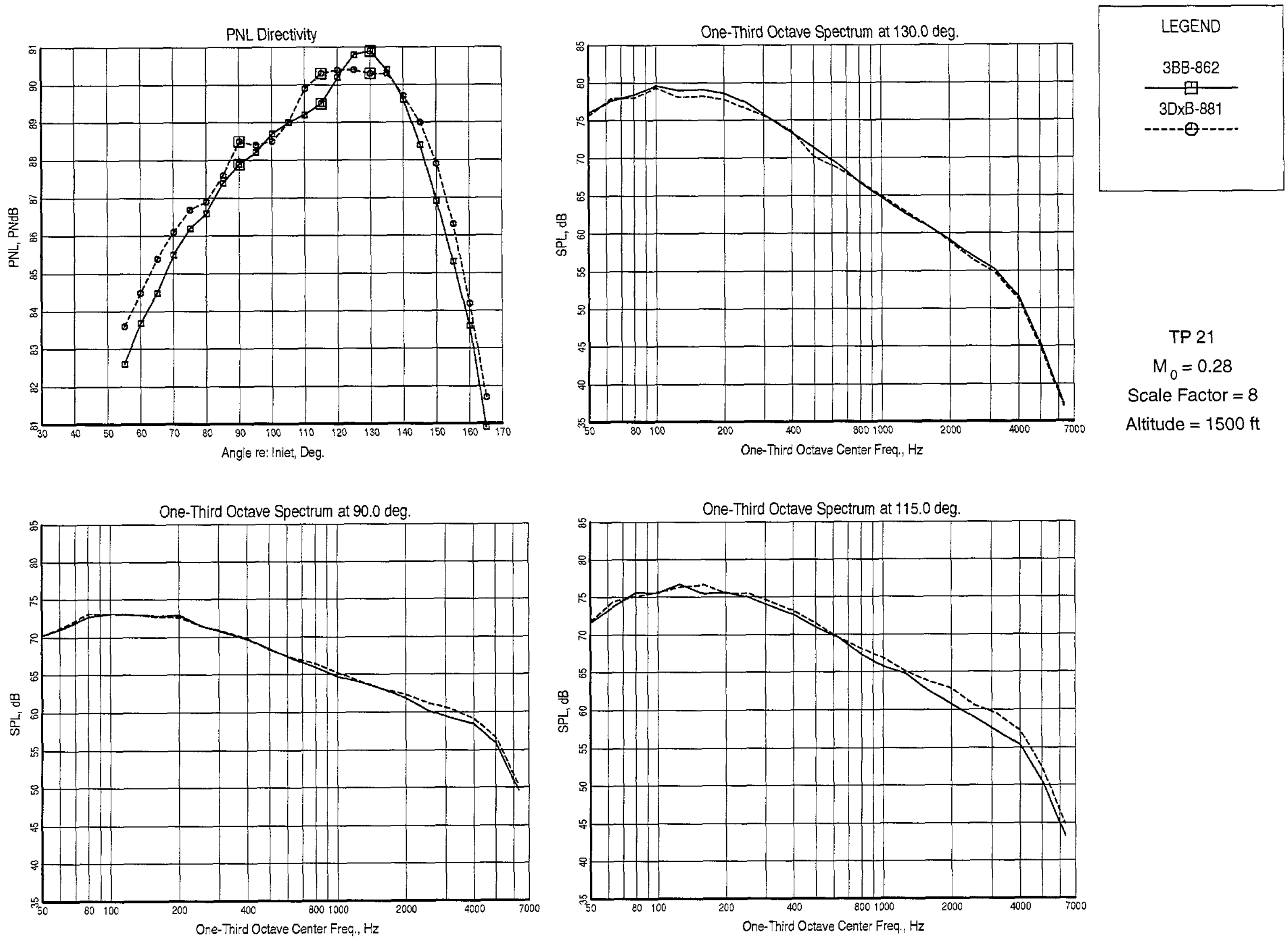


**Figure 94. PNL Directivity and SPL Spectra: Baseline BPR = 5 External Plug Nozzle (3BB); 64 Internal Doublets on Core Nozzle (3DxB)**

with the internal doublets slightly higher at the forward and aft angles and slightly lower near the peak PNL angles. The spectra are very similar and show no obvious trends. The PNL directivities of 3BB and 3DxB also show that the external doublets have a higher PNL value at forward and aft angles, and the levels around the peak PNL angle are lower. The spectral comparisons are again very similar, although the doublets result in more noise at high frequencies.

#### 6.1.3.2.2 Fan Nozzle Concepts

This section discusses results of a mixing-enhancement device on the fan nozzle of the external plug BPR = 5 configuration. The tested fan nozzle device was configuration 3BC, the 24-chevron fan nozzle (page 167).

Figure 95 is a comparison of the normalized EPNL of 3BC and baseline 3BB configurations as a function of normalized $V_{mix}$ for the Mach 0.28 flight simulation condition. On an EPNL basis, it is clear that the fan chevron had little acoustic impact relative to the baseline configuration, unlike the result for the internal plug nozzle. Recall that for the internal plug, configurations 2BB versus 2BC (Figure 77) a 0.5 to 1.0 EPNdB reduction was observed.

Figures 96 and 97 compare the PNL directivity along with 1/3-octave and Noy spectra for 3BB and 3BC for the test point 21 Mach 0.28 condition. The fan chevron PNL is higher in the forward quadrant but lower at the other locations. In terms of spectra, the fan chevron reduces noise at lower frequencies but generates additional high-frequency noise relative to the baseline. A similar observation can be made from the PWL comparisons in Figure 98. This is in contrast to the results with the internal plug nozzle, where no significant high-frequency noise increase was observed as illustrated in Figures 79 through 81. We thus have the puzzling result that the internal and external plug baseline nozzles exhibit very similar acoustic characteristics, but addition of a fan chevron produces different noise impacts.

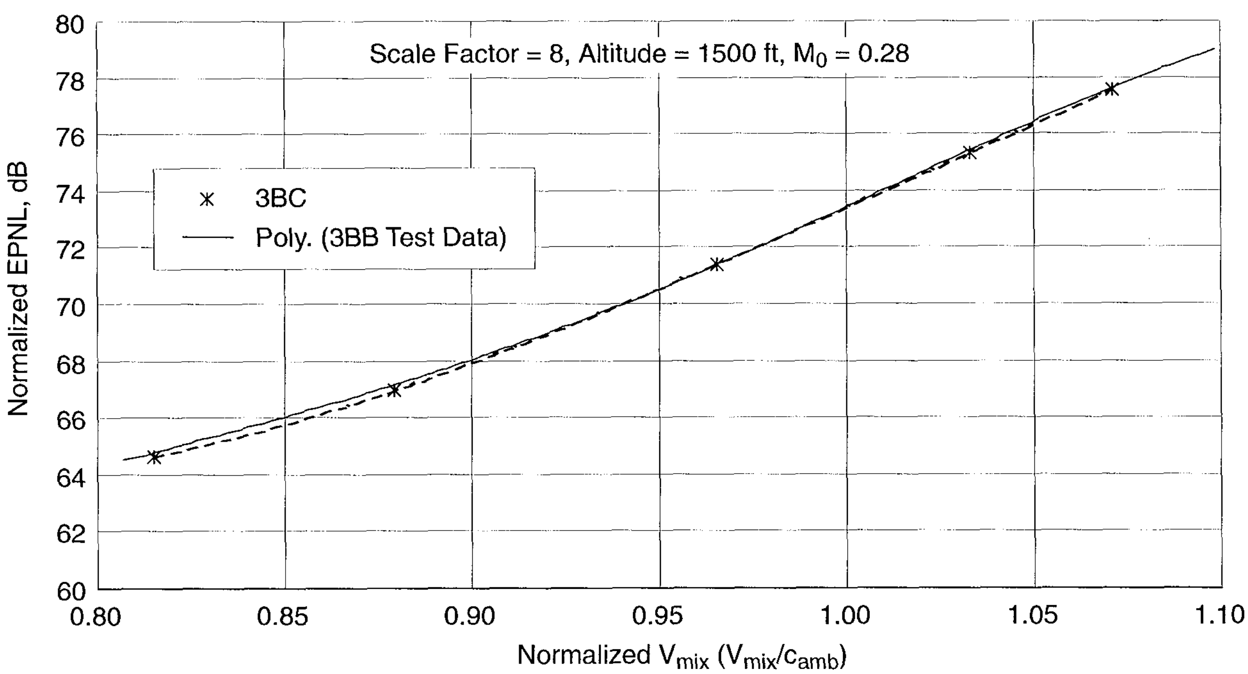


**Figure 95. Normalized EPNL Variation with Normalized $V_{mix}$: Baseline BPR = 5 Nozzle with External Plug (3BB); 24-Chevron Fan Nozzle (3BC)**

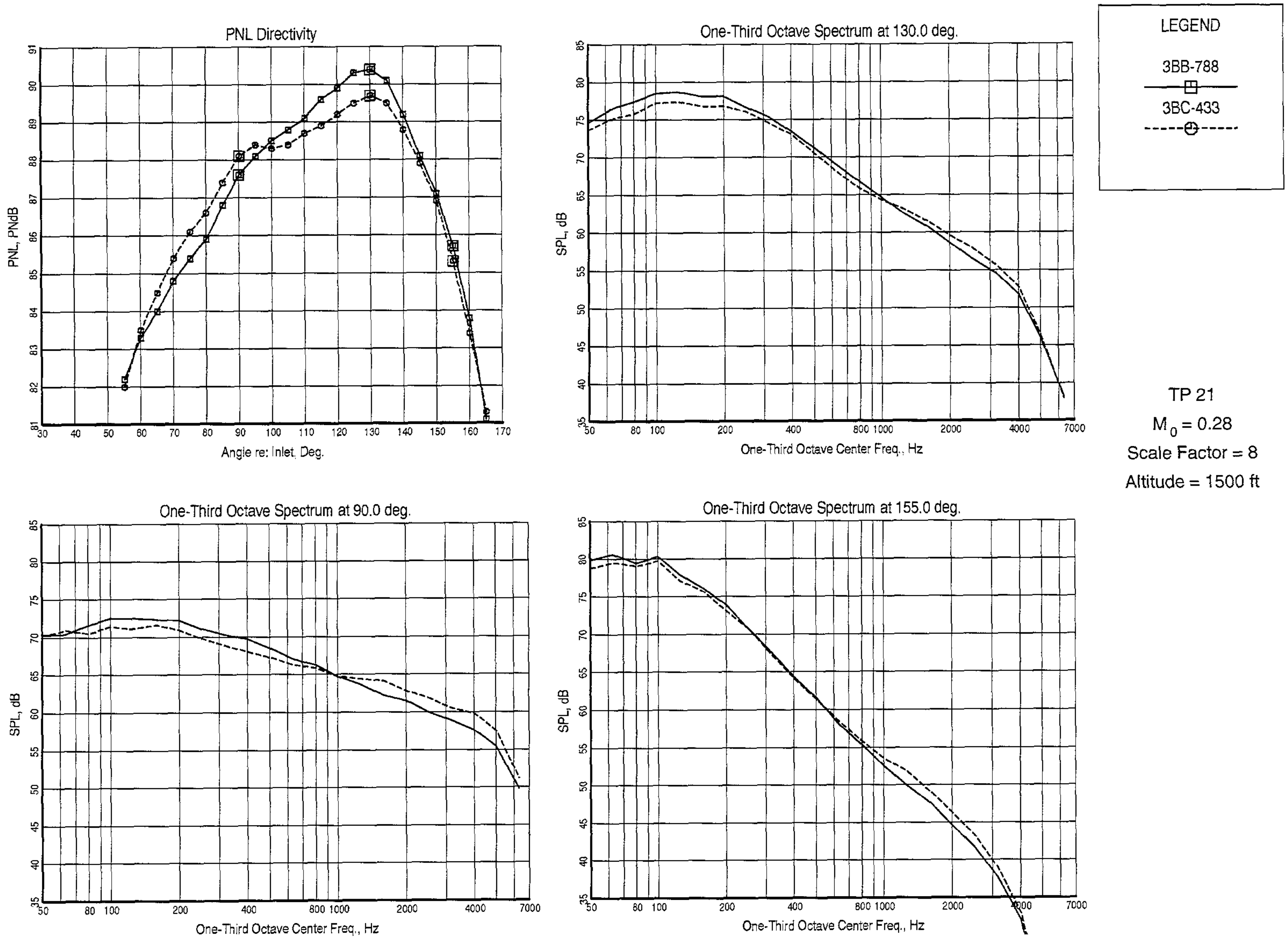


**Figure 96. PNL Directivity and SPL Spectra: Baseline BPR = 5 External Plug Nozzle (3BB); 24-Chevron Fan Nozzle (3BC)**

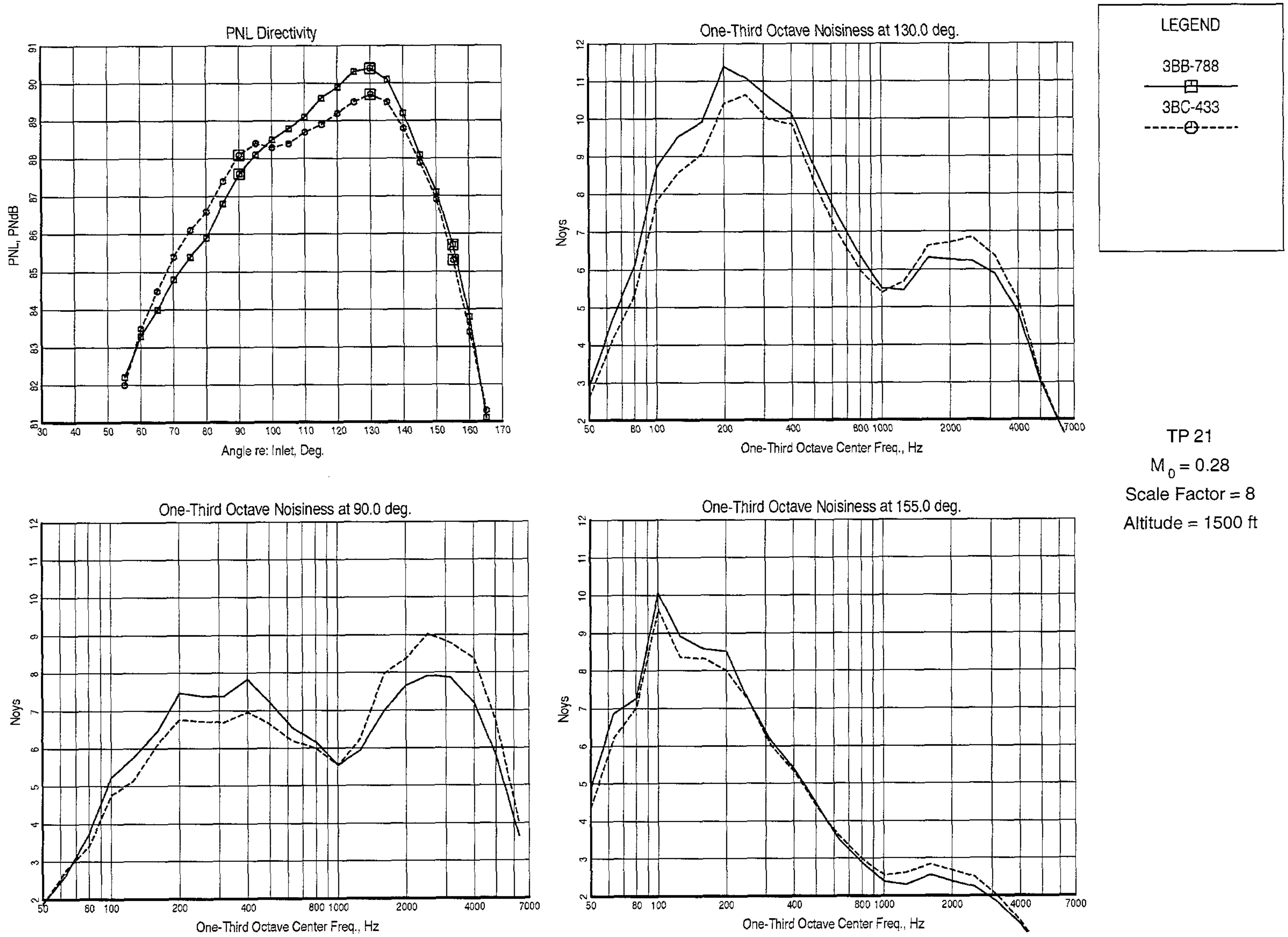


Figure 97. PNL Directivity and Noy Spectra: Baseline BPR = 5 External Plug Nozzle (3BB); 24-Chevron Fan Nozzle (3BC)

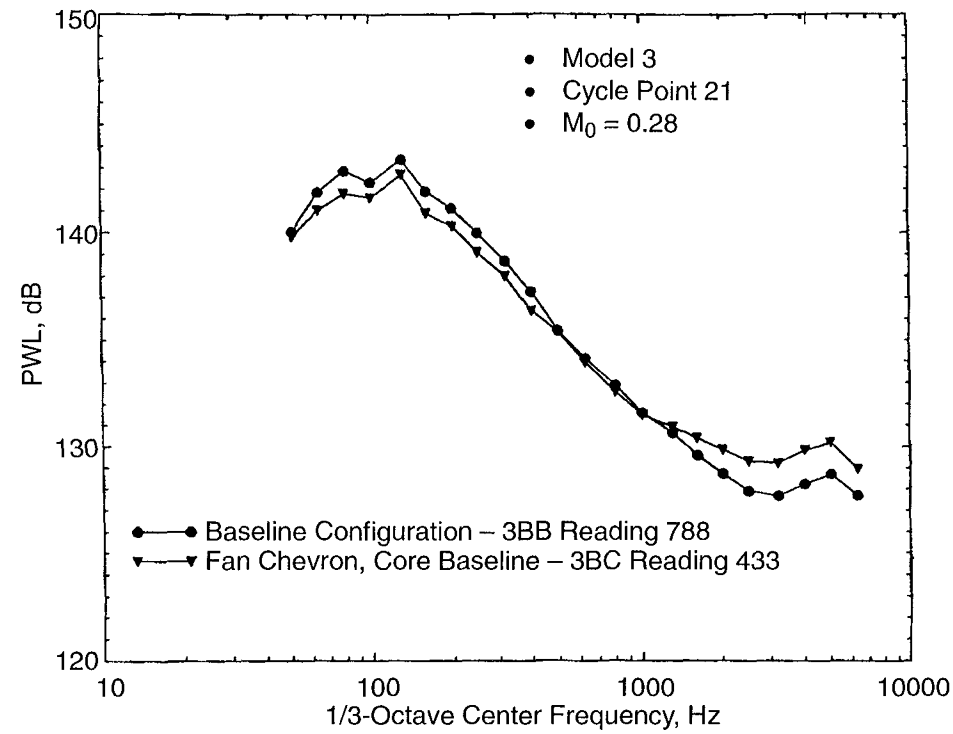


**Figure 98. Comparison of Sound Power for Fan Nozzle Chevrons (3BB and 3BC)**

### 6.1.3.2.3 Combined Core and Fan Nozzle Concepts

The results of testing the BPR = 5 external plug nozzle with combinations of fan and core mixing-enhancer concepts are discussed in this section. The tested nozzle combinations included the following:

1. Configuration 3C8C, 12-straight-core-chevron nozzle and 24-straight-fan-chevron nozzle (page 183)
2. Configuration 3C12C, 12-straight-core-chevron nozzle and 24-straight-fan-chevron nozzle (page 182)
3. Configuration 3IC, 12 inward-bent-core-chevron nozzle and 24-straight-fan-chevron nozzle (page 186)
4. Configuration 3AC, 12-alternating-bent-core-chevron nozzle and 24-straight-fan-chevron nozzle (page 187)

Figure 99 compares normalized EPNL for 3C8C, 3C12C, 3IC, 3AC, and the baseline 3BB configurations as a function of normalized $V_{mix}$ for the Mach 0.28 flight-simulation condition. Use of the chevron devices simultaneously on the fan and core nozzles reduces jet noise significantly. At the highest jet velocity points, configurations 3C8C, 3IC, and 3AC each provide a noise reduction in the neighborhood of 3 EPNdB. This is considered a major break-through in subsonic jet noise reduction technology.

While the fan chevron nozzle showed little benefit when used by itself, it is interesting to note that it increased the configuration noise benefits when combined with core chevron nozzles. Another interesting observation is that 3C12C provided approximately half the noise benefit relative to 3C8C. The difference between C8 and C12 lies solely in the number of chevrons. When these two configurations were individually tested on the core nozzle, with no

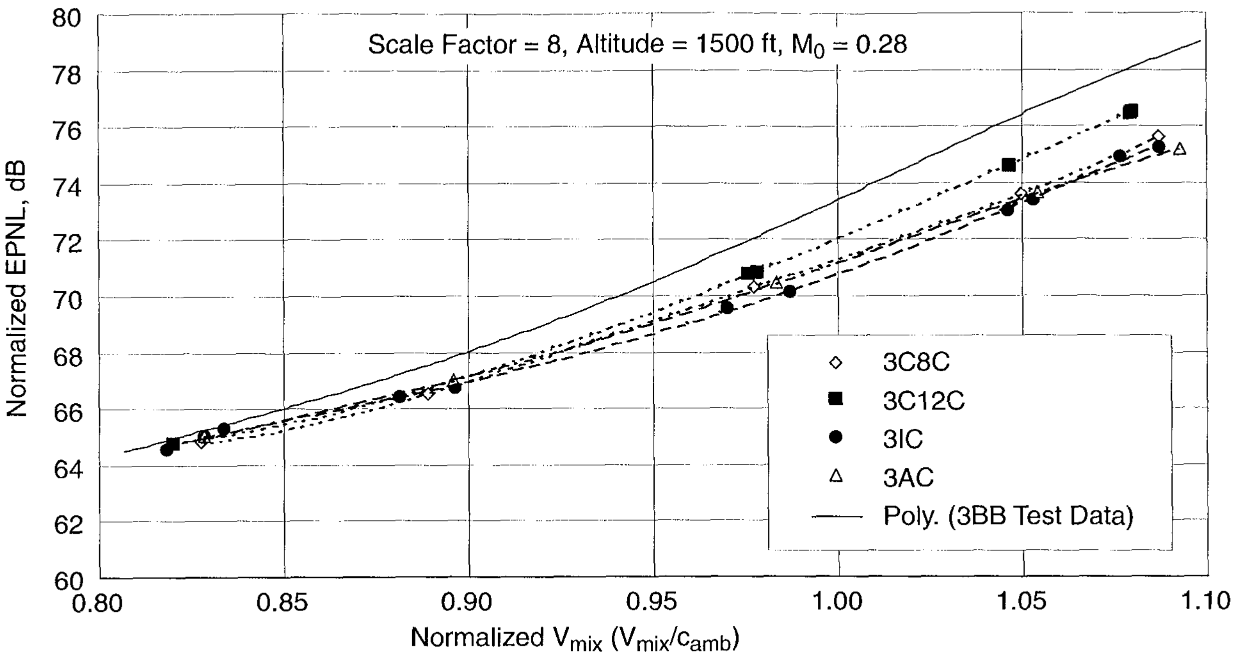


**Figure 99. Normalized EPNL Variation with Normalized $V_{mix}$: Baseline BPR = 5 External Plug Nozzle (3BB); Combined Core and Fan Chevron Nozzles (3C8C, 3C12C, 3IC, and 3AC)**

devices on the fan nozzle, there were no significant differences in the EPNL values of 3C8B and 3C12B (see Figure 88). This indicates that (1) there is a relationship between the number of chevrons on the core and the number of chevrons on the fan and (2) there is an interaction between the flow induced by the fan chevrons and that induced by the core devices.

The observation of an interactive effect between the core chevrons and fan chevrons is further clarified by the EPNL results presented in Figure 100. Here, the normalized EPNL of 3C8B and 3C12B are compared with the normalized EPNL of 3C8C and 3C12C as a function of normalized $V_{mix}$ for the Mach 0.28 flight-simulation condition. The open symbols are for core chevrons alone, and the closed symbols correspond to the same core configurations with the 24-chevron fan nozzle. The core-only configurations are very close in terms of EPNL. However, when the 24-chevron fan nozzle is added, the 8-chevron core becomes much more effective in jet noise reduction compared to the 12-chevron core. Hence, if the chevron noise-reduction concepts are to be applied both to the fan and core nozzles, this relationship between the number of chevrons on the core and the number of chevrons on the fan needs to be further investigated, understood, and optimized.

A comparison of the PNL directivities, the 1/3-octave spectra, and the Noy spectra (at three angles) for 3BB, 3C8C, 3C12C, 3IC, and 3AC configurations at cycle point 21 (Cycle 2) and Mach 0.28 flight-simulation conditions are presented in Figures 101 and 102 (see Appendix D for comparisons at all angles). The PNL directivity comparison indicates that core and fan chevron devices offer significant benefits. The peak PNL of 3IC (12 inward-flip chevrons on the core and 24 straight chevrons on the fan) is reduced by 3.5 dB relative to the 3BB baseline, and the peak PNL angle of 3IC is shifted to 110° relative to the 3BB peak PNL angle of 130°. Spectrally, observed low-frequency jet noise reduction is very impressive; SPL is reduced more than 5 dB. Configuration 3AC (12 alternating flip chevrons on the

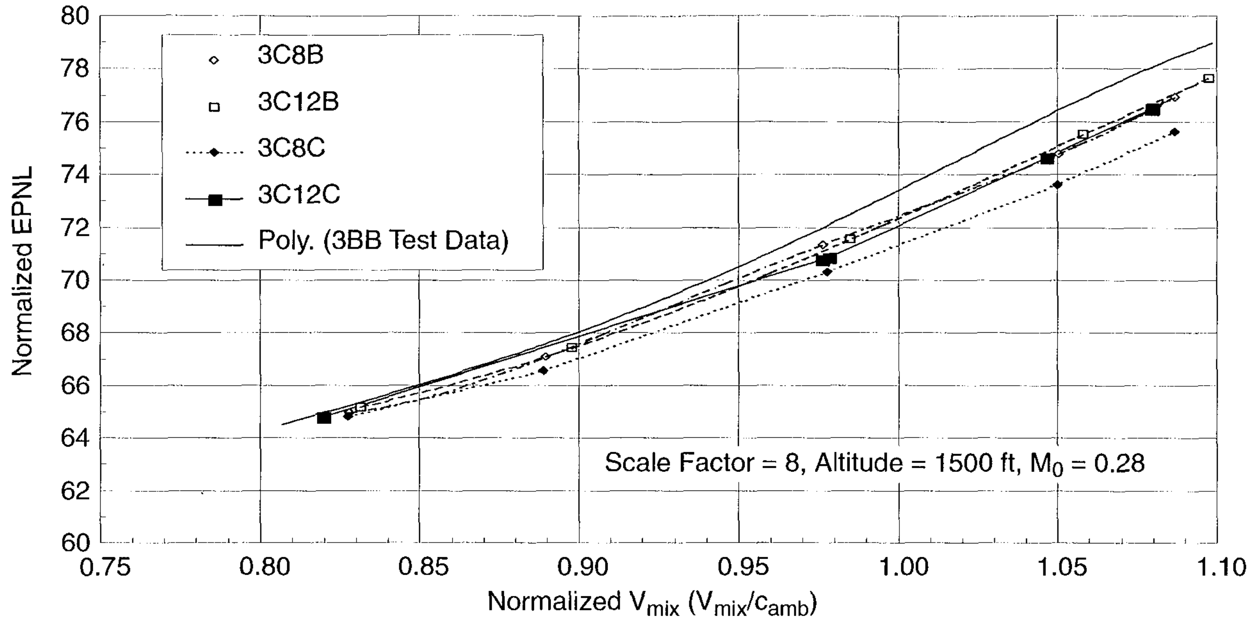


**Figure 100. Normalized EPNL Variation with Normalized $V_{mix}$: Baseline BPR = 5 Nozzle with External Plug (3BB); Effect of Fan Chevrons on Core Chevrons (3C8B, 3C12B, 3C8C, and 3C12C)**

core and 24 straight chevrons on the fan) provides the maximum jet noise reduction at low frequencies. It also generates significant noise in the medium- to high-frequency range. Configuration 3C8C does not show any increase in noise at high frequency.

Some of the above trends are also observed in the sound power spectra comparisons in Figure 103. This figure shows over 10 dB reduction in low-frequency noise for configuration 3AC; the next best configuration, 3IC, exhibits about 6 dB reduction in low-frequency noise. Configuration 3AC shows a high-frequency noise increase of 2 to 3 dB on a power spectrum basis. Configuration 3IC shows a smaller high-frequency noise increase of 1 to 1.5 dB in the power spectrum, and this does not show up in the SPL spectra.

In conclusion, several noise-reduction concepts tested on the BPR = 5 external plug nozzle were effective. Figure 104 is a summary of the EPNL benefits of all mixing devices tested with this model. At typical takeoff conditions, reductions of 1 to 2.5 EPNdB were observed for core devices only, with the inward-bent chevrons and alternating chevrons giving the best noise reduction. The fan nozzle chevrons by themselves did not yield significant noise reduction but significantly increased total exhaust system noise reduction when added to the core nozzle devices. As much as 3.5 EPNdB noise reduction was achieved with the combination of inward-bent chevrons on the core and straight chevrons on the fan. The straight 8-chevron core nozzle also gave good suppression in combination with 24 straight chevrons on the fan nozzle. An interactive effect of fan and core chevron number was deduced, but additional study is needed to enable exploitation of the effect.

#### 6.1.3.3 External Plug BPR=8 Configurations

A limited number of noise-reduction concepts were tested on the BPR = 8 external plug nozzle, Model 5 shown in Figure 14. The configurations tested included the following:

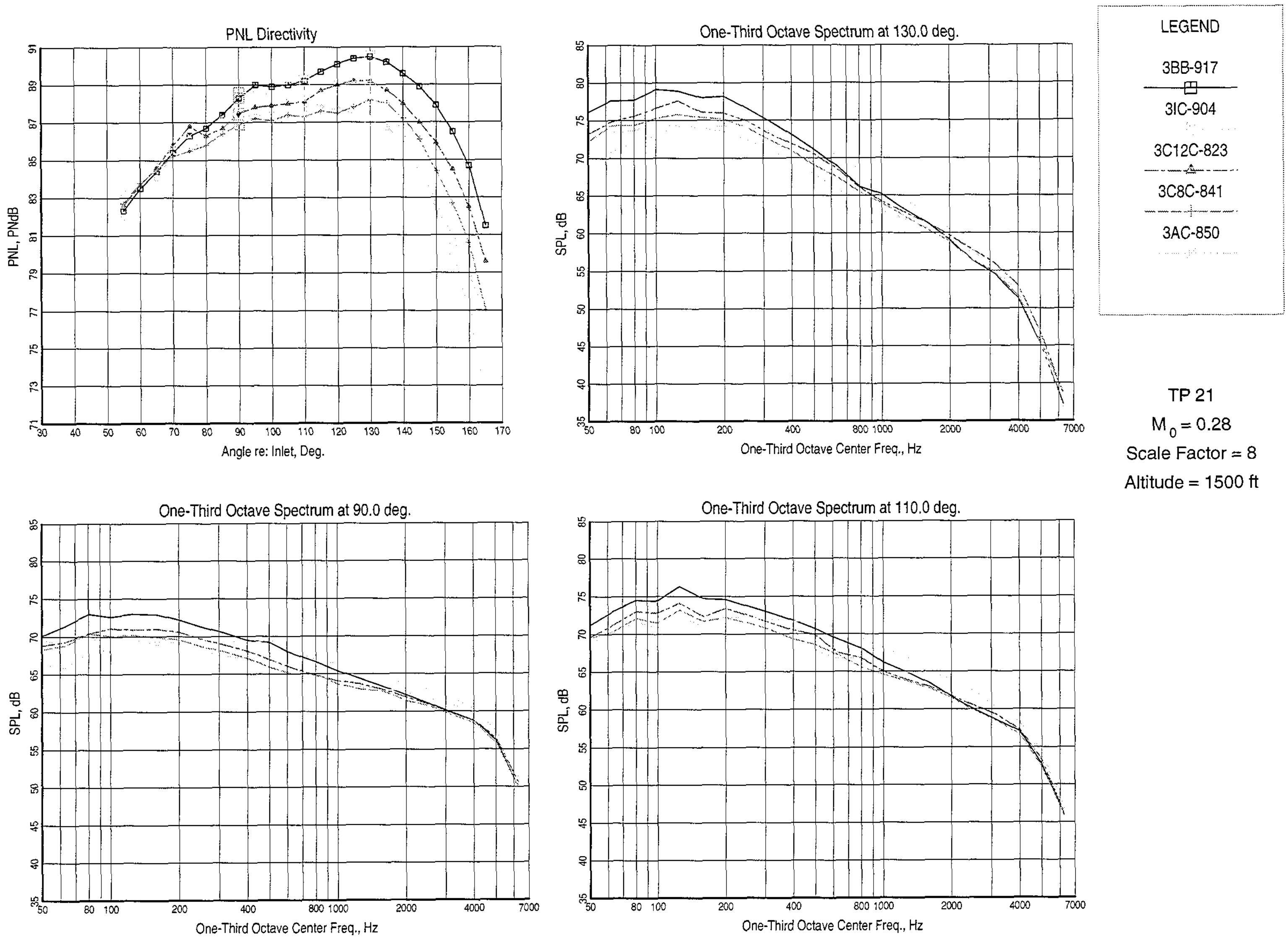


**Figure 101. PNL Directivity and SPL Spectra: Baseline BPR = 5 External Plug Nozzle (3BB); Combined Fan and Core Chevron Nozzles (3C8C, 3C12C, 3IC, and 3AC)**

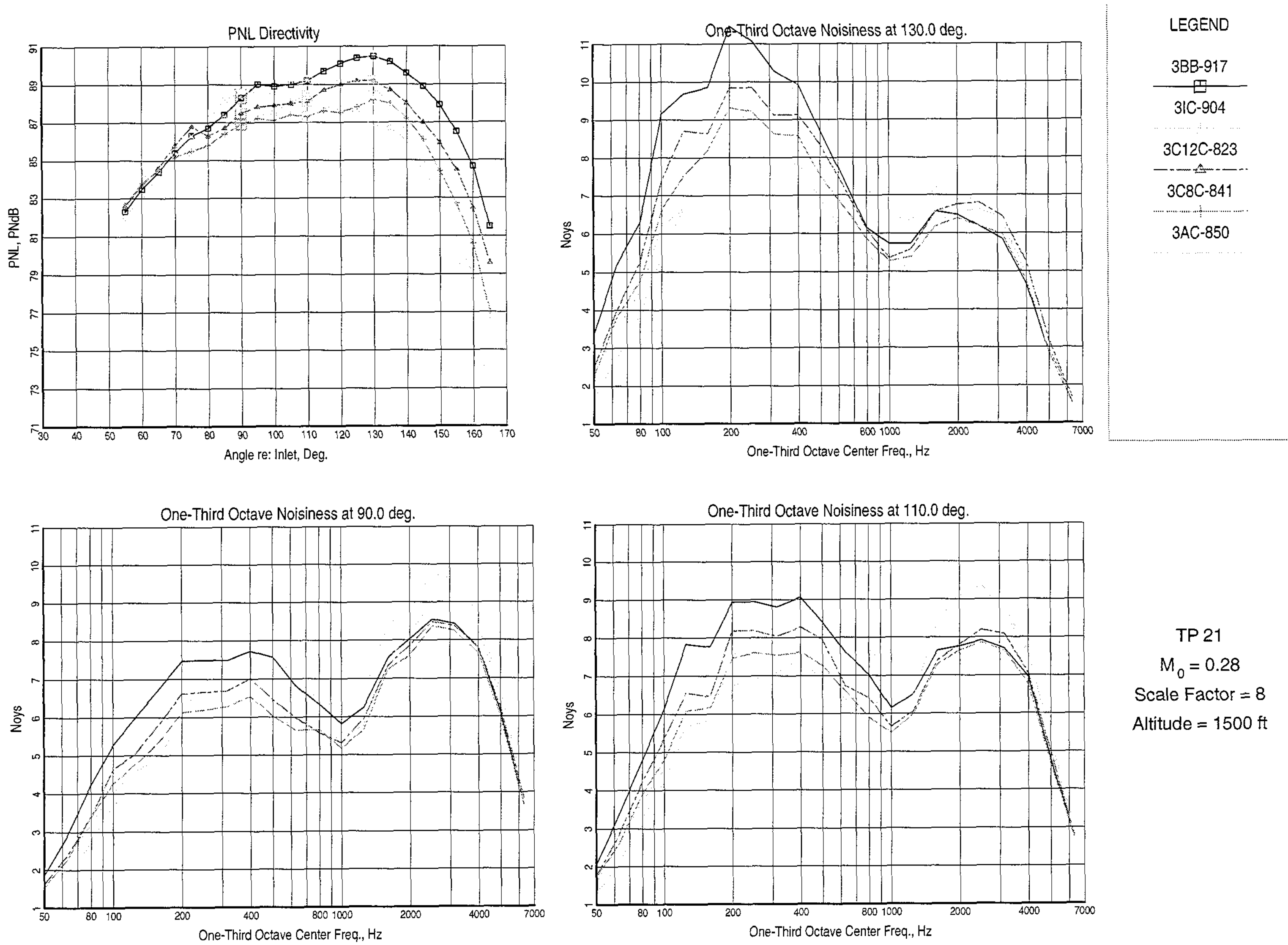


**Figure 102. PNL Directivity and Noy Spectra: Baseline BPR = 5 External Plug Nozzle (3BB); Combined Fan and Core Chevron Nozzles (3C8C, 3C12C, 3IC, and 3AC)**

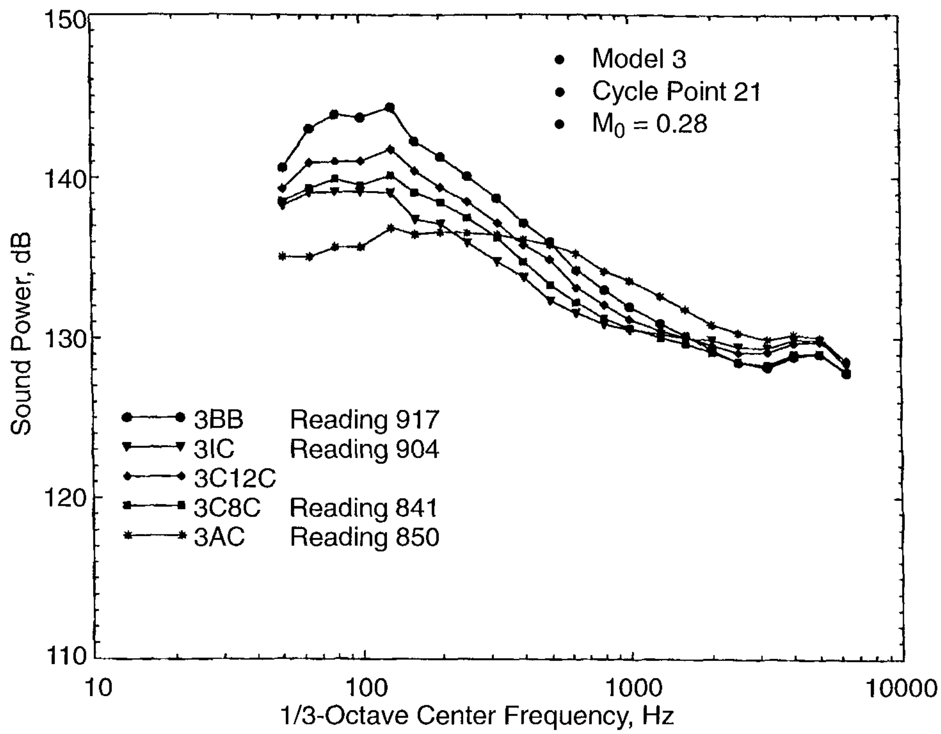


**Figure 103. Comparison of Sound Power for Combined Fan and Core Chevron Nozzles (3BB, 3C8C, 3C12C, and 3AC)**

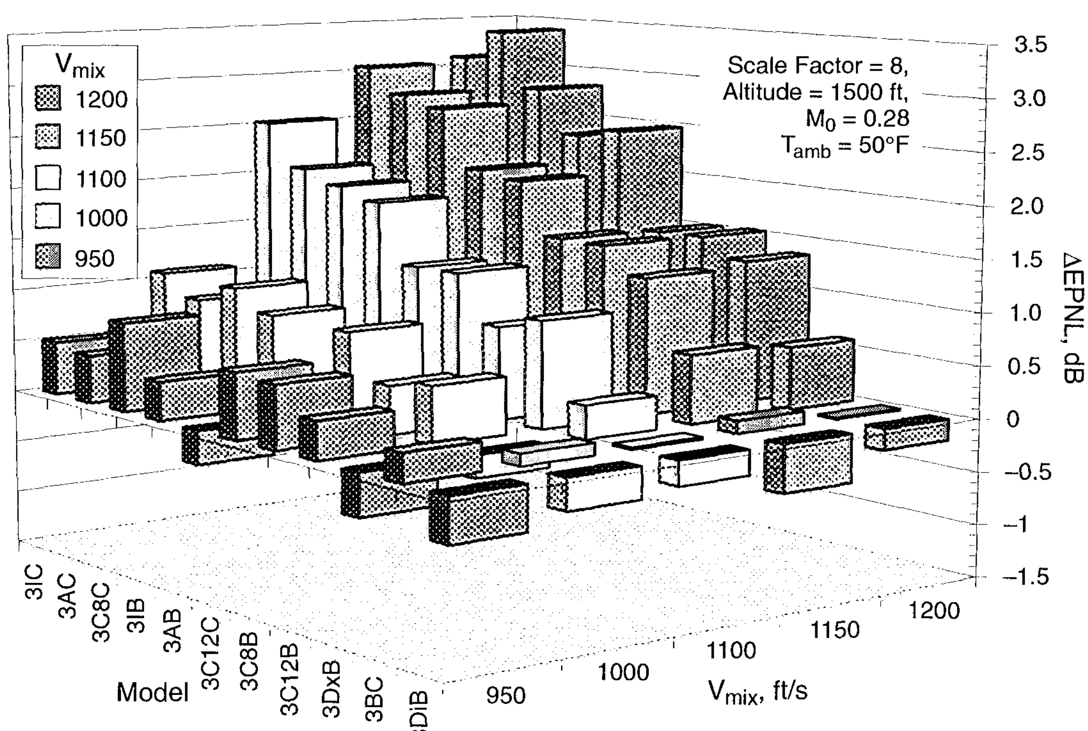


**Figure 104. Mixing Enhancer Noise Benefits Relative to Baseline BPR = 5 External Plug Nozzle (Model 3)**

1. Configuration 5C12B, 12-straight-chevron core nozzle (page 194)
2. Configuration 5BC, 24-chevron fan nozzle (page 192)
3. Configuration 5C12C, 12-straight-chevron core nozzle and 24-chevron fan nozzle (page 193)

Figure 105 compares the normalized EPNL of 5C12B, 5BC, 5C12C, and the baseline 5BB nozzle as a function of normalized $V_{mix}$ for the Mach 0.28 flight–simulation condition. The results for the BPR = 8 model are somewhat different than those of the BPR = 5 model. When separately tested, the fan-chevron configuration (5BC) is more effective than the core-chevron configuration (5C12B). When tested together (5C12C), there is no significant increase in the noise benefit when compared to the fan-alone chevron configuration (5BC). The fan-chevron alone configuration 5BC seems to give the best noise reduction, around 0.8 to 1.2 EPNdB at high power. It is to be expected that, as bypass ratio increases, fan nozzle mixing-enhancement devices will be more effective than core nozzle mixing devices because core flow is a smaller fraction of the total flow, and core velocity is lower for a given thrust. In addition, the fan-to-ambient shear layer contribution to the jet mixing noise increases with increasing bypass ratio.

Comparisons of the PNL directivity, 1/3-octave SPL spectra, and Noy spectra (at three angles) for 5BB, 5C12B, 5BC, and 5C12C at cycle point 41 (Cycle 4) and Mach 0.28 conditions are presented in Figures 106 and 107. The PNL directivity shows that the chevrons affect angle as well as the magnitude of peak PNL. Because of a noise decrease in the aft quadrant, the chevron configurations move the peak PNL forward to about 95°. In terms of SPL, the fan chevrons provide the most benefit at the lower frequencies. Some noise increases at high frequency and at some aft angles were also observed. Overall, the core chevrons were less effective for the higher bypass ratio nozzle. This probably is to be expected, since the jet velocities are generally lower for higher bypass ratio nozzles.

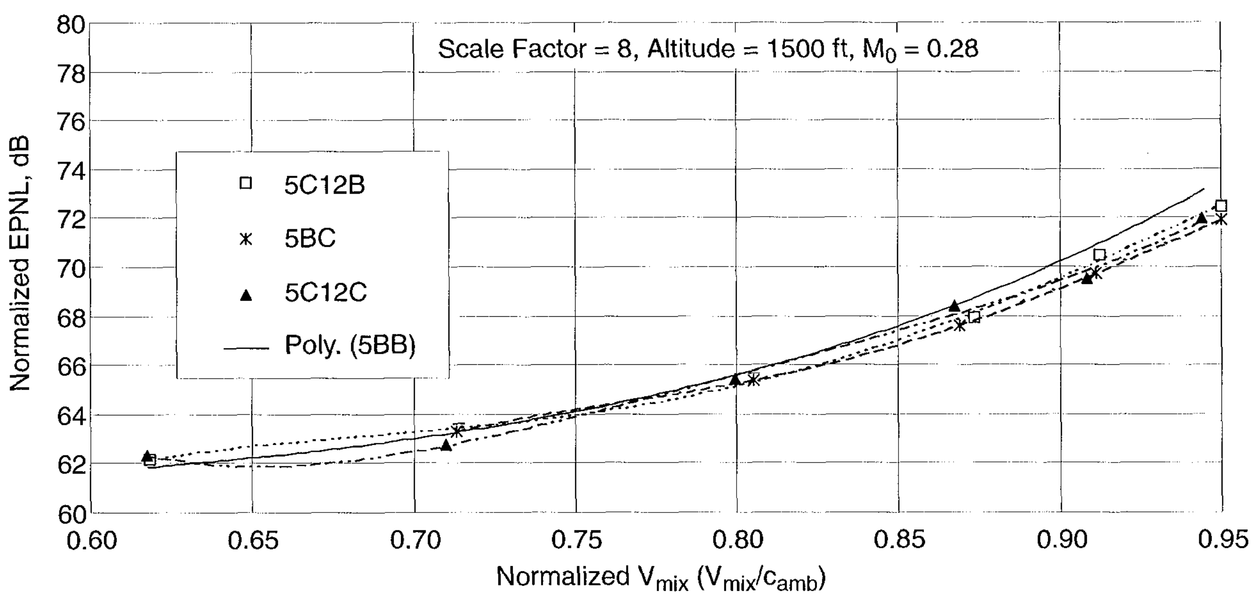


**Figure 105. Normalized EPNL Variation with Normalized $V_{mix}$: Baseline BPR = 8 Nozzle with External Plug (5BB); Fan, Core, and Combined Chevron Nozzles (5C12B, 5BC, 5C12C)**

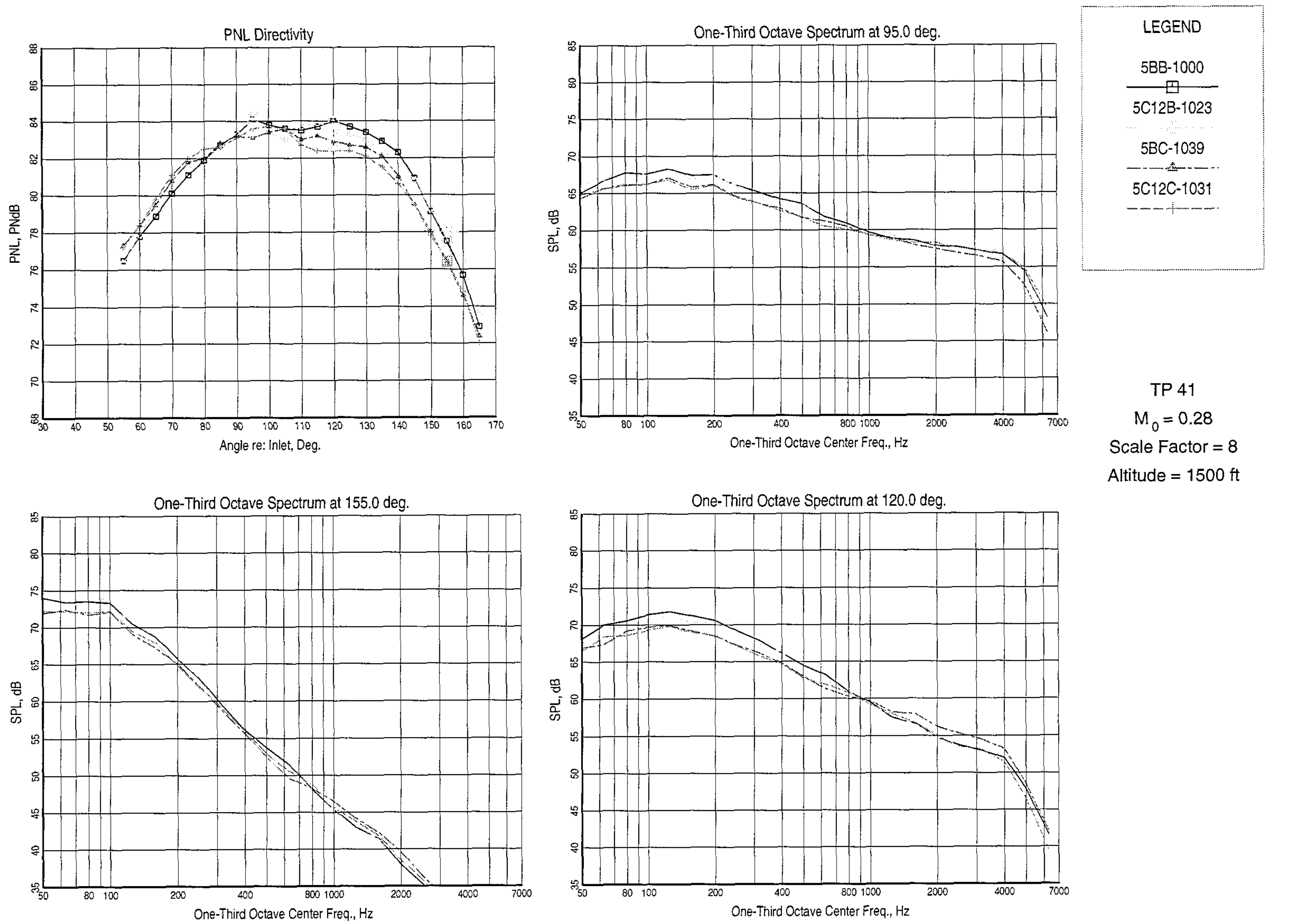


**Figure 106. PNL Directivity and SPL Spectra: Baseline BPR = 8 External Plug Nozzle (5BB); Core, Fan, and Combined Chevron Nozzles (5BB, 5C12B, 5BC, and 5C12C)**

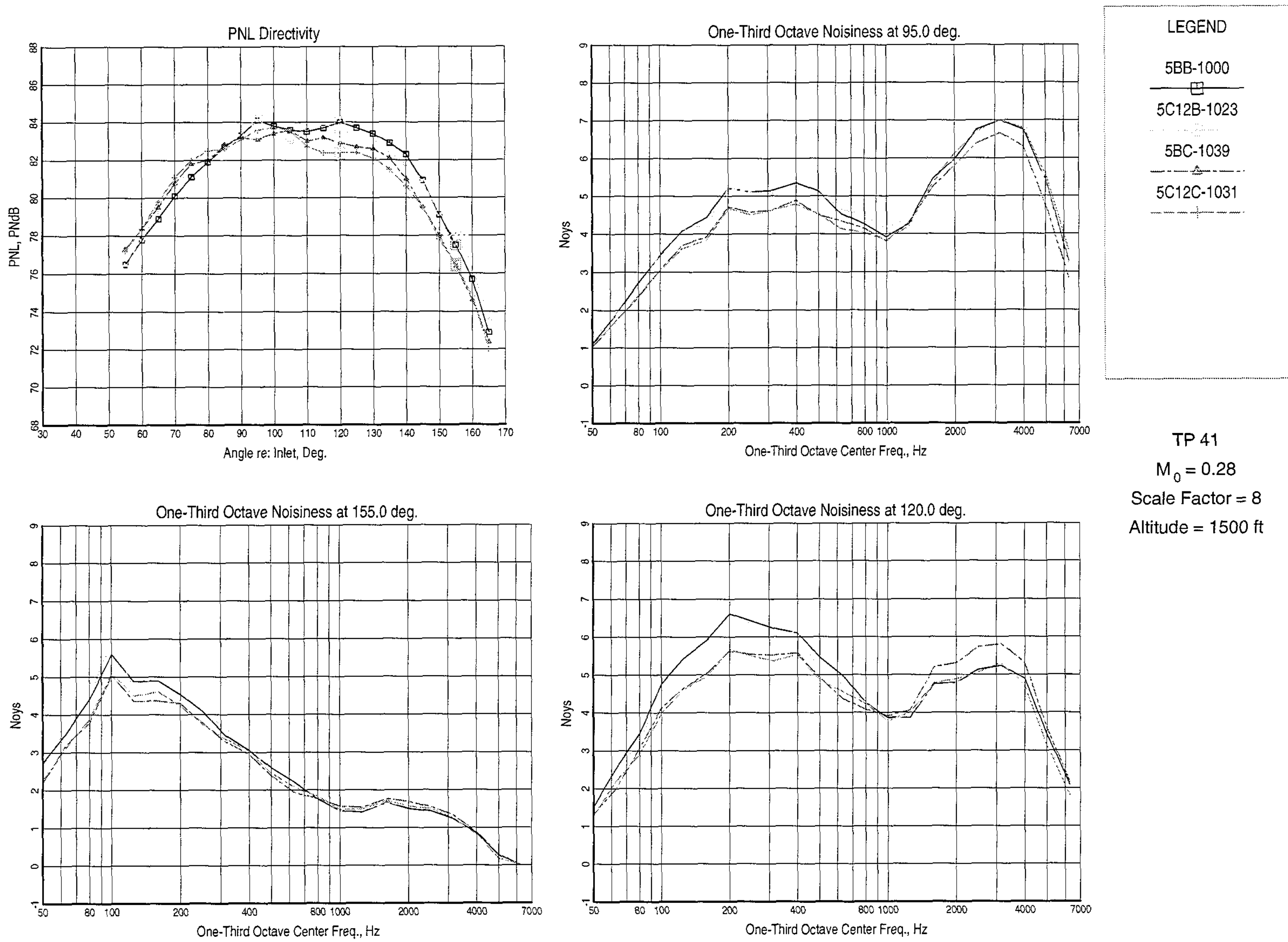


**Figure 107. PNL Directivity and Noy Spectra: Baseline BPR = 8 External Plug Nozzle (5BB); Core, Fan, and Combined Chevron Nozzles (5BB, 5C12B, 5BC, and 5C12C)**

Some of the above trends are again observed in the sound power spectra comparisons presented in Figure 108. The fan chevron configurations give the best noise reduction at the lower frequencies.

## 6.2 Nozzle Plume Survey Results

Jet plume temperature and total pressure surveys were made by NASA Lewis on the BPR = 5 external plug nozzle configurations, following the acoustic tests, to provide diagnostic information on how the mixing devices alter or change the jet mixing process and jet plume development. In turn, the changes in jet plume mixing and structure can offer additional insight as to why some mixing devices were successful and some were not. Ultimately, it was hoped that the changes in flow field can be related to the jet noise generation process through theoretical notions of the fundamental physics. In this section, selected results of the temperature survey measurements for 3BB and 3IB configurations are summarized. The data are compared in terms of an axial temperature profile and cross-sectional temperature profiles at a number of axial locations (refer to Section 5.5 for details).

Temperature profiles along a nozzle radial/axial center plane, ranging from 0.5 to approximately 88 inches downstream of the plug trailing edge, are shown in Figure 109 for configurations 3BB and 3IB. The inward-flip chevron has clearly decreased the length of the hot potential core by a factor of two, indicating that the inward-bent-chevron device dramatically increases the jet plume mixing rate.

Figure 110 compares cross-sectional (radial/circumferential plane) temperature profiles at a

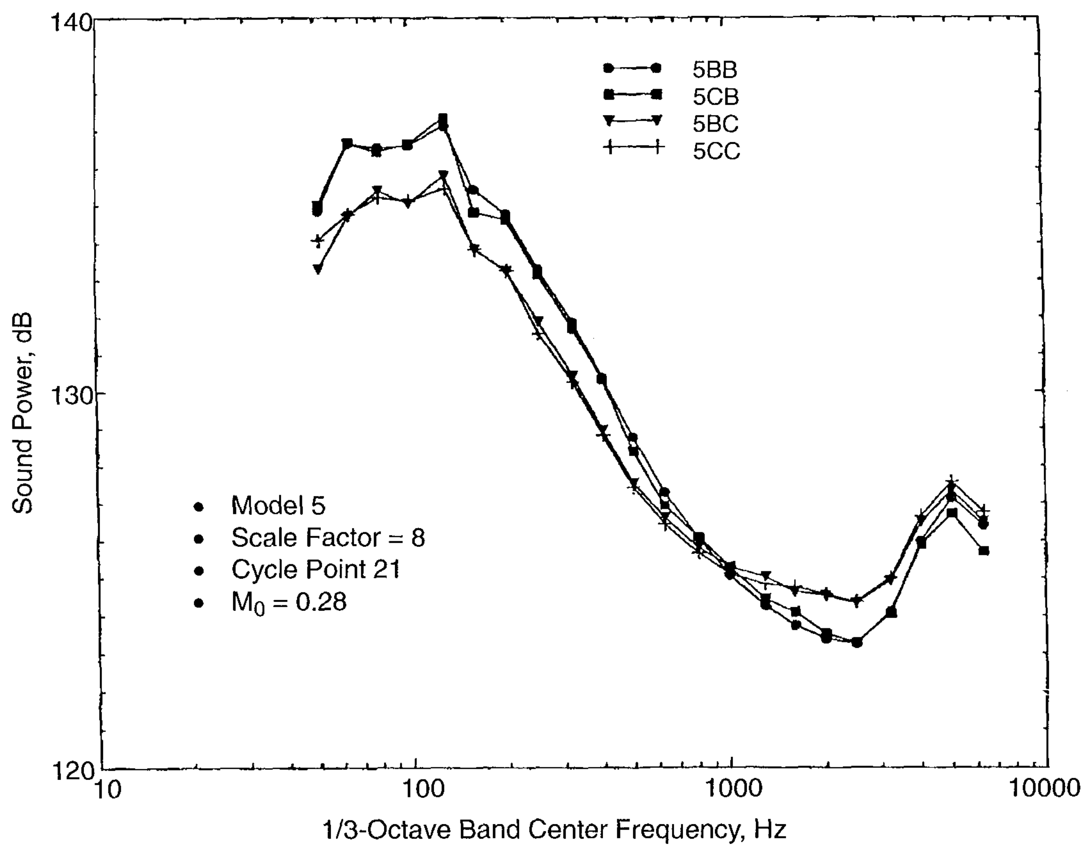


**Figure 108. Comparison of Sound Power for Core, Fan, and Combined Chevron Nozzles (5BB, 5C12B, 5BC, and 5C12C)**

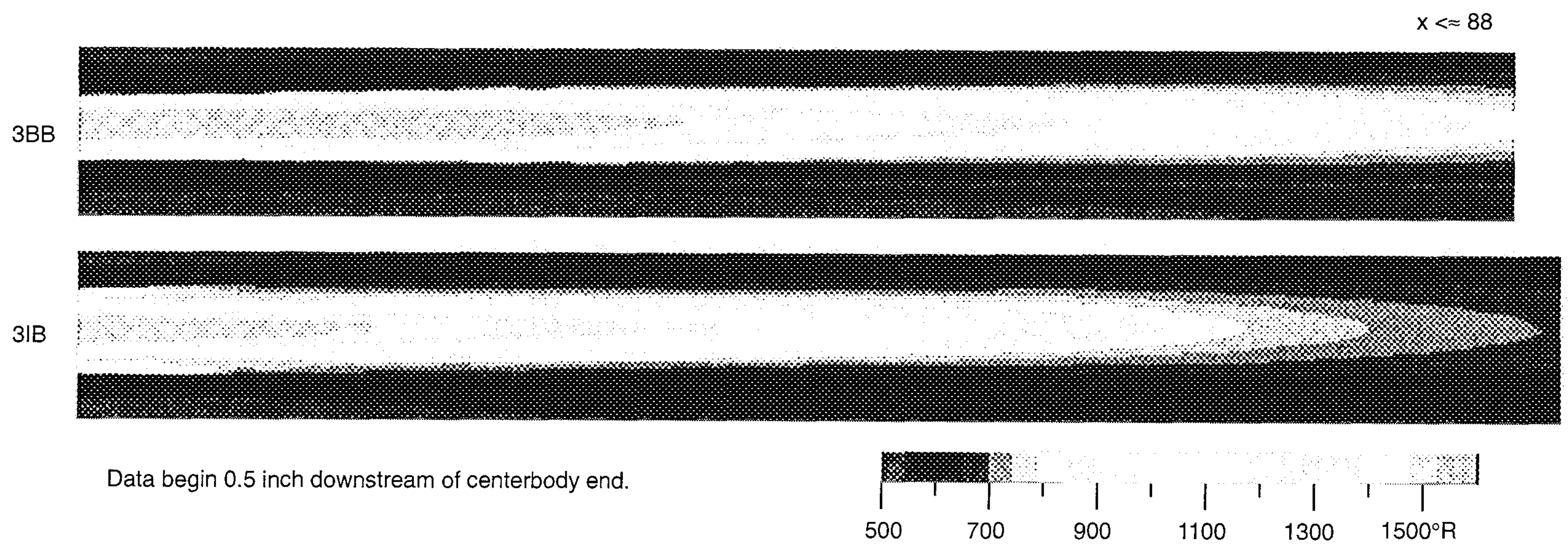


**Figure 109. Total Temperature Profiles Along the Nozzle Centerline (3BB and 3IB)**

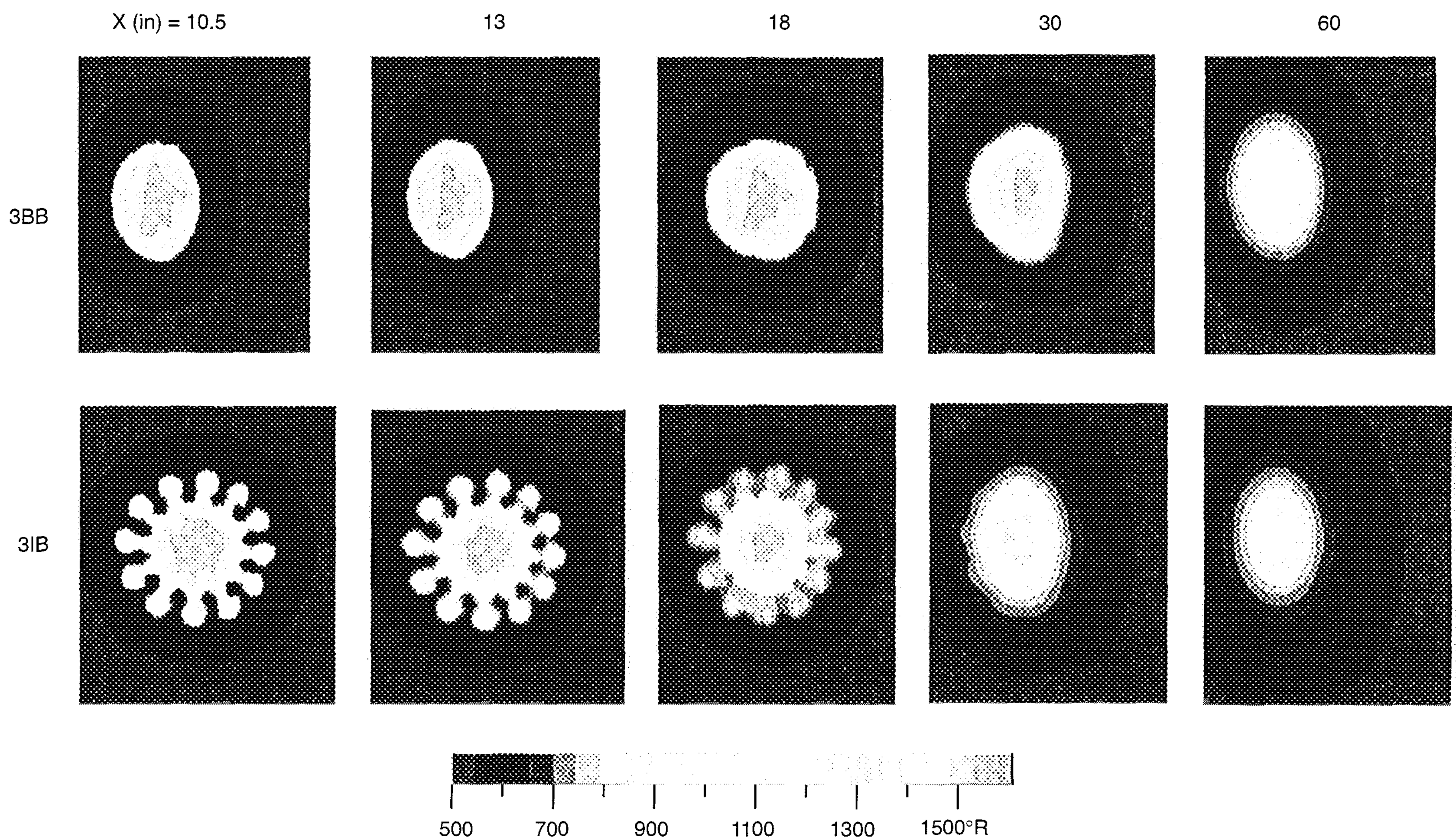


Figure 110. Total Temperature Plume Survey Axial Slices (3BB and 3IB)

number of axial locations corresponding to the results for configurations 3BB and 3IB shown in Figure 109. A round, hot, core flow; a round, cooler, fan flow; and a shear layer between the core and fan streams are discernible for the 3BB baseline nozzle. The hot core persists for a significant axial distance downstream of the exhaust. The cross-sectional temperature profiles of the 3IB configuration indicate cross flow of the hot core and cooler fan streams. The cross-sectional temperature profiles exhibit patterns similar to those of a 12-lobed forced mixer. Each of the 12 chevrons has created a strong vortex pattern, and this has greatly increased the mixing between the core and fan streams, thus reducing the hot potential-core length relative to that of the baseline nozzle. At the fourth measurement location (x = 30 in), there is no identifiable hot core for the 3IB configuration. For the baseline 3BB configuration, a significant amount of hot core flow still exists at this location.

The above flow field surveys support the hypothesis that the chevrons generate large-scale longitudinal vortices that entrain fan flow into the core flow on one side of the vortex and entrain core flow into the fan stream on the other side of the vortex. This results in a lobular structure like that produced by a forced lobe-mixer. The effective perimeter of the mixing layer between the two streams is therefore increased and produces more rapid jet plume decay with axial distance. The successive axial slices shown in Figure 110 support the hypothesis of increased mixing perimeter.

Additional contour plots of this type were published by NASA at the Separate Flow Nozzle Test Status Meeting Proceedings (Reference 29). Velocity contours were deduced from total pressure and total temperature surveys, in both a centerplane along the plume, and at selected axial stations normal to the plume axis, as shown in Figure 111 (see Section 5.5 for details). Selected samples of these types of plots are shown in Figures 112 through 116 for configurations 3BB, 3AB, 3C8B, 3IB, and 3IC24. On these plots, the "yellow" contour areas represent midway between the core

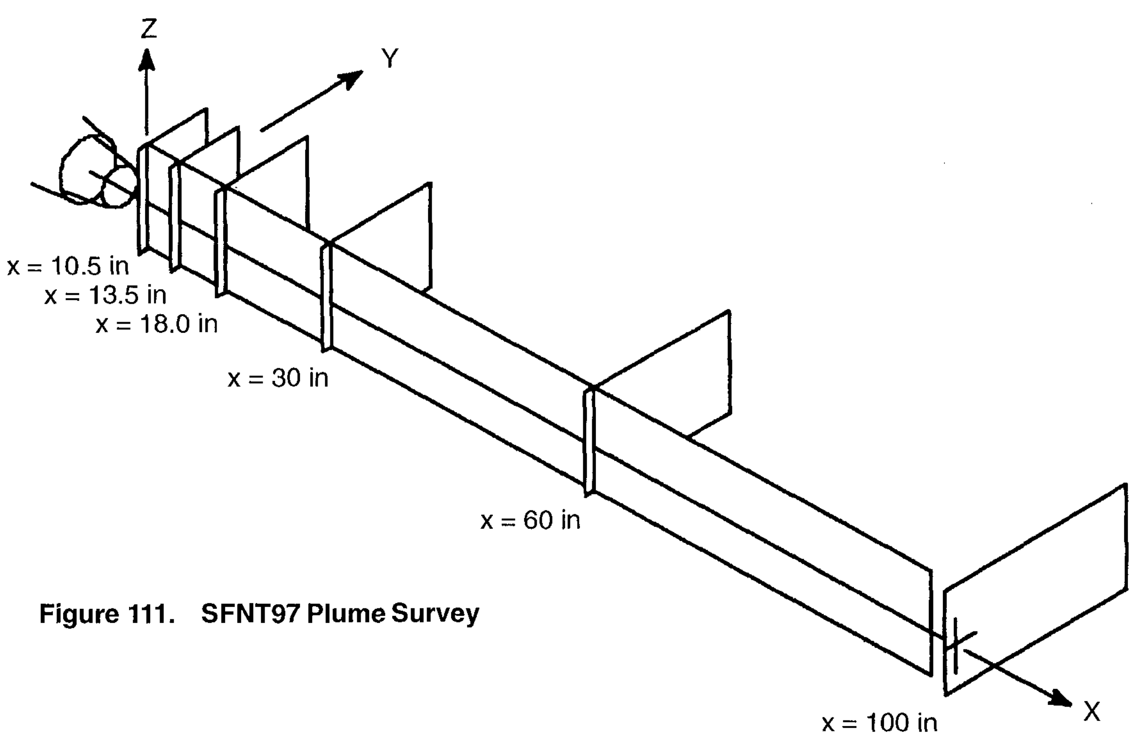


**Figure 111. SFNT97 Plume Survey**

velocity and the fan velocity. This yellow band can be considered a measure of the mixing-layer perimeter.

Figure 112 shows the cross-sectional velocity contours, at a station 10.5 inches downstream of the plug tip, for the above five configurations. Note that, relative to the baseline 3BB nozzle, the yellow band representing mixing-layer perimeter is considerably longer for the chevron nozzles, thus validating the hypothesis that the mixing layer perimeter is increased by the vortex entrainment process. It is observed that the alternating chevron produces 6 lobes around the perimeter, rather than 12, and that the 3IB nozzle actually forms discrete jets rather than lobes, as a result of the stronger vortex formations due to the chevron inward bend. The CFD analysis results reported in Sections 3.3 and 3.4 predicted formation of a longitudinal vortex by the chevrons, and this is certainly substantiated by these flow field measurements.

Figure 113 shows the cross–section velocity contours at a station 13.5 inches downstream of the plug tip. These contours look similar to those in Figure 112, but the lobes have grown in size and extent, and the regions of highest velocity are smaller for the 3IB and 3IC24 nozzles relative to the baseline 3BB nozzle. Contour plots for stations 18 inches, 30 inches, and 60 inches downstream of the plug tip are shown in Figures 114, 115, and 116, respectively. At farther downstream stations, the lobular structure loses its identity, and the plume becomes more axisymmetric in velocity profile, while the regions of highest velocity from the core stream are smaller relative to the baseline plume.

Figure 117 shows a distribution of the jet plume maximum velocity near the core centerline, as a function of axial distance downstream of the plug tip, for Configurations 3BB, 3C8B, 3C12B, 3AB, and 3IB. The 3IB configuration produces a modest reduction in peak velocity in the range of 40 to 60 inches downstream, but configuration 3AB produces a much more dramatic reduction over most of the jet plume axial extent. In contrast, the straight-chevron configurations, 3C8B and 3C12B, have only a small effect on the plume centerline velocity decay.

Figure 118 is a similar plot for configurations 3IB, 3IC24, 3C12B, and 3C12C24. This plot shows the influence of the fan chevrons (24 in both cases) on plume development for two core chevron types: 12 inward flip and 12 straight. In both cases, the addition of the fan chevron retarded plume maximum velocity decay, particularly beyond 40 inches downstream. This is in spite of the fact that lower noise levels were achieved with the addition of fan chevrons to the core chevron configurations.

## 6.3 Diagnostic Evaluation of Noise Reductions

It is of interest to see if observed noise reductions for the various concepts tested can be explained by the observed and/or computed flow field changes and, further, be related to the prevailing theoretical concepts for how jet-mixing noise is generated. The framework selected for this diagnostic evaluation is the MGB jet noise prediction model, documented in References 30–33. This model is based on the jet being acoustically equivalent to a distribution of uncorrelated, convecting sources. These sources are assumed to be turbulent shear stress quadrupoles; the source strengths and frequency spectra are related to the mean (steady) flow field velocity and temperature distributions and uses an isotropic turbulence model for defining the turbulent shear stresses and corresponding noise source strengths.

In Reference 33, a systematic study was carried out, using the MGB model, to explain the differences between an unsuppressed baseline nozzle and a multichute suppressor nozzle. The

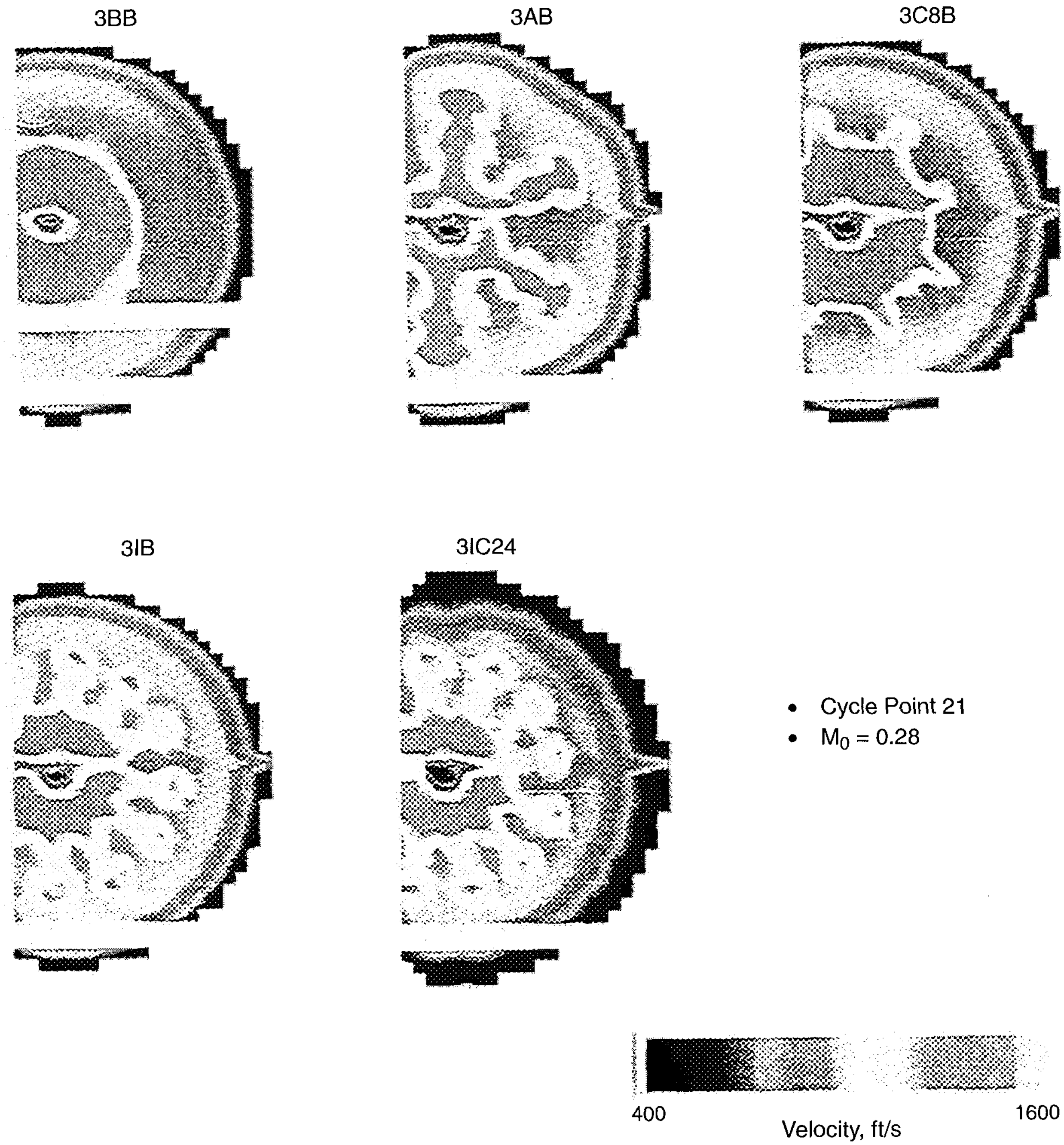


**Figure 112. Mean Velocity Field Contours 10.5 Inches Downstream of Plug Tip**

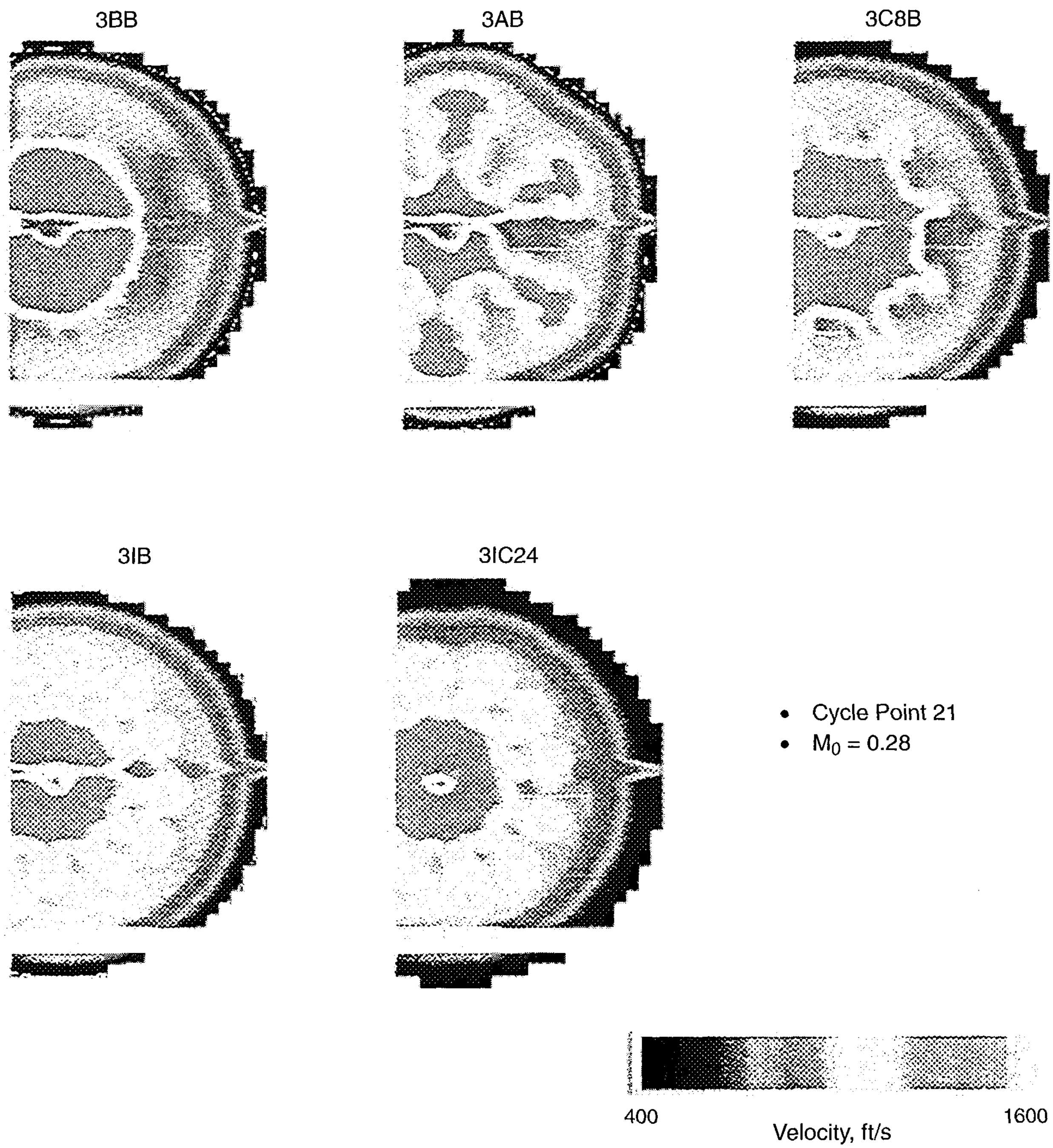


**Figure 113. Mean Velocity Field Contours 13.5 Inches Downstream of Plug Tip**

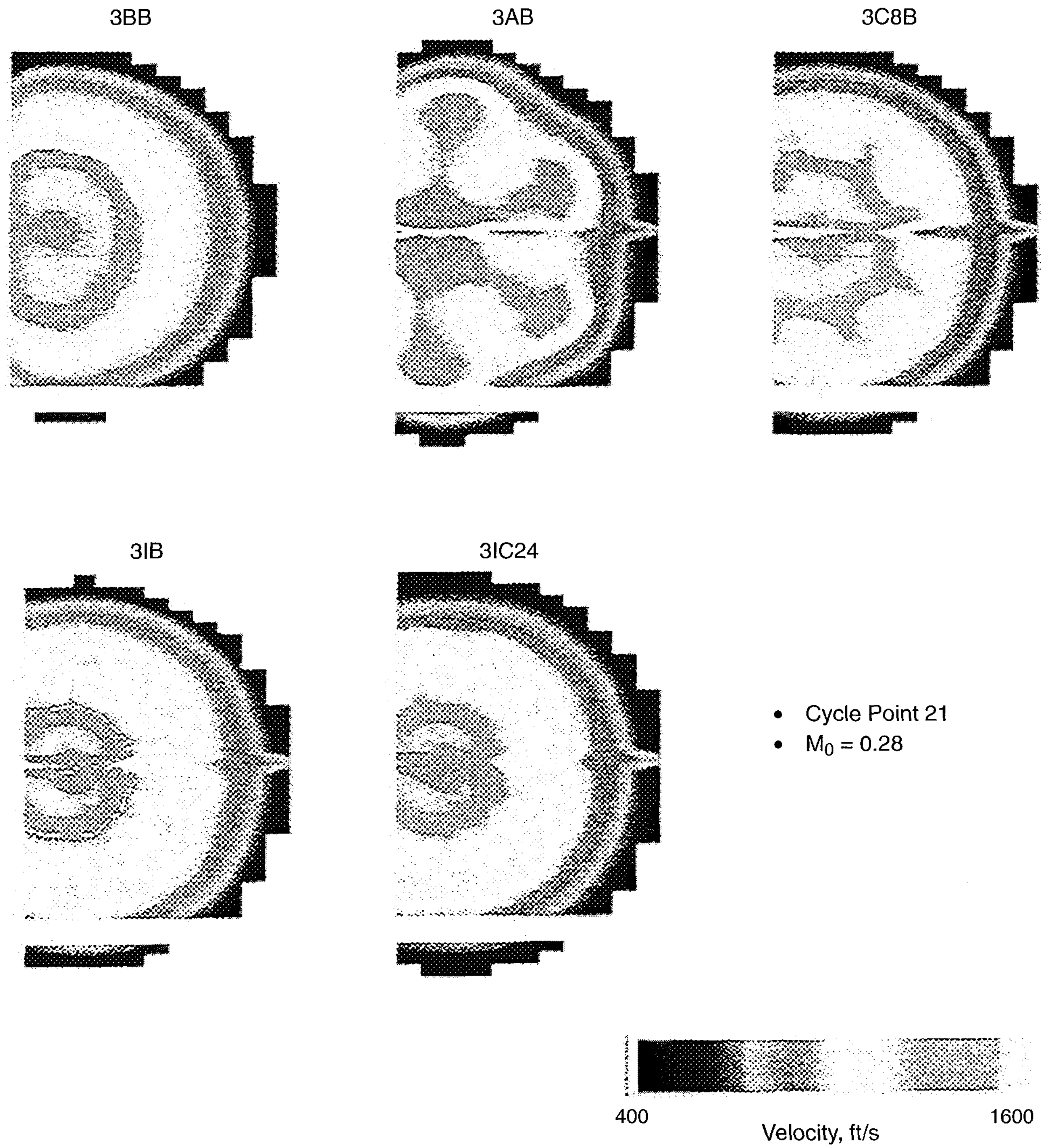


**Figure 114. Mean Velocity Field Contours 18 Inches Downstream of Plug Tip**

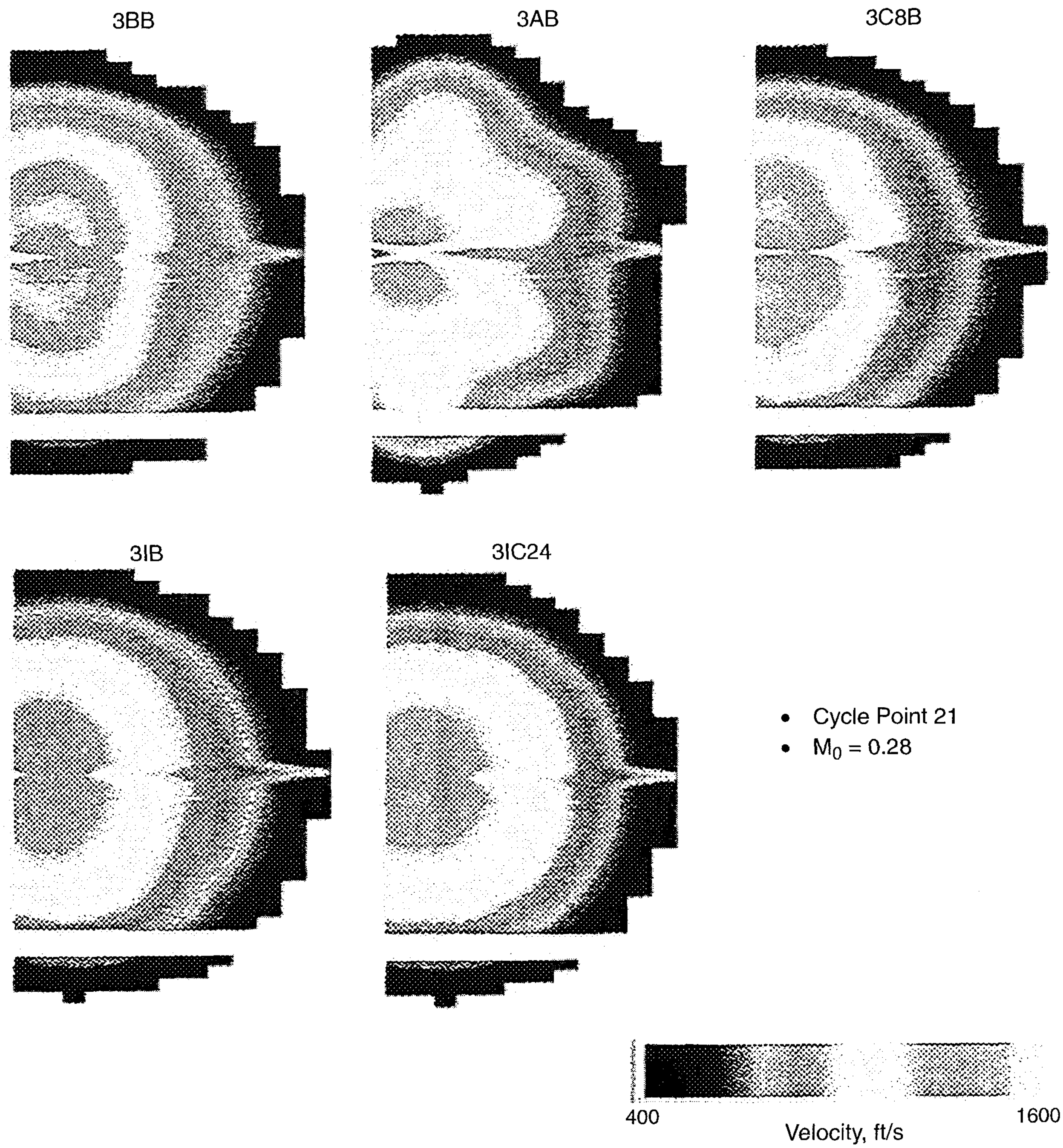


**Figure 115. Mean Velocity Field Contours 30 Inches Downstream of Plug Tip**

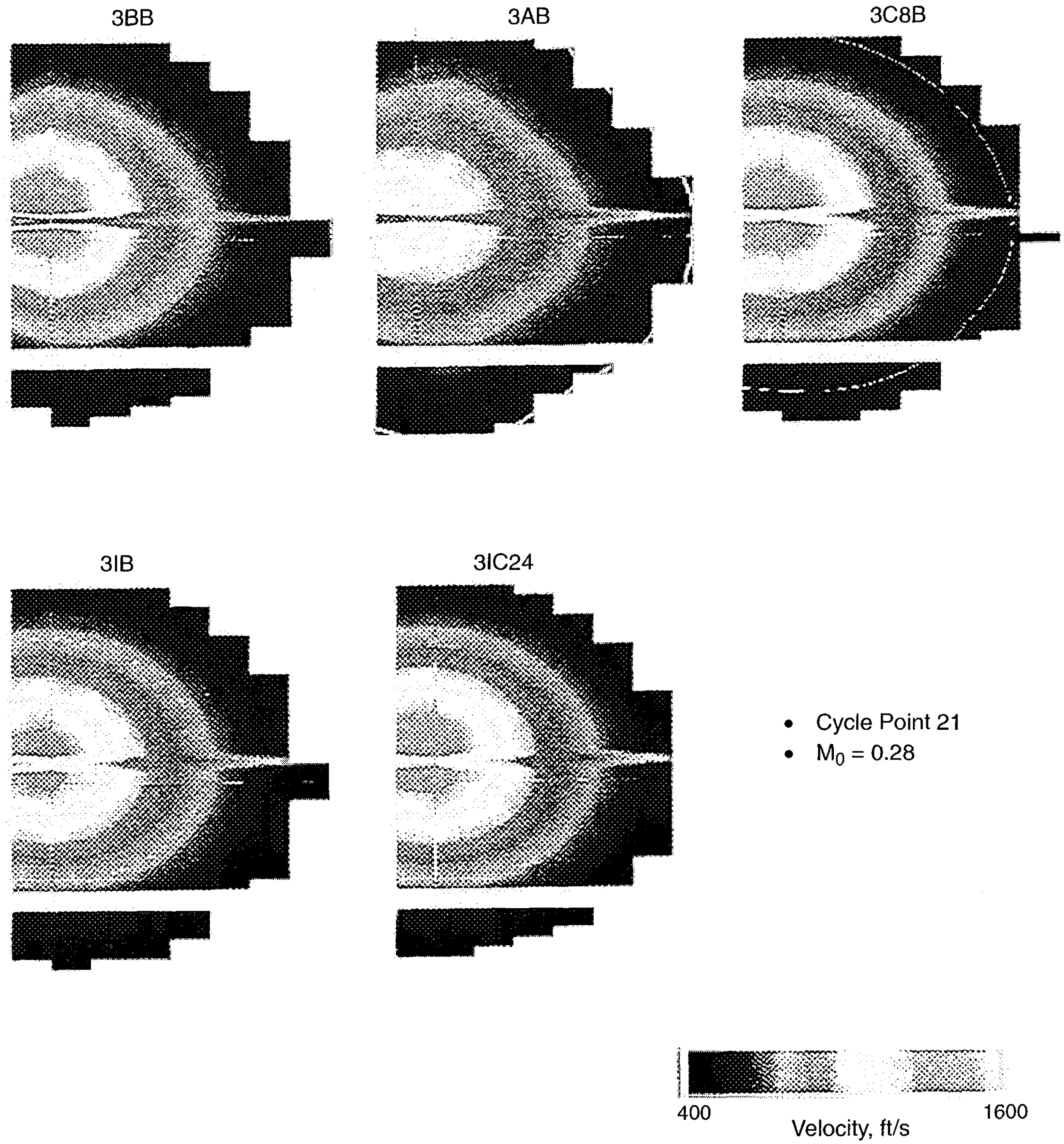


**Figure 116. Mean Velocity Field Contours 60 Inches Downstream of Plug Tip**

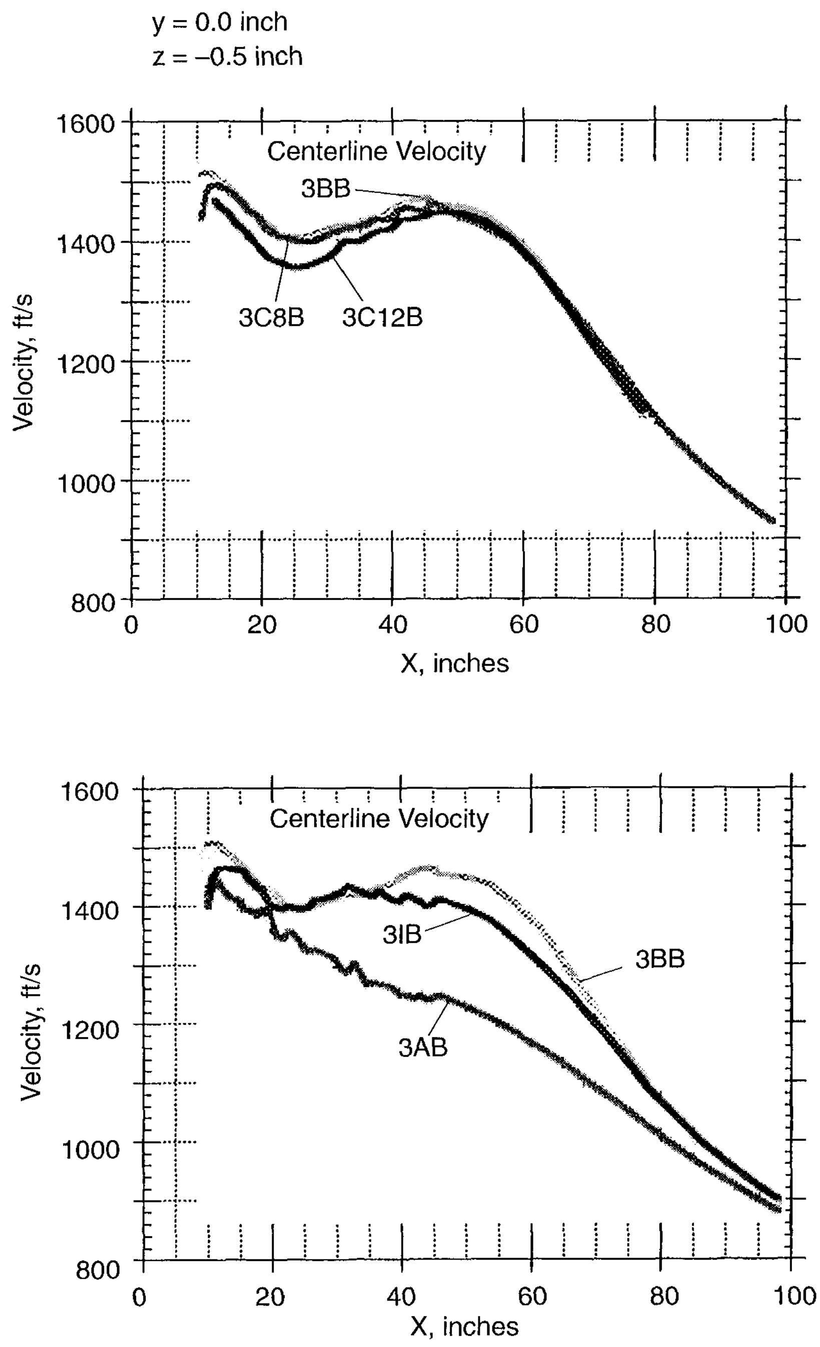


**Figure 117. Velocity Profiles: Core Chevron Comparisons**

y = 0.0 inch
z = –0.5 inch

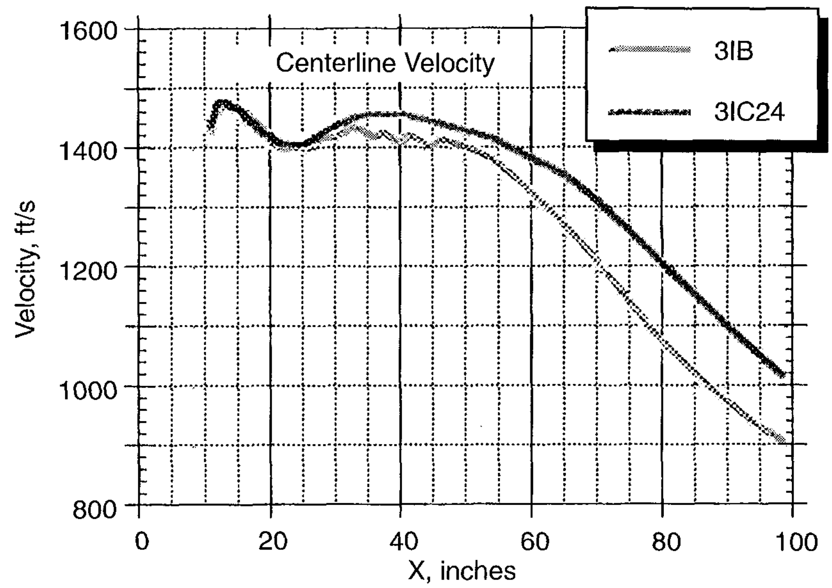


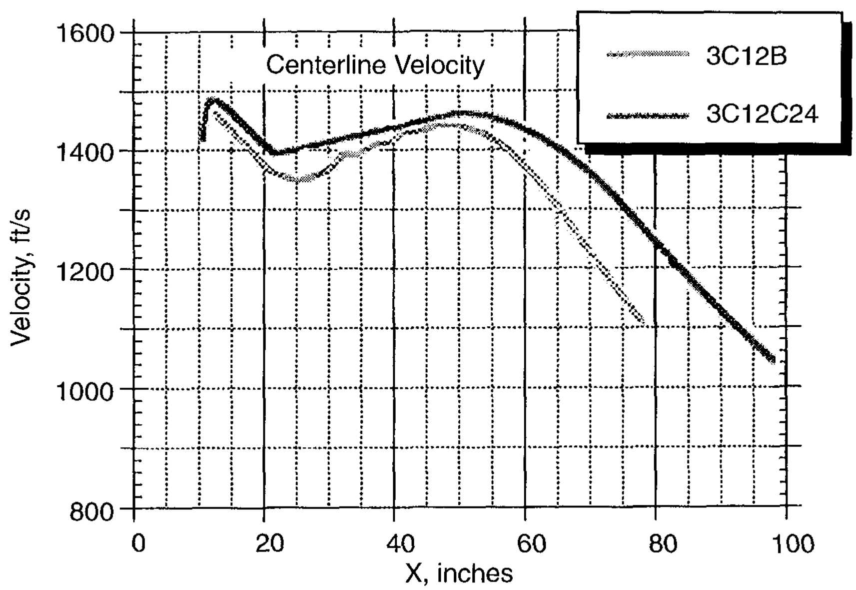


**Figure 118. Velocity Profiles: Fan Chevron Comparisons**

study showed that the basic noise characteristics were dependent on three physical processes involved in jet mixing:

1. Noise source generation
2. Noise source convective amplification
3. Noise source jet shielding (refraction and shielding)

These processes depend on the flow field characteristics: jet radial velocity profiles, temperature profiles, shear gradients, axial plume decay rates, etc. The MGB code quantifies these relationships, and the code can be used to separate the effects of these basic processes. Although the limitations of MGB may preclude quantitatively accurate simulation of, for example, chevron-nozzle noise generation, the modeling concepts can be used in a qualitative sense to rationalize the results of this test program. The following paragraphs discuss the observed noise reductions in relation to the measured flow field survey results and attempt to establish a plausible connection to the MGB paradigm for jet noise generation and reduction.

All of the flow field survey data were taken on Model 3, the BPR = 5 external plug nozzle, because it was on this baseline that the best noise-reduction devices were tested. The following diagnostic evaluations will therefore be confined to the Model 3 baseline nozzle and selected noise-reduction devices tested on that configuration.

### 6.3.1 Source Intensity Noise Generation Diagnostic Evaluation

As discussed previously, three basic physical processes determine the noise produced by jet mixing. The first process, turbulent source sound generation, is a function of the turbulence intensities produced in the jet mixing process. The dominant frequencies of the volume-element sources distributed throughout the jet plume are proportional to the mean velocity shear or velocity gradient, in the MGB framework. Thus, flow regions containing high shear will produce high turbulence intensities; the corresponding noise source strength will be high and have high radiation frequencies.

Conversely, the regions of small velocity gradients will produce volume-eddy sources of low amplitude and low frequency. However, the regions of high shear are typically thin, occur close to the nozzle exit, and are of small volume while the regions of low shear are typically thick, occur far downstream of the nozzle, and are of large volume. Thus, even though the eddies generated in low-shear regions are low in amplitude, they are larger, radiate at low frequencies because of large scale, and there are many more of them.

The formal expression for the noise source intensity produced by a volume element imbedded in a jet plume is, from Reference 33:

$$dI(\omega) = \left[\frac{\rho_0 \ell^3}{c_0^5 R^2}\right](u')^4 \omega^4 H(\mu) \cdot dV \qquad (6)$$

In this expression, $dI$ is the source sound intensity spectrum for the volume element $dV$. The density, speed of sound, and emission frequency are denoted by $\varrho_0$, $c_0$, and $\omega$. Turbulence intensity is represented by $u'$. $H(\mu)$ is the Fourier transform of the moving-frame, space-time crosscorrelation of $u'$, and $\mu$ is the ratio of the emission frequency to the characteristic frequency, given by the expression:

$$\omega_0 \approx \frac{dU}{dr} \qquad (7)$$

Characteristic turbulent eddy size is given by:

$$\ell \approx u'/\omega_0 \qquad (8)$$

The term $dU/dr$ is the local turbulent eddy location crossstream mean velocity gradient or shear. In the MGB model, turbulence intensity is related to the three components of shear stress:

$$u' = \sqrt{\tau/\rho} \qquad (9)$$

It can be seen from the above expressions that noise source intensity per unit volume is a complex function of mean velocity, mean velocity gradients, turbulence intensity, and mean shear stress distribution. At any given emission frequency, the local eddy volume sound intensity given by Equation 6 is summed over all eddy volumes in the jet plume to give the total sound intensity.

It was observed (and speculated) in Section 6.1 that the noise-reduction devices generate higher turbulence intensities close to the nozzle exit but, because of the enhanced plume decay (as evidenced from the flow survey results shown in Section 6.2), reduce low-frequency noise. The MGB paradigm says that the effects of convective amplification and fluid shielding/refraction are negligible at 90° observer angles. Thus, we can examine SPL spectra at 90° to assess whether the source generation notions described above are apparent in the data. Figures 119 and 120 show 90° SPL spectra for four core chevron devices, without and with the fan chevrons, respectively. The data are for cycle point 21, corresponding to a typical sideline or full-power takeoff point.

For the cases without fan chevrons, Figure 119, there is little high-frequency noise increase (above 2 kHz) — with the exception that the alternating-chevron arrangement (bent-in, bent-out, bent-in, bent-out, …) exhibits a considerable high-frequency noise increase, on the order of 2 dB. This is consistent with the notion that increasing the mixing layer perimeter close to the jet exit will increase high-frequency noise generation. The plume survey data shown in Figures 112, 113, and 114 corroborate this, where the "yellow" contour for 3AB is about 2 to 3 times the length of the baseline contour. The other chevron device contours, although lobular in nature, are not nearly as dramatically contorted as 3AB. Note also that the contours have very large crossstream gradients that, as Equation 7 implies, are associated with higher source frequencies.

For the cases with fan chevrons, as shown in Figure 120, the trends are qualitatively the same, but the fan chevrons have reduced the mid-to-high-frequency noise increase of the alternating core chevrons and provided greater reduction in low-frequency noise for all the core chevron devices. If we look at axial stations somewhat downstream of the nozzle exit, say 18 and 30 inches as shown in Figures 114 and 115, the "yellow" contours are much thicker for the 3IC24 configuration compared to the baseline. Additionally, the crossstream mean velocity gradients appear weaker, implying lower intensities and at lower emission frequencies, based on the MGB formulations given by equations 7, 8, and 9.

It may be possible to correlate directly the differences in mixing layer contour length and thickness with the changes in high- and low-frequency noise for those slices of jet close to and far away from the nozzle exit, respectively.

### 6.3.2 Noise Source Convective Amplification Diagnostic Evaluation

The second physical process that plays a strong role in mixing noise radiation from a jet is convective amplification, due to relative motion, of the source intensity. Turbulent eddies are assumed to be convecting quadrupole sources, moving at a convection speed proportional to the local flow velocity in the plume at the location of the eddy. The convective amplification of the local turbulent eddy, in the MGB formulation, has the form:

$$CA = [(1 - M_c \cos\theta)^2 + \alpha \cdot (u'/c_0)^2]^{n/2} \tag{10}$$

*CA*, the convective amplification factor given by Equation 10, is applied locally to each eddy volume. The exponent $n$ is a function of the quadrupole type and varies from 0 to 4 for the

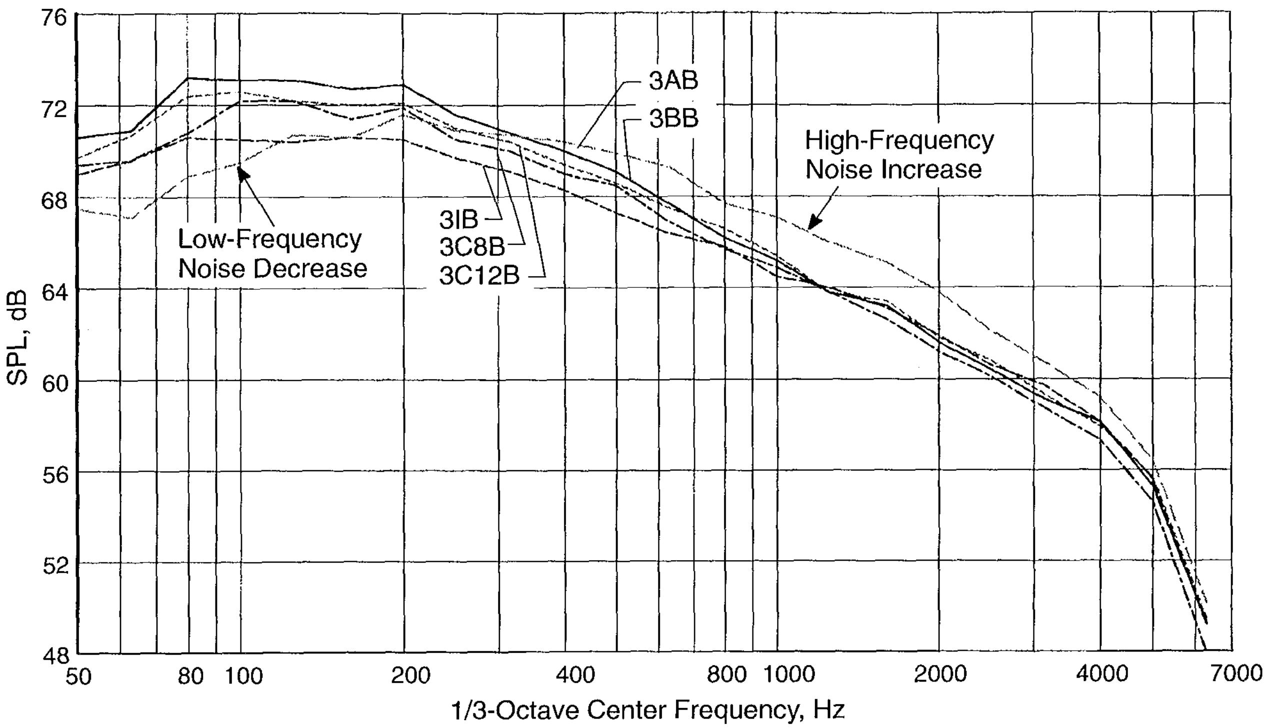


**Figure 119. One-Third Octave Spectrum at 90° for Core Chevron Devices Without Fan Chevrons**

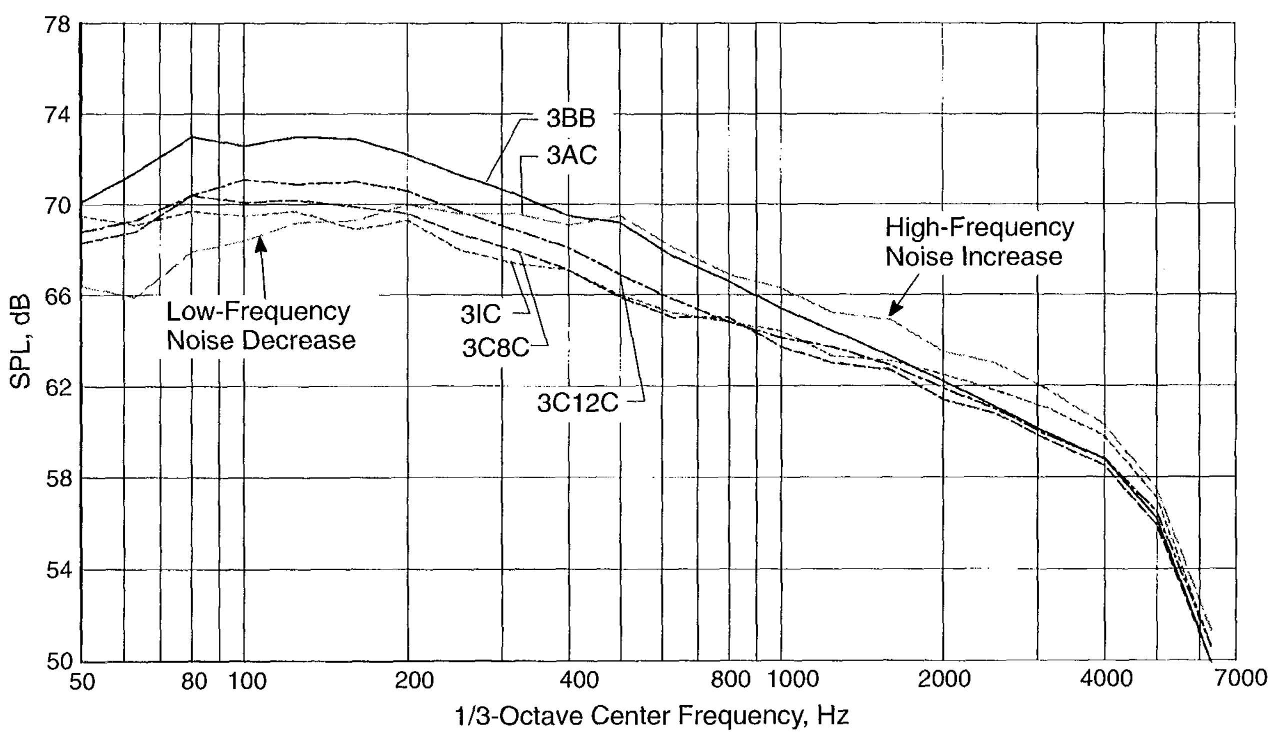


**Figure 120. One-Third Octave Spectrum at 90° for Core Chevron Devices With Fan Chevrons**

various quadrupole orientations: x–x, x–r, x–ϕ, ϕ–ϕ, r–ϕ, r–r, etc. In Equation 10, $M_c$ is the eddy convection Mach number, typically about 0.6 to 0.8 of the local flow, and $\theta$ is emission angle relative to the jet exhaust axis. For subsonic convection speeds, *CA* is approximated by the expression:

$$CA \approx (1 - M_c \cos\theta)^n \qquad (11)$$

Thus, for high flow velocities, we would expect high eddy convection Mach numbers; therefore, a lift in noise should occur in the aft quadrant and a reduction in noise in the forward quadrant, in addition to a Doppler shift of the source frequency due to convection. The slope of the directivity pattern, especially the OASPL directivity pattern, is therefore a good indicator of eddy convection Mach number.

Figures 121 and 122 show OASPL directivity patterns for the nozzle device combinations examined in subsection 6.3.1. Since, for the most part, the spectral peaks occur at low frequencies, OASPL is dominated by the lowest frequencies. Therefore, the OASPL directivity patterns are a good indicator of the low-frequency source convection speeds. The plots show that, below a directivity angle of 130°, the directivity patterns are not significantly altered, even though the levels are reduced significantly by the various chevron devices. The peak mean velocity decay trends shown in Figures 117 and 118 show very little reduction in peak velocity far downstream of the nozzle exit, where low-frequency noise sources typically dominate. The one exception is the alternating chevron 3AB, Figure 117, which also shows a much larger drop in OASPL at angles above 130°, as seen in Figures 121 and 122. This reduction in convective amplification "lift" at angles close to jet axis is due, at least in part, to the reduced convection velocities in the far-downstream regions of the plume, resulting from the more rapid plume decay.

It can therefore be concluded that: if the noise reduction device significantly reduces the mean velocity, it will also reduce the convective amplification of the noise sources in the aft quadrant, thus reducing peak noise levels in the aft quadrant.

### 6.3.3 Refraction and Fluid Shielding Diagnostic Evaluation

The MGB code paradigm as described in References 30 through 33 include the physical processes of refraction and shielding of sources as the sound emitted by the imbedded source propagates through the jet flow to the surrounding ambient medium. For example, in the limiting case of a "slug flow" jet, a source convecting along the jet axis will radiate at all angles. Sound radiating at 90° to the jet axis will pass through the discontinuity boundary between the jet flow and the surrounding medium without alteration. If the sound impinges on the boundary at other than normal incidence, the sound wave will be refracted, as it passes through the flow-discontinuity boundary, and emerge at a different radiation angle. If the incident impingement angle becomes very shallow in the flow direction, the refraction process may reflect the sound totally back into the jet flow, and any emission angle smaller than this critical angle will not pass through the slip layer; the situation would produce an effective "zone of silence."

In real jets, however, the jet is not a slug flow; it has a finite velocity gradient in the radial direction. When the gradient is large, the sound refraction, as described qualitatively for a slug flow jet above, will be large. For small mean velocity gradients, it can be expected that the sound refraction will be small. Since the velocity gradients are not infinite, pure reflection and creation of a zone of silence will not usually occur, and there will always be some "leakage" of the sound at shallow angles.

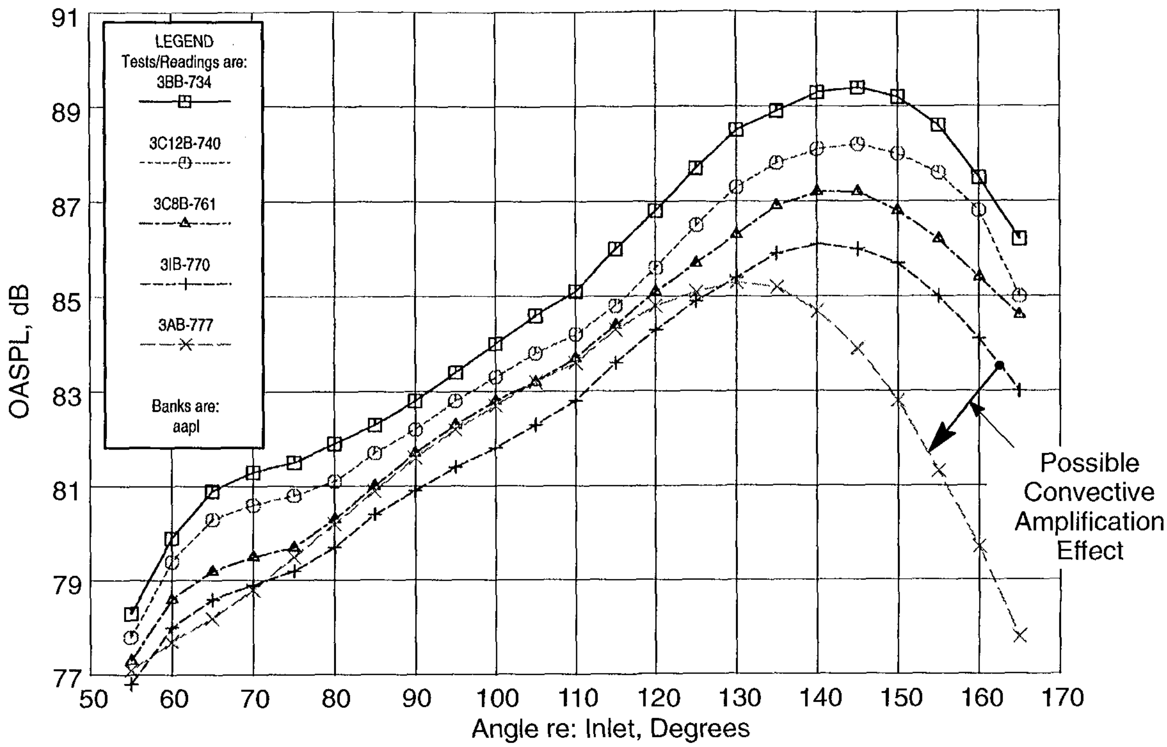


**Figure 121. OASPL Directivity for Core Chevron Devices Without Fan Chevrons**

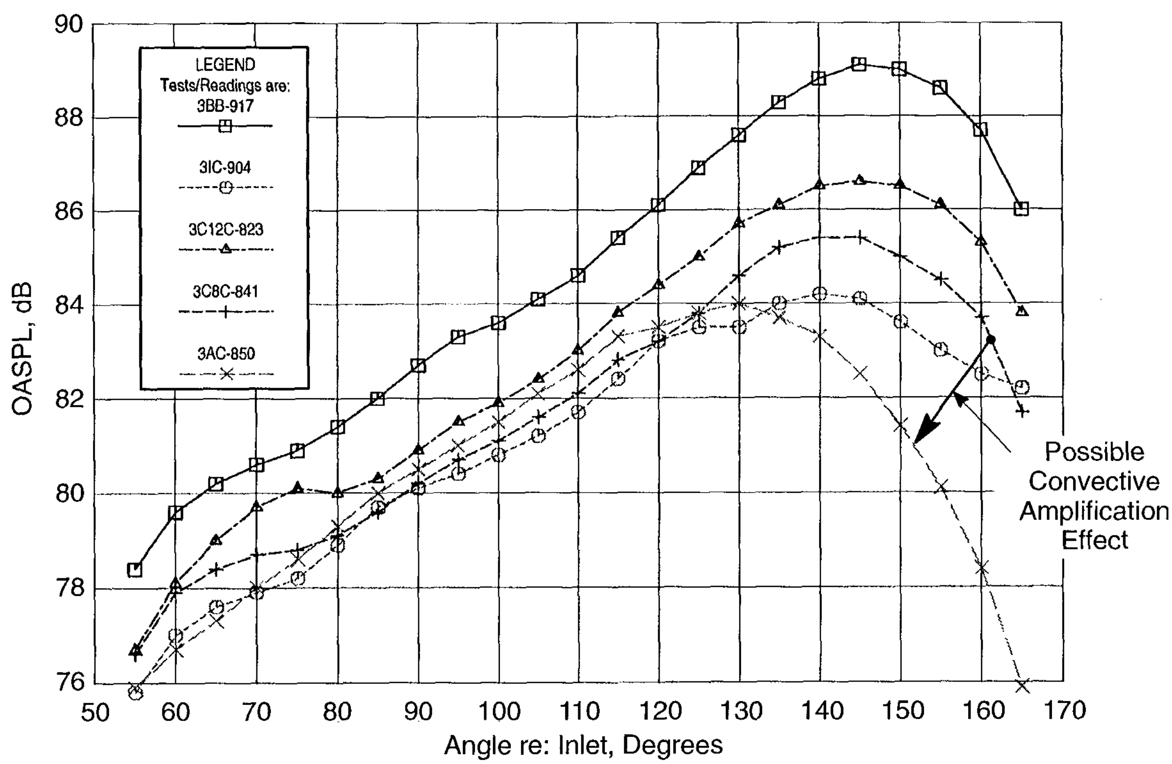


**Figure 122. OASPL Directivity for Core Chevron Devices With Fan Chevrons**

MGB modeling of this effect uses a limiting high-frequency approximation that attempts to quantify the amount of fluid "shielding" provided by the jet flow field around the embedded source. The shielding effect is a function of the source location in the jet (how much flow the emitted sound must propagate through along the emission path) and how much the flow gradients refract and absorb the sound energy along that path. In general, the MGB formulation would say that high velocity gradients and high frequencies radiating at angles close to the jet axis experience the greatest shielding attenuation. No attenuation occurs below 90°, and the shielding attenuation drops off rapidly as frequency is reduced.

One indication of the shielding effect is the amount of noise drop-off at high frequencies and angles close to the jet axis. Examination of the SPL spectra in the range of 130° to 160° (see Appendixes C and D) shows very little difference in SPL over the frequency range of 1 to 10 kHz among the nine nozzle configurations tested. Two exceptions are 3AB and 3AC, where slightly higher levels, on the order of 1 to 2 dB, are observed. This could be attributed to reduced fluid shielding effects or, as discussed in subsection 6.3.1, an actual source noise increase. From the observation that the high-frequency increase is greatest at 90° and the fact that it seems to diminish as observer angle increases in the aft arc, it can be speculated that the source noise increase observed at 90° is mitigated by enhanced fluid shielding. This could possibly be a result of entrainment of the high-velocity core flow to a much larger radius, thus shielding the sources "inside" this core flow. The velocity contour plots at axial stations close to the nozzle exit, such as Figures 112, 113, and 114 for configuration 3AB, suggest that this is a plausible explanation.

In summary, it can be concluded that the fundamental mixing noise conceptual model provided by the MGB paradigm is not inconsistent with experimental evidence for the impacts of mixing devices in reducing jet mixing noise. Notions of turbulent, convecting, quadrupole-source distributions in the jet can at least qualitatively explain some of the observed effects. It was concluded from this study that the effectiveness of a mixing device is related to:

1. reduction in convective amplification produced by more rapid plume decay,
2. reduction in far-downstream turbulence intensities and shear stresses that produce a source reduction at low frequency, and
3. increased shear layer perimeter near the nozzle exit causing an increase in high-frequency noise.

There is no clear indication that fluid shielding is either increased or decreased, although one core chevron device (3AB) seemed to exhibit an increase in fluid shielding. The best noise-reduction device contains an optimum combination of the sometimes competing influences of effects 1, 2, and 3 above. It was also concluded that the MGB framework, with some additional development and refinement, holds significant potential for providing a tool to quantitatively predict the effects observed in this test program. Thus it offers the hope for a design tool that can identify even greater noise reductions than were observed in this program.

# 7.0 Conclusions

Five baseline axisymmetric separate-flow nozzle models having bypass ratios of 5 and 8, and eleven different mixing-enhancer model nozzles were designed and fabricated. The mixing-enhancer devices consisted of various chevrons, vortex-generator doublets, and a tongue mixer. With various combinations of core and fan nozzle hardware, 28 separate-flow-nozzle/mixing-enhancer configurations were tested, and the acoustic benefits were measured over a range of simulated operating cycle and flight conditions. Most of the mixing-enhancer tests were conducted with the external plug and internal plug BPR = 5 configurations. All the tests were conducted in the NASA Lewis Aeroacoustic and Propulsion Laboratory (AAPL) facility during the March through June 1997 time period. The following conclusions, regarding scale-model testing of high-bypass, separate-flow exhaust systems and the effectiveness of mixing enhancers in reducing these exhaust systems jet noise, were drawn based on the experimental test results and subsequent analysis of the data.

**Repeatability:** The external-plug, BPR = 5, baseline nozzle was tested on 15 different days during this program. For a given cycle point, noise level (including EPNL) was found to be dependent both on variations in the ambient temperature and on nozzle conditions of repeat test points. Repeatability of EPNL data was established by normalizing the results to account for variations in ambient and nozzle test conditions. It was concluded that there are several ways to normalize scale-model data for ambient and charging station conditions, but the best approach from a physics point of view is not yet resolved.

**Baseline Nozzles:** No significant acoustic differences in the normalized EPNL results were noted between the data of baseline coplanar, internal-plug, and external-plug configurations of BPR = 5 and baseline internal-plug and external-plug configurations of BPR = 8. Small differences among these configurations were noted in the measured spectral results. When compared to baseline coplanar and internal-plug nozzles, the external plug nozzle showed higher noise in the forward arc and at low frequencies but lower noise in the aft arc and at higher frequencies. It was concluded that, on an EPNL basis, there is no significant noise difference between internal-plug, external-plug, and coplanar exhaust systems.

**Tongue Mixer:** The tongue mixer appeared to produce an aggressive vortex system and thus promoted more rapid decay of the fully merged plume. For the selected reference engine size, while the straight-chevron concept was more effective than the tongue mixer at a given nozzle pressure ratio, the data trends were different when the comparison was made at a given thrust — due to differences in the core mass flow characteristics between the chevron and tongue mixer devices. At very high thrusts, both straight chevrons and tongue mixer concepts produced similar EPNL reductions relative to the baseline nozzle, but the tongue mixer was considerably noisier at moderate and low thrusts. It was concluded that the tongue mixer was not effective in reducing noise globally and was less effective than the chevrons on a specific thrust basis.

**Doublets:** The doublet configurations showed little or no benefit. The external doublets (3DxB) provided a slight benefit at the highest velocities, and the internal doublets (3DiB) showed a small increase in noise. There was a shift in the spectral peak level frequency relative to the baseline without any reduction in the level. The doublets increased higher frequency noise. The doublets had no effect on the directivity or the angular location of peak PNL. It was concluded that the doublet concept was ineffective in reducing noise relative to other concepts and does not warrant any further consideration.

**Chevrons:** Core chevrons introduced a vortex into the shear layer between the fan and core streams, and fan chevrons introduced a vortex between the free-jet and fan streams. This vortex enhanced the decay of the plume. Most of the chevron designs significantly improved mixing without inducing additional turbulence near the nozzle exit. The inward-flip core chevron configuration reduced the axial length of the hot potential core of the baseline configuration by a factor of two. The temperature survey data of the inward-flip chevron indicated that the 12-lobed mixer profile provided impressive mixing enhancement. In general, the strength of the vortex, rate of decay of the plume, and any additional turbulence were strongly dependent upon the chevron design characteristics. Chevron devices were most effective with BPR = 5 configurations; effectiveness decreased when they were tested with BPR = 8 nozzles. It was concluded that the chevron concept, especially the inward-flip chevron, was the most successful device tested and warrants further development.

Straight chevrons on the fan nozzle reduced EPNL less, compared to those on the core nozzle. Fan chevrons alone were more effective at higher bypass ratios compared to core chevrons. It was concluded that, if only fan nozzle or core nozzle mixing devices were being contemplated, then the core nozzle offers the best potential; however, if the bypass ratio is very high (say, greater than 7 or 8), then fan nozzle chevrons might be more effective.

The combination of fan nozzle chevrons with the core nozzle devices produced a significant additional decrease in farfield noise. The benefits with the straight core chevrons were approximately doubled by the addition of fan chevrons. Significant noise benefits were achieved by addition of fan chevrons to the eight-core-chevron configuration (3C8C). Reductions of 3 EPNdB and more were measured when the fan chevron nozzle was added to the inward-flip and alternating-flip chevrons (3IC and 3AC). The benefit of 3C8C approached that of the inward- and alternating-flip chevron configurations (3IC and 3AC). It was concluded that there is a relationship, between the number of chevrons on the core nozzle relative to the number of fan nozzle chevrons, that significantly impacts the noise-reduction potential.

It was concluded that chevron nozzles —core only, fan only, or in combination — do not significantly alter the shape of the noise directivity patterns, nor do they (necessarily) reduce low-frequency noise at the expense of increasing high-frequency noise. An impressive jet noise spectral benefit is very clearly indicated in Figure 123. In this figure, the noise benefit (indicated by green, yellow, and red) of the configuration with inward-flip chevron on the core and straight chevron on the fan nozzle (3IC) — relative to the baseline nozzle (3BB) — is plotted as a function of both frequency and microphone angle for a typical takeoff condition.

**Summary:** A number of core and fan mixing-enhancer devices and combinations tested during this program reduced jet noise significantly relative to separate-flow baseline nozzles. Figure 124 is a bar graph summary of these benefits measured at a typical takeoff power point with BPR = 5, external-plug configurations. The figure indicates that the inward flip and alternating flip core chevrons, when combined with straight fan chevron nozzle, exceeded the NASA stretch goal of 3 EPNdB jet noise reduction at typical sideline certification conditions.

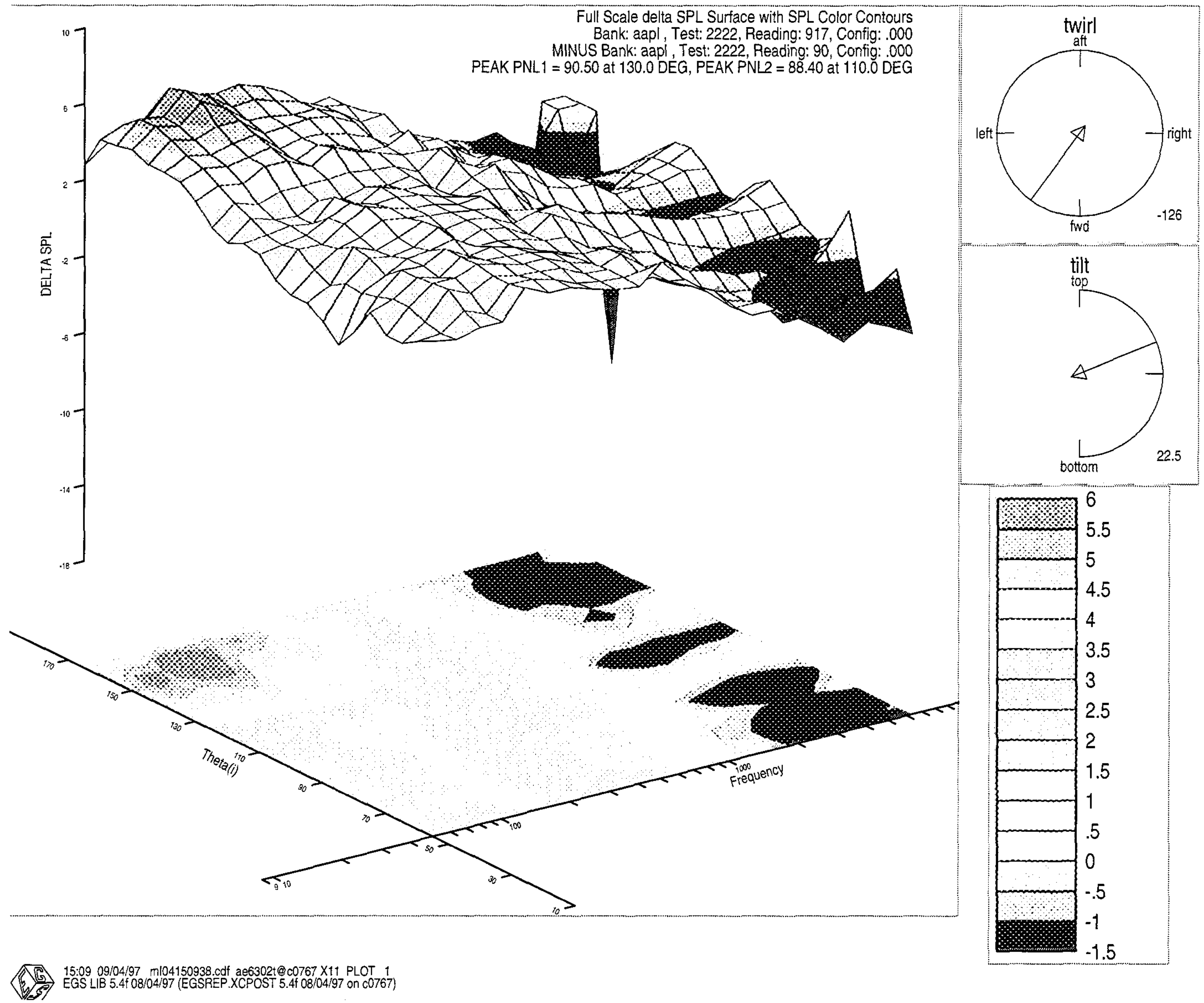


**Figure 123. Spectral Noise Reduction: Configuration 3BB Minus Configuration 3IC SPL**

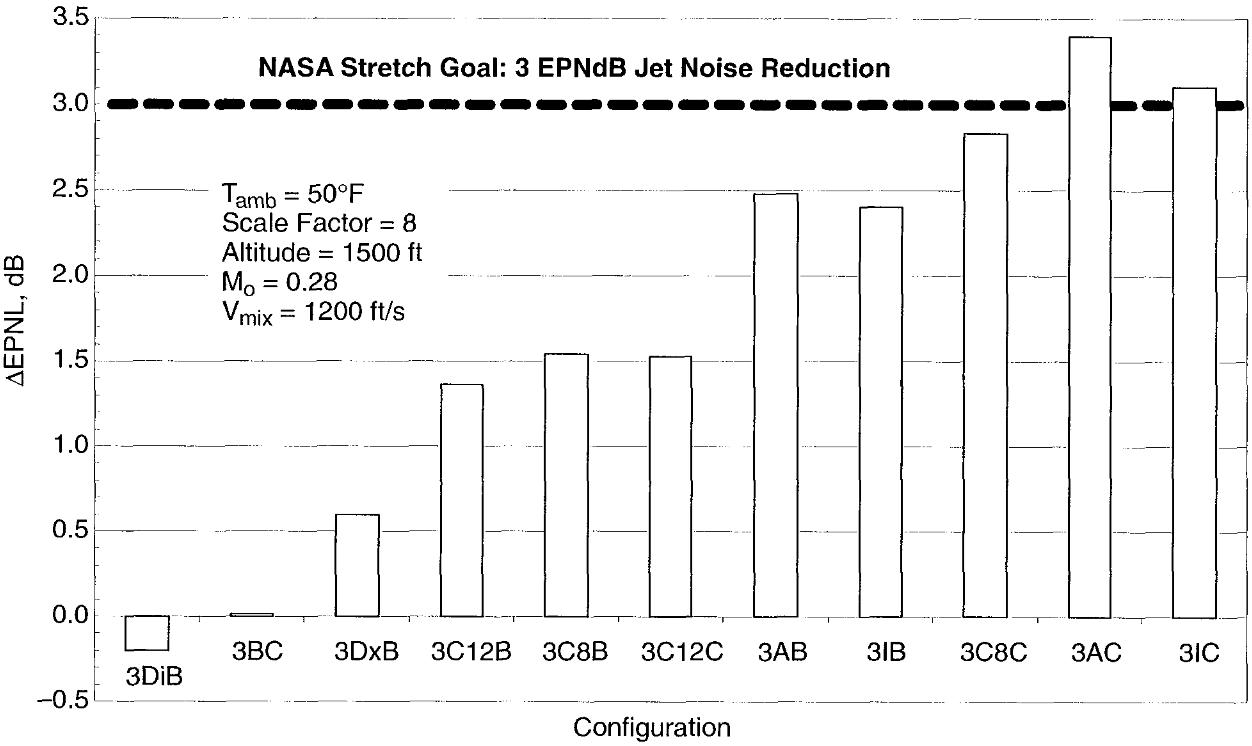


**Figure 124. EPNL Noise Benefits of Mixing-Enhancer Concepts Relative to Baseline BPR = 5 External Plug Nozzle (3BB)**

# 8.0 Recommendations

The following recommendations are made relative to the results and conclusions of this test program.

The five most promising configurations should be evaluated for exhaust system performance, at both takeoff and cruise conditions, including thrust coefficient and flow coefficient:

1 Straight-chevron core, baseline fan (3C12B)

2 Inward-flip-chevron core, baseline fan (3IB)

3 Alternating-flip-chevron core, baseline fan (3AB)

4 Straight-chevron core, baseline fan (3C8B)

5 Repeat (1–4) above with 24-chevron fan nozzle

A detailed study of the NASA-acquired flowfield measurements, the GEAE CFD results, and the measured acoustic results is recommended, using the MGB code as a *diagnostic tool*, for three of the best mixing-device configurations, at three cycle conditions, along with the baseline nozzle cases, for the purpose of:

a. quantifying the relationship between fluid mechanics (mixing processes, vortex formation and structure, etc.) and acoustics

b. substantiating the aeroacoustics model in MGB.

Since the MGB code has been less than successful in predicting the noise benefits of internal mixer nozzles, this detailed study would help to identify shortcomings in the MGB model and provide direction for further development or improvement in the MGB model. This will help provide an effective design tool for external mixing-enhancer devices on separate-flow exhaust systems.

# 9.0 Transition of Technology to Product Lines

GE Aircraft Engine's plan to transition the technology developed under this program to GEAE's product lines was provided to NASA in the "Commercialization Plan" dated February 2, 1998. This document, which contains GEAE proprietary information, describes GEAE's plans for the entire NAS3–27720 contract.

To enable transition of jet noise-reduction technology to product engines, the plan recommends a follow-on, in-house, scale-model effort for optimization of the chevron concept. It is suggested that this effort aim at refining the chevron noise-reduction concept from an acoustic and aerodynamic performance perspective.

The plan, following the suggested scale-model effort, also recommends a program comprising full-scale design, fabrication, and development testing on a GEAE engine. Use of the chevron technology in a GEAE product turbofan eventually will depend upon a successful engine demonstration; acoustic needs of current engines and growth applications; the results of trade studies involving cost, weight, and benefit; and market requirements.

# 10.0 New Technology

The chevron concept is a new technology conceived and developed under GEAE IR&D and demonstrated under this program. The concept provides impressive mixing enhancement and thus a significant jet noise reduction. Initially conceived during an in-house GEAE investigation, the chevron concept was further developed during this program. GEAE has applied for a patent.

# 11.0 References


1. Gliebe, P.R., Sandusky, G.T., and Chamberlin, R., "Mixer Nozzle Aeroacoustic Characteristics for the Energy Efficient Engine," AIAA Paper 81–1994, 1981.
2. Goodykoontz, J.H., "Experiments of High Bypass Internal Mixer Nozzle Jet Noise," NASA TM 83020, 1982.
3. Seiner, J.M., "Fluid Dynamics and Noise Emission Associated with Supersonic Jets," *Studies in Turbulence,* Springer Verlag, 1991.
4. Krejsa, E.A. and Saiyed, N.H., "Characteristics of Residual Mixing Noise from Internal Fan/Core Mixers," AIAA Paper 97–0382, 1997.
5. Bradbury, L.J.S. and Khadem, A.H., "The Distortion of a Jet by Tabs," J. Fluid Mechanics, Vol. 70, pp 801–813.
6. Ahuja, K.K. and Brown, W.H., "Shear Flow Control by Mechanical Tabs," AIAA Paper 89–0994, 1989.
7. Zaman, K.B.M.Q., Samimy, M., and Reeder, M.F., "Effect of Tabs on the Evolution of an Axisymmetric Jet," NASA TM 104472, 1991.
8. Zaman, K.B.M.Q., Reeder, M.F., and Samimy, M., "Supersonic Jet Mixing Enhancement by Delta–Tabs," AIAA Paper 92–3548, 1992.
9. Seiner, J.M. and Grosch, C.E., "Mixing Enhancement by Tabs in Round Supersonic Jets," AIAA Paper 98–2326, 1998.
10. Longmire, E.K., Eaton, J.K., and Elkins, C.J., "Control of Jet Structure by Crown Shaped Nozzles," AIAA Journal, Vol. 30, 1992, pp 505–512.
11. Samimy, M., Kim, J.H., and Clancy, P.S., "Mixing Enhancement in Supersonic Jets via Nozzle Trailing Edge Modifications," AIAA Paper 97–1877, 1997.
12. Ho, C.M. and Gutmark, E., "Vortex Induction and Mass Entrainment in a Small Aspect Ratio Elliptic Jet," J. Fluid Mechanics, 1979, pp 383–405.
13. McCormick, D.C., "Shock–Boundary Layer Interaction Control with Low–Profile Vortex Generators and Passive Cavity," AIAA Paper 92–0064, 1992.
14. Barber, T.J., Mounts, J.S., and McCormick, D.C., "Boundary Layer Energization by Means of Optimized Vortex Generators," AIAA Paper 93–0445, 1993.
15. Barter, J.W., "Prediction and Passive Control of Fluctuation Pressure Loads Produced by Shock Wave Turbulent Boundary Layer Separation," PhD Dissertation, Dept. of Aerospace Engineering and Engineering Mechanics, University of Texas at Austin, 1995.
16. Compton, W.B. and Abdol–Hamid, K. S., "Navier–Stokes Simulation of Nozzle Afterbody Flows at Off–Design Conditions," AIAA Paper 91–3207, 1991.
17. Carlson, J.R., "Computational Prediction of Isolated Performance of an Axisymmetric Nozzle at Mach Number 0.90," NASA TM 4506, 1994.
18. Carlson, J.R., "High Reynolds Number Analysis of Flat Plate and Separated Afterbody Flow Using Non–Linear Turbulence Models," AIAA Paper 96–2544, 1996.

19. *A User's Guide to NPARC Version 3.0,* The NPARC Alliance, Arnold Engineering Development Center, Tullahoma, Tennessee, 1996.

20. *GRIDGEN User's Guide,* Pointwise Inc., Bedford, Texas.

21. Merchen, R.L., "Design Report – General Electric/NASA High Bypass Ratio Exhaust Model NAS3 27720 AoI 14.3," 1997.

22. Hoff, G.E., Janardan B.A., Low J., et al., "Test Plan Report for Scale Model Separate Flow Exhaust System Models with Jet Mixing Enhancer Concepts in the NASA Lewis Research Center Aeroacoustic Propulsion Laboratory," February 1997.

23. Castner, R.S., "The Nozzle Acoustic Test Rig; An Acoustic and Aerodynamic Free-Jet Facility," AIAA 94–2565, 1994.

24. Hoch, R.E., Duponchel, J.P., Cocking, B.J., and Bryce, W.D., "Studies of the Influence of Density on Jet Noise," Journal of Sound and Vibration, 28, pp 649–668.

25. Amiet, R.K., "Refraction of Sound by Shear Layer Refraction," AIAA Paper 77–54, 1977.

26. Gliebe, P.R. et al., "High Velocity Jet Noise Source Location and Reduction," U.S. Dept. of Transportation Report FAA–RD–76–79, Task III, Vol. I, 1978.

27. Gliebe, P.R. and Janardan, B.A., "Ultra-High Bypass Engine Aeroacoustic Study," Report Prepared by GEAE for NASA, Contract NAS3–25269, Task Order 4, 1993.

28. Fisher, Preston, Bryce, "Modeling of Noise from Simple Coaxial Jets," AIAA Paper 93–4413, 1993.

29. *Separate Flow Nozzle Test Status Meeting Proceedings,* NASA Lewis Research Center, September 10, 1997.

30. Balsa, T.F., Gliebe, P.R., Kantola, R.A., Mani, R., Stringas, E.J., and Wang, J.C.F., "High Velocity Jet Noise Source Location and Reduction, Task 2 – Theoretical Development and Basic Experiments," FAA Report FAA–RD–76–79, II, 1978.

31. Gliebe, P.R., "High Velocity Jet Noise Source Location and Reduction, Task 2 Supplement – Computer Program for Calculating the Aeroacoustic Characteristics of Jets from Nozzles of Arbitrary Shape," FAA Report FAA–RD–76–79, IIa, 1977.

32. Balsa, T.F. and Gliebe, P.R., "Aerodynamics and Noise of Coaxial Jets," AIAA Journal, Vol. 15, 1977, pp 1550–1558.

33. Gliebe, P.R., "Diagnostic Evaluation of Jet Noise Suppression Mechanisms," Journal of Aircraft, Vol. 17, 1980, pp 837–842.

# Appendix A
# AAPL SFN Test Configurations

The AAPL SFN test configurations are listed below, and engineering drawings are replicated on the following pages — as indicated in the tabulation.

Model 1 – Coplanar, BPR = 5
Model 2 – Internal Plug, BPR = 5
Model 3 – External Plug, BPR = 5
Model 4 – Internal Plug, BPR = 8
Model 5 – External Plug, BPR = 8
Model 6 – Tongue Mixer Core Nozzle with Extended Internal Plug
Model 7 – Model 4 Core Nozzle with Extended Internal Plug (BPR = 14)

| Page | Designation | Description |
|---|---|---|
| 158 | 1 (also called 1BB) | Model 1<br>Core: Baseline<br>Fan: Baseline |
| 159 | 2BB | Model 2<br>Core: Baseline<br>Fan: Baseline |
| 160 | 2BD | Model 2<br>Core: Baseline<br>Fan: 96 Internal Doublets |
| 161 | 2BC (also called 2BC24) | Model 2<br>Core: Baseline<br>Fan: 24 Chevrons |
| 162 | 2CC (also called 2C12C) | Model 2<br>Core: 12 Chevrons<br>Fan: 24 Chevrons |
| 163 | 2CB (also called 2C12B) | Model 2<br>Core: 12 Chevrons<br>Fan: Baseline |
| 164 | 2TmB | Model 2<br>Core: Tongue Mixer<br>Fan: Baseline |
| 165 | 2TmC | Model 2<br>Core: Tongue Mix<br>Fan: 24 Chevrons |
| 166 | 3BB | Model 3<br>Core: Baseline<br>Fan: Baseline |
| 167 | 3BC | Model 3<br>Core: Baseline<br>Fan: 24 Chevrons |
| 168 | 3BS | Model 3<br>Core: Baseline<br>Fan: Scarf Nozzle |
| 169 | 3BOmax | Model 3<br>Core: Baseline<br>Fan: Max. Offset Nozzle |
| 170 | 3BT24 | Model 3<br>Core: Baseline<br>Fan: 24 Flip Tabs |
| 171 | 3BT48 | Model 3<br>Core: Baseline<br>Fan: 48 Flip Tabs |
| 172 | 3T24T24 | Model 3<br>Core: 24 Flip Tabs<br>Fan: 24 Flip Tabs |
| 173 | 3T24B | Model 3<br>Core: 24 Flip Tabs<br>Fan: Baseline |
| 174 | 3T48B | Model 3<br>Core: 48 Flip Tabs<br>Fan: Baseline |
| 175 | 3T48T48 | Model 3<br>Core: 48 Flip Tabs<br>Fan: 48 Flip Tabs |
| 176 | 3T48C | Model 3<br>Core: 48 Flip Tabs<br>Fan: 24 Chevrons |
| 177 | 3HmB | Model 3<br>Core: Half Mixer<br>Fan: Baseline |
| 178 | 3HmS(0) | Model 3<br>Core: Half Mixer<br>Fan: Scarf Nozzle |

| Page | Designation | Description |
|---|---|---|
| 179 | 3HmC | Model 3<br>Core: Half Mixer<br>Fan: 24 Chevrons |
| 180 | 3HmOmax | Model 3<br>Core: Half Mixer<br>Fan: Max. Offset Nozzle |
| 181 | 3C12B | Model 3<br>Core: 12 Chevrons<br>Fan: Baseline |
| 182 | 3C12C | Model 3<br>Core: 12 Chevrons<br>Fan: 24 Chevrons |
| 183 | 3C8C | Model 3<br>Core: 8 Chevrons<br>Fan: 24 Chevrons |
| 184 | 3C8B | Model 3<br>Core: 8 Chevrons<br>Fan: Baseline |
| 185 | 3IB | Model 3<br>Core: 12 In-Flip Chev<br>Fan: Baseline |
| 186 | 3IC | Model 3<br>Core: 12 In-Flip Chev<br>Fan: 24 Chevrons |
| 187 | 3AC | Model 3<br>Core: 12 Alt-Flip Chev<br>Fan: 24 Chevrons |
| 188 | 3AB | Model 3<br>Core: 12 Alt-Flip Chev<br>Fan: Baseline |
| 189 | 3DiB | Model 3<br>Core: 64 Int Doublets<br>Fan: Baseline |
| 190 | 3DxB | Model 3<br>Core: 20 Ext Doublets<br>Fan: Baseline |

| Page | Designation | Description |
|---|---|---|
| 191 | 5BB | Model 5<br>Core: Baseline<br>Fan: Baseline |
| 192 | 5BC | Model 5<br>Core: Baseline<br>Fan: 24 Chevrons |
| 193 | 5CC<br>(also called 5C12C) | Model 5<br>Core: 12 Chevrons<br>Fan: 24 Chevrons |
| 194 | 5CB<br>(also called 5C12B) | Model 5<br>Core: 12 Chevrons<br>Fan: Baseline |
| 195 | 4BB | Model 4<br>Core: Baseline<br>Fan: Baseline |
| 196 | 6TmB | Model 6<br>Core: Tongue Mixer<br>Fan: Baseline |
| 197 | 6TmC | Model 6<br>Core: Tongue Mixer<br>Fan: 24 Chevrons |
| 198 | 7BB | Model 7<br>Core: Baseline<br>Fan: Baseline |
| 199 | 3FB<br>(also called 3FMB) | Model 3<br>Core: Full Mixer<br>Fan: Baseline |
| 200 | 3FC<br>(also called 3FMC) | Model 3<br>Core: Full Mixer<br>Fan: 24 Chevrons |
| 201 | 3T24T48 | Model 3<br>Core: 24 Flip Tabs<br>Fan: 48 Flip Tabs |
| 202 | 3T24C | Model 3<br>Core: 24 Flip Tabs<br>Fan: 24 Chevrons |

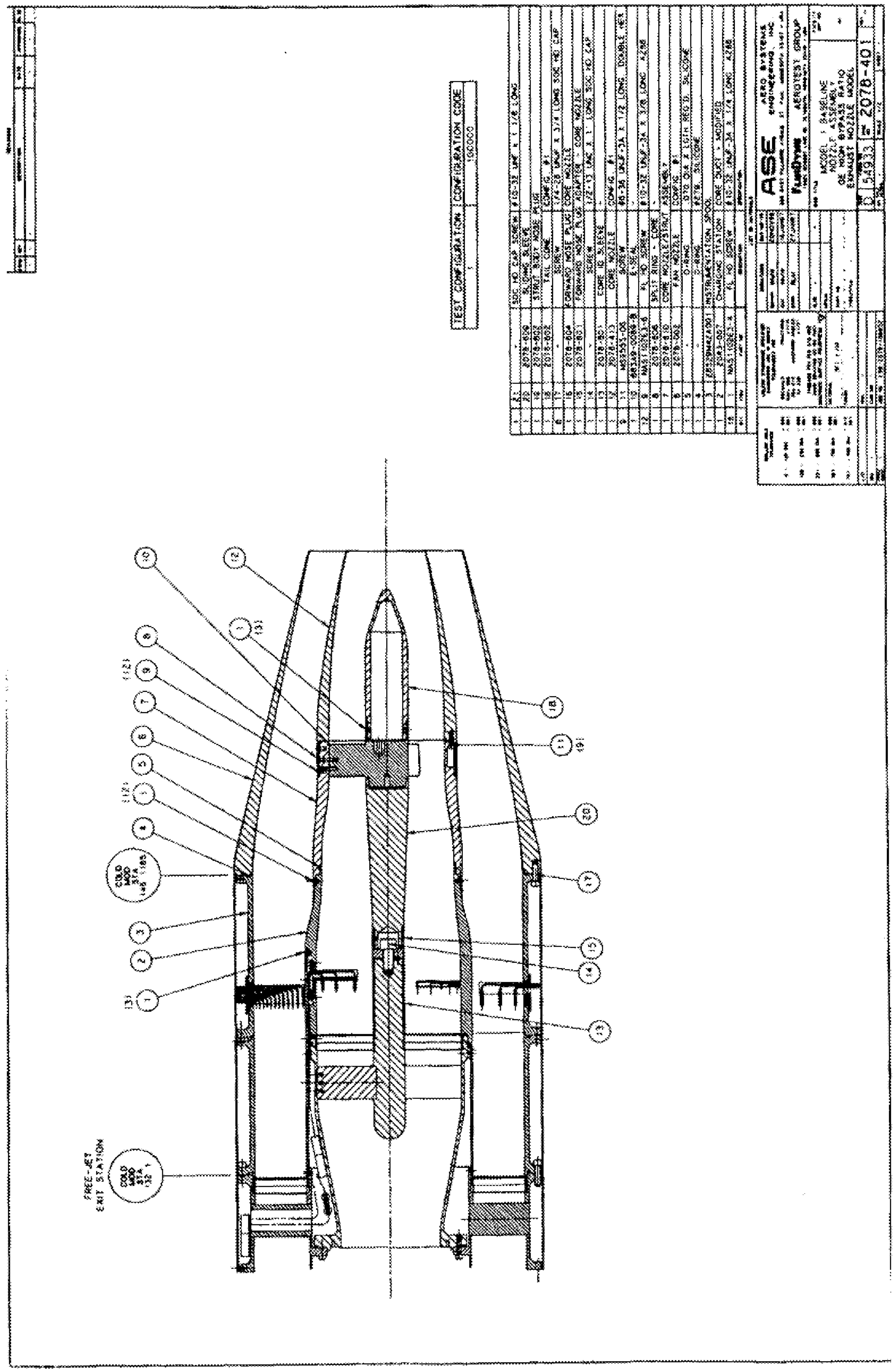

TEST CONFIGURATION
CONFIGURATION CODE
FREE-JET EXIT STATION
ASE
AEROTEST GROUP
2078-401

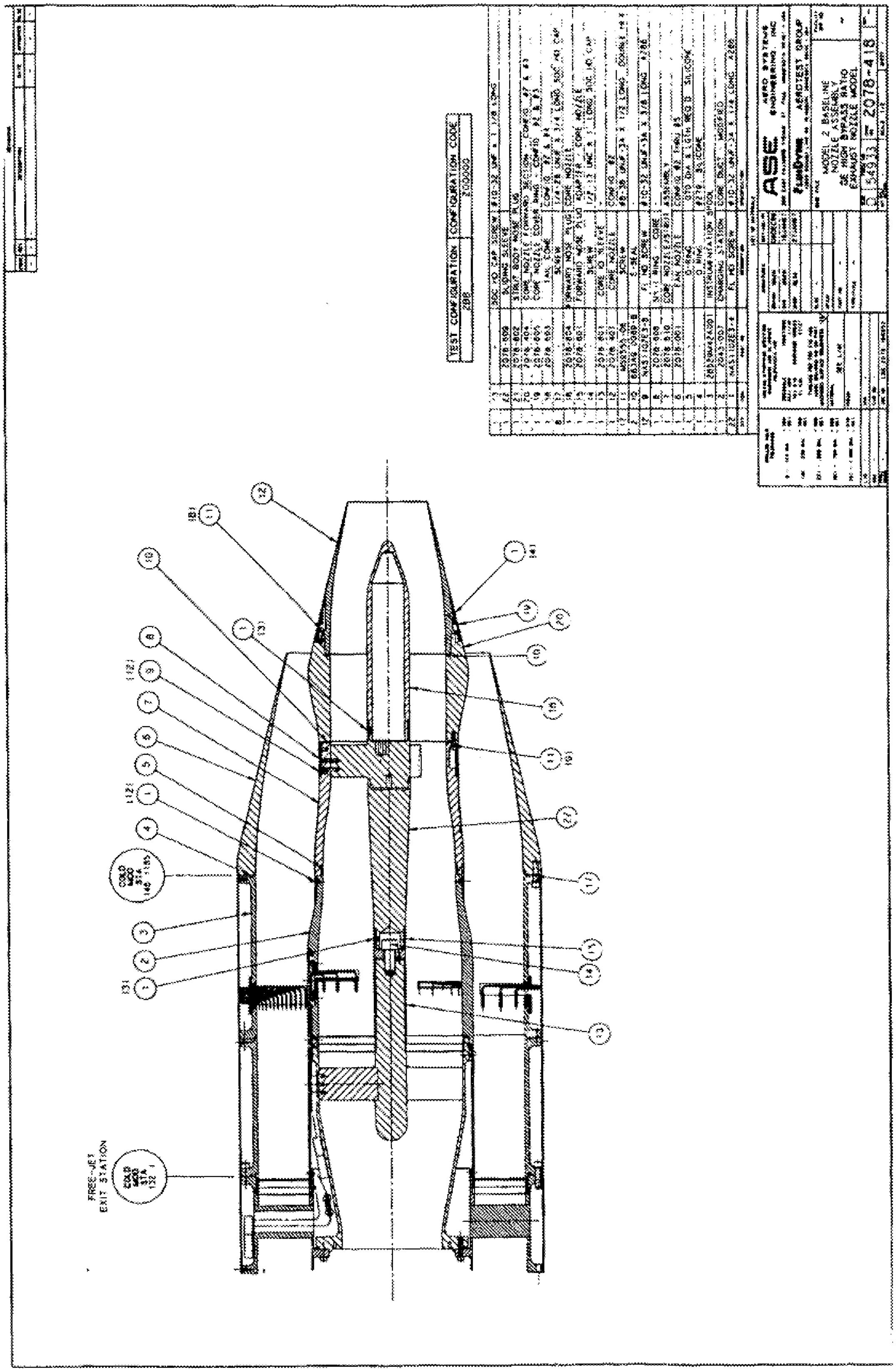

TEST CONFIGURATION
CONFIGURATION CODE
MODEL 2 BASELINE NOZZLE ASSEMBLY
GE HIGH BYPASS RATIO EXHAUST NOZZLE MODEL
2078-418
FREE-JET EXIT STATION

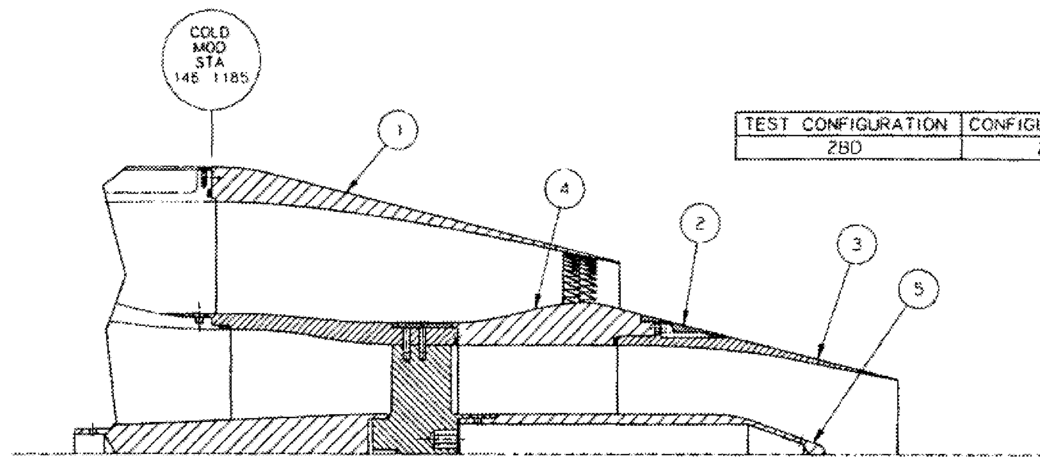


| TEST CONFIGURATION | CONFIGURATION CODE |
|---|---|
| 2BD | 200200 |

NOTE:

1. SEE DRAWING 2078-418 FOR ITEMS NOT SHOWN ON THIS DRAWING

| QTY | ITEM | PART NO | DESCRIPTION | SPECIFICATION |
|---|---|---|---|---|
| 1 | 5 | 2078-603 | TAIL CONE | CONFIG #2 & #4 |
| 1 | 4 | 2078-404 | CORE NOZZLE FORWARD SECTION - CONFIG #2 & #3 | |
| 1 | 3 | 2078-407 | CORE NOZZLE CONFIG #2 | |
| 1 | 2 | 2078-605 | CORE NOZZLE COVER RING CONFIG #2 & #3 | |
| 1 | 1 | 2078-004 | FAN NOZZLE #7D | INTERNAL VORTEX GENERATOR DOUBLET |

LIST OF MATERIALS

| SIGNATURES | | DAY-MO-YR |
|---|---|---|
| DRAWN | WMW | 15JAN97 |
| CHK | WMW | 16JAN97 |
| ENGR | RLM | 28JAN97 |

ASE AERO SYSTEMS ENGINEERING, INC
358 EAST FILLMORE AVENUE ST. PAUL MINNESOTA 55107 USA

FLUIDYNE AEROTEST GROUP

DWG TITLE
96 INT. DOUB. FAN/BASE CORE
MODEL 2 NOZZLE ASSEMBLY
GE HIGH BYPASS RATIO
EXHAUST NOZZLE MODEL

SIZE D | FSCM NO 54933 | DWG NO 2078-618

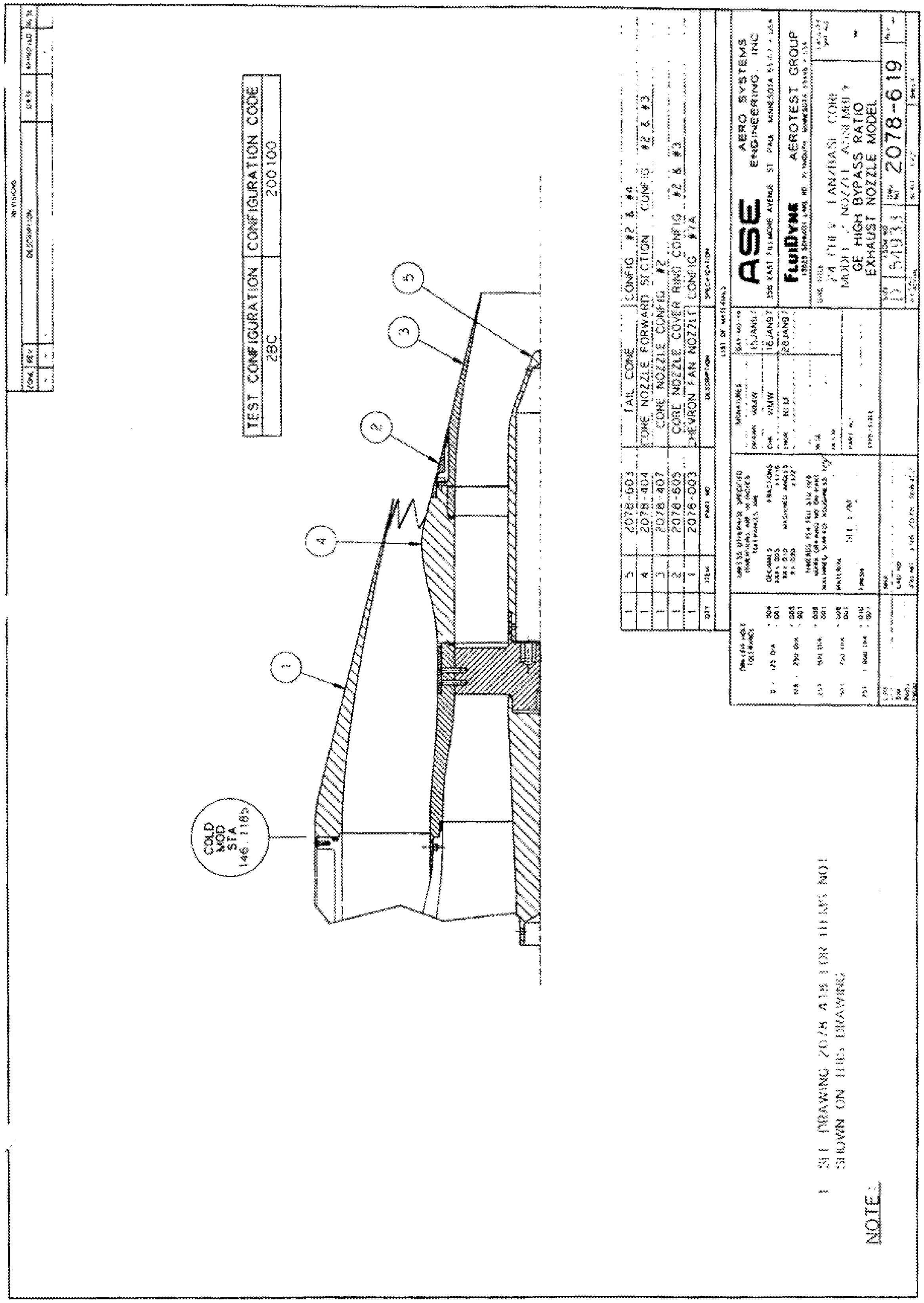

TEST CONFIGURATION
CONFIGURATION CODE
2BC
200100
COLD MOD STA 146.1165
2078-603 TAIL CONE CONFIG #2 & #4
2078-404 CORE NOZZLE FORWARD SECTION CONFIG #2 & #3
2078-407 CORE NOZZLE CONFIG #2
2078-605 CORE NOZZLE COVER RING CONFIG #2 & #3
2078-003 CHEVRON FAN NOZZLE CONFIG #7A
ASE AERO SYSTEMS ENGINEERING, INC
FLUIDYNE AEROTEST GROUP
GE HIGH BYPASS RATIO
EXHAUST NOZZLE MODEL
2078-619
NOTE:
1. SEE DRAWING 2078-418 FOR ITEMS NOT SHOWN ON THIS DRAWING

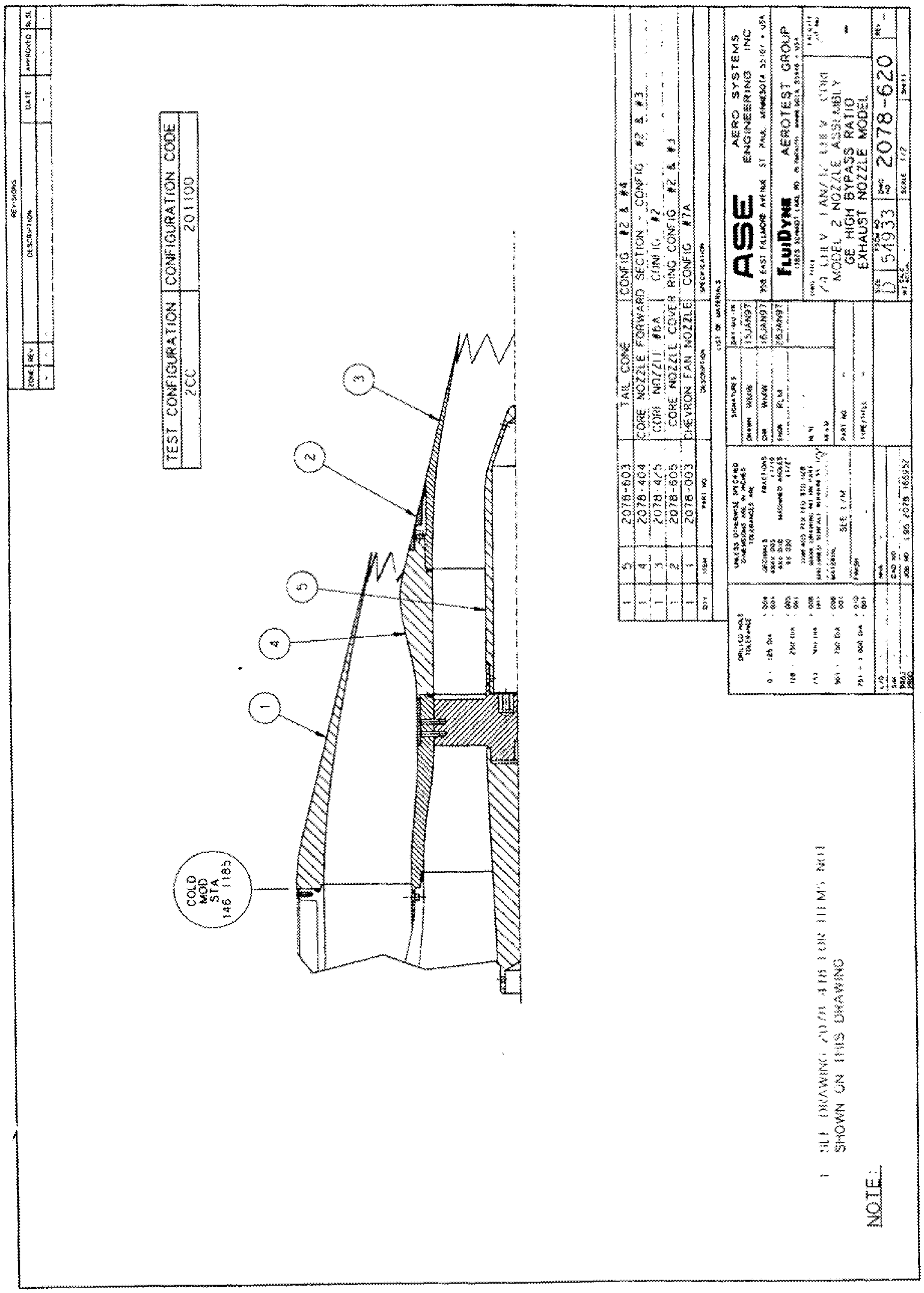
TEST CONFIGURATION
2CC
CONFIGURATION CODE
201100
COLD MOD STA 146.1185
5 2078-603 TAIL CONE CONFIG #2 & #4
4 2078-404 CORE NOZZLE FORWARD SECTION - CONFIG #2 & #3
3 2078-425 CORE NOZZLE #6A CONFIG #2
2 2078-605 CORE NOZZLE COVER RING CONFIG #2 & #3
1 2078-003 CHEVRON FAN NOZZLE CONFIG #7A
LIST OF MATERIALS
ASE AERO SYSTEMS ENGINEERING INC
FLUIDYNE AEROTEST GROUP
MODEL 2 NOZZLE ASSEMBLY
GE HIGH BYPASS RATIO
EXHAUST NOZZLE MODEL
2078-620
NOTE:
SHOWN ON THIS DRAWING

| TEST CONFIGURATION | CONFIGURATION CODE |
|---|---|
| 2C8 | 201000 |

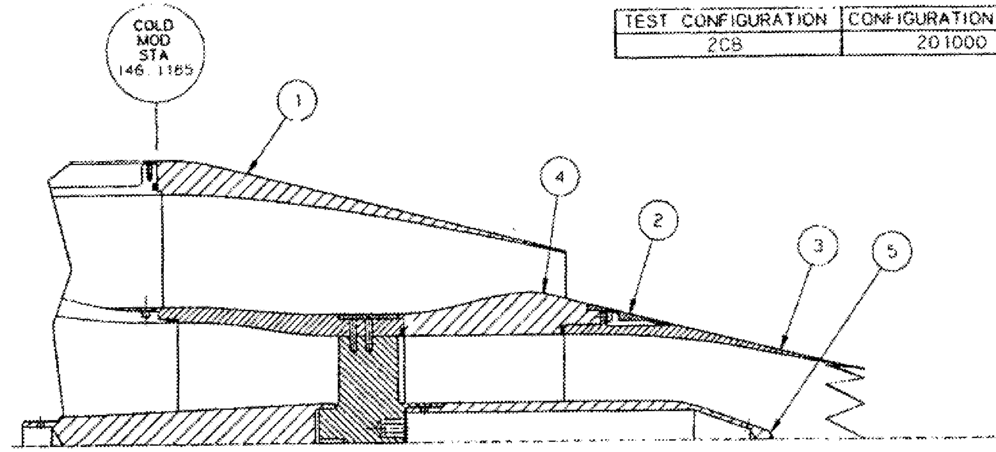


| QTY | ITEM | PART NO | DESCRIPTION | SPECIFICATION |
|---|---|---|---|---|
| 1 | 5 | 2078-603 | TAIL CONE | CONFIG #2 & #4 |
| 1 | 4 | 2078-404 | CORE NOZZLE FORWARD SECTION - CONFIG #2 & #3 | |
| 1 | 3 | 2078-425 | CORE NOZZLE #6A | CONFIG #2 |
| 1 | 2 | 2078-605 | CORE NOZZLE COVER RING CONFIG #2 & #3 | |
| 1 | 1 | 2078-001 | FAN NO/21F | CONFIG #2 THRU #5 |

LIST OF MATERIALS

ASE AERO SYSTEMS ENGINEERING, INC

FLUIDYNE AEROTEST GROUP

BASE FAN/12 CHEV. CORE
MODEL 2 NOZZLE ASSEMBLY
GE HIGH BYPASS RATIO
EXHAUST NOZZLE MODEL

SIZE D FSCM NO 54933 DWG NO 2078-621

SCALE 1/2

DRAWN WMW 15JAN97
CHK WMW 16JAN97
ENGR RLM 28JAN97

MATERIAL SEE L/M

REF 1.98-2078-188952

NOTE:

1 SEE DRAWING 2078-418 FOR ITEMS NOT SHOWN ON THIS DRAWING

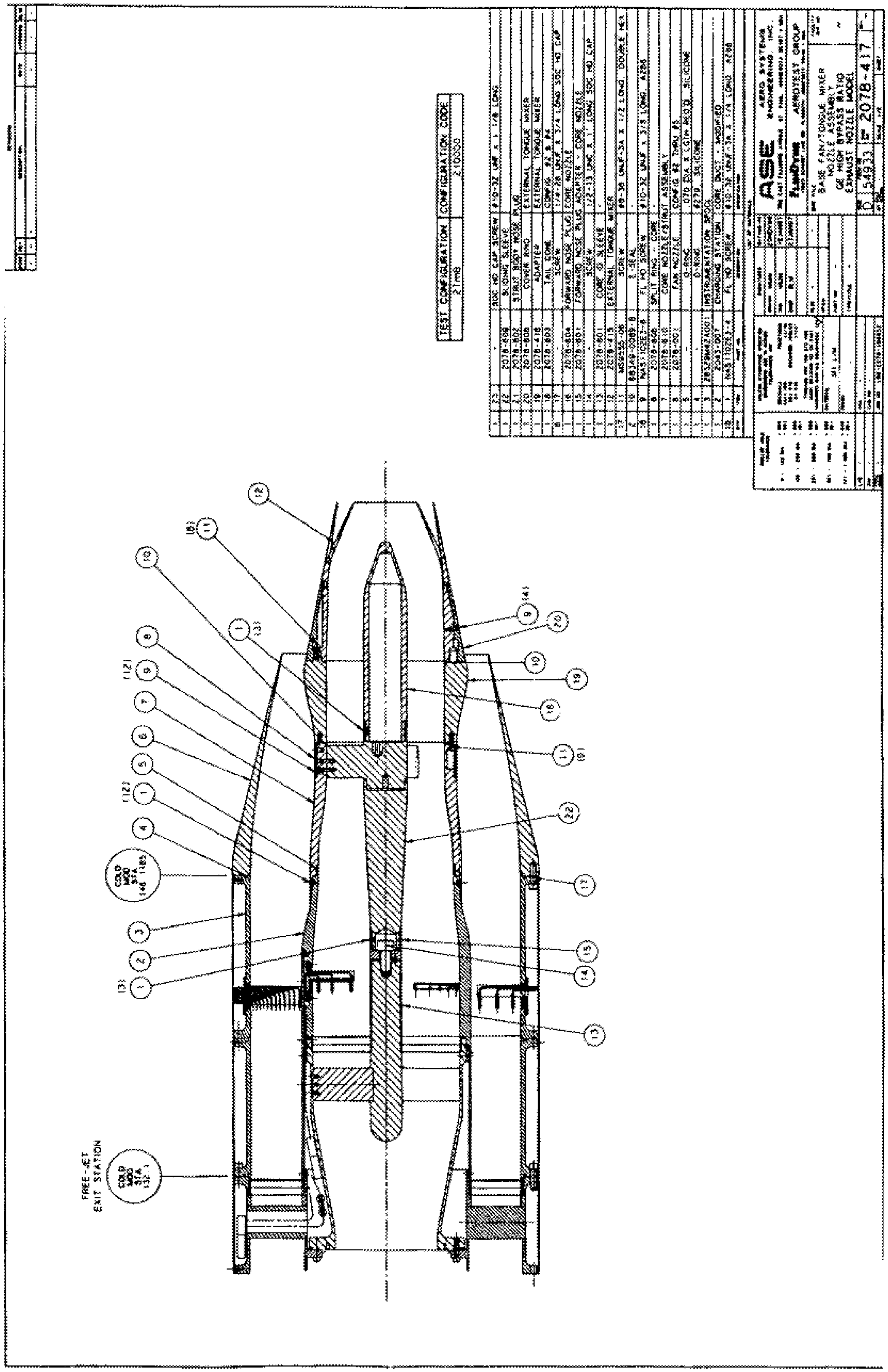

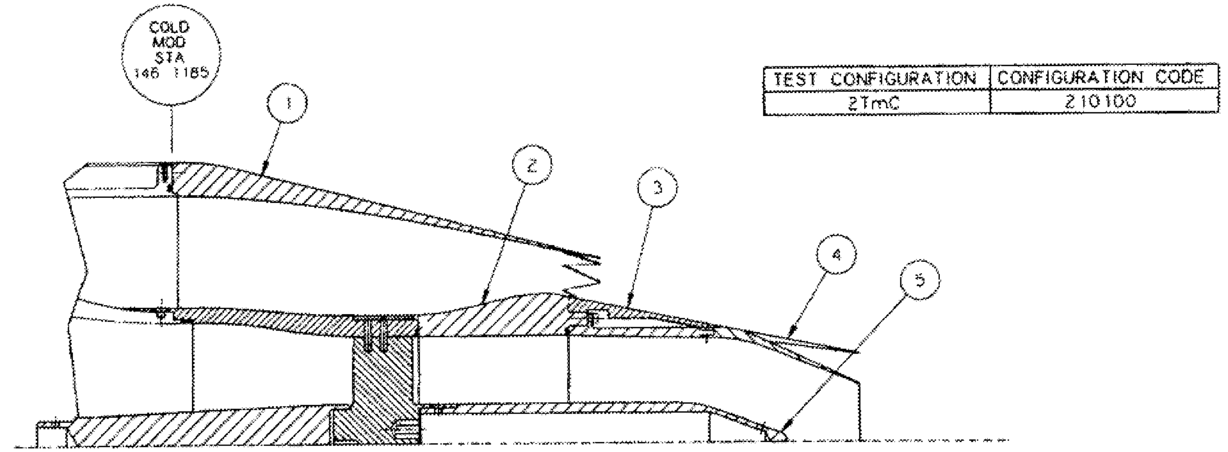


| TEST CONFIGURATION | CONFIGURATION CODE |
|---|---|
| 2TmC | 210100 |

| QTY | ITEM | PART NO | DESCRIPTION | SPECIFICATION |
|---|---|---|---|---|
| 1 | 5 | 2078-603 | TAIL CONE | CONFIG #2 & #4 |
| 1 | 4 | 2078-415 | EXTERNAL TONGUE MIXER | |
| 1 | 3 | 2078-608 | COVER RING | EXTERNAL TONGUE MIXER |
| 1 | 2 | 2078-416 | ADAPTER | EXTERNAL TONGUE MIXER |
| 1 | 1 | 2078-003 | CHEVRON FAN NOZZLE | CONFIG #7A |

LIST OF MATERIALS

| SIGNATURES | | DAY-MO-YR |
|---|---|---|
| DRAWN | WMW | 15JAN97 |
| CHK | WMW | 16JAN97 |
| ENGR | RLM | 28JAN97 |

MATERIAL: SEE L/M

ASE AERO SYSTEMS ENGINEERING, INC
358 EAST FILLMORE AVENUE, ST. PAUL, MINNESOTA 55107 USA

FLUIDYNE AEROTEST GROUP

DWG TITLE: 24 CHEV FAN/TONGUE MIXER MODEL 2 NOZZLE ASSEMBLY GE HIGH BYPASS RATIO EXHAUST NOZZLE MODEL

SIZE D | FSCM NO 54933 | DWG NO 2078-622 | REV –

NOTE:

1 SEE DRAWING 2078-417 FOR ITEMS NOT SHOWN ON THIS DRAWING

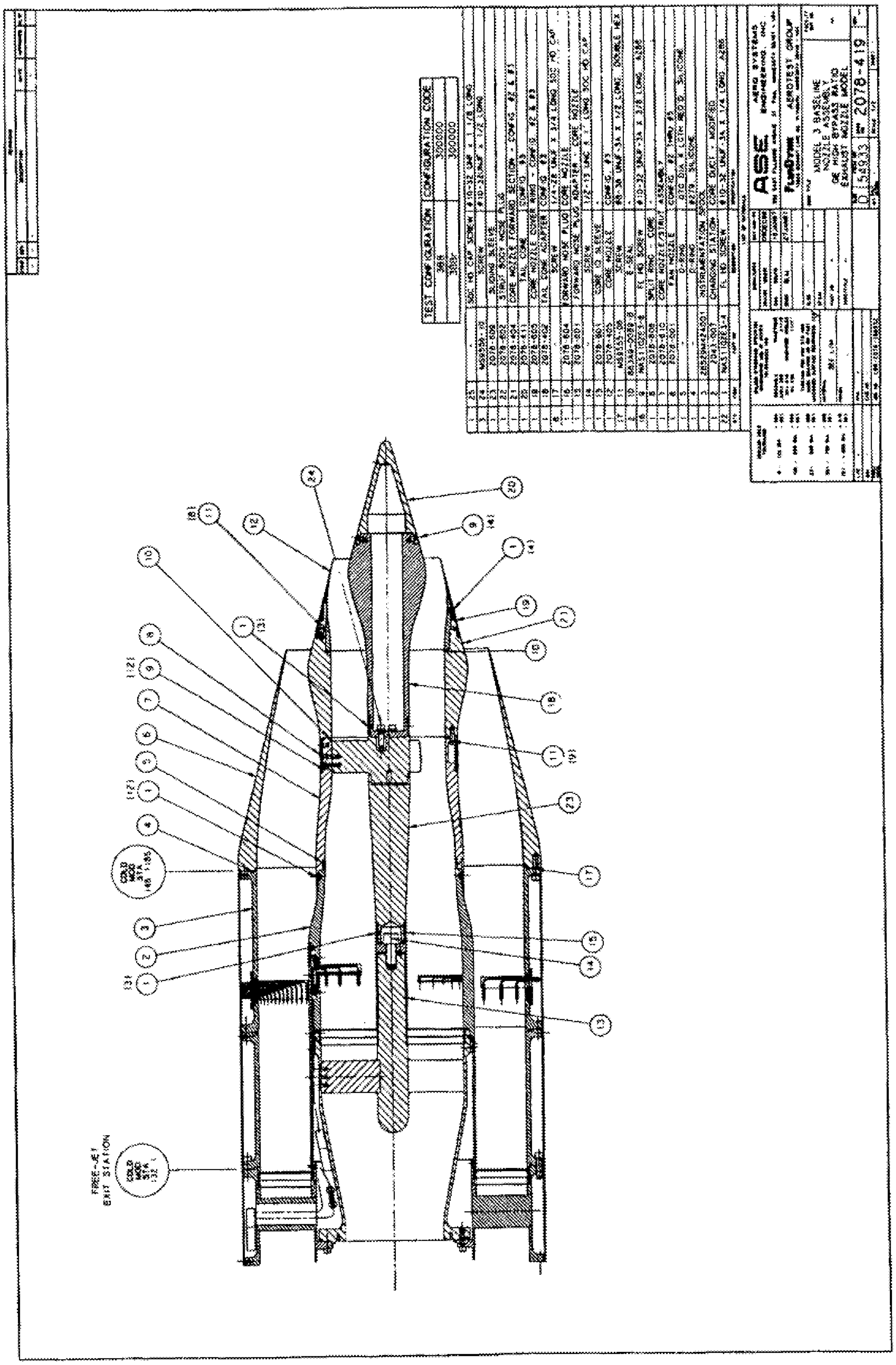

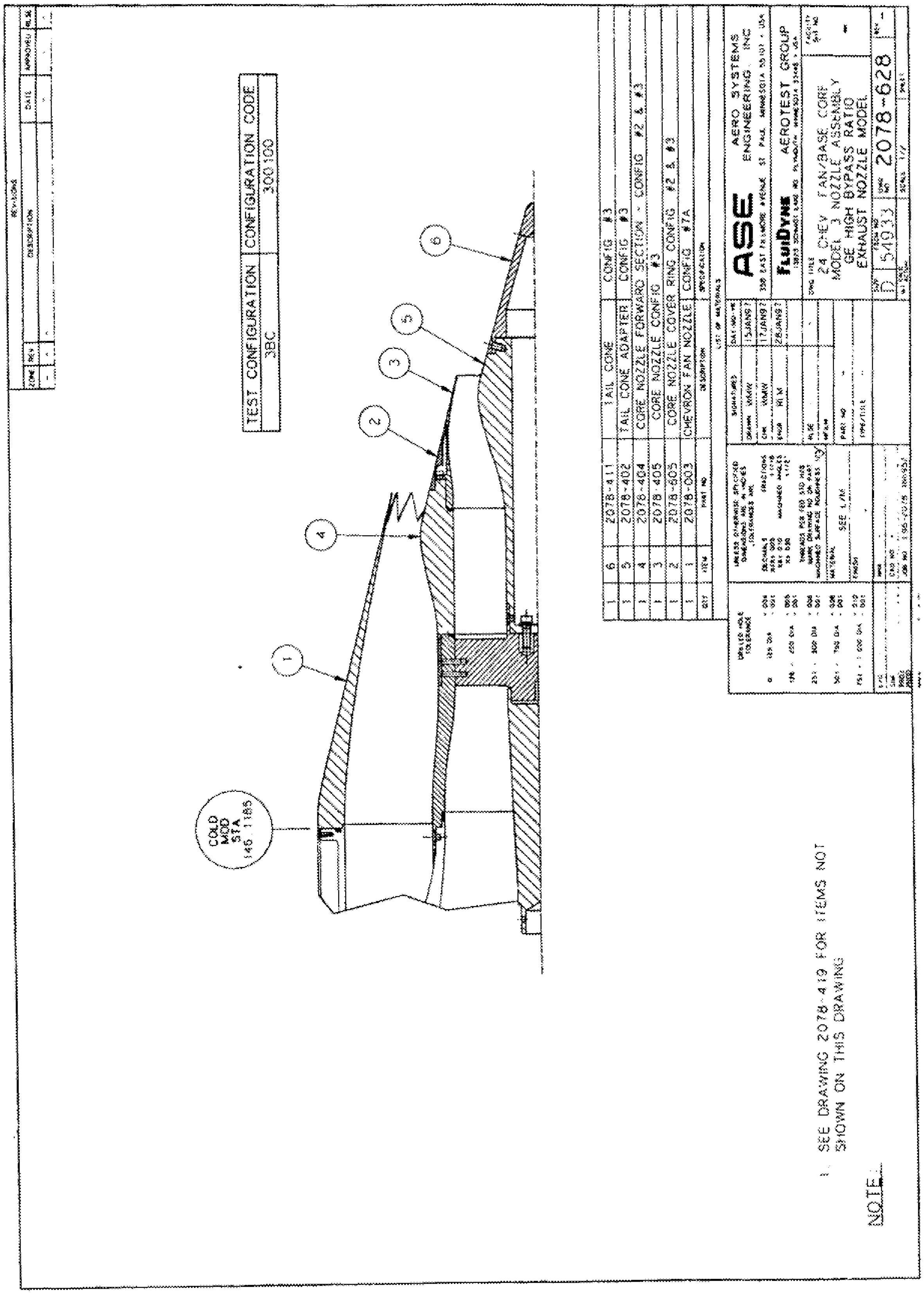
REVISIONS
ZONE
REV
DESCRIPTION
DATE
APPROVED
TEST CONFIGURATION
CONFIGURATION CODE
3BC
300100
COLD MOD STA 145.1185
1
2
3
4
5
6
1 6 2078-411 TAIL CONE CONFIG #3
1 5 2078-402 TAIL CONE ADAPTER CONFIG #3
1 4 2078-404 CORE NOZZLE FORWARD SECTION - CONFIG #2 & #3
1 3 2078-405 CORE NOZZLE CONFIG #3
1 2 2078-605 CORE NOZZLE COVER RING CONFIG #2 & #3
1 1 2078-003 CHEVRON FAN NOZZLE CONFIG #7A
QTY
ITEM
PART NO
DESCRIPTION
SPECIFICATION
LIST OF MATERIALS
DRILLED HOLE TOLERANCE
UNLESS OTHERWISE SPECIFIED DIMENSIONS ARE IN INCHES TOLERANCES ARE
DECIMALS
FRACTIONS
MACHINED ANGLES
MATERIAL
SEE L/M
FINISH
SIGNATURES
DATE
DRAWN WMW 15JAN97
CHK WMW 17JAN97
ENGR RLM 28JAN97
PART NO
ASE
AERO SYSTEMS ENGINEERING, INC
FLUIDYNE
AEROTEST GROUP
DWG TITLE
24 CHEV FAN/BASE CORE
MODEL 3 NOZZLE ASSEMBLY
GE HIGH BYPASS RATIO
EXHAUST NOZZLE MODEL
SIZE D
FSCM NO 54933
DWG NO 2078-628
SCALE 1/2
1. SEE DRAWING 2078-419 FOR ITEMS NOT SHOWN ON THIS DRAWING
NOTE:

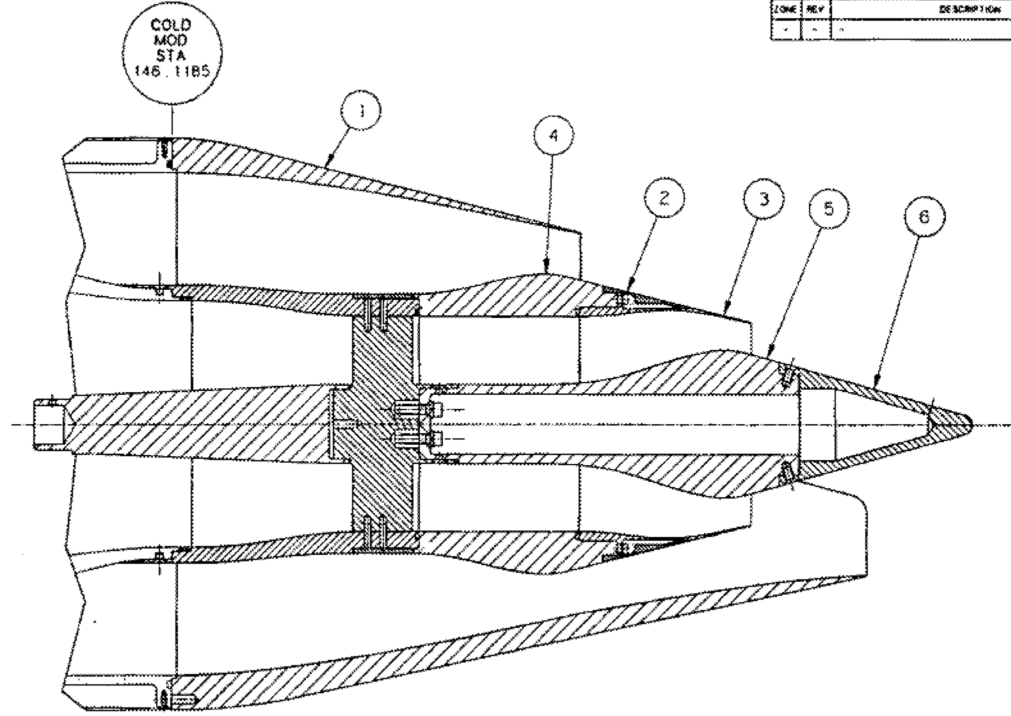


| TEST CONFIGURATION | CONFIGURATION CODE | FAN NOZZLE CLOCKING POSITION |
|---|---|---|
| 3BS | 300700 | 0° |
| 3BS | 300709 | 90° |
| 3BS | 300718 | 180° |

1. SEE DRAWING 2078-419 FOR ITEMS NOT CALLED OUT ON THIS DRAWING

NOTE:

| QTY | ITEM | PART NO. | DESCRIPTION | SPECIFICATION |
|---|---|---|---|---|
| 1 | 6 | 2078-411 | TAIL CONE | CONFIG. #3 |
| 1 | 5 | 2078-402 | TAIL CONE ADAPTER | CONFIG. #3 |
| 1 | 4 | 2078-404 | CORE NOZZLE FORWARD SECTION - CONFIG. #2 & #3 | |
| 1 | 3 | 2078-405 | CORE NOZZLE CONFIG. #3 | |
| 1 | 2 | 2078-605 | CORE NOZZLE COVER RING CONFIG. #2 & #3 | |
| 1 | 1 | 2087-008 | SCARF NOZZLE | |

LIST OF MATERIALS

| SIGNATURES | | DAY-MO-YR |
|---|---|---|
| DRAWN | WMW | 14JAN97 |
| CHK | WMW | 20JAN97 |
| ENGR | RLM | 28JAN97 |

MATERIAL: SEE L/M

ASE AERO SYSTEMS ENGINEERING, INC.
358 EAST FILLMORE AVENUE, ST. PAUL, MINNESOTA 55107 • USA

FLUIDYNE AEROTEST GROUP

DWG TITLE: SCARF FAN/BASE CORE MODEL 3 NOZZLE ASSEMBLY PRATT & WHITNEY MIXING ENHANCMENT NOZZLES

SIZE D | FSCM NO 54933 | DWG NO 2087-601 | REV -

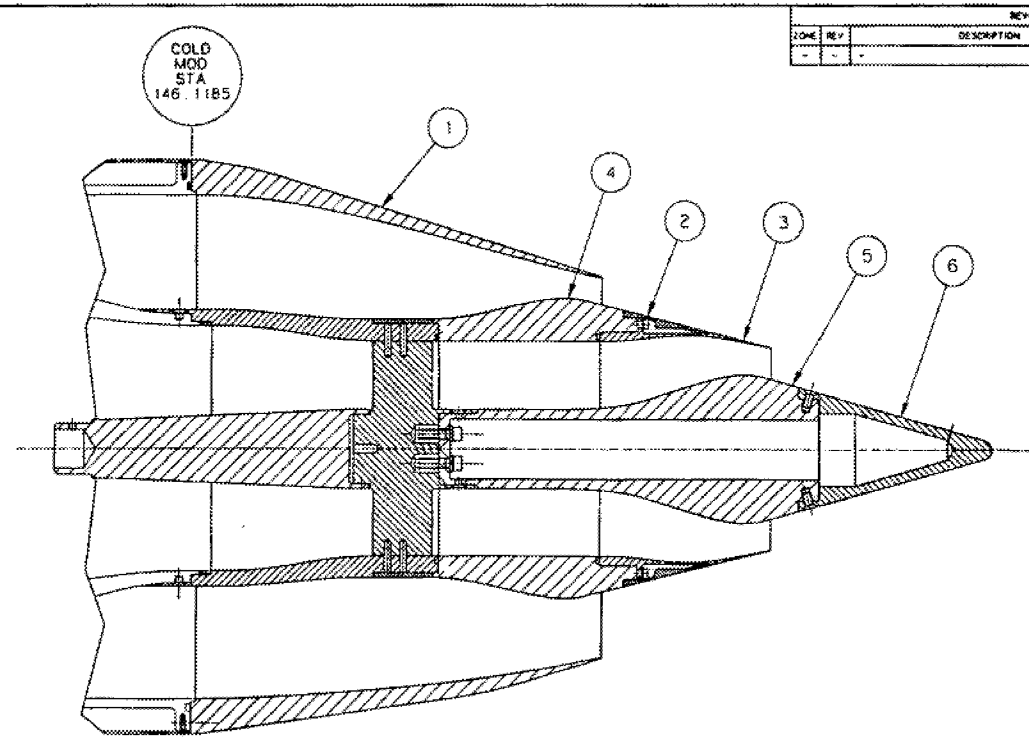


| TEST CONFIGURATION | CONFIGURATION CODE | FAN NOZZLE CLOCKING POSITION |
|---|---|---|
| 380max | 3000500 | 0° |
| 380max | 3000509 | 90° |
| 380max | 3000518 | 180° |

| QTY | ITEM | PART NO | DESCRIPTION | SPECIFICATION |
|---|---|---|---|---|
| 1 | 6 | 2078-411 | TAIL CONE | CONFIG. #3 |
| 1 | 5 | 2078-402 | TAIL CONE ADAPTER | CONFIG. #3 |
| 1 | 4 | 2078-404 | CORE NOZZLE FORWARD SECTION - CONFIG. #2 & #3 | |
| 1 | 3 | 2078-405 | CORE NOZZLE CONFIG. #3 | |
| 1 | 2 | 2078-605 | CORE NOZZLE COVER RING CONFIG. #2 & #3 | |
| 1 | 1 | 2087-004 | FAN NOZZLE #2 | OFFSET - CENTERLINE |

LIST OF MATERIALS

REVISIONS

| ZONE | REV | DESCRIPTION | DATE | APPROVED | RLSE |
|---|---|---|---|---|---|
| - | - | - | - | - | - |

DRILLED HOLE TOLERANCE
0 - .125 DIA +.004 -.001
.126 - .250 DIA +.005 -.001
.251 - .500 DIA +.006 -.001
.501 - .750 DIA +.008 -.001
.751 - 1.000 DIA +.010 -.001

UNLESS OTHERWISE SPECIFIED DIMENSIONS ARE IN INCHES TOLERANCES ARE
DECIMALS .XXX± .005 .XX± .010 .X± .030
FRACTIONS ±1/16
MACHINED ANGLES ±1/2°
THREADS PER FED STD H28
MARK DRAWING NO ON PART
MACHINED SURFACE ROUGHNESS 125

MATERIAL SEE L/M
FINISH -

| SIGNATURES | | DAY-MO-YR |
|---|---|---|
| DRAWN | WMW | 14JAN97 |
| CHK | WMW | 20JAN97 |
| ENGR | RLM | 28JAN97 |
| RLSE | - | - |
| MFXM | | |
| PART NO | - | |
| TYPE/STYLE | - | |

AERO SYSTEMS ENGINEERING, INC.
358 EAST FILLMORE AVENUE, ST. PAUL, MINNESOTA 55107 • USA

FLUIDYNE AEROTEST GROUP
13822 SCHMIDT LAKE RD, PLYMOUTH, MINNESOTA 55446 • USA

L/O -
SIM -
NASA -
CAD NO -
AIR NO 128 7087 NS/R64

1. SEE DRAWING 2078-419 FOR ITEMS NOT CALLED OUT ON THIS DRAWING

NOTE:

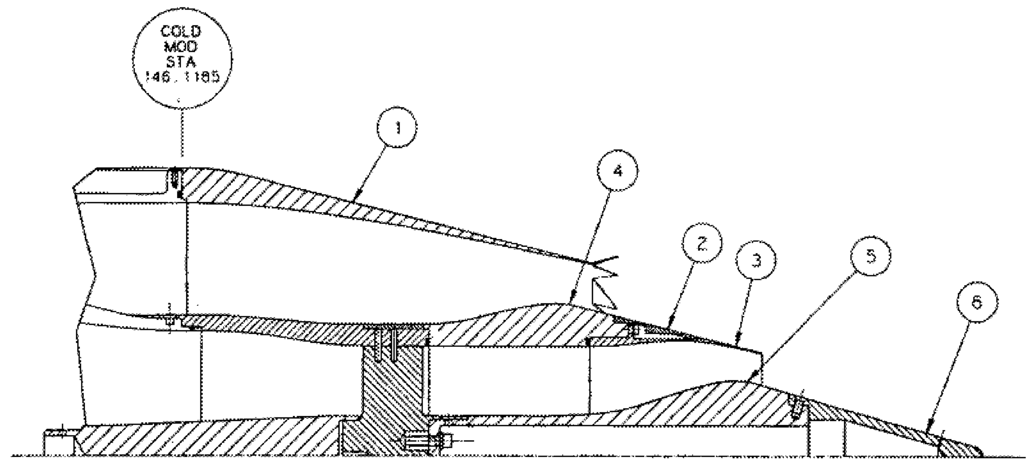


| QTY | ITEM | PART NO | DESCRIPTION | SPECIFICATION |
|---|---|---|---|---|
| 1 | 6 | 2078-411 | TAIL CONE | CONFIG. #3 |
| 1 | 5 | 2078-402 | TAIL CONE ADAPTER | CONFIG. #3 |
| 1 | 4 | 2078-404 | CORE NOZZLE FORWARD SECTION - CONFIG. #2 & #3 | |
| 1 | 3 | 2078-405 | CORE NOZZLE CONFIG. #3 | |
| 1 | 2 | 2078-605 | CORE NOZZLE COVER RING CONFIG. #2 & #3 | |
| 1 | 1 | 2087-002 | 24 FLIPPER TAB - FAN NOZZLE MODEL #4 | |

LIST OF MATERIALS

| TEST CONFIGURATION |
|---|
| 3BT24 |

NOTE:

1. SEE DRAWING 2078-419 FOR ITEMS NOT CALLED OUT ON THIS DRAWING

MATERIAL: SEE L/M

JOB NO. L98-2087-167664

| SIGNATURES | | DAY-MO-YR |
|---|---|---|
| DRAWN | WMW | 14JAN97 |
| CHK | WMW | 20JAN97 |
| ENGR | RLM | 28JAN97 |

AERO SYSTEMS ENGINEERING, INC.
358 EAST FILLMORE AVENUE, ST. PAUL, MINNESOTA 55107 • USA

FLUIDYNE AEROTEST GROUP

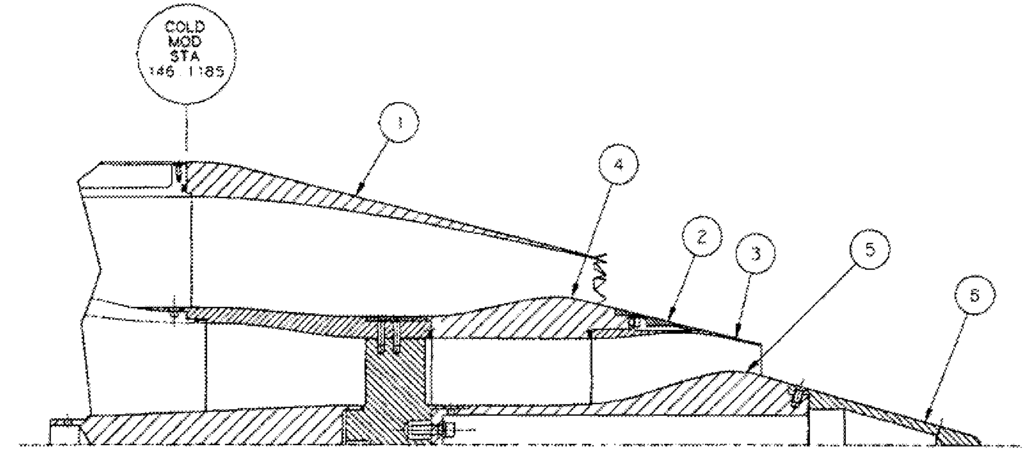


| QTY | ITEM | PART NO | DESCRIPTION | SPECIFICATION |
|---|---|---|---|---|
| 1 | 6 | 2078-411 | TAIL CONE | CONFIG #3 |
| 1 | 5 | 2078-402 | TAIL CONE ADAPTER | CONFIG #3 |
| 1 | 4 | 2078-404 | CORE NOZZLE FORWARD SECTION - CONFIG #2 & #3 | |
| 1 | 3 | 2078-405 | CORE NOZZLE CONFIG. #3 | |
| 1 | 2 | 2078-605 | CORE NOZZLE COVER RING CONFIG. #2 & #3 | |
| 1 | 1 | 2087-001 | 48 FLIPPER TAB - FAN NOZZLE MODEL #3 | |

LIST OF MATERIALS

| TEST CONFIGURATION |
|---|
| 3BT48 |

AERO SYSTEMS ENGINEERING, INC.
358 EAST FILLMORE AVENUE, ST. PAUL, MINNESOTA 55107 • USA

FLUIDYNE AEROTEST GROUP

NOTE:
1. SEE DRAWING 2078-419 FOR ITEMS NOT CALLED OUT ON THIS DRAWING

| REVISIONS | | | | | |
|---|---|---|---|---|---|
| ZONE | REV | DESCRIPTION | DATE | APPROVED | RLSE |
| - | A | REVISED ITEM 3 | 05MAY97 | RLM | - |

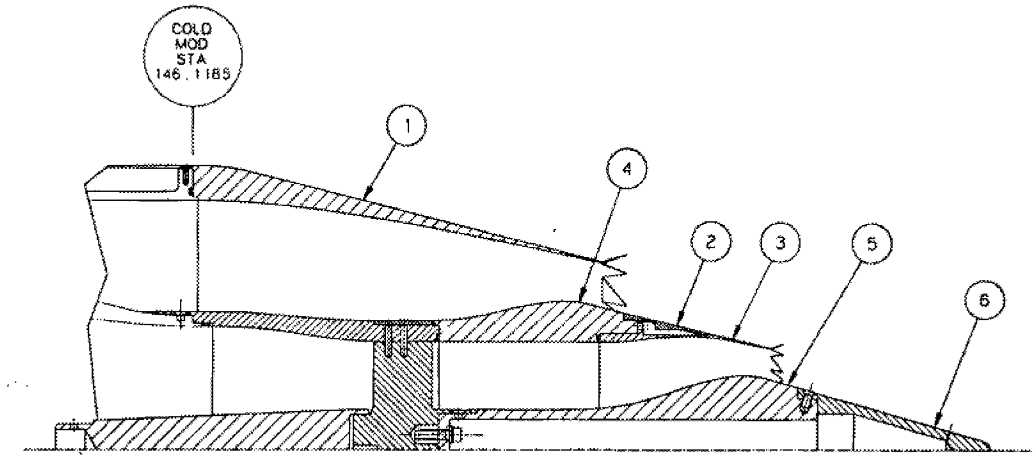


| TEST CONFIGURATION |
|---|
| 3T24T24 |

| QTY | ITEM | PART NO | DESCRIPTION | SPECIFICATION |
|---|---|---|---|---|
| 1 | 6 | 2078-411 | TAIL CONE | CONFIG. #3 |
| 1 | 5 | 2078-402 | TAIL CONE ADAPTER | CONFIG. #3 |
| 1 | 4 | 2078-404 | CORE NOZZLE FORWARD SECTION - CONFIG. #2 & #3 | |
| 1 | 3 | 2087-406 | 24 FLIPPER TAB | |
| 1 | 2 | 2078-605 | CORE NOZZLE COVER RING CONFIG. #2 & #3 | |
| 1 | 1 | 2087-002 | 24 FLIPPER TAB - FAN NOZZLE MODEL #4 | |

LIST OF MATERIALS

| SIGNATURES | | DAY-MO-YR |
|---|---|---|
| DRAWN | WMW | 14JAN97 |
| CHK | WMW | 20JAN97 |
| ENGR | RLM | 28JAN97 |
| RLSE | - | - |
| MFG/M | | |
| PART NO | - | |
| TYPE/TITLE | - | |

UNLESS OTHERWISE SPECIFIED DIMENSIONS ARE IN INCHES TOLERANCES ARE
DECIMALS .XXX± .005 .XX± .010 .X± .030
FRACTIONS ±1/16
MACHINED ANGLES ±1/2°
THREADS PER FED STD H28
MARK DRAWING NO ON PART
MACHINED SURFACE ROUGHNESS 125
MATERIAL SEE L/M
FINISH -
JOB NO 195-2087-167684

AERO SYSTEMS ENGINEERING, INC.
358 EAST FILLMORE AVENUE . ST. PAUL, MINNESOTA 55107 • USA
FLUIDYNE AEROTEST GROUP

NOTE:
1. SEE DRAWING 2078-419 FOR ITEMS NOT CALLED OUT ON THIS DRAWING

| ZONE | REV | DESCRIPTION | DATE | APPROVED | RLSE |
|---|---|---|---|---|---|
| - | A | REVISED ITEM 3 | 05MAY97 | RLM | - |

REVISIONS

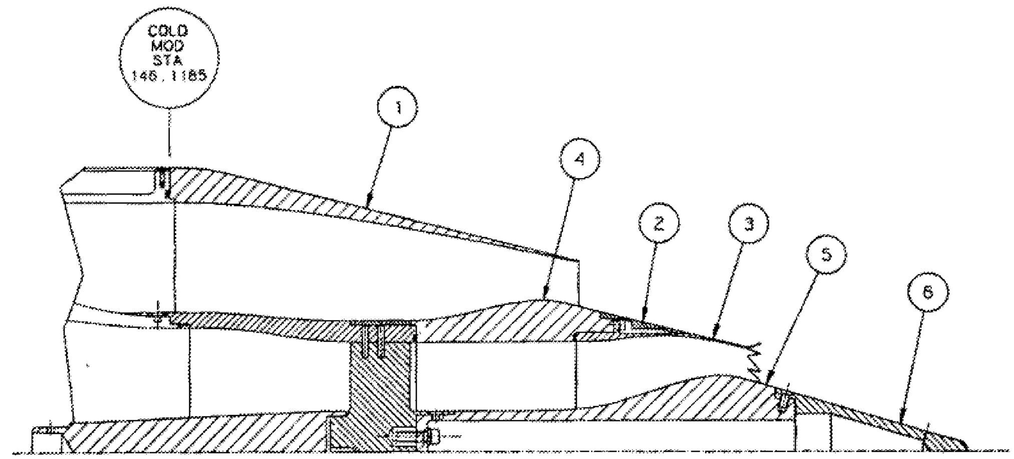


| QTY | ITEM | PART NO | DESCRIPTION | SPECIFICATION |
|---|---|---|---|---|
| 1 | 6 | 2078-411 | TAIL CONE | CONFIG. #3 |
| 1 | 5 | 2078-402 | TAIL CONE ADAPTER | CONFIG. #3 |
| 1 | 4 | 2078-404 | CORE NOZZLE FORWARD SECTION - CONFIG. #2 & #3 | |
| 1 | 3 | 2087-406 | 24 FLIPPER TAB | |
| 1 | 2 | 2078-605 | CORE NOZZLE COVER RING CONFIG. #2 & #3 | |
| 1 | 1 | 2078-001 | FAN NOZZLE CONFIG. #2 THRU #5 | |

LIST OF MATERIALS

| TEST CONFIGURATION |
|---|
| 3T24B |

NOTE:

1. SEE DRAWING 2078-419 FOR ITEMS NOT CALLED OUT ON THIS DRAWING

| SIGNATURES | | DAY-MO-YR |
|---|---|---|
| DRAWN | WMW | 14JAN97 |
| CHK | WMW | 20JAN97 |
| ENGR | RLM | 28JAN97 |

MATERIAL: SEE L/M

AERO SYSTEMS ENGINEERING, INC.
358 EAST FILLMORE AVENUE, ST. PAUL, MINNESOTA 55107 • USA

FLUIDYNE AEROTEST GROUP

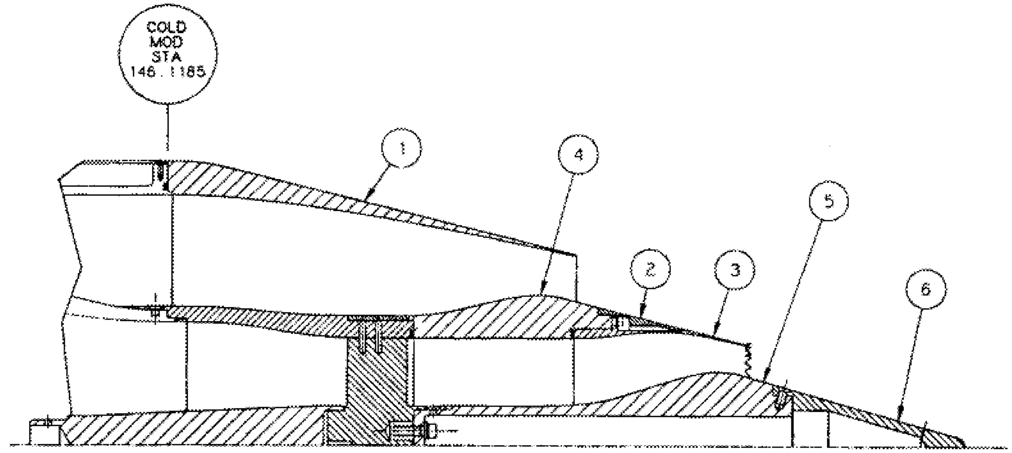


| ZONE | REV | DESCRIPTION | DATE | APPROVED | RLSE |
|---|---|---|---|---|---|
| - | A | REVISED ITEM 3 | 25APR97 | RLM | - |

| QTY | ITEM | PART NO | DESCRIPTION | SPECIFICATION |
|---|---|---|---|---|
| 1 | 6 | 2078-411 | TAIL CONE | CONFIG. #3 |
| 1 | 5 | 2078-402 | TAIL CONE ADAPTER | CONFIG. #3 |
| 1 | 4 | 2078-404 | CORE NOZZLE FORWARD SECTION - CONFIG. #2 & #3 | |
| 1 | 3 (Ⓐ) | 2087-405 | 48 FLIPPER TAB | |
| 1 | 2 | 2078-605 | CORE NOZZLE COVER RING CONFIG. #2 & #3 | |
| 1 | 1 | 2078-001 | FAN NOZZLE CONFIG. #2 THRU #5 | |

LIST OF MATERIALS

| TEST CONFIGURATION |
|---|
| 3T48B |

| SIGNATURES | | DAY-MO-YR |
|---|---|---|
| DRAWN | WMW | 14JAN97 |
| CHK | WMW | 20JAN97 |
| ENGR | RLM | 28JAN97 |

MATERIAL: SEE L/M

JOB NO. L96-2087-167664

AERO SYSTEMS ENGINEERING, INC.
358 EAST FILLMORE AVENUE, ST. PAUL, MINNESOTA 55107 • USA

FLUIDYNE AEROTEST GROUP

NOTE:

1. SEE DRAWING 2078-419 FOR ITEMS NOT CALLED OUT ON THIS DRAWING

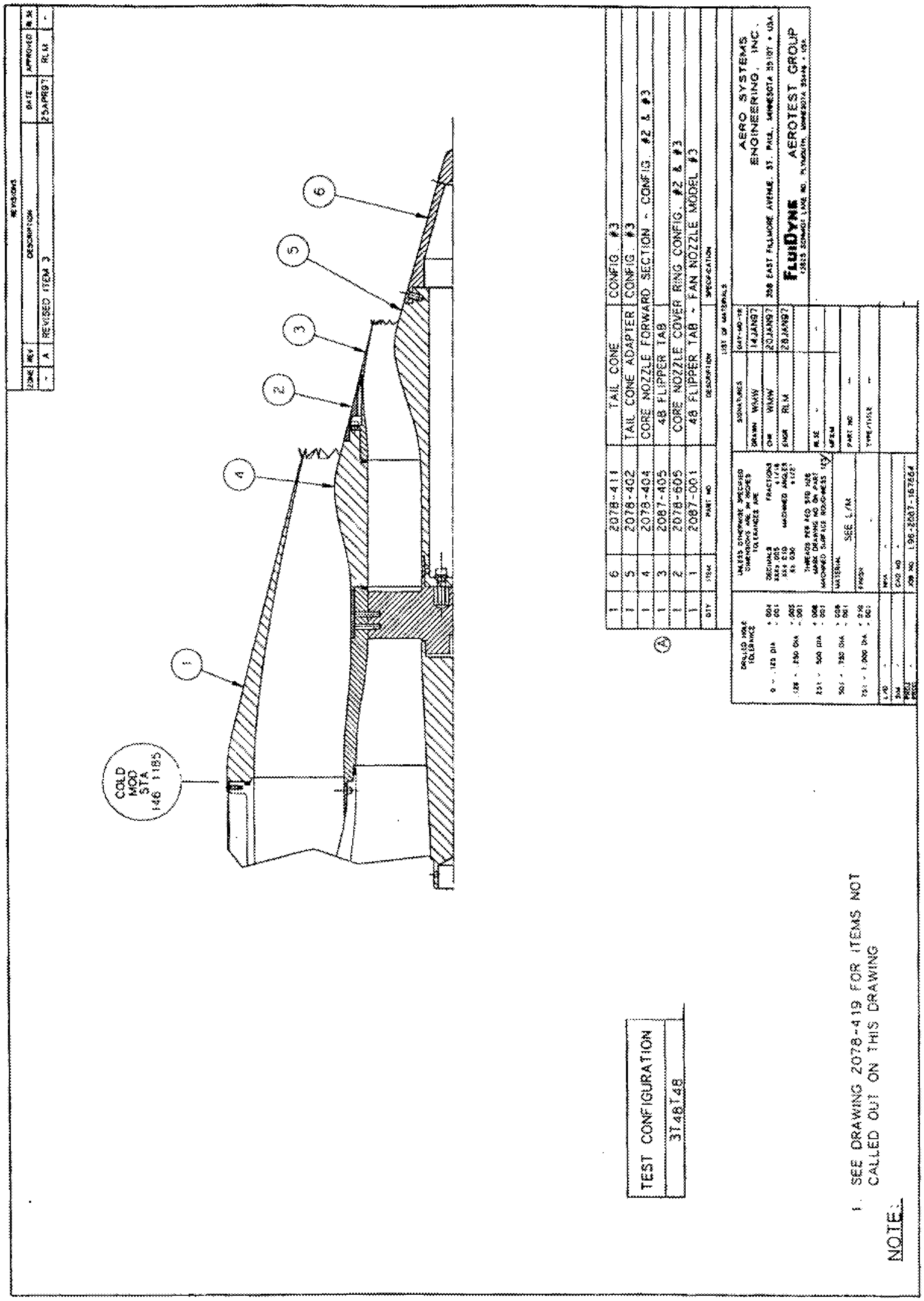
REVISIONS
ZONE | REV | DESCRIPTION | DATE | APPROVED | RLSE
- | A | REVISED ITEM 3 | 25APR97 | RLM | -
COLD MOD STA 146.1185
1
2
3
4
5
6
TEST CONFIGURATION
3T48T48
NOTE:
1. SEE DRAWING 2078-419 FOR ITEMS NOT CALLED OUT ON THIS DRAWING
1 | 6 | 2078-411 | TAIL CONE | CONFIG. #3
1 | 5 | 2078-402 | TAIL CONE ADAPTER | CONFIG. #3
1 | 4 | 2078-404 | CORE NOZZLE FORWARD SECTION - CONFIG. #2 & #3
1 | 3 | 2087-405 | 48 FLIPPER TAB
1 | 2 | 2078-605 | CORE NOZZLE COVER RING CONFIG. #2 & #3
1 | 1 | 2087-001 | 48 FLIPPER TAB - FAN NOZZLE MODEL #3
QTY | ITEM | PART NO | DESCRIPTION | SPECIFICATION
LIST OF MATERIALS
DRAWN WAW 14JAN97
CHK WAW 20JAN97
ENGR RLM 28JAN97
SEE L/M
AERO SYSTEMS ENGINEERING, INC.
358 EAST FILLMORE AVENUE, ST. PAUL, MINNESOTA 55107 • USA
FLUIDYNE
AEROTEST GROUP

| REVISIONS | | | | | |
|---|---|---|---|---|---|
| ZONE | REV | DESCRIPTION | DATE | APPROVED | RLSE |
| - | A | REVISED ITEM 3 | 23APR97 | RLM | - |

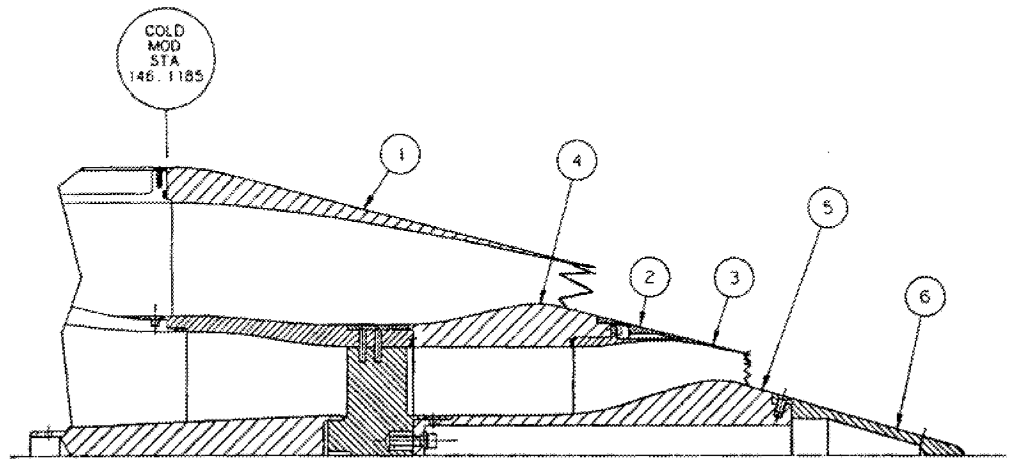


| TEST CONFIGURATION |
|---|
| 3T48C |

| QTY | ITEM | PART NO | DESCRIPTION | SPECIFICATION |
|---|---|---|---|---|
| 1 | 6 | 2078-411 | TAIL CONE | CONFIG. #3 |
| 1 | 5 | 2078-402 | TAIL CONE ADAPTER | CONFIG. #3 |
| 1 | 4 | 2078-404 | CORE NOZZLE FORWARD SECTION - CONFIG. #2 & #3 | |
| 1 | 3 | 2087-405 | 48 FLIPPER TAB (A) | |
| 1 | 2 | 2078-605 | CORE NOZZLE COVER RING CONFIG. #2 & #3 | |
| 1 | 1 | 2078-003 | CHEVRON FAN NOZZLE | CONFIG #7A |

LIST OF MATERIALS

| SIGNATURES | | DAY-MO-YR |
|---|---|---|
| DRAWN | WMW | 14JAN97 |
| CHK | WMW | 20JAN97 |
| ENGR | RLM | 28JAN97 |
| RLSE | - | - |

MATERIAL SEE L/M

PART NO. -

TYPE/TITLE -

JOB NO L98-2087-167884

AERO SYSTEMS ENGINEERING, INC.
358 EAST FILLMORE AVENUE, ST. PAUL, MINNESOTA 55107 USA

FLUIDYNE AEROTEST GROUP

NOTE:

1. SEE DRAWING 2078-419 FOR ITEMS NOT CALLED OUT ON THIS DRAWING

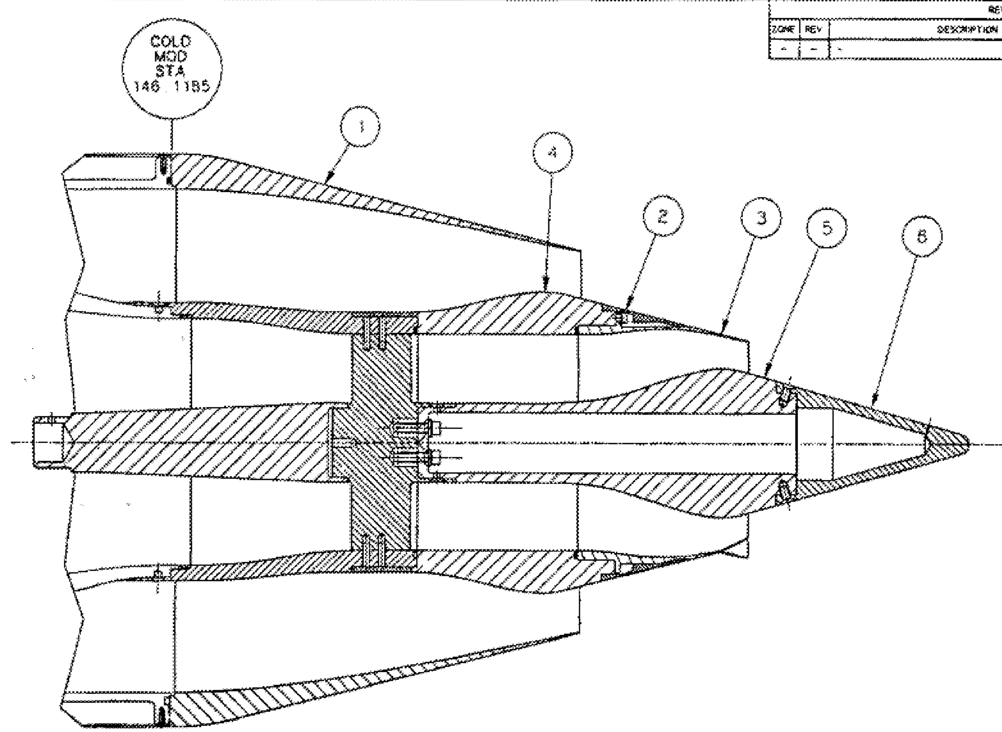


| TEST CONFIGURATION | CONFIGURATION CODE | Fan Nozzle Clocking Position |
|---|---|---|
| 3HmB(0) | 3090000 | 0° |
| 3HmB(90) | 3090009 | 90° |
| 3HmB(180) | 3090018 | 180° |
| 3HmB(45) | 3090045 | 45° |

| QTY | ITEM | PART NO | DESCRIPTION | SPECIFICATION |
|---|---|---|---|---|
| 1 | 6 | 2078-411 | TAIL CONE | CONFIG. #3 |
| 1 | 5 | 2078-402 | TAIL CONE ADAPTER | CONFIG. #3 |
| 1 | 4 | 2078-404 | CORE NOZZLE FORWARD SECTION - CONFIG. #2 & #3 | |
| 1 | 3 | 2087-404 | HALF MIXER | |
| 1 | 2 | 2078-605 | CORE NOZZLE COVER RING CONFIG. #2 & #3 | |
| 1 | 1 | 2078-001 | FAN NOZZLE | CONFIG. #2 THRU #5 |

LIST OF MATERIALS

| SIGNATURES | | DAY-MO-YR |
|---|---|---|
| DRAWN | WMW | 20JAN97 |
| CHK | WMW | 29JAN97 |
| ENGR | RLM | 30JAN97 |

MATERIAL SEE L/M

JOB NO L96-2078-166952

ASE AERO SYSTEMS ENGINEERING, INC.
358 EAST FILLMORE AVENUE, ST. PAUL, MINNESOTA 55107 • USA

FLUIDYNE AEROTEST GROUP

NOTE:

1. SEE DRAWING 2078-419 FOR ITEMS NOT CALLED OUT ON THIS DRAWING

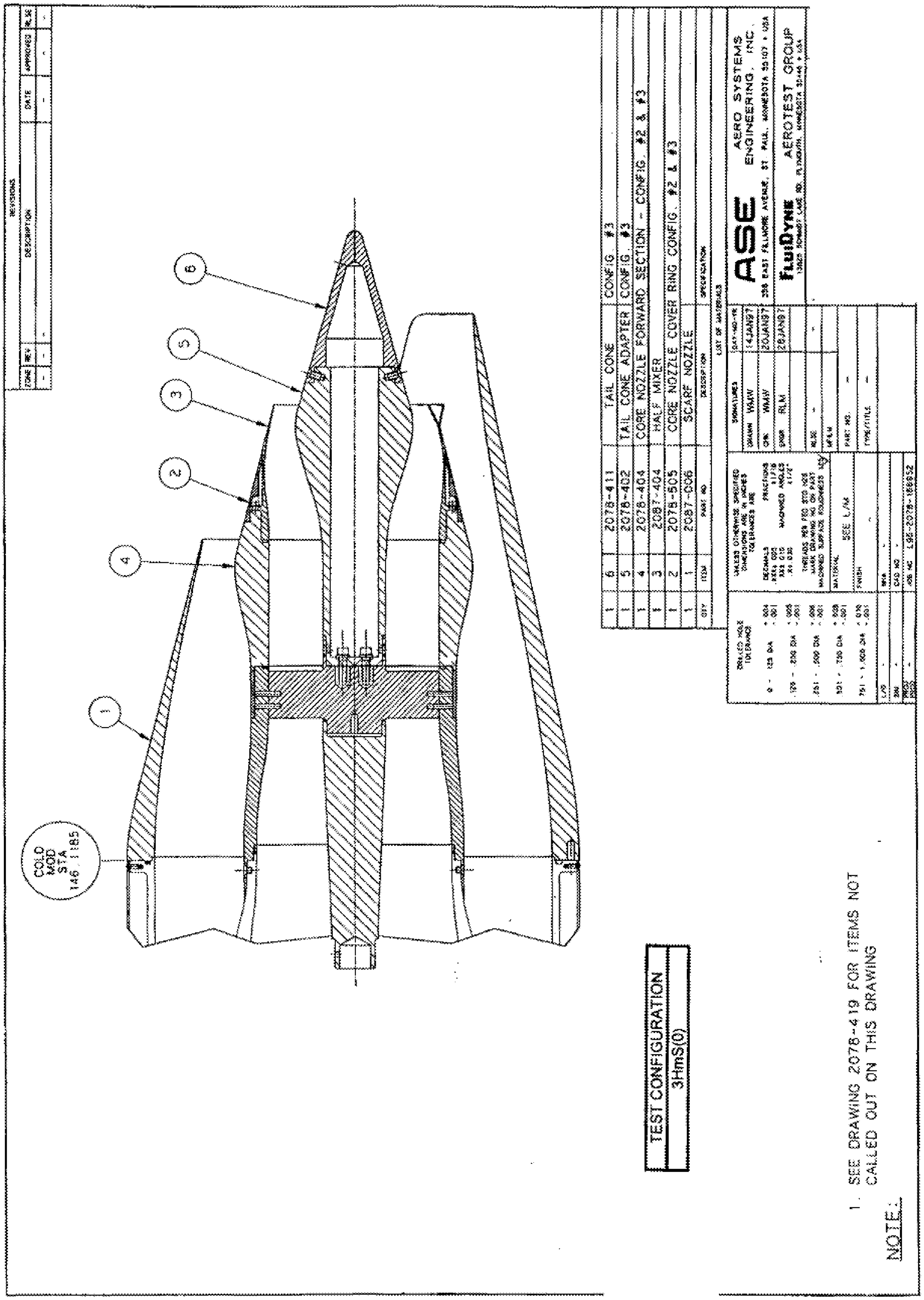

REVISIONS
ZONE REV DESCRIPTION DATE APPROVED RLSE
1
2
3
4
5
6
COLD MOD STA 146.1185
1 6 2078-411 TAIL CONE CONFIG #3
1 5 2078-402 TAIL CONE ADAPTER CONFIG #3
1 4 2078-404 CORE NOZZLE FORWARD SECTION - CONFIG #2 & #3
1 3 2087-404 HALF MIXER
1 2 2078-505 CORE NOZZLE COVER RING CONFIG #2 & #3
1 1 2087-006 SCARF NOZZLE
QTY ITEM PART NO DESCRIPTION SPECIFICATION
LIST OF MATERIALS
SIGNATURES DATE
DRAWN WAW 14JAN97
CHK WAW 20JAN97
ENGR RLM 28JAN97
ASE AERO SYSTEMS ENGINEERING, INC.
358 EAST FILLMORE AVENUE, ST PAUL, MINNESOTA 55107 USA
FLUIDYNE AEROTEST GROUP
TEST CONFIGURATION
3HmS(0)
NOTE:
1. SEE DRAWING 2078-419 FOR ITEMS NOT CALLED OUT ON THIS DRAWING

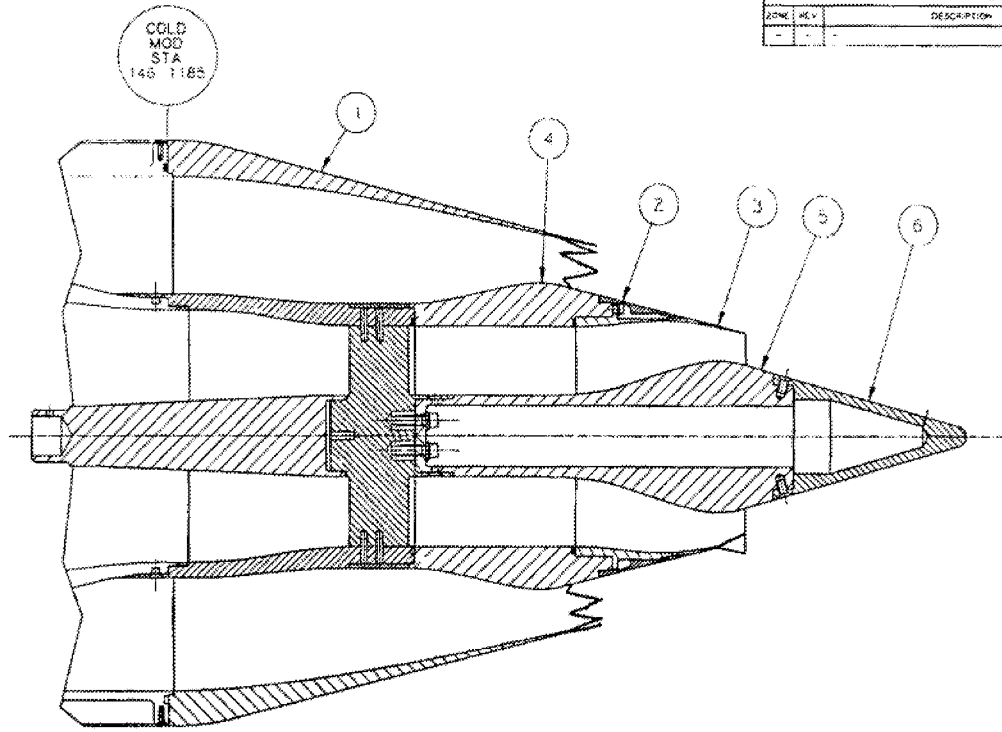


| TEST CONFIGURATION | CONFIGURATION CODE | Fan Nozzle Clocking Position |
|---|---|---|
| 3HmC(0) | 3090100 | 0° |
| 3HmC(45) | 3090145 | 45° |

| QTY | ITEM | PART NO | DESCRIPTION | SPECIFICATION |
|---|---|---|---|---|
| 1 | 6 | 2078-411 | TAIL CONE | CONFIG. #3 |
| 1 | 5 | 2078-402 | TAIL CONE ADAPTER | CONFIG. #3 |
| 1 | 4 | 2078-404 | CORE NOZZLE FORWARD SECTION - CONFIG. #2 & #3 | |
| 1 | 3 | 2087-404 | HALF MIXER | |
| 1 | 2 | 2078-605 | CORE NOZZLE COVER RING CONFIG. #2 & #3 | |
| 1 | 1 | 2078-003 | CHEVRON FAN NOZZLE | CONFIG. #7A |

LIST OF MATERIALS

DRILLED HOLE TOLERANCE
0 - .125 DIA +.004 -.001
.126 - .250 DIA +.005 -.001
.251 - .500 DIA +.006 -.001
.501 - .750 DIA +.008 -.001
.751 - 1.000 DIA +.010 -.001

UNLESS OTHERWISE SPECIFIED DIMENSIONS ARE IN INCHES TOLERANCES ARE
DECIMALS .XXX ±.005 .XX ±.010 .X ±.030
FRACTIONS ±1/16
MACHINED ANGLES ±1/2°
THREADS PER FED STD H28
MASK DRAWING NO ON PART
MACHINED SURFACE ROUGHNESS 125
MATERIAL SEE L/M
FINISH -

SIGNATURES / DAY-MO-YR
DRAWN WMW 20JAN97
CHK WMW 29JAN97
ENGR RLM 30JAN97
RLSE -
MFG/M
PART NO -
TYPE/TITLE -

L/D -
SM -
PROJ/PROD -
WHA -
CAD NO -
JOB NO L96-2078-186932

ASE AERO SYSTEMS ENGINEERING, INC.
358 EAST FILLMORE AVENUE ST. PAUL, MINNESOTA 55107 • USA
FLUIDYNE AEROTEST GROUP
13825 SCHMIDT LAKE RD. PLYMOUTH, MINNESOTA 55446 • USA

NOTE:

1. SEE DRAWING 2078-419 FOR ITEMS NOT CALLED OUT ON THIS DRAWING

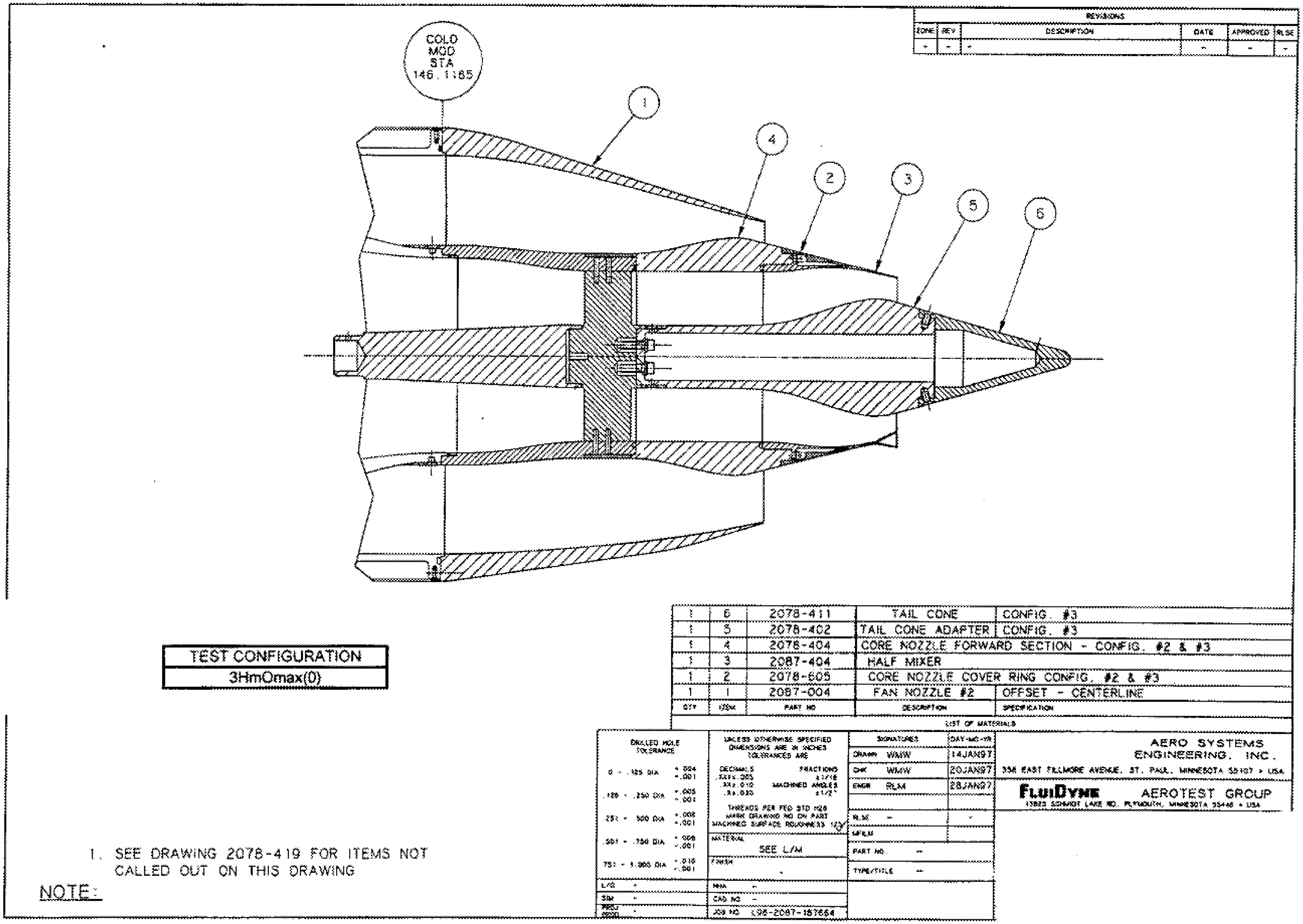
REVISIONS
ZONE
REV
DESCRIPTION
DATE
APPROVED
RLSE
COLD MOD STA 146.1185
1
2
3
4
5
6
TEST CONFIGURATION
3HmOmax(0)
1 | 6 | 2078-411 | TAIL CONE | CONFIG. #3
1 | 5 | 2078-402 | TAIL CONE ADAPTER | CONFIG. #3
1 | 4 | 2078-404 | CORE NOZZLE FORWARD SECTION - CONFIG. #2 & #3
1 | 3 | 2087-404 | HALF MIXER
1 | 2 | 2078-605 | CORE NOZZLE COVER RING CONFIG. #2 & #3
1 | 1 | 2087-004 | FAN NOZZLE #2 | OFFSET - CENTERLINE
QTY | ITEM | PART NO | DESCRIPTION | SPECIFICATION
LIST OF MATERIALS
SIGNATURES
DAY-MO-YR
DRAWN WMW 14JAN97
CHK WMW 20JAN97
ENGR RLM 28JAN97
AERO SYSTEMS ENGINEERING, INC.
358 EAST FILLMORE AVENUE, ST. PAUL, MINNESOTA 55107 • USA
FLUIDYNE AEROTEST GROUP
SEE L/M
1. SEE DRAWING 2078-419 FOR ITEMS NOT CALLED OUT ON THIS DRAWING
NOTE:

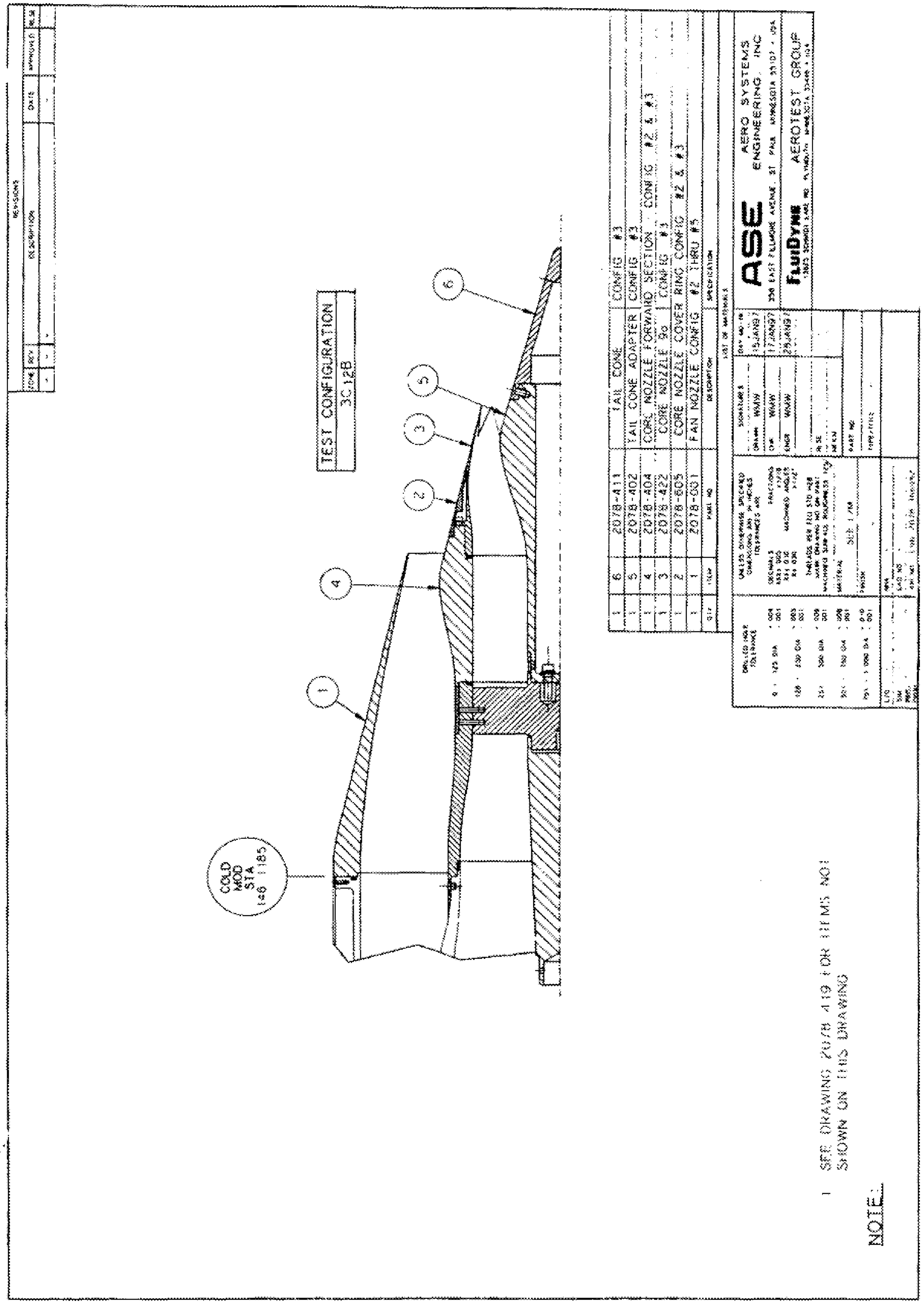
REVISIONS
ZONE REV DESCRIPTION DATE APPROVED RLSE
COLD MOD STA 146 1185
TEST CONFIGURATION
3C12B
1
2
3
4
5
6
1 6 2078-411 TAIL CONE CONFIG #3
1 5 2078-402 TAIL CONE ADAPTER CONFIG #3
1 4 2078-404 CORE NOZZLE FORWARD SECTION - CONFIG #2 & #3
1 3 2078-422 CORE NOZZLE 9o CONFIG #3
1 2 2078-605 CORE NOZZLE COVER RING CONFIG #2 & #3
1 1 2078-001 FAN NOZZLE CONFIG #2 THRU #5
QTY ITEM PART NO DESCRIPTION SPECIFICATION
LIST OF MATERIALS
DRAWN WMW 15JAN97
CHK WMW 17JAN97
ENGR WMW 25JAN97
ASE AERO SYSTEMS ENGINEERING, INC
358 EAST FILLMORE AVENUE, ST. PAUL MINNESOTA 55107 - USA
FLUIDYNE AEROTEST GROUP
1 SEE DRAWING 2078-419 FOR ITEMS NOT SHOWN ON THIS DRAWING
NOTE:

| ZONE | REV | DESCRIPTION | DATE | APPROVED |
|---|---|---|---|---|
| - | A | REVISED ITEM 3 PICTURE | 14APR97 | RLM |

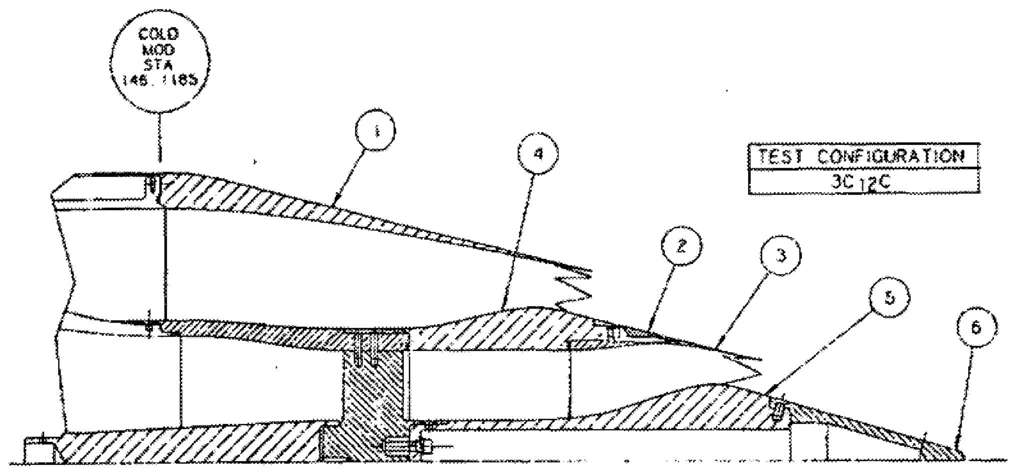


| QTY | ITEM | PART NO | DESCRIPTION | SPECIFICATION |
|---|---|---|---|---|
| 1 | 6 | 2078-411 | TAIL CONE | CONFIG #3 |
| 1 | 5 | 2078-402 | TAIL CONE ADAPTER | CONFIG #3 |
| 1 | 4 | 2078-404 | CORE NOZZLE FORWARD SECTION - CONFIG. #2 & #3 | |
| 1 | 3 | 2078-422 | CORE NOZZLE 9A | CONFIG. #3 |
| 1 | 2 | 2078-805 | CORE NOZZLE COVER RING CONFIG. #2 & #3 | |
| 1 | 1 | 2078-003 | CONFIG. #7A | CHEVRON FAN NOZZLE |

LIST OF MATERIALS

DRAWN WAW 14JAN97
CHK WAW 18JAN97
CHKR RLM 28JAN97

MATERIAL SEE L/M

JOB NO E96-2078-186832

ASE AERO SYSTEMS ENGINEERING, INC.

FLUIDYNE AEROTEST GROUP

NOTE:

1. SEE DRAWING 2078-419 FOR ITEMS NOT CALLED OUT ON THIS DRAWING

| Zone | Rev | Description | Date | Approved |
|---|---|---|---|---|

**TEST CONFIGURATION**
3CHC

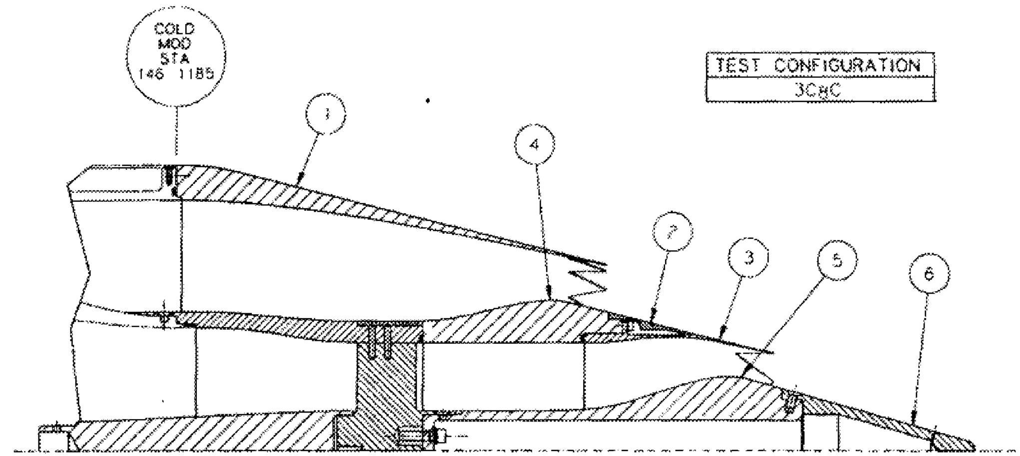


| QTY | ITEM | PART NO | DESCRIPTION | SPECIFICATION |
|---|---|---|---|---|
| 1 | 6 | 2078-411 | TAIL CONE | CONFIG #3 |
| 1 | 5 | 2078-402 | TAIL CONE ADAPTER | CONFIG #3 |
| 1 | 4 | 2078-404 | CORE NOZZLE FORWARD SECTION | CONFIG #2 & #3 |
| 1 | 3 | 2078-423 | CORE NOZZLE 9b | CONFIG #3 |
| 1 | 2 | 2078-605 | CORE NOZZLE COVER RING CONFIG #2 & #3 | |
| 1 | 1 | 2078-003 | CONFIG #7A | CHEVRON FAN NOZZLE |

LIST OF MATERIALS

| SIGNATURES | | DAY-MO-YR |
|---|---|---|
| DRAWN | WMW | 15JAN97 |
| CHK | WMW | 17JAN97 |
| ENGR | RLM | 28JAN97 |

UNLESS OTHERWISE SPECIFIED DIMENSIONS ARE IN INCHES TOLERANCES ARE

MATERIAL: SEE L/M

ASE AERO SYSTEMS ENGINEERING, INC.
358 EAST FILLMORE AVENUE ST. PAUL, MINNESOTA 55107 • USA

FLUIDYNE AEROTEST GROUP

1. SEE DRAWING 2078-419 FOR ITEMS NOT SHOWN ON THIS DRAWING

NOTE:

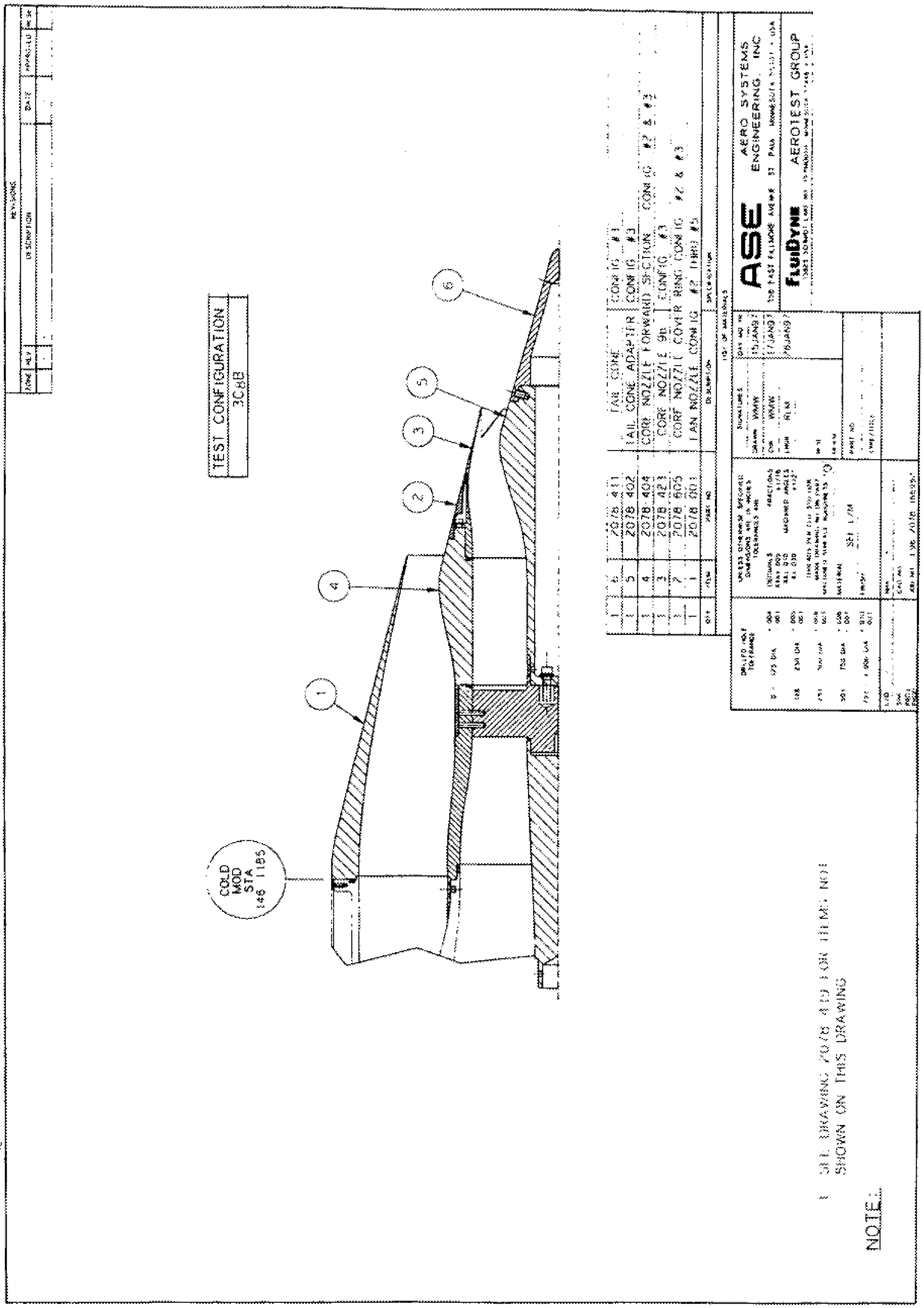
TEST CONFIGURATION
3C8B
COLD MOD STA 146.1185
1
2
3
4
5
6
TAIL CONE CONFIG #1
TAIL CONE ADAPTER CONFIG #3
CORE NOZZLE FORWARD SECTION CONFIG #2 & #3
CORE NOZZLE 9B CONFIG #3
CORE NOZZLE COVER RING CONFIG #2 & #3
FAN NOZZLE CONFIG #2 THRU #5
ASE
AERO SYSTEMS ENGINEERING, INC.
FLUIDYNE
AEROTEST GROUP
NOTE:
SEE DRAWING 2078-400 FOR ITEMS NOT SHOWN ON THIS DRAWING

| TEST CONFIGURATION |
| --- |
| 318 |

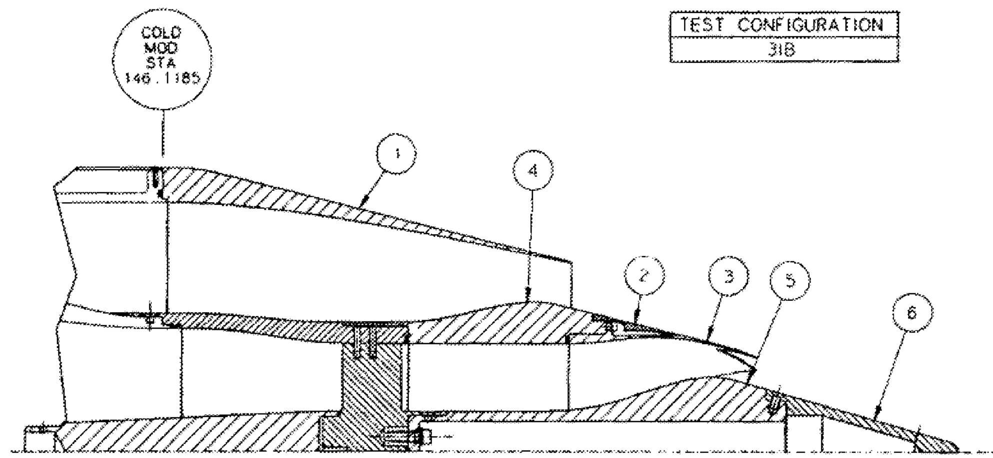


| QTY | ITEM | PART NO | DESCRIPTION | SPECIFICATION |
| --- | --- | --- | --- | --- |
| 1 | 6 | 2078-411 | TAIL CONE | CONFIG #3 |
| 1 | 5 | 2078-402 | TAIL CONE ADAPTER | CONFIG #3 |
| 1 | 4 | 2078-404 | CORE NOZZLE FORWARD SECTION - CONFIG #2 & #3 | |
| 1 | 3 | 2078-427 | CORE NOZZLE 9C | CONFIG #3 |
| 1 | 2 | 2078-605 | CORE NOZZLE COVER RING CONFIG #2 & #3 | |
| 1 | 1 | 2078-001 | FAN NOZZLE CONFIG #2 THRU #5 | |

LIST OF MATERIALS

ASE AERO SYSTEMS ENGINEERING, INC.
358 EAST FILLMORE AVENUE ST. PAUL, MINNESOTA 55107 • USA

FLUIDYNE AEROTEST GROUP

NOTE:

1 SEE DRAWING 2078-419 FOR ITEMS NOT SHOWN ON THIS DRAWING

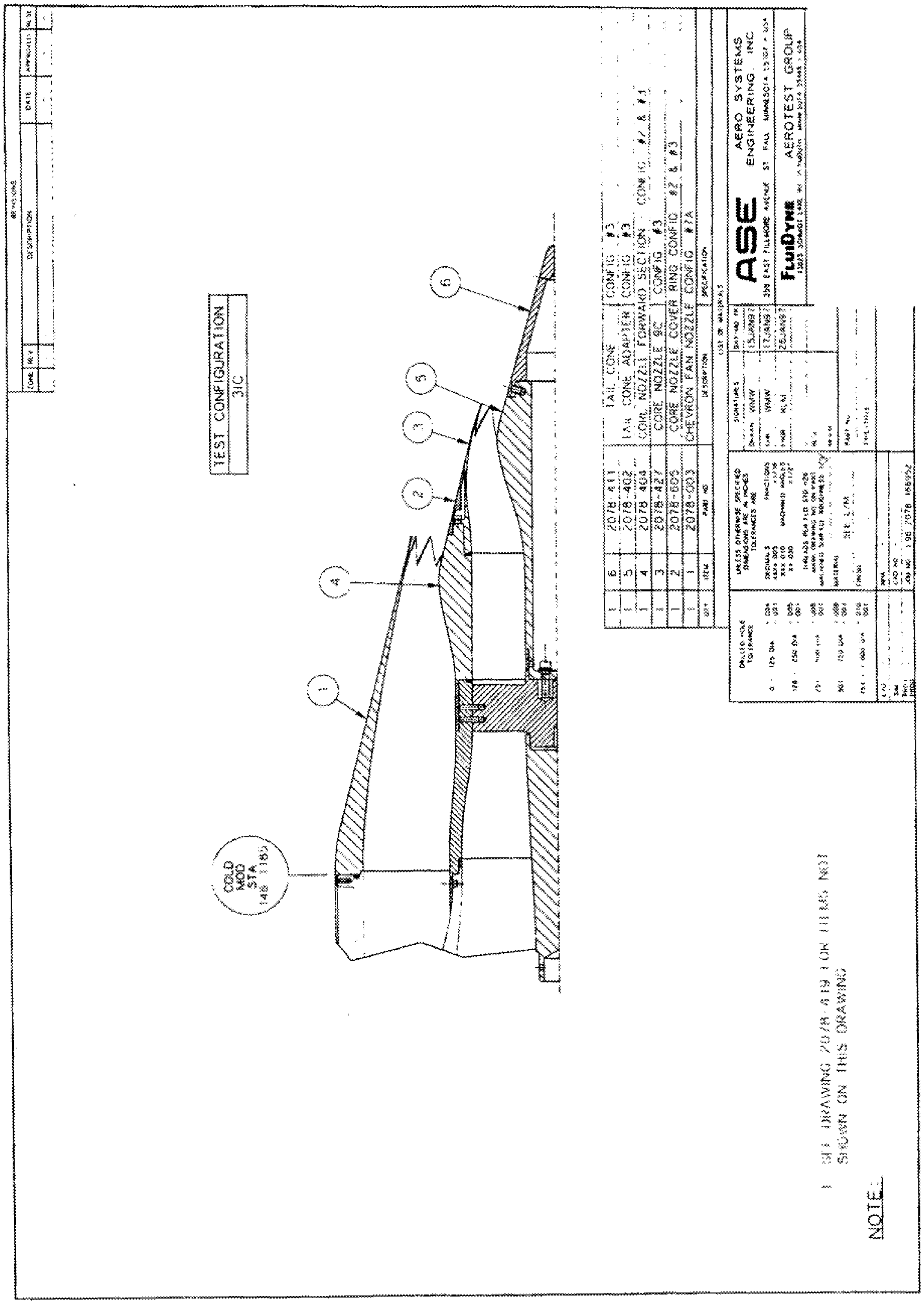
TEST CONFIGURATION
31C
6 2078-411 TAIL CONE CONFIG #3
5 2078-402 TAIL CONE ADAPTER CONFIG #3
4 2078-404 CORE NOZZLE FORWARD SECTION CONFIG #2 & #3
3 2078-427 CORE NOZZLE 9C CONFIG #3
2 2078-605 CORE NOZZLE COVER RING CONFIG #2 & #3
1 2078-003 CHEVRON FAN NOZZLE CONFIG #7A
ASE
AERO SYSTEMS ENGINEERING, INC.
FLUIDYNE
AEROTEST GROUP
NOTE:
SHOWN ON THIS DRAWING

| REVISIONS | | | | | |
|---|---|---|---|---|---|
| ZONE | REV | DESCRIPTION | DATE | APPROVED | BY |
| - | - | - | | - | |

| TEST CONFIGURATION |
|---|
| 3AC |

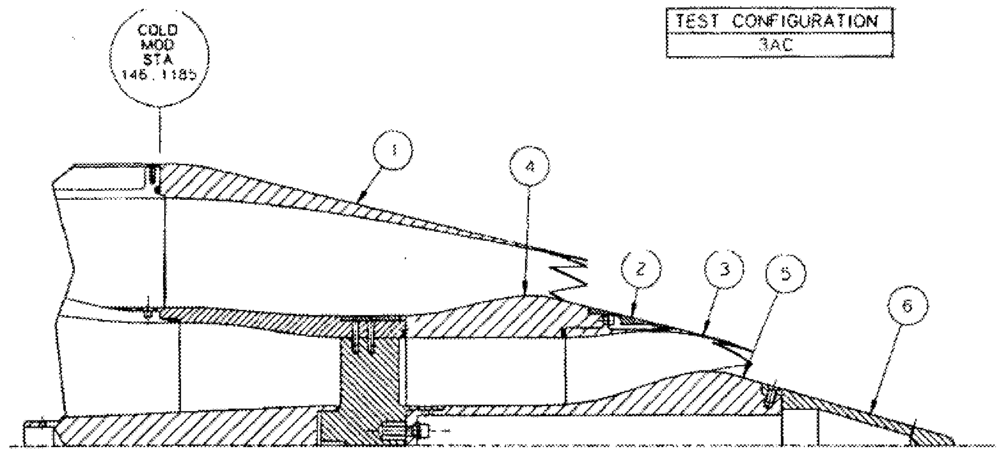


| QTY | ITEM | PART NO | DESCRIPTION | SPECIFICATION |
|---|---|---|---|---|
| 1 | 6 | 2078-411 | TAIL CONE | CONFIG. #3 |
| 1 | 5 | 2078-402 | TAIL CONE ADAPTER | CONFIG. #3 |
| 1 | 4 | 2078-404 | CORE NOZZLE FORWARD SECTION - CONFIG. #2 & #3 | |
| 1 | 3 | 2078-429 | CORE NOZZLE 9D | CONFIG. #3 |
| 1 | 2 | 2078-605 | CORE NOZZLE COVER RING CONFIG. #2 & #3 | |
| 1 | 1 | 2078-003 | CHEVRON FAN NOZZLE CONFIG. #7A | |

LIST OF MATERIALS

UNLESS OTHERWISE SPECIFIED DIMENSIONS ARE IN INCHES TOLERANCES ARE

MATERIAL: SEE L/M

| SIGNATURES | | DAY-MO-YR |
|---|---|---|
| DRAWN | WMW | 15JAN97 |
| CHK | WMW | 17JAN97 |
| ENGR | RLM | 28JAN97 |

**ASE** AERO SYSTEMS ENGINEERING, INC
358 EAST FILLMORE AVENUE · ST. PAUL, MINNESOTA 55107 · USA

**FLUIDYNE** AEROTEST GROUP

NOTE:

1. SEE DRAWING 2078-419 FOR ITEMS NOT SHOWN ON THIS DRAWING

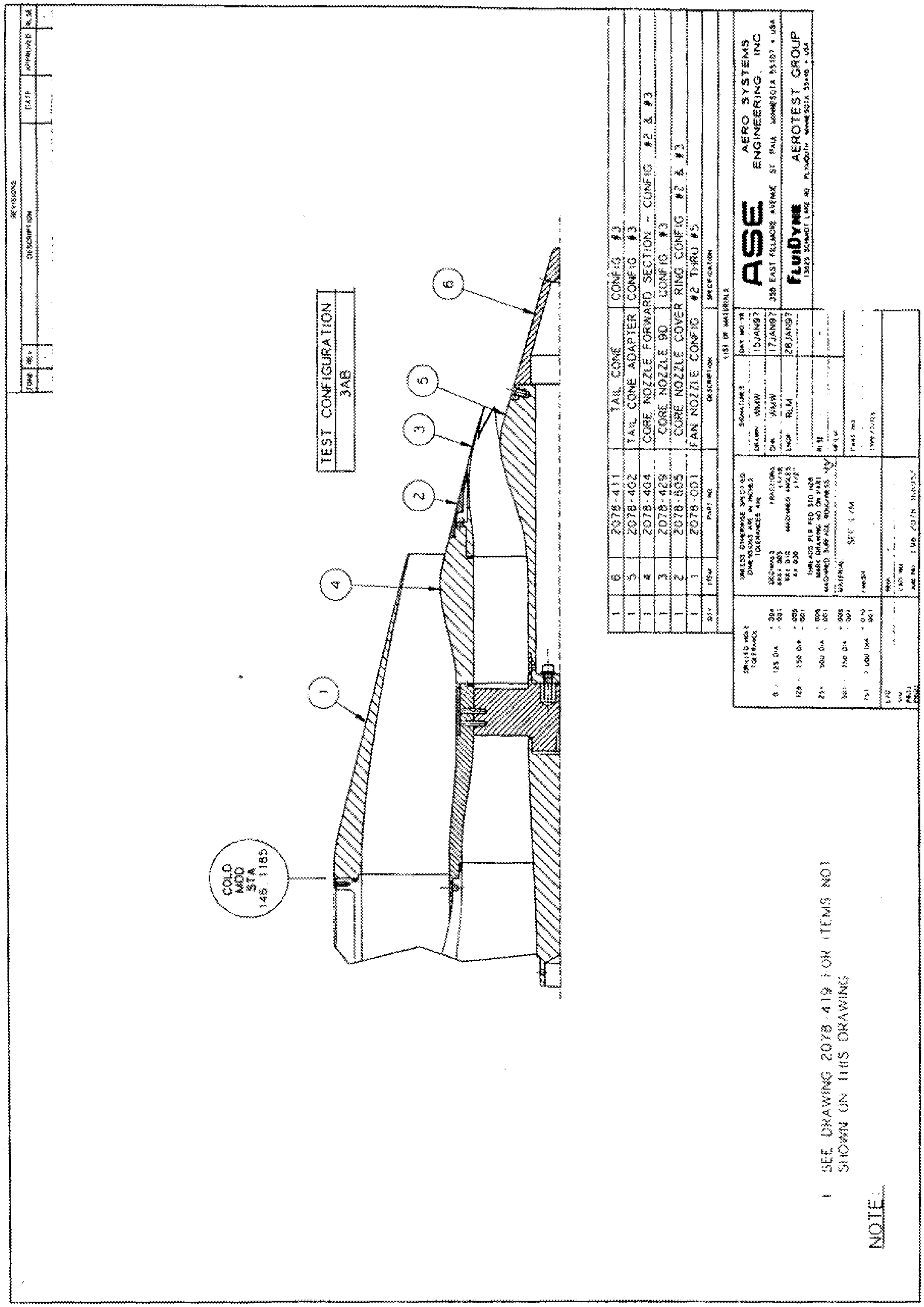
TEST CONFIGURATION
3AB
COLD MOD STA 146.1185
1
2
3
4
5
6
REVISIONS
ZONE
REV
DESCRIPTION
DATE
APPROVED
1 | 6 | 2078-411 | TAIL CONE | CONFIG #3
1 | 5 | 2078-402 | TAIL CONE ADAPTER | CONFIG #3
1 | 4 | 2078-404 | CORE NOZZLE FORWARD SECTION - CONFIG #2 & #3
1 | 3 | 2078-429 | CORE NOZZLE 9D | CONFIG #3
1 | 2 | 2078-605 | CORE NOZZLE COVER RING CONFIG #2 & #3
1 | 1 | 2078-001 | FAN NOZZLE CONFIG #2 THRU #5
QTY
ITEM
PART NO.
DESCRIPTION
SPECIFICATION
LIST OF MATERIALS
DRAWN
CHK
ENGR
WMW
RLM
13JAN97
17JAN97
28JAN97
ASE
AERO SYSTEMS ENGINEERING, INC
358 EAST FILLMORE AVENUE ST. PAUL MINNESOTA 55107 USA
FLUIDYNE
AEROTEST GROUP
NOTE:
1. SEE DRAWING 2078-419 FOR ITEMS NOT SHOWN ON THIS DRAWING

| TEST CONFIGURATION |
|---|
| 3D18 |

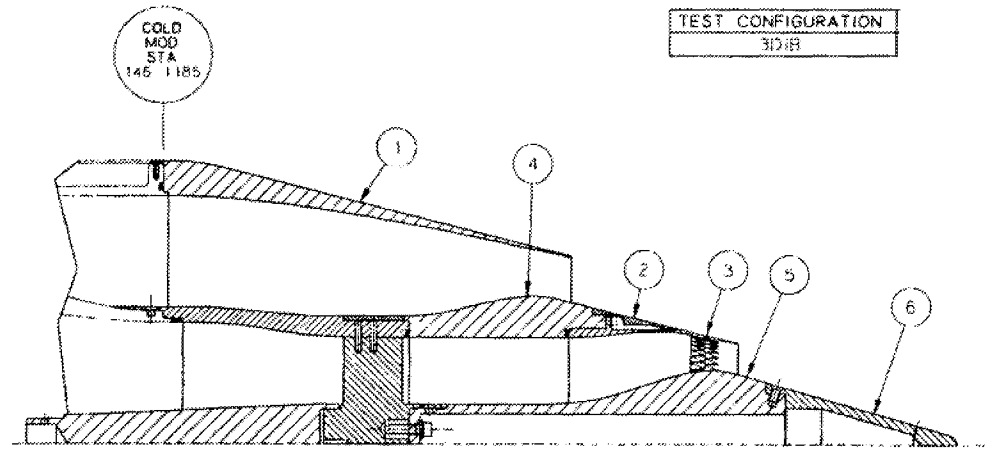


| QTY | ITEM | PART NO | DESCRIPTION | SPECIFICATION |
|---|---|---|---|---|
| 1 | 6 | 2078-411 | TAIL CONE | CONFIG #3 |
| 1 | 5 | 2078-402 | TAIL CONE ADAPTER | CONFIG #3 |
| 1 | 4 | 2078-404 | CORE NOZZLE FORWARD SECTION | CONFIG #2 & #3 |
| 1 | 3 | 2078-426 | CORE NOZZLE 90 | INTERNAL VORTEX GENERATOR DOUBLET |
| 1 | 2 | 2078-605 | CORE NOZZLE COVER RING | CONFIG #2 & #3 |
| 1 | 1 | 2078-001 | FAN NOZZLE | CONFIG #2 THRU #5 |

LIST OF MATERIALS

UNLESS OTHERWISE SPECIFIED DIMENSIONS ARE IN INCHES

MATERIAL SEE L/M

| SIGNATURES | | DAY MO YR |
|---|---|---|
| DRAWN | WMW | 15JAN97 |
| CHK | WMW | 17JAN97 |
| ENGR | WMW | 28JAN97 |

ASE AERO SYSTEMS ENGINEERING, INC

FLUIDYNE AEROTEST GROUP

NOTE:

1 SEE DRAWING 2078-419 FOR ITEMS NOT SHOWN ON THIS DRAWING

| | |
|---|---|
| TEST CONFIGURATION | |
| 3DxB | |

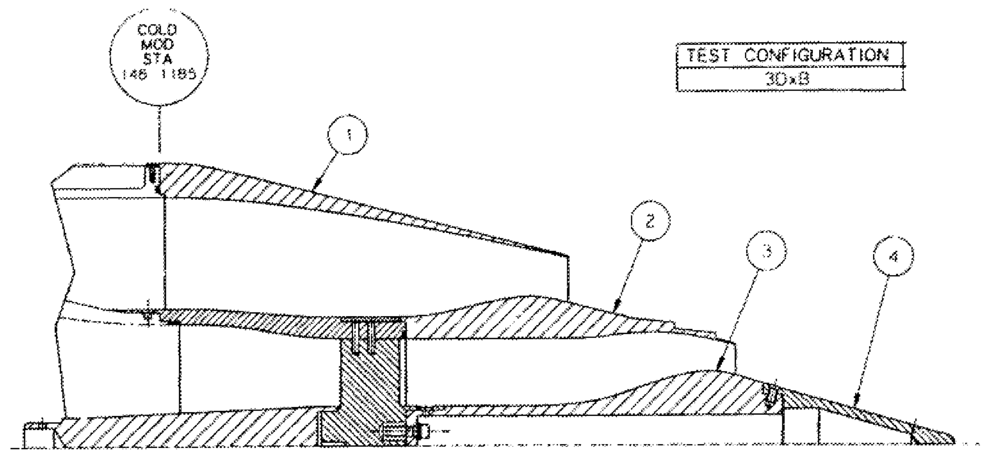


| QTY | ITEM | PART NO | DESCRIPTION | SPECIFICATION |
|---|---|---|---|---|
| 1 | 4 | 2078-411 | TAIL CONE | CONFIG #1 |
| 1 | 3 | 2078-402 | TAIL CONE ADAPTER | CONFIG #3 |
| 1 | 2 | 2078-005 | CORE NOZZLE 9: | EXTERNAL VORTEX GENERATOR DOUBLET |
| 1 | 1 | 2078-001 | FAN NOZZLE CONFIG | #2 THRU #5 |

LIST OF MATERIALS

| SIGNATURES | | DAY MO YR |
|---|---|---|
| DRAWN | WMW | 15JAN97 |
| CHK | WMW | 17JAN97 |
| ENGR | RLM | 28JAN97 |

ASE AERO SYSTEMS ENGINEERING, INC

FLUIDYNE AEROTEST GROUP

NOTE:

1. SEE DRAWING 2078-419 FOR ITEMS NOT SHOWN ON THIS DRAWING

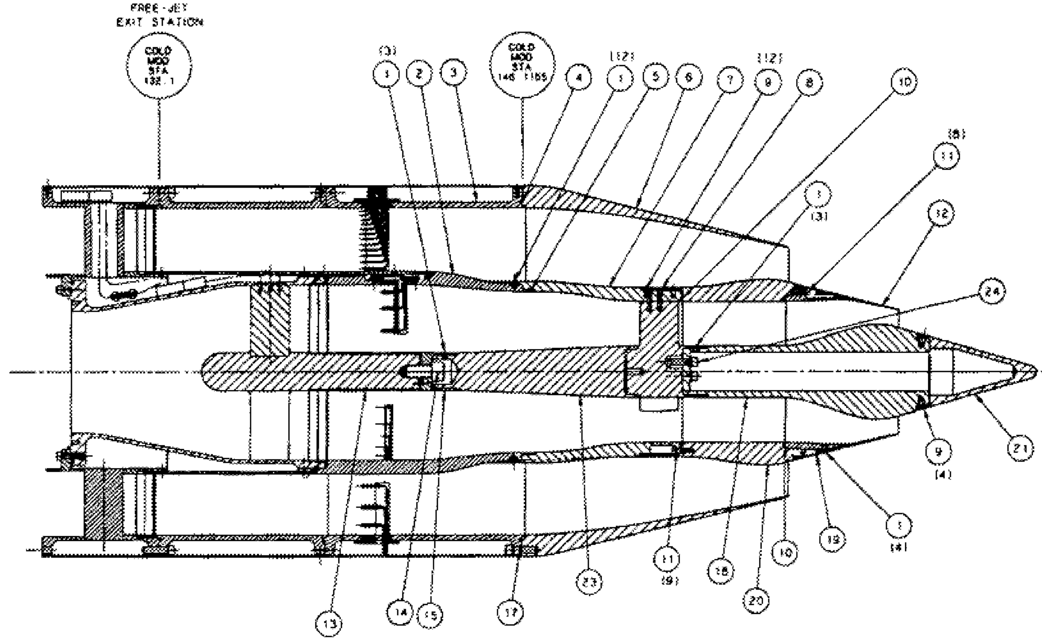


TEST CONFIGURATION
588

| | | | | |
|---|---|---|---|---|
| 1 | 25 | - | SOC HD CAP SCREW | #10-32 UNF x 1 1/8 LONG |
| 3 | 24 | MS9558-10 | SCREW | #10-32UNF x 1/2 LONG |
| 1 | 23 | 2078-509 | SLIDING SLEEVE | |
| 1 | 22 | 2078-502 | STRUT BODY NOSE PLUG | |
| 1 | 21 | 2078-408 | TAIL CONE | CONFIG. #5 |
| 1 | 20 | 2078-409 | CORE NOZZLE FORWARD SECTION CONFIG. #4 & #5 | |
| 1 | 19 | 2078-507 | CORE NOZZLE COVER RING - CONFIG. #4 & #5 | |
| 1 | 18 | 2078-406 | TAIL CONE ADAPTER | CONFIG. #5 |
| 8 | 17 | - | SCREW | 1/4-28 UNF X 3/4 LONG SOC HD CAP |
| 1 | 16 | 2078-604 | FORWARD NOSE PLUG | CORE NOZZLE |
| 1 | 15 | 2078-601 | FORWARD NOSE PLUG ADAPTER - CORE NOZZLE | |
| 1 | 14 | - | SCREW | 1/2-13 UNC X 1" LONG SOC HD CAP |
| 1 | 13 | 2078-801 | CORE ID SLEEVE | - |
| 1 | 12 | 2078-410 | CORE NOZZLE | CONFIG. #5 |
| 17 | 11 | MS9555-08 | SCREW | #8-36 UNF-3A X 1/2 LONG. DOUBLE HEX |
| 2 | 10 | 883A9-0089-8 | E-SEAL | - |
| 16 | 9 | NAS1102E3-6 | FL HD SCREW | #10-32 UNF-3A X 3/8 LONG. A286 |
| 1 | 8 | 2078-606 | SPLIT RING - CORE | - |
| 1 | 7 | 2078-610 | CORE NOZZLE/STRUT ASSEMBLY | |
| 1 | 6 | 2078-601 | FAN NOZZLE | CONFIG. #2 THRU #5 |
| 1 | 5 | - | O-RING | .070 DIA X LGTH REQ'D. SILICONE |
| 1 | 4 | - | O-RING | #279. SILICONE |
| 1 | 3 | Z852 9M42A001 | INSTRUMENTATION SPOOL | |
| 1 | 2 | 2043-007 | CHARGING STATION | CORE DUCT - MODIFIED |
| 22 | 1 | NAS1102E3-4 | FL HD SCREW | #10-32 UNF-3A X 1/4 LONG. A286 |

ASE AERO SYSTEMS ENGINEERING, INC.
FluiDyne AEROTEST GROUP

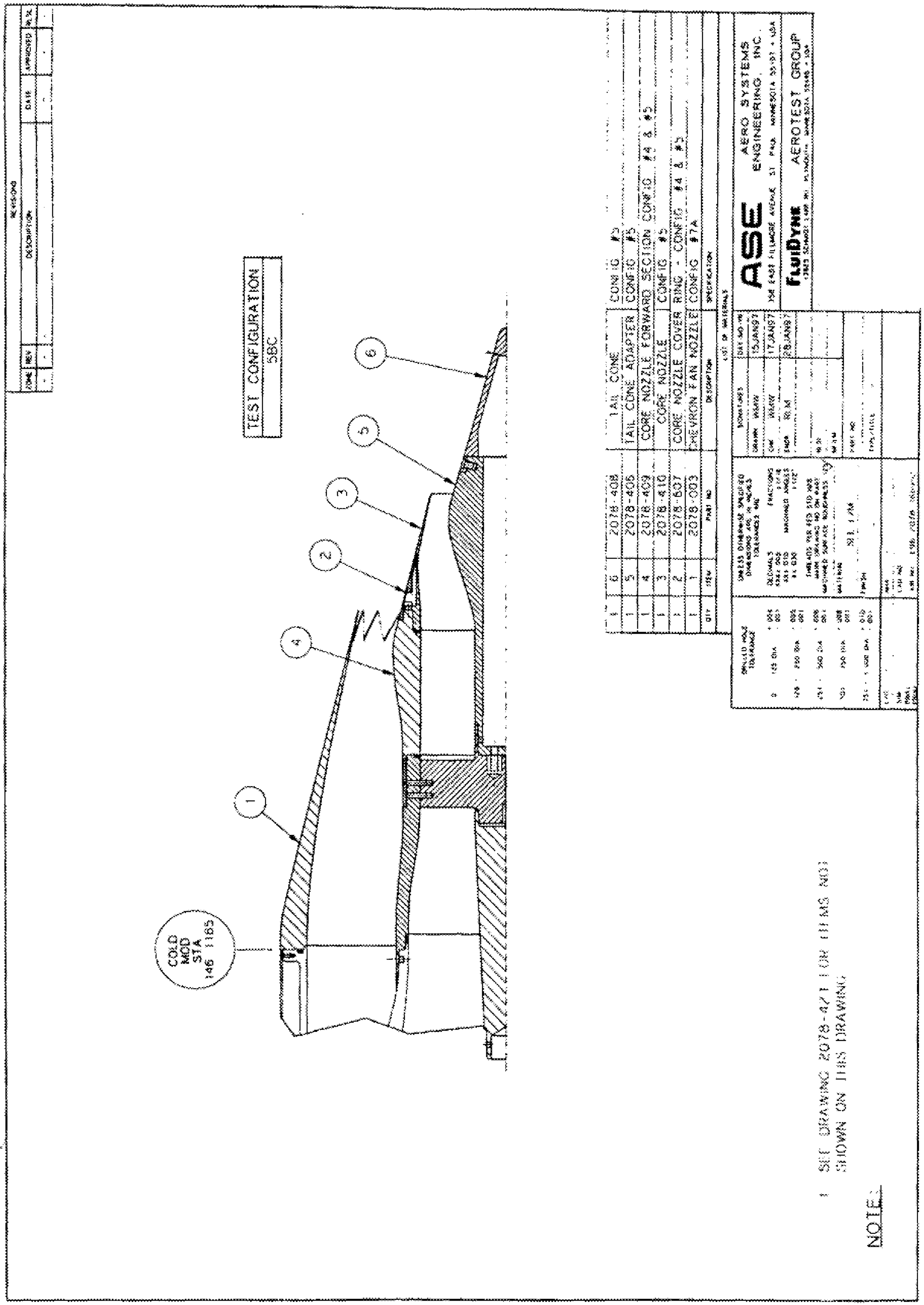
TEST CONFIGURATION
5BC
COLD MOD STA 146 1185
1
2
3
4
5
6
NOTE:
1 SEE DRAWING 2078-421 FOR ITEMS NOT SHOWN ON THIS DRAWING
1 6 2078-408 TAIL CONE CONFIG #5
1 5 2078-406 TAIL CONE ADAPTER CONFIG #5
1 4 2078-409 CORE NOZZLE FORWARD SECTION CONFIG #4 & #5
1 3 2078-410 CORE NOZZLE CONFIG #5
1 2 2078-607 CORE NOZZLE COVER RING - CONFIG #4 & #5
1 1 2078-003 CHEVRON FAN NOZZLE CONFIG #7A
QTY ITEM PART NO DESCRIPTION SPECIFICATION
LIST OF MATERIALS
REVISIONS
ZONE REV DESCRIPTION DATE APPROVED
DRAWN WMW 15JAN97
CHK WMW 17JAN97
ENGR RLM 28JAN97
ASE AERO SYSTEMS ENGINEERING, INC.
FLUIDYNE AEROTEST GROUP

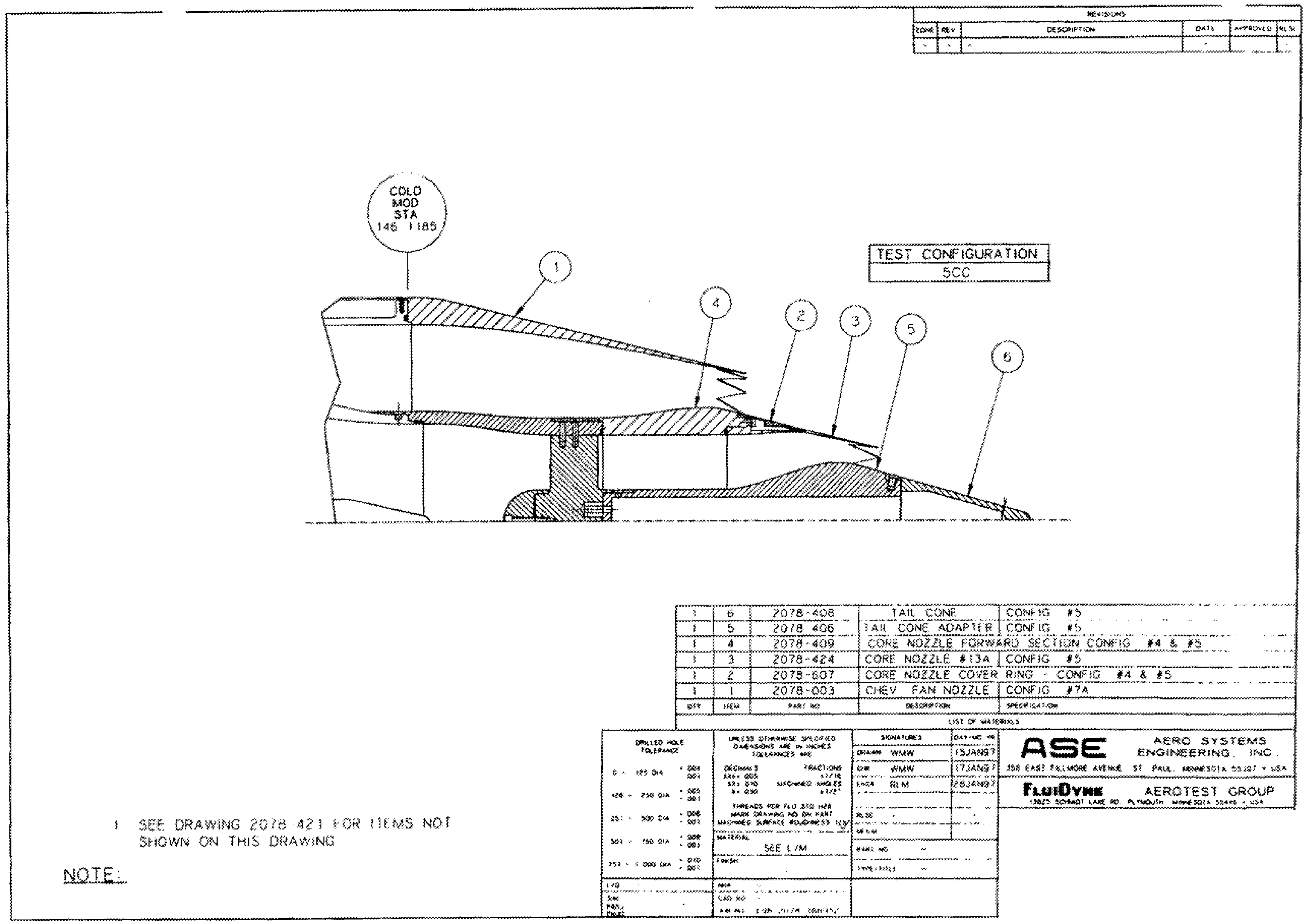
REVISIONS
ZONE | REV | DESCRIPTION | DATE | APPROVED
COLD MOD STA 146.1185
TEST CONFIGURATION
5CC
1
2
3
4
5
6
1 | 6 | 2078-408 | TAIL CONE | CONFIG #5
1 | 5 | 2078-406 | TAIL CONE ADAPTER | CONFIG #5
1 | 4 | 2078-409 | CORE NOZZLE FORWARD SECTION CONFIG #4 & #5
1 | 3 | 2078-424 | CORE NOZZLE #13A | CONFIG #5
1 | 2 | 2078-607 | CORE NOZZLE COVER RING - CONFIG #4 & #5
1 | 1 | 2078-003 | CHEV FAN NOZZLE | CONFIG #7A
QTY | ITEM | PART NO | DESCRIPTION | SPECIFICATION
LIST OF MATERIALS
DRAWN WMW 15JAN97
WMW 17JAN97
RLM 28JAN97
MATERIAL SEE L/M
ASE
AERO SYSTEMS ENGINEERING, INC.
358 EAST FILLMORE AVENUE ST. PAUL, MINNESOTA 55107 USA
FLUIDYNE
AEROTEST GROUP
1. SEE DRAWING 2078-421 FOR ITEMS NOT SHOWN ON THIS DRAWING
NOTE:

TEST CONFIGURATION
5CB

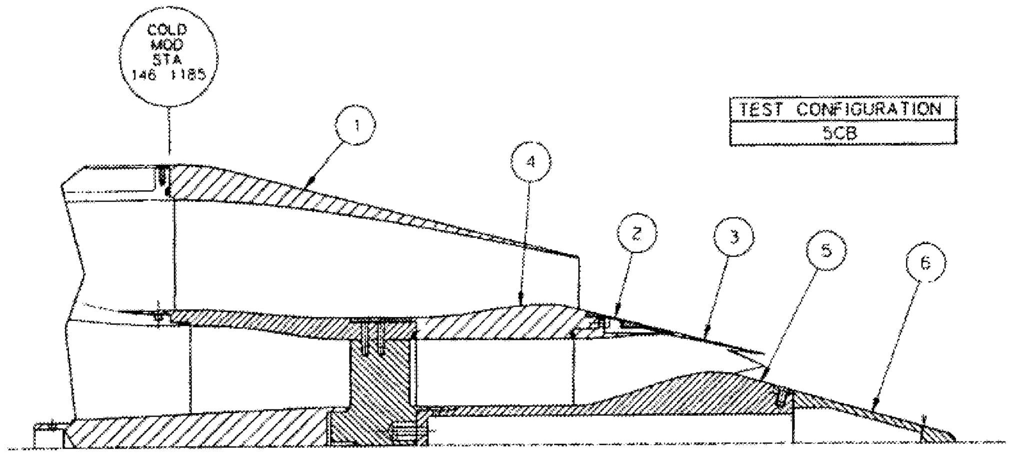


| QTY | ITEM | PART NO | DESCRIPTION | SPECIFICATION |
|---|---|---|---|---|
| 1 | 6 | 2078-408 | TAIL CONE | CONFIG #5 |
| 1 | 5 | 2078-406 | TAIL CONE ADAPTER | CONFIG #5 |
| 1 | 4 | 2078-409 | CORE NOZZLE FORWARD SECTION | CONFIG #4 & #5 |
| 1 | 3 | 2078-424 | CORE NOZZLE #13A | CONFIG #5 |
| 1 | 2 | 2078-607 | CORE NOZZLE COVER RING - | CONFIG #4 & #5 |
| 1 | 1 | 2078-001 | FAN NOZZLE | CONFIG #2 THRU #5 |

LIST OF MATERIALS

| SIGNATURES | | DATE |
|---|---|---|
| DRAWN | WMW | 15JAN97 |
| CHK | WMW | 17JAN97 |
| ENGR | RLM | 28JAN97 |

MATERIAL: SEE L/M

JOB NO L98-2078-166952

ASE AERO SYSTEMS ENGINEERING INC
358 EAST FILLMORE AVENUE ST PAUL MINNESOTA 55107 USA

FLUIDYNE AEROTEST GROUP

REVISIONS

NOTE:

1 SEE DRAWING 2078-421 FOR ITEMS NOT SHOWN ON THIS DRAWING

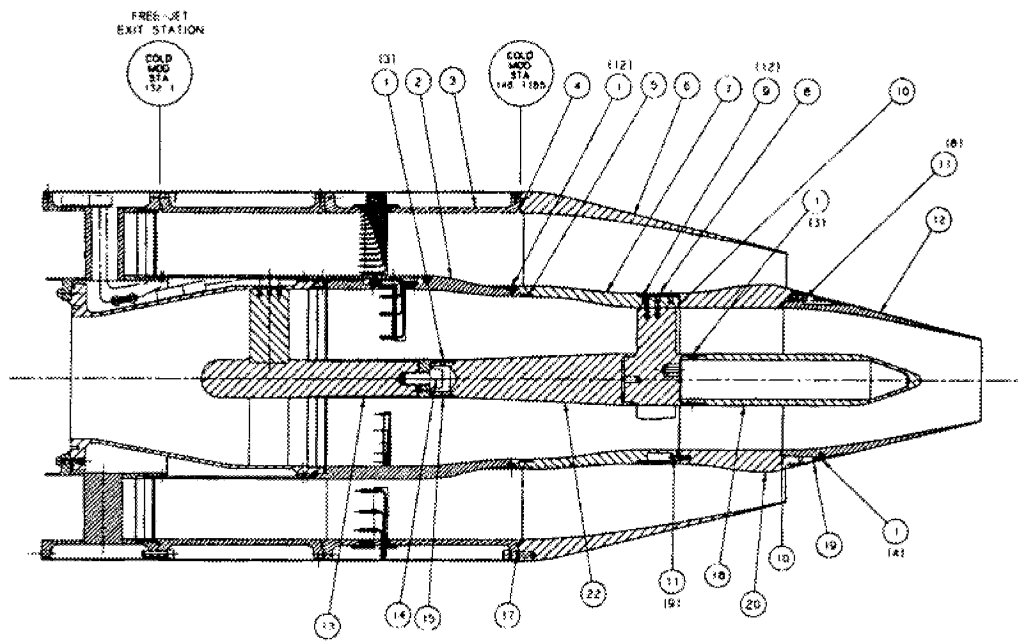


TEST CONFIGURATION 488

| | | | | |
|---|---|---|---|---|
| 1 | 23 | - | SOC HD CAP SCREW | #10-32 UNF x 1 1/8 LONG |
| 1 | 22 | Z078-609 | SLIDING SLEEVE | |
| 1 | 21 | Z078-502 | STRUT BODY NOSE PLUG | |
| 1 | 20 | Z078-409 | CORE NOZZLE FORWARD SECTION CONFIG #4 & #5 | |
| 1 | 19 | Z078-607 | CORE NOZZLE COVER RING - CONFIG #4 & #5 | |
| 1 | 18 | Z078-603 | TAIL CONE | CONFIG #3 & #4 |
| 8 | 17 | - | SCREW | 1/4-28 UNF x 3/4 LONG SOC HD CAP |
| 1 | 16 | Z078-604 | FORWARD NOSE PLUG | CORE NOZZLE |
| 1 | 15 | Z078-601 | FORWARD NOSE PLUG ADAPTER - CORE NOZZLE | |
| 1 | 14 | - | SCREW | 1/2-13 UNC x 1" LONG SOC HD CAP |
| 1 | 13 | Z078-601 | CORE ID SLEEVE | - |
| 1 | 12 | Z078-412 | CORE NOZZLE | CONFIG #4 |
| 17 | 11 | MS9555-06 | SCREW | #6 38 UNF-3A x 1/2 LONG DOUBLE HEX |
| 2 | 10 | 8B3A9-0089-8 | E-SEAL | - |
| 12 | 9 | NAS1102E3-6 | FL HD SCREW | #10-32 UNF-3A x 3/8 LONG A286 |
| 1 | 8 | Z078-606 | SPLIT RING - CORE | - |
| 1 | 7 | Z078-610 | CORE NOZZLE/STRUT ASSEMBLY | |
| 1 | 6 | Z078-001 | FAN NOZZLE | CONFIG #2 THRU #5 |
| 1 | 5 | - | O-RING | .070 DIA x LGTH REQ'D SILICONE |
| 1 | 4 | - | O-RING | #279 SILICONE |
| 1 | 3 | Z652PM4ZA001 | INSTRUMENTATION SPOOL | |
| 1 | 2 | Z043-007 | CHARGING STATION | CORE DUCT - MODIFIED |
| 22 | 1 | NAS1102E3-4 | FL HD SCREW | #10-32 UNF-3A x 1/4 LONG A286 |

ASE AERO SYSTEMS ENGINEERING, INC.

FluiDyne AEROTEST GROUP

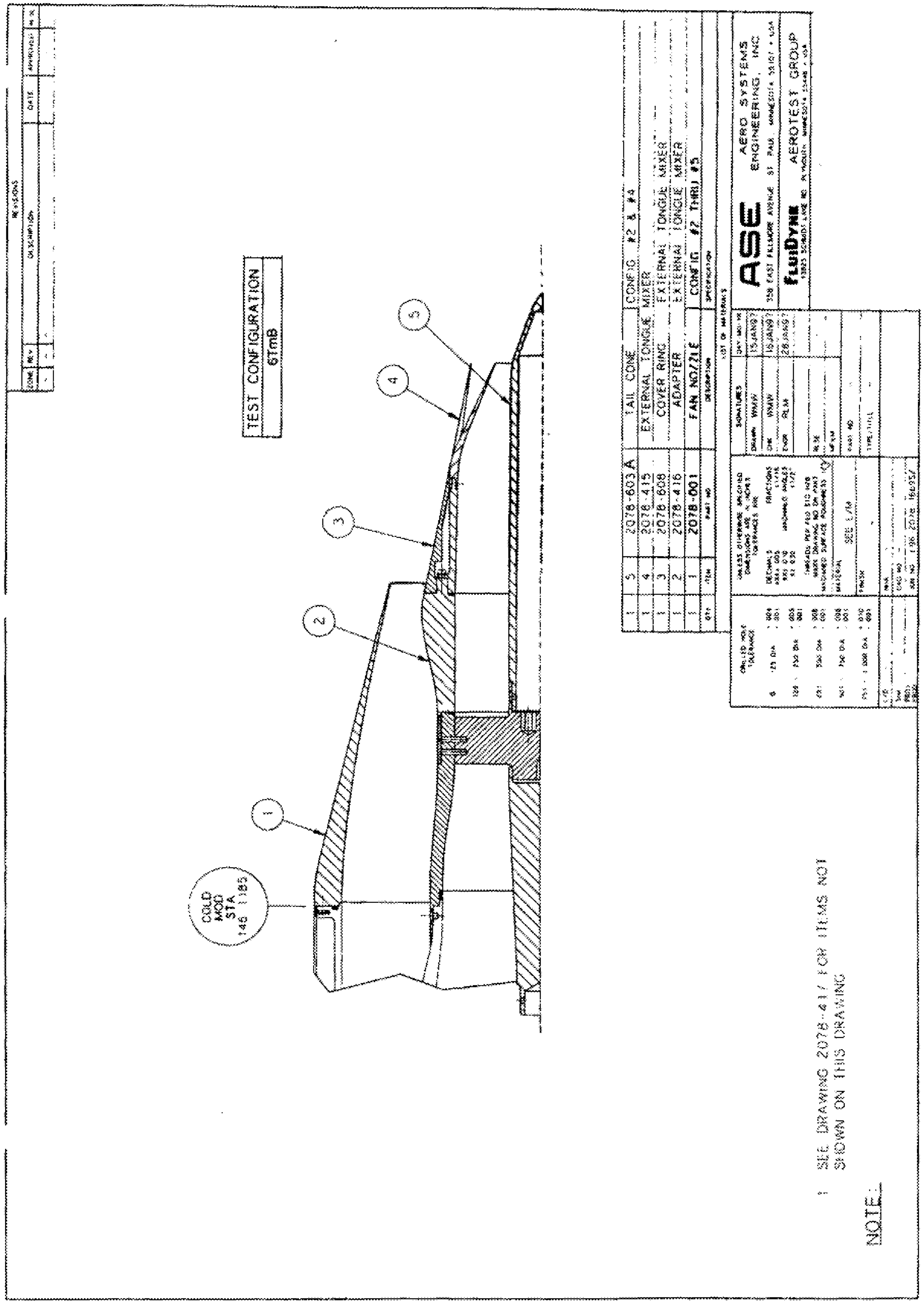
TEST CONFIGURATION
6TmB
COLD MOD STA
1
2
3
4
5
NOTE:
1. SEE DRAWING 2078-417 FOR ITEMS NOT SHOWN ON THIS DRAWING
2078-603 A TAIL CONE CONFIG #2 & #4
2078-415 EXTERNAL TONGUE MIXER
2078-608 COVER RING EXTERNAL TONGUE MIXER
2078-416 ADAPTER EXTERNAL TONGUE MIXER
2078-001 FAN NOZZLE CONFIG #2 THRU #5
ASE AERO SYSTEMS ENGINEERING, INC
FLUIDYNE AEROTEST GROUP

REVISIONS

| ZONE | REV | DESCRIPTION | DATE | APPROVED |
|---|---|---|---|---|
| - | - | - | | |

TEST CONFIGURATION
6TmC

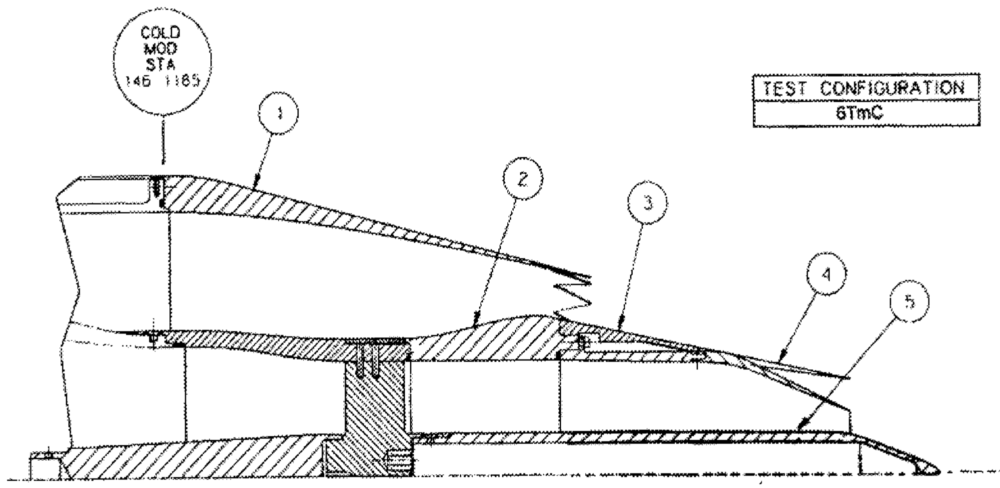


| QTY | ITEM | PART NO | DESCRIPTION | SPECIFICATION |
|---|---|---|---|---|
| 1 | 5 | 2078-603 A | TAIL CONE | CONFIG #2 & #4 |
| 1 | 4 | 2078-415 | EXTERNAL TONGUE MIXER | |
| 1 | 3 | 2078-608 | COVER RING | EXTERNAL TONGUE MIXER |
| 1 | 2 | 2078-416 | ADAPTER | EXTERNAL TONGUE MIXER |
| 1 | 1 | 2078-003 | CHEVRON FAN NOZZLE | CONFIG #7A |

LIST OF MATERIALS

| SIGNATURES | | DATE |
|---|---|---|
| DRAWN | WMW | 15JAN97 |
| CHK | WMW | 16JAN97 |
| ENGR | RLM | 28JAN97 |

UNLESS OTHERWISE SPECIFIED DIMENSIONS ARE IN INCHES
MATERIAL SEE L/M
JOB NO 198-2078-186932

ASE AERO SYSTEMS ENGINEERING, INC
358 EAST FILLMORE AVENUE ST PAUL MINNESOTA 55107 USA

FLUIDYNE AEROTEST GROUP

NOTE:

1 SEE DRAWING 2078-417 FOR ITEMS NOT SHOWN ON THIS DRAWING

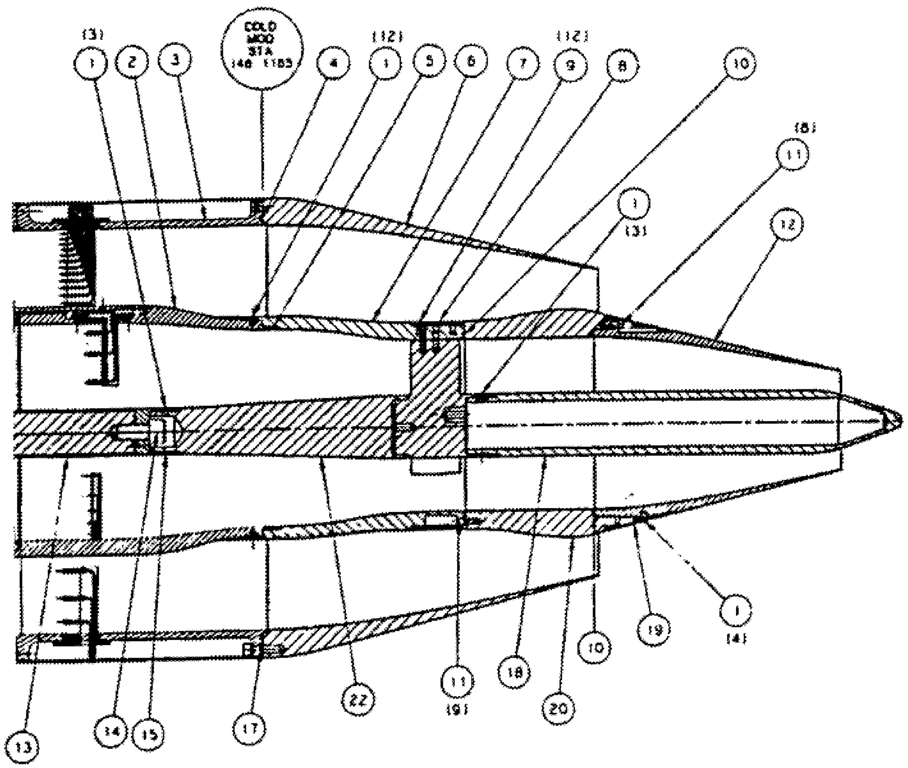


| TEST CONFIGURATION |
| --- |
| 7BB |

| | | | | |
| --- | --- | --- | --- | --- |
| 1 | 23 | - | SOC HD CAP SCREW | #10-32 UNF x 1 1/8 LONG |
| 1 | 22 | 2078-809 | SLIDING SLEEVE | |
| 1 | 21 | 2078-802 | STRUT BODY NOSE PLUG | |
| 1 | 20 | 2078-408 | CORE NOZZLE FORWARD SECTION CONFIG #4 & #5 | |
| 1 | 19 | 2078-807 | CORE NOZZLE COVER RING - CONFIG #4 & #5 | |
| 1 | 18 | 2078-803A | TAIL CONE | |
| 8 | 17 | - | SCREW | 1/4-28 UNF X 3/4 LONG SOC HD CAP |
| 1 | 16 | 2078-804 | FORWARD NOSE PLUG | CORE NOZZLE |
| 1 | 15 | 2078-801 | FORWARD NOSE PLUG ADAPTER - CORE NOZZLE | |
| 1 | 14 | - | SCREW | 1/2-13 UNC X 1" LONG SOC HD CAP |
| 1 | 13 | 2078-801 | CORE ID SLEEVE | - |
| 1 | 12 | 2078-412 | CORE NOZZLE | CONFIG. #4 |
| 17 | 11 | MS9555-06 | SCREW | #8-36 UNF-3A X 1/2 LONG DOUBLE HEX |
| 2 | 10 | 683A9-0089-B | E-SEAL | - |
| 12 | 9 | NAS1102E3-8 | FL HD SCREW | #10-32 UNF-3A X 3/8 LONG A286 |
| 1 | 8 | 2078-808 | SPLIT RING - CORE | - |
| 1 | 7 | 2078-810 | CORE NOZZLE/STRUT ASSEMBLY | |
| 1 | 6 | 2078-001 | FAN NOZZLE | CONFIG #2 THRU #5 |
| 1 | 5 | - | O-RING | .070 DIA X LGTH REQ'D SILICONE |
| 1 | 4 | - | O-RING | #279 SILICONE |
| 1 | 3 | 28529M42A001 | INSTRUMENTATION SPOOL | |
| 1 | 2 | 2043-007 | CHARGING STATION | CORE DUCT - MODIFIED |
| 22 | 1 | NAS1102E3-4 | FL HD SCREW | #10-32 UNF-3A X 1/4 LONG A286 |

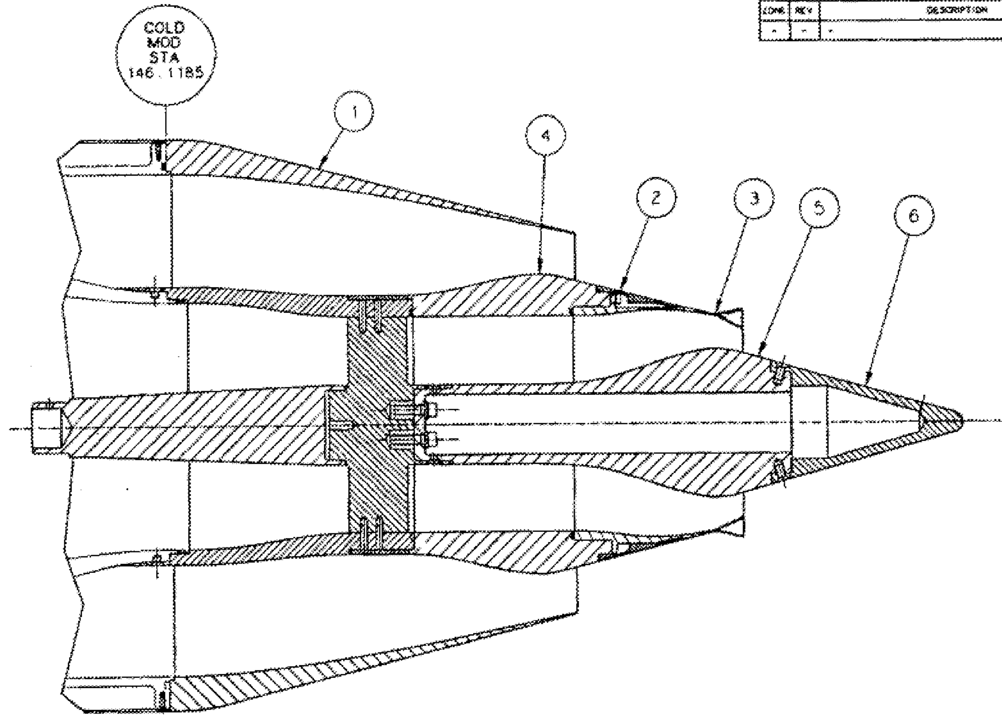


| REVISIONS | | | | | |
|---|---|---|---|---|---|
| CONF | REV | DESCRIPTION | DATE | APPROVED | RLSE |
| - | - | - | - | - | - |

TEST CONFIGURATION

3FB

| QTY | ITEM | PART NO | DESCRIPTION | SPECIFICATION |
|---|---|---|---|---|
| 1 | 6 | 2078-411 | TAIL CONE | CONFIG. #3 |
| 1 | 5 | 2078-402 | TAIL CONE ADAPTER | CONFIG. #3 |
| 1 | 4 | 2078-404 | CORE NOZZLE FORWARD SECTION - CONFIG. #2 & #3 | |
| 1 | 3 | 2087-407 | FULL MIXER | |
| 1 | 2 | 2078-605 | CORE NOZZLE COVER RING CONFIG. #2 & #3 | |
| 1 | 1 | 2078-001 | FAN NOZZLE | CONFIG. #2 THRU #5 |

LIST OF MATERIALS

| SIGNATURES | | DAY-MO-YR |
|---|---|---|
| DRAWN | WMW | 20JAN97 |
| CHK | WMW | 29JAN97 |
| ENGR | RLM | 30JAN97 |
| RLSE | - | - |
| MFEM | | |
| PART NO | - | |
| TYPE/STYLE | - | |

UNLESS OTHERWISE SPECIFIED DIMENSIONS ARE IN INCHES TOLERANCES ARE

MATERIAL SEE L/M

FINISH -

JOB NO L96-2078-166852

ASE AERO SYSTEMS ENGINEERING, INC.
358 EAST FILLMORE AVENUE, ST. PAUL, MINNESOTA 55107 • USA

FLUIDYNE AEROTEST GROUP

NOTE:

1. SEE DRAWING 2078-419 FOR ITEMS NOT CALLED OUT ON THIS DRAWING

| ZONE | REV | DESCRIPTION | DATE | APPROVED | RLSE |
|---|---|---|---|---|---|
| - | - | - | - | - | - |

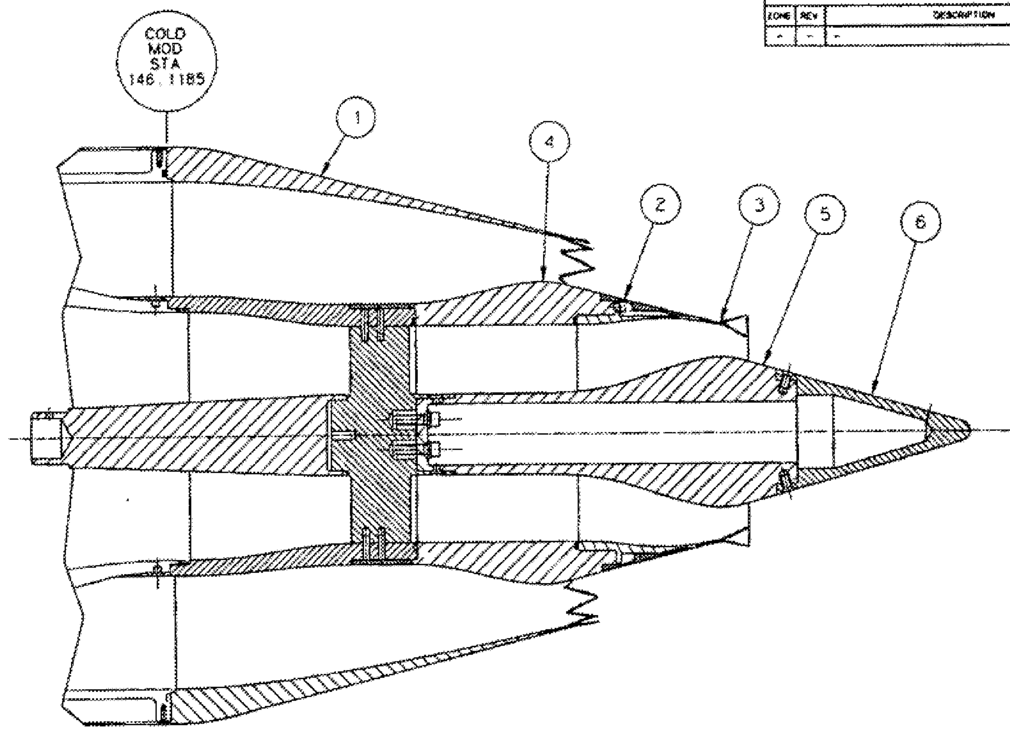


| QTY | ITEM | PART NO | DESCRIPTION | SPECIFICATION |
|---|---|---|---|---|
| 1 | 6 | 2078-411 | TAIL CONE | CONFIG. #3 |
| 1 | 5 | 2078-402 | TAIL CONE ADAPTER | CONFIG. #3 |
| 1 | 4 | 2078-404 | CORE NOZZLE FORWARD SECTION - CONFIG #2 & #3 | |
| 1 | 3 | 2087-407 | FULL MIXER | |
| 1 | 2 | 2078-605 | CORE NOZZLE COVER RING CONFIG. #2 & #3 | |
| 1 | 1 | 2078-003 | CHEVRON FAN NOZZLE | |

LIST OF MATERIALS

| TEST CONFIGURATION |
|---|
| 3FC |

| SIGNATURES | | DAY-MO-YR |
|---|---|---|
| DRAWN | WMW | 20JAN97 |
| CHK | WMW | 29JAN97 |
| ENGR | RLM | 30JAN97 |

MATERIAL: SEE L/M

JOB NO: L96-2078-168952

ASE AERO SYSTEMS ENGINEERING, INC.
358 EAST FILLMORE AVENUE, ST. PAUL, MINNESOTA 55107 • USA

FLUIDYNE AEROTEST GROUP

NOTE:

1. SEE DRAWING 2078-419 FOR ITEMS NOT CALLED OUT ON THIS DRAWING

| ZONE | REV | DESCRIPTION | DATE | APPROVED | RLSE |
|---|---|---|---|---|---|
| - | A | REVISED ITEM 3 | 05MAY97 | RLM | - |

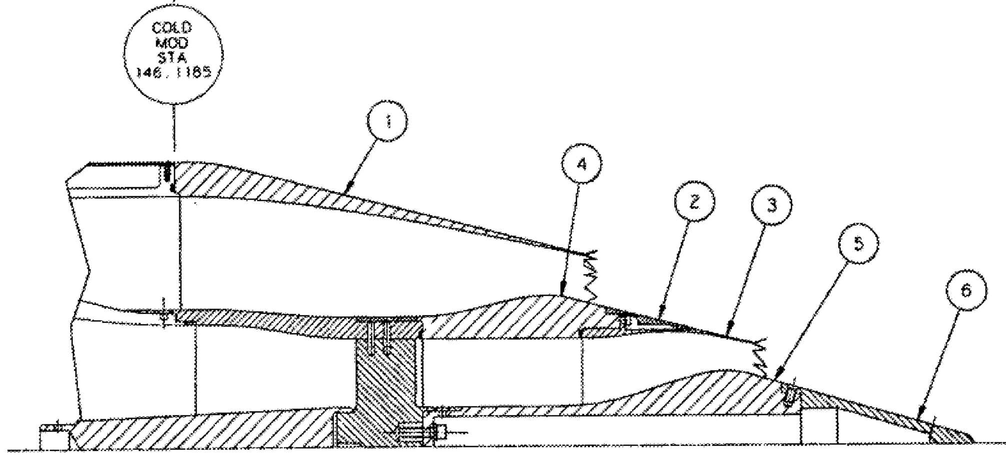


| TEST CONFIGURATION |
|---|
| $3T_{24}T_{48}$ |

| QTY | ITEM | PART NO | DESCRIPTION | SPECIFICATION |
|---|---|---|---|---|
| 1 | 6 | 2078-411 | TAIL CONE | CONFIG. #3 |
| 1 | 5 | 2078-402 | TAIL CONE ADAPTER | CONFIG. #3 |
| 1 | 4 | 2078-404 | CORE NOZZLE FORWARD SECTION - CONFIG. #2 & #3 | |
| 1 | 3 | 2087-406 | 24 FLIPPER TAB | |
| 1 | 2 | 2078-605 | CORE NOZZLE COVER RING CONFIG. #2 & #3 | |
| 1 | 1 | 2087-001 | 48 FLIPPER TAB - FAN NOZZLE MODEL #3 | |

LIST OF MATERIALS

| SIGNATURES | | DAY-MO-YR |
|---|---|---|
| DRAWN | WMW | 31JAN97 |
| CHK | WMW | 3FEB97 |
| ENGR | - | - |
| RLSE | - | - |
| MFG/AP | | |
| PART NO. | - | |
| TYPE/TITLE | - | |

UNLESS OTHERWISE SPECIFIED DIMENSIONS ARE IN INCHES TOLERANCES ARE

MATERIAL: SEE L/M

FINISH: -

JOB NO. L96-2087-167884

AERO SYSTEMS ENGINEERING, INC.
358 EAST FILLMORE AVENUE ST. PAUL, MINNESOTA 55107 USA

FLUIDYNE AEROTEST GROUP

NOTE:

1. SEE DRAWING 2078-419 FOR ITEMS NOT CALLED OUT ON THIS DRAWING

| REVISIONS | | | | | |
|---|---|---|---|---|---|
| ZONE | REV | DESCRIPTION | DATE | APPROVED | RLSE |
| - | A | REVISED ITEM 3 | 05MAY97 | RLM | - |

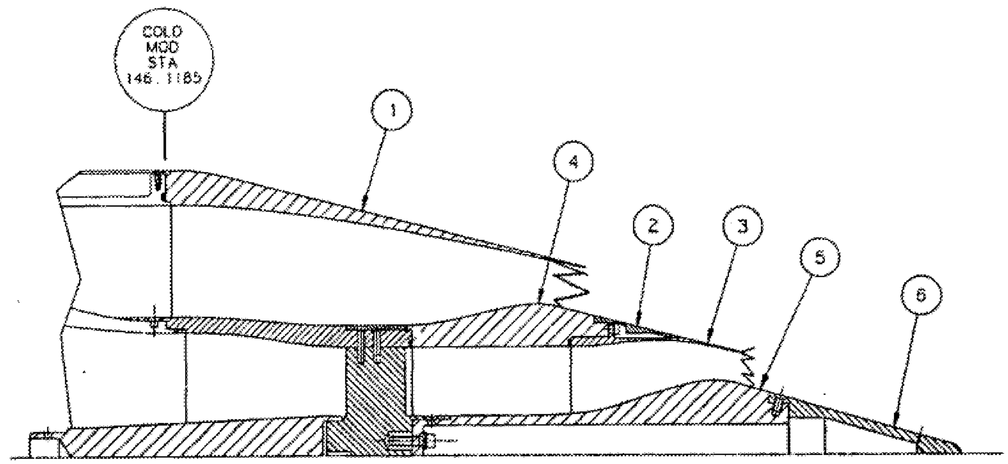


| TEST CONFIGURATION |
|---|
| 3T24C |

| QTY | ITEM | PART NO | DESCRIPTION | SPECIFICATION |
|---|---|---|---|---|
| 1 | 6 | 2078-411 | TAIL CONE | CONFIG. #3 |
| 1 | 5 | 2078-402 | TAIL CONE ADAPTER | CONFIG. #3 |
| 1 | 4 | 2078-404 | CORE NOZZLE FORWARD SECTION - CONFIG. #2 & #3 | |
| 1 | 3 | 2087-406 | 24 FLIPPER TAB | |
| 1 | 2 | 2078-605 | CORE NOZZLE COVER RING CONFIG. #2 & #3 | |
| 1 | 1 | 2078-003 | CHEVRON FAN NOZZLE | CONFIG #7A |

LIST OF MATERIALS

| SIGNATURES | | DAY-MO-YR |
|---|---|---|
| DRAWN | WMW | 14JAN97 |
| CHK | WMW | 20JAN97 |
| ENGR | RLM | 28JAN97 |
| RLSE | - | - |
| MFG | | |

MATERIAL: SEE L/M
PART NO. -
TYPE/TITLE -
JOB NO. L98-2087-167664

AERO SYSTEMS ENGINEERING, INC.
358 EAST FILLMORE AVENUE, ST. PAUL, MINNESOTA 55107 • USA

FLUIDYNE AEROTEST GROUP
13625 SCHMIDT LAKE RD, PLYMOUTH, MINNESOTA 55446 • USA

NOTE:

1. SEE DRAWING 2078-419 FOR ITEMS NOT CALLED OUT ON THIS DRAWING

# Appendix B
# Aeroacoustic Summary Data Tables

Aeroacoustic summary data tables are presented in this appendix for:

- Model 1 (Coplanar, BPR = 5)
- Model 2 (Internal Plug, BPR = 5)
- Model 3 (External Plug, BPR = 5)
- Model 4 (Internal Plug, BPR = 8)
- Model 5 (External Plug, BPR = 8)
- Model 6 (Tongue Mixer with Extended Internal Plug, BPR = 5)
- Model 7 (External Plug, BPR $\simeq$ 14)

Blank cells in the tables indicate missing data from the supplied data files. The following parameter names and definitions are used.

| | |
|---|---|
| **Configuration** | See Section 5 for naming convention and Appendix A for description |
| **Date** | Test date |
| **Point** | Reading or test point number identified in AAPL Escort system |
| **Cycle** | Condition number of test point (identifies condition on test cycle). |
| **XMA** | Free-jet Mach number |
| $\mathbf{T_{amb}}$ | Ambient temperature in test chamber (°F) |
| $\mathbf{P_{amb}}$ | Ambient pressure in test chamber, inches of Hg |
| **RH** | Relative humidity in test chamber (%) |
| $\mathbf{P_{18}}$ | Fan (secondary) nozzle total pressure, psia |
| **PFPQA** | Fan (secondary) nozzle pressure ratio |
| $\mathbf{T_{18}}$ | Fan (secondary) nozzle total temperature (°F) |
| $\mathbf{W_{18}}$ | Fan (secondary) nozzle weight flow, lb/s |
| $\mathbf{V_{18}}$ | Fan (secondary) nozzle ideal exit velocity (ft/s) |
| $\mathbf{CD_{18}}$ | Fan (secondary) nozzle flow coefficient |
| $\mathbf{P_8}$ | Core (primary) nozzle total pressure, psia |
| **P8PQA** | Core (primary) nozzle pressure ratio |
| $\mathbf{T_8}$ | Core (primary) nozzle total temperature (°F) |
| $\mathbf{W_8}$ | Core (primary) nozzle model weight flow (lb/s) |
| $\mathbf{V_8}$ | Core (primary) nozzle ideal exit velocity (ft/s) |
| $\mathbf{CD_8}$ | Core (primary) nozzle flow coefficient |
| $\mathbf{V_{mix}}$ | Mass-averaged model ideal mixed velocity (ft/s) |
| $\mathbf{V_{mix}/V_{amb}}$ | Normalised mass-averaged model ideal mixed velocity |
| $\mathbf{F_N}$ | Net thrust, lbf |
| **EPNL** | Scaled (scale factor = 8) effective perceived noise level with 1500-ft flyover, dB |
| **NF** | Correction factor, 10 log (F/1000) |
| **NEPNL** | Normalized EPNL, EPNL – 10 log (F/1000), dB |

| Page | Designation | Description |
|---|---|---|
| 205 | 1 (also called 1BB) | Model 1<br>Core: Baseline<br>Fan: Baseline |
| 206 | 2BB | Model 2<br>Core: Baseline<br>Fan: Baseline |
| 207 | 2BD | Model 2<br>Core: Baseline<br>Fan: 96 Internal Doublets |
| 208 | 2TmB | Model 2<br>Core: Tongue Mixer<br>Fan: Baseline |
| 208 | 2TmC | Model 2<br>Core: Tongue Mix<br>Fan: 24 Chevrons |
| 209 | 2CB (also called 2C12B) | Model 2<br>Core: 12 Chevrons<br>Fan: Baseline |
| 210 | 2CC (also called 2C12C) | Model 2<br>Core: 12 Chevrons<br>Fan: 24 Chevrons |
| 211 | 2BC (also called 2BC24) | Model 2<br>Core: Baseline<br>Fan: 24 Chevrons |
| 211 | 3BB | Model 3<br>Core: Baseline<br>Fan: Baseline |
| 216 | 3BC | Model 3<br>Core: Baseline<br>Fan: 24 Chevrons |
| 216 | 3C12B | Model 3<br>Core: 12 Chevrons<br>Fan: Baseline |
| 217 | 3C8B | Model 3<br>Core: 8 Chevrons<br>Fan: Baseline |
| 217 | 3IB | Model 3<br>Core: 12 In-Flip Chev<br>Fan: Baseline |
| 217 | 3AB | Model 3<br>Core: 12 Alt-Flip Chev<br>Fan: Baseline |

| Page | Designation | Description |
|---|---|---|
| 218 | 3DiB | Model 3<br>Core: 64 Int Doublets<br>Fan: Baseline |
| 218 | 3IC | Model 3<br>Core: 12 In-Flip Chev<br>Fan: 24 Chevrons |
| 219 | 3C12C | Model 3<br>Core: 12 Chevrons<br>Fan: 24 Chevrons |
| 219 | 3C8C | Model 3<br>Core: 8 Chevrons<br>Fan: 24 Chevrons |
| 219 | 3AC | Model 3<br>Core: 12 Alt-Flip Chev<br>Fan: 24 Chevrons |
| 219 | 3DxB | Model 3<br>Core: 20 Ext Doublets<br>Fan: Baseline |
| 220 | 4BB | Model 4<br>Core: Baseline<br>Fan: Baseline |
| 221 | 5BB | Model 5<br>Core: Baseline<br>Fan: Baseline |
| 221 | 5CB (also called 5C12B) | Model 5<br>Core: 12 Chevrons<br>Fan: Baseline |
| 222 | 5CC (also called 5C12C) | Model 5<br>Core: 12 Chevrons<br>Fan: 24 Chevrons |
| 222 | 5BC | Model 5<br>Core: Baseline<br>Fan: 24 Chevrons |
| 222 | 6TmB | Model 6<br>Core: Tongue Mixer<br>Fan: Baseline |
| 223 | 6TmC | Model 6<br>Core: Tongue Mixer<br>Fan: 24 Chevrons |
| 223 | 7BB | Model 7<br>Core: Baseline<br>Fan: Baseline |

## Aeroacoustic Summary Data

## Model 1 – Configuration 1BB, Baseline Core Nozzle, Baseline Fan Nozzle

| Date | Point | Cycle | XMA | $T_{amb}$ | $P_{amb}$ | RH | $P_{18}$ | PFQPA | $T_{18}$ | $W_{18}$ | $V_{18}$ | $CD_{18}$ | $P_8$ | P8QPA | $T_8$ | $W_8$ | $V_8$ | $CD_8$ | $V_{mix}$ | $V_{mix}/c_{amb}$ | $F_N$ | EPNL | NF | NEPNL |
|---|---|---|---|---|---|---|---|---|---|---|---|---|---|---|---|---|---|---|---|---|---|---|---|---|
| 3/20/97 | 122 | 52 | 0.28 | 48.3 | 29.06 | 46.3 | 20.320 | 1.425 | 142 | 11.20 | 835 | 0.924 | 17.17 | 1.204 | 846 | 1.50 | 902 | 0.682 | 843 | 0.762 | 13453 | 74.70 | 11.29 | 63.4 |
| | 121 | 51 | 0.28 | 48.3 | 29.06 | 46.3 | 22.910 | 1.607 | 139 | 13.47 | 955 | 0.933 | 19.37 | 1.359 | 989 | 2.05 | 1211 | 0.748 | 989 | 0.895 | 20949 | 82.00 | 13.21 | 68.8 |
| | 120 | 50 | 0.28 | 48.3 | 29.06 | 46.3 | 26.220 | 1.839 | 142 | 15.82 | 1075 | 0.942 | 23.95 | 1.680 | 1177 | 2.90 | 1652 | 0.834 | 1164 | 1.053 | 31805 | 97.30 | 15.02 | 82.3 |
| | 105 | 24 | 0.28 | 48.3 | 29.06 | 46.3 | 21.590 | 1.513 | 136 | 12.44 | 894 | 0.931 | 18.13 | 1.271 | 837 | 1.80 | 1017 | 0.714 | 910 | 0.823 | 16981 | 77.40 | 12.30 | 65.1 |
| | 106 | 23 | 0.28 | 48.3 | 29.06 | 46.3 | 22.860 | 1.602 | 140 | 13.45 | 953 | 0.936 | 19.26 | 1.350 | 886 | 2.09 | 1154 | 0.744 | 980 | 0.887 | 20711 | 80.70 | 13.16 | 67.5 |
| | 107 | 22 | 0.28 | 48.3 | 29.06 | 46.3 | 24.760 | 1.736 | 146 | 14.84 | 1030 | 0.943 | 21.52 | 1.509 | 961 | 2.59 | 1379 | 0.792 | 1082 | 0.979 | 26762 | 86.70 | 14.28 | 72.4 |
| | 108 | 21 | 0.28 | 48.3 | 29.06 | 46.3 | 26.150 | 1.834 | 144 | 15.82 | 1074 | 0.946 | 23.99 | 1.682 | 1043 | 3.04 | 1584 | 0.835 | 1157 | 1.046 | 31755 | 91.40 | 15.02 | 76.4 |
| | 109 | 20 | 0.28 | 42.3 | 29.04 | 61.0 | 27.011 | 1.894 | 145 | 16.36 | 1100 | 0.947 | 25.62 | 1.796 | 1081 | 3.32 | 1695 | 0.858 | 1201 | 1.093 | 34935 | 94.00 | 15.43 | 78.6 |
| | 92 | 13 | 0.28 | 48.3 | 29.06 | 46.3 | 19.850 | 1.391 | 137 | 10.76 | 803 | 0.920 | 17.74 | 1.243 | 781 | 1.80 | 948 | 0.735 | 824 | 0.746 | 12849 | 74.30 | 11.09 | 63.2 |
| | 93 | 12 | 0.28 | 48.3 | 29.06 | 46.3 | 21.690 | 1.519 | 141 | 12.42 | 902 | 0.928 | 19.03 | 1.333 | 838 | 2.11 | 1111 | 0.756 | 932 | 0.844 | 17997 | 79.00 | 12.55 | 66.4 |
| | 94 | 11 | 0.28 | 48.3 | 29.06 | 46.3 | 23.270 | 1.630 | 142 | 13.72 | 971 | 0.935 | 20.69 | 1.449 | 932 | 2.45 | 1300 | 0.788 | 1021 | 0.924 | 22860 | 83.60 | 13.59 | 70.0 |
| | 95 | 10 | 0.28 | 48.3 | 29.06 | 46.3 | 24.970 | 1.750 | 145 | 14.94 | 1037 | 0.940 | 22.42 | 1.571 | 1032 | 2.74 | 1477 | 0.813 | 1105 | 1.000 | 27937 | 88.80 | 14.46 | 74.3 |
| | 102 | 24 | 0.20 | 48.3 | 29.06 | 46.3 | 21.600 | 1.514 | 134 | 12.50 | 893 | 0.934 | 18.17 | 1.273 | 840 | 1.83 | 1021 | 0.724 | 910 | 0.823 | 19614 | 81.60 | 12.93 | 68.7 |
| | 101 | 21 | 0.20 | 48.3 | 29.06 | 46.3 | 26.140 | 1.832 | 135 | 15.95 | 1065 | 0.947 | 23.95 | 1.678 | 1041 | 3.05 | 1580 | 0.837 | 1148 | 1.039 | 35000 | 95.10 | 15.44 | 79.7 |
| | 96 | 14 | 0.20 | 48.3 | 29.06 | 46.3 | 18.070 | 1.266 | 136 | 8.88 | 683 | 0.915 | 16.40 | 1.149 | 731 | 1.39 | 746 | 0.707 | 691 | 0.625 | 9604 | 72.30 | 9.82 | 62.5 |
| | 104 | 14 | 0.20 | 48.3 | 29.06 | 46.3 | 18.280 | 1.281 | 135 | 9.18 | 699 | 0.920 | 16.04 | 1.124 | 741 | 1.18 | 689 | 0.659 | 698 | 0.631 | 9810 | 72.30 | 9.92 | 62.4 |
| | 97 | 13 | 0.20 | 48.3 | 29.06 | 46.3 | 19.880 | 1.392 | 141 | 10.82 | 807 | 0.926 | 17.82 | 1.248 | 784 | 1.85 | 958 | 0.748 | 829 | 0.750 | 15309 | 78.00 | 11.85 | 66.2 |
| | 103 | 13 | 0.20 | 48.3 | 29.06 | 46.3 | 20.260 | 1.419 | 139 | 11.23 | 828 | 0.930 | 17.21 | 1.206 | 797 | 1.57 | 888 | 0.698 | 835 | 0.756 | 15630 | 78.10 | 11.94 | 66.2 |
| | 98 | 12 | 0.20 | 48.3 | 29.06 | 46.3 | 21.560 | 1.510 | 147 | 12.29 | 900 | 0.931 | 19.04 | 1.334 | 844 | 2.13 | 1114 | 0.765 | 932 | 0.843 | 20382 | 82.80 | 13.09 | 69.7 |
| | 99 | 11 | 0.20 | 48.3 | 29.06 | 46.3 | 23.270 | 1.630 | 145 | 13.71 | 973 | 0.936 | 20.55 | 1.439 | 933 | 2.43 | 1289 | 0.788 | 1021 | 0.923 | 25641 | 87.90 | 14.09 | 73.8 |
| | 100 | 10 | 0.20 | 48.3 | 29.06 | 46.3 | 25.010 | 1.752 | 138 | 15.07 | 1031 | 0.940 | 22.45 | 1.573 | 1032 | 2.75 | 1480 | 0.816 | 1100 | 0.996 | 31149 | 92.80 | 14.93 | 77.9 |
| | 117 | 52 | 0.00 | 48.3 | 29.06 | 46.3 | 20.270 | 1.421 | 143 | 11.22 | 832 | 0.931 | 17.21 | 1.207 | 840 | 1.57 | 904 | 0.708 | 841 | 0.761 | 21373 | 83.70 | 13.30 | 70.4 |
| | 118 | 51 | 0.00 | 48.3 | 29.06 | 46.3 | 22.850 | 1.602 | 142 | 13.42 | 955 | 0.936 | 19.29 | 1.353 | 991 | 2.05 | 1203 | 0.756 | 988 | 0.893 | 30372 | 91.80 | 14.82 | 77.0 |
| | 119 | 50 | 0.00 | 48.3 | 29.06 | 46.3 | 26.180 | 1.835 | 142 | 15.82 | 1073 | 0.943 | 24.09 | 1.689 | 1182 | 2.95 | 1663 | 0.842 | 1166 | 1.055 | 43481 | 101.10 | 16.38 | 84.7 |
| | 115 | 24 | 0.00 | 48.3 | 29.06 | 46.3 | 21.600 | 1.514 | 141 | 12.46 | 898 | 0.936 | 18.20 | 1.276 | 844 | 1.86 | 1027 | 0.733 | 915 | 0.828 | 26064 | 87.60 | 14.16 | 73.4 |
| | 114 | 23 | 0.00 | 48.3 | 29.06 | 46.3 | 22.840 | 1.601 | 142 | 13.46 | 954 | 0.939 | 19.11 | 1.339 | 885 | 2.07 | 1139 | 0.748 | 979 | 0.885 | 30196 | 90.80 | 14.80 | 76.0 |
| | 113 | 22 | 0.00 | 48.3 | 29.06 | 46.3 | 24.740 | 1.735 | 145 | 14.86 | 1029 | 0.944 | 21.51 | 1.508 | 960 | 2.61 | 1377 | 0.798 | 1081 | 0.978 | 37520 | 96.10 | 15.74 | 80.4 |
| | 112 | 21 | 0.00 | 48.3 | 29.06 | 46.3 | 26.170 | 1.835 | 146 | 15.84 | 1076 | 0.948 | 24.02 | 1.684 | 1046 | 3.06 | 1587 | 0.840 | 1159 | 1.049 | 43544 | 100.10 | 16.39 | 83.7 |
| | 110 | 20 | 0.00 | 43.1 | 29.04 | 60.9 | 27.008 | 1.893 | 148 | 16.37 | 1103 | 0.950 | 25.61 | 1.796 | 1083 | 3.33 | 1696 | 0.862 | 1203 | 1.094 | 47115 | 101.80 | 16.73 | 85.1 |
| | 111 | 20 | 0.00 | 48.3 | 29.06 | 46.3 | 26.800 | 1.879 | 146 | 16.24 | 1096 | 0.949 | 25.27 | 1.771 | 1069 | 3.32 | 1670 | 0.868 | 1194 | 1.080 | 46406 | 101.90 | 16.67 | 85.2 |
| | 87 | 14 | 0.00 | 48.5 | 29.06 | 46.4 | 18.103 | 1.269 | 130 | 8.98 | 683 | 0.916 | 16.45 | 1.153 | 727 | 1.43 | 754 | 0.716 | 693 | 0.626 | 14326 | 76.90 | 11.56 | 65.3 |
| | 116 | 14 | 0.00 | 48.3 | 29.06 | 46.3 | 18.250 | 1.279 | 139 | 9.17 | 699 | 0.926 | 16.02 | 1.123 | 742 | 1.21 | 687 | 0.677 | 697 | 0.631 | 14384 | 76.80 | 11.58 | 65.2 |
| | 88 | 13 | 0.00 | 48.3 | 29.06 | 46.3 | 19.850 | 1.391 | 140 | 10.85 | 805 | 0.929 | 17.72 | 1.242 | 781 | 1.83 | 946 | 0.750 | 826 | 0.747 | 20812 | 83.40 | 13.18 | 70.2 |
| | 89 | 12 | 0.00 | 48.3 | 29.06 | 46.3 | 21.650 | 1.517 | 144 | 12.45 | 903 | 0.935 | 19.01 | 1.332 | 841 | 2.14 | 1110 | 0.767 | 933 | 0.844 | 27053 | 88.90 | 14.32 | 74.6 |
| | 90 | 11 | 0.00 | 48.3 | 29.06 | 46.3 | 23.260 | 1.630 | 147 | 13.71 | 975 | 0.938 | 20.56 | 1.441 | 932 | 2.45 | 1290 | 0.794 | 1022 | 0.925 | 32826 | 93.50 | 15.16 | 78.3 |
| | 91 | 10 | 0.00 | 48.3 | 29.06 | 46.3 | 25.010 | 1.752 | 140 | 15.06 | 1033 | 0.942 | 22.45 | 1.573 | 1031 | 2.76 | 1479 | 0.819 | 1103 | 0.998 | 39048 | 97.50 | 15.92 | 81.6 |

## Aeroacoustic Summary Data

## Model 2 – Configuration 2BB, Baseline Core Nozzle, Baseline Fan Nozzle

| Date | Point | Cycle | XMA | $T_{amb}$ | $P_{amb}$ | RH | $P_{18}$ | PFQPA | $T_{18}$ | $W_{18}$ | $V_{18}$ | $CD_{18}$ | $P_8$ | P8QPA | $T_8$ | $W_8$ | $V_8$ | $CD_8$ | $V_{mix}$ | $V_{mix}/c_{amb}$ | $F_N$ | EPNL | NF | NEPNL |
|---|---|---|---|---|---|---|---|---|---|---|---|---|---|---|---|---|---|---|---|---|---|---|---|---|
| 3/25/97 | 233 | 51 | 0.28 | 47.9 | 28.98 | 91.1 | 22.809 | 1.603 | 140 | 13.74 | 955 | 0.980 | 19.12 | 1.344 | 990 | 2.07 | 1190 | 0.783 | 985 | 0.891 | 21279 | 81.10 | 13.28 | 67.8 |
| | 234 | 50 | 0.28 | 47.6 | 28.98 | 91.8 | 25.994 | 1.827 | 144 | 15.77 | 1071 | 0.971 | 23.76 | 1.670 | 1182 | 2.94 | 1646 | 0.861 | 1161 | 1.051 | 31648 | 92.20 | 15.00 | 77.2 |
| | 232 | 25 | 0.28 | 48.2 | 28.96 | 91.3 | 20.250 | 1.424 | 140 | 11.68 | 832 | 0.987 | 17.11 | 1.203 | 834 | 1.59 | 896 | 0.734 | 840 | 0.760 | 14014 | 74.60 | 11.47 | 63.1 |
| | 198 | 24 | 0.28 | 57.8 | 28.92 | 82.1 | 21.469 | 1.512 | 141 | 12.75 | 897 | 0.986 | 17.98 | 1.266 | 840 | 1.87 | 1009 | 0.758 | 911 | 0.817 | 17519 | 76.80 | 12.44 | 64.4 |
| | 199 | 23 | 0.28 | 57.7 | 28.94 | 84.3 | 22.748 | 1.601 | 144 | 13.74 | 956 | 0.985 | 19.19 | 1.351 | 887 | 2.20 | 1156 | 0.794 | 983 | 0.881 | 21328 | 80.10 | 13.29 | 66.8 |
| | 200 | 22 | 0.28 | 56.5 | 28.94 | 87.6 | 24.622 | 1.733 | 142 | 15.11 | 1025 | 0.984 | 21.40 | 1.506 | 960 | 2.66 | 1376 | 0.827 | 1077 | 0.967 | 27149 | 85.60 | 14.34 | 71.3 |
| | 201 | 21 | 0.28 | 56.2 | 28.94 | 88.8 | 26.092 | 1.836 | 139 | 16.06 | 1071 | 0.980 | 23.78 | 1.674 | 1046 | 3.07 | 1579 | 0.860 | 1152 | 1.034 | 32004 | 90.80 | 15.05 | 75.7 |
| | 202 | 20 | 0.28 | 55.8 | 28.94 | 92.3 | 26.956 | 1.897 | 139 | 16.56 | 1096 | 0.975 | 25.48 | 1.793 | 1081 | 3.37 | 1694 | 0.884 | 1197 | 1.075 | 35016 | 93.30 | 15.44 | 77.9 |
| | 231 | 13 | 0.28 | 49.0 | 28.96 | 90.6 | 19.797 | 1.392 | 139 | 11.25 | 806 | 0.986 | 17.65 | 1.242 | 791 | 1.86 | 950 | 0.776 | 827 | 0.747 | 13464 | 73.60 | 11.29 | 62.3 |
| | 230 | 12 | 0.28 | 49.9 | 28.96 | 90.2 | 21.502 | 1.512 | 144 | 12.71 | 899 | 0.984 | 18.86 | 1.327 | 845 | 2.16 | 1103 | 0.793 | 929 | 0.839 | 18305 | 78.00 | 12.63 | 65.4 |
| | 229 | 11 | 0.28 | 50.4 | 28.96 | 89.9 | 23.176 | 1.630 | 146 | 13.99 | 974 | 0.982 | 20.58 | 1.448 | 936 | 2.51 | 1300 | 0.821 | 1023 | 0.924 | 23460 | 82.80 | 13.70 | 69.1 |
| | 228 | 10 | 0.28 | 51.3 | 28.96 | 89.5 | 24.818 | 1.746 | 145 | 15.13 | 1034 | 0.979 | 22.15 | 1.558 | 1032 | 2.76 | 1465 | 0.841 | 1100 | 0.993 | 28082 | 87.60 | 14.48 | 73.1 |
| | 204 | 21 | 0.20 | 56.1 | 28.94 | 90.1 | 26.084 | 1.835 | 141 | 15.99 | 1073 | 0.978 | 23.91 | 1.683 | 1045 | 3.11 | 1586 | 0.866 | 1156 | 1.038 | 35597 | 94.80 | 15.51 | 79.3 |
| | 205 | 21 | 0.20 | 56.0 | 28.94 | 90.1 | 26.078 | 1.835 | 142 | 16.01 | 1073 | 0.978 | 23.91 | 1.682 | 1045 | 3.11 | 1586 | 0.866 | 1156 | 1.038 | 35642 | 80.90 | 15.52 | 65.4 |
| | 208 | 14 | 0.20 | 56.3 | 28.92 | 88.0 | 18.205 | 1.282 | 142 | 9.58 | 703 | 0.990 | 15.91 | 1.120 | 739 | 1.22 | 678 | 0.705 | 700 | 0.629 | 10072 | 71.60 | 10.03 | 61.6 |
| | 206 | 14 | 0.20 | 56.3 | 28.94 | 88.8 | 18.203 | 1.281 | 142 | 9.57 | 703 | 0.990 | 15.92 | 1.120 | 742 | 1.23 | 680 | 0.706 | 700 | 0.628 | 10325 | 77.40 | 10.14 | 67.3 |
| | 207 | 14 | 0.20 | 56.3 | 28.92 | 88.0 | 18.197 | 1.281 | 142 | 9.58 | 702 | 0.991 | 15.91 | 1.120 | 739 | 1.22 | 676 | 0.705 | 700 | 0.628 | 10159 | 72.20 | 10.07 | 62.1 |
| | 223 | 14 | 0.20 | 55.2 | 28.92 | 87.1 | 18.043 | 1.270 | 140 | 9.39 | 690 | 0.989 | 16.45 | 1.158 | 732 | 1.52 | 767 | 0.760 | 701 | 0.630 | 10334 | 72.20 | 10.14 | 62.1 |
| | 224 | 13 | 0.20 | 54.2 | 28.94 | 87.9 | 19.903 | 1.401 | 141 | 11.38 | 814 | 0.990 | 17.66 | 1.243 | 782 | 1.89 | 949 | 0.781 | 833 | 0.750 | 16161 | 77.60 | 12.08 | 65.5 |
| | 225 | 12 | 0.20 | 53.7 | 28.94 | 88.9 | 21.496 | 1.513 | 141 | 12.80 | 897 | 0.989 | 18.93 | 1.332 | 842 | 2.20 | 1111 | 0.801 | 929 | 0.836 | 21114 | 82.00 | 13.25 | 68.8 |
| | 226 | 11 | 0.20 | 53.1 | 28.94 | 90.4 | 23.234 | 1.635 | 142 | 14.13 | 973 | 0.985 | 20.49 | 1.442 | 932 | 2.51 | 1291 | 0.824 | 1021 | 0.920 | 26429 | 87.30 | 14.22 | 73.1 |
| | 227 | 10 | 0.20 | 52.1 | 28.96 | 90.2 | 24.862 | 1.749 | 143 | 15.23 | 1034 | 0.979 | 22.22 | 1.563 | 1032 | 2.79 | 1470 | 0.845 | 1101 | 0.993 | 31513 | 91.90 | 14.98 | 76.9 |
| | 237 | 52 | 0.00 | 48.8 | 28.98 | 88.0 | 20.137 | 1.415 | 140 | 11.55 | 825 | 0.985 | 17.00 | 1.195 | 845 | 1.58 | 883 | 0.747 | 832 | 0.752 | 21599 | 82.60 | 13.34 | 69.3 |
| | 236 | 51 | 0.00 | 48.6 | 28.98 | 89.1 | 22.727 | 1.597 | 140 | 13.71 | 950 | 0.981 | 19.26 | 1.354 | 990 | 2.14 | 1204 | 0.797 | 985 | 0.891 | 30846 | 90.60 | 14.89 | 75.7 |
| | 235 | 50 | 0.00 | 47.8 | 28.98 | 91.9 | 26.023 | 1.829 | 143 | 15.81 | 1072 | 0.971 | 23.77 | 1.671 | 1182 | 2.95 | 1646 | 0.865 | 1162 | 1.052 | 43248 | 104.80 | 16.36 | 88.4 |
| | 210 | 24 | 0.00 | 56.9 | 28.94 | 85.9 | 21.576 | 1.519 | 144 | 12.87 | 903 | 0.990 | 18.13 | 1.276 | 846 | 1.95 | 1028 | 0.778 | 920 | 0.825 | 27001 | 86.50 | 14.31 | 72.2 |
| | 211 | 23 | 0.00 | 56.8 | 28.94 | 85.8 | 22.737 | 1.600 | 142 | 13.82 | 953 | 0.989 | 19.25 | 1.354 | 890 | 2.22 | 1162 | 0.800 | 982 | 0.881 | 31145 | 90.10 | 14.93 | 75.2 |
| | 212 | 22 | 0.00 | 56.8 | 28.92 | 85.7 | 24.627 | 1.734 | 146 | 15.06 | 1029 | 0.984 | 21.38 | 1.505 | 961 | 2.68 | 1375 | 0.834 | 1081 | 0.970 | 38086 | 95.30 | 15.81 | 79.5 |
| | 213 | 21 | 0.00 | 57.2 | 28.92 | 84.8 | 25.987 | 1.830 | 137 | 16.03 | 1067 | 0.979 | 23.88 | 1.681 | 1039 | 3.13 | 1580 | 0.870 | 1151 | 1.032 | 43735 | 99.70 | 16.41 | 83.3 |
| | 217 | 20 | 0.00 | 57.1 | 28.92 | 84.6 | 26.961 | 1.899 | 145 | 16.47 | 1103 | 0.975 | 25.49 | 1.795 | 1086 | 3.38 | 1698 | 0.888 | 1204 | 1.080 | 47458 | 101.40 | 16.76 | 84.6 |
| | 209 | 14 | 0.00 | 56.5 | 28.94 | 87.6 | 18.183 | 1.280 | 142 | 9.59 | 702 | 0.995 | 15.86 | 1.116 | 739 | 1.23 | 667 | 0.717 | 698 | 0.626 | 14802 | 75.90 | 11.70 | 64.2 |
| | 222 | 14 | 0.00 | 56.1 | 28.94 | 85.8 | 18.030 | 1.269 | 141 | 9.39 | 689 | 0.992 | 16.43 | 1.156 | 737 | 1.53 | 764 | 0.771 | 699 | 0.628 | 15113 | 76.20 | 11.79 | 64.4 |
| | 221 | 13 | 0.00 | 56.9 | 28.94 | 83.2 | 19.725 | 1.388 | 138 | 11.25 | 802 | 0.991 | 17.64 | 1.242 | 787 | 1.90 | 949 | 0.792 | 823 | 0.738 | 21466 | 82.60 | 13.32 | 69.3 |
| | 220 | 12 | 0.00 | 57.7 | 28.92 | 83.0 | 21.436 | 1.509 | 138 | 12.76 | 893 | 0.986 | 18.90 | 1.331 | 843 | 2.21 | 1110 | 0.806 | 925 | 0.829 | 27450 | 87.70 | 14.39 | 73.3 |
| | 219 | 11 | 0.00 | 57.5 | 28.92 | 82.7 | 23.130 | 1.629 | 138 | 14.08 | 967 | 0.984 | 20.68 | 1.456 | 931 | 2.57 | 1307 | 0.833 | 1019 | 0.914 | 33769 | 92.70 | 15.29 | 77.4 |
| | 218 | 10 | 0.00 | 57.3 | 28.92 | 83.3 | 24.913 | 1.755 | 135 | 15.36 | 1029 | 0.980 | 22.23 | 1.566 | 1032 | 2.80 | 1472 | 0.848 | 1098 | 0.985 | 39562 | 96.50 | 15.97 | 80.5 |

## Aeroacoustic Summary Data — Model 2 – Configuration 2BB, Baseline Core Nozzle, Baseline Fan Nozzle (Concluded)

| Date | Point | Cycle | XMA | $T_{amb}$ | $P_{amb}$ | RH | $P_{18}$ | PFQPA | $T_{18}$ | $W_{18}$ | $V_{18}$ | $CD_{18}$ | $P_8$ | P8QPA | $T_8$ | $W_8$ | $V_8$ | $CD_8$ | $V_{mix}$ | $V_{mix}/c_{amb}$ | $F_N$ | EPNL | NF | NEPNL |
|---|---|---|---|---|---|---|---|---|---|---|---|---|---|---|---|---|---|---|---|---|---|---|---|---|
| 4/21/97 | 940 | 24 | 0.28 | 59.2 | 28.90 | 36.8 | 21.407 | 1.509 | 139 | 12.89 | 893 | | 18.07 | 1.273 | 838 | 1.91 | 1019 | | 909 | 0.814 | 17554 | 77.10 | 12.44 | 64.7 |
| | 954 | 24 | 0.28 | 58.3 | 28.88 | 36.1 | 21.389 | 1.508 | 138 | 12.94 | 892 | | 18.08 | 1.275 | 846 | 1.90 | 1025 | | 909 | 0.815 | 17664 | 77.40 | 12.47 | 64.9 |
| | 941 | 23 | 0.28 | 59.1 | 28.90 | 37.5 | 22.737 | 1.603 | 141 | 13.88 | 954 | | 19.24 | 1.356 | 891 | 2.20 | 1163 | | 983 | 0.880 | 21509 | 80.70 | 13.33 | 67.4 |
| | 955 | 23 | 0.28 | 57.8 | 28.88 | 36.4 | 22.657 | 1.598 | 138 | 13.98 | 949 | | 19.27 | 1.359 | 887 | 2.21 | 1165 | | 979 | 0.877 | 21517 | 80.20 | 13.33 | 66.9 |
| | 942 | 22 | 0.28 | 58.7 | 28.90 | 37.8 | 24.691 | 1.741 | 142 | 15.24 | 1029 | | 21.50 | 1.515 | 956 | 2.69 | 1380 | | 1082 | 0.969 | 27556 | 86.30 | 14.40 | 71.9 |
| | 943 | 21 | 0.28 | 59.6 | 28.88 | 37.5 | 26.170 | 1.845 | 142 | 16.07 | 1078 | | 23.83 | 1.681 | 1040 | 3.09 | 1576 | | 1159 | 1.037 | 32297 | 91.00 | 15.09 | 75.9 |
| | 944 | 20 | 0.28 | 59.4 | 28.88 | 37.6 | 26.926 | 1.899 | 143 | 16.52 | 1101 | | 25.36 | 1.788 | 1081 | 3.34 | 1682 | | 1200 | 1.074 | 35080 | 93.70 | 15.45 | 78.2 |
| | 945 | 20 | 0.28 | 58.9 | 28.88 | 38.7 | 26.976 | 1.902 | 143 | 16.51 | 1102 | | 25.43 | 1.793 | 1081 | 3.36 | 1687 | | 1202 | 1.076 | 35229 | 93.80 | 15.47 | 78.3 |
| | 950 | 13 | 0.28 | 60.4 | 28.88 | 39.7 | 19.650 | 1.386 | 139 | 11.15 | 800 | | 17.67 | 1.246 | 772 | 1.90 | 949 | | 822 | 0.735 | 13248 | 73.60 | 11.22 | 62.4 |
| | 951 | 12 | 0.28 | 60.8 | 28.88 | 40.6 | 21.463 | 1.513 | 140 | 12.80 | 896 | | 18.94 | 1.335 | 835 | 2.19 | 1110 | | 928 | 0.830 | 18368 | 78.20 | 12.64 | 65.6 |
| | 952 | 11 | 0.28 | 60.0 | 28.88 | 40.9 | 23.143 | 1.632 | 140 | 14.10 | 970 | | 20.43 | 1.440 | 920 | 2.49 | 1281 | | 1017 | 0.910 | 23262 | 82.60 | 13.67 | 68.9 |
| | 953 | 10 | 0.28 | 60.2 | 28.88 | 40.6 | 24.906 | 1.756 | 140 | 15.31 | 1035 | | 22.11 | 1.559 | 1018 | 2.76 | 1454 | | 1100 | 0.984 | 28335 | 90.30 | 14.52 | 75.8 |
| | 946 | 21 | 0.20 | 59.1 | 28.90 | 39.0 | 26.089 | 1.839 | 142 | 16.00 | 1075 | | 23.76 | 1.675 | 1043 | 3.08 | 1573 | | 1156 | 1.035 | 35395 | 94.80 | 15.49 | 79.3 |
| | 947 | 21 | 0.00 | 59.6 | 28.90 | 39.2 | 26.164 | 1.845 | 142 | 16.00 | 1077 | | 23.77 | 1.675 | 1046 | 3.08 | 1574 | | 1159 | 1.037 | 43570 | 99.10 | 16.39 | 82.7 |
| | 949 | 13 | 0.00 | 59.2 | 28.90 | 40.7 | 19.644 | 1.385 | 140 | 11.16 | 800 | | 17.67 | 1.246 | 782 | 1.92 | 953 | | 823 | 0.736 | 21082 | 82.40 | 13.24 | 69.2 |
| | 948 | 11 | 0.00 | 60.6 | 28.90 | 38.8 | 23.122 | 1.630 | 142 | 14.06 | 970 | | 20.48 | 1.443 | 922 | 2.52 | 1285 | | 1019 | 0.911 | 33197 | 92.60 | 15.21 | 77.4 |
| 5/12/97 | 1233 | 24 | 0.28 | 54.2 | 28.88 | 58.4 | 21.501 | 1.516 | 140 | 12.92 | 899 | | 18.04 | 1.272 | 839 | 1.90 | 1018 | | 915 | 0.823 | 17897 | 77.60 | 12.53 | 65.1 |
| | 1234 | 23 | 0.28 | 54.4 | 28.88 | 56.5 | 22.701 | 1.601 | 141 | 13.80 | 953 | | 19.11 | 1.348 | 888 | 2.16 | 1151 | | 980 | 0.882 | 21284 | 80.40 | 13.28 | 67.1 |
| | 1235 | 22 | 0.28 | 55.1 | 28.88 | 54.5 | 24.556 | 1.732 | 143 | 15.10 | 1026 | | 21.46 | 1.514 | 962 | 2.68 | 1381 | | 1080 | 0.970 | 27224 | 86.10 | 14.35 | 71.8 |
| | 1236 | 21 | 0.28 | 55.6 | 28.88 | 54.7 | 25.892 | 1.826 | 143 | 15.85 | 1070 | | 23.81 | 1.679 | 1041 | 3.10 | 1575 | | 1154 | 1.036 | 31807 | 90.50 | 15.03 | 75.5 |
| | 1237 | 20 | 0.28 | 55.5 | 28.88 | 54.7 | 26.882 | 1.896 | 144 | 16.44 | 1101 | | 25.34 | 1.787 | 1081 | 3.35 | 1682 | | 1200 | 1.078 | 35088 | 93.20 | 15.45 | 77.7 |
| | 1238 | 21 | 0.20 | 54.9 | 28.88 | 55.6 | 25.873 | 1.825 | 144 | 15.82 | 1070 | | 23.74 | 1.674 | 1038 | 3.10 | 1569 | | 1153 | 1.036 | 34924 | 94.60 | 15.43 | 79.2 |
| | 1239 | 21 | 0.00 | 55.0 | 28.88 | 55.8 | 26.014 | 1.835 | 143 | 15.95 | 1074 | | 23.78 | 1.677 | 1037 | 3.11 | 1571 | | 1156 | 1.039 | 43608 | 99.30 | 16.40 | 82.9 |

## Aeroacoustic Summary Data — Model 2 – Configuration 2BD, Baseline Core Nozzle, 96-Internal-Doublets Fan Nozzle

| Date | Point | Cycle | XMA | $T_{amb}$ | $P_{amb}$ | RH | $P_{18}$ | PFQPA | $T_{18}$ | $W_{18}$ | $V_{18}$ | $CD_{18}$ | $P_8$ | P8QPA | $T_8$ | $W_8$ | $V_8$ | $CD_8$ | $V_{mix}$ | $V_{mix}/c_{amb}$ | $F_N$ | EPNL | NF | NEPNL |
|---|---|---|---|---|---|---|---|---|---|---|---|---|---|---|---|---|---|---|---|---|---|---|---|---|
| 3/25/97 | 241 | 23A | 0.28 | 42.4 | 29.02 | 88.3 | 22.838 | 1.602 | 159 | 13.59 | 969 | 0.983 | 19.19 | 1.346 | 892 | 2.16 | 1152 | 0.784 | 994 | 0.904 | 21389 | 80.70 | 13.30 | 67.4 |
| | 242 | 22A | 0.28 | 42.0 | 29.02 | 87.7 | 24.680 | 1.732 | 179 | 14.65 | 1056 | 0.981 | 21.63 | 1.518 | 962 | 2.71 | 1389 | 0.831 | 1108 | 1.009 | 27510 | 86.40 | 14.39 | 72.0 |
| | 243 | 21A | 0.28 | 41.6 | 29.02 | 87.5 | 26.068 | 1.829 | 190 | 15.37 | 1112 | 0.979 | 24.00 | 1.685 | 1037 | 3.14 | 1583 | 0.866 | 1192 | 1.086 | 32401 | 91.60 | 15.11 | 76.5 |
| | 249 | 24 | 0.28 | 40.3 | 29.04 | 86.0 | 21.566 | 1.513 | 141 | 12.74 | 897 | 0.981 | 18.11 | 1.271 | 848 | 1.89 | 1021 | 0.761 | 914 | 0.833 | 17462 | 80.40 | 12.42 | 68.0 |
| | 248 | 23 | 0.28 | 40.4 | 29.04 | 86.0 | 22.803 | 1.600 | 141 | 13.71 | 952 | 0.978 | 19.23 | 1.349 | 879 | 2.18 | 1150 | 0.784 | 980 | 0.893 | 21028 | 80.20 | 13.23 | 67.0 |
| | 247 | 22 | 0.28 | 40.6 | 29.04 | 86.2 | 24.690 | 1.732 | 142 | 15.04 | 1025 | 0.977 | 21.45 | 1.504 | 957 | 2.66 | 1372 | 0.826 | 1077 | 0.982 | 26913 | 85.60 | 14.30 | 71.3 |
| | 246 | 21 | 0.28 | 40.7 | 29.02 | 86.5 | 26.066 | 1.829 | 143 | 15.91 | 1071 | 0.975 | 24.01 | 1.685 | 1034 | 3.14 | 1582 | 0.865 | 1155 | 1.053 | 31943 | 91.00 | 15.04 | 76.0 |
| | 244 | 20 | 0.28 | 41.3 | 29.04 | 87.6 | 26.991 | 1.893 | 145 | 16.41 | 1101 | 0.971 | 25.73 | 1.805 | 1076 | 3.41 | 1699 | 0.886 | 1204 | 1.097 | 35198 | 94.50 | 15.47 | 79.0 |
| | 251 | 23 | 0.00 | 41.5 | 29.04 | 81.9 | 22.838 | 1.602 | 142 | 13.79 | 955 | 0.983 | 19.36 | 1.358 | 888 | 2.24 | 1166 | 0.800 | 984 | 0.896 | 31282 | 90.20 | 14.95 | 75.2 |
| | 252 | 22 | 0.00 | 41.7 | 29.02 | 81.6 | 24.717 | 1.734 | 143 | 15.12 | 1026 | 0.980 | 21.59 | 1.514 | 964 | 2.71 | 1387 | 0.836 | 1081 | 0.985 | 38269 | 95.20 | 15.83 | 79.4 |

## Aeroacoustic Summary Data

## Model 2 – Configuration 2TmB, Tongue-Mixer Core Nozzle, Baseline Fan Nozzle

| Date | Point | Cycle | XMA | $T_{amb}$ | $P_{amb}$ | RH | $P_{18}$ | PFQPA | $T_{18}$ | $W_{18}$ | $V_{18}$ | $CD_{18}$ | $P_8$ | P8QPA | $T_8$ | $W_8$ | $V_8$ | $CD_8$ | $V_{mix}$ | $V_{mix}/c_{amb}$ | $F_N$ | EPNL | NF | NEPNL |
|---|---|---|---|---|---|---|---|---|---|---|---|---|---|---|---|---|---|---|---|---|---|---|---|---|
| 3/26/97 | 267 | 21A | 0.28 | 43.0 | 29.19 | 61.0 | 26.129 | 1.823 | 140 | 15.99 | 1066 | 0.975 | 19.92 | 1.390 | 1037 | 3.02 | 1273 | 1.084 | 1099 | 1.000 | 29795 | 86.50 | 14.74 | 71.8 |
| | 266 | 20A | 0.28 | 43.0 | 29.21 | 59.3 | 27.076 | 1.889 | 141 | 16.58 | 1095 | 0.975 | 20.78 | 1.450 | 1076 | 3.28 | 1365 | 1.114 | 1140 | 1.037 | 32829 | 89.00 | 15.16 | 73.8 |
| | 262 | 24 | 0.28 | 41.4 | 29.21 | 62.8 | 21.706 | 1.513 | 141 | 12.76 | 897 | 0.975 | 18.21 | 1.270 | 841 | 2.67 | 1017 | 1.064 | 918 | 0.836 | 18658 | 78.80 | 12.71 | 66.1 |
| | 263 | 23 | 0.28 | 41.9 | 29.21 | 61.2 | 23.022 | 1.605 | 140 | 13.81 | 955 | 0.974 | 19.36 | 1.350 | 890 | 3.07 | 1156 | 1.100 | 991 | 0.903 | 22874 | 82.20 | 13.59 | 68.6 |
| | 264 | 22 | 0.28 | 42.0 | 29.21 | 61.7 | 24.738 | 1.725 | 143 | 15.01 | 1022 | 0.974 | 21.67 | 1.511 | 958 | 3.79 | 1381 | 1.159 | 1094 | 0.996 | 29433 | 87.60 | 14.69 | 72.9 |
| | 265 | 21 | 0.28 | 42.8 | 29.21 | 60.9 | 26.225 | 1.829 | 134 | 16.08 | 1063 | 0.972 | 24.14 | 1.684 | 1039 | 4.42 | 1583 | 1.215 | 1175 | 1.069 | 35277 | 92.00 | 15.47 | 76.5 |
| | 268 | 21A | 0.20 | 43.1 | 29.21 | 61.9 | 26.274 | 1.832 | 140 | 16.10 | 1071 | 0.976 | 19.92 | 1.389 | 1039 | 3.03 | 1273 | 1.089 | 1103 | 1.003 | 33660 | 90.30 | 15.27 | 75.0 |
| | 272 | 26 | 0.20 | 43.4 | 29.19 | 61.1 | 18.357 | 1.281 | 139 | 9.49 | 701 | 0.972 | 16.07 | 1.121 | 743 | 1.76 | 681 | 0.999 | 698 | 0.634 | 10696 | 73.50 | 10.29 | 63.2 |
| | 271 | 25 | 0.20 | 43.2 | 29.19 | 61.6 | 20.369 | 1.421 | 139 | 11.60 | 829 | 0.976 | 17.22 | 1.201 | 808 | 2.27 | 884 | 1.030 | 838 | 0.762 | 17002 | 78.50 | 12.30 | 66.2 |
| | 270 | 24 | 0.20 | 43.3 | 29.21 | 61.4 | 21.647 | 1.510 | 140 | 12.69 | 894 | 0.973 | 18.23 | 1.271 | 840 | 2.70 | 1019 | 1.076 | 916 | 0.833 | 21316 | 82.20 | 13.29 | 68.9 |
| | 269 | 21 | 0.20 | 43.3 | 29.21 | 61.1 | 26.346 | 1.838 | 141 | 16.08 | 1073 | 0.973 | 24.16 | 1.685 | 1034 | 4.44 | 1582 | 1.216 | 1183 | 1.076 | 39395 | 95.50 | 15.95 | 79.5 |
| | 273 | 26 | 0.00 | 43.6 | 29.21 | 60.7 | 18.340 | 1.279 | 140 | 9.51 | 700 | 0.977 | 16.12 | 1.124 | 740 | 1.84 | 690 | 1.030 | 698 | 0.635 | 15671 | 76.70 | 11.95 | 64.7 |
| | 274 | 24 | 0.00 | 43.8 | 29.21 | 60.5 | 21.729 | 1.516 | 141 | 12.83 | 899 | 0.978 | 18.25 | 1.273 | 842 | 2.75 | 1022 | 1.091 | 921 | 0.837 | 28489 | 87.30 | 14.55 | 72.8 |
| | 279 | 22 | 0.00 | 43.2 | 29.19 | 62.7 | 26.383 | 1.841 | 141 | 16.16 | 1075 | 0.977 | 20.03 | 1.398 | 1042 | 3.09 | 1286 | 1.101 | 1109 | 1.008 | 42450 | 95.30 | 16.28 | 79.0 |
| | 275 | 11 | 0.00 | 43.7 | 29.19 | 61.4 | 22.976 | 1.603 | 141 | 13.79 | 954 | 0.977 | 19.33 | 1.349 | 887 | 3.12 | 1153 | 1.118 | 991 | 0.901 | 33279 | 90.50 | 15.22 | 75.3 |
| | 276 | 10 | 0.00 | 43.4 | 29.19 | 61.8 | 24.780 | 1.729 | 141 | 15.09 | 1023 | 0.975 | 21.55 | 1.504 | 962 | 3.78 | 1374 | 1.169 | 1093 | 0.994 | 41005 | 95.20 | 16.13 | 79.1 |
| | 277 | 10 | 0.00 | 43.5 | 29.19 | 61.8 | 26.338 | 1.838 | 142 | 16.11 | 1074 | 0.974 | 24.09 | 1.681 | 1039 | 4.43 | 1581 | 1.221 | 1183 | 1.076 | 48299 | 99.10 | 16.84 | 82.3 |
| | 278 | 10 | 0.00 | 43.5 | 29.19 | 61.9 | 27.085 | 1.890 | 139 | 16.59 | 1095 | 0.975 | 20.94 | 1.461 | 1084 | 3.36 | 1383 | 1.132 | 1143 | 1.039 | 45361 | 97.20 | 16.57 | 80.6 |

## Aeroacoustic Summary Data

## Model 2 – Configuration 2TmC, Tongue-Mixer Core Nozzle, 24-Chevron Fan Nozzle

| Date | Point | Cycle | XMA | $T_{amb}$ | $P_{amb}$ | RH | $P_{18}$ | PFQPA | $T_{18}$ | $W_{18}$ | $V_{18}$ | $CD_{18}$ | $P_8$ | P8QPA | $T_8$ | $W_8$ | $V_8$ | $CD_8$ | $V_{mix}$ | $V_{mix}/c_{amb}$ | $F_N$ | EPNL | NF | NEPNL |
|---|---|---|---|---|---|---|---|---|---|---|---|---|---|---|---|---|---|---|---|---|---|---|---|---|
| 3/26/97 | 286 | 21A | 0.28 | 40.1 | 29.17 | 71.4 | 26.247 | 1.833 | 143 | 16.33 | 1074 | 0.993 | 19.90 | 1.390 | 1042 | 3.00 | 1276 | 1.080 | 1105 | 1.008 | 30572 | 86.30 | 14.85 | 71.4 |
| | 282 | 24 | 0.28 | 40.2 | 29.17 | 70.9 | 21.729 | 1.517 | 134 | 13.11 | 895 | 0.994 | 18.24 | 1.274 | 838 | 2.70 | 1021 | 1.071 | 917 | 0.837 | 19104 | 78.90 | 12.81 | 66.1 |
| | 283 | 23 | 0.28 | 40.3 | 29.17 | 70.6 | 22.934 | 1.601 | 142 | 14.01 | 953 | 0.994 | 19.32 | 1.349 | 888 | 3.07 | 1154 | 1.104 | 990 | 0.903 | 23176 | 83.10 | 13.65 | 69.4 |
| | 284 | 22 | 0.28 | 40.1 | 29.17 | 71.4 | 24.877 | 1.737 | 144 | 15.38 | 1029 | 0.993 | 21.47 | 1.499 | 962 | 3.72 | 1369 | 1.158 | 1095 | 0.999 | 29950 | 87.00 | 14.76 | 72.2 |
| | 285 | 21 | 0.28 | 40.1 | 29.17 | 71.5 | 26.294 | 1.836 | 144 | 16.28 | 1075 | 0.989 | 24.10 | 1.683 | 1049 | 4.40 | 1588 | 1.215 | 1184 | 1.080 | 36024 | 91.60 | 15.57 | 76.0 |
| | 287 | 20A | 0.28 | 40.0 | 29.14 | 71.2 | 27.088 | 1.892 | 141 | 16.88 | 1097 | 0.990 | 20.86 | 1.457 | 1079 | 3.31 | 1376 | 1.119 | 1143 | 1.042 | 33485 | 88.70 | 15.25 | 73.5 |
| | 288 | 21A | 0.20 | 40.1 | 29.17 | 71.6 | 26.288 | 1.836 | 141 | 16.37 | 1073 | 0.993 | 19.91 | 1.391 | 1041 | 3.04 | 1276 | 1.091 | 1104 | 1.007 | 34117 | 90.10 | 15.33 | 74.8 |
| | 292 | 26 | 0.20 | 39.8 | 29.14 | 71.9 | 18.370 | 1.284 | 139 | 9.65 | 704 | 0.985 | 16.09 | 1.124 | 740 | 1.78 | 689 | 1.000 | 702 | 0.640 | 10948 | 73.40 | 10.39 | 63.0 |
| | 290 | 24 | 0.20 | 40.0 | 29.14 | 71.6 | 21.613 | 1.510 | 141 | 12.85 | 895 | 0.987 | 18.16 | 1.269 | 845 | 2.67 | 1017 | 1.073 | 916 | 0.836 | 21526 | 82.10 | 13.33 | 68.8 |
| | 291 | 25 | 0.20 | 39.9 | 29.14 | 71.9 | 20.344 | 1.421 | 140 | 11.74 | 830 | 0.988 | 17.20 | 1.202 | 805 | 2.30 | 883 | 1.042 | 839 | 0.765 | 17282 | 78.70 | 12.38 | 66.3 |
| | 289 | 21 | 0.20 | 40.0 | 29.14 | 71.6 | 26.314 | 1.838 | 141 | 16.33 | 1074 | 0.989 | 24.06 | 1.681 | 1046 | 4.40 | 1584 | 1.216 | 1182 | 1.078 | 39736 | 94.60 | 15.99 | 78.6 |
| | 300 | 20 | 0.00 | 40.8 | 29.17 | 70.8 | 26.972 | 1.884 | 141 | 16.77 | 1093 | 0.993 | 25.64 | 1.791 | 1081 | 4.80 | 1692 | 1.252 | 1226 | 1.118 | 52541 | 100.50 | 17.20 | 83.3 |
| | 293 | 26 | 0.00 | 40.2 | 29.14 | 71.5 | 18.320 | 1.280 | 139 | 9.64 | 700 | 0.991 | 16.02 | 1.120 | 739 | 1.79 | 676 | 1.023 | 696 | 0.635 | 15783 | 76.90 | 11.98 | 64.9 |
| | 294 | 24 | 0.00 | 40.6 | 29.14 | 70.6 | 21.678 | 1.515 | 140 | 12.98 | 898 | 0.992 | 18.12 | 1.266 | 846 | 2.70 | 1013 | 1.089 | 918 | 0.837 | 28566 | 86.70 | 14.56 | 72.1 |
| | 295 | 23 | 0.00 | 40.7 | 29.14 | 70.6 | 22.967 | 1.605 | 141 | 14.01 | 955 | 0.992 | 19.28 | 1.347 | 886 | 3.11 | 1151 | 1.120 | 990 | 0.903 | 33697 | 90.00 | 15.28 | 74.7 |
| | 296 | 22 | 0.00 | 40.7 | 29.14 | 70.6 | 24.842 | 1.736 | 141 | 15.37 | 1025 | 0.992 | 21.58 | 1.508 | 966 | 3.80 | 1380 | 1.173 | 1096 | 0.999 | 41705 | 94.90 | 16.20 | 78.7 |
| | 297 | 21B | 0.00 | 40.6 | 29.14 | 71.2 | 26.298 | 1.837 | 141 | 16.39 | 1073 | 0.993 | 24.02 | 1.678 | 945 | 4.56 | 1528 | 1.219 | 1172 | 1.069 | 48743 | 97.90 | 16.88 | 81.0 |
| | 298 | 21 | 0.00 | 40.7 | 29.17 | 71.1 | 26.355 | 1.841 | 141 | 16.40 | 1074 | 0.990 | 24.14 | 1.686 | 1046 | 4.45 | 1589 | 1.226 | 1184 | 1.080 | 49103 | 98.60 | 16.91 | 81.7 |
| | 299 | 20A | 0.00 | 40.8 | 29.17 | 70.9 | 27.035 | 1.888 | 141 | 16.84 | 1095 | 0.992 | 20.94 | 1.462 | 1070 | 3.40 | 1379 | 1.138 | 1142 | 1.041 | 45974 | 96.80 | 16.63 | 80.2 |

## Aeroacoustic Summary Data — Model 2 – Configuration 2C12B, 12-Chevron Core Nozzle, Baseline Fan Nozzle

| Date | Point | Cycle | XMA | $T_{amb}$ | $P_{amb}$ | RH | $P_{18}$ | PFQPA | $T_{18}$ | $W_{18}$ | $V_{18}$ | $CD_{18}$ | $P_8$ | P8QPA | $T_8$ | $W_8$ | $V_8$ | $CD_8$ | $V_{mix}$ | $V_{mix}/c_{amb}$ | $F_N$ | EPNL | NF | NEPNL |
|---|---|---|---|---|---|---|---|---|---|---|---|---|---|---|---|---|---|---|---|---|---|---|---|---|
| 3/27/97 | 314 | 24 | 0.28 | 68.2 | 29.06 | 33.3 | 21.528 | 1.509 | 141 | 12.81 | 895 | 0.988 | 18.09 | 1.268 | 844 | 1.98 | 1016 | 0.798 | 911 | 0.809 | 17636 | 76.60 | 12.46 | 64.1 |
| | 315 | 23 | 0.28 | 68.3 | 29.06 | 33.8 | 22.799 | 1.598 | 142 | 13.81 | 952 | 0.987 | 19.36 | 1.357 | 890 | 2.32 | 1166 | 0.828 | 983 | 0.872 | 21598 | 80.10 | 13.34 | 66.8 |
| | 316 | 22 | 0.28 | 68.4 | 29.06 | 34.8 | 24.670 | 1.729 | 141 | 15.15 | 1022 | 0.983 | 21.52 | 1.508 | 961 | 2.80 | 1379 | 0.867 | 1078 | 0.956 | 27354 | 85.00 | 14.37 | 70.6 |
| | 318 | 21 | 0.28 | 68.9 | 29.04 | 33.9 | 26.198 | 1.837 | 141 | 16.06 | 1073 | 0.978 | 24.02 | 1.684 | 1044 | 3.27 | 1586 | 0.904 | 1160 | 1.029 | 32493 | 89.70 | 15.12 | 74.6 |
| | 319 | 20 | 0.28 | 68.9 | 29.04 | 33.0 | 27.138 | 1.903 | 141 | 16.67 | 1100 | 0.976 | 25.56 | 1.792 | 1081 | 3.53 | 1692 | 0.923 | 1204 | 1.068 | 35864 | 92.30 | 15.55 | 76.8 |
| | 313 | 26 | 0.20 | 67.9 | 29.06 | 34.7 | 18.241 | 1.278 | 141 | 9.59 | 699 | 0.991 | 15.98 | 1.120 | 743 | 1.30 | 679 | 0.744 | 697 | 0.619 | 10234 | 72.00 | 10.10 | 61.9 |
| | 312 | 25 | 0.20 | 68.3 | 29.06 | 33.9 | 20.308 | 1.423 | 141 | 11.75 | 832 | 0.990 | 17.08 | 1.197 | 809 | 1.68 | 874 | 0.775 | 837 | 0.743 | 16416 | 77.30 | 12.15 | 65.1 |
| | 311 | 24 | 0.20 | 68.3 | 29.06 | 35.7 | 21.525 | 1.509 | 141 | 12.73 | 897 | 0.979 | 18.11 | 1.269 | 842 | 2.00 | 1017 | 0.803 | 911 | 0.809 | 20132 | 80.40 | 13.04 | 67.4 |
| | 310 | 21 | 0.20 | 68.2 | 29.06 | 35.2 | 26.125 | 1.831 | 143 | 16.02 | 1072 | 0.980 | 23.99 | 1.681 | 1042 | 3.27 | 1583 | 0.906 | 1159 | 1.029 | 35938 | 94.10 | 15.56 | 78.5 |
| | 306 | 23 | 0.00 | 67.7 | 29.06 | 38.6 | 22.909 | 1.606 | 142 | 13.93 | 957 | 0.988 | 19.21 | 1.347 | 889 | 2.30 | 1152 | 0.833 | 984 | 0.874 | 31677 | 89.60 | 15.01 | 74.6 |
| | 307 | 22 | 0.00 | 68.1 | 29.06 | 37.3 | 24.718 | 1.733 | 143 | 15.17 | 1026 | 0.984 | 21.54 | 1.510 | 962 | 2.83 | 1381 | 0.874 | 1082 | 0.960 | 38739 | 94.60 | 15.88 | 78.7 |
| | 308 | 21 | 0.00 | 68.4 | 29.04 | 37.2 | 26.132 | 1.832 | 143 | 16.05 | 1072 | 0.980 | 23.99 | 1.682 | 1044 | 3.27 | 1585 | 0.907 | 1159 | 1.029 | 44473 | 98.30 | 16.48 | 81.8 |
| | 309 | 20 | 0.00 | 68.8 | 29.06 | 36.7 | 26.965 | 1.890 | 143 | 16.47 | 1098 | 0.978 | 25.55 | 1.791 | 1084 | 3.54 | 1693 | 0.927 | 1203 | 1.067 | 47886 | 100.50 | 16.80 | 83.7 |
| | 304 | 13 | 0.00 | 67.1 | 29.06 | 38.0 | 18.222 | 1.277 | 140 | 9.61 | 697 | 0.995 | 15.98 | 1.120 | 749 | 1.32 | 680 | 0.762 | 695 | 0.618 | 15006 | 75.90 | 11.76 | 64.1 |
| | 305 | 12 | 0.00 | 67.6 | 29.06 | 38.7 | 21.506 | 1.507 | 141 | 12.83 | 894 | 0.992 | 18.06 | 1.266 | 842 | 2.01 | 1010 | 0.811 | 909 | 0.808 | 26787 | 86.00 | 14.28 | 71.7 |

## Aeroacoustic Summary Data — Model 2 – Configuration 2C12C(BLT), 12-Chevron Core Nozzle, Boundary Layer Tip Fan Nozzle

| Date | Point | Cycle | XMA | $T_{amb}$ | $P_{amb}$ | RH | $P_{18}$ | PFQPA | $T_{18}$ | $W_{18}$ | $V_{18}$ | $CD_{18}$ | $P_8$ | P8QPA | $T_8$ | $W_8$ | $V_8$ | $CD_8$ | $V_{mix}$ | $V_{mix}/c_{amb}$ | $F_N$ | EPNL | NF | NEPNL |
|---|---|---|---|---|---|---|---|---|---|---|---|---|---|---|---|---|---|---|---|---|---|---|---|---|
| 3/27/97 | 323 | 24 | 0.28 | 65.3 | 29.06 | 39.5 | 21.599 | 1.514 | 141 | 13.07 | 898 | 1.003 | 18.10 | 1.268 | 840 | 1.97 | 1015 | 0.791 | 913 | 0.813 | 17948 | 78.00 | 12.54 | 65.5 |
| | 324 | 23 | 0.28 | 64.9 | 29.06 | 39.4 | 22.814 | 1.599 | 142 | 14.01 | 952 | 1.001 | 19.34 | 1.355 | 888 | 2.32 | 1162 | 0.829 | 982 | 0.875 | 21811 | 81.10 | 13.39 | 67.7 |
| | 325 | 22 | 0.28 | 64.6 | 29.06 | 40.6 | 24.793 | 1.737 | 143 | 15.42 | 1028 | 0.998 | 21.60 | 1.514 | 962 | 2.83 | 1383 | 0.871 | 1083 | 0.965 | 28050 | 86.00 | 14.48 | 71.5 |
| | 326 | 21 | 0.28 | 64.5 | 29.06 | 40.8 | 26.225 | 1.838 | 143 | 16.31 | 1075 | 0.994 | 24.05 | 1.686 | 1045 | 3.27 | 1588 | 0.904 | 1161 | 1.034 | 32899 | 90.10 | 15.17 | 74.9 |
| | 327 | 20 | 0.28 | 63.8 | 29.06 | 42.0 | 26.995 | 1.892 | 144 | 16.77 | 1099 | 0.990 | 25.71 | 1.802 | 1087 | 3.55 | 1703 | 0.926 | 1204 | 1.073 | 36014 | 92.80 | 15.56 | 77.2 |

## Aeroacoustic Summary Data

## Model 2 – Configuration 2C12C, 12-Chevron Core Nozzle, 24-Chevron Fan Nozzle

| Date | Point | Cycle | XMA | $T_{amb}$ | $P_{amb}$ | RH | $P_{18}$ | PFQPA | $T_{18}$ | $W_{18}$ | $V_{18}$ | $CD_{18}$ | $P_8$ | P8QPA | $T_8$ | $W_8$ | $V_8$ | $CD_8$ | $V_{mix}$ | $V_{mix}/c_{amb}$ | $F_N$ | EPNL | NF | NEPNL |
|---|---|---|---|---|---|---|---|---|---|---|---|---|---|---|---|---|---|---|---|---|---|---|---|---|
| 3/27/97 | 334 | 24 | 0.28 | 60.8 | 29.08 | 45.1 | 21.645 | 1.516 | 144 | 13.04 | 901 | 1.000 | 18.20 | 1.274 | 847 | 2.01 | 1025 | 0.799 | 918 | 0.820 | 18031 | 76.90 | 12.56 | 64.3 |
| | 335 | 23 | 0.28 | 60.5 | 29.08 | 45.8 | 22.863 | 1.601 | 144 | 14.03 | 955 | 1.001 | 19.32 | 1.353 | 888 | 2.30 | 1159 | 0.825 | 984 | 0.880 | 21870 | 80.00 | 13.40 | 66.6 |
| | 336 | 22 | 0.28 | 60.2 | 29.08 | 46.3 | 24.789 | 1.735 | 145 | 15.43 | 1029 | 1.000 | 21.65 | 1.515 | 965 | 2.83 | 1388 | 0.868 | 1084 | 0.970 | 27980 | 84.80 | 14.47 | 70.3 |
| | 337 | 21 | 0.28 | 60.3 | 29.08 | 45.3 | 26.264 | 1.839 | 145 | 16.33 | 1077 | 0.995 | 24.06 | 1.684 | 1043 | 3.27 | 1586 | 0.904 | 1162 | 1.040 | 33167 | 89.50 | 15.21 | 74.3 |
| | 338 | 20 | 0.28 | 60.0 | 29.08 | 45.0 | 27.008 | 1.891 | 146 | 16.76 | 1101 | 0.990 | 25.65 | 1.796 | 1086 | 3.54 | 1698 | 0.925 | 1205 | 1.078 | 36132 | 92.20 | 15.58 | 76.6 |
| | 339 | 20 | 0.28 | 60.3 | 29.08 | 44.0 | 26.998 | 1.890 | 146 | 16.75 | 1100 | 0.990 | 25.59 | 1.792 | 1086 | 3.53 | 1696 | 0.923 | 1204 | 1.076 | 35843 | 91.80 | 15.54 | 76.3 |
| | 333 | 26 | 0.20 | 61.0 | 29.08 | 45.2 | 18.256 | 1.278 | 142 | 9.69 | 700 | 1.002 | 16.01 | 1.121 | 740 | 1.31 | 681 | 0.745 | 697 | 0.623 | 10347 | 72.10 | 10.15 | 62.0 |
| | 332 | 25 | 0.20 | 61.1 | 29.08 | 45.5 | 20.326 | 1.423 | 143 | 11.88 | 833 | 1.002 | 17.16 | 1.202 | 795 | 1.71 | 879 | 0.777 | 839 | 0.750 | 16605 | 77.40 | 12.20 | 65.2 |
| | 330 | 24 | 0.20 | 62.1 | 29.08 | 43.8 | 21.688 | 1.519 | 142 | 13.12 | 902 | 1.003 | 18.18 | 1.273 | 854 | 2.01 | 1028 | 0.805 | 919 | 0.820 | 20904 | 80.70 | 13.20 | 67.5 |
| | 331 | 21 | 0.20 | 61.5 | 29.08 | 44.8 | 26.256 | 1.839 | 144 | 16.39 | 1077 | 0.997 | 24.03 | 1.682 | 1047 | 3.27 | 1586 | 0.907 | 1162 | 1.038 | 36741 | 93.30 | 15.65 | 77.6 |
| | 345 | 26 | 0.00 | 60.0 | 29.08 | 42.0 | 18.286 | 1.280 | 141 | 9.76 | 701 | 1.005 | 16.08 | 1.126 | 744 | 1.38 | 694 | 0.771 | 700 | 0.626 | 15379 | 76.10 | 11.87 | 64.2 |
| | 344 | 24 | 0.00 | 60.1 | 29.08 | 42.2 | 21.588 | 1.511 | 140 | 13.04 | 896 | 1.002 | 18.20 | 1.274 | 848 | 2.05 | 1026 | 0.816 | 913 | 0.817 | 27271 | 86.10 | 14.36 | 71.7 |
| | 343 | 23 | 0.00 | 60.2 | 29.08 | 42.2 | 22.860 | 1.600 | 140 | 14.08 | 952 | 1.001 | 19.34 | 1.354 | 888 | 2.34 | 1161 | 0.838 | 982 | 0.878 | 31937 | 89.60 | 15.04 | 74.6 |
| | 341 | 22 | 0.00 | 59.8 | 29.10 | 44.5 | 24.778 | 1.734 | 141 | 15.45 | 1025 | 0.998 | 21.57 | 1.510 | 958 | 2.84 | 1379 | 0.874 | 1080 | 0.966 | 39056 | 94.20 | 15.92 | 78.3 |
| | 342 | 21 | 0.00 | 60.2 | 29.10 | 42.5 | 26.180 | 1.833 | 142 | 16.29 | 1072 | 0.994 | 24.09 | 1.687 | 1040 | 3.32 | 1584 | 0.913 | 1159 | 1.036 | 45014 | 98.40 | 16.53 | 81.9 |
| | 340 | 20 | 0.00 | 60.5 | 29.08 | 43.7 | 27.033 | 1.892 | 140 | 16.86 | 1095 | 0.991 | 25.52 | 1.786 | 1082 | 3.53 | 1689 | 0.927 | 1198 | 1.072 | 48249 | 100.00 | 16.83 | 83.2 |
| 4/21/97 | 961 | 24 | 0.28 | 55.1 | 28.88 | 37.5 | 21.478 | 1.515 | 141 | 13.01 | 899 | | 18.04 | 1.272 | 851 | 1.98 | 1023 | | 915 | 0.823 | 17986 | 77.60 | 12.55 | 65.1 |
| | 962 | 23 | 0.28 | 55.7 | 28.88 | 37.4 | 22.670 | 1.599 | 141 | 13.95 | 952 | | 19.16 | 1.351 | 890 | 2.27 | 1156 | | 981 | 0.881 | 21690 | 80.20 | 13.36 | 66.8 |
| | 963 | 22 | 0.28 | 56.0 | 28.88 | 36.9 | 24.582 | 1.734 | 142 | 15.31 | 1025 | | 21.44 | 1.512 | 962 | 2.79 | 1380 | | 1081 | 0.970 | 27838 | 84.90 | 14.45 | 70.5 |
| | 964 | 21 | 0.28 | 56.1 | 28.88 | 37.2 | 25.944 | 1.830 | 141 | 16.18 | 1070 | | 23.88 | 1.684 | 1044 | 3.25 | 1581 | | 1156 | 1.038 | 32815 | 89.50 | 15.16 | 74.3 |
| | 965 | 20 | 0.28 | 56.4 | 28.88 | 37.2 | 26.820 | 1.891 | 141 | 16.73 | 1096 | | 25.39 | 1.791 | 1082 | 3.50 | 1686 | | 1200 | 1.077 | 35948 | 91.90 | 15.56 | 76.3 |
| | 966 | 21 | 0.20 | 56.3 | 28.88 | 37.7 | 25.940 | 1.829 | 141 | 16.18 | 1070 | | 23.91 | 1.686 | 1041 | 3.26 | 1581 | | 1157 | 1.038 | 35975 | 93.40 | 15.56 | 77.8 |
| | 967 | 21 | 0.00 | 56.2 | 28.88 | 38.0 | 25.943 | 1.829 | 141 | 16.17 | 1070 | | 23.77 | 1.677 | 1043 | 3.25 | 1574 | | 1155 | 1.037 | 44432 | 97.90 | 16.48 | 81.4 |

## Aeroacoustic Summary Data

## Model 2 – Configuration 2BC, Baseline Core Nozzle, 24-Chevron Fan Nozzle

| Date | Point | Cycle | XMA | $T_{amb}$ | $P_{amb}$ | RH | $P_{18}$ | PFQPA | $T_{18}$ | $W_{18}$ | $V_{18}$ | $CD_{18}$ | $P_8$ | P8QPA | $T_8$ | $W_8$ | $V_8$ | $CD_8$ | $V_{mix}$ | $V_{mix}/c_{amb}$ | $F_N$ | EPNL | NF | NEPNL |
|---|---|---|---|---|---|---|---|---|---|---|---|---|---|---|---|---|---|---|---|---|---|---|---|---|
| 3/28/97 | 357 | 24 | 0.28 | 69.7 | 28.78 | 35.5 | 21.345 | 1.511 | 139 | 12.87 | 895 | 0.999 | 17.99 | 1.273 | 840 | 1.89 | 1022 | 0.761 | 911 | 0.808 | 17551 | 76.80 | 12.44 | 64.4 |
| | 356 | 23 | 0.28 | 69.5 | 28.78 | 35.3 | 22.605 | 1.600 | 141 | 13.87 | 952 | 0.998 | 19.09 | 1.351 | 887 | 2.17 | 1156 | 0.786 | 980 | 0.869 | 21277 | 79.70 | 13.28 | 66.4 |
| | 355 | 22 | 0.28 | 69.4 | 28.78 | 35.1 | 24.478 | 1.733 | 142 | 15.22 | 1024 | 0.997 | 21.43 | 1.517 | 960 | 2.68 | 1387 | 0.830 | 1079 | 0.956 | 27257 | 84.70 | 14.35 | 70.3 |
| | 354 | 21 | 0.28 | 68.9 | 28.78 | 35.1 | 25.839 | 1.829 | 144 | 16.04 | 1072 | 0.993 | 23.74 | 1.680 | 1043 | 3.09 | 1583 | 0.865 | 1154 | 1.024 | 32037 | 89.70 | 15.06 | 74.6 |
| | 353 | 20 | 0.28 | 69.1 | 28.78 | 34.8 | 26.698 | 1.889 | 145 | 16.60 | 1099 | 0.991 | 25.35 | 1.794 | 1080 | 3.35 | 1693 | 0.884 | 1199 | 1.063 | 35212 | 92.70 | 15.47 | 77.2 |
| | 362 | 26 | 0.20 | 69.8 | 28.76 | 38.0 | 18.060 | 1.279 | 140 | 9.60 | 699 | 1.002 | 15.89 | 1.125 | 740 | 1.26 | 690 | 0.713 | 698 | 0.619 | 10241 | 71.90 | 10.10 | 61.8 |
| | 361 | 25 | 0.20 | 70.0 | 28.76 | 36.6 | 20.050 | 1.420 | 140 | 11.72 | 829 | 1.002 | 16.99 | 1.203 | 795 | 1.62 | 881 | 0.742 | 835 | 0.740 | 16228 | 77.10 | 12.10 | 65.0 |
| | 358 | 24 | 0.20 | 69.7 | 28.78 | 35.9 | 21.368 | 1.512 | 140 | 12.92 | 896 | 1.002 | 17.97 | 1.272 | 843 | 1.90 | 1021 | 0.767 | 912 | 0.808 | 20283 | 82.70 | 13.07 | 69.6 |
| | 360 | 24 | 0.20 | 70.0 | 28.76 | 36.7 | 21.335 | 1.511 | 141 | 12.85 | 896 | 0.999 | 17.98 | 1.273 | 838 | 1.91 | 1021 | 0.768 | 912 | 0.808 | 20153 | 80.30 | 13.04 | 67.3 |
| | 359 | 21 | 0.20 | 70.2 | 28.78 | 36.2 | 25.984 | 1.839 | 142 | 16.18 | 1075 | 0.994 | 23.84 | 1.688 | 1038 | 3.12 | 1586 | 0.867 | 1158 | 1.025 | 35759 | 93.90 | 15.53 | 78.4 |
| | 347 | 26 | 0.00 | 68.2 | 28.82 | 30.1 | 18.120 | 1.280 | 143 | 9.69 | 703 | 1.008 | 15.87 | 1.121 | 742 | 1.27 | 682 | 0.728 | 700 | 0.622 | 15164 | 76.00 | 11.81 | 64.2 |
| | 348 | 24 | 0.00 | 69.6 | 28.82 | 28.9 | 21.369 | 1.511 | 145 | 12.87 | 899 | 1.002 | 17.99 | 1.272 | 843 | 1.93 | 1021 | 0.777 | 915 | 0.811 | 26781 | 85.80 | 14.28 | 71.5 |
| | 349 | 23 | 0.00 | 69.9 | 28.82 | 28.6 | 22.556 | 1.595 | 145 | 13.82 | 953 | 1.001 | 19.07 | 1.348 | 885 | 2.19 | 1151 | 0.798 | 980 | 0.868 | 31144 | 89.10 | 14.93 | 74.2 |
| | 350 | 22 | 0.00 | 69.7 | 28.80 | 28.7 | 24.465 | 1.730 | 143 | 15.22 | 1025 | 0.998 | 21.26 | 1.504 | 960 | 2.66 | 1373 | 0.833 | 1076 | 0.954 | 38251 | 94.30 | 15.83 | 78.5 |
| | 351 | 21 | 0.00 | 69.8 | 28.80 | 29.3 | 25.856 | 1.829 | 144 | 16.10 | 1072 | 0.993 | 23.80 | 1.684 | 1039 | 3.12 | 1583 | 0.871 | 1155 | 1.024 | 44068 | 98.40 | 16.44 | 82.0 |
| | 352 | 20 | 0.00 | 70.3 | 28.80 | 29.3 | 26.711 | 1.889 | 144 | 16.57 | 1098 | 0.992 | 25.35 | 1.793 | 1077 | 3.37 | 1691 | 0.889 | 1199 | 1.062 | 47373 | 100.60 | 16.76 | 83.8 |
| 4/21/97 | 956 | 22 | 0.28 | 57.3 | 28.88 | 37.1 | 24.545 | 1.731 | 139 | 15.35 | 1022 | | 21.52 | 1.518 | 960 | 2.69 | 1385 | | 1076 | 0.965 | 27485 | 85.30 | 14.39 | 70.9 |
| | 957 | 21 | 0.28 | 56.7 | 28.88 | 37.7 | 25.940 | 1.829 | 140 | 16.21 | 1068 | | 23.90 | 1.685 | 1040 | 3.12 | 1580 | | 1152 | 1.033 | 32348 | 90.20 | 15.10 | 75.1 |
| | 958 | 20 | 0.28 | 56.6 | 28.88 | 37.7 | 26.888 | 1.896 | 139 | 16.75 | 1096 | | 25.45 | 1.795 | 1086 | 3.36 | 1691 | | 1197 | 1.074 | 35450 | 92.90 | 15.50 | 77.4 |
| | 959 | 21 | 0.20 | 55.9 | 28.88 | 37.6 | 26.062 | 1.838 | 141 | 16.26 | 1073 | | 23.90 | 1.685 | 1047 | 3.11 | 1583 | | 1156 | 1.038 | 35903 | 94.00 | 15.55 | 78.4 |
| | 960 | 21 | 0.00 | 55.9 | 28.88 | 38.1 | 26.019 | 1.835 | 141 | 16.23 | 1072 | | 23.72 | 1.672 | 1047 | 3.08 | 1572 | | 1153 | 1.035 | 44065 | 98.60 | 16.44 | 82.2 |

## Aeroacoustic Summary Data

## Model 3 – Configuration 3BB, Baseline Core Nozzle, Baseline Fan Nozzle

| Date | Point | Cycle | XMA | $T_{amb}$ | $P_{amb}$ | RH | $P_{18}$ | PFQPA | $T_{18}$ | $W_{18}$ | $V_{18}$ | $CD_{18}$ | $P_8$ | P8QPA | $T_8$ | $W_8$ | $V_8$ | $CD_8$ | $V_{mix}$ | $V_{mix}/c_{amb}$ | $F_N$ | EPNL | NF | NEPNL |
|---|---|---|---|---|---|---|---|---|---|---|---|---|---|---|---|---|---|---|---|---|---|---|---|---|
| 4/1/97 | 400 | 24 | 0.28 | 46.3 | 29.51 | 18.7 | 21.853 | 1.508 | 138 | 13.00 | 892 | 0.986 | 18.42 | 1.272 | 842 | 2.13 | 1020 | 0.894 | 910 | 0.825 | 17918 | 77.40 | 12.53 | 64.9 |
| | 398 | 23 | 0.28 | 46.1 | 29.51 | 17.0 | 23.186 | 1.601 | 140 | 14.02 | 952 | 0.983 | 19.53 | 1.349 | 892 | 2.40 | 1155 | 0.907 | 982 | 0.890 | 21803 | 80.70 | 13.39 | 67.3 |
| | 399 | 23 | 0.28 | 46.2 | 29.51 | 18.2 | 23.138 | 1.597 | 138 | 14.03 | 948 | 0.985 | 19.56 | 1.350 | 885 | 2.41 | 1155 | 0.908 | 979 | 0.887 | 21712 | 80.70 | 13.37 | 67.3 |
| | 397 | 22 | 0.28 | 46.2 | 29.51 | 16.5 | 25.050 | 1.729 | 140 | 15.36 | 1022 | 0.982 | 22.00 | 1.518 | 964 | 2.89 | 1391 | 0.929 | 1080 | 0.979 | 27891 | 86.60 | 14.45 | 72.1 |
| | 395 | 21 | 0.28 | 46.0 | 29.49 | 16.0 | 26.583 | 1.835 | 141 | 16.30 | 1072 | 0.979 | 24.40 | 1.685 | 1043 | 3.25 | 1586 | 0.941 | 1158 | 1.050 | 33039 | 91.70 | 15.19 | 76.5 |
| | 396 | 20 | 0.28 | 46.0 | 29.49 | 13.8 | 27.326 | 1.887 | 141 | 16.71 | 1094 | 0.976 | 26.07 | 1.800 | 1082 | 3.47 | 1698 | 0.948 | 1198 | 1.087 | 35684 | 94.10 | 15.52 | 78.6 |
| | 369 | 13 | 0.28 | 45.4 | 29.51 | 19.4 | 20.208 | 1.394 | 139 | 11.50 | 807 | 0.986 | 17.94 | 1.238 | 791 | 2.06 | 944 | 0.899 | 828 | 0.751 | 14052 | 74.50 | 11.48 | 63.0 |
| | 370 | 12 | 0.28 | 45.5 | 29.51 | 21.2 | 21.901 | 1.512 | 139 | 13.05 | 895 | 0.987 | 19.29 | 1.331 | 835 | 2.41 | 1106 | 0.915 | 928 | 0.842 | 19185 | 79.20 | 12.83 | 66.4 |
| | 371 | 11 | 0.28 | 46.1 | 29.51 | 20.7 | 23.615 | 1.630 | 140 | 14.36 | 969 | 0.983 | 20.93 | 1.445 | 931 | 2.71 | 1294 | 0.925 | 1020 | 0.925 | 24259 | 84.00 | 13.85 | 70.2 |
| | 372 | 10 | 0.28 | 46.1 | 29.51 | 20.6 | 25.406 | 1.754 | 141 | 15.56 | 1035 | 0.980 | 22.58 | 1.559 | 1037 | 2.90 | 1469 | 0.922 | 1103 | 1.000 | 29274 | 88.40 | 14.66 | 73.7 |
| | 401 | | 0.28 | 45.6 | 29.51 | 20.2 | 21.703 | 1.498 | 137 | 13.05 | 884 | 0.999 | 19.58 | 1.351 | 448 | 3.03 | 949 | 0.932 | 896 | 0.813 | 18627 | 76.70 | 12.70 | 64.0 |
| | 402 | | 0.28 | 45.2 | 29.51 | 20.1 | 21.696 | 1.497 | 142 | 12.76 | 888 | 0.981 | 19.40 | 1.339 | 1021 | 2.28 | 1195 | 0.916 | 934 | 0.848 | 18566 | 79.70 | 12.69 | 67.0 |
| | 403 | | 0.28 | 44.7 | 29.51 | 23.0 | 21.799 | 1.504 | 143 | 12.75 | 893 | 0.974 | 22.99 | 1.586 | 1054 | 3.02 | 1503 | 0.944 | 1010 | 0.917 | 21838 | 86.90 | 13.39 | 73.5 |
| | 404 | | 0.28 | 45.1 | 29.51 | 21.8 | 21.564 | 1.488 | 141 | 12.75 | 880 | 0.988 | 23.42 | 1.616 | 463 | 4.03 | 1193 | 0.953 | 955 | 0.867 | 21434 | 79.70 | 13.31 | 66.4 |
| | 405 | | 0.28 | 44.4 | 29.51 | 24.5 | 21.764 | 1.502 | 141 | 12.90 | 890 | 0.987 | 21.35 | 1.473 | 720 | 3.10 | 1222 | 0.942 | 954 | 0.866 | 20346 | 80.00 | 13.08 | 66.9 |

## Aeroacoustic Summary Data

## Model 3 – Configuration 3BB, Baseline Core Nozzle, Baseline Fan Nozzle (Continued)

| Date | Point | Cycle | XMA | $T_{amb}$ | $P_{amb}$ | RH | $P_{18}$ | PFQPA | $T_{18}$ | $W_{18}$ | $V_{18}$ | $CD_{18}$ | $P_8$ | P8QPA | $T_8$ | $W_8$ | $V_8$ | $CD_8$ | $V_{mix}$ | $V_{mix}/c_{amb}$ | $F_N$ | EPNL | NF | NEPNL |
|---|---|---|---|---|---|---|---|---|---|---|---|---|---|---|---|---|---|---|---|---|---|---|---|---|
| 4/1/97 | 389 | 26 | 0.20 | 46.4 | 29.49 | 16.6 | 18.572 | 1.282 | 141 | 9.79 | 704 | 0.990 | 16.30 | 1.125 | 743 | 1.48 | 693 | 0.868 | 702 | 0.636 | 10731 | 72.70 | 10.31 | 62.4 |
| | 390 | 25 | 0.20 | 45.9 | 29.49 | 17.5 | 20.589 | 1.421 | 141 | 11.89 | 831 | 0.990 | 17.38 | 1.200 | 803 | 1.85 | 878 | 0.887 | 837 | 0.759 | 16813 | 78.20 | 12.26 | 65.9 |
| | 391 | 24 | 0.20 | 45.9 | 29.51 | 16.2 | 21.816 | 1.506 | 142 | 12.96 | 894 | 0.988 | 18.38 | 1.269 | 843 | 2.14 | 1016 | 0.902 | 911 | 0.826 | 20673 | 81.50 | 13.15 | 68.3 |
| | 392 | 21 | 0.20 | 46.1 | 29.51 | 16.0 | 26.530 | 1.831 | 141 | 16.30 | 1071 | 0.980 | 24.30 | 1.678 | 1041 | 3.25 | 1580 | 0.945 | 1155 | 1.047 | 36278 | 95.60 | 15.60 | 80.0 |
| | 377 | 14 | 0.20 | 46.4 | 29.49 | 14.9 | 18.470 | 1.275 | 138 | 9.67 | 695 | 0.989 | 16.72 | 1.155 | 730 | 1.69 | 758 | 0.890 | 704 | 0.638 | 10824 | 73.10 | 10.34 | 62.8 |
| | 376 | 13 | 0.20 | 45.8 | 29.49 | 17.0 | 20.157 | 1.392 | 139 | 11.47 | 805 | 0.988 | 18.02 | 1.244 | 781 | 2.11 | 950 | 0.909 | 828 | 0.751 | 16309 | 77.90 | 12.12 | 65.8 |
| | 375 | 12 | 0.20 | 46.2 | 29.51 | 16.8 | 21.904 | 1.512 | 140 | 13.04 | 896 | 0.987 | 19.31 | 1.333 | 842 | 2.42 | 1112 | 0.917 | 930 | 0.843 | 21692 | 83.00 | 13.36 | 69.6 |
| | 374 | 11 | 0.20 | 46.0 | 29.51 | 17.8 | 23.638 | 1.632 | 141 | 14.36 | 970 | 0.983 | 20.97 | 1.447 | 930 | 2.73 | 1295 | 0.931 | 1023 | 0.927 | 27122 | 89.10 | 14.33 | 74.8 |
| | 373 | 10 | 0.20 | 45.8 | 29.51 | 18.1 | 25.355 | 1.750 | 142 | 15.53 | 1033 | 0.980 | 22.68 | 1.566 | 1033 | 2.96 | 1472 | 0.933 | 1104 | 1.001 | 32283 | 92.70 | 15.09 | 77.6 |
| | 388 | 26 | 0.00 | 46.7 | 29.51 | 17.0 | 18.552 | 1.281 | 139 | 9.79 | 701 | 0.992 | 16.23 | 1.120 | 745 | 1.46 | 680 | 0.879 | 698 | 0.632 | 15599 | 76.80 | 11.93 | 64.9 |
| | 387 | 24 | 0.00 | 46.0 | 29.49 | 19.8 | 21.869 | 1.510 | 139 | 13.03 | 894 | 0.989 | 18.38 | 1.269 | 843 | 2.15 | 1016 | 0.906 | 911 | 0.826 | 27469 | 87.60 | 14.39 | 73.2 |
| | 386 | 23 | 0.00 | 46.4 | 29.49 | 18.8 | 23.155 | 1.599 | 139 | 14.06 | 950 | 0.986 | 19.56 | 1.351 | 888 | 2.43 | 1156 | 0.917 | 981 | 0.889 | 32109 | 90.60 | 15.07 | 75.5 |
| | 385 | 22 | 0.00 | 46.3 | 29.49 | 19.1 | 25.118 | 1.734 | 140 | 15.43 | 1024 | 0.982 | 21.86 | 1.509 | 963 | 2.88 | 1380 | 0.931 | 1080 | 0.979 | 39341 | 95.80 | 15.95 | 79.9 |
| | 384 | 21 | 0.00 | 46.5 | 29.49 | 21.4 | 26.544 | 1.833 | 141 | 16.30 | 1071 | 0.977 | 24.37 | 1.682 | 1045 | 3.25 | 1585 | 0.942 | 1156 | 1.048 | 44938 | 99.80 | 16.53 | 83.3 |
| | 383 | 20 | 0.00 | 46.7 | 29.49 | 21.3 | 27.425 | 1.893 | 141 | 16.76 | 1097 | 0.976 | 25.98 | 1.793 | 1088 | 3.46 | 1697 | 0.949 | 1200 | 1.087 | 48133 | 102.30 | 16.82 | 85.5 |
| | 378 | 14 | 0.00 | 46.8 | 29.49 | 16.6 | 18.429 | 1.272 | 138 | 9.65 | 691 | 0.993 | 16.68 | 1.152 | 732 | 1.70 | 753 | 0.903 | 701 | 0.635 | 15757 | 77.10 | 11.97 | 65.1 |
| | 379 | 13 | 0.00 | 47.2 | 29.49 | 16.7 | 20.149 | 1.391 | 138 | 11.52 | 804 | 0.991 | 17.95 | 1.239 | 784 | 2.11 | 944 | 0.917 | 826 | 0.748 | 22316 | 83.00 | 13.49 | 69.5 |
| | 380 | 12 | 0.00 | 47.4 | 29.49 | 16.9 | 21.848 | 1.508 | 139 | 13.02 | 893 | 0.988 | 19.30 | 1.332 | 841 | 2.44 | 1110 | 0.924 | 927 | 0.840 | 28457 | 88.60 | 14.54 | 74.1 |
| | 381 | 11 | 0.00 | 47.2 | 29.49 | 17.6 | 23.615 | 1.630 | 140 | 14.39 | 969 | 0.986 | 20.95 | 1.447 | 932 | 2.74 | 1297 | 0.933 | 1021 | 0.925 | 34796 | 93.40 | 15.42 | 78.0 |
| | 382 | 10 | 0.00 | 47.6 | 29.49 | 18.5 | 25.351 | 1.750 | 141 | 15.56 | 1032 | 0.983 | 22.63 | 1.562 | 1033 | 2.97 | 1469 | 0.939 | 1102 | 0.998 | 40560 | 97.50 | 16.08 | 81.4 |
| | 406 | | 0.00 | 44.6 | 29.53 | 22.3 | 21.696 | 1.497 | 141 | 12.89 | 887 | 0.991 | 21.38 | 1.475 | 725 | 3.12 | 1225 | 0.950 | 952 | 0.865 | 30135 | 90.40 | 14.79 | 75.6 |
| 4/4/97 | 545 | 24 | 0.28 | 74.4 | 29.19 | 37.5 | 21.722 | 1.515 | 139 | 12.97 | 897 | 0.987 | 18.24 | 1.272 | 836 | 2.13 | 1019 | 0.898 | 914 | 0.807 | 18018 | 76.60 | 12.56 | 64.0 |
| | 546 | 23 | 0.28 | 74.2 | 29.21 | 38.2 | 22.948 | 1.601 | 139 | 13.93 | 952 | 0.986 | 19.43 | 1.355 | 880 | 2.42 | 1159 | 0.910 | 982 | 0.867 | 21718 | 80.00 | 13.37 | 66.6 |
| | 547 | 22 | 0.28 | 74.1 | 29.19 | 38.0 | 24.746 | 1.727 | 140 | 15.19 | 1020 | 0.983 | 21.68 | 1.513 | 954 | 2.86 | 1379 | 0.928 | 1077 | 0.951 | 27276 | 85.40 | 14.36 | 71.0 |
| | 548 | 21 | 0.28 | 74.4 | 29.19 | 37.5 | 26.332 | 1.837 | 142 | 16.17 | 1074 | 0.980 | 24.10 | 1.682 | 1036 | 3.22 | 1580 | 0.942 | 1158 | 1.022 | 32459 | 90.50 | 15.11 | 75.4 |
| | 549 | 20 | 0.28 | 73.8 | 29.19 | 41.7 | 27.073 | 1.889 | 144 | 16.58 | 1098 | 0.976 | 25.67 | 1.791 | 1077 | 3.43 | 1689 | 0.947 | 1199 | 1.059 | 35133 | 93.30 | 15.46 | 77.8 |
| | 553 | 26 | 0.20 | 70.5 | 29.21 | 49.8 | 18.325 | 1.278 | 142 | 9.59 | 700 | 0.987 | 16.10 | 1.123 | 742 | 1.44 | 688 | 0.863 | 698 | 0.618 | 10379 | 71.70 | 10.16 | 61.5 |
| | 552 | 25 | 0.20 | 70.8 | 29.19 | 48.6 | 20.463 | 1.428 | 142 | 11.82 | 836 | 0.988 | 17.22 | 1.201 | 801 | 1.83 | 880 | 0.882 | 842 | 0.746 | 16750 | 77.70 | 12.24 | 65.5 |
| | 551 | 24 | 0.20 | 71.2 | 29.19 | 48.2 | 21.730 | 1.516 | 142 | 12.89 | 901 | 0.984 | 18.31 | 1.278 | 838 | 2.15 | 1028 | 0.897 | 919 | 0.813 | 20755 | 80.90 | 13.17 | 67.7 |
| | 550 | 21 | 0.20 | 71.2 | 29.19 | 47.8 | 26.288 | 1.834 | 143 | 16.11 | 1074 | 0.977 | 24.10 | 1.681 | 1043 | 3.21 | 1583 | 0.940 | 1158 | 1.025 | 35927 | 94.70 | 15.55 | 79.1 |
| | 562 | 21 | 0.20 | 68.4 | 29.21 | 53.2 | 26.300 | 1.834 | 143 | 16.11 | 1074 | 0.978 | 24.21 | 1.688 | 1043 | 3.23 | 1589 | 0.942 | 1160 | 1.029 | 35982 | 94.90 | 15.56 | 79.3 |
| | 554 | 26 | 0.00 | 70.4 | 29.21 | 50.2 | 18.272 | 1.274 | 142 | 9.57 | 695 | 0.993 | 16.01 | 1.117 | 741 | 1.43 | 670 | 0.877 | 692 | 0.613 | 14937 | 75.60 | 11.74 | 63.9 |
| | 555 | 24 | 0.00 | 70.2 | 29.21 | 50.4 | 21.563 | 1.504 | 142 | 12.85 | 892 | 0.991 | 18.28 | 1.275 | 835 | 2.18 | 1023 | 0.912 | 911 | 0.807 | 27103 | 86.10 | 14.33 | 71.8 |
| | 556 | 23 | 0.00 | 70.2 | 29.21 | 50.2 | 23.016 | 1.605 | 142 | 13.99 | 956 | 0.988 | 19.40 | 1.353 | 881 | 2.43 | 1156 | 0.919 | 986 | 0.873 | 32062 | 92.10 | 15.06 | 77.0 |
| | 557 | 22 | 0.00 | 69.8 | 29.21 | 50.9 | 24.838 | 1.732 | 142 | 15.26 | 1025 | 0.987 | 21.59 | 1.506 | 951 | 2.86 | 1371 | 0.935 | 1080 | 0.957 | 38669 | 94.90 | 15.87 | 79.0 |
| | 558 | 21 | 0.00 | 69.6 | 29.21 | 51.1 | 26.414 | 1.842 | 143 | 16.24 | 1077 | 0.981 | 24.21 | 1.688 | 1035 | 3.26 | 1586 | 0.947 | 1162 | 1.030 | 44756 | 99.10 | 16.51 | 82.6 |
| | 559 | 20 | 0.00 | 69.1 | 29.21 | 51.9 | 27.220 | 1.898 | 143 | 16.64 | 1102 | 0.975 | 25.71 | 1.793 | 1079 | 3.43 | 1692 | 0.949 | 1202 | 1.066 | 47874 | 101.40 | 16.80 | 84.6 |
| | 565 | 26 | 0.00 | 43.6 | 29.27 | 33.1 | 18.370 | 1.279 | 144 | 9.67 | 701 | 0.996 | 15.99 | 1.113 | 736 | 1.42 | 658 | 0.881 | 696 | 0.633 | 15346 | 76.80 | 11.86 | 64.9 |
| | 575 | 26 | 0.00 | 42.9 | 29.29 | 33.9 | 18.407 | 1.280 | 142 | 9.68 | 702 | 0.991 | 16.05 | 1.116 | 747 | 1.42 | 670 | 0.874 | 698 | 0.635 | 15376 | 76.80 | 11.87 | 64.9 |
| | 566 | 24 | 0.00 | 43.8 | 29.27 | 32.7 | 21.774 | 1.516 | 144 | 12.99 | 901 | 0.992 | 18.30 | 1.273 | 841 | 2.17 | 1022 | 0.915 | 919 | 0.835 | 27617 | 87.30 | 14.41 | 72.9 |

## Aeroacoustic Summary Data

## Model 3 – Configuration 3BB, Baseline Core Nozzle, Baseline Fan Nozzle (Continued)

| Date | Point | Cycle | XMA | $T_{amb}$ | $P_{amb}$ | RH | $P_{18}$ | PFQPA | $T_{18}$ | $W_{18}$ | $V_{18}$ | $CD_{18}$ | $P_8$ | P8QPA | $T_8$ | $W_8$ | $V_8$ | $CD_8$ | $V_{mix}$ | $V_{mix}/c_{amb}$ | $F_N$ | EPNL | NF | NEPNL |
|---|---|---|---|---|---|---|---|---|---|---|---|---|---|---|---|---|---|---|---|---|---|---|---|---|
| 4/4/97 | 569 | 24 | 0.00 | 43.1 | 29.27 | 33.9 | 21.648 | 1.506 | 143 | 12.85 | 895 | 0.989 | 18.24 | 1.269 | 847 | 2.13 | 1017 | 0.907 | 912 | 0.830 | 27110 | 87.10 | 14.33 | 72.8 |
| | 567 | 23 | 0.00 | 43.3 | 29.27 | 33.6 | 23.055 | 1.604 | 144 | 13.95 | 957 | 0.986 | 19.44 | 1.353 | 883 | 2.43 | 1157 | 0.916 | 987 | 0.897 | 32052 | 91.00 | 15.06 | 75.9 |
| | 574 | 23 | 0.00 | 42.6 | 29.29 | 34.2 | 22.976 | 1.598 | 143 | 13.89 | 953 | 0.985 | 19.43 | 1.351 | 886 | 2.42 | 1156 | 0.915 | 983 | 0.895 | 31842 | 90.80 | 15.03 | 75.8 |
| | 570 | 22 | 0.00 | 43.3 | 29.27 | 33.7 | 24.904 | 1.733 | 144 | 15.31 | 1027 | 0.986 | 21.76 | 1.514 | 964 | 2.88 | 1386 | 0.935 | 1084 | 0.985 | 39158 | 96.20 | 15.93 | 80.3 |
| | 571 | 21 | 0.00 | 43.3 | 29.27 | 33.3 | 26.250 | 1.827 | 144 | 16.13 | 1071 | 0.982 | 24.16 | 1.681 | 1045 | 3.24 | 1584 | 0.947 | 1157 | 1.052 | 44494 | 100.20 | 16.48 | 83.7 |
| | 573 | 21 | 0.00 | 42.7 | 29.29 | 34.2 | 26.389 | 1.836 | 144 | 16.11 | 1075 | 0.975 | 24.06 | 1.674 | 1030 | 3.19 | 1571 | 0.932 | 1157 | 1.052 | 44374 | 99.80 | 16.47 | 83.3 |
| 4/7/97 | 572 | 20 | 0.00 | 42.8 | 29.27 | 33.8 | 27.207 | 1.893 | 144 | 16.56 | 1100 | 0.974 | 25.60 | 1.781 | 1085 | 3.40 | 1686 | 0.946 | 1200 | 1.091 | 47599 | 101.90 | 16.78 | 85.1 |
| | 576 | | 0.00 | 42.7 | 29.29 | 34.8 | 21.539 | 1.498 | 144 | 12.51 | 890 | 0.970 | 27.10 | 1.885 | 1080 | 3.67 | 1757 | 0.960 | 1086 | 0.988 | 34891 | 101.50 | 15.43 | 86.1 |
| | 577 | | 0.00 | 41.7 | 29.29 | 35.5 | 21.589 | 1.501 | 140 | 12.98 | 889 | 1.000 | 22.45 | 1.561 | 446 | 3.91 | 1141 | 0.967 | 948 | 0.863 | 31798 | 88.60 | 15.02 | 73.6 |
| | 578 | | 0.00 | 40.9 | 29.29 | 36.9 | 21.539 | 1.498 | 140 | 12.95 | 887 | 1.001 | 18.69 | 1.299 | 440 | 2.79 | 884 | 0.932 | 886 | 0.808 | 27717 | 85.50 | 14.43 | 71.1 |
| | 579 | | 0.00 | 41.2 | 29.29 | 36.8 | 21.626 | 1.504 | 141 | 12.92 | 892 | 0.993 | 17.49 | 1.216 | 744 | 1.98 | 888 | 0.898 | 891 | 0.812 | 26389 | 85.60 | 14.21 | 71.4 |
| | 580 | | 0.00 | 41.2 | 29.29 | 37.1 | 21.649 | 1.505 | 141 | 12.83 | 894 | 0.985 | 17.22 | 1.198 | 851 | 1.79 | 890 | 0.885 | 892 | 0.813 | 25880 | 85.80 | 14.13 | 71.7 |
| | 582 | | 0.00 | 41.3 | 29.29 | 37.5 | 21.673 | 1.507 | 141 | 12.84 | 894 | 0.985 | 20.12 | 1.399 | 889 | 2.62 | 1220 | 0.934 | 949 | 0.865 | 29161 | 93.10 | 14.65 | 78.5 |
| | 583 | | 0.00 | 41.1 | 29.29 | 37.8 | 21.692 | 1.508 | 141 | 12.87 | 894 | 0.986 | 24.29 | 1.689 | 798 | 3.63 | 1453 | 0.961 | 1017 | 0.927 | 33291 | 95.40 | 15.22 | 80.2 |
| | 584 | | 0.00 | 40.9 | 29.29 | 38.5 | 21.554 | 1.499 | 140 | 12.88 | 887 | 0.994 | 23.29 | 1.620 | 528 | 3.90 | 1238 | 0.960 | 968 | 0.883 | 32216 | 90.60 | 15.08 | 75.5 |
| | 585 | | 0.00 | 40.5 | 29.29 | 39.3 | 21.674 | 1.507 | 139 | 13.18 | 892 | 1.009 | 21.64 | 1.505 | 134 | 4.57 | 887 | 0.959 | 891 | 0.812 | 31410 | 85.80 | 14.97 | 70.8 |
| | 586 | | 0.00 | 40.3 | 29.29 | 39.5 | 21.606 | 1.502 | 139 | 13.16 | 888 | 1.011 | 14.60 | 1.015 | 131 | 0.25 | 193 | 0.343 | 875 | 0.798 | 23295 | 84.10 | 13.67 | 70.4 |
| 4/8/97 | 591 | 24 | 0.28 | 40.0 | 29.29 | 45.0 | 21.767 | 1.513 | 145 | 12.94 | 900 | 0.990 | 18.32 | 1.274 | 845 | 2.14 | 1025 | 0.900 | 918 | 0.838 | 18309 | 78.10 | 12.63 | 65.5 |
| | 592 | 23 | 0.28 | 40.0 | 29.31 | 45.2 | 22.978 | 1.597 | 142 | 13.90 | 951 | 0.986 | 19.39 | 1.348 | 892 | 2.39 | 1154 | 0.910 | 981 | 0.895 | 21777 | 81.30 | 13.38 | 67.9 |
| | 593 | 22 | 0.28 | 40.2 | 29.31 | 45.1 | 24.799 | 1.724 | 142 | 15.22 | 1021 | 0.984 | 21.64 | 1.504 | 969 | 2.84 | 1378 | 0.932 | 1077 | 0.983 | 27558 | 87.00 | 14.40 | 72.6 |
| | 594 | 21 | 0.28 | 40.0 | 29.31 | 46.0 | 26.205 | 1.822 | 142 | 16.10 | 1067 | 0.982 | 24.09 | 1.675 | 1048 | 3.21 | 1580 | 0.944 | 1152 | 1.051 | 32373 | 91.50 | 15.10 | 76.4 |
| | 595 | 20 | 0.28 | 39.9 | 29.31 | 46.1 | 27.212 | 1.892 | 142 | 16.66 | 1097 | 0.977 | 25.74 | 1.790 | 1087 | 3.43 | 1694 | 0.950 | 1199 | 1.094 | 35546 | 94.40 | 15.51 | 78.9 |
| | 596 | 21 | 0.20 | 40.1 | 29.31 | 45.9 | 26.173 | 1.819 | 141 | 16.05 | 1065 | 0.977 | 24.22 | 1.684 | 1046 | 3.23 | 1588 | 0.942 | 1153 | 1.052 | 35877 | 95.60 | 15.55 | 80.1 |
| | 597 | 21 | 0.00 | 40.7 | 29.31 | 45.9 | 26.323 | 1.830 | 141 | 16.17 | 1069 | 0.979 | 24.34 | 1.692 | 1036 | 3.27 | 1588 | 0.944 | 1157 | 1.054 | 44352 | 99.90 | 16.47 | 83.4 |
| 4/9/97 | 646 | 24 | 0.28 | 31.1 | 29.55 | 42.3 | 21.930 | 1.511 | 138 | 13.05 | 894 | 0.984 | 18.47 | 1.273 | 850 | 2.14 | 1026 | 0.893 | 913 | 0.840 | 18246 | 78.20 | 12.61 | 65.6 |
| | 645 | 23 | 0.28 | 31.5 | 29.55 | 41.0 | 23.187 | 1.598 | 137 | 14.07 | 948 | 0.985 | 19.59 | 1.350 | 886 | 2.41 | 1155 | 0.907 | 978 | 0.900 | 21929 | 81.50 | 13.41 | 68.1 |
| | 644 | 22 | 0.28 | 31.5 | 29.55 | 41.4 | 25.187 | 1.736 | 138 | 15.45 | 1023 | 0.980 | 21.82 | 1.504 | 955 | 2.85 | 1371 | 0.923 | 1078 | 0.991 | 28080 | 87.20 | 14.48 | 72.7 |
| | 642 | 21 | 0.28 | 32.8 | 29.55 | 41.5 | 26.503 | 1.827 | 140 | 16.24 | 1067 | 0.978 | 24.29 | 1.674 | 1034 | 3.24 | 1573 | 0.940 | 1151 | 1.058 | 32693 | 92.00 | 15.14 | 76.9 |
| | 643 | 20 | 0.28 | 32.1 | 29.55 | 42.5 | 27.406 | 1.889 | 139 | 16.82 | 1093 | 0.976 | 25.92 | 1.787 | 1075 | 3.46 | 1685 | 0.948 | 1195 | 1.098 | 35823 | 94.40 | 15.54 | 78.9 |
| | 648 | | 0.28 | 31.2 | 29.55 | 40.6 | 26.677 | 1.838 | 137 | 16.98 | 1070 | 1.012 | 24.30 | 1.675 | 128 | 5.32 | 984 | 0.959 | 1050 | 0.966 | 32988 | 85.10 | 15.18 | 69.9 |
| | 641 | 21 | 0.20 | 33.7 | 29.55 | 38.4 | 26.561 | 1.831 | 138 | 16.32 | 1067 | 0.978 | 24.40 | 1.682 | 1031 | 3.27 | 1577 | 0.942 | 1153 | 1.058 | 36307 | 95.70 | 15.60 | 80.1 |
| | 639 | 24 | 0.00 | 34.6 | 29.55 | 38.5 | 21.957 | 1.513 | 146 | 13.07 | 901 | 0.991 | 18.34 | 1.264 | 850 | 2.16 | 1010 | 0.916 | 917 | 0.841 | 27766 | 87.70 | 14.44 | 73.3 |
| | 640 | 21 | 0.00 | 34.1 | 29.55 | 38.7 | 26.616 | 1.834 | 140 | 16.33 | 1071 | 0.978 | 24.54 | 1.691 | 1041 | 3.28 | 1590 | 0.943 | 1158 | 1.062 | 45078 | 100.40 | 16.54 | 83.9 |
| 4/10/97 | 679 | 24 | 0.28 | 38.0 | 29.51 | 42.3 | 22.006 | 1.519 | 141 | 13.13 | 902 | 0.989 | 18.49 | 1.276 | 843 | 2.18 | 1027 | 0.905 | 919 | 0.840 | 18762 | 78.50 | 12.73 | 65.8 |
| | 680 | 23 | 0.28 | 37.9 | 29.51 | 40.5 | 23.197 | 1.601 | 141 | 14.05 | 953 | 0.985 | 19.49 | 1.345 | 881 | 2.41 | 1145 | 0.911 | 981 | 0.897 | 22079 | 81.60 | 13.44 | 68.2 |
| | 681 | 22 | 0.28 | 38.1 | 29.51 | 40.0 | 25.096 | 1.732 | 141 | 15.40 | 1024 | 0.983 | 21.88 | 1.509 | 964 | 2.88 | 1381 | 0.930 | 1080 | 0.987 | 28129 | 86.80 | 14.49 | 72.3 |
| | 682 | 21 | 0.28 | 37.7 | 29.53 | 39.8 | 26.695 | 1.842 | 142 | 16.39 | 1075 | 0.978 | 24.33 | 1.679 | 1043 | 3.24 | 1582 | 0.942 | 1159 | 1.060 | 33328 | 92.10 | 15.23 | 76.9 |
| | 683 | 20 | 0.28 | 38.0 | 29.51 | 39.4 | 27.388 | 1.890 | 141 | 16.80 | 1096 | 0.974 | 25.95 | 1.791 | 1080 | 3.47 | 1691 | 0.949 | 1198 | 1.095 | 36000 | 94.90 | 15.56 | 79.3 |
| | 684 | 21 | 0.20 | 38.2 | 29.51 | 41.5 | 26.771 | 1.847 | 143 | 16.41 | 1079 | 0.975 | 24.42 | 1.685 | 1043 | 3.25 | 1587 | 0.941 | 1163 | 1.063 | 37120 | 96.30 | 15.70 | 80.6 |
| | 685 | 21 | 0.00 | 38.5 | 29.51 | 42.7 | 26.548 | 1.832 | 142 | 16.28 | 1071 | 0.979 | 24.35 | 1.680 | 1043 | 3.25 | 1582 | 0.942 | 1156 | 1.056 | 44693 | 100.20 | 16.50 | 83.7 |

## Aeroacoustic Summary Data

## Model 3 – Configuration 3BB, Baseline Core Nozzle, Baseline Fan Nozzle (Continued)

| Date | Point | Cycle | XMA | $T_{amb}$ | $P_{amb}$ | RH | $P_{18}$ | PFQPA | $T_{18}$ | $W_{18}$ | $V_{18}$ | $CD_{18}$ | $P_8$ | P8QPA | $T_8$ | $W_8$ | $V_8$ | $CD_8$ | $V_{mix}$ | $V_{mix}/c_{amb}$ | $F_N$ | EPNL | NF | NEPNL |
|---|---|---|---|---|---|---|---|---|---|---|---|---|---|---|---|---|---|---|---|---|---|---|---|---|
| 4/11/97 | 730 | 24 | 0.28 | 43.7 | 29.31 | 48.2 | 21.749 | 1.511 | 140 | 12.94 | 896 | 0.987 | 18.31 | 1.272 | 845 | 2.13 | 1022 | 0.898 | 914 | 0.830 | 18189 | 78.30 | 12.60 | 65.7 |
| | 731 | 23 | 0.28 | 43.3 | 29.31 | 48.7 | 23.124 | 1.607 | 141 | 14.04 | 956 | 0.986 | 19.41 | 1.348 | 885 | 2.40 | 1152 | 0.909 | 985 | 0.895 | 22156 | 81.40 | 13.45 | 67.9 |
| | 732 | 22 | 0.28 | 43.4 | 29.31 | 48.4 | 24.899 | 1.730 | 141 | 15.28 | 1023 | 0.983 | 21.81 | 1.515 | 964 | 2.87 | 1387 | 0.930 | 1081 | 0.982 | 27998 | 87.10 | 14.47 | 72.6 |
| | 734 | 21 | 0.28 | 43.5 | 29.31 | 48.8 | 26.363 | 1.832 | 141 | 16.16 | 1071 | 0.978 | 24.19 | 1.681 | 1041 | 3.22 | 1583 | 0.940 | 1156 | 1.051 | 32750 | 91.80 | 15.15 | 76.6 |
| | 733 | 20 | 0.28 | 43.4 | 29.31 | 48.6 | 27.367 | 1.902 | 141 | 16.75 | 1101 | 0.979 | 25.87 | 1.798 | 1078 | 3.47 | 1695 | 0.952 | 1203 | 1.094 | 36169 | 94.40 | 15.58 | 78.8 |
| | 735 | 21 | 0.20 | 43.4 | 29.31 | 49.0 | 26.375 | 1.833 | 142 | 16.17 | 1072 | 0.976 | 24.18 | 1.681 | 1040 | 3.23 | 1581 | 0.944 | 1157 | 1.052 | 36250 | 95.90 | 15.59 | 80.3 |
| | 736 | 21 | 0.00 | 43.2 | 29.31 | 48.7 | 26.270 | 1.826 | 142 | 16.11 | 1069 | 0.977 | 24.14 | 1.677 | 1044 | 3.21 | 1581 | 0.941 | 1154 | 1.049 | 44153 | 99.70 | 16.45 | 83.3 |
| 4/14/97 | 751 | 24 | 0.28 | 48.1 | 29.41 | 29.8 | 21.897 | 1.517 | 140 | 13.06 | 899 | 0.987 | 18.35 | 1.271 | 844 | 2.14 | 1020 | 0.900 | 916 | 0.829 | 18376 | 77.90 | 12.64 | 65.3 |
| | 752 | 23 | 0.28 | 48.4 | 29.41 | 31.5 | 23.175 | 1.605 | 141 | 14.06 | 955 | 0.986 | 19.52 | 1.352 | 883 | 2.42 | 1156 | 0.911 | 985 | 0.891 | 22186 | 80.90 | 13.46 | 67.4 |
| | 753 | 22 | 0.28 | 48.3 | 29.41 | 30.5 | 25.041 | 1.735 | 143 | 15.35 | 1027 | 0.983 | 21.83 | 1.512 | 964 | 2.87 | 1384 | 0.930 | 1083 | 0.980 | 28011 | 86.90 | 14.47 | 72.4 |
| | 754 | 21 | 0.28 | 48.5 | 29.41 | 30.2 | 26.528 | 1.838 | 143 | 16.27 | 1076 | 0.979 | 24.30 | 1.683 | 1040 | 3.25 | 1583 | 0.943 | 1160 | 1.049 | 33053 | 94.10 | 15.19 | 78.9 |
| | 755 | 20 | 0.28 | 48.2 | 29.39 | 28.7 | 27.216 | 1.886 | 141 | 16.65 | 1094 | 0.975 | 25.81 | 1.788 | 1078 | 3.44 | 1688 | 0.948 | 1196 | 1.082 | 35414 | 95.60 | 15.49 | 80.1 |
| | 756 | 21 | 0.20 | 48.3 | 29.41 | 28.8 | 26.482 | 1.834 | 141 | 16.24 | 1072 | 0.976 | 24.25 | 1.680 | 1042 | 3.23 | 1582 | 0.940 | 1156 | 1.046 | 36279 | 95.60 | 15.60 | 80.0 |
| | 757 | 21 | 0.00 | 48.4 | 29.41 | 28.5 | 26.481 | 1.834 | 141 | 16.23 | 1072 | 0.977 | 24.25 | 1.679 | 1041 | 3.24 | 1580 | 0.943 | 1156 | 1.046 | 44491 | 99.80 | 16.48 | 83.3 |
| 4/15/97 | 785 | 24 | 0.28 | 56.1 | 29.43 | 30.0 | 21.838 | 1.512 | 140 | 12.99 | 897 | 0.987 | 18.41 | 1.275 | 841 | 2.18 | 1024 | 0.908 | 914 | 0.821 | 18198 | 78.10 | 12.60 | 65.5 |
| | 786 | 23 | 0.28 | 56.4 | 29.43 | 29.3 | 23.030 | 1.594 | 141 | 13.95 | 949 | 0.987 | 19.49 | 1.349 | 888 | 2.41 | 1154 | 0.912 | 979 | 0.879 | 21780 | 80.60 | 13.38 | 67.2 |
| | 787 | 22 | 0.28 | 56.2 | 29.43 | 29.9 | 25.002 | 1.731 | 141 | 15.34 | 1024 | 0.984 | 21.79 | 1.509 | 960 | 2.87 | 1378 | 0.930 | 1079 | 0.969 | 27762 | 86.10 | 14.43 | 71.7 |
| | 788 | 21 | 0.28 | 56.8 | 29.41 | 30.2 | 26.530 | 1.837 | 142 | 16.31 | 1074 | 0.979 | 24.29 | 1.681 | 1039 | 3.24 | 1582 | 0.940 | 1158 | 1.039 | 32883 | 90.80 | 15.17 | 75.6 |
| | 789 | 20 | 0.28 | 56.6 | 29.43 | 28.9 | 27.244 | 1.886 | 143 | 16.61 | 1095 | 0.975 | 25.84 | 1.789 | 1082 | 3.44 | 1691 | 0.947 | 1198 | 1.075 | 35425 | 93.70 | 15.49 | 78.2 |
| | 791 | 21 | 0.20 | 57.5 | 29.43 | 29.1 | 26.434 | 1.830 | 142 | 16.22 | 1071 | 0.977 | 24.20 | 1.675 | 1039 | 3.22 | 1576 | 0.940 | 1154 | 1.035 | 35953 | 94.80 | 15.56 | 79.2 |
| | 792 | 21 | 0.00 | 56.9 | 29.43 | 30.3 | 26.440 | 1.830 | 142 | 16.22 | 1071 | 0.979 | 24.26 | 1.679 | 1038 | 3.25 | 1577 | 0.946 | 1156 | 1.037 | 44437 | 99.40 | 16.48 | 82.9 |
| | 793 | | 0.00 | 58.1 | 29.41 | 28.2 | 14.445 | 1.000 | 141 | 0.14 | 14 | 0.718 | 21.74 | 1.505 | 134 | 4.71 | 887 | 0.984 | 862 | 0.773 | 8230 | 80.90 | 9.15 | 71.7 |
| 4/16/97 | 832 | 24 | 0.28 | 49.0 | 29.14 | 85.7 | 21.520 | 1.504 | 141 | 12.80 | 892 | 0.989 | 18.18 | 1.271 | 843 | 2.12 | 1019 | 0.902 | 910 | 0.823 | 17703 | 77.30 | 12.48 | 64.8 |
| | 834 | 23 | 0.28 | 48.5 | 29.14 | 86.1 | 22.905 | 1.601 | 143 | 13.89 | 955 | 0.988 | 19.40 | 1.356 | 889 | 2.40 | 1164 | 0.909 | 986 | 0.892 | 21774 | 80.70 | 13.38 | 67.3 |
| | 835 | 22 | 0.28 | 47.9 | 29.12 | 88.3 | 24.712 | 1.728 | 143 | 15.16 | 1023 | 0.986 | 21.70 | 1.517 | 963 | 2.85 | 1390 | 0.927 | 1081 | 0.979 | 27551 | 86.00 | 14.40 | 71.6 |
| | 836 | 21 | 0.28 | 47.9 | 29.14 | 88.0 | 26.278 | 1.837 | 145 | 16.11 | 1077 | 0.981 | 24.12 | 1.686 | 1047 | 3.21 | 1590 | 0.941 | 1162 | 1.052 | 32779 | 91.10 | 15.16 | 75.9 |
| | 837 | 20 | 0.28 | 48.0 | 29.12 | 87.5 | 27.069 | 1.893 | 144 | 16.54 | 1100 | 0.977 | 25.64 | 1.792 | 1086 | 3.41 | 1695 | 0.947 | 1201 | 1.087 | 35197 | 93.30 | 15.47 | 77.8 |
| 4/17/97 | 859 | 24 | 0.28 | 40.1 | 29.12 | 61.6 | 21.580 | 1.509 | 143 | 12.83 | 896 | 0.989 | 18.25 | 1.276 | 830 | 2.14 | 1023 | 0.897 | 914 | 0.834 | 18092 | 78.10 | 12.57 | 65.5 |
| | 860 | 23 | 0.28 | 39.7 | 29.12 | 61.4 | 22.843 | 1.598 | 140 | 13.86 | 950 | 0.988 | 19.38 | 1.355 | 892 | 2.40 | 1164 | 0.909 | 982 | 0.896 | 21783 | 81.30 | 13.38 | 67.9 |
| | 861 | 22 | 0.28 | 39.4 | 29.12 | 63.2 | 24.694 | 1.727 | 140 | 15.19 | 1020 | 0.984 | 21.64 | 1.513 | 963 | 2.84 | 1385 | 0.927 | 1078 | 0.984 | 27622 | 87.00 | 14.41 | 72.6 |
| | 862 | 21 | 0.28 | 39.2 | 29.12 | 65.2 | 26.153 | 1.829 | 142 | 16.05 | 1070 | 0.979 | 23.93 | 1.674 | 1044 | 3.18 | 1577 | 0.939 | 1154 | 1.054 | 32453 | 91.00 | 15.11 | 75.9 |
| | 863 | 20 | 0.28 | 39.1 | 29.12 | 68.3 | 27.003 | 1.888 | 142 | 16.55 | 1096 | 0.977 | 25.61 | 1.791 | 1084 | 3.41 | 1694 | 0.946 | 1198 | 1.094 | 35379 | 94.20 | 15.49 | 78.7 |

## Aeroacoustic Summary Data

## Model 3 – Configuration 3BB, Baseline Core Nozzle, Baseline Fan Nozzle (Concluded)

| Date | Point | Cycle | XMA | $T_{amb}$ | $P_{amb}$ | RH | $P_{18}$ | PFQPA | $T_{18}$ | $W_{18}$ | $V_{18}$ | $CD_{18}$ | $P_8$ | P8QPA | $T_8$ | $W_8$ | $V_8$ | $CD_8$ | $V_{mix}$ | $V_{mix}/c_{amb}$ | $F_N$ | EPNL | NF | NEPNL |
|---|---|---|---|---|---|---|---|---|---|---|---|---|---|---|---|---|---|---|---|---|---|---|---|---|
| 4/18/97 | 927 | 64 | 0.28 | 44.1 | 28.98 | 33.6 | 21.633 | 1.521 | 140 | 12.95 | 902 | | 17.41 | 1.224 | 809 | 1.89 | 925 | | 905 | 0.822 | 17535 | 77.40 | 12.44 | 65.0 |
| | 928 | 63 | 0.28 | 44.0 | 28.96 | 34.0 | 23.097 | 1.624 | 140 | 14.13 | 965 | | 18.19 | 1.279 | 839 | 2.10 | 1029 | | 974 | 0.885 | 21421 | 80.10 | 13.31 | 66.8 |
| | 929 | 62 | 0.28 | 43.8 | 28.98 | 34.7 | 25.134 | 1.767 | 140 | 15.57 | 1040 | | 20.42 | 1.435 | 923 | 2.62 | 1276 | | 1074 | 0.976 | 27676 | 85.20 | 14.42 | 70.8 |
| | 930 | 61 | 0.28 | 43.6 | 28.98 | 35.4 | 26.466 | 1.861 | 140 | 16.34 | 1082 | | 21.90 | 1.540 | 988 | 2.86 | 1421 | | 1133 | 1.030 | 31410 | 88.80 | 14.97 | 73.8 |
| | 931 | 60 | 0.28 | 43.5 | 28.98 | 35.9 | 27.377 | 1.924 | 140 | 16.86 | 1108 | | 23.11 | 1.624 | 1017 | 3.07 | 1515 | | 1172 | 1.065 | 34167 | 90.90 | 15.34 | 75.6 |
| | 914 | 24 | 0.28 | 45.5 | 28.98 | 36.1 | 21.441 | 1.507 | 140 | 12.82 | 891 | 0.995 | 18.11 | 1.273 | 843 | 2.11 | 1023 | 0.899 | 911 | 0.826 | 17841 | 78.10 | 12.51 | 65.6 |
| | 925 | 24 | 0.28 | 44.5 | 28.98 | 34.6 | 21.507 | 1.512 | 140 | 12.82 | 896 | | 18.13 | 1.274 | 838 | 2.11 | 1021 | | 914 | 0.830 | 17862 | 77.90 | 12.52 | 65.4 |
| | 915 | 23 | 0.28 | 45.0 | 28.98 | 33.9 | 22.932 | 1.612 | 141 | 13.95 | 959 | 0.988 | 19.17 | 1.347 | 888 | 2.36 | 1152 | 0.907 | 987 | 0.896 | 21984 | 81.00 | 13.42 | 67.6 |
| | 916 | 22 | 0.28 | 45.2 | 28.98 | 36.7 | 24.560 | 1.726 | 144 | 15.03 | 1023 | 0.985 | 21.48 | 1.510 | 962 | 2.82 | 1381 | 0.928 | 1080 | 0.980 | 27303 | 86.40 | 14.36 | 72.0 |
| | 917 | 21 | 0.28 | 45.4 | 28.98 | 34.4 | 26.061 | 1.832 | 141 | 16.00 | 1070 | 0.979 | 23.84 | 1.675 | 1043 | 3.17 | 1579 | 0.939 | 1154 | 1.048 | 32191 | 91.30 | 15.08 | 76.2 |
| | 918 | 20 | 0.28 | 45.2 | 28.98 | 35.1 | 26.964 | 1.895 | 141 | 16.47 | 1098 | 0.975 | 25.58 | 1.798 | 1081 | 3.41 | 1697 | 0.947 | 1200 | 1.089 | 35094 | 93.80 | 15.45 | 78.3 |
| | 926 | 13 | 0.28 | 44.3 | 28.96 | 34.3 | 19.702 | 1.385 | 140 | 11.16 | 800 | | 17.70 | 1.244 | 786 | 2.05 | 952 | | 824 | 0.748 | 13449 | 74.90 | 11.29 | 63.6 |
| | 924 | 12 | 0.28 | 44.5 | 28.96 | 33.9 | 21.515 | 1.513 | 140 | 12.80 | 896 | 0.986 | 18.92 | 1.330 | 847 | 2.34 | 1110 | 0.909 | 929 | 0.844 | 18551 | 78.90 | 12.68 | 66.2 |
| | 923 | 11 | 0.28 | 44.8 | 28.98 | 34.5 | 23.209 | 1.631 | 140 | 14.11 | 970 | 0.984 | 20.54 | 1.443 | 928 | 2.65 | 1291 | 0.922 | 1021 | 0.927 | 23688 | 83.70 | 13.75 | 70.0 |
| | 921 | 10 | 0.28 | 45.1 | 28.98 | 34.0 | 24.901 | 1.750 | 140 | 15.25 | 1032 | 0.979 | 22.13 | 1.555 | 1030 | 2.87 | 1461 | 0.929 | 1100 | 0.999 | 28498 | 88.60 | 14.55 | 74.1 |
| | 919 | 21 | 0.20 | 45.6 | 28.98 | 32.9 | 26.096 | 1.834 | 141 | 16.01 | 1072 | 0.977 | 23.97 | 1.684 | 1043 | 3.19 | 1586 | 0.941 | 1157 | 1.050 | 35763 | 95.40 | 15.53 | 79.9 |
| | 933 | 63 | 0.00 | 43.9 | 28.98 | 36.4 | 23.119 | 1.625 | 140 | 14.11 | 966 | | 18.19 | 1.279 | 846 | 2.12 | 1032 | | 975 | 0.886 | 31370 | 89.50 | 14.97 | 74.5 |
| | 932 | 61 | 0.00 | 43.5 | 28.98 | 36.5 | 26.491 | 1.862 | 140 | 16.38 | 1082 | | 21.98 | 1.545 | 988 | 2.89 | 1426 | | 1135 | 1.031 | 43283 | 97.40 | 16.36 | 81.0 |
| | 920 | 21 | 0.00 | 45.5 | 28.98 | 33.2 | 26.006 | 1.828 | 141 | 15.95 | 1069 | 0.979 | 23.94 | 1.682 | 1045 | 3.19 | 1586 | 0.941 | 1155 | 1.048 | 43839 | 102.40 | 16.42 | 86.0 |
| | 935 | 13 | 0.00 | 43.8 | 28.98 | 37.4 | 19.712 | 1.385 | 140 | 11.19 | 800 | | 17.61 | 1.238 | 768 | 2.07 | 934 | | 821 | 0.746 | 21626 | 85.70 | 13.35 | 72.4 |
| | 936 | 13 | 0.00 | 43.6 | 28.98 | 37.7 | 19.679 | 1.383 | 140 | 11.19 | 798 | | 17.60 | 1.237 | 772 | 2.06 | 934 | | 820 | 0.745 | 21593 | 83.00 | 13.34 | 69.7 |
| | 934 | 11 | 0.00 | 43.9 | 28.98 | 36.8 | 23.213 | 1.631 | 140 | 14.16 | 969 | | 20.59 | 1.447 | 931 | 2.68 | 1294 | | 1022 | 0.928 | 34110 | 96.30 | 15.33 | 81.0 |
| 4/23/97 | 1069 | 24 | 0.28 | 51.0 | 28.84 | 74.0 | 21.483 | 1.517 | 141 | 12.83 | 900 | | 17.97 | 1.269 | 840 | 2.08 | 1014 | | 916 | 0.827 | 17955 | 77.70 | 12.54 | 65.2 |
| | 1070 | 23 | 0.28 | 51.1 | 28.84 | 73.2 | 22.684 | 1.602 | 142 | 13.77 | 954 | | 19.11 | 1.350 | 885 | 2.36 | 1152 | | 984 | 0.888 | 21528 | 80.60 | 13.33 | 67.3 |
| | 1071 | 22 | 0.28 | 51.2 | 28.84 | 74.1 | 24.522 | 1.732 | 142 | 15.07 | 1025 | | 21.31 | 1.505 | 965 | 2.79 | 1374 | | 1080 | 0.974 | 27093 | 85.80 | 14.33 | 71.5 |
| | 1072 | 21 | 0.28 | 51.2 | 28.84 | 72.6 | 25.968 | 1.834 | 143 | 15.94 | 1073 | | 23.64 | 1.669 | 1051 | 3.14 | 1572 | | 1156 | 1.043 | 32245 | 91.20 | 15.08 | 76.1 |
| | 1073 | 20 | 0.28 | 51.4 | 28.84 | 73.2 | 26.810 | 1.893 | 143 | 16.38 | 1099 | | 25.35 | 1.790 | 1086 | 3.37 | 1687 | | 1200 | 1.083 | 35021 | 93.50 | 15.44 | 78.1 |
| | 1074 | 21 | 0.20 | 51.5 | 28.84 | 72.3 | 26.034 | 1.839 | 142 | 15.93 | 1075 | | 23.98 | 1.694 | 1051 | 3.19 | 1593 | | 1162 | 1.048 | 35814 | 95.00 | 15.54 | 79.5 |
| | 1075 | 21 | 0.00 | 51.6 | 28.84 | 70.6 | 25.929 | 1.831 | 142 | 15.88 | 1071 | | 23.74 | 1.676 | 1053 | 3.15 | 1579 | | 1156 | 1.043 | 43644 | 99.00 | 16.40 | 82.6 |
| 5/13/97 | 1272 | 24 | 0.28 | 62.1 | 28.84 | 35.8 | 21.506 | 1.519 | 139 | 12.91 | 900 | | 18.02 | 1.273 | 845 | 2.12 | 1022 | | 917 | 0.819 | 18093 | 77.50 | 12.58 | 64.9 |
| | 1273 | 23 | 0.28 | 61.3 | 28.84 | 37.0 | 22.715 | 1.604 | 139 | 13.85 | 953 | | 19.24 | 1.359 | 881 | 2.41 | 1162 | | 984 | 0.879 | 21759 | 80.60 | 13.38 | 67.2 |
| | 1274 | 22 | 0.28 | 60.8 | 28.86 | 38.4 | 24.523 | 1.731 | 141 | 15.09 | 1023 | | 21.42 | 1.512 | 952 | 2.83 | 1375 | | 1079 | 0.965 | 27360 | 86.10 | 14.37 | 71.7 |
| | 1275 | 21 | 0.28 | 60.3 | 28.84 | 39.5 | 26.001 | 1.836 | 141 | 15.97 | 1073 | | 23.87 | 1.685 | 1037 | 3.19 | 1578 | | 1158 | 1.035 | 32239 | 90.70 | 15.08 | 75.6 |
| | 1276 | 20 | 0.28 | 59.6 | 28.84 | 40.3 | 26.826 | 1.894 | 141 | 16.45 | 1097 | | 25.50 | 1.801 | 1079 | 3.41 | 1691 | | 1201 | 1.075 | 35149 | 93.20 | 15.46 | 77.7 |
| | 1278 | 21 | 0.20 | 58.4 | 28.84 | 42.1 | 25.950 | 1.832 | 140 | 15.94 | 1070 | | 24.00 | 1.695 | 1042 | 3.22 | 1589 | | 1159 | 1.038 | 35632 | 94.80 | 15.52 | 79.3 |
| | 1279 | 21 | 0.00 | 57.7 | 28.86 | 43.8 | 25.969 | 1.833 | 141 | 15.96 | 1071 | | 24.02 | 1.696 | 1048 | 3.21 | 1593 | | 1159 | 1.039 | 43884 | 99.60 | 16.42 | 83.2 |

## Aeroacoustic Summary Data

### Model 3 – Configuration 3BC, Baseline Core Nozzle, 24-Chevron Fan Nozzle

| Date | Point | Cycle | XMA | $T_{amb}$ | $P_{amb}$ | RH | $P_{18}$ | PFQPA | $T_{18}$ | $W_{18}$ | $V_{18}$ | $CD_{18}$ | $P_8$ | P8QPA | $T_8$ | $W_8$ | $V_8$ | $CD_8$ | $V_{mix}$ | $V_{mix}/c_{amb}$ | $F_N$ | EPNL | NF | NEPNL |
|---|---|---|---|---|---|---|---|---|---|---|---|---|---|---|---|---|---|---|---|---|---|---|---|---|
| 4/2/97 | 430 | 24 | 0.28 | 60.4 | 29.45 | 20.0 | 21.867 | 1.512 | 140 | 13.19 | 896 | 1.000 | 18.30 | 1.266 | 840 | 2.10 | 1010 | 0.891 | 911 | 0.815 | 18065 | 77.20 | 12.57 | 64.6 |
| | 431 | 23 | 0.28 | 60.5 | 29.45 | 19.9 | 23.207 | 1.605 | 140 | 14.30 | 954 | 1.002 | 19.52 | 1.350 | 886 | 2.41 | 1154 | 0.908 | 983 | 0.879 | 22132 | 80.40 | 13.45 | 66.9 |
| | 432 | 22 | 0.28 | 60.0 | 29.45 | 21.1 | 25.018 | 1.730 | 140 | 15.58 | 1022 | 0.996 | 21.93 | 1.517 | 965 | 2.89 | 1389 | 0.929 | 1080 | 0.966 | 28243 | 85.90 | 14.51 | 71.4 |
| | 433 | 21 | 0.28 | 60.4 | 29.45 | 20.4 | 26.474 | 1.831 | 140 | 16.51 | 1070 | 0.992 | 24.38 | 1.686 | 1043 | 3.25 | 1587 | 0.942 | 1155 | 1.033 | 33116 | 90.50 | 15.20 | 75.3 |
| | 434 | 20 | 0.28 | 59.9 | 29.45 | 20.6 | 27.374 | 1.893 | 141 | 17.05 | 1097 | 0.993 | 25.92 | 1.792 | 1082 | 3.46 | 1693 | 0.948 | 1197 | 1.071 | 36066 | 93.10 | 15.57 | 77.5 |
| | 429 | 26 | 0.20 | 60.5 | 29.45 | 20.1 | 18.550 | 1.283 | 139 | 9.88 | 703 | 0.999 | 16.23 | 1.122 | 735 | 1.44 | 683 | 0.857 | 700 | 0.626 | 10747 | 72.70 | 10.31 | 62.4 |
| | 428 | 25 | 0.20 | 60.7 | 29.47 | 19.3 | 20.492 | 1.417 | 140 | 14.20 | 826 | 1.082 | 17.33 | 1.198 | 803 | 1.82 | 875 | 0.877 | 832 | 0.743 | 19394 | 77.70 | 12.88 | 64.8 |
| | 426 | 24 | 0.20 | 61.0 | 29.47 | 18.7 | 21.876 | 1.512 | 140 | 13.21 | 896 | 1.001 | 18.37 | 1.270 | 840 | 2.14 | 1016 | 0.900 | 913 | 0.816 | 21110 | 81.30 | 13.24 | 68.1 |
| | 427 | 21 | 0.20 | 60.9 | 29.47 | 19.3 | 26.487 | 1.831 | 141 | 16.51 | 1070 | 0.992 | 24.16 | 1.670 | 1044 | 3.21 | 1576 | 0.940 | 1152 | 1.030 | 36449 | 94.20 | 15.62 | 78.6 |
| | 415 | 26 | 0.00 | 60.9 | 29.49 | 16.9 | 18.470 | 1.275 | 139 | 9.78 | 695 | 1.000 | 16.19 | 1.118 | 742 | 1.45 | 675 | 0.877 | 692 | 0.619 | 15425 | 76.20 | 11.88 | 64.3 |
| | 416 | 24 | 0.00 | 61.1 | 29.49 | 17.5 | 21.915 | 1.514 | 139 | 13.26 | 896 | 1.002 | 18.37 | 1.269 | 839 | 2.16 | 1015 | 0.908 | 913 | 0.816 | 27981 | 86.40 | 14.47 | 71.9 |
| | 417 | 23 | 0.00 | 60.9 | 29.49 | 17.5 | 23.199 | 1.602 | 139 | 14.30 | 952 | 1.001 | 19.52 | 1.348 | 884 | 2.43 | 1151 | 0.917 | 981 | 0.877 | 32525 | 90.00 | 15.12 | 74.9 |
| | 418 | 22 | 0.00 | 61.1 | 29.49 | 17.4 | 25.101 | 1.734 | 140 | 15.68 | 1024 | 0.996 | 21.86 | 1.510 | 960 | 2.89 | 1380 | 0.933 | 1079 | 0.964 | 39686 | 95.00 | 15.99 | 79.0 |
| | 419 | 21 | 0.00 | 60.7 | 29.49 | 17.1 | 26.475 | 1.829 | 140 | 16.51 | 1069 | 0.991 | 24.32 | 1.680 | 1043 | 3.24 | 1582 | 0.943 | 1153 | 1.031 | 45173 | 98.80 | 16.55 | 82.3 |
| | 420 | 20 | 0.00 | 61.0 | 29.47 | 17.1 | 27.451 | 1.897 | 141 | 17.05 | 1098 | 0.992 | 25.93 | 1.791 | 1084 | 3.45 | 1695 | 0.946 | 1198 | 1.071 | 48735 | 101.20 | 16.88 | 84.3 |
| | 421 | | 0.00 | 62.1 | 29.47 | 18.2 | 21.748 | 1.503 | 138 | 13.28 | 888 | 1.013 | 19.48 | 1.346 | 441 | 3.04 | 938 | 0.940 | 898 | 0.801 | 29109 | 85.10 | 14.64 | 70.5 |
| | 422 | | 0.00 | 62.3 | 29.47 | 17.0 | 21.794 | 1.506 | 140 | 13.06 | 892 | 0.996 | 19.64 | 1.357 | 1020 | 2.36 | 1221 | 0.926 | 943 | 0.841 | 28865 | 89.70 | 14.60 | 75.1 |
| | 423 | | 0.00 | 62.1 | 29.47 | 17.0 | 21.769 | 1.505 | 141 | 12.97 | 892 | 0.991 | 23.06 | 1.594 | 1049 | 3.05 | 1508 | 0.946 | 1009 | 0.901 | 32055 | 95.60 | 15.06 | 80.5 |
| | 424 | | 0.00 | 61.8 | 29.47 | 16.8 | 21.693 | 1.499 | 139 | 13.09 | 887 | 1.004 | 23.33 | 1.612 | 476 | 3.97 | 1200 | 0.950 | 959 | 0.857 | 32565 | 89.10 | 15.13 | 74.0 |
| | 425 | | 0.00 | 61.9 | 29.47 | 17.9 | 21.720 | 1.501 | 140 | 13.76 | 889 | 0.983 | 21.31 | 1.473 | 724 | 3.10 | 1222 | 0.946 | 950 | 0.848 | 31790 | 89.40 | 15.02 | 74.4 |

## Aeroacoustic Summary Data

### Model 3 – Configuration 3C12B, 12-Chevron Core Nozzle, Baseline Fan Nozzle

| Date | Point | Cycle | XMA | $T_{amb}$ | $P_{amb}$ | RH | $P_{18}$ | PFQPA | $T_{18}$ | $W_{18}$ | $V_{18}$ | $CD_{18}$ | $P_8$ | P8QPA | $T_8$ | $W_8$ | $V_8$ | $CD_8$ | $V_{mix}$ | $V_{mix}/c_{amb}$ | $F_N$ | EPNL | NF | NEPNL |
|---|---|---|---|---|---|---|---|---|---|---|---|---|---|---|---|---|---|---|---|---|---|---|---|---|
| 4/11/97 | 737 | 24 | 0.28 | 42.0 | 29.27 | 50.7 | 21.767 | 1.514 | 138 | 13.00 | 896 | 0.988 | 18.23 | 1.268 | 841 | 2.20 | 1015 | 0.931 | 913 | 0.831 | 18224 | 77.80 | 12.61 | 65.2 |
| | 738 | 23 | 0.28 | 41.3 | 29.29 | 52.4 | 23.159 | 1.611 | 140 | 14.08 | 958 | 0.985 | 19.30 | 1.343 | 885 | 2.46 | 1144 | 0.941 | 985 | 0.898 | 22236 | 80.90 | 13.47 | 67.4 |
| | 739 | 22 | 0.28 | 41.1 | 29.27 | 53.3 | 24.869 | 1.730 | 141 | 15.25 | 1024 | 0.983 | 21.63 | 1.505 | 968 | 2.93 | 1379 | 0.961 | 1081 | 0.985 | 27899 | 86.00 | 14.46 | 71.5 |
| | 740 | 21 | 0.28 | 41.1 | 29.27 | 53.2 | 26.332 | 1.833 | 142 | 16.13 | 1072 | 0.975 | 24.23 | 1.686 | 1047 | 3.34 | 1590 | 0.975 | 1161 | 1.058 | 32993 | 90.70 | 15.18 | 75.5 |
| | 741 | 20 | 0.28 | 41.0 | 29.27 | 53.6 | 27.217 | 1.894 | 143 | 16.61 | 1099 | 0.974 | 25.76 | 1.793 | 1091 | 3.54 | 1698 | 0.980 | 1204 | 1.098 | 35891 | 93.20 | 15.55 | 77.7 |
| | 742 | 21 | 0.20 | 40.7 | 29.27 | 54.8 | 26.236 | 1.826 | 142 | 16.05 | 1069 | 0.977 | 24.02 | 1.672 | 1048 | 3.30 | 1579 | 0.972 | 1156 | 1.054 | 36059 | 94.80 | 15.57 | 79.2 |
| | 743 | 21 | 0.00 | 40.6 | 29.27 | 55.5 | 26.378 | 1.836 | 142 | 16.17 | 1073 | 0.977 | 24.24 | 1.687 | 1050 | 3.34 | 1592 | 0.975 | 1162 | 1.059 | 44913 | 99.20 | 16.52 | 82.7 |
| | 746 | 26 | 0.20 | 40.2 | 29.25 | 58.5 | 18.331 | 1.276 | 139 | 9.57 | 696 | 0.986 | 16.02 | 1.116 | 747 | 1.44 | 668 | 0.888 | 692 | 0.631 | 10332 | 72.70 | 10.14 | 62.6 |
| | 745 | 25 | 0.20 | 40.2 | 29.25 | 58.2 | 20.444 | 1.423 | 140 | 11.79 | 831 | 0.987 | 17.26 | 1.201 | 812 | 1.89 | 884 | 0.915 | 838 | 0.765 | 16834 | 78.40 | 12.26 | 66.1 |
| | 744 | 24 | 0.20 | 40.3 | 29.25 | 57.3 | 21.742 | 1.514 | 140 | 12.94 | 897 | 0.986 | 18.25 | 1.271 | 851 | 2.19 | 1022 | 0.931 | 915 | 0.835 | 20956 | 81.70 | 13.21 | 68.5 |

## Aeroacoustic Summary Data — Model 3 – Configuration 3C8B, 8-Chevron Core Nozzle, Baseline Fan Nozzle

| Date | Point | Cycle | XMA | $T_{amb}$ | $P_{amb}$ | RH | $P_{18}$ | PFQPA | $T_{18}$ | $W_{18}$ | $V_{18}$ | $CD_{18}$ | $P_8$ | P8QPA | $T_8$ | $W_8$ | $V_8$ | $CD_8$ | $V_{mix}$ | $V_{mix}/c_{amb}$ | $F_N$ | EPNL | NF | NEPNL |
|---|---|---|---|---|---|---|---|---|---|---|---|---|---|---|---|---|---|---|---|---|---|---|---|---|
| 4/14/97 | 758 | 24 | 0.28 | 47.8 | 29.41 | 26.9 | 21.865 | 1.514 | 139 | 13.06 | 897 | 0.988 | 18.33 | 1.270 | 843 | 2.20 | 1017 | 0.928 | 915 | 0.828 | 18312 | 77.60 | 12.63 | 65.0 |
| | 759 | 23 | 0.28 | 47.5 | 29.41 | 26.1 | 23.085 | 1.599 | 141 | 13.99 | 951 | 0.986 | 19.52 | 1.352 | 885 | 2.49 | 1157 | 0.938 | 982 | 0.890 | 22006 | 80.50 | 13.43 | 67.1 |
| | 760 | 22 | 0.28 | 47.6 | 29.41 | 26.2 | 24.938 | 1.727 | 143 | 15.27 | 1023 | 0.982 | 21.66 | 1.500 | 961 | 2.91 | 1370 | 0.952 | 1078 | 0.976 | 27857 | 85.80 | 14.45 | 71.4 |
| | 761 | 21 | 0.28 | 47.4 | 29.41 | 26.0 | 26.515 | 1.836 | 143 | 16.27 | 1074 | 0.979 | 24.17 | 1.674 | 1043 | 3.32 | 1577 | 0.970 | 1160 | 1.050 | 33202 | 90.00 | 15.21 | 74.8 |
| | 762 | 20 | 0.28 | 47.9 | 29.41 | 25.6 | 27.263 | 1.888 | 143 | 16.66 | 1097 | 0.976 | 25.80 | 1.787 | 1082 | 3.54 | 1689 | 0.976 | 1201 | 1.087 | 35814 | 92.50 | 15.54 | 77.0 |
| | 763 | 21 | 0.20 | 47.6 | 29.41 | 26.6 | 26.490 | 1.835 | 143 | 16.19 | 1074 | 0.975 | 24.30 | 1.683 | 1049 | 3.32 | 1587 | 0.968 | 1162 | 1.052 | 36561 | 94.10 | 15.63 | 78.5 |
| | 764 | 21 | 0.00 | 47.9 | 29.41 | 25.9 | 26.421 | 1.830 | 143 | 16.15 | 1071 | 0.976 | 24.17 | 1.674 | 1052 | 3.31 | 1582 | 0.969 | 1158 | 1.049 | 44586 | 98.50 | 16.49 | 82.0 |

## Aeroacoustic Summary Data — Model 3 – Configuration 3IB, 12-Chevron (In-Flip) Core Nozzle, Baseline Fan Nozzle

| Date | Point | Cycle | XMA | $T_{amb}$ | $P_{amb}$ | RH | $P_{18}$ | PFQPA | $T_{18}$ | $W_{18}$ | $V_{18}$ | $CD_{18}$ | $P_8$ | P8QPA | $T_8$ | $W_8$ | $V_8$ | $CD_8$ | $V_{mix}$ | $V_{mix}/c_{amb}$ | $F_N$ | EPNL | NF | NEPNL |
|---|---|---|---|---|---|---|---|---|---|---|---|---|---|---|---|---|---|---|---|---|---|---|---|---|
| 4/14/97 | 765 | 24 | 0.28 | 46.3 | 29.41 | 26.9 | 21.797 | 1.510 | 140 | 13.08 | 894 | 0.996 | 18.41 | 1.275 | 846 | 2.16 | 1027 | 0.903 | 913 | 0.828 | 18368 | 77.60 | 12.64 | 65.0 |
| | 766 | 23 | 0.28 | 46.2 | 29.41 | 26.9 | 23.125 | 1.602 | 141 | 14.03 | 953 | 0.987 | 19.46 | 1.348 | 888 | 2.38 | 1153 | 0.904 | 982 | 0.891 | 21963 | 80.30 | 13.42 | 66.9 |
| | 769 | 22 | 0.28 | 46.2 | 29.41 | 28.0 | 24.990 | 1.731 | 141 | 15.32 | 1024 | 0.983 | 21.83 | 1.512 | 961 | 2.85 | 1382 | 0.922 | 1080 | 0.979 | 27961 | 84.70 | 14.47 | 70.2 |
| | 770 | 21 | 0.28 | 45.8 | 29.41 | 28.4 | 26.426 | 1.830 | 142 | 16.20 | 1071 | 0.979 | 24.33 | 1.685 | 1039 | 3.25 | 1584 | 0.941 | 1157 | 1.049 | 32872 | 89.30 | 15.17 | 74.1 |
| | 771 | 20 | 0.28 | 45.2 | 29.41 | 29.4 | 27.293 | 1.890 | 141 | 16.70 | 1096 | 0.974 | 25.89 | 1.793 | 1078 | 3.47 | 1692 | 0.951 | 1198 | 1.087 | 35734 | 91.60 | 15.53 | 76.1 |
| | 772 | 21 | 0.20 | 45.2 | 29.41 | 29.3 | 26.383 | 1.827 | 141 | 16.17 | 1068 | 0.976 | 24.20 | 1.676 | 1039 | 3.22 | 1577 | 0.939 | 1153 | 1.046 | 36076 | 93.20 | 15.57 | 77.6 |
| | 773 | 21 | 0.00 | 45.3 | 29.41 | 29.0 | 26.360 | 1.825 | 141 | 16.19 | 1067 | 0.977 | 24.35 | 1.686 | 1044 | 3.24 | 1589 | 0.939 | 1154 | 1.047 | 44595 | 97.70 | 16.49 | 81.2 |
| 4/15/97 | 805 | 24 | 0.28 | 60.4 | 29.35 | 26.4 | 21.754 | 1.509 | 138 | 12.98 | 893 | 0.989 | 18.32 | 1.271 | 840 | 2.12 | 1018 | 0.891 | 910 | 0.814 | 18025 | 77.00 | 12.56 | 64.4 |
| | 806 | 23 | 0.28 | 60.5 | 29.37 | 26.0 | 23.035 | 1.598 | 140 | 14.00 | 950 | 0.988 | 19.37 | 1.344 | 885 | 2.36 | 1145 | 0.902 | 978 | 0.875 | 21851 | 79.90 | 13.39 | 66.5 |
| | 807 | 22 | 0.28 | 60.4 | 29.37 | 26.3 | 24.850 | 1.724 | 140 | 15.27 | 1019 | 0.985 | 21.68 | 1.504 | 956 | 2.84 | 1371 | 0.925 | 1074 | 0.961 | 27385 | 84.00 | 14.38 | 69.6 |
| | 808 | 21 | 0.28 | 60.6 | 29.37 | 26.7 | 26.359 | 1.828 | 141 | 16.21 | 1070 | 0.981 | 24.10 | 1.671 | 1041 | 3.21 | 1574 | 0.941 | 1153 | 1.031 | 32632 | 88.50 | 15.14 | 73.4 |
| | 809 | 20 | 0.28 | 59.9 | 29.37 | 28.1 | 27.202 | 1.886 | 142 | 16.66 | 1095 | 0.976 | 25.72 | 1.784 | 1080 | 3.45 | 1685 | 0.952 | 1196 | 1.070 | 35305 | 90.70 | 15.48 | 75.2 |
| | 810 | 21 | 0.20 | 59.8 | 29.37 | 28.4 | 26.430 | 1.833 | 142 | 16.20 | 1072 | 0.978 | 24.24 | 1.681 | 1042 | 3.23 | 1583 | 0.941 | 1157 | 1.035 | 36113 | 92.50 | 15.58 | 76.9 |
| | 811 | 21 | 0.00 | 59.6 | 29.37 | 28.7 | 26.414 | 1.832 | 142 | 16.17 | 1072 | 0.978 | 24.29 | 1.684 | 1046 | 3.24 | 1587 | 0.944 | 1158 | 1.036 | 44605 | 97.00 | 16.49 | 80.5 |

## Aeroacoustic Summary Data — Model 3 – Configuration 3AB, 12-Chevron (Alt-Flip) Core Nozzle, Baseline Fan Nozzle

| Date | Point | Cycle | XMA | $T_{amb}$ | $P_{amb}$ | RH | $P_{18}$ | PFQPA | $T_{18}$ | $W_{18}$ | $V_{18}$ | $CD_{18}$ | $P_8$ | P8QPA | $T_8$ | $W_8$ | $V_8$ | $CD_8$ | $V_{mix}$ | $V_{mix}/c_{amb}$ | $F_N$ | EPNL | NF | NEPNL |
|---|---|---|---|---|---|---|---|---|---|---|---|---|---|---|---|---|---|---|---|---|---|---|---|---|
| 4/14/97 | 774 | 24 | 0.28 | 44.5 | 29.43 | 31.7 | 21.872 | 1.514 | 140 | 13.07 | 897 | 0.989 | 18.29 | 1.266 | 847 | 2.35 | 1013 | 0.997 | 915 | 0.831 | 18806 | 78.60 | 12.74 | 65.9 |
| | 775 | 23 | 0.28 | 44.5 | 29.43 | 32.3 | 23.177 | 1.604 | 142 | 14.08 | 955 | 0.988 | 19.55 | 1.353 | 893 | 2.66 | 1161 | 1.002 | 988 | 0.897 | 22657 | 81.50 | 13.55 | 67.9 |
| | 776 | 22 | 0.28 | 44.4 | 29.43 | 32.0 | 24.991 | 1.730 | 142 | 15.36 | 1023 | 0.986 | 21.84 | 1.512 | 968 | 3.11 | 1385 | 1.008 | 1085 | 0.985 | 28554 | 85.90 | 14.56 | 71.3 |
| | 777 | 21 | 0.28 | 44.4 | 29.43 | 33.2 | 26.553 | 1.838 | 143 | 16.28 | 1075 | 0.980 | 24.22 | 1.676 | 1048 | 3.44 | 1581 | 1.006 | 1164 | 1.057 | 33643 | 89.80 | 15.27 | 74.5 |
| | 778 | 20 | 0.28 | 44.4 | 29.43 | 33.1 | 27.345 | 1.893 | 144 | 16.70 | 1100 | 0.976 | 25.92 | 1.794 | 1086 | 3.65 | 1697 | 1.002 | 1207 | 1.096 | 36456 | 92.00 | 15.62 | 76.4 |
| | 779 | 21 | 0.20 | 44.1 | 29.43 | 32.6 | 26.609 | 1.842 | 144 | 16.27 | 1078 | 0.977 | 24.37 | 1.687 | 1051 | 3.45 | 1592 | 1.002 | 1168 | 1.061 | 37308 | 93.60 | 15.72 | 77.9 |
| | 780 | 21 | 0.00 | 44.3 | 29.43 | 32.3 | 26.518 | 1.835 | 144 | 16.22 | 1075 | 0.978 | 24.24 | 1.678 | 1055 | 3.43 | 1587 | 1.003 | 1164 | 1.057 | 44951 | 96.50 | 16.53 | 80.0 |

## Aeroacoustic Summary Data — Model 3 – Configuration 3DIB, 64-Internal-Doublet Core Nozzle, Baseline Fan Nozzle

| Date | Point | Cycle | XMA | $T_{amb}$ | $P_{amb}$ | RH | $P_{18}$ | PFQPA | $T_{18}$ | $W_{18}$ | $V_{18}$ | $CD_{18}$ | $P_8$ | P8QPA | $T_8$ | $W_8$ | $V_8$ | $CD_8$ | $V_{mix}$ | $V_{mix}/c_{amb}$ | $F_N$ | EPNL | NF | NEPNL |
|---|---|---|---|---|---|---|---|---|---|---|---|---|---|---|---|---|---|---|---|---|---|---|---|---|
| 4/15/97 | 797 | 24 | 0.28 | 58.3 | 29.37 | 28.4 | 21.833 | 1.514 | 136 | 13.15 | 894 | 0.995 | 18.40 | 1.276 | 831 | 2.15 | 1023 | 0.891 | 912 | 0.818 | 18382 | 77.40 | 12.64 | 64.8 |
| | 798 | 23 | 0.28 | 58.4 | 29.37 | 28.6 | 23.060 | 1.599 | 140 | 13.99 | 950 | 0.987 | 19.45 | 1.349 | 886 | 2.36 | 1152 | 0.893 | 980 | 0.878 | 21830 | 80.90 | 13.39 | 67.5 |
| | 799 | 22 | 0.28 | 58.6 | 29.37 | 27.9 | 24.964 | 1.731 | 141 | 15.34 | 1023 | 0.983 | 21.85 | 1.515 | 956 | 2.83 | 1384 | 0.912 | 1079 | 0.967 | 27749 | 86.00 | 14.43 | 71.6 |
| | 800 | 21 | 0.28 | 58.4 | 29.37 | 27.9 | 26.412 | 1.831 | 141 | 16.22 | 1071 | 0.981 | 24.14 | 1.674 | 1039 | 3.17 | 1575 | 0.926 | 1153 | 1.033 | 32681 | 91.00 | 15.14 | 75.9 |
| | 801 | 20 | 0.28 | 58.6 | 29.37 | 27.2 | 27.307 | 1.893 | 142 | 16.69 | 1098 | 0.977 | 25.83 | 1.791 | 1080 | 3.40 | 1691 | 0.935 | 1198 | 1.073 | 35552 | 93.60 | 15.51 | 78.1 |
| | 802 | 21 | 0.20 | 58.7 | 29.37 | 27.7 | 26.317 | 1.825 | 143 | 16.15 | 1069 | 0.978 | 24.05 | 1.668 | 1043 | 3.14 | 1572 | 0.923 | 1151 | 1.031 | 35636 | 94.90 | 15.52 | 79.4 |
| | 803 | 21 | 0.20 | 58.5 | 29.37 | 27.7 | 26.443 | 1.833 | 143 | 16.17 | 1073 | 0.978 | 24.18 | 1.677 | 1044 | 3.16 | 1580 | 0.925 | 1156 | 1.036 | 35970 | 94.90 | 15.56 | 79.3 |
| | 804 | 21 | 0.00 | 58.6 | 29.37 | 28.2 | 26.514 | 1.838 | 143 | 16.24 | 1075 | 0.979 | 24.37 | 1.690 | 1039 | 3.21 | 1589 | 0.928 | 1160 | 1.039 | 44730 | 99.40 | 16.51 | 82.9 |

## Aeroacoustic Summary Data — Model 3 – Configuration 3IC, 12-Chevron (In-Flip) Core Nozzle, 24-Chevron Fan Nozzle

| Date | Point | Cycle | XMA | $T_{amb}$ | $P_{amb}$ | RH | $P_{18}$ | PFQPA | $T_{18}$ | $W_{18}$ | $V_{18}$ | $CD_{18}$ | $P_8$ | P8QPA | $T_8$ | $W_8$ | $V_8$ | $CD_8$ | $V_{mix}$ | $V_{mix}/c_{amb}$ | $F_N$ | EPNL | NF | NEPNL |
|---|---|---|---|---|---|---|---|---|---|---|---|---|---|---|---|---|---|---|---|---|---|---|---|---|
| 4/15/97 | 812 | 24 | 0.28 | 56.8 | 29.35 | 31.6 | 21.743 | 1.509 | 139 | 13.13 | 893 | 1.002 | 18.39 | 1.276 | 844 | 2.14 | 1027 | 0.893 | 912 | 0.818 | 18233 | 77.20 | 12.61 | 64.6 |
| | 813 | 23 | 0.28 | 56.3 | 29.35 | 32.7 | 23.057 | 1.600 | 140 | 14.19 | 951 | 1.000 | 19.51 | 1.354 | 890 | 2.39 | 1161 | 0.901 | 982 | 0.881 | 22099 | 79.90 | 13.44 | 66.5 |
| | 814 | 22 | 0.28 | 56.1 | 29.35 | 32.9 | 25.007 | 1.735 | 141 | 15.58 | 1025 | 0.999 | 21.80 | 1.512 | 961 | 2.85 | 1382 | 0.924 | 1080 | 0.970 | 28232 | 84.10 | 14.51 | 69.6 |
| | 816 | 20 | 0.28 | 55.8 | 29.35 | 33.1 | 27.266 | 1.892 | 141 | 16.97 | 1097 | 0.991 | 25.90 | 1.797 | 1084 | 3.46 | 1698 | 0.952 | 1199 | 1.077 | 36098 | 90.50 | 15.57 | 74.9 |
| | 817 | 21 | 0.20 | 55.6 | 29.35 | 33.5 | 26.438 | 1.834 | 142 | 16.47 | 1072 | 0.992 | 24.33 | 1.688 | 1043 | 3.25 | 1588 | 0.942 | 1157 | 1.040 | 36778 | 92.20 | 15.66 | 76.5 |
| | 818 | 21 | 0.00 | 55.7 | 29.37 | 33.4 | 26.279 | 1.823 | 141 | 16.37 | 1066 | 0.992 | 24.20 | 1.678 | 1036 | 3.25 | 1576 | 0.947 | 1151 | 1.034 | 44777 | 96.20 | 16.51 | 79.7 |
| 4/18/97 | 906 | 64 | 0.28 | 43.1 | 29.00 | 41.7 | 21.682 | 1.522 | 140 | 13.18 | 902 | 1.003 | 17.40 | 1.222 | 806 | 1.85 | 920 | 0.858 | 905 | 0.823 | 17862 | 77.60 | 12.52 | 65.1 |
| | 907 | 63 | 0.28 | 43.5 | 29.00 | 41.1 | 23.086 | 1.621 | 140 | 14.30 | 963 | 1.004 | 18.25 | 1.281 | 840 | 2.09 | 1034 | 0.872 | 973 | 0.884 | 21696 | 80.10 | 13.36 | 66.7 |
| | 909 | 62 | 0.28 | 43.5 | 29.02 | 39.2 | 25.151 | 1.765 | 142 | 15.73 | 1041 | 1.000 | 20.49 | 1.438 | 923 | 2.60 | 1283 | 0.906 | 1075 | 0.977 | 28029 | 84.20 | 14.48 | 69.7 |
| | 910 | 61 | 0.28 | 43.7 | 29.00 | 40.7 | 26.562 | 1.865 | 142 | 16.64 | 1086 | 0.999 | 21.85 | 1.534 | 986 | 2.83 | 1418 | 0.919 | 1134 | 1.031 | 32041 | 86.90 | 15.06 | 71.8 |
| | 911 | 60 | 0.28 | 44.0 | 29.00 | 39.9 | 27.425 | 1.925 | 142 | 17.18 | 1111 | 0.998 | 23.12 | 1.623 | 1012 | 3.06 | 1517 | 0.930 | 1172 | 1.065 | 34841 | 88.50 | 15.42 | 73.1 |
| | 888 | 24 | 0.28 | 41.9 | 29.02 | 48.7 | 21.515 | 1.510 | 144 | 13.03 | 897 | 1.007 | 18.19 | 1.276 | 845 | 2.12 | 1028 | 0.898 | 916 | 0.834 | 18594 | 78.00 | 12.69 | 65.3 |
| | 905 | 24 | 0.28 | 43.3 | 29.02 | 40.0 | 21.501 | 1.509 | 140 | 12.96 | 894 | 1.001 | 18.08 | 1.269 | 844 | 2.05 | 1016 | 0.879 | 911 | 0.828 | 18062 | 77.60 | 12.57 | 65.0 |
| | 889 | 23 | 0.28 | 42.0 | 29.02 | 47.8 | 22.830 | 1.602 | 146 | 14.03 | 957 | 1.003 | 19.17 | 1.345 | 876 | 2.36 | 1143 | 0.904 | 984 | 0.896 | 22106 | 80.20 | 13.45 | 66.8 |
| | 890 | 22 | 0.28 | 42.2 | 29.02 | 45.0 | 24.740 | 1.736 | 144 | 15.48 | 1027 | 1.005 | 21.68 | 1.521 | 951 | 2.86 | 1386 | 0.927 | 1084 | 0.987 | 28473 | 84.70 | 14.54 | 70.2 |
| | 891 | 21 | 0.28 | 42.3 | 29.02 | 47.0 | 26.137 | 1.834 | 144 | 16.29 | 1074 | 0.996 | 23.96 | 1.681 | 1031 | 3.22 | 1578 | 0.943 | 1157 | 1.053 | 33045 | 88.60 | 15.19 | 73.4 |
| | 904 | 21 | 0.28 | 44.1 | 29.02 | 40.0 | 26.070 | 1.830 | 141 | 16.28 | 1070 | 0.993 | 23.84 | 1.673 | 1036 | 3.17 | 1573 | 0.937 | 1151 | 1.046 | 32747 | 88.20 | 15.15 | 73.0 |
| | 892 | 20 | 0.28 | 42.2 | 29.02 | 46.1 | 26.874 | 1.886 | 143 | 16.73 | 1095 | 0.995 | 25.36 | 1.779 | 1075 | 3.40 | 1680 | 0.950 | 1194 | 1.087 | 35581 | 90.80 | 15.51 | 75.3 |
| | 896 | 26 | 0.20 | 42.8 | 29.02 | 43.8 | 18.308 | 1.285 | 141 | 9.79 | 706 | 1.005 | 16.07 | 1.127 | 734 | 1.44 | 695 | 0.852 | 705 | 0.641 | 10808 | 73.50 | 10.34 | 63.2 |
| | 895 | 25 | 0.20 | 42.8 | 29.04 | 45.2 | 20.238 | 1.420 | 142 | 11.80 | 830 | 1.000 | 17.21 | 1.207 | 797 | 1.82 | 890 | 0.871 | 838 | 0.762 | 16706 | 77.80 | 12.23 | 65.6 |
| | 894 | 24 | 0.20 | 42.6 | 29.02 | 46.3 | 21.532 | 1.511 | 143 | 12.93 | 897 | 0.998 | 18.17 | 1.275 | 846 | 2.09 | 1028 | 0.883 | 915 | 0.833 | 20729 | 81.10 | 13.17 | 67.9 |
| | 893 | 21 | 0.20 | 42.4 | 29.02 | 46.4 | 26.264 | 1.843 | 143 | 16.33 | 1077 | 0.993 | 24.12 | 1.692 | 1038 | 3.22 | 1590 | 0.940 | 1161 | 1.057 | 36532 | 92.50 | 15.63 | 76.9 |
| | 912 | 63 | 0.00 | 44.0 | 29.00 | 40.0 | 23.134 | 1.624 | 141 | 14.33 | 967 | 1.004 | 18.28 | 1.283 | 843 | 2.13 | 1038 | 0.888 | 976 | 0.887 | 31513 | 88.40 | 14.98 | 73.4 |
| | 913 | 61 | 0.00 | 45.1 | 29.02 | 39.0 | 26.534 | 1.863 | 142 | 16.68 | 1085 | 0.999 | 21.80 | 1.530 | 986 | 2.85 | 1414 | 0.927 | 1133 | 1.028 | 43621 | 95.70 | 16.40 | 79.3 |
| | 897 | 26 | 0.00 | 42.7 | 29.04 | 43.6 | 18.265 | 1.281 | 141 | 9.77 | 703 | 1.008 | 16.01 | 1.123 | 734 | 1.44 | 684 | 0.868 | 700 | 0.637 | 15384 | 76.60 | 11.87 | 64.7 |
| | 898 | 24 | 0.00 | 43.6 | 29.04 | 45.0 | 21.595 | 1.515 | 141 | 13.09 | 899 | 1.005 | 18.21 | 1.277 | 853 | 2.12 | 1033 | 0.898 | 918 | 0.834 | 27430 | 87.10 | 14.38 | 72.7 |
| | 899 | 23 | 0.00 | 44.5 | 29.04 | 44.0 | 22.844 | 1.602 | 141 | 14.09 | 954 | 1.004 | 19.18 | 1.346 | 890 | 2.35 | 1150 | 0.907 | 982 | 0.892 | 31732 | 88.80 | 15.01 | 73.8 |
| | 900 | 23 | 0.00 | 45.0 | 29.04 | 41.6 | 22.908 | 1.607 | 141 | 14.13 | 957 | 1.003 | 19.20 | 1.347 | 891 | 2.35 | 1152 | 0.905 | 985 | 0.894 | 31879 | 92.80 | 15.03 | 77.8 |
| | 901 | 22 | 0.00 | 45.0 | 29.02 | 41.0 | 24.619 | 1.727 | 142 | 15.33 | 1022 | 1.000 | 21.52 | 1.510 | 957 | 2.82 | 1378 | 0.927 | 1078 | 0.978 | 38411 | 93.60 | 15.84 | 77.8 |
| | 902 | 21 | 0.00 | 45.4 | 29.02 | 39.8 | 26.136 | 1.834 | 141 | 16.33 | 1071 | 0.994 | 23.99 | 1.683 | 1039 | 3.21 | 1583 | 0.944 | 1155 | 1.048 | 44548 | 97.10 | 16.49 | 80.6 |
| | 903 | 20 | 0.00 | 45.2 | 29.02 | 40.3 | 26.997 | 1.894 | 141 | 16.84 | 1097 | 0.993 | 25.53 | 1.791 | 1078 | 3.43 | 1690 | 0.953 | 1197 | 1.087 | 47909 | 98.70 | 16.80 | 81.9 |

## Aeroacoustic Summary Data — Model 3 – Configuration 3C12C, 12-Chevron Core Nozzle, 24-Chevron Fan Nozzle

| Date | Point | Cycle | XMA | $T_{amb}$ | $P_{amb}$ | RH | $P_{18}$ | PFQPA | $T_{18}$ | $W_{18}$ | $V_{18}$ | $CD_{18}$ | $P_8$ | P8QPA | $T_8$ | $W_8$ | $V_8$ | $CD_8$ | $V_{mix}$ | $V_{mix}/c_{amb}$ | $F_N$ | EPNL | NF | NEPNL |
|---|---|---|---|---|---|---|---|---|---|---|---|---|---|---|---|---|---|---|---|---|---|---|---|---|
| 4/15/97 | 819 | 24 | 0.28 | 52.8 | 29.37 | 39.5 | 21.744 | 1.508 | 139 | 13.15 | 893 | 1.002 | 18.29 | 1.268 | 835 | 2.23 | 1010 | 0.941 | 910 | 0.820 | 18234 | 77.40 | 12.61 | 64.8 |
| | 821 | 22 | 0.28 | 52.6 | 29.37 | 39.4 | 24.964 | 1.732 | 142 | 15.53 | 1025 | 0.998 | 21.85 | 1.515 | 966 | 2.98 | 1388 | 0.964 | 1083 | 0.976 | 28326 | 85.30 | 14.52 | 70.8 |
| | 822 | 22 | 0.28 | 52.3 | 29.37 | 39.8 | 25.033 | 1.736 | 142 | 15.57 | 1027 | 0.996 | 21.91 | 1.519 | 970 | 2.96 | 1397 | 0.954 | 1085 | 0.978 | 28560 | 85.40 | 14.56 | 70.8 |
| | 823 | 21 | 0.28 | 52.3 | 29.37 | 40.2 | 26.452 | 1.834 | 142 | 16.45 | 1073 | 0.991 | 24.35 | 1.689 | 1048 | 3.36 | 1592 | 0.976 | 1161 | 1.046 | 33566 | 89.90 | 15.26 | 74.6 |
| | 825 | 20 | 0.28 | 51.9 | 29.37 | 41.8 | 27.107 | 1.880 | 142 | 16.84 | 1093 | 0.988 | 25.79 | 1.788 | 1089 | 3.54 | 1694 | 0.979 | 1197 | 1.079 | 35535 | 92.00 | 15.51 | 76.5 |
| | 826 | 20 | 0.28 | 51.8 | 29.37 | 41.5 | 27.200 | 1.886 | 142 | 16.89 | 1095 | 0.990 | 25.68 | 1.781 | 1083 | 3.53 | 1686 | 0.979 | 1197 | 1.080 | 36117 | 92.10 | 15.58 | 76.5 |
| | 827 | 21 | 0.20 | 51.7 | 29.37 | 41.3 | 26.495 | 1.837 | 144 | 16.45 | 1075 | 0.993 | 24.19 | 1.677 | 1050 | 3.32 | 1584 | 0.973 | 1161 | 1.047 | 36899 | 93.70 | 15.67 | 78.0 |
| | 828 | 21 | 0.00 | 51.6 | 29.37 | 41.1 | 26.395 | 1.830 | 144 | 16.39 | 1072 | 0.992 | 24.06 | 1.668 | 1053 | 3.30 | 1578 | 0.974 | 1157 | 1.044 | 44959 | 98.10 | 16.53 | 81.6 |

## Aeroacoustic Summary Data — Model 3 – Configuration 3C8C, 8-Chevron Core Nozzle, 24-Chevron Fan Nozzle

| Date | Point | Cycle | XMA | $T_{amb}$ | $P_{amb}$ | RH | $P_{18}$ | PFQPA | $T_{18}$ | $W_{18}$ | $V_{18}$ | $CD_{18}$ | $P_8$ | P8QPA | $T_8$ | $W_8$ | $V_8$ | $CD_8$ | $V_{mix}$ | $V_{mix}/c_{amb}$ | $F_N$ | EPNL | NF | NEPNL |
|---|---|---|---|---|---|---|---|---|---|---|---|---|---|---|---|---|---|---|---|---|---|---|---|---|
| 4/16/97 | 838 | 24 | 0.28 | 47.9 | 29.10 | 91.1 | 21.636 | 1.514 | 138 | 13.14 | 896 | 1.005 | 18.20 | 1.274 | 851 | 2.19 | 1027 | 0.931 | 914 | 0.828 | 18554 | 77.50 | 12.68 | 64.8 |
| | 839 | 23 | 0.28 | 48.0 | 29.10 | 91.1 | 22.866 | 1.600 | 140 | 14.08 | 952 | 1.003 | 19.32 | 1.351 | 885 | 2.46 | 1156 | 0.937 | 982 | 0.889 | 22132 | 80.00 | 13.45 | 66.5 |
| | 840 | 22 | 0.28 | 47.8 | 29.12 | 91.6 | 24.663 | 1.725 | 143 | 15.36 | 1023 | 0.999 | 21.60 | 1.511 | 963 | 2.91 | 1382 | 0.954 | 1080 | 0.978 | 27983 | 84.80 | 14.47 | 70.3 |
| | 841 | 21 | 0.28 | 47.7 | 29.10 | 91.6 | 26.226 | 1.835 | 144 | 16.31 | 1074 | 0.995 | 23.99 | 1.679 | 1045 | 3.28 | 1582 | 0.968 | 1160 | 1.050 | 33052 | 88.80 | 15.19 | 73.6 |
| | 843 | 20 | 0.28 | 47.5 | 29.10 | 91.6 | 27.055 | 1.893 | 142 | 16.84 | 1098 | 0.992 | 25.62 | 1.792 | 1085 | 3.50 | 1694 | 0.973 | 1200 | 1.087 | 35985 | 91.20 | 15.56 | 75.6 |
| | 844 | 21 | 0.20 | 47.4 | 29.12 | 91.2 | 26.207 | 1.833 | 142 | 16.34 | 1072 | 0.995 | 24.13 | 1.688 | 1045 | 3.31 | 1590 | 0.968 | 1159 | 1.050 | 36898 | 94.10 | 15.67 | 78.4 |
| | 845 | 21 | 0.20 | 47.5 | 29.10 | 90.8 | 26.207 | 1.833 | 142 | 16.31 | 1072 | 0.994 | 24.07 | 1.684 | 1046 | 3.30 | 1587 | 0.968 | 1159 | 1.049 | 36469 | 93.00 | 15.62 | 77.4 |
| | 846 | 21 | 0.00 | 47.7 | 29.12 | 90.1 | 26.159 | 1.830 | 141 | 16.31 | 1071 | 0.995 | 24.05 | 1.682 | 1048 | 3.29 | 1586 | 0.969 | 1157 | 1.047 | 44644 | 97.50 | 16.50 | 81.0 |

## Aeroacoustic Summary Data — Model 3 – Configuration 3AC, 12-Chevron (Alt-Flip) Core Nozzle, 24-Chevron Fan Nozzle

| Date | Point | Cycle | XMA | $T_{amb}$ | $P_{amb}$ | RH | $P_{18}$ | PFQPA | $T_{18}$ | $W_{18}$ | $V_{18}$ | $CD_{18}$ | $P_8$ | P8QPA | $T_8$ | $W_8$ | $V_8$ | $CD_8$ | $V_{mix}$ | $V_{mix}/c_{amb}$ | $F_N$ | EPNL | NF | NEPNL |
|---|---|---|---|---|---|---|---|---|---|---|---|---|---|---|---|---|---|---|---|---|---|---|---|---|
| 4/16/97 | 847 | 24 | 0.28 | 47.0 | 29.12 | 91.1 | 21.624 | 1.513 | 139 | 13.07 | 896 | 1.001 | 18.15 | 1.269 | 846 | 2.33 | 1018 | 0.994 | 915 | 0.829 | 18492 | 77.70 | 12.67 | 65.0 |
| | 848 | 23 | 0.28 | 46.6 | 29.12 | 91.3 | 22.970 | 1.607 | 141 | 14.16 | 957 | 1.001 | 19.38 | 1.355 | 880 | 2.63 | 1159 | 0.995 | 988 | 0.896 | 22672 | 80.60 | 13.55 | 67.0 |
| | 849 | 22 | 0.28 | 46.7 | 29.12 | 91.7 | 24.713 | 1.729 | 144 | 15.37 | 1025 | 0.999 | 21.70 | 1.518 | 965 | 3.08 | 1390 | 1.002 | 1085 | 0.984 | 28411 | 85.00 | 14.53 | 70.5 |
| | 850 | 21 | 0.28 | 46.3 | 29.12 | 91.5 | 26.227 | 1.835 | 145 | 16.29 | 1075 | 0.994 | 23.98 | 1.677 | 1044 | 3.41 | 1580 | 1.006 | 1163 | 1.054 | 33494 | 88.90 | 15.25 | 73.7 |
| | 851 | 20 | 0.28 | 46.4 | 29.10 | 91.9 | 27.029 | 1.891 | 146 | 16.74 | 1100 | 0.993 | 25.59 | 1.790 | 1085 | 3.60 | 1693 | 1.001 | 1205 | 1.093 | 36192 | 90.80 | 15.59 | 75.2 |
| | 852 | 21 | 0.20 | 46.3 | 29.12 | 91.3 | 26.280 | 1.838 | 145 | 16.34 | 1077 | 0.994 | 24.24 | 1.696 | 1047 | 3.44 | 1597 | 1.002 | 1168 | 1.059 | 37215 | 92.30 | 15.71 | 76.6 |
| | 853 | 21 | 0.00 | 46.2 | 29.12 | 91.7 | 26.257 | 1.837 | 144 | 16.33 | 1076 | 0.994 | 23.85 | 1.668 | 1045 | 3.38 | 1574 | 1.002 | 1161 | 1.053 | 45428 | 95.80 | 16.57 | 79.2 |

## Aeroacoustic Summary Data — Model 3 – Configuration 3DXB, 20-External-Doublet Core Nozzle, Baseline Fan Nozzle

| Date | Point | Cycle | XMA | $T_{amb}$ | $P_{amb}$ | RH | $P_{18}$ | PFQPA | $T_{18}$ | $W_{18}$ | $V_{18}$ | $CD_{18}$ | $P_8$ | P8QPA | $T_8$ | $W_8$ | $V_8$ | $CD_8$ | $V_{mix}$ | $V_{mix}/c_{amb}$ | $F_N$ | EPNL | NF | NEPNL |
|---|---|---|---|---|---|---|---|---|---|---|---|---|---|---|---|---|---|---|---|---|---|---|---|---|
| 4/17/97 | 878 | 24 | 0.28 | 35.3 | 29.12 | 86.6 | 21.612 | 1.512 | 142 | 12.85 | 897 | 0.988 | 18.26 | 1.277 | 850 | 2.13 | 1032 | 0.898 | 916 | 0.840 | 18111 | 78.80 | 12.58 | 66.2 |
| | 879 | 23 | 0.28 | 35.2 | 29.12 | 86.5 | 22.880 | 1.600 | 142 | 13.86 | 954 | 0.987 | 19.29 | 1.349 | 887 | 2.38 | 1154 | 0.909 | 983 | 0.901 | 21845 | 81.70 | 13.39 | 68.3 |
| | 880 | 22 | 0.28 | 34.7 | 29.12 | 87.8 | 24.716 | 1.729 | 140 | 15.18 | 1021 | 0.984 | 21.55 | 1.507 | 959 | 2.83 | 1377 | 0.928 | 1077 | 0.988 | 27547 | 86.80 | 14.40 | 72.4 |
| | 881 | 21 | 0.28 | 34.8 | 29.12 | 88.4 | 26.210 | 1.833 | 140 | 16.11 | 1071 | 0.978 | 23.99 | 1.678 | 1044 | 3.20 | 1581 | 0.943 | 1156 | 1.060 | 32483 | 91.40 | 15.12 | 76.3 |
| | 882 | 20 | 0.28 | 34.7 | 29.12 | 88.4 | 27.086 | 1.894 | 143 | 16.53 | 1099 | 0.974 | 25.56 | 1.788 | 1080 | 3.41 | 1689 | 0.948 | 1200 | 1.101 | 35450 | 94.20 | 15.50 | 78.7 |
| | 883 | 21 | 0.20 | 34.6 | 29.12 | 90.6 | 26.218 | 1.833 | 142 | 16.05 | 1072 | 0.978 | 24.19 | 1.691 | 1042 | 3.23 | 1592 | 0.942 | 1159 | 1.063 | 36121 | 95.80 | 15.58 | 80.2 |
| | 884 | 21 | 0.00 | 34.6 | 29.12 | 90.6 | 26.108 | 1.826 | 141 | 16.00 | 1068 | 0.977 | 23.98 | 1.677 | 1044 | 3.20 | 1580 | 0.943 | 1153 | 1.058 | 43827 | 99.50 | 16.42 | 83.1 |

## Aeroacoustic Summary Data

## Model 4 – Configuration 4BB, Baseline Core Nozzle, Baseline Fan Nozzle

| Date | Point | Cycle | XMA | $T_{amb}$ | $P_{amb}$ | RH | $P_{18}$ | PFQPA | $T_{18}$ | $W_{18}$ | $V_{18}$ | $CD_{18}$ | $P_8$ | P8QPA | $T_8$ | $W_8$ | $V_8$ | $CD_8$ | $V_{mix}$ | $V_{mix}/c_{amb}$ | $F_N$ | EPNL | NF | NEPNL |
|---|---|---|---|---|---|---|---|---|---|---|---|---|---|---|---|---|---|---|---|---|---|---|---|---|
| 4/21/97 | 971 | 45 | 0.28 | 53.9 | 28.88 | 44.2 | 17.762 | 1.253 | 140 | 10.23 | 670 | | 16.66 | 1.175 | 815 | 1.10 | 830 | | 686 | 0.617 | 8408 | 71.10 | 9.25 | 61.9 |
| | 972 | 44 | 0.28 | 54.0 | 28.88 | 44.8 | 19.026 | 1.342 | 140 | 11.90 | 762 | | 17.26 | 1.217 | 856 | 1.20 | 929 | | 777 | 0.699 | 12214 | 73.80 | 10.87 | 62.9 |
| | 973 | 43 | 0.28 | 54.1 | 28.88 | 45.2 | 20.451 | 1.442 | 141 | 13.49 | 847 | | 18.89 | 1.332 | 948 | 1.50 | 1153 | | 878 | 0.790 | 16974 | 77.30 | 12.30 | 65.0 |
| | 974 | 42 | 0.28 | 54.0 | 28.90 | 45.3 | 21.650 | 1.526 | 141 | 14.63 | 906 | | 20.28 | 1.430 | 996 | 1.72 | 1304 | | 949 | 0.853 | 20847 | 80.70 | 13.19 | 67.5 |
| | 975 | 41 | 0.28 | 54.0 | 28.88 | 45.5 | 22.273 | 1.571 | 141 | 15.15 | 935 | | 21.60 | 1.523 | 1069 | 1.90 | 1442 | | 992 | 0.892 | 23171 | 83.50 | 13.65 | 69.9 |
| | 976 | 40 | 0.28 | 54.5 | 28.88 | 45.4 | 23.034 | 1.624 | 141 | 15.77 | 966 | | 22.57 | 1.591 | 1129 | 1.98 | 1540 | | 1031 | 0.927 | 25482 | 85.90 | 14.06 | 71.8 |
| | 980 | 33 | 0.28 | 53.5 | 28.90 | 48.3 | 17.833 | 1.257 | 140 | 10.34 | 675 | | 15.76 | 1.110 | 774 | 0.78 | 660 | | 674 | 0.607 | 8038 | 70.60 | 9.05 | 61.5 |
| | 979 | 32 | 0.28 | 53.3 | 28.90 | 47.9 | 19.276 | 1.359 | 141 | 12.19 | 778 | | 16.64 | 1.173 | 814 | 1.02 | 826 | | 781 | 0.704 | 12376 | 73.70 | 10.93 | 62.8 |
| | 978 | 31 | 0.28 | 54.0 | 28.90 | 46.2 | 20.820 | 1.468 | 141 | 13.87 | 866 | | 17.79 | 1.254 | 872 | 1.27 | 1001 | | 877 | 0.789 | 17060 | 76.80 | 12.32 | 64.5 |
| | 977 | 30 | 0.28 | 55.0 | 28.90 | 44.6 | 22.176 | 1.563 | 141 | 15.12 | 930 | | 19.16 | 1.351 | 925 | 1.52 | 1170 | | 952 | 0.856 | 21265 | 79.80 | 13.28 | 66.5 |
| | 982 | 44 | 0.20 | 53.6 | 28.90 | 48.2 | 19.050 | 1.343 | 140 | 11.97 | 763 | | 17.24 | 1.215 | 858 | 1.21 | 926 | | 778 | 0.700 | 14560 | 76.50 | 11.63 | 64.9 |
| | 981 | 32 | 0.20 | 53.3 | 28.90 | 47.9 | 19.227 | 1.355 | 140 | 12.20 | 774 | | 16.60 | 1.170 | 818 | 1.02 | 821 | | 778 | 0.700 | 14591 | 76.50 | 11.64 | 64.9 |
| | 983 | 44 | 0.00 | 54.2 | 28.90 | 47.1 | 19.032 | 1.341 | 142 | 11.94 | 762 | | 17.17 | 1.210 | 864 | 1.20 | 918 | | 777 | 0.699 | 19897 | 80.40 | 12.99 | 67.4 |
| | 991 | 43 | 0.00 | 53.6 | 28.90 | 50.2 | 20.473 | 1.443 | 143 | 13.50 | 848 | | 18.92 | 1.333 | 953 | 1.52 | 1157 | | 880 | 0.792 | 26176 | 86.50 | 14.18 | 72.3 |
| | 984 | 42 | 0.00 | 54.3 | 28.90 | 47.8 | 21.641 | 1.525 | 142 | 14.67 | 906 | | 20.55 | 1.448 | 1007 | 1.78 | 1330 | | 952 | 0.857 | 31066 | 90.70 | 14.92 | 75.8 |
| | 989 | 41 | 0.00 | 53.9 | 28.90 | 49.7 | 22.245 | 1.568 | 143 | 15.17 | 934 | | 21.63 | 1.525 | 1069 | 1.91 | 1444 | | 992 | 0.892 | 33567 | 93.10 | 15.26 | 77.8 |
| | 985 | 40 | 0.00 | 54.4 | 28.90 | 47.2 | 23.126 | 1.630 | 143 | 15.88 | 971 | | 22.68 | 1.598 | 1129 | 2.02 | 1547 | | 1037 | 0.932 | 36824 | 95.30 | 15.66 | 79.6 |
| | 992 | 33 | 0.00 | 53.3 | 28.90 | 52.5 | 17.881 | 1.260 | 142 | 10.47 | 679 | | 15.84 | 1.116 | 764 | 0.86 | 674 | | 679 | 0.612 | 15284 | 76.30 | 11.84 | 64.5 |
| | 986 | 32 | 0.00 | 54.8 | 28.90 | 46.8 | 19.254 | 1.357 | 142 | 12.16 | 777 | | 16.67 | 1.175 | 830 | 1.05 | 835 | | 782 | 0.703 | 20406 | 80.70 | 13.10 | 67.6 |
| | 990 | 31 | 0.00 | 53.5 | 28.90 | 50.4 | 20.657 | 1.456 | 143 | 13.70 | 858 | | 17.85 | 1.258 | 879 | 1.31 | 1011 | | 871 | 0.784 | 26001 | 85.30 | 14.15 | 71.2 |
| | 987 | 30 | 0.00 | 54.4 | 28.90 | 47.8 | 22.105 | 1.558 | 142 | 15.13 | 928 | | 19.06 | 1.343 | 918 | 1.52 | 1157 | | 949 | 0.853 | 31310 | 97.60 | 14.96 | 82.6 |
| | 988 | 30 | 0.00 | 54.6 | 28.90 | 48.5 | 22.100 | 1.558 | 142 | 15.10 | 928 | | 19.05 | 1.342 | 922 | 1.52 | 1157 | | 949 | 0.853 | 31321 | 89.10 | 14.96 | 74.1 |

## Aeroacoustic Summary Data

## Model 5 – Configuration 5BB, Baseline Core Nozzle, Baseline Fan Nozzle

| Date | Point | Cycle | XMA | $T_{amb}$ | $P_{amb}$ | RH | $P_{18}$ | PFQPA | $T_{18}$ | $W_{18}$ | $V_{18}$ | $CD_{18}$ | $P_8$ | P8QPA | $T_8$ | $W_8$ | $V_8$ | $CD_8$ | $V_{mix}$ | $V_{mix}/c_{amb}$ | $F_N$ | EPNL | NF | NEPNL |
|---|---|---|---|---|---|---|---|---|---|---|---|---|---|---|---|---|---|---|---|---|---|---|---|---|
| 4/22/97 | 996 | 45 | 0.28 | 44.8 | 28.92 | 79.0 | 17.778 | 1.252 | 138 | 10.24 | 668 | | 16.35 | 1.152 | 819 | 1.28 | 780 | | 681 | 0.618 | 8576 | 71.20 | 9.33 | 61.9 |
| | 997 | 44 | 0.28 | 45.0 | 28.92 | 78.6 | 19.098 | 1.345 | 140 | 11.93 | 765 | | 17.27 | 1.217 | 868 | 1.51 | 933 | | 784 | 0.711 | 12761 | 74.20 | 11.06 | 63.1 |
| | 998 | 43 | 0.28 | 44.8 | 28.92 | 78.8 | 20.546 | 1.446 | 140 | 13.54 | 849 | | 18.94 | 1.333 | 946 | 1.85 | 1154 | | 886 | 0.804 | 17683 | 78.40 | 12.48 | 65.9 |
| | 999 | 42 | 0.28 | 44.7 | 28.92 | 78.9 | 21.663 | 1.525 | 140 | 14.61 | 904 | | 20.47 | 1.441 | 998 | 2.11 | 1318 | | 957 | 0.869 | 21547 | 81.70 | 13.33 | 68.4 |
| | 1000 | 41 | 0.28 | 45.3 | 28.92 | 78.6 | 22.346 | 1.573 | 140 | 15.20 | 935 | | 21.45 | 1.511 | 1063 | 2.22 | 1427 | | 998 | 0.906 | 23824 | 84.30 | 13.77 | 70.5 |
| | 1001 | 40 | 0.28 | 45.5 | 28.92 | 78.4 | 23.040 | 1.622 | 140 | 15.77 | 964 | | 22.80 | 1.605 | 1124 | 2.37 | 1551 | | 1041 | 0.945 | 26343 | 87.40 | 14.21 | 73.2 |
| | 1005 | 33 | 0.28 | 43.2 | 28.92 | 83.9 | 17.912 | 1.261 | 139 | 10.43 | 679 | | 15.79 | 1.112 | 780 | 1.06 | 667 | | 678 | 0.616 | 8442 | 71.70 | 9.26 | 62.4 |
| | 1004 | 32 | 0.28 | 43.7 | 28.94 | 83.1 | 19.305 | 1.359 | 140 | 12.21 | 777 | | 16.53 | 1.164 | 816 | 1.29 | 807 | | 780 | 0.709 | 12632 | 74.00 | 11.01 | 63.0 |
| | 1003 | 31 | 0.28 | 44.2 | 28.94 | 81.1 | 20.796 | 1.464 | 140 | 13.81 | 862 | | 17.97 | 1.265 | 871 | 1.66 | 1019 | | 879 | 0.799 | 17522 | 77.40 | 12.44 | 65.0 |
| | 1002 | 30 | 0.28 | 44.8 | 28.94 | 79.4 | 22.093 | 1.555 | 141 | 15.02 | 924 | | 19.15 | 1.348 | 922 | 1.88 | 1165 | | 952 | 0.864 | 21565 | 80.30 | 13.34 | 67.0 |
| | 1006 | 44 | 0.20 | 43.0 | 28.94 | 83.6 | 19.061 | 1.341 | 139 | 11.95 | 760 | | 17.25 | 1.213 | 870 | 1.51 | 926 | | 779 | 0.709 | 14939 | 76.90 | 11.74 | 65.2 |
| | 1007 | 32 | 0.20 | 43.0 | 28.94 | 83.8 | 19.296 | 1.358 | 140 | 12.21 | 777 | | 16.48 | 1.160 | 820 | 1.28 | 799 | | 779 | 0.709 | 14993 | 77.00 | 11.76 | 65.2 |
| | 1012 | 44 | 0.00 | 45.0 | 28.94 | 79.2 | 19.066 | 1.342 | 140 | 11.94 | 762 | | 17.44 | 1.227 | 865 | 1.58 | 951 | | 784 | 0.712 | 20797 | 81.80 | 13.18 | 68.6 |
| | 1014 | 43 | 0.00 | 44.9 | 28.94 | 78.8 | 20.528 | 1.445 | 140 | 13.56 | 848 | | 18.93 | 1.332 | 952 | 1.86 | 1155 | | 885 | 0.804 | 26839 | 87.50 | 14.29 | 73.2 |
| | 1015 | 42 | 0.00 | 45.1 | 28.94 | 78.7 | 21.686 | 1.526 | 141 | 14.67 | 906 | | 20.46 | 1.439 | 1002 | 2.12 | 1317 | | 958 | 0.870 | 31609 | 91.70 | 15.00 | 76.7 |
| | 1016 | 41 | 0.00 | 45.3 | 28.96 | 77.5 | 22.330 | 1.571 | 141 | 15.23 | 934 | | 21.58 | 1.518 | 1063 | 2.25 | 1434 | | 999 | 0.907 | 34405 | 94.10 | 15.37 | 78.7 |
| | 1017 | 40 | 0.00 | 45.2 | 28.96 | 78.8 | 23.086 | 1.624 | 141 | 15.83 | 966 | | 22.94 | 1.614 | 1124 | 2.40 | 1559 | | 1045 | 0.948 | 37520 | 96.40 | 15.74 | 80.7 |
| | 1008 | 33 | 0.00 | 44.0 | 28.94 | 82.1 | 17.900 | 1.260 | 140 | 10.49 | 678 | | 15.65 | 1.101 | 776 | 1.04 | 635 | | 674 | 0.613 | 15220 | 77.00 | 11.82 | 65.2 |
| | 1009 | 32 | 0.00 | 44.3 | 28.94 | 81.2 | 19.230 | 1.353 | 140 | 12.19 | 772 | | 16.54 | 1.164 | 818 | 1.33 | 807 | | 776 | 0.705 | 20601 | 81.10 | 13.14 | 68.0 |
| | 1010 | 31 | 0.00 | 44.3 | 28.94 | 80.2 | 20.725 | 1.459 | 140 | 13.81 | 859 | | 17.91 | 1.260 | 872 | 1.68 | 1011 | | 875 | 0.795 | 26661 | 85.90 | 14.26 | 71.6 |
| | 1011 | 30 | 0.00 | 44.5 | 28.94 | 79.4 | 22.098 | 1.555 | 140 | 15.10 | 924 | | 19.33 | 1.360 | 931 | 1.95 | 1185 | | 955 | 0.867 | 32017 | 90.30 | 15.05 | 75.2 |

## Aeroacoustic Summary Data

## Model 5 – Configuration 5C12B, 12-Chevron Core Nozzle, Baseline Fan Nozzle

| Date | Point | Cycle | XMA | $T_{amb}$ | $P_{amb}$ | RH | $P_{18}$ | PFQPA | $T_{18}$ | $W_{18}$ | $V_{18}$ | $CD_{18}$ | $P_8$ | P8QPA | $T_8$ | $W_8$ | $V_8$ | $CD_8$ | $V_{mix}$ | $V_{mix}/c_{amb}$ | $F_N$ | EPNL | NF | NEPNL |
|---|---|---|---|---|---|---|---|---|---|---|---|---|---|---|---|---|---|---|---|---|---|---|---|---|
| 4/22/97 | 1018 | 45 | 0.28 | 43.5 | 28.96 | 82.6 | 17.782 | 1.251 | 139 | 10.23 | 668 | | 16.39 | 1.153 | 814 | 1.34 | 781 | | 680 | 0.618 | 8567 | 71.50 | 9.33 | 62.2 |
| | 1019 | 44 | 0.28 | 43.4 | 28.96 | 83.0 | 19.122 | 1.345 | 141 | 11.97 | 765 | | 17.34 | 1.220 | 863 | 1.58 | 937 | | 785 | 0.714 | 12802 | 74.50 | 11.07 | 63.4 |
| | 1021 | 43 | 0.28 | 43.5 | 28.96 | 83.5 | 20.548 | 1.445 | 141 | 13.48 | 849 | | 18.90 | 1.329 | 949 | 1.89 | 1149 | | 886 | 0.805 | 17669 | 77.90 | 12.47 | 65.4 |
| | 1022 | 42 | 0.28 | 43.5 | 28.96 | 83.4 | 21.696 | 1.526 | 141 | 14.62 | 906 | | 20.56 | 1.446 | 1004 | 2.17 | 1326 | | 961 | 0.873 | 21812 | 81.30 | 13.39 | 67.9 |
| | 1023 | 41 | 0.28 | 43.9 | 28.96 | 82.7 | 22.346 | 1.571 | 143 | 15.17 | 936 | | 21.69 | 1.525 | 1063 | 2.32 | 1441 | | 1004 | 0.912 | 24237 | 84.30 | 13.84 | 70.5 |
| | 1024 | 40 | 0.28 | 43.5 | 28.96 | 83.8 | 23.055 | 1.622 | 142 | 15.74 | 966 | | 22.81 | 1.604 | 1124 | 2.43 | 1550 | | 1045 | 0.950 | 26469 | 86.70 | 14.23 | 72.5 |
| | 1025 | 44 | 0.20 | 43.4 | 28.96 | 84.4 | 19.104 | 1.344 | 140 | 11.94 | 764 | | 17.37 | 1.222 | 861 | 1.58 | 940 | | 784 | 0.713 | 15146 | 77.20 | 11.80 | 65.4 |
| | 1026 | 44 | 0.00 | 43.5 | 28.96 | 84.1 | 19.034 | 1.338 | 140 | 11.91 | 758 | | 17.37 | 1.221 | 864 | 1.60 | 939 | | 780 | 0.709 | 20560 | 82.00 | 13.13 | 68.9 |

## Aeroacoustic Summary Data

## Model 5 – Configuration 5C12C, 12-Chevron Core Nozzle, 24-Chevron Fan Nozzle

| Date | Point | Cycle | XMA | $T_{amb}$ | $P_{amb}$ | RH | $P_{18}$ | PFQPA | $T_{18}$ | $W_{18}$ | $V_{18}$ | $CD_{18}$ | $P_8$ | P8QPA | $T_8$ | $W_8$ | $V_8$ | $CD_8$ | $V_{mix}$ | $V_{mix}/c_{amb}$ | $F_N$ | EPNL | NF | NEPNL |
|---|---|---|---|---|---|---|---|---|---|---|---|---|---|---|---|---|---|---|---|---|---|---|---|---|
| 4/22/97 | 1027 | 45 | 0.28 | 45.3 | 28.94 | 78.6 | 17.796 | 1.252 | 137 | 10.39 | 668 | | 16.37 | 1.152 | 816 | 1.33 | 779 | | 681 | 0.618 | 8599 | 71.70 | 9.34 | 62.4 |
| | 1028 | 44 | 0.28 | 44.2 | 28.96 | 82.4 | 19.064 | 1.341 | 139 | 12.07 | 760 | | 17.36 | 1.221 | 859 | 1.59 | 937 | | 781 | 0.710 | 12915 | 73.90 | 11.11 | 62.8 |
| | 1029 | 43 | 0.28 | 44.2 | 28.96 | 85.8 | 20.466 | 1.440 | 140 | 13.67 | 844 | 1.003 | 18.83 | 1.325 | 939 | 1.89 | 1141 | 0.937 | 880 | 0.800 | 17709 | 77.90 | 12.48 | 65.4 |
| | 1030 | 42 | 0.28 | 43.2 | 28.94 | 89.5 | 21.565 | 1.517 | 140 | 14.75 | 899 | | 20.50 | 1.442 | 999 | 2.17 | 1319 | | 954 | 0.867 | 21775 | 81.80 | 13.38 | 68.4 |
| | 1031 | 41 | 0.28 | 43.0 | 28.94 | 90.8 | 22.322 | 1.571 | 140 | 15.44 | 934 | | 21.52 | 1.514 | 1062 | 2.29 | 1430 | | 999 | 0.908 | 24390 | 83.40 | 13.87 | 69.5 |
| | 1032 | 40 | 0.28 | 42.7 | 28.96 | 91.3 | 22.899 | 1.611 | 141 | 15.91 | 958 | | 22.80 | 1.604 | 1124 | 2.44 | 1550 | | 1038 | 0.944 | 26612 | 86.20 | 14.25 | 71.9 |
| | 1033 | 44 | 0.20 | 42.7 | 28.94 | 91.2 | 19.158 | 1.348 | 140 | 12.16 | 767 | | 17.34 | 1.220 | 865 | 1.57 | 938 | | 787 | 0.716 | 15303 | 76.60 | 11.85 | 64.8 |
| | 1034 | 44 | 0.00 | 43.2 | 28.94 | 90.4 | 19.059 | 1.341 | 140 | 12.09 | 761 | | 17.28 | 1.216 | 866 | 1.58 | 930 | | 780 | 0.710 | 21042 | 80.90 | 13.23 | 67.7 |

## Aeroacoustic Summary Data

## Model 5 – Configuration 5BC, Baseline Core Nozzle, 24-Chevron Fan Nozzle

| Date | Point | Cycle | XMA | $T_{amb}$ | $P_{amb}$ | RH | $P_{18}$ | PFQPA | $T_{18}$ | $W_{18}$ | $V_{18}$ | $CD_{18}$ | $P_8$ | P8QPA | $T_8$ | $W_8$ | $V_8$ | $CD_8$ | $V_{mix}$ | $V_{mix}/c_{amb}$ | $F_N$ | EPNL | NF | NEPNL |
|---|---|---|---|---|---|---|---|---|---|---|---|---|---|---|---|---|---|---|---|---|---|---|---|---|
| 4/22/97 | 1036 | 44 | 0.28 | 42.2 | 28.92 | 88.3 | 19.077 | 1.343 | 141 | 12.04 | 764 | | 17.35 | 1.221 | 861 | 1.53 | 938 | | 784 | 0.713 | 12864 | 74.40 | 11.09 | 63.3 |
| | 1037 | 43 | 0.28 | 42.2 | 28.94 | 88.4 | 20.477 | 1.441 | 142 | 13.65 | 846 | | 19.02 | 1.338 | 945 | 1.87 | 1161 | | 884 | 0.805 | 17814 | 77.90 | 12.51 | 65.4 |
| | 1038 | 42 | 0.28 | 42.2 | 28.94 | 88.0 | 21.605 | 1.520 | 142 | 14.80 | 903 | | 20.44 | 1.438 | 1002 | 2.10 | 1316 | | 955 | 0.869 | 21806 | 81.00 | 13.39 | 67.6 |
| | 1039 | 41 | 0.28 | 42.6 | 28.96 | 87.3 | 22.377 | 1.574 | 141 | 15.46 | 937 | | 21.67 | 1.524 | 1060 | 2.25 | 1439 | | 1001 | 0.911 | 24445 | 83.60 | 13.88 | 69.7 |
| | 1040 | 40 | 0.28 | 42.7 | 28.96 | 87.6 | 23.102 | 1.625 | 142 | 16.04 | 967 | | 22.91 | 1.611 | 1122 | 2.38 | 1556 | | 1044 | 0.950 | 26968 | 86.20 | 14.31 | 71.9 |
| | 1041 | 44 | 0.20 | 42.8 | 28.96 | 87.4 | 19.022 | 1.338 | 141 | 12.01 | 759 | | 17.33 | 1.219 | 860 | 1.53 | 934 | | 779 | 0.709 | 15021 | 76.70 | 11.77 | 64.9 |
| | 1042 | 44 | 0.00 | 43.0 | 28.96 | 87.6 | 19.016 | 1.338 | 141 | 12.04 | 759 | | 17.42 | 1.225 | 866 | 1.57 | 947 | | 781 | 0.710 | 20820 | 81.10 | 13.18 | 67.9 |

## Aeroacoustic Summary Data

## Model 6 – Configuration 6TmB, Tongue-Mixer Core Nozzle, Baseline Fan Nozzle

| Date | Point | Cycle | XMA | $T_{amb}$ | $P_{amb}$ | RH | $P_{18}$ | PFQPA | $T_{18}$ | $W_{18}$ | $V_{18}$ | $CD_{18}$ | $P_8$ | P8QPA | $T_8$ | $W_8$ | $V_8$ | $CD_8$ | $V_{mix}$ | $V_{mix}/c_{amb}$ | $F_N$ | EPNL | NF | NEPNL |
|---|---|---|---|---|---|---|---|---|---|---|---|---|---|---|---|---|---|---|---|---|---|---|---|---|
| 5/12/97 | 1240 | 24 | 0.28 | 58.5 | 28.86 | 45.3 | 21.321 | 1.505 | 138 | 12.60 | 890 | | 17.86 | 1.261 | 843 | 2.14 | 1002 | | 906 | 0.812 | 17526 | 78.20 | 12.44 | 65.8 |
| | 1248 | 24 | 0.28 | 59.4 | 28.86 | 41.6 | 21.280 | 1.502 | 138 | 12.58 | 888 | | 17.91 | 1.264 | 833 | 2.17 | 1003 | | 905 | 0.810 | 17359 | 78.10 | 12.40 | 65.7 |
| | 1241 | 23 | 0.28 | 58.3 | 28.86 | 45.4 | 22.716 | 1.603 | 140 | 13.69 | 953 | | 19.05 | 1.345 | 885 | 2.48 | 1145 | | 983 | 0.881 | 21598 | 81.50 | 13.34 | 68.2 |
| | 1249 | 23 | 0.28 | 59.2 | 28.86 | 40.6 | 22.652 | 1.599 | 140 | 13.66 | 951 | | 18.97 | 1.339 | 875 | 2.46 | 1133 | | 979 | 0.876 | 21469 | 81.40 | 13.32 | 68.1 |
| | 1242 | 22 | 0.28 | 58.5 | 28.84 | 45.7 | 24.520 | 1.731 | 141 | 14.98 | 1023 | | 21.35 | 1.507 | 958 | 3.05 | 1372 | | 1083 | 0.970 | 27708 | 86.90 | 14.43 | 72.5 |
| | 1250 | 22 | 0.28 | 58.8 | 28.86 | 41.4 | 24.445 | 1.726 | 141 | 14.93 | 1021 | | 21.33 | 1.506 | 957 | 3.05 | 1371 | | 1081 | 0.968 | 27464 | 86.60 | 14.39 | 72.2 |
| | 1243 | 21 | 0.28 | 58.5 | 28.84 | 45.1 | 25.944 | 1.832 | 141 | 15.89 | 1071 | | 23.88 | 1.686 | 1030 | 3.57 | 1575 | | 1164 | 1.043 | 33027 | 91.30 | 15.19 | 76.1 |
| | 1251 | 21 | 0.28 | 58.9 | 28.86 | 41.2 | 25.875 | 1.826 | 142 | 15.85 | 1069 | | 23.78 | 1.679 | 1033 | 3.55 | 1571 | | 1162 | 1.040 | 32735 | 91.00 | 15.15 | 75.8 |
| | 1244 | 20 | 0.28 | 58.8 | 28.84 | 44.8 | 26.851 | 1.896 | 141 | 16.41 | 1098 | | 25.50 | 1.800 | 1075 | 3.86 | 1689 | | 1212 | 1.085 | 36226 | 92.70 | 15.59 | 77.1 |
| | 1245 | 20 | 0.28 | 58.6 | 28.84 | 44.7 | 26.785 | 1.891 | 141 | 16.34 | 1096 | | 25.35 | 1.790 | 1077 | 3.82 | 1682 | | 1209 | 1.083 | 35969 | 94.00 | 15.56 | 78.4 |
| | 1252 | 20 | 0.28 | 58.8 | 28.86 | 41.5 | 26.779 | 1.890 | 142 | 16.38 | 1097 | | 25.34 | 1.789 | 1071 | 3.84 | 1678 | | 1208 | 1.082 | 35950 | 93.70 | 15.56 | 78.1 |
| | 1246 | 21 | 0.20 | 58.5 | 28.84 | 44.6 | 26.036 | 1.838 | 141 | 15.90 | 1074 | | 23.92 | 1.689 | 1038 | 3.56 | 1582 | | 1168 | 1.046 | 36589 | 94.50 | 15.63 | 78.9 |
| | 1253 | 21 | 0.20 | 59.2 | 28.86 | 41.2 | 26.045 | 1.839 | 143 | 15.91 | 1075 | | 23.89 | 1.686 | 1036 | 3.55 | 1578 | | 1168 | 1.046 | 36505 | 94.30 | 15.62 | 78.7 |
| | 1247 | 21 | 0.00 | 59.1 | 28.84 | 44.5 | 26.008 | 1.836 | 142 | 15.86 | 1073 | | 23.84 | 1.683 | 1040 | 3.55 | 1578 | | 1167 | 1.044 | 44771 | 97.40 | 16.51 | 80.9 |
| | 1254 | 21 | 0.00 | 59.5 | 28.86 | 40.3 | 25.987 | 1.834 | 143 | 15.89 | 1073 | | 23.77 | 1.677 | 1037 | 3.54 | 1571 | | 1165 | 1.043 | 44691 | 97.30 | 16.50 | 80.8 |

## Aeroacoustic Summary Data

## Model 6 – Configuration 6TmC, Tongue-Mixer Core Nozzle, 24-Chevron Fan Nozzle

| Date | Point | Cycle | XMA | $T_{amb}$ | $P_{amb}$ | RH | $P_{18}$ | PFQPA | $T_{18}$ | $W_{18}$ | $V_{18}$ | $CD_{18}$ | $P_8$ | P8QPA | $T_8$ | $W_8$ | $V_8$ | $CD_8$ | $V_{mix}$ | $V_{mix}/c_{amb}$ | $F_N$ | EPNL | NF | NEPNL |
|---|---|---|---|---|---|---|---|---|---|---|---|---|---|---|---|---|---|---|---|---|---|---|---|---|
| 5/12/97 | 1255 | 24 | 0.28 | 58.6 | 28.88 | 39.0 | 21.435 | 1.512 | 139 | 12.88 | 895 | | 18.06 | 1.274 | 847 | 2.21 | 1024 | | 915 | 0.819 | 18248 | 78.70 | 12.61 | 66.1 |
| | 1256 | 23 | 0.28 | 58.6 | 28.86 | 39.5 | 22.704 | 1.602 | 141 | 13.91 | 953 | | 19.18 | 1.353 | 887 | 2.52 | 1157 | | 985 | 0.882 | 22157 | 81.80 | 13.46 | 68.3 |
| | 1257 | 22 | 0.28 | 58.5 | 28.88 | 39.6 | 24.569 | 1.733 | 142 | 15.27 | 1025 | | 21.36 | 1.507 | 962 | 3.05 | 1374 | | 1084 | 0.971 | 28166 | 86.50 | 14.50 | 72.0 |
| | 1258 | 21 | 0.28 | 58.4 | 28.88 | 39.2 | 25.989 | 1.833 | 143 | 16.17 | 1073 | | 23.83 | 1.681 | 1039 | 3.55 | 1576 | | 1165 | 1.044 | 33461 | 90.70 | 15.25 | 75.5 |
| | 1259 | 20 | 0.28 | 58.3 | 28.86 | 39.7 | 26.786 | 1.890 | 142 | 16.57 | 1097 | | 25.42 | 1.793 | 1082 | 3.84 | 1687 | | 1209 | 1.083 | 36381 | 93.30 | 15.61 | 77.7 |
| | 1260 | 21 | 0.20 | 57.6 | 28.88 | 40.6 | 26.005 | 1.834 | 141 | 16.24 | 1071 | | 23.85 | 1.682 | 1040 | 3.56 | 1577 | | 1163 | 1.043 | 37055 | 93.40 | 15.69 | 77.7 |
| | 1261 | 21 | 0.00 | 57.6 | 28.88 | 40.7 | 25.911 | 1.827 | 140 | 16.12 | 1068 | | 23.72 | 1.673 | 1041 | 3.54 | 1570 | | 1159 | 1.039 | 45082 | 96.60 | 16.54 | 80.1 |

## Aeroacoustic Summary Data

## Model 7 – Configuration 7BB, Baseline Core Nozzle, Baseline Fan Nozzle

| Date | Point | Cycle | XMA | $T_{amb}$ | $P_{amb}$ | RH | $P_{18}$ | PFQPA | $T_{18}$ | $W_{18}$ | $V_{18}$ | $CD_{18}$ | $P_8$ | P8QPA | $T_8$ | $W_8$ | $V_8$ | $CD_8$ | $V_{mix}$ | $V_{mix}/c_{amb}$ | $F_N$ | EPNL | NF | NEPNL |
|---|---|---|---|---|---|---|---|---|---|---|---|---|---|---|---|---|---|---|---|---|---|---|---|---|
| 5/12/97 | 1267 | 71 | 0.28 | 52.5 | 28.92 | 52.2 | 20.162 | 1.420 | 140 | 13.16 | 829 | | 19.09 | 1.345 | 979 | 0.99 | 1185 | | 854 | 0.769 | 15334 | 76.10 | 11.86 | 64.2 |
| | 1262 | 74 | 0.20 | 53.5 | 28.92 | 48.9 | 17.515 | 1.234 | 141 | 9.93 | 649 | | 16.30 | 1.148 | 832 | 0.67 | 775 | | 657 | 0.591 | 9239 | 72.30 | 9.66 | 62.6 |
| | 1263 | 73 | 0.20 | 53.4 | 28.92 | 48.9 | 18.270 | 1.287 | 141 | 10.96 | 709 | | 17.39 | 1.225 | 899 | 0.82 | 959 | | 726 | 0.654 | 11877 | 74.70 | 10.75 | 64.0 |
| | 1264 | 72 | 0.20 | 53.0 | 28.92 | 49.8 | 19.040 | 1.341 | 143 | 11.89 | 763 | | 18.15 | 1.278 | 944 | 0.90 | 1068 | | 785 | 0.707 | 14415 | 76.80 | 11.59 | 65.2 |
| | 1265 | 71 | 0.20 | 53.2 | 28.92 | 51.0 | 19.923 | 1.403 | 143 | 12.90 | 817 | | 19.07 | 1.343 | 979 | 1.00 | 1182 | | 844 | 0.760 | 17264 | 79.30 | 12.37 | 66.9 |
| | 1266 | 70 | 0.20 | 53.0 | 28.92 | 52.3 | 20.634 | 1.453 | 141 | 13.64 | 855 | | 20.21 | 1.423 | 1016 | 1.11 | 1304 | | 889 | 0.801 | 19610 | 81.80 | 12.92 | 68.9 |
| | 1268 | 71 | 0.00 | 52.7 | 28.92 | 51.5 | 20.122 | 1.417 | 139 | 13.15 | 826 | | 19.01 | 1.338 | 984 | 0.99 | 1177 | | 850 | 0.766 | 23592 | 84.30 | 13.73 | 70.6 |

# Appendix C
# Selected Acoustic Data: Baseline BPR=5 External Plug Nozzle with Various Core Nozzle Noise-Reduction Concepts

This appendix presents comparison plots of data measured for Model 3 with baseline fan nozzle and various core nozzle noise-reduction concepts. Model operating conditions were:

- Test Point 21, Cycle 2
- Takeoff Thrust ≈ 33,000 lbf (One Engine)
- Altitude = 1500 ft
- Simulated Flight Mach Number = 0.28

The following comparisons are included:

1. Overall Sound Pressure Lavel (OASPL) Directivity
2. Perceived Noise Level (PNL) Directivity
3. Sound Pressure Level (SPL) Spectra at 60°, 70°, 80°, 90°, 100°, 110°, 120°, 130°, 140°, 150°, and 160° (11 Plots)
4. Noy Spectra at 60°, 70°, 80°, 90°, 100°, 110°, 120°, 130°, 140°, 150°, and 160° (11 Plots)

| | Configuration | | | | |
|---|---|---|---|---|---|
| | **3BB** | **3C12B** | **3C8B** | **3IB** | **3AB** |
| Data Symbol | □ | ○ | Δ | + | × |
| Core Nozzle | Base | 12 Chevrons | 8 Chevrons | 12 In-Flip Chevrons | 12 Alt-Flip Chevrons |
| Fan Nozzle | Base | Base | Base | Base | Base |
| Test Point | 734 | 740 | 761 | 770 | 777 |
| Total Temperature, °F | | | | | |
| Ambient ($T_{amb}$) | 43.5 | 41.1 | 47.4 | 45.8 | 44.4 |
| Core Nozzle ($T_8$) | 1041.2 | 1046.7 | 1043 | 1038.9 | 1047.8 |
| Fan Nozzle ($T_{18}$) | 141.4 | 142.2 | 142.9 | 141.6 | 143 |
| Pressure Ratio | | | | | |
| Core Nozzle (P8PQA) | 1.681 | 1.686 | 1.674 | 1.685 | 1.676 |
| Fan Nozzle (PFQPA) | 1.832 | 1.833 | 1.836 | 1.830 | 1.838 |
| Ideal Exit Velocity, ft/s | | | | | |
| Core Nozzle ($V_8$) | 1583 | 1590 | 1577 | 1584 | 1581 |
| Fan Nozzle ($V_{18}$) | 1071 | 1072 | 1074 | 1071 | 1075 |
| Mass-Averaged (Vmix) | 1156 | 1161 | 1160 | 1157 | 1164 |
| Net Thrust ($F_N$), lbf | 32,750 | 32,993 | 33,202 | 32,872 | 33,643 |
| 1500-ft EPNL | 91.8 | 90.7 | 90.0 | 89.3 | 89.8 |

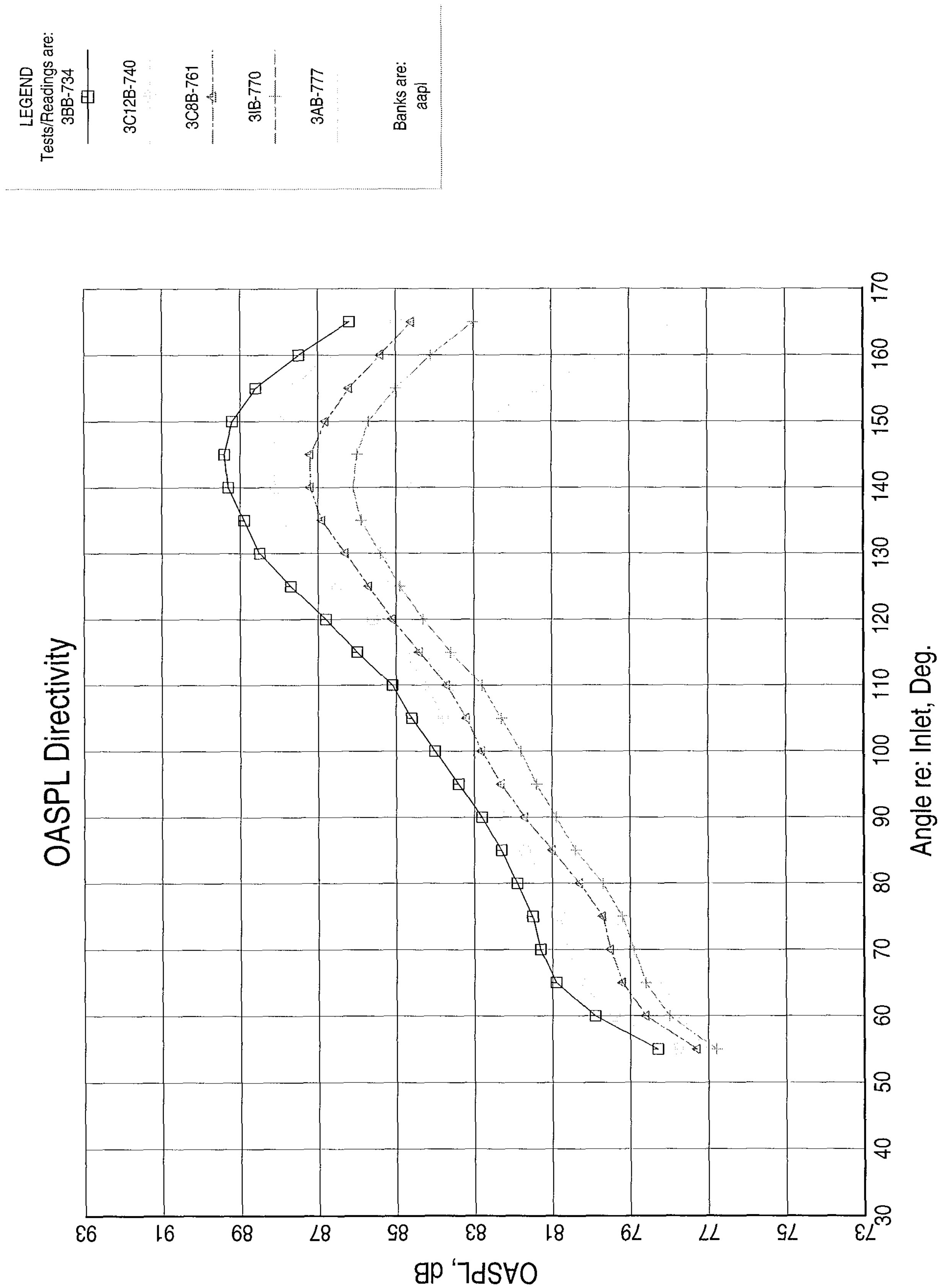
OASPL Directivity
OASPL, dB
93
91
89
87
85
83
81
79
77
75
73
30
40
50
60
70
80
90
100
110
120
130
140
150
160
170
Angle re: Inlet, Deg.
LEGEND
Tests/Readings are:
3BB-734
3C12B-740
3C8B-761
3IB-770
3AB-777
Banks are:
aapl

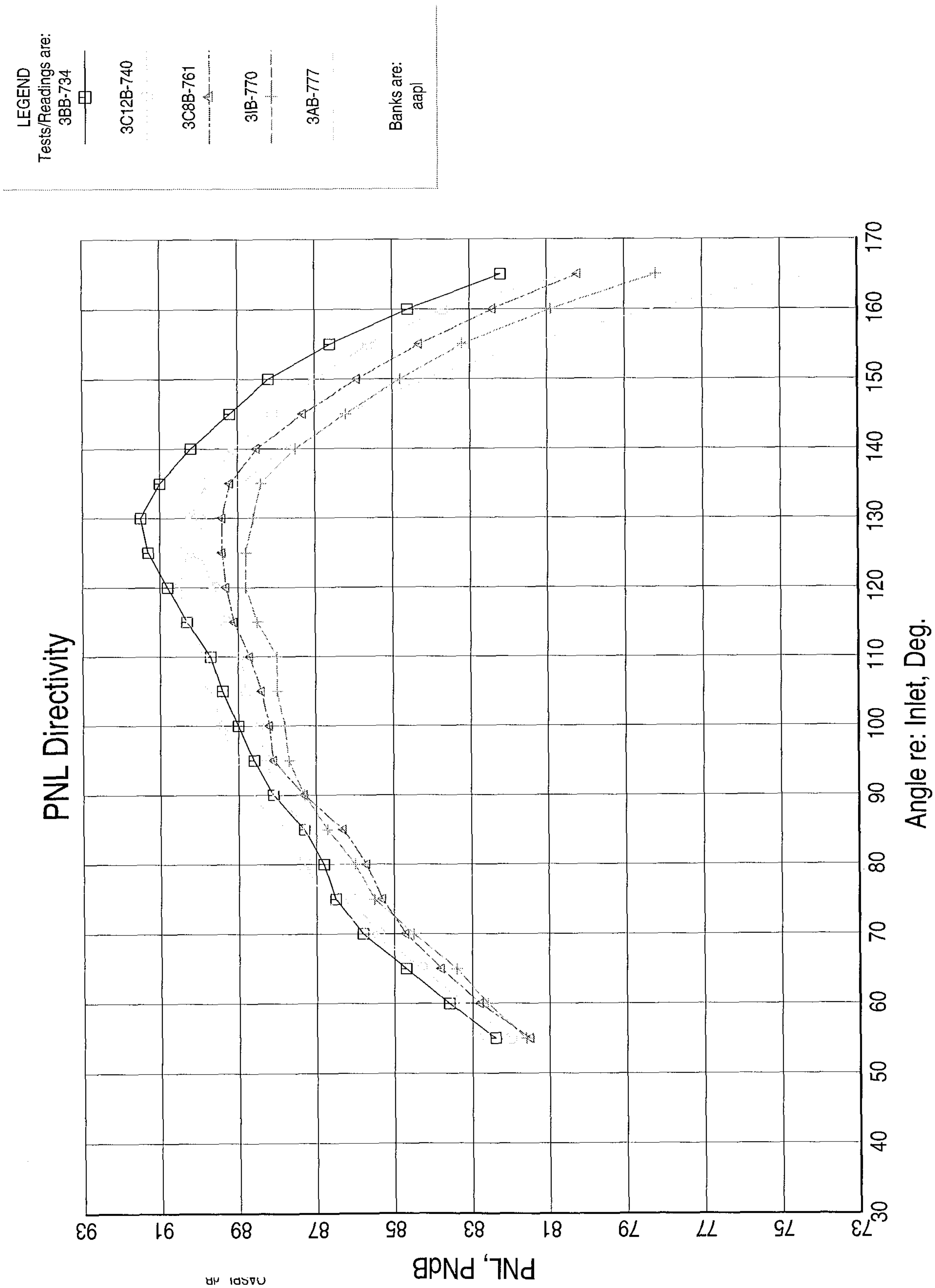
PNL Directivity
LEGEND
Tests/Readings are:
3BB-734
3C12B-740
3C8B-761
3IB-770
3AB-777
Banks are:
aapl
PNL, PNdB
Angle re: Inlet, Deg.
93
91
89
87
85
83
81
79
77
75
73
30
40
50
60
70
80
90
100
110
120
130
140
150
160
170

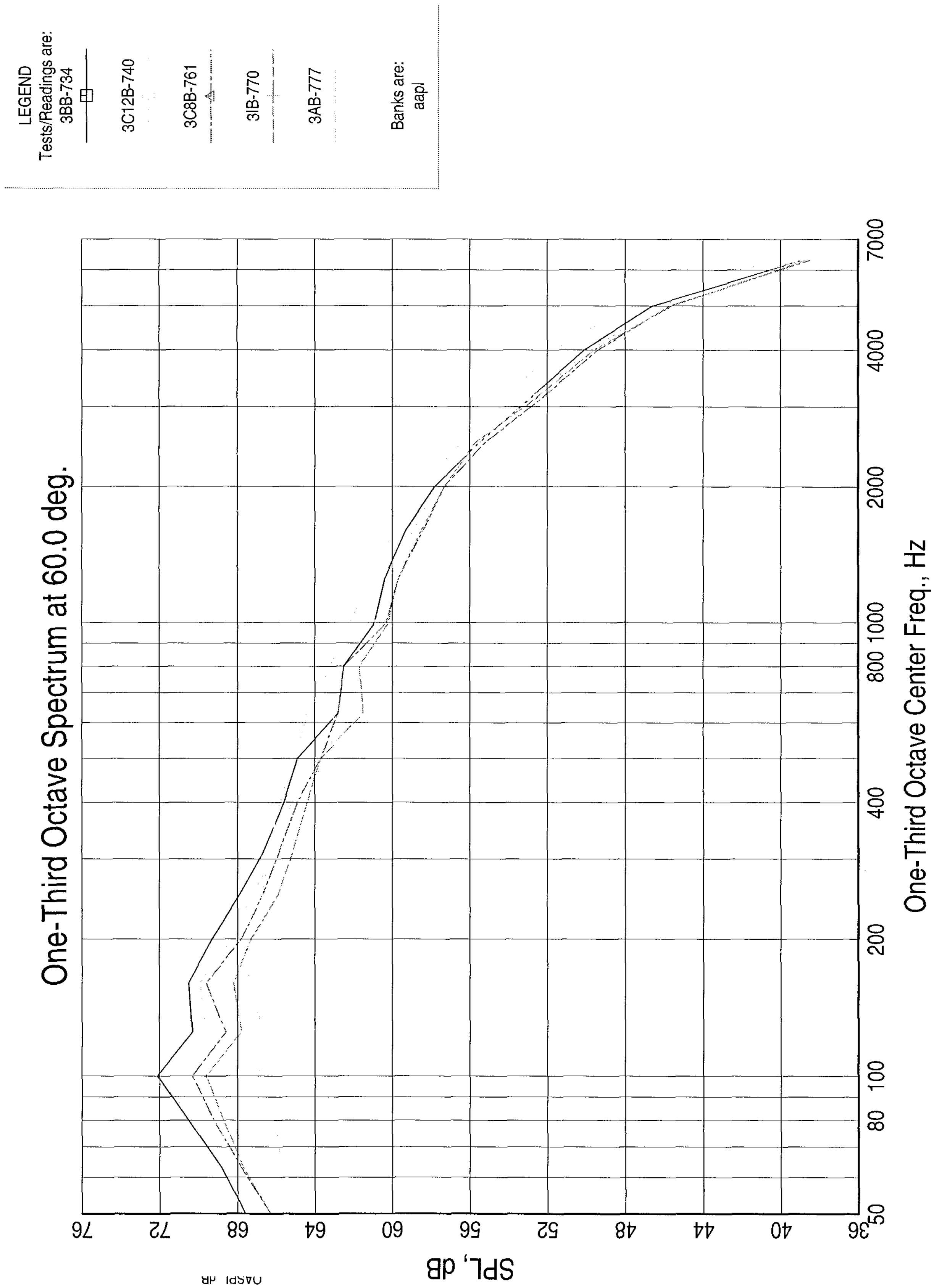
One-Third Octave Spectrum at 60.0 deg.
LEGEND
Tests/Readings are:
3BB-734
3C12B-740
3C8B-761
3IB-770
3AB-777
Banks are:
aapl
SPL, dB
One-Third Octave Center Freq., Hz
76
72
68
64
60
56
52
48
44
40
36
50
80
100
200
400
800 1000
2000
4000
7000

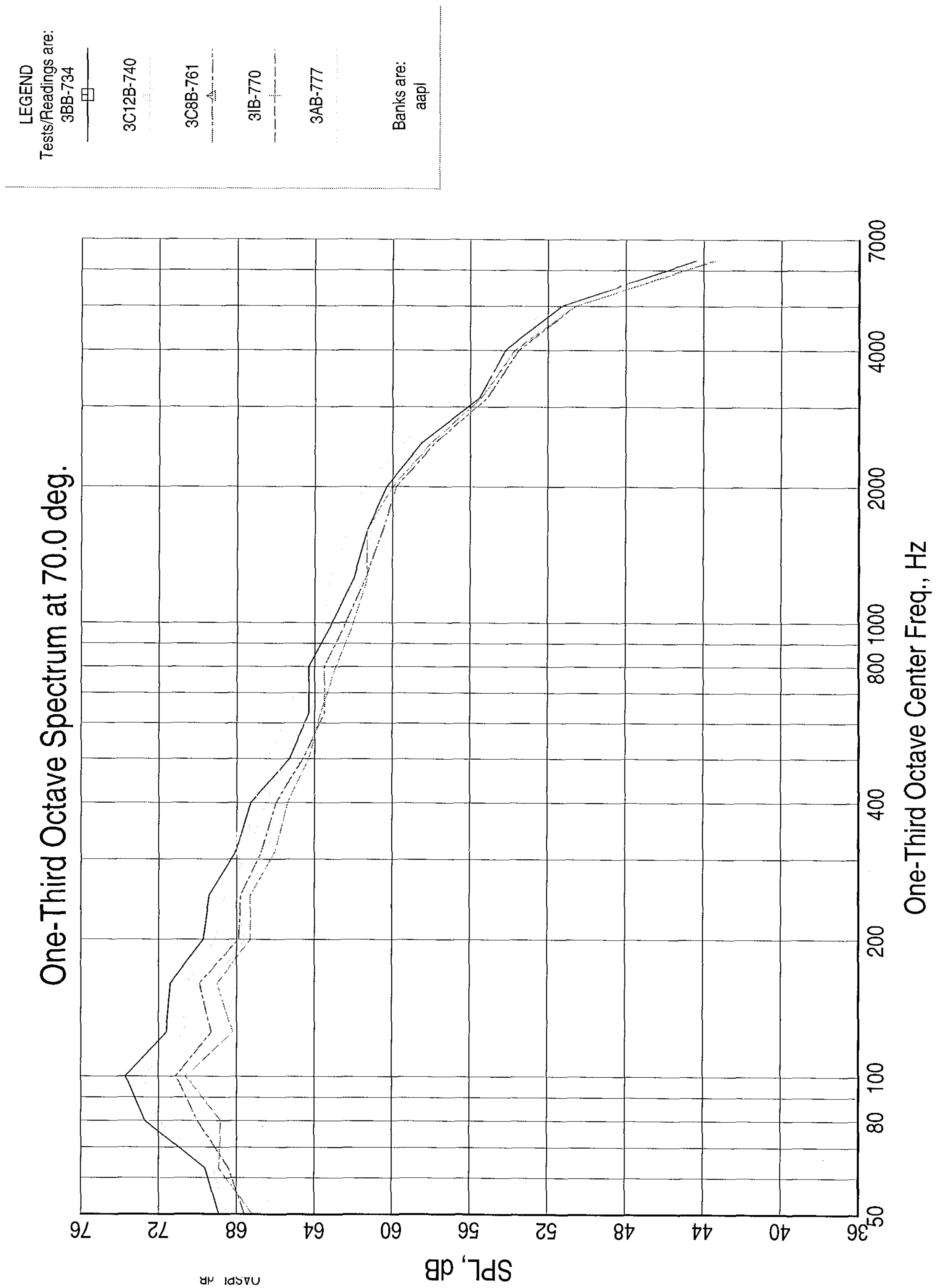

One-Third Octave Spectrum at 70.0 deg.
LEGEND
Tests/Readings are:
3BB-734
3C12B-740
3C8B-761
3IB-770
3AB-777
Banks are:
aapl
SPL, dB
76
72
68
64
60
56
52
48
44
40
36
50
80
100
200
400
800
1000
2000
4000
7000
One-Third Octave Center Freq., Hz

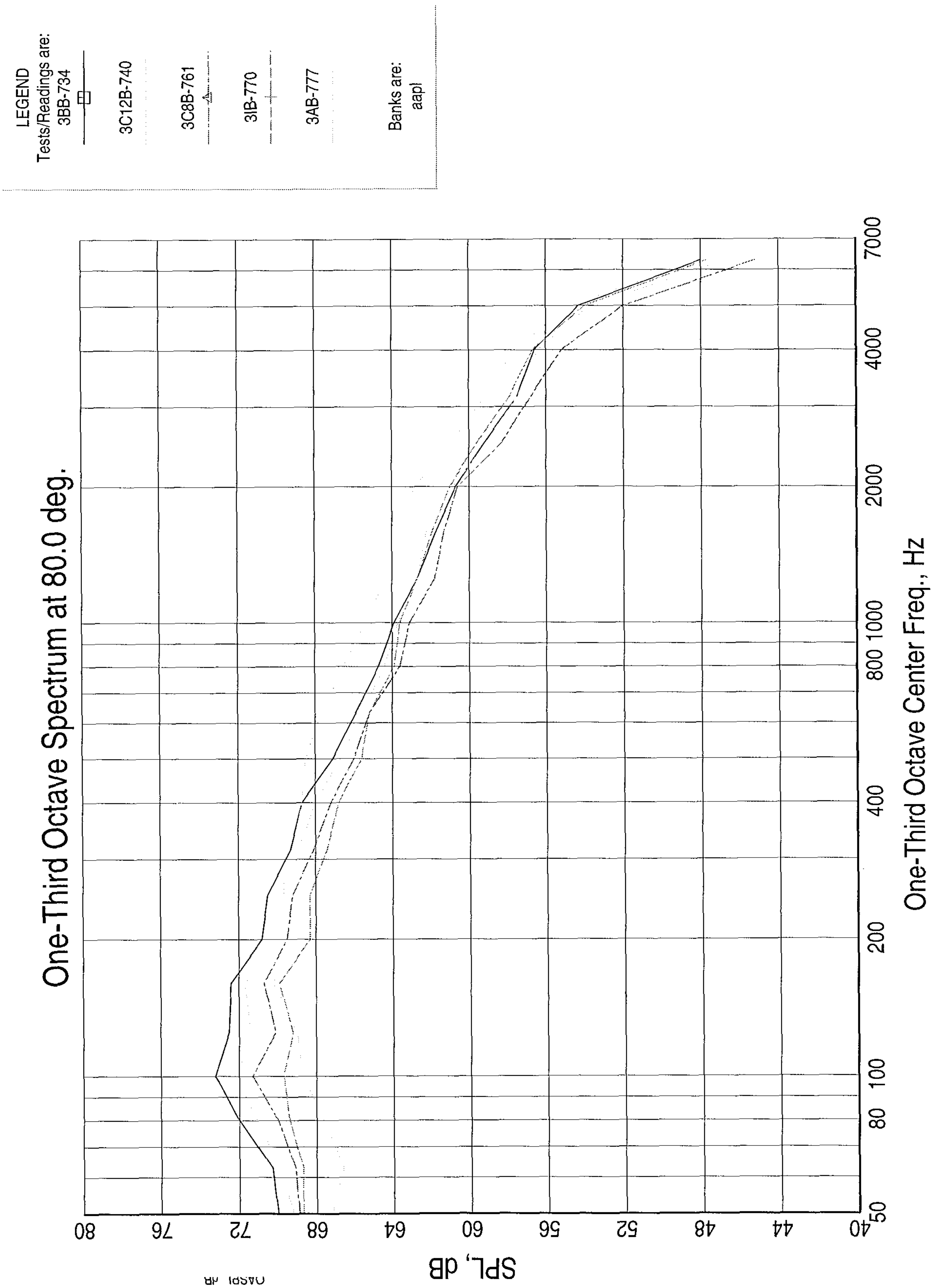
One-Third Octave Spectrum at 80.0 deg.
LEGEND
Tests/Readings are:
3BB-734
3C12B-740
3C8B-761
3IB-770
3AB-777
Banks are:
aapl
SPL, dB
One-Third Octave Center Freq., Hz
80
76
72
68
64
60
56
52
48
44
40
50
80
100
200
400
800 1000
2000
4000
7000

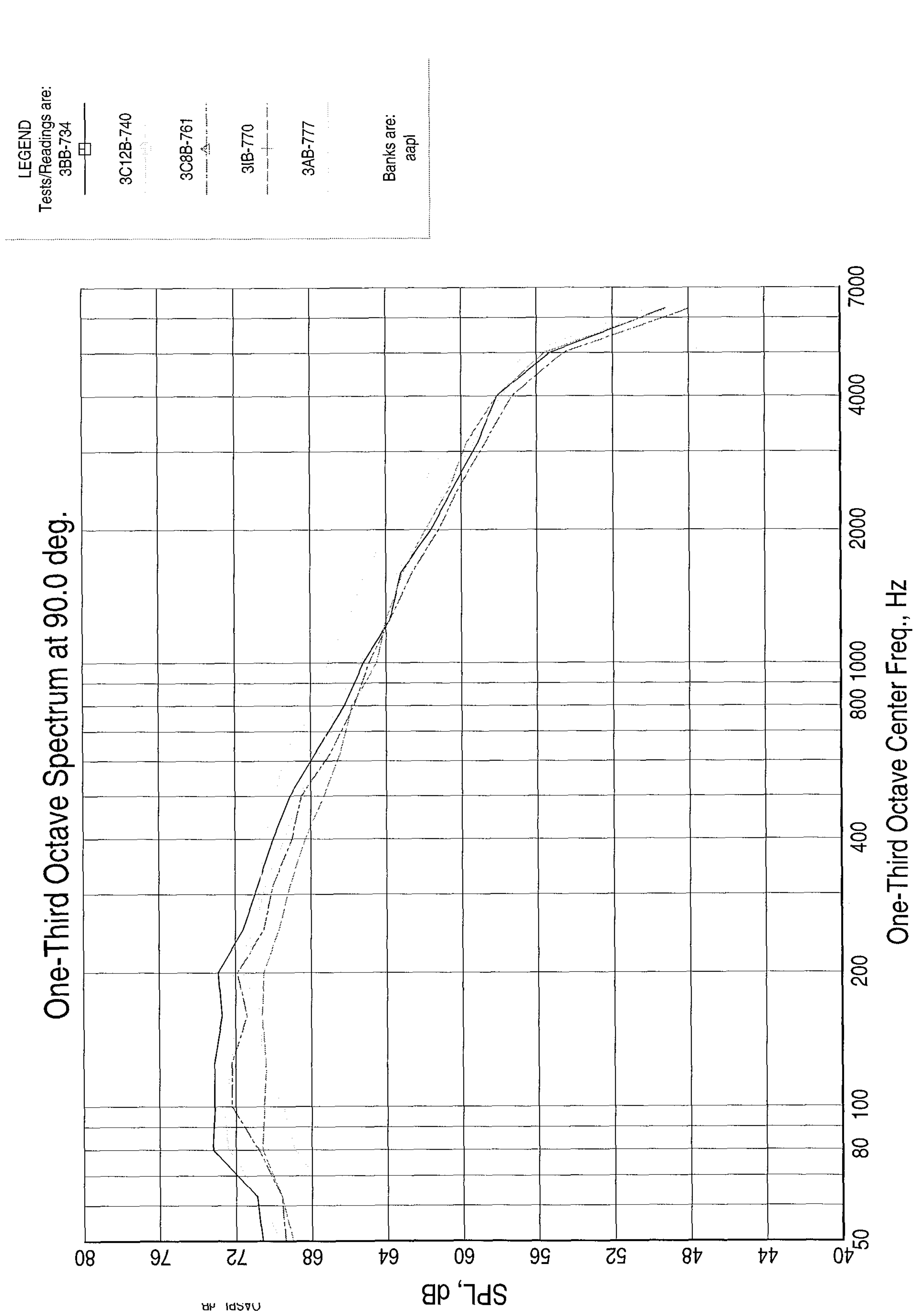
One-Third Octave Spectrum at 90.0 deg.
LEGEND
Tests/Readings are:
3BB-734
3C12B-740
3C8B-761
3IB-770
3AB-777
Banks are:
aapl
SPL, dB
80
76
72
68
64
60
56
52
48
44
40
50
80
100
200
400
800 1000
2000
4000
7000
One-Third Octave Center Freq., Hz

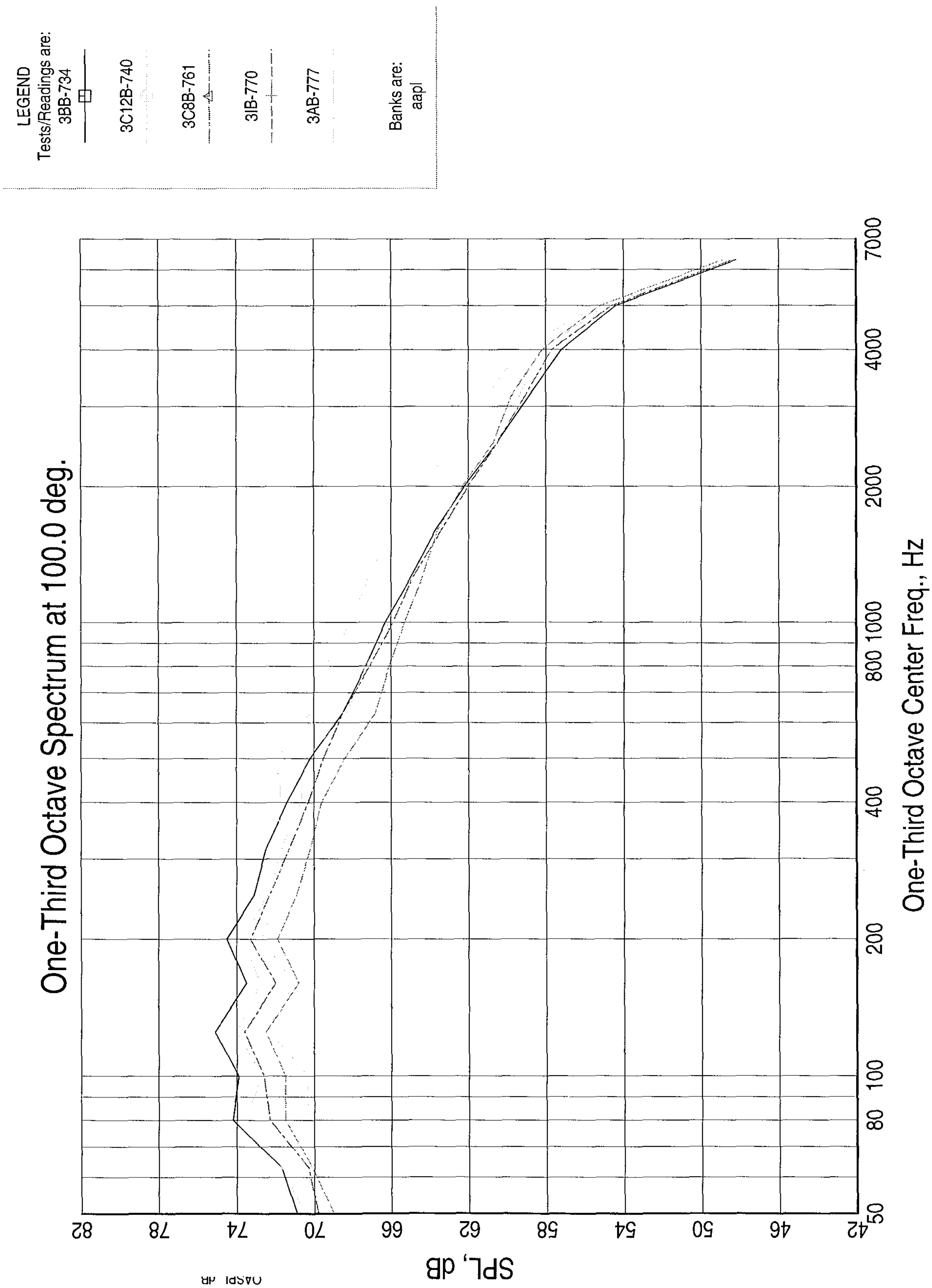

One-Third Octave Spectrum at 100.0 deg.
LEGEND
Tests/Readings are:
3BB-734
3C12B-740
3C8B-761
3IB-770
3AB-777
Banks are:
aapl
SPL, dB
One-Third Octave Center Freq., Hz
42
46
50
54
58
62
66
70
74
78
82
50
80
100
200
400
800
1000
2000
4000
7000

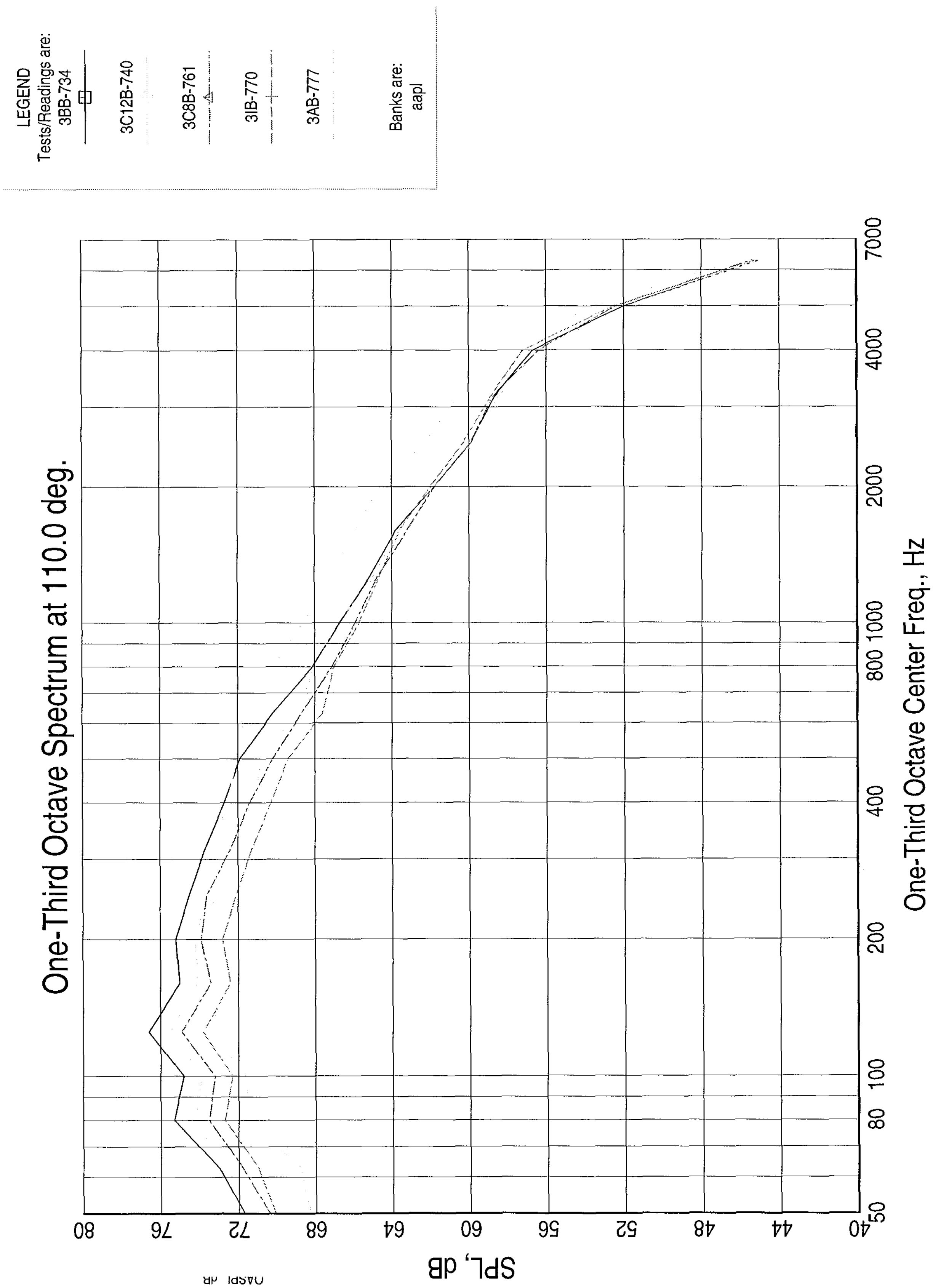
One-Third Octave Spectrum at 110.0 deg.
LEGEND
Tests/Readings are:
3BB-734
3C12B-740
3C8B-761
3IB-770
3AB-777
Banks are:
aapl
SPL, dB
80
76
72
68
64
60
56
52
48
44
40
50
80
100
200
400
800
1000
2000
4000
7000
One-Third Octave Center Freq., Hz

## One-Third Octave Spectrum at 120.0 deg.

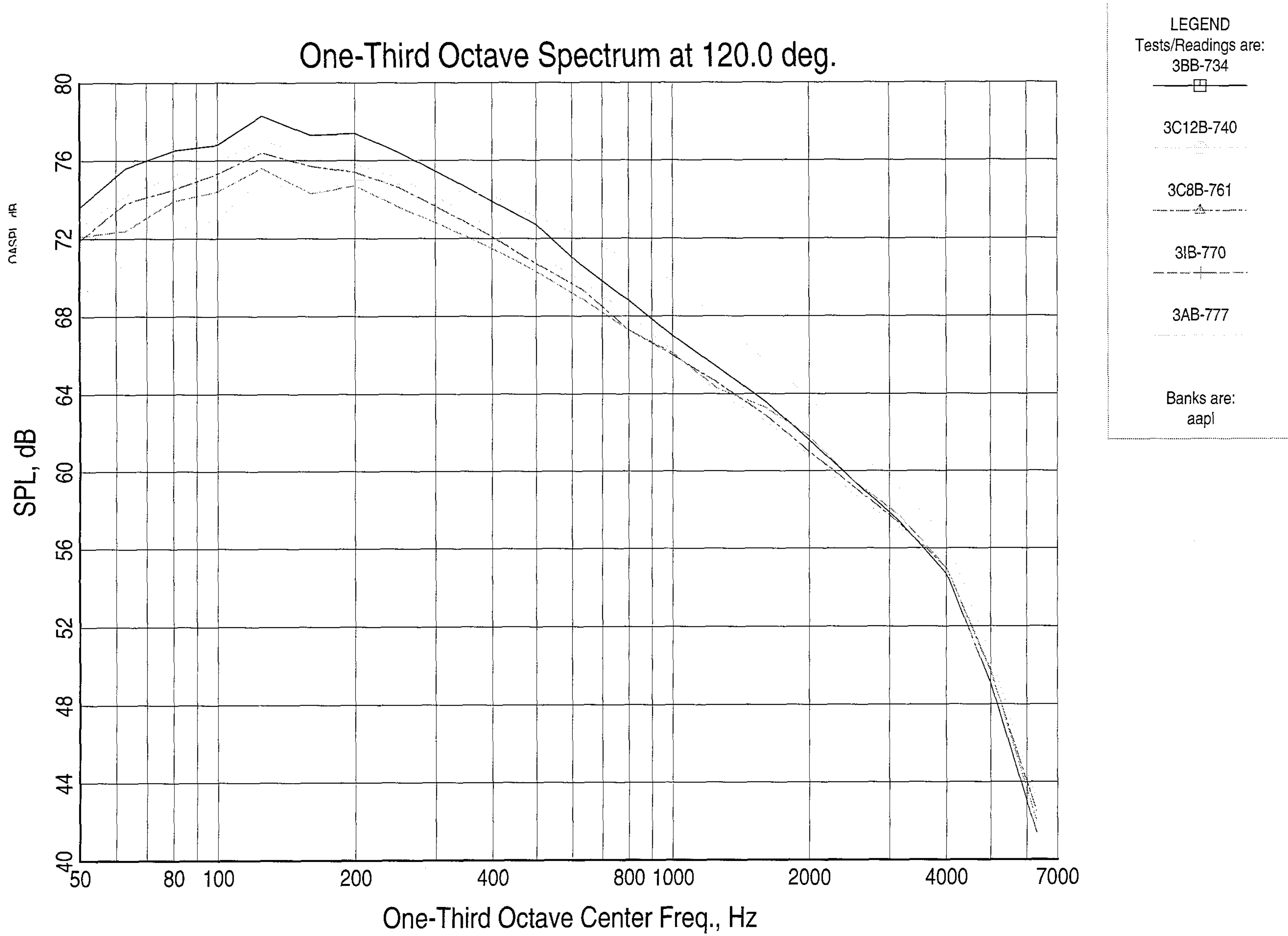

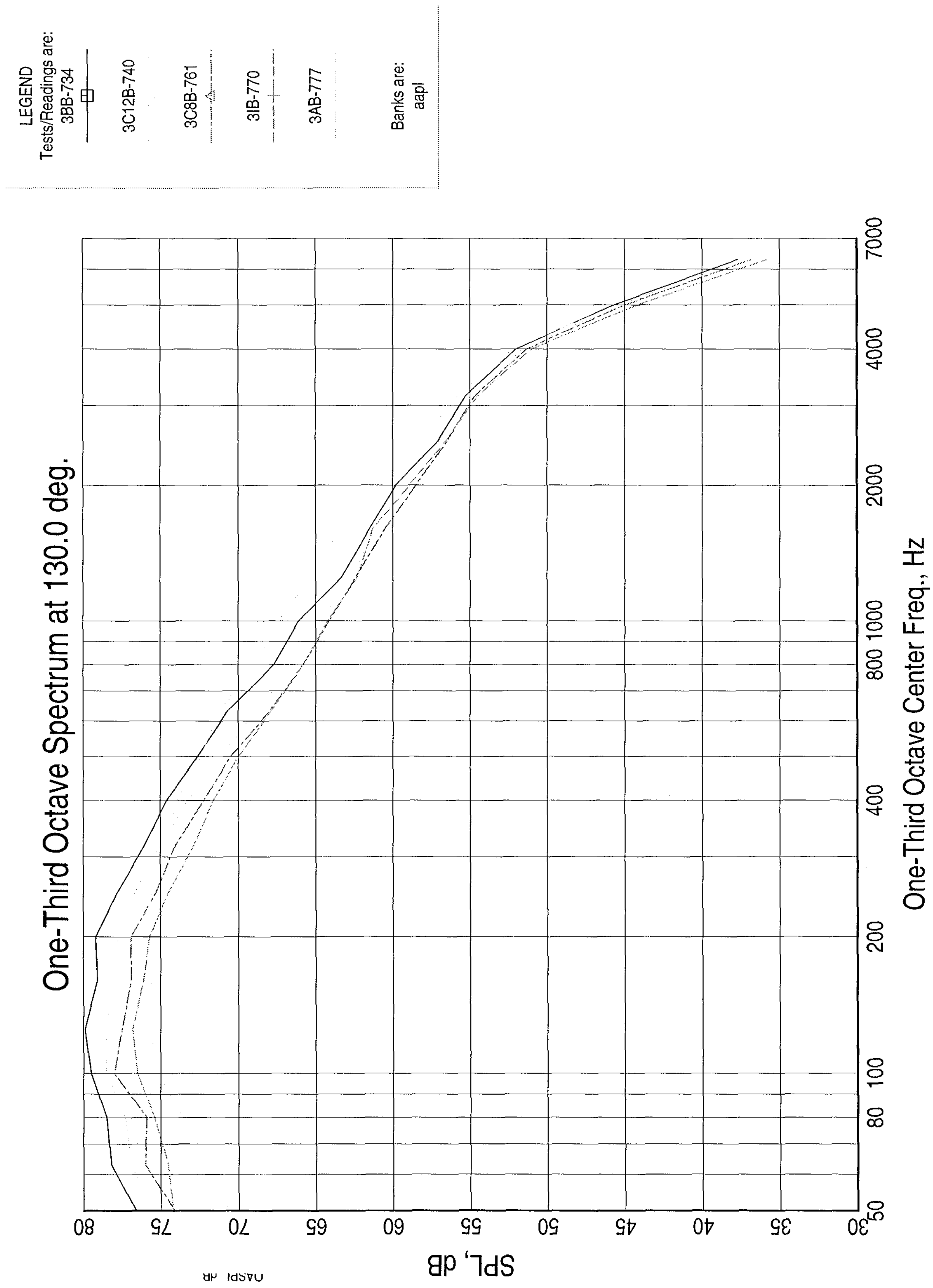
One-Third Octave Spectrum at 130.0 deg.
SPL, dB
One-Third Octave Center Freq., Hz
80
75
70
65
60
55
50
45
40
35
30
50
80
100
200
400
800 1000
2000
4000
7000
LEGEND
Tests/Readings are:
3BB-734
3C12B-740
3C8B-761
3IB-770
3AB-777
Banks are:
aapl

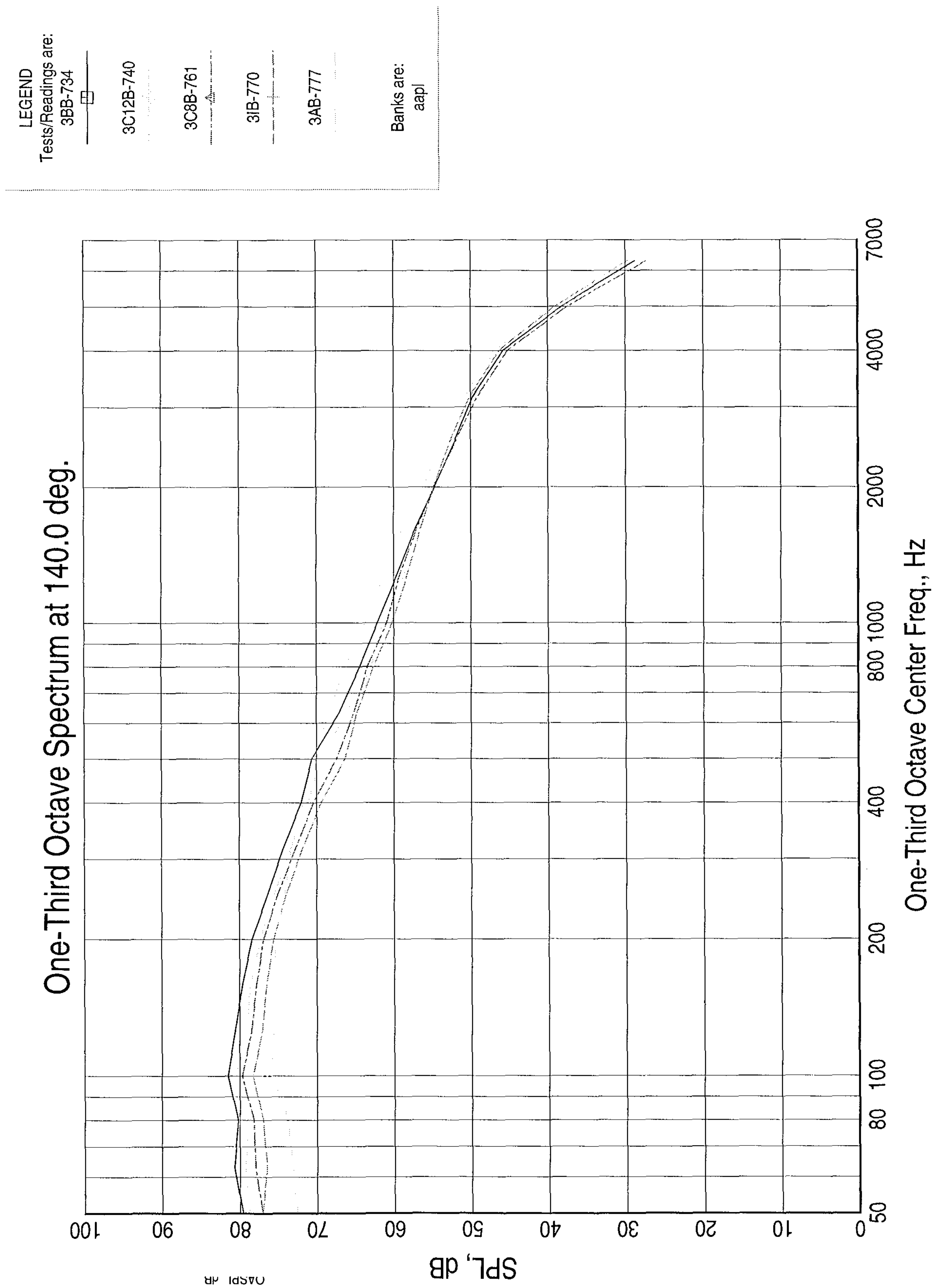

One-Third Octave Spectrum at 140.0 deg.
LEGEND
Tests/Readings are:
3BB-734
3C12B-740
3C8B-761
3IB-770
3AB-777
Banks are:
aapl
SPL, dB
One-Third Octave Center Freq., Hz
0
10
20
30
40
50
60
70
80
90
100
50
80
100
200
400
800 1000
2000
4000
7000

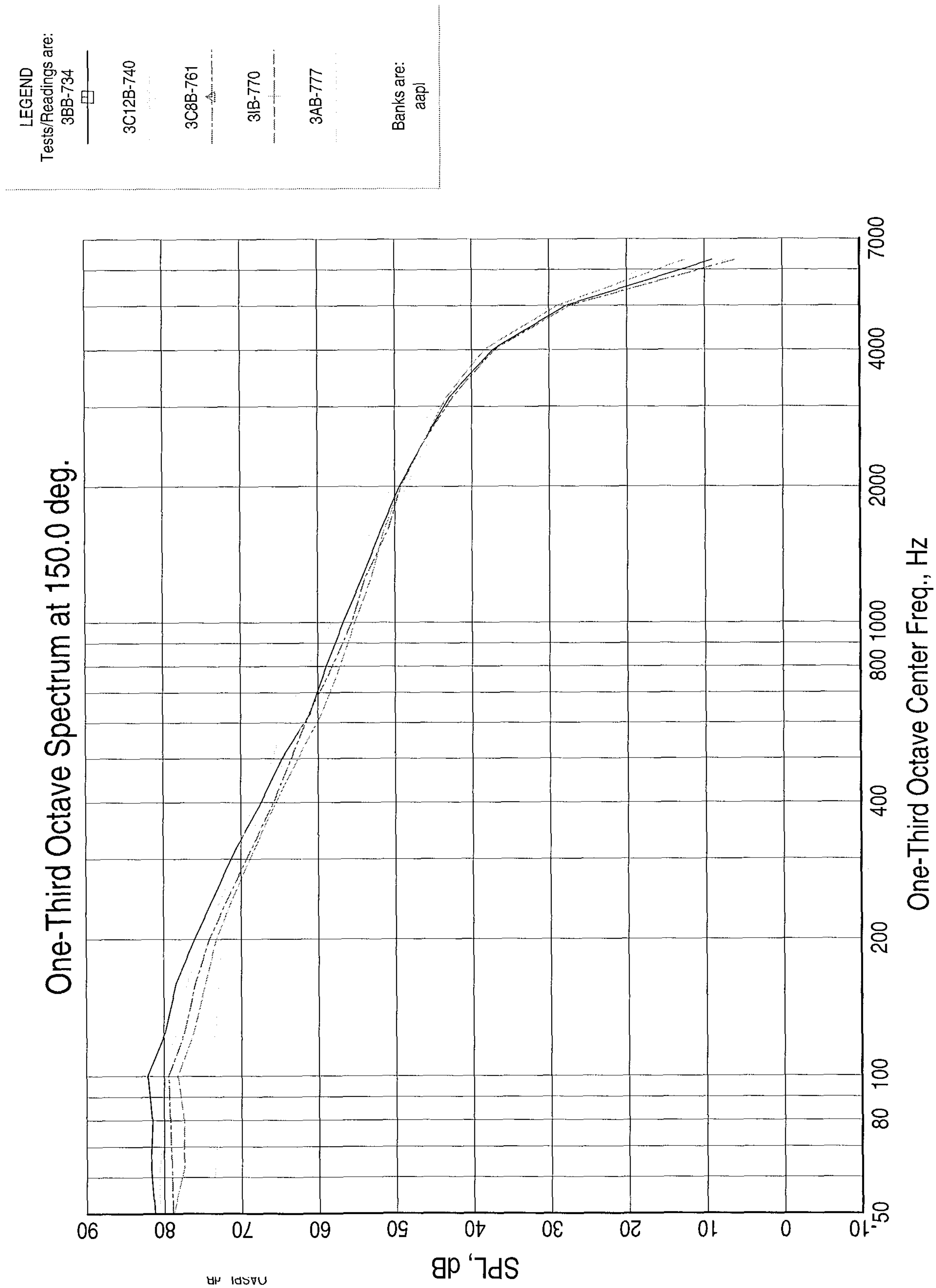
One-Third Octave Spectrum at 150.0 deg.
LEGEND
Tests/Readings are:
3BB-734
3C12B-740
3C8B-761
3IB-770
3AB-777
Banks are:
aapl
SPL, dB
One-Third Octave Center Freq., Hz
90
80
70
60
50
40
30
20
10
0
-10
50
80
100
200
400
800
1000
2000
4000
7000

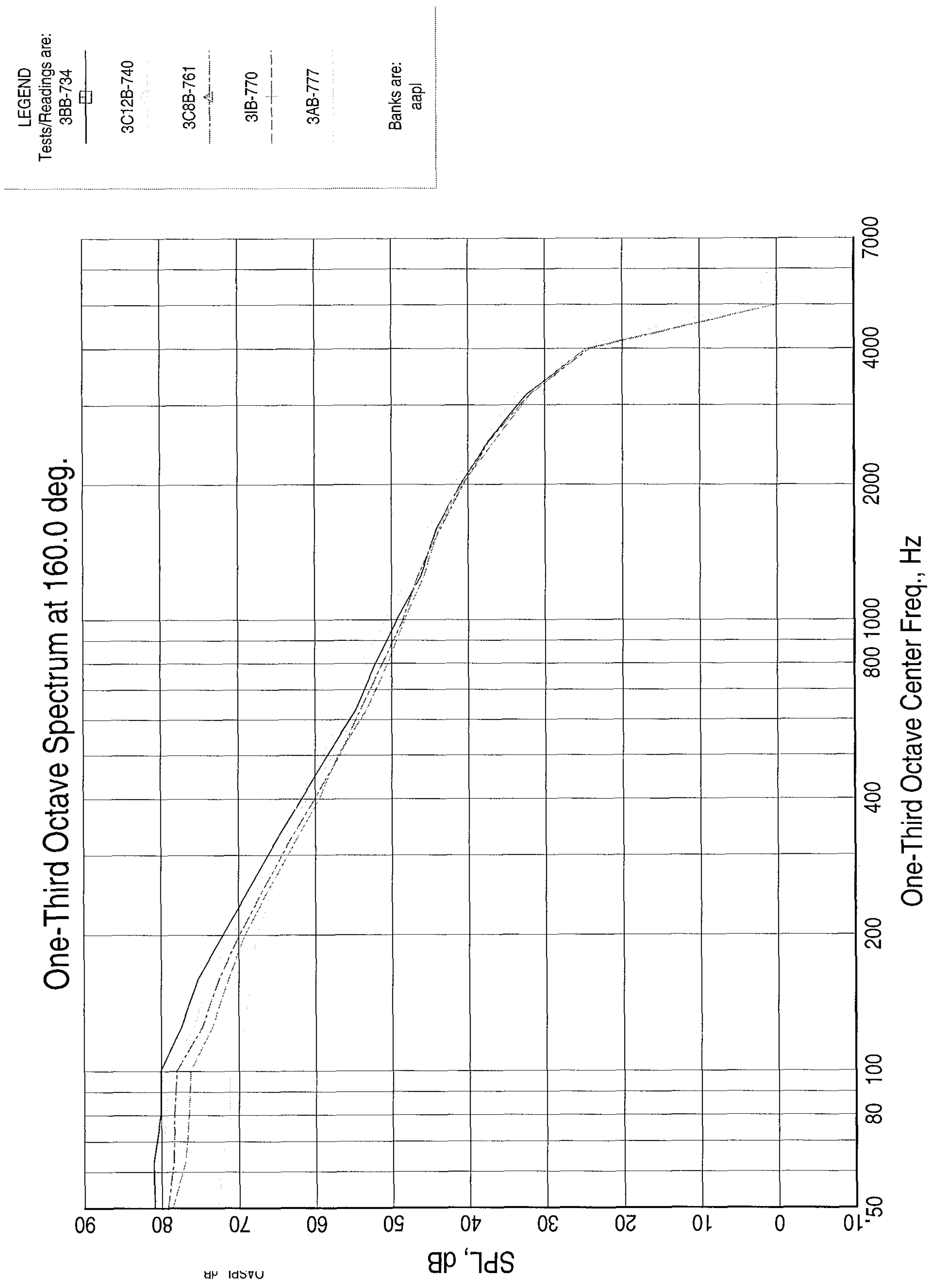
One-Third Octave Spectrum at 160.0 deg.
LEGEND
Tests/Readings are:
3BB-734
3C12B-740
3C8B-761
3IB-770
3AB-777
Banks are:
aapl
SPL, dB
One-Third Octave Center Freq., Hz
90
80
70
60
50
40
30
20
10
0
-10
50
80
100
200
400
800
1000
2000
4000
7000

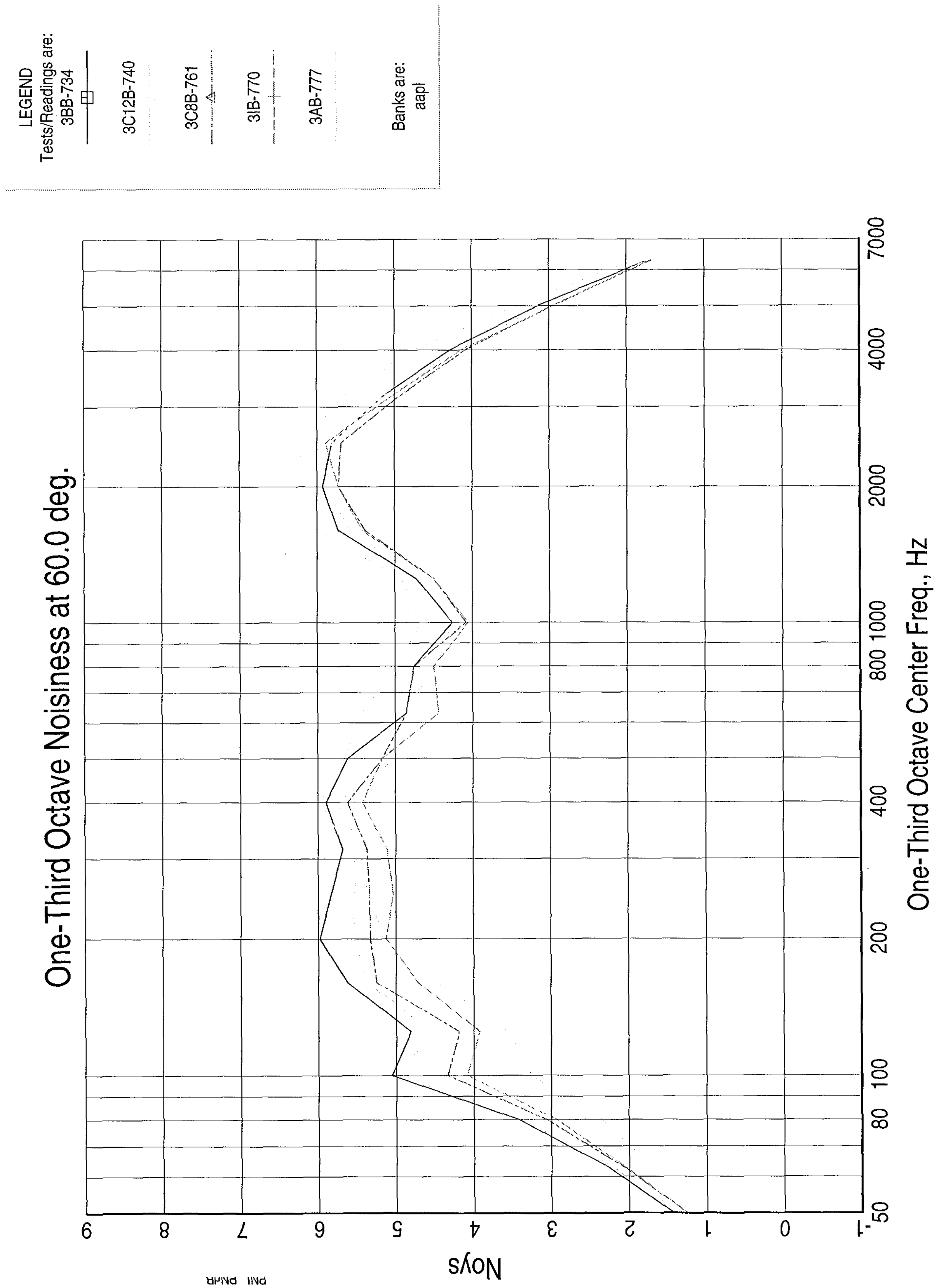
One-Third Octave Noisiness at 60.0 deg.
LEGEND
Tests/Readings are:
3BB-734
3C12B-740
3C8B-761
3IB-770
3AB-777
Banks are:
aapl
Noys
One-Third Octave Center Freq., Hz
50
80
100
200
400
800
1000
2000
4000
7000
-1
0
1
2
3
4
5
6
7
8
9

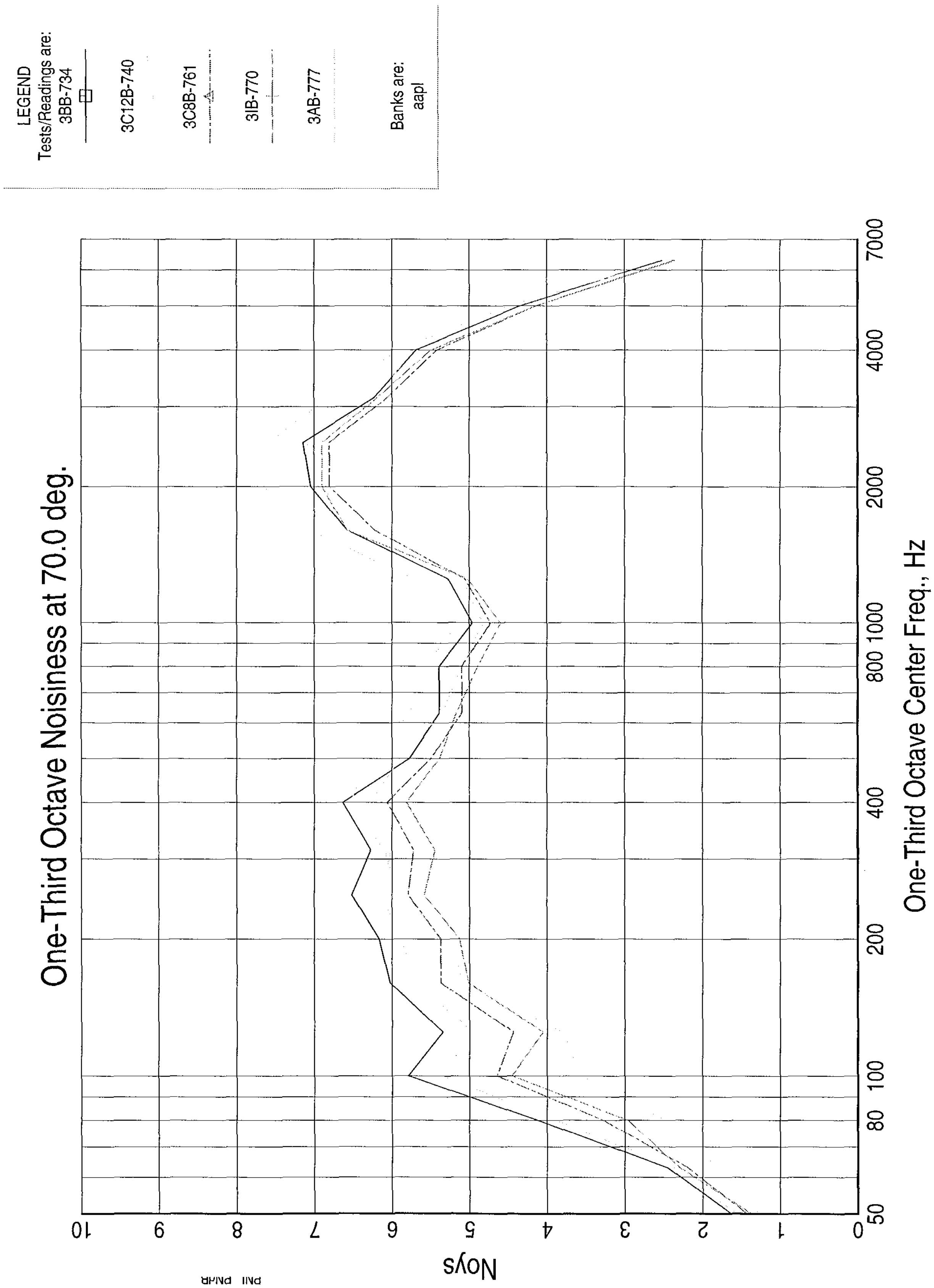
One-Third Octave Noisiness at 70.0 deg.
LEGEND
Tests/Readings are:
3BB-734
3C12B-740
3C8B-761
3IB-770
3AB-777
Banks are:
aapl
Noys
PNI PNAR
0
1
2
3
4
5
6
7
8
9
10
50
80
100
200
400
800 1000
2000
4000
7000
One-Third Octave Center Freq., Hz

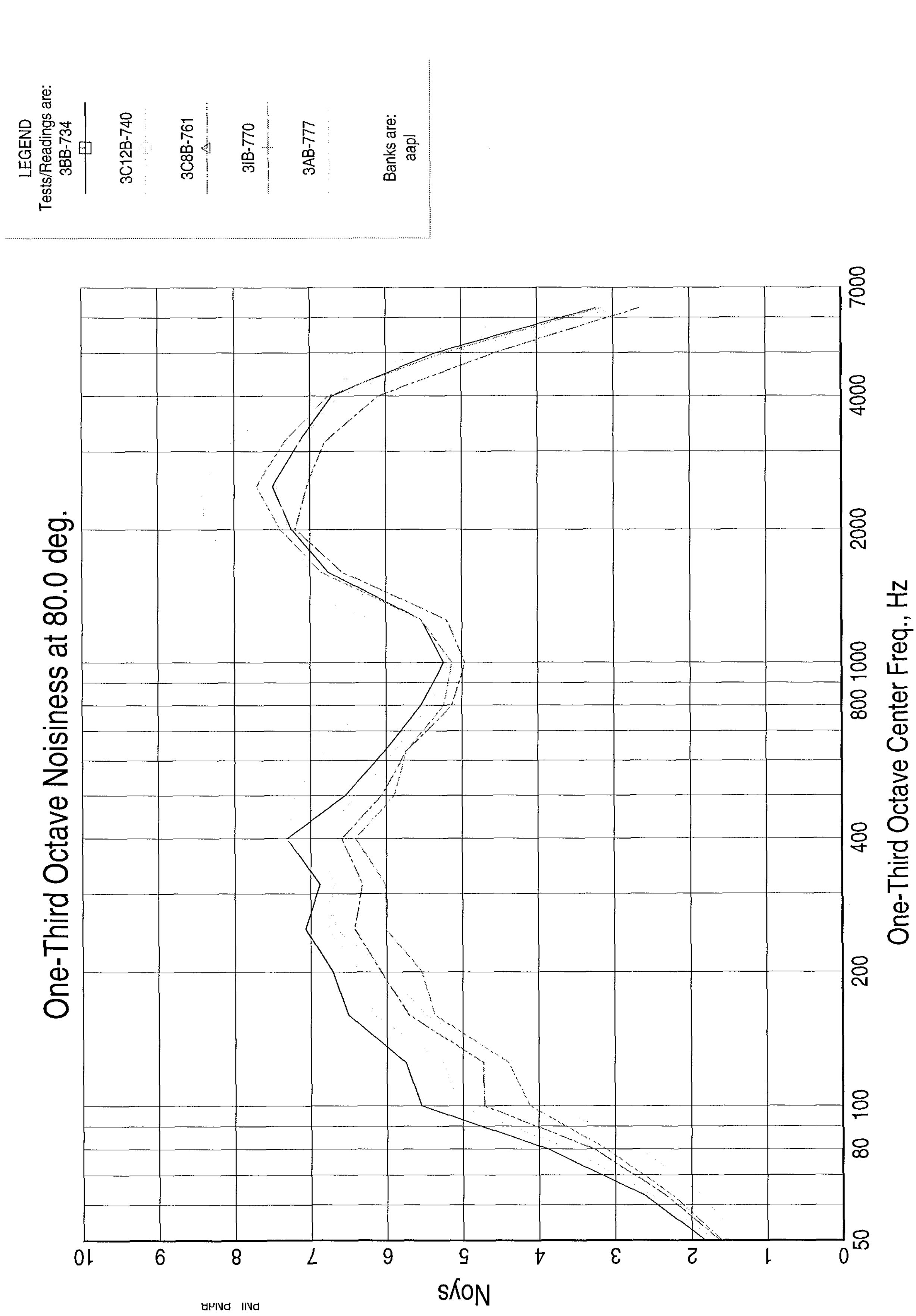
One-Third Octave Noisiness at 80.0 deg.
LEGEND
Tests/Readings are:
3BB-734
3C12B-740
3C8B-761
3IB-770
3AB-777
Banks are:
aapl
Noys
PNI PNdR
0
1
2
3
4
5
6
7
8
9
10
50
80
100
200
400
800 1000
2000
4000
7000
One-Third Octave Center Freq., Hz

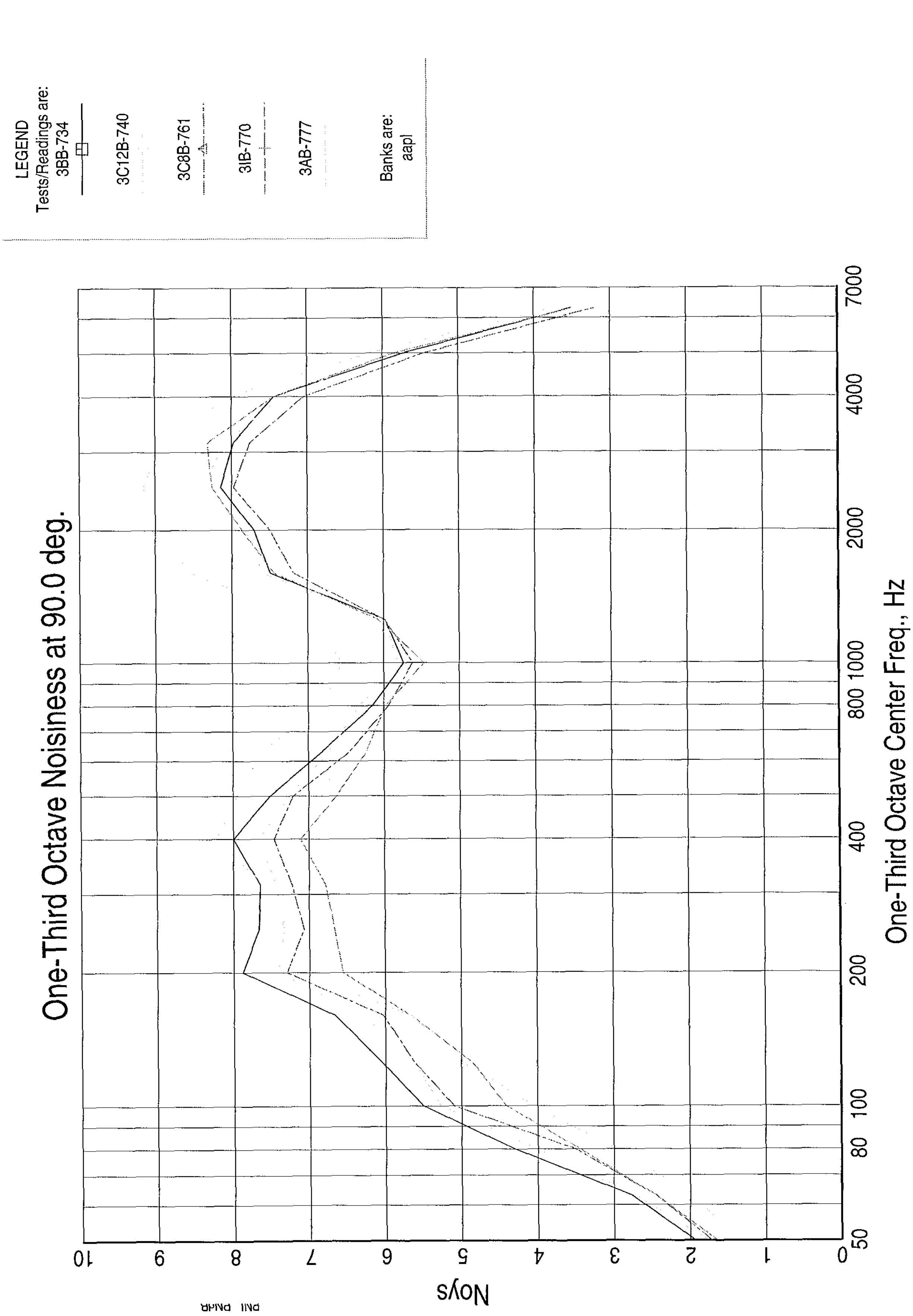

One-Third Octave Noisiness at 90.0 deg.
LEGEND
Tests/Readings are:
3BB-734
3C12B-740
3C8B-761
3IB-770
3AB-777
Banks are:
aapl
Noys
0
1
2
3
4
5
6
7
8
9
10
50
80
100
200
400
800
1000
2000
4000
7000
One-Third Octave Center Freq., Hz

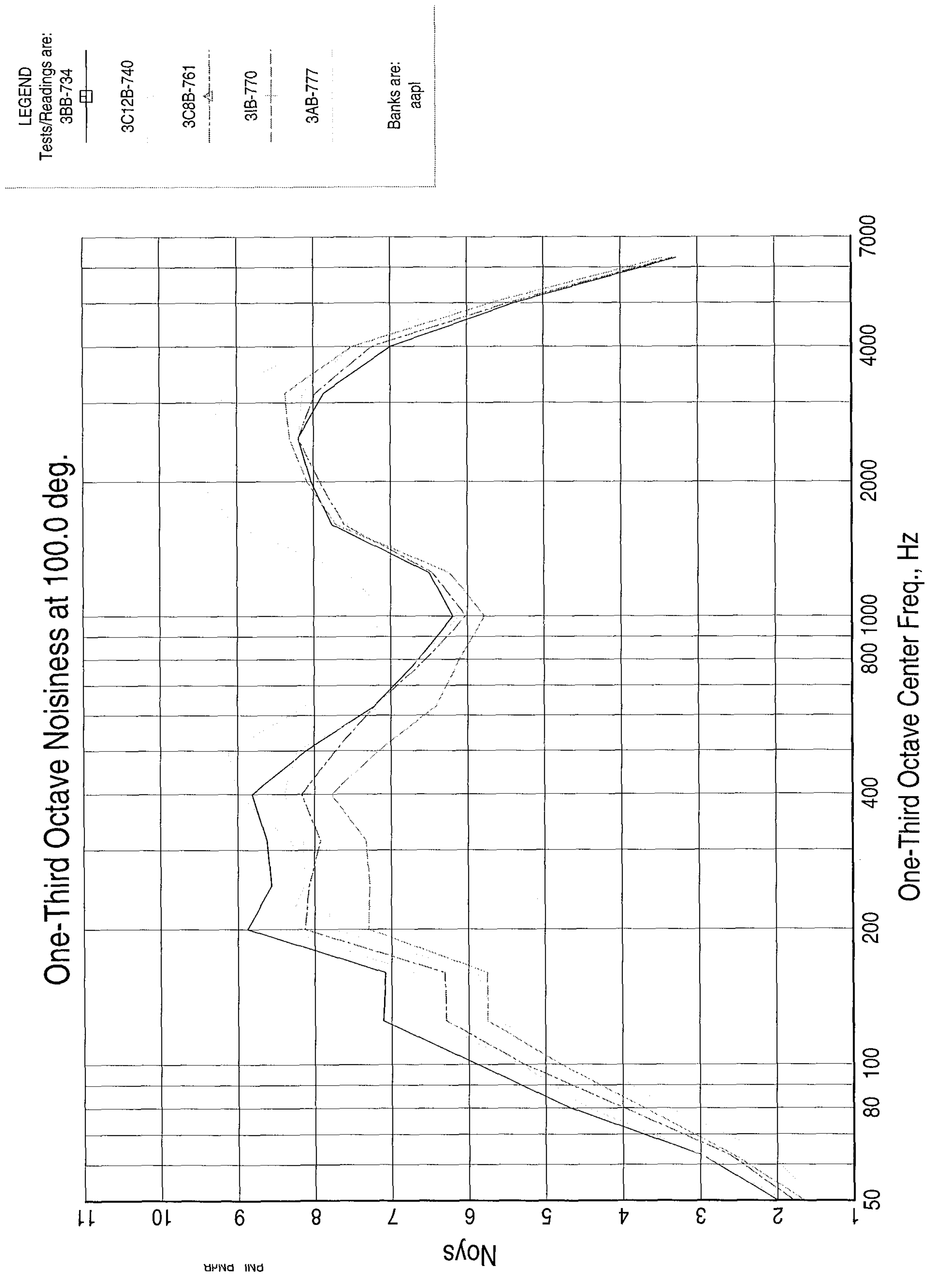
One-Third Octave Noisiness at 100.0 deg.
LEGEND
Tests/Readings are:
3BB-734
3C12B-740
3C8B-761
3IB-770
3AB-777
Banks are:
aapl
Noys
One-Third Octave Center Freq., Hz
50
80
100
200
400
800
1000
2000
4000
7000
1
2
3
4
5
6
7
8
9
10
11
PNI PNdB

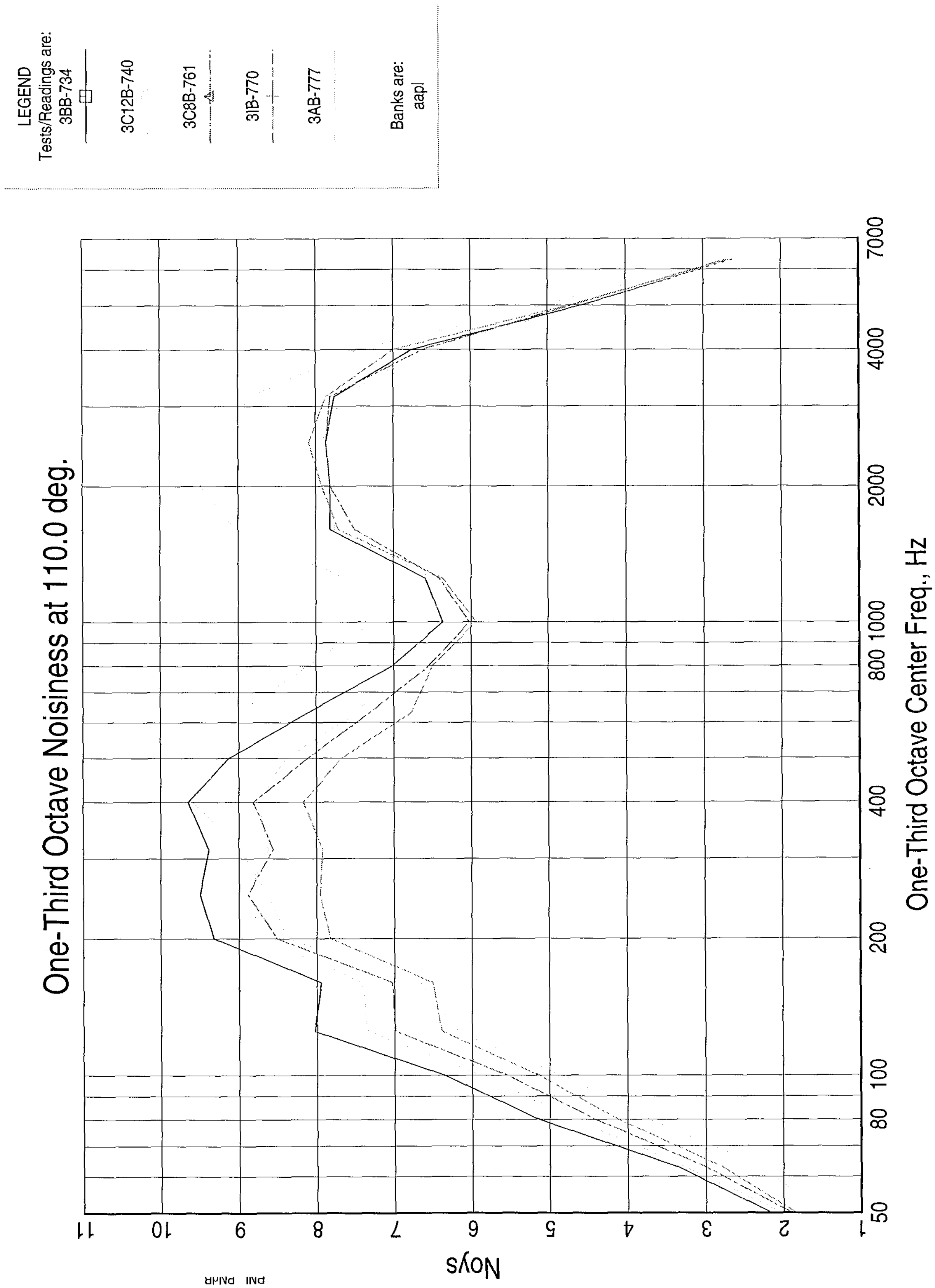
One-Third Octave Noisiness at 110.0 deg.
Noys
One-Third Octave Center Freq., Hz
1
2
3
4
5
6
7
8
9
10
11
50
80
100
200
400
800 1000
2000
4000
7000
LEGEND
Tests/Readings are:
3BB-734
3C12B-740
3C8B-761
3IB-770
3AB-777
Banks are:
aapl
PNI PNdR

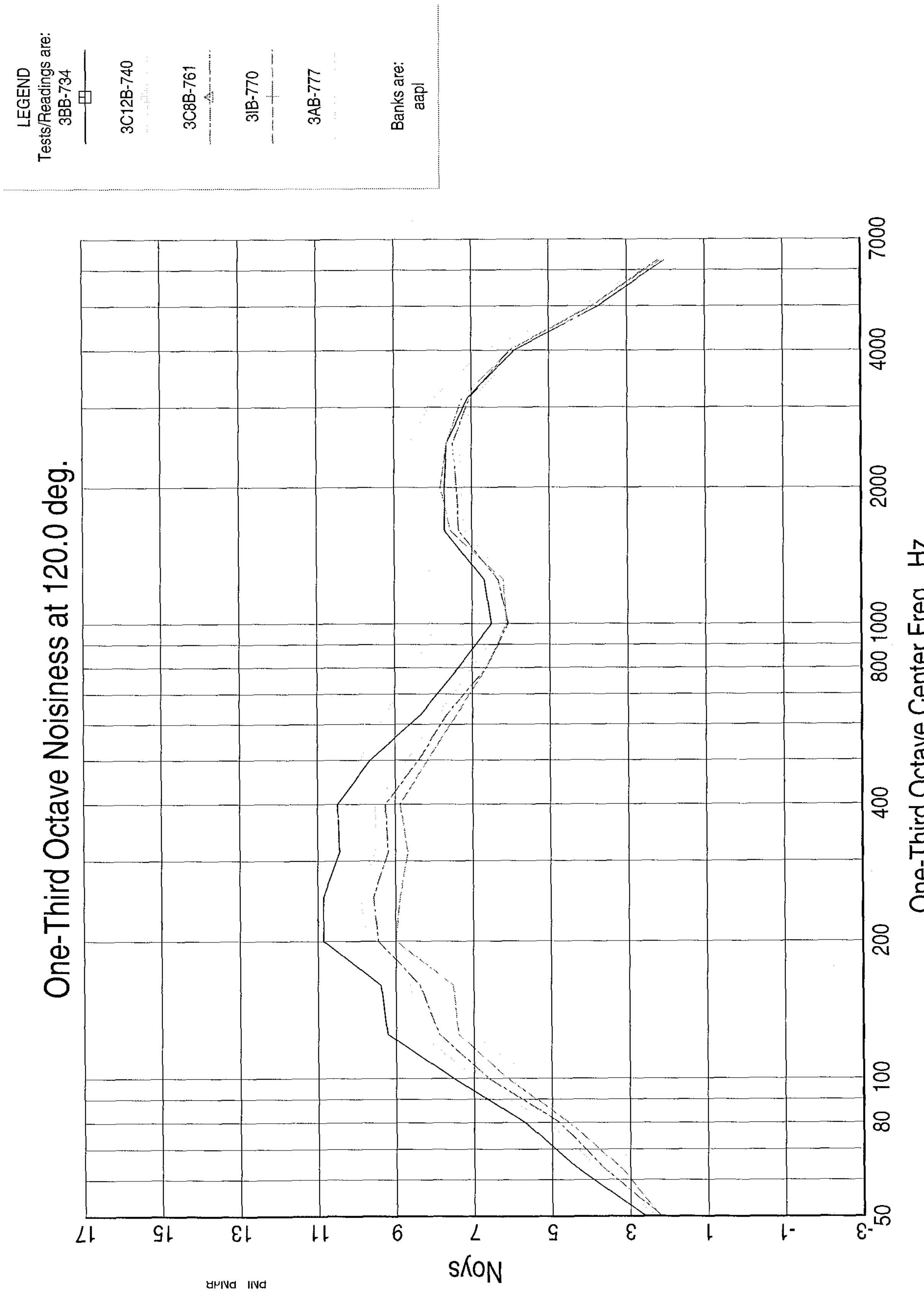

One-Third Octave Noisiness at 120.0 deg.
LEGEND
Tests/Readings are:
3BB-734
3C12B-740
3C8B-761
3IB-770
3AB-777
Banks are:
aapl
Noys
PNI PNdB
17
15
13
11
9
7
5
3
1
-1
-3
50
80
100
200
400
800
1000
2000
4000
7000
One-Third Octave Center Freq., Hz

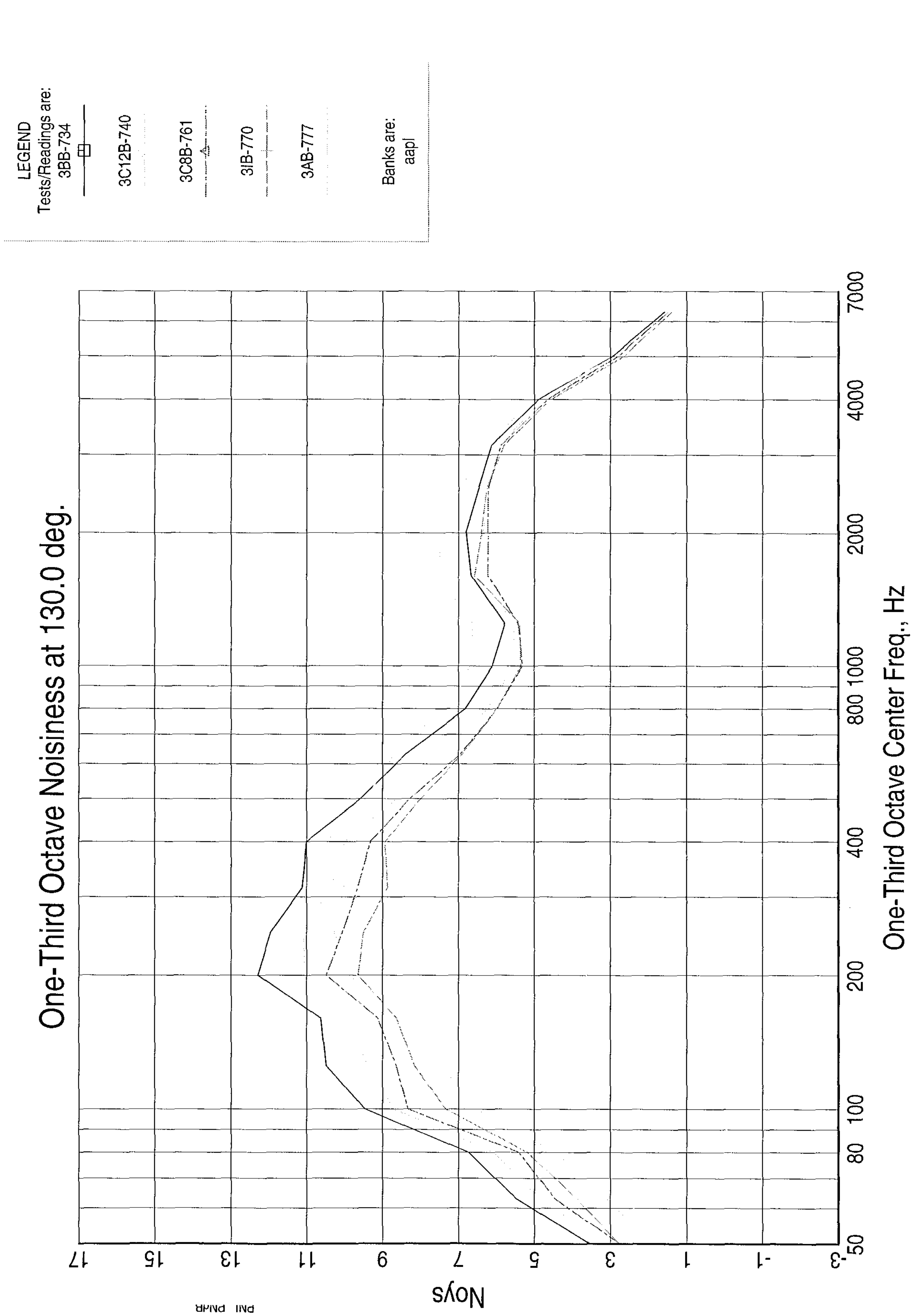
One-Third Octave Noisiness at 130.0 deg.
LEGEND
Tests/Readings are:
3BB-734
3C12B-740
3C8B-761
3IB-770
3AB-777
Banks are:
aapl
Noys
One-Third Octave Center Freq., Hz
17
15
13
11
9
7
5
3
1
-1
-3
50
80
100
200
400
800
1000
2000
4000
7000
PNL PNdB

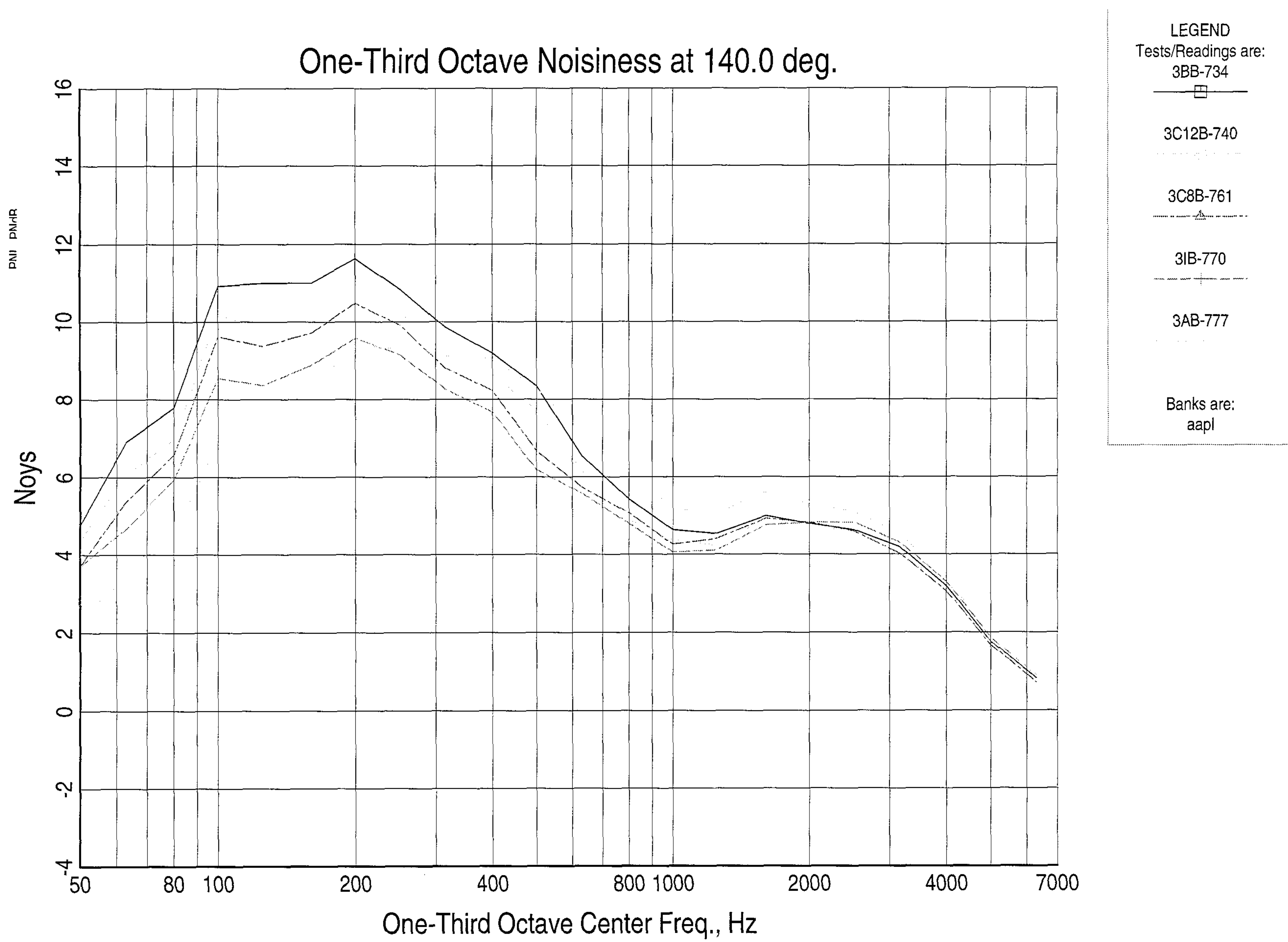
One-Third Octave Noisiness at 140.0 deg.
Noys
16
14
12
10
8
6
4
2
0
-2
-4
50
80
100
200
400
800
1000
2000
4000
7000
One-Third Octave Center Freq., Hz
LEGEND
Tests/Readings are:
3BB-734
3C12B-740
3C8B-761
3IB-770
3AB-777
Banks are:
aapl

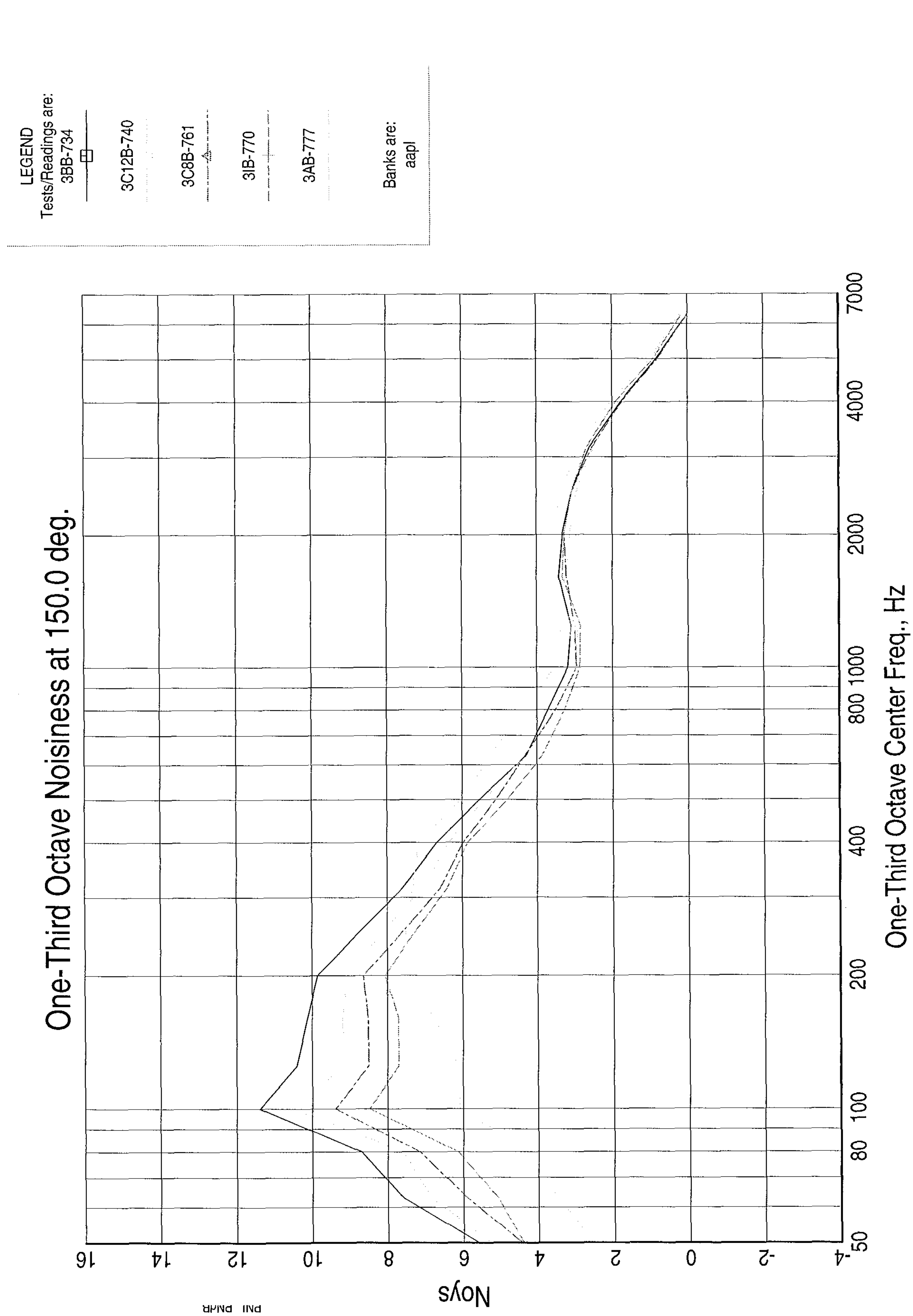

One-Third Octave Noisiness at 150.0 deg.
LEGEND
Tests/Readings are:
3BB-734
3C12B-740
3C8B-761
3IB-770
3AB-777
Banks are:
aapl
Noys
One-Third Octave Center Freq., Hz
16
14
12
10
8
6
4
2
0
-2
-4
50
80
100
200
400
800 1000
2000
4000
7000
PNI PNHR

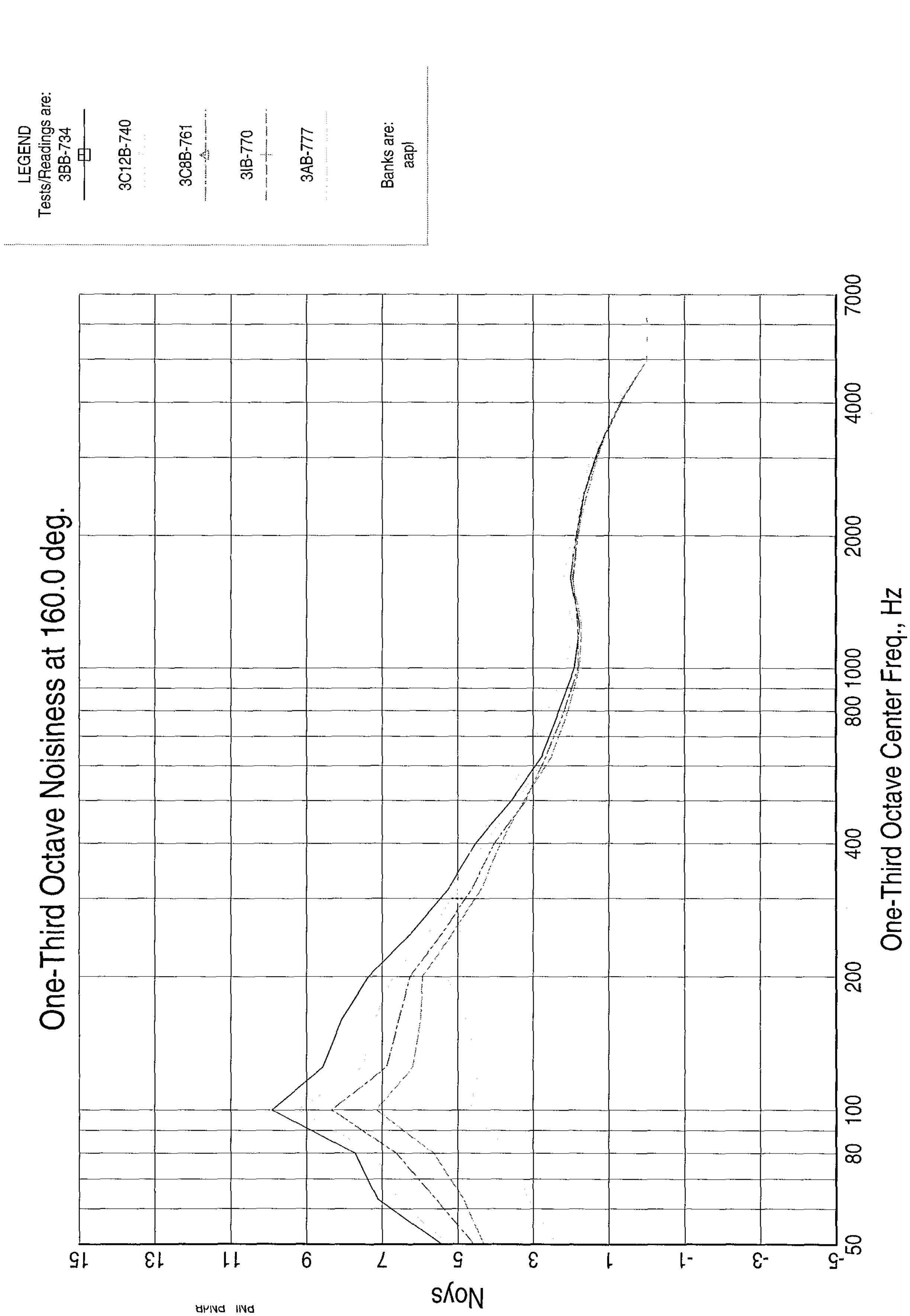

One-Third Octave Noisiness at 160.0 deg.
LEGEND
Tests/Readings are:
3BB-734
3C12B-740
3C8B-761
3IB-770
3AB-777
Banks are:
aapl
Noys
One-Third Octave Center Freq., Hz
50
80
100
200
400
800
1000
2000
4000
7000
15
13
11
9
7
5
3
1
-1
-3
-5
PNI PN4B

# Appendix D
# Selected Acoustic Data: Baseline BPR=5 External Plug Nozzle with Various Combined Core and Fan Nozzle Noise-Reduction Concepts

This appendix presents comparison plots of data measured for Model 3 with a 24-chevron fan nozzle and various core nozzle noise-reduction concepts. Model operating conditions were:

- Test Point 21, Cycle 2
- Takeoff Thrust ≃ 33,000 lbf (One Engine)
- Altitude = 1500 ft
- Simulated Flight Mach Number = 0.28

The following comparisons are included:

1. Overall Sound Pressure Lavel (OASPL) Directivity
2. Perceived Noise Level (PNL) Directivity
3. Sound Pressure Level (SPL) Spectra at 60°, 70°, 80°, 90°, 100°, 110°, 120°, 130°, 140°, 150°, and 160° (11 Plots)
4. Noy Spectra at 60°, 70°, 80°, 90°, 100°, 110°, 120°, 130°, 140°, 150°, and 160° (11 Plots)

| | Configuration | | | | |
|---|---|---|---|---|---|
| | 3BB | 3IC | 3C12C | 3C8C | 3AC |
| Data Symbol | □ | ○ | Δ | + | × |
| Core Nozzle | Base | 12 In-Flip Chevrons | 12 Chevrons | 8 Chevrons | 12 Alt–Flip Chevrons |
| Fan Nozzle | Base | 24 Chevrons | 24 Chevrons | 24 Chevrons | 24 Chevrons |
| Test Point | 917 | 904 | 823 | 841 | 850 |
| Total Temperature, °F | | | | | |
| Ambient ($T_{amb}$) | 45.4 | 44.1 | 52.3 | 47.7 | 46.3 |
| Core Nozzle ($T_8$) | 1042.8 | 1035.6 | 1048.2 | 1045 | 1044.3 |
| Fan Nozzle ($T_{18}$) | 140.8 | 140.6 | 142.1 | 143.6 | 144.8 |
| Pressure Ratio | | | | | |
| Core Nozzle (P8PQA) | 1.675 | 1.673 | 1.689 | 1.679 | 1.677 |
| Fan Nozzle (PFQPA) | 1.832 | 1.830 | 1.834 | 1.835 | 1.835 |
| Ideal Exit Velocity, ft/s | | | | | |
| Core Nozzle ($V_8$) | 1579 | 1573 | 1592 | 1582 | 1580 |
| Fan Nozzle ($V_{18}$) | 1070 | 1070 | 1073 | 1074 | 1075 |
| Mass-Averaged ($V_{mix}$) | 1154 | 1151 | 1161 | 1160 | 1163 |
| Net Thrust ($F_N$), lbf | 32,191 | 32,747 | 33,566 | 33,052 | 33,494 |
| 1500-ft EPNL | 91.3 | 88.2 | 89.9 | 88.8 | 88.9 |

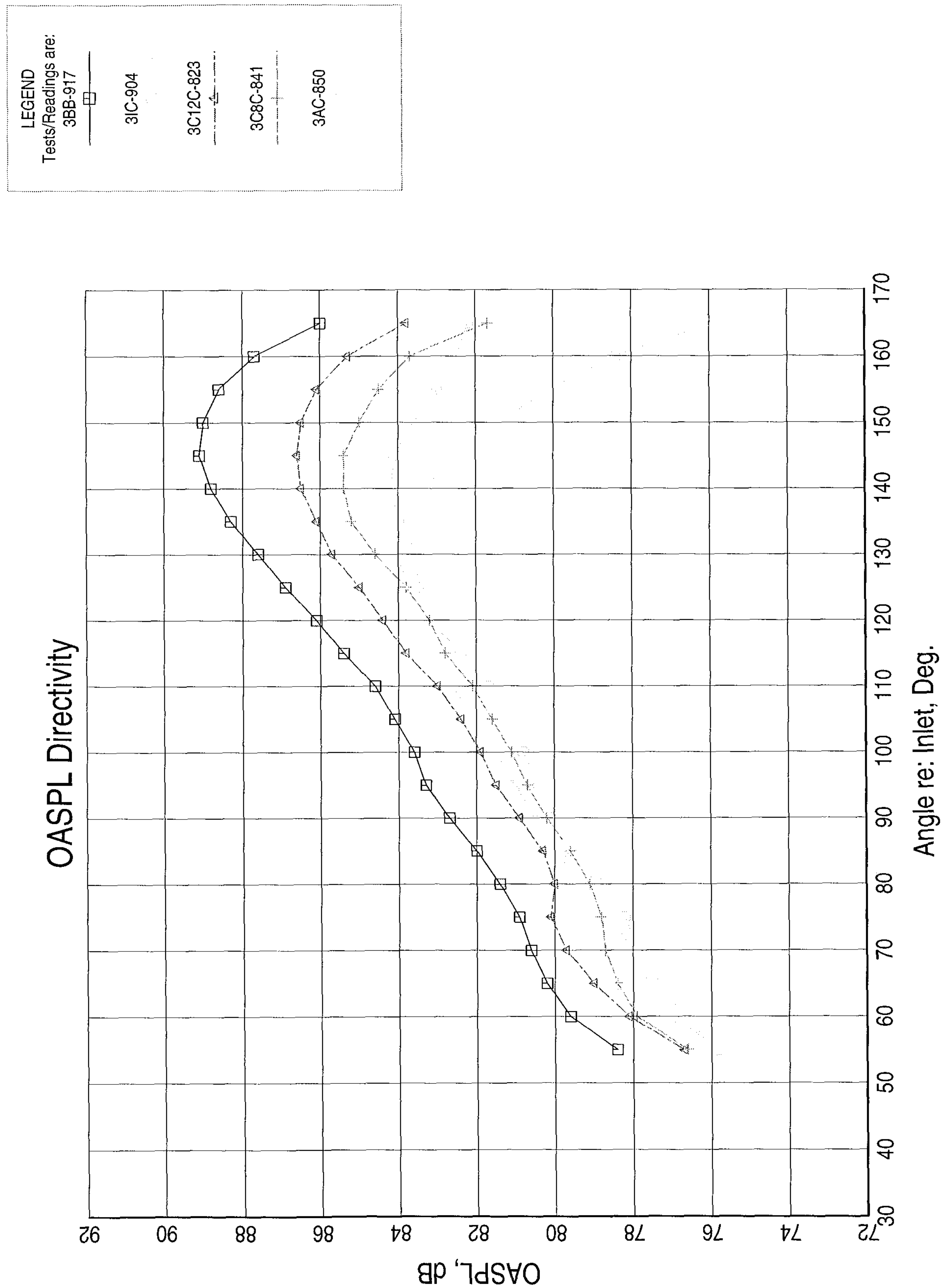
OASPL Directivity
LEGEND
Tests/Readings are:
3BB-917
3IC-904
3C12C-823
3C8C-841
3AC-850
OASPL, dB
Angle re: Inlet, Deg.
72
74
76
78
80
82
84
86
88
90
92
30
40
50
60
70
80
90
100
110
120
130
140
150
160
170

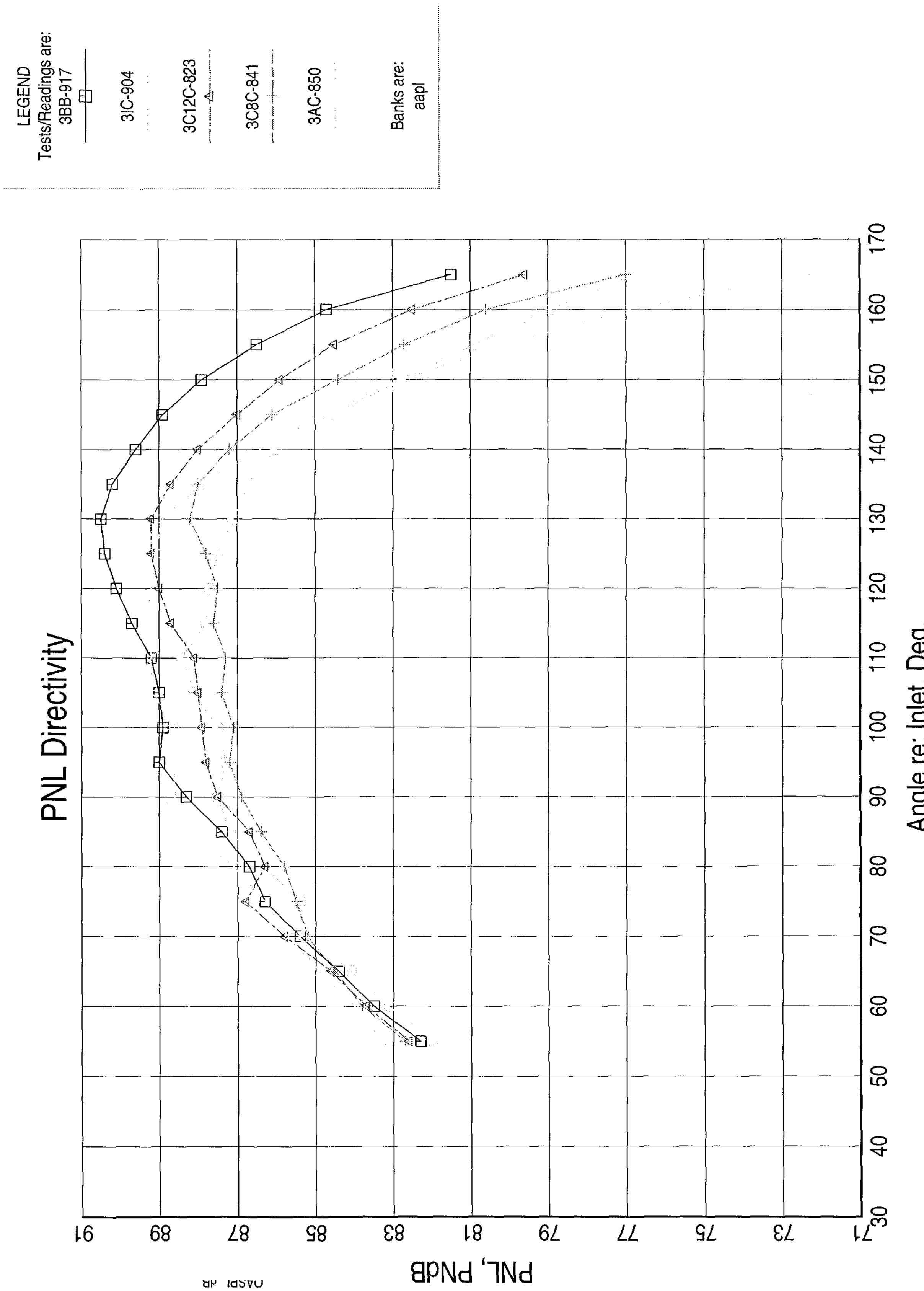
PNL Directivity
LEGEND
Tests/Readings are:
3BB-917
3IC-904
3C12C-823
3C8C-841
3AC-850
Banks are:
aapl
Angle re: Inlet, Deg.
PNL, PNdB
30
40
50
60
70
80
90
100
110
120
130
140
150
160
170
71
73
75
77
79
81
83
85
87
89
91

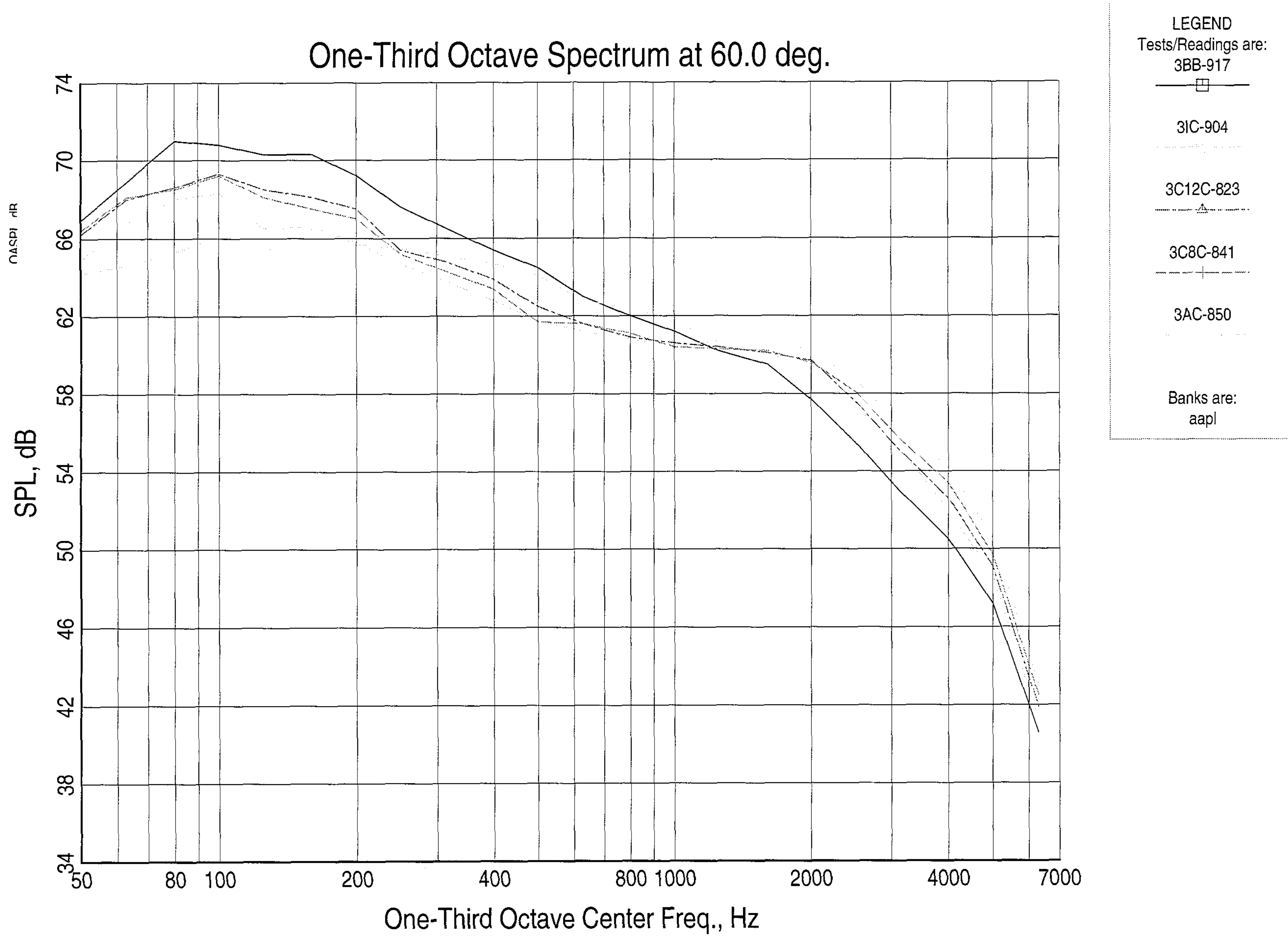
One-Third Octave Spectrum at 60.0 deg.
SPL, dB
74
70
66
62
58
54
50
46
42
38
34
50
80
100
200
400
800
1000
2000
4000
7000
One-Third Octave Center Freq., Hz
LEGEND
Tests/Readings are:
3BB-917
3IC-904
3C12C-823
3C8C-841
3AC-850
Banks are:
aapl

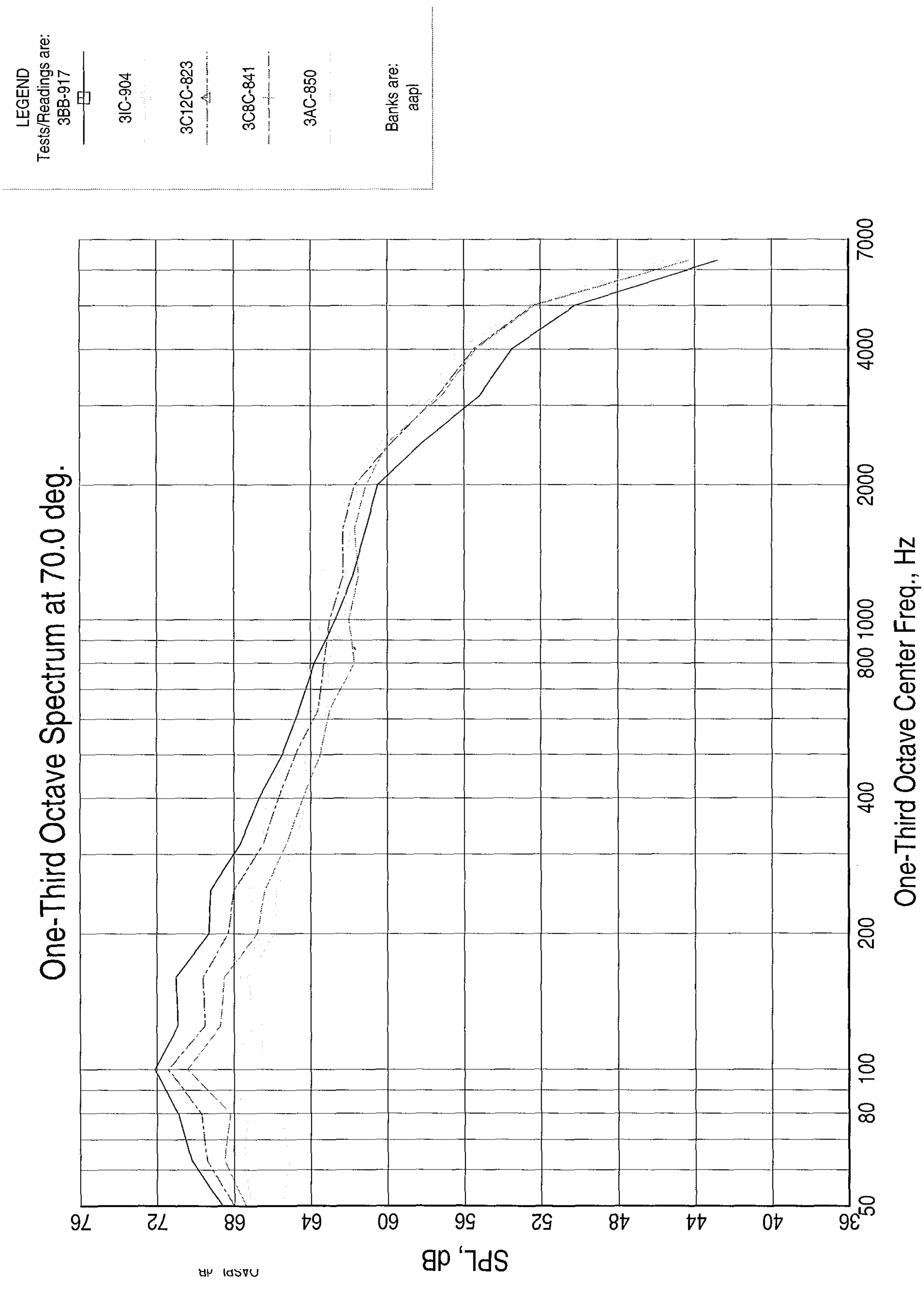
One-Third Octave Spectrum at 70.0 deg.
LEGEND
Tests/Readings are:
3BB-917
3IC-904
3C12C-823
3C8C-841
3AC-850
Banks are:
aapl
SPL, dB
One-Third Octave Center Freq., Hz
36
40
44
48
52
56
60
64
68
72
76
50
80
100
200
400
800
1000
2000
4000
7000

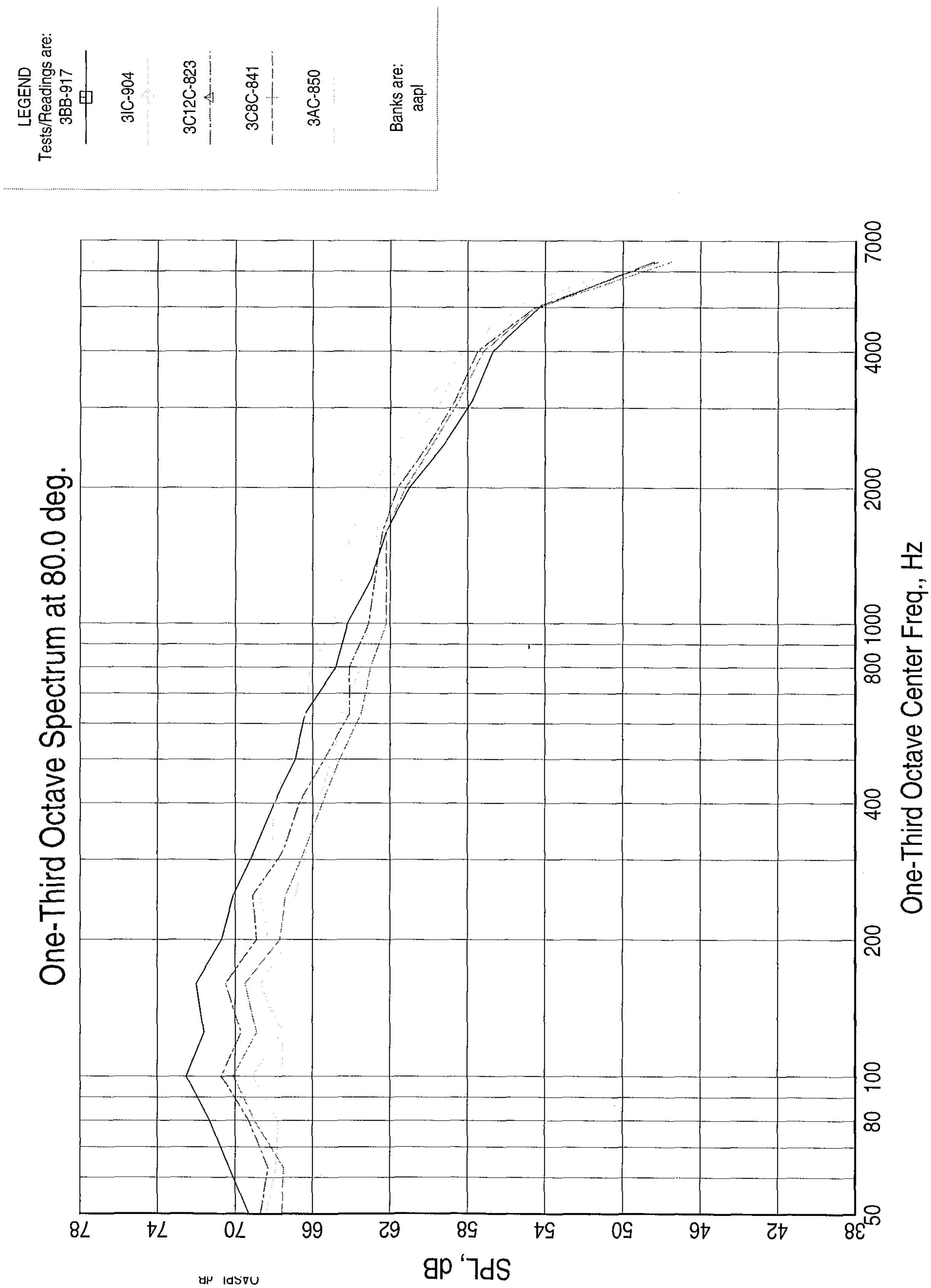
One-Third Octave Spectrum at 80.0 deg.
LEGEND
Tests/Readings are:
3BB-917
3IC-904
3C12C-823
3C8C-841
3AC-850
Banks are:
aapl
SPL, dB
One-Third Octave Center Freq., Hz
38
42
46
50
54
58
62
66
70
74
78
50
80
100
200
400
800
1000
2000
4000
7000

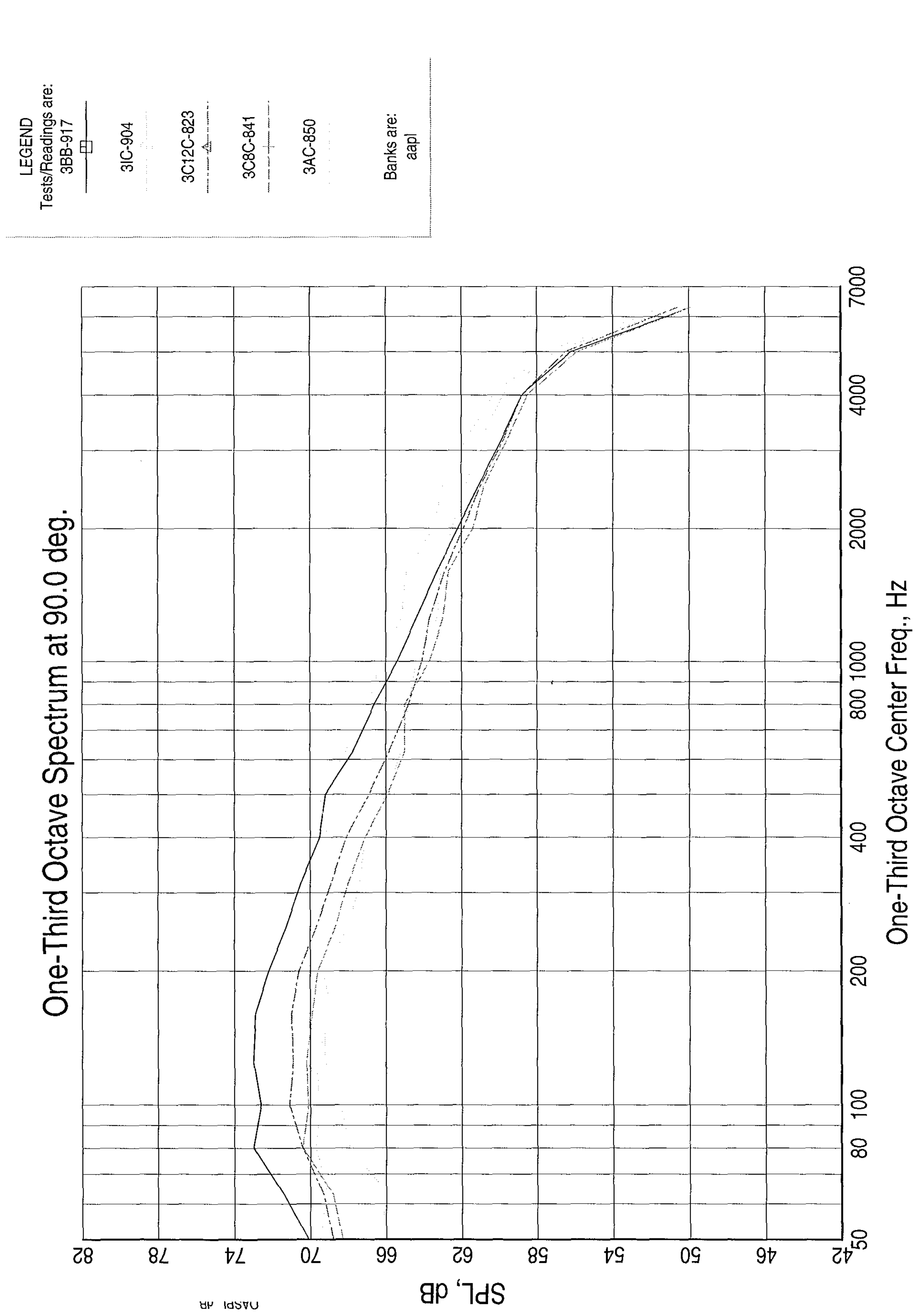
One-Third Octave Spectrum at 90.0 deg.
LEGEND
Tests/Readings are:
3BB-917
3IC-904
3C12C-823
3C8C-841
3AC-850
Banks are:
aapl
SPL, dB
OASPL dB
82
78
74
70
66
62
58
54
50
46
42
50
80
100
200
400
800
1000
2000
4000
7000
One-Third Octave Center Freq., Hz

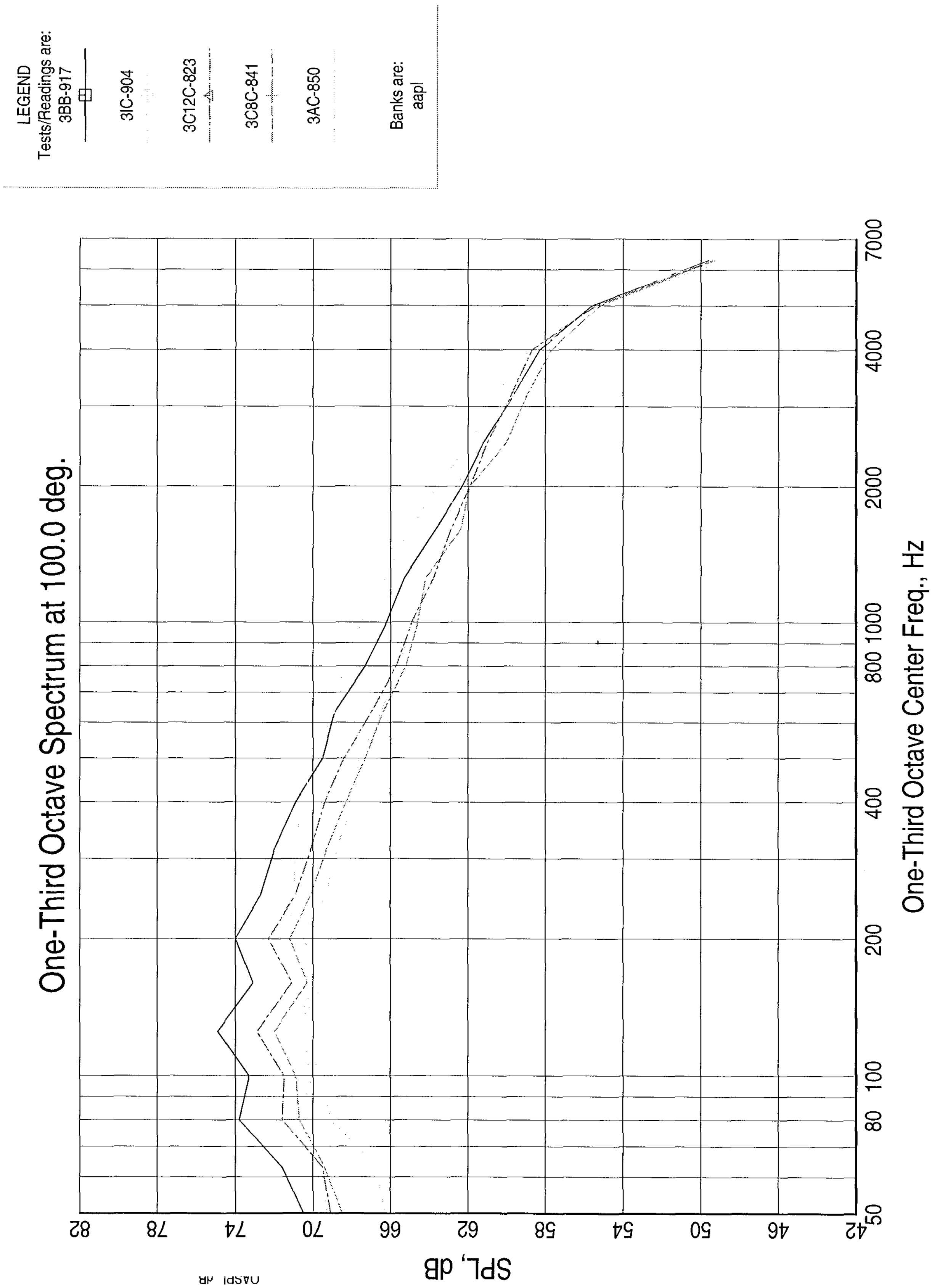

One-Third Octave Spectrum at 100.0 deg.
LEGEND
Tests/Readings are:
3BB-917
3IC-904
3C12C-823
3C8C-841
3AC-850
Banks are:
aapl
SPL, dB
OASPL dB
One-Third Octave Center Freq., Hz
42
46
50
54
58
62
66
70
74
78
82
50
80
100
200
400
800
1000
2000
4000
7000

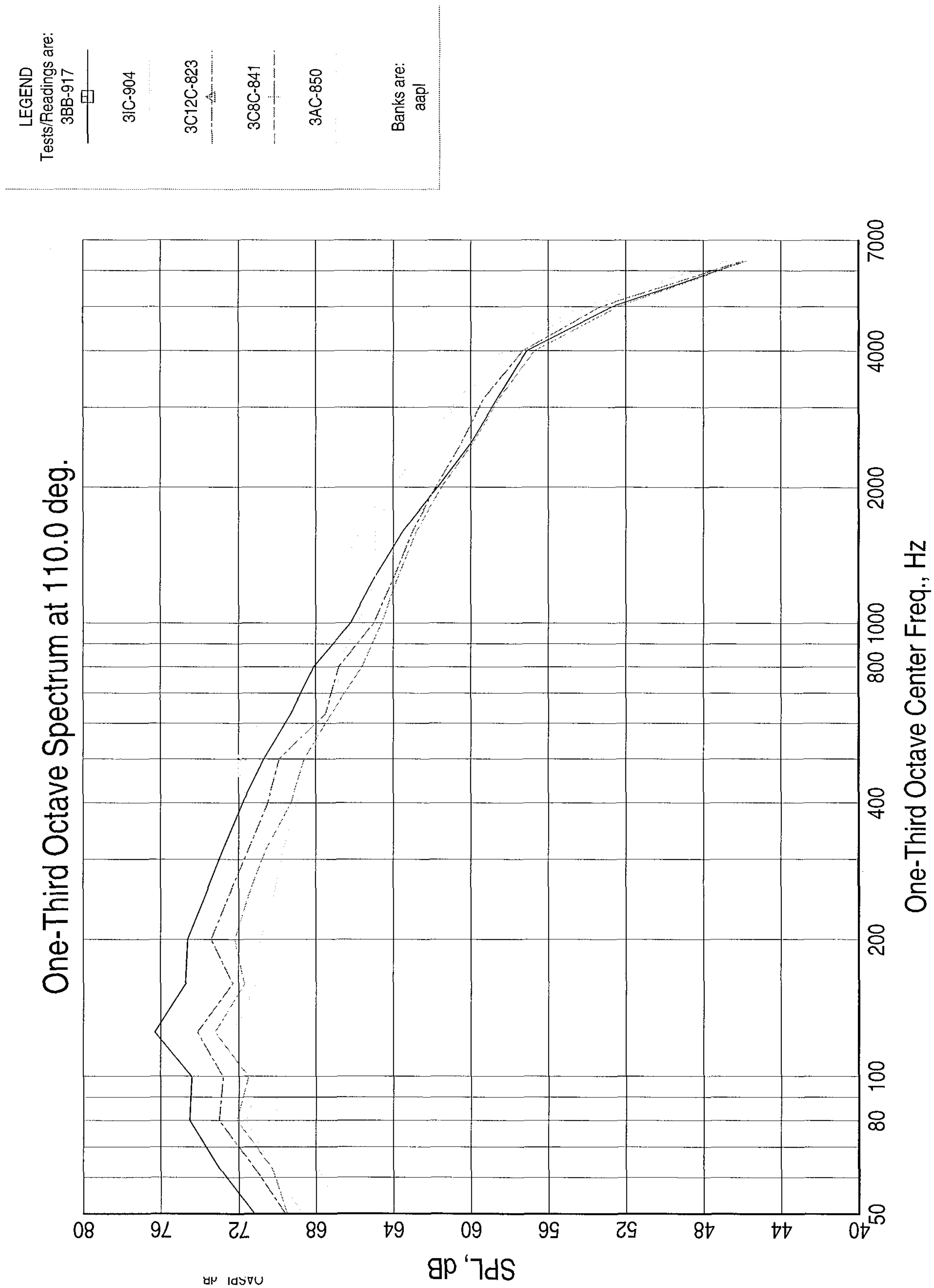

One-Third Octave Spectrum at 110.0 deg.
LEGEND
Tests/Readings are:
3BB-917
3IC-904
3C12C-823
3C8C-841
3AC-850
Banks are:
aapl
SPL, dB
OASPL dB
80
76
72
68
64
60
56
52
48
44
40
50
80
100
200
400
800 1000
2000
4000
7000
One-Third Octave Center Freq., Hz

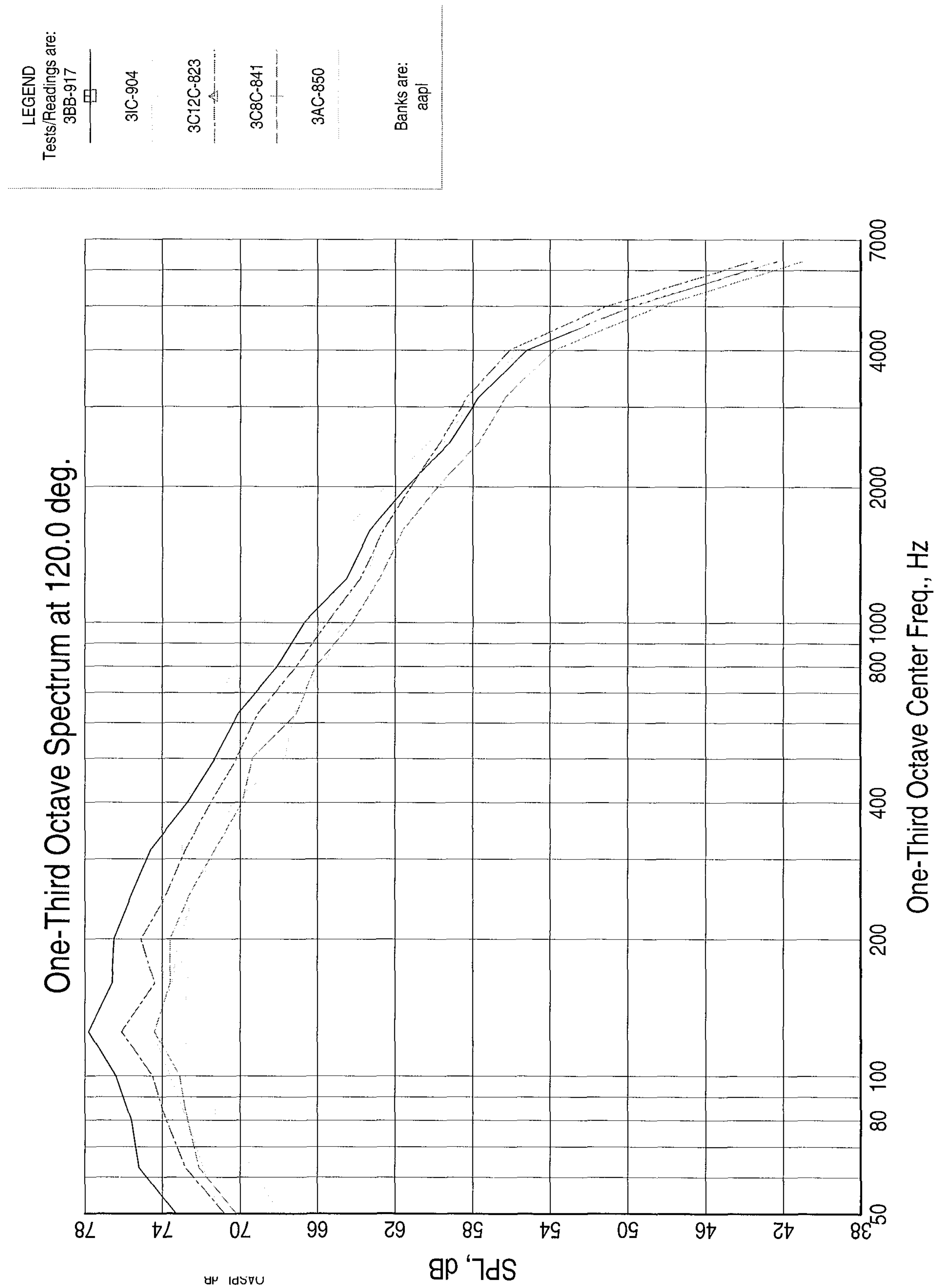
One-Third Octave Spectrum at 120.0 deg.
LEGEND
Tests/Readings are:
3BB-917
3IC-904
3C12C-823
3C8C-841
3AC-850
Banks are:
aapl
SPL, dB
78
74
70
66
62
58
54
50
46
42
38
50
80
100
200
400
800
1000
2000
4000
7000
One-Third Octave Center Freq., Hz

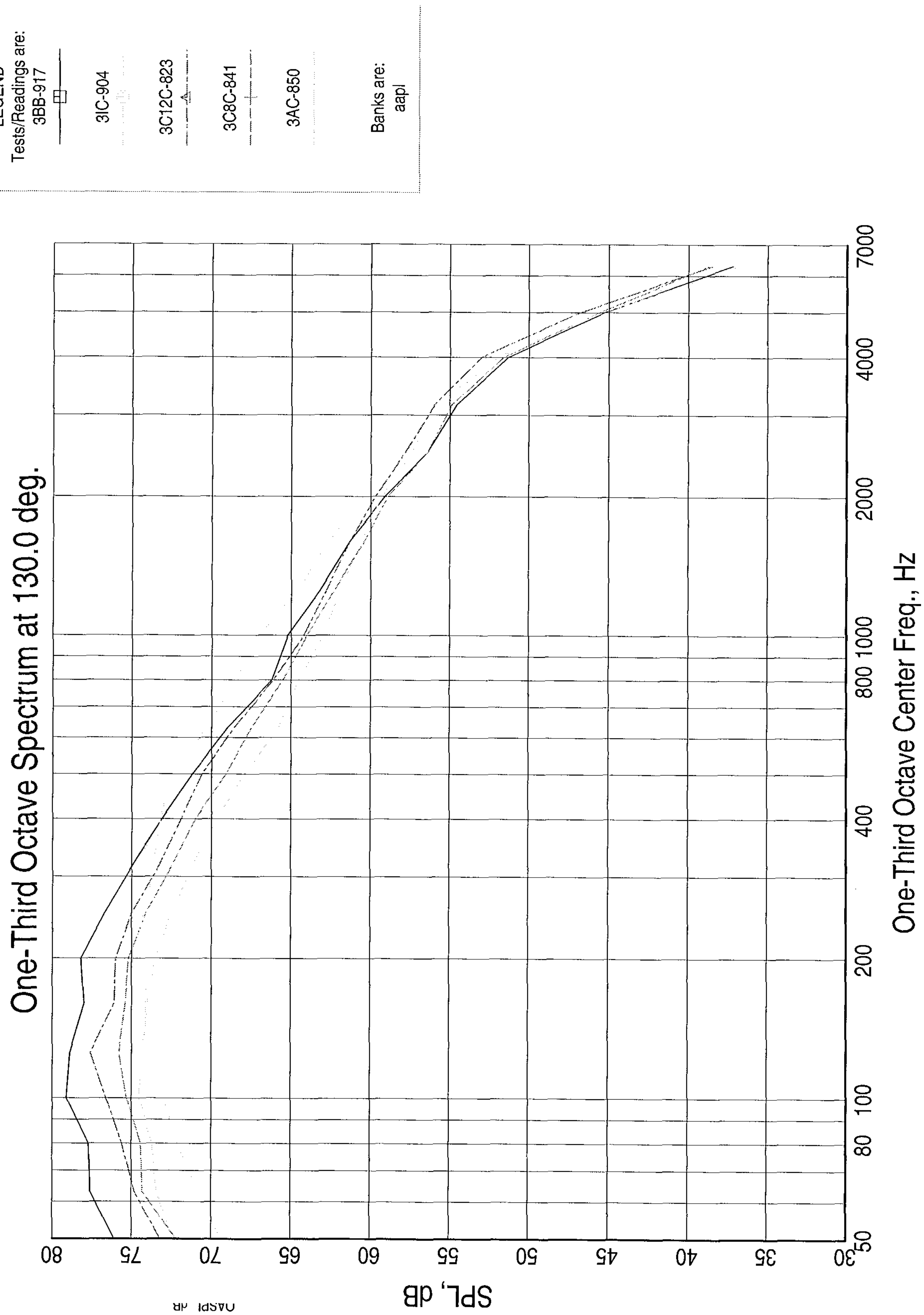
One-Third Octave Spectrum at 130.0 deg.
LEGEND
Tests/Readings are:
3BB-917
3IC-904
3C12C-823
3C8C-841
3AC-850
Banks are:
aapl
SPL, dB
One-Third Octave Center Freq., Hz
80
75
70
65
60
55
50
45
40
35
30
50
80
100
200
400
800 1000
2000
4000
7000

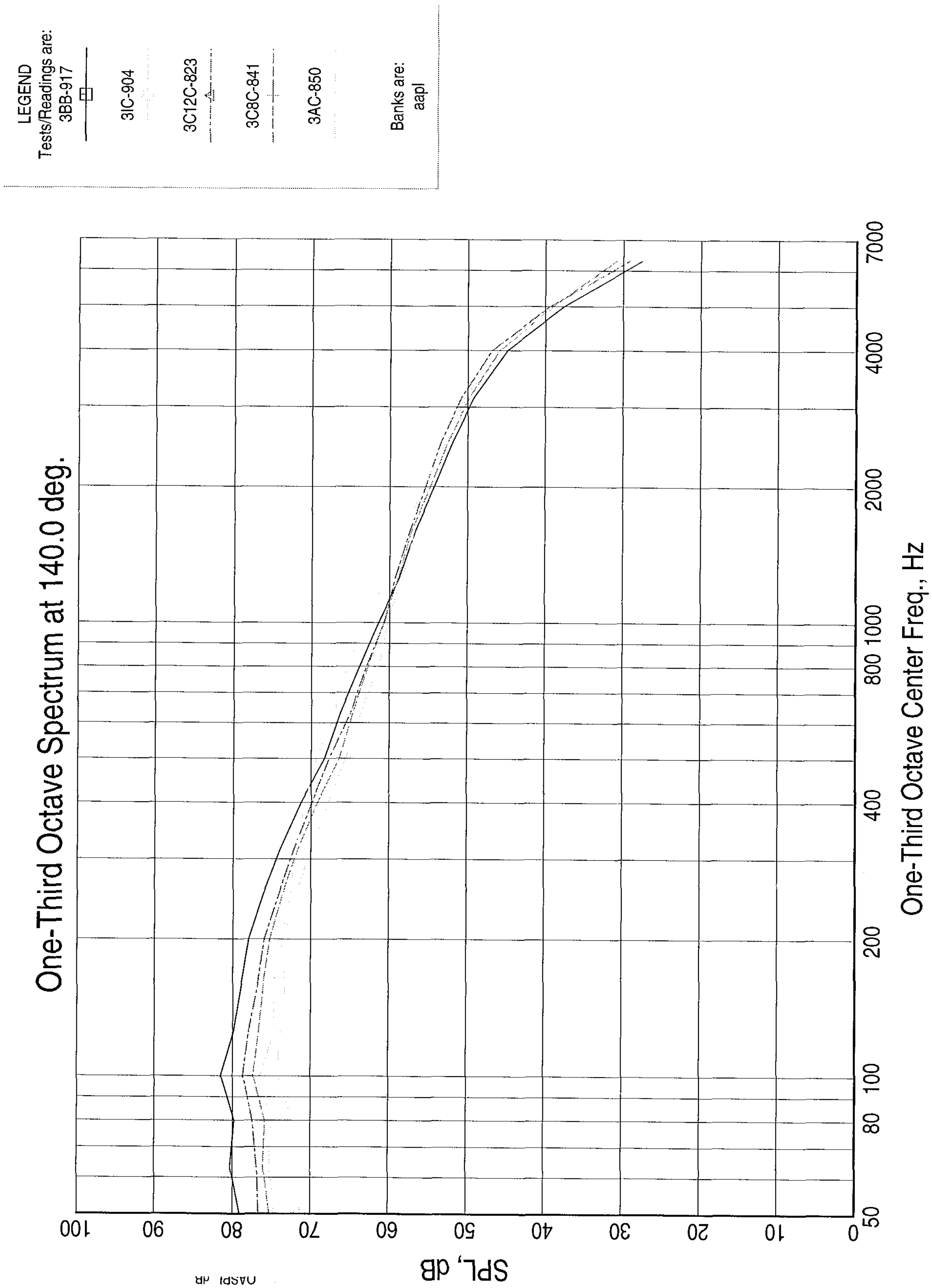
One-Third Octave Spectrum at 140.0 deg.
LEGEND
Tests/Readings are:
3BB-917
3IC-904
3C12C-823
3C8C-841
3AC-850
Banks are:
aapl
SPL, dB
0 10 20 30 40 50 60 70 80 90 100
50 80 100 200 400 800 1000 2000 4000 7000
One-Third Octave Center Freq., Hz

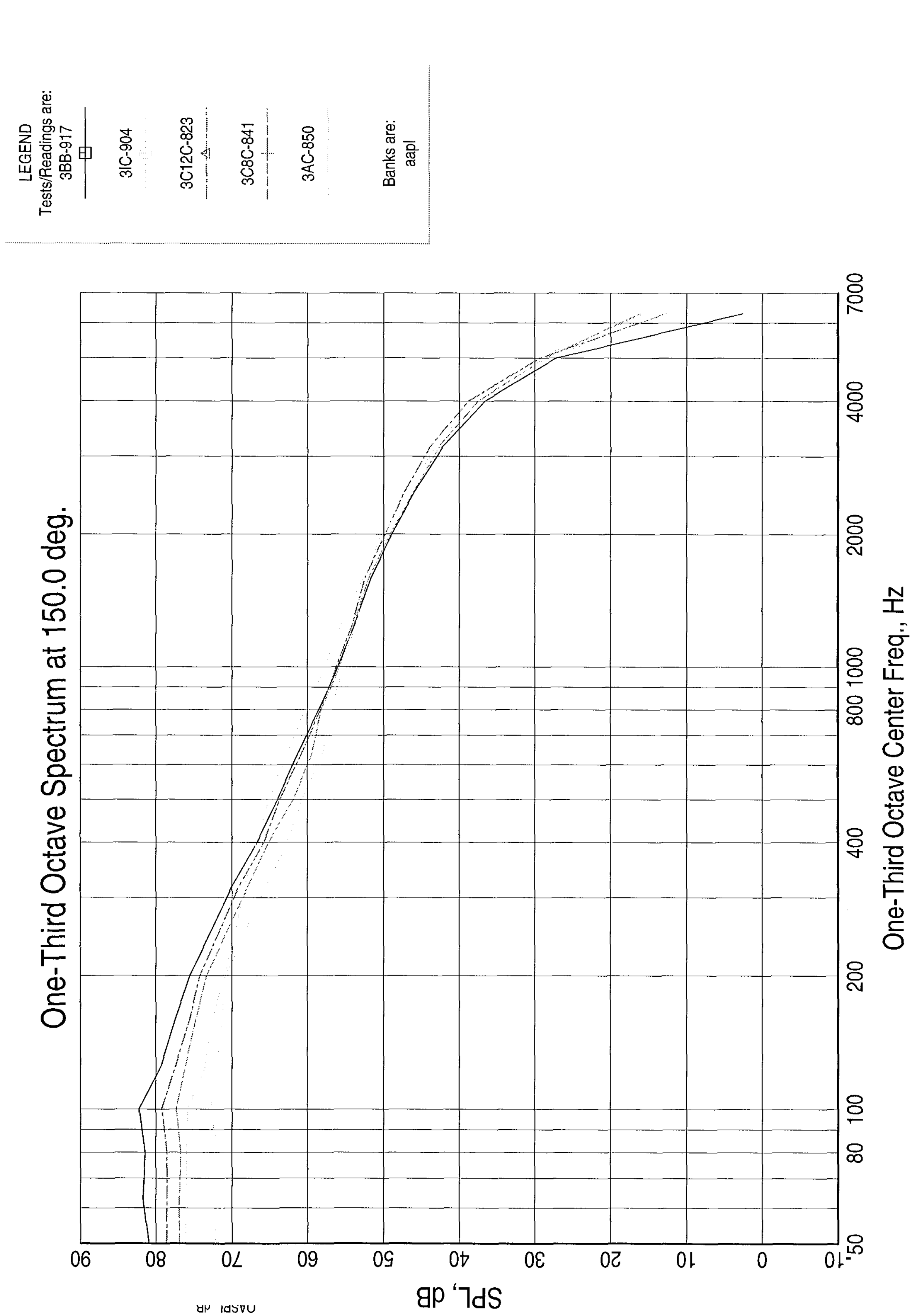

One-Third Octave Spectrum at 150.0 deg.
LEGEND
Tests/Readings are:
3BB-917
3IC-904
3C12C-823
3C8C-841
3AC-850
Banks are:
aapl
SPL, dB
90
80
70
60
50
40
30
20
10
0
-10
50
80
100
200
400
800
1000
2000
4000
7000
One-Third Octave Center Freq., Hz

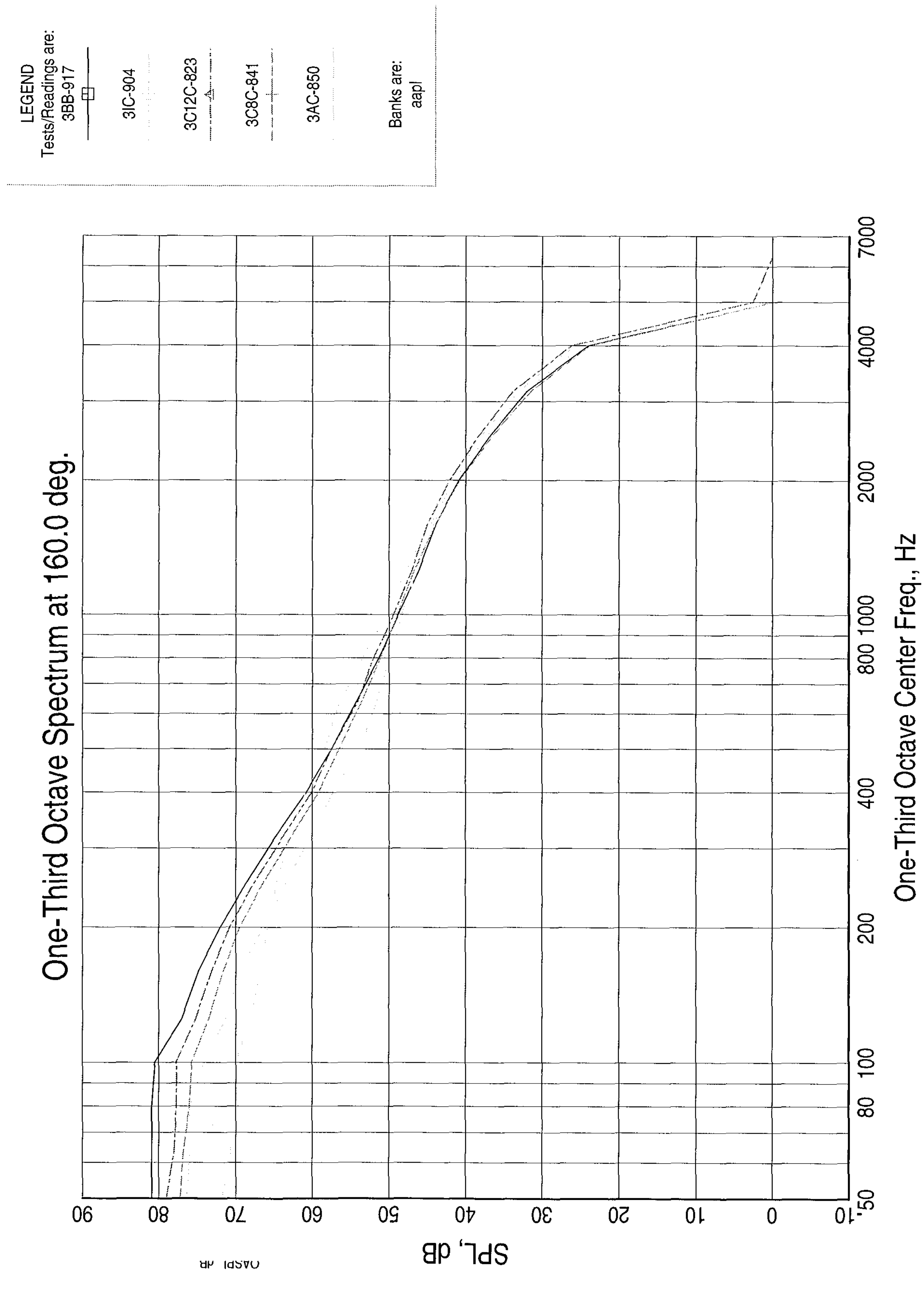
One-Third Octave Spectrum at 160.0 deg.
LEGEND
Tests/Readings are:
3BB-917
3IC-904
3C12C-823
3C8C-841
3AC-850
Banks are:
aapl
SPL, dB
OASPL dB
One-Third Octave Center Freq., Hz
90
80
70
60
50
40
30
20
10
0
-10
50
80
100
200
400
800
1000
2000
4000
7000

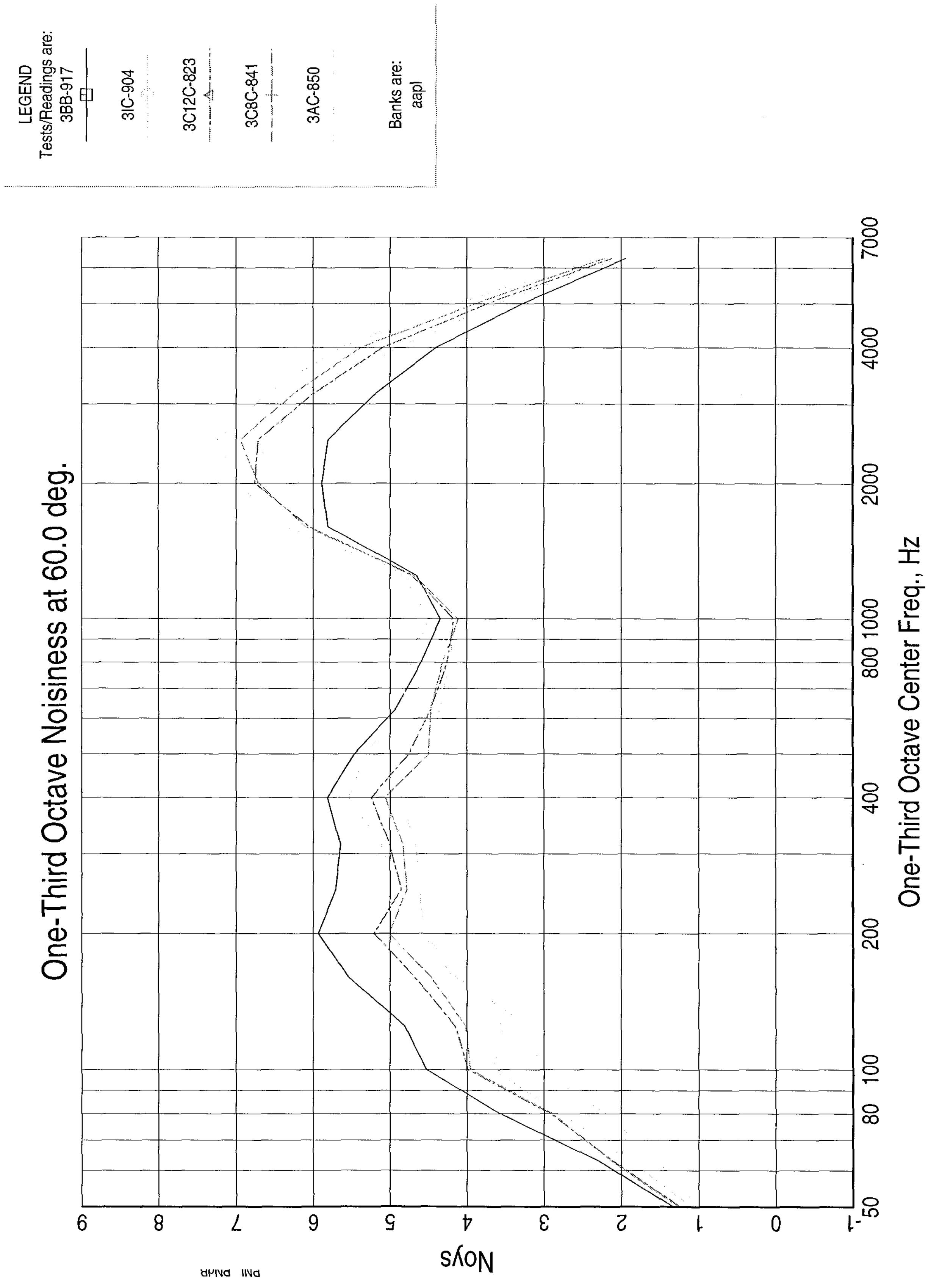
One-Third Octave Noisiness at 60.0 deg.
LEGEND
Tests/Readings are:
3BB-917
3IC-904
3C12C-823
3C8C-841
3AC-850
Banks are:
aapl
Noys
One-Third Octave Center Freq., Hz
50
80
100
200
400
800 1000
2000
4000
7000
-1
0
1
2
3
4
5
6
7
8
9

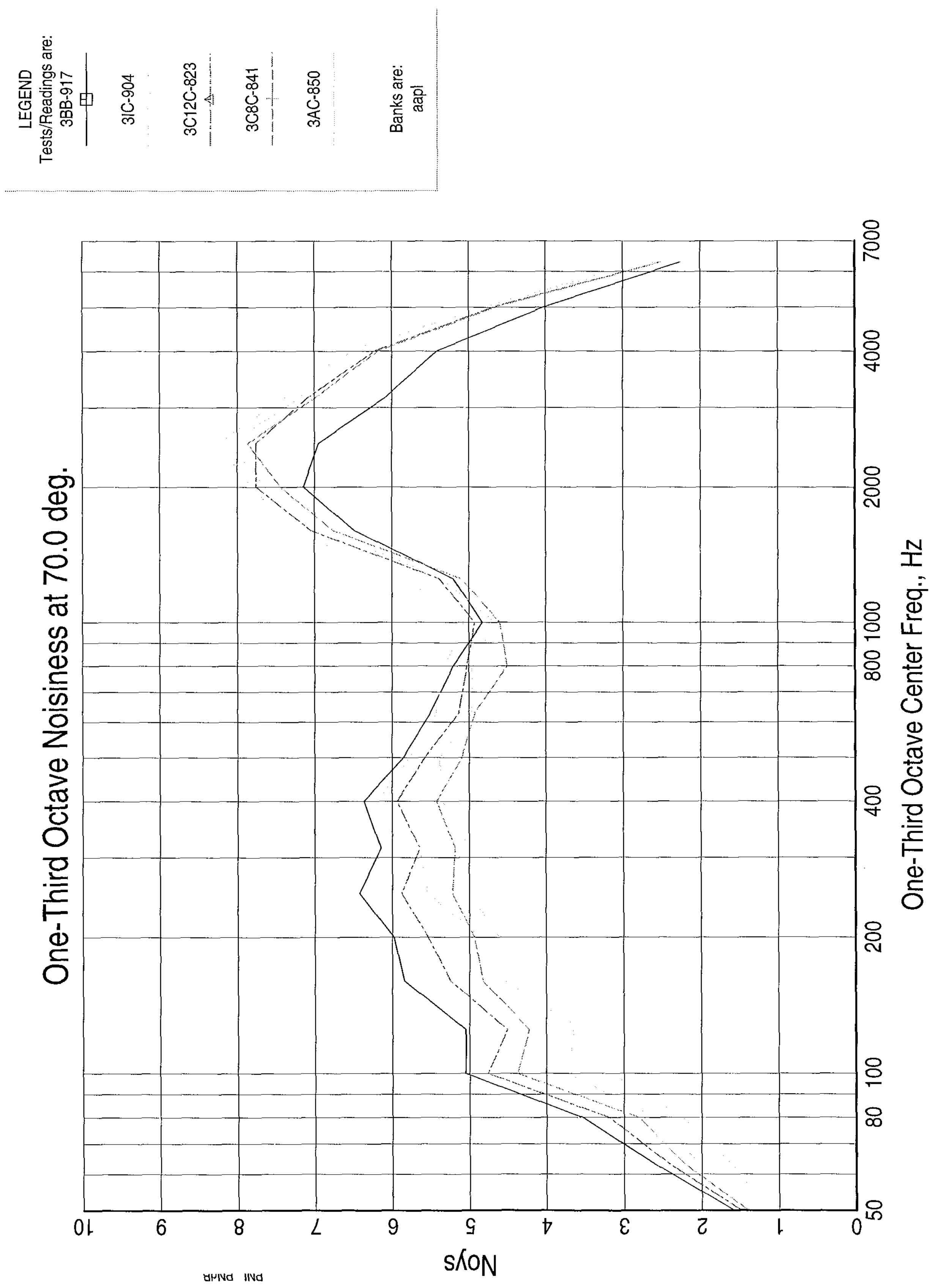
One-Third Octave Noisiness at 70.0 deg.
LEGEND
Tests/Readings are:
3BB-917
3IC-904
3C12C-823
3C8C-841
3AC-850
Banks are:
aapl
Noys
0
1
2
3
4
5
6
7
8
9
10
50
80
100
200
400
800 1000
2000
4000
7000
One-Third Octave Center Freq., Hz
PNI PNdB

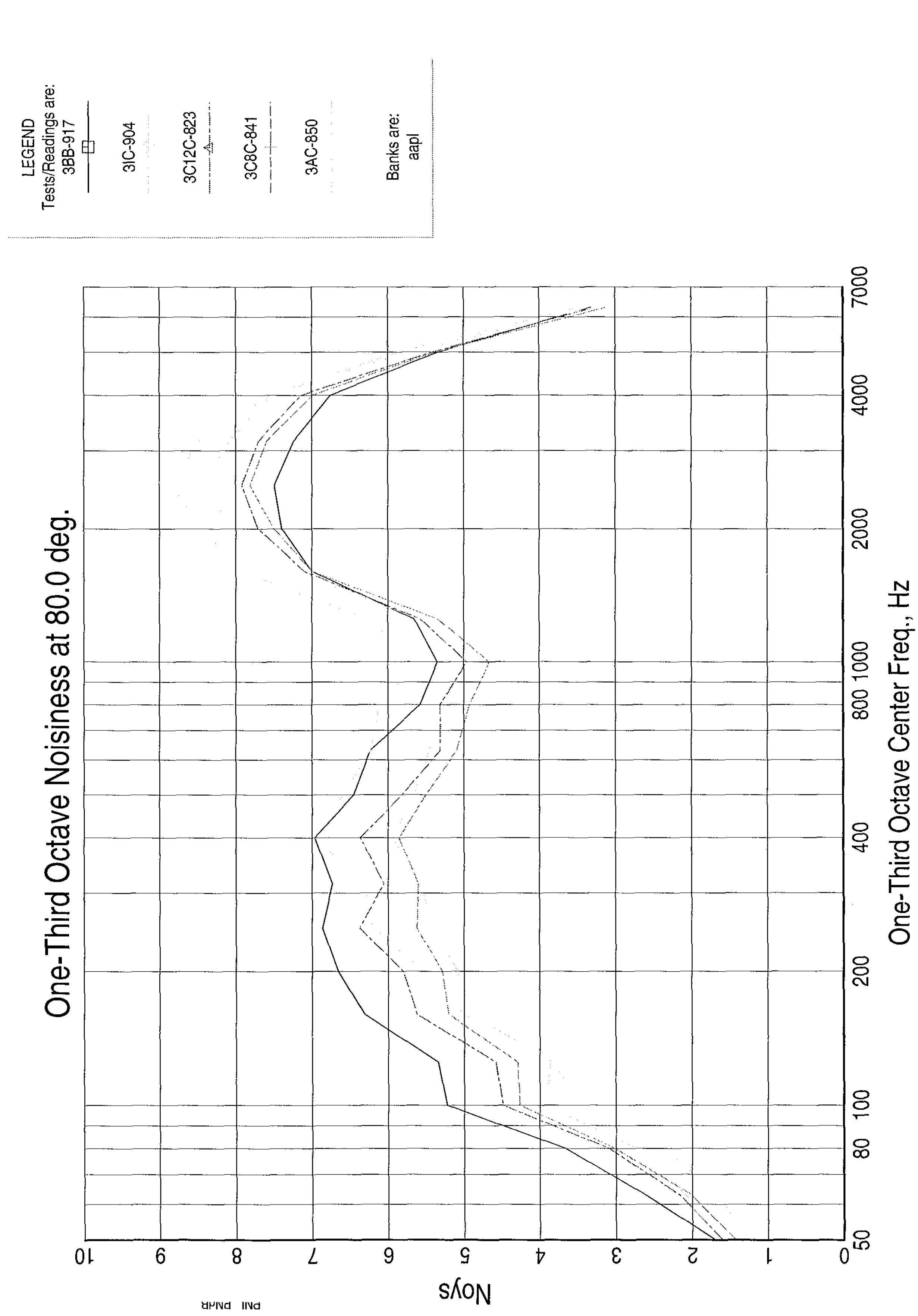

One-Third Octave Noisiness at 80.0 deg.
LEGEND
Tests/Readings are:
3BB-917
3IC-904
3C12C-823
3C8C-841
3AC-850
Banks are:
aapl
Noys
PNL PNdB
0
1
2
3
4
5
6
7
8
9
10
50
80
100
200
400
800
1000
2000
4000
7000
One-Third Octave Center Freq., Hz

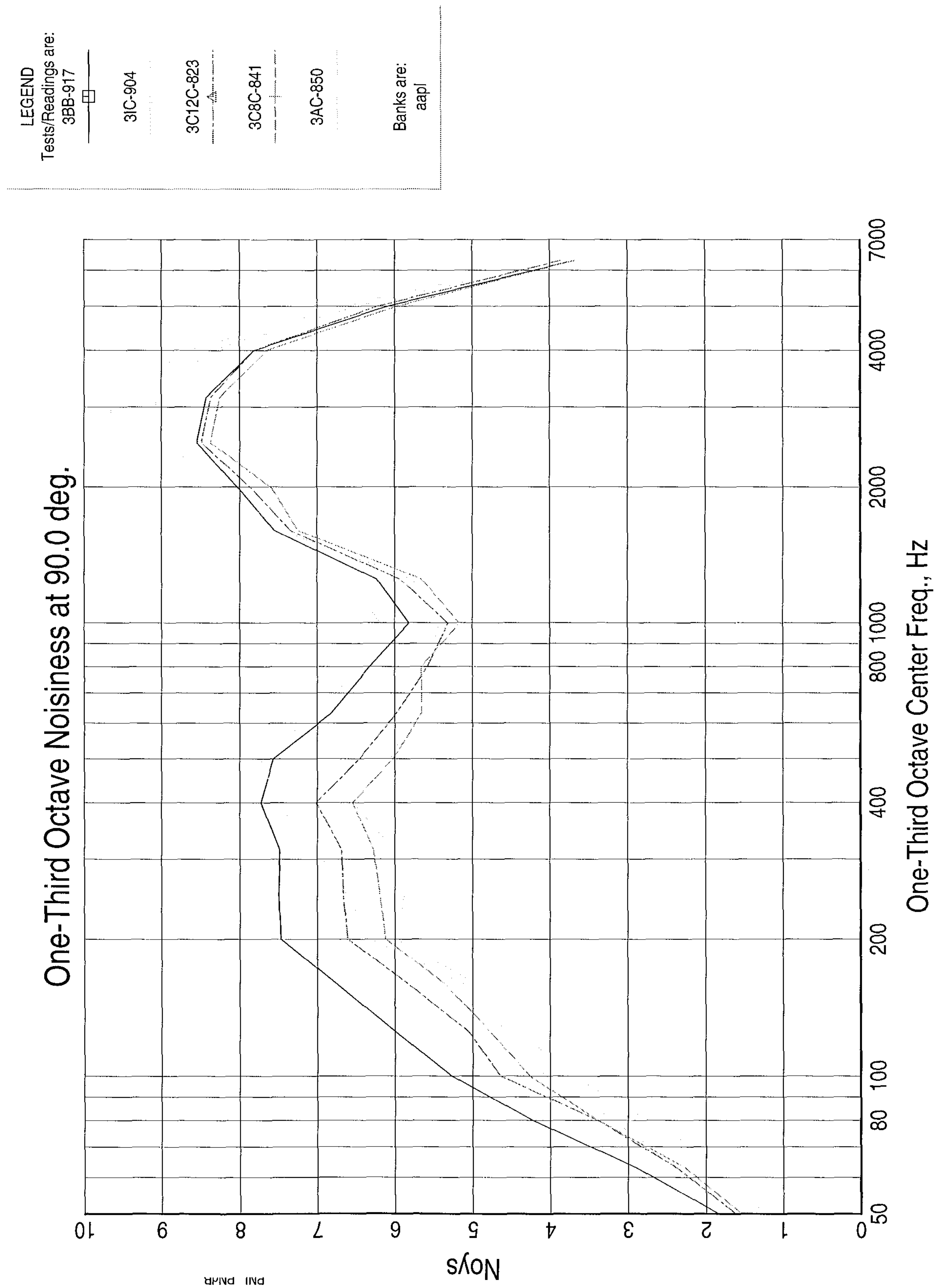
One-Third Octave Noisiness at 90.0 deg.
LEGEND
Tests/Readings are:
3BB-917
3IC-904
3C12C-823
3C8C-841
3AC-850
Banks are:
aapl
Noys
One-Third Octave Center Freq., Hz
0
1
2
3
4
5
6
7
8
9
10
50
80
100
200
400
800
1000
2000
4000
7000
PNI PNdB

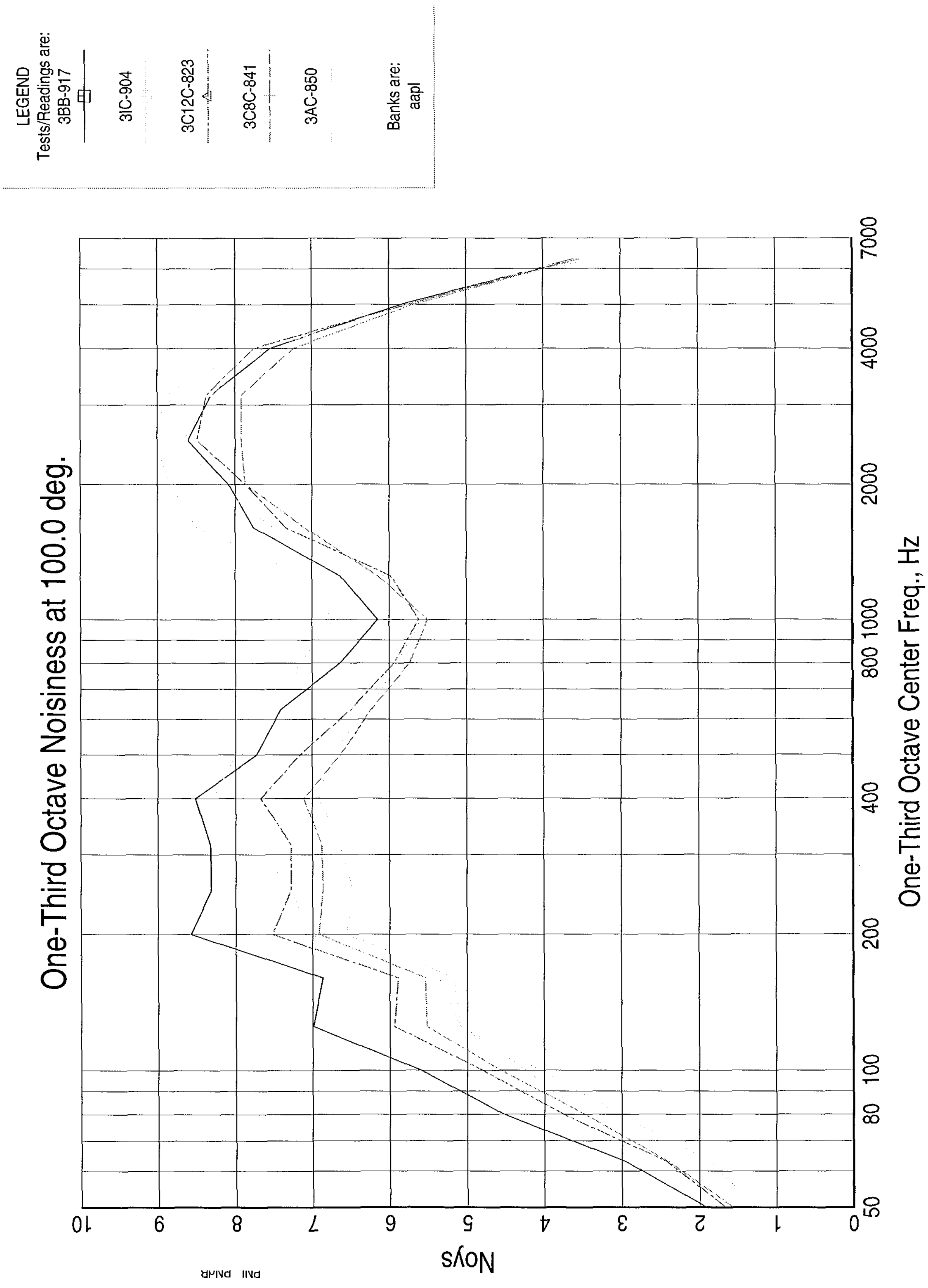
One-Third Octave Noisiness at 100.0 deg.
Noys
One-Third Octave Center Freq., Hz
LEGEND
Tests/Readings are:
3BB-917
3IC-904
3C12C-823
3C8C-841
3AC-850
Banks are:
aapl
0
1
2
3
4
5
6
7
8
9
10
50
80
100
200
400
800
1000
2000
4000
7000

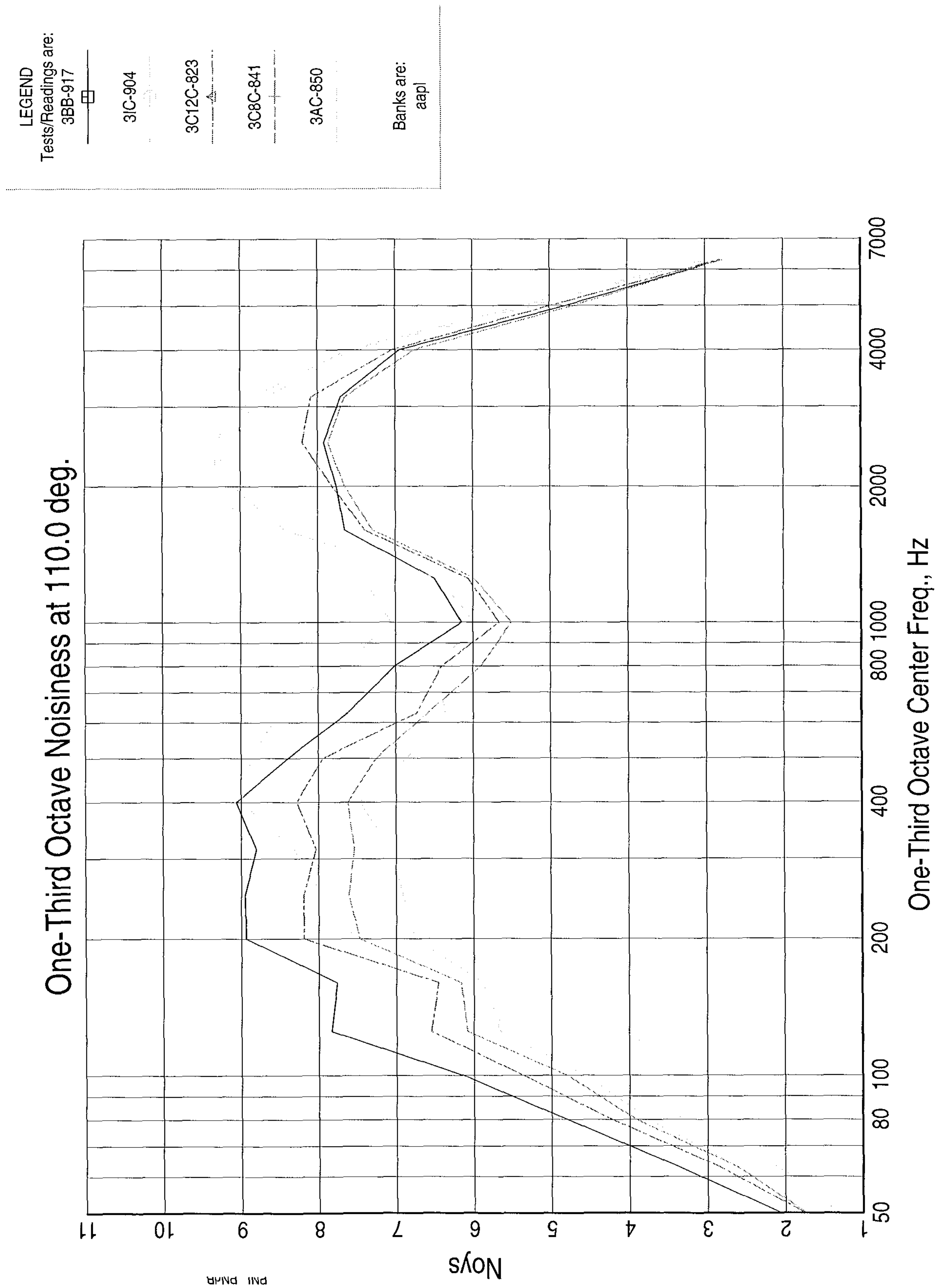
One-Third Octave Noisiness at 110.0 deg.
LEGEND
Tests/Readings are:
3BB-917
3IC-904
3C12C-823
3C8C-841
3AC-850
Banks are:
aapl
Noys
1
2
3
4
5
6
7
8
9
10
11
50
80
100
200
400
800
1000
2000
4000
7000
One-Third Octave Center Freq., Hz
PNL PNdB

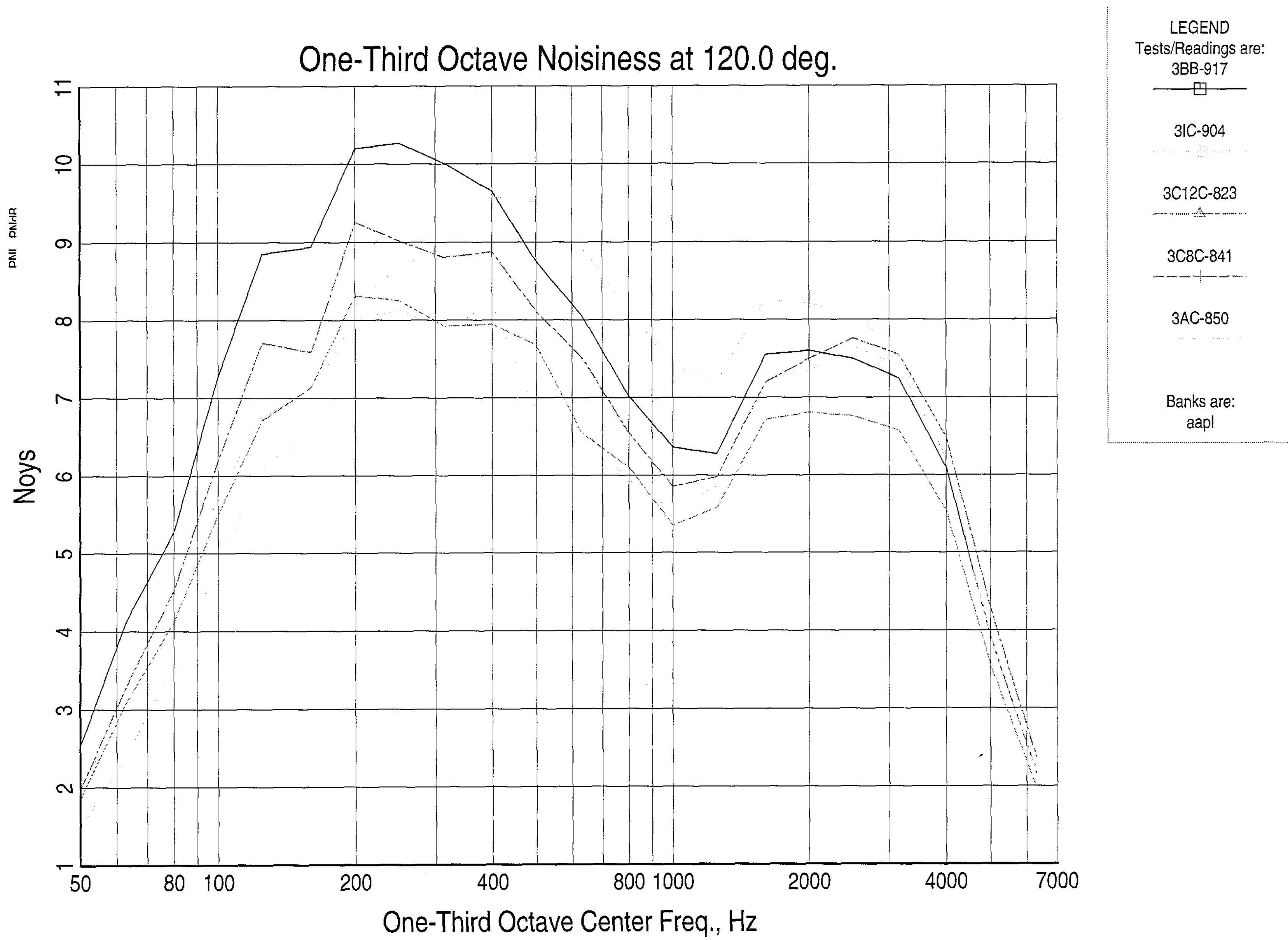
One-Third Octave Noisiness at 120.0 deg.
LEGEND
Tests/Readings are:
3BB-917
3IC-904
3C12C-823
3C8C-841
3AC-850
Banks are:
aapl
Noys
11
10
9
8
7
6
5
4
3
2
1
50
80
100
200
400
800
1000
2000
4000
7000
One-Third Octave Center Freq., Hz

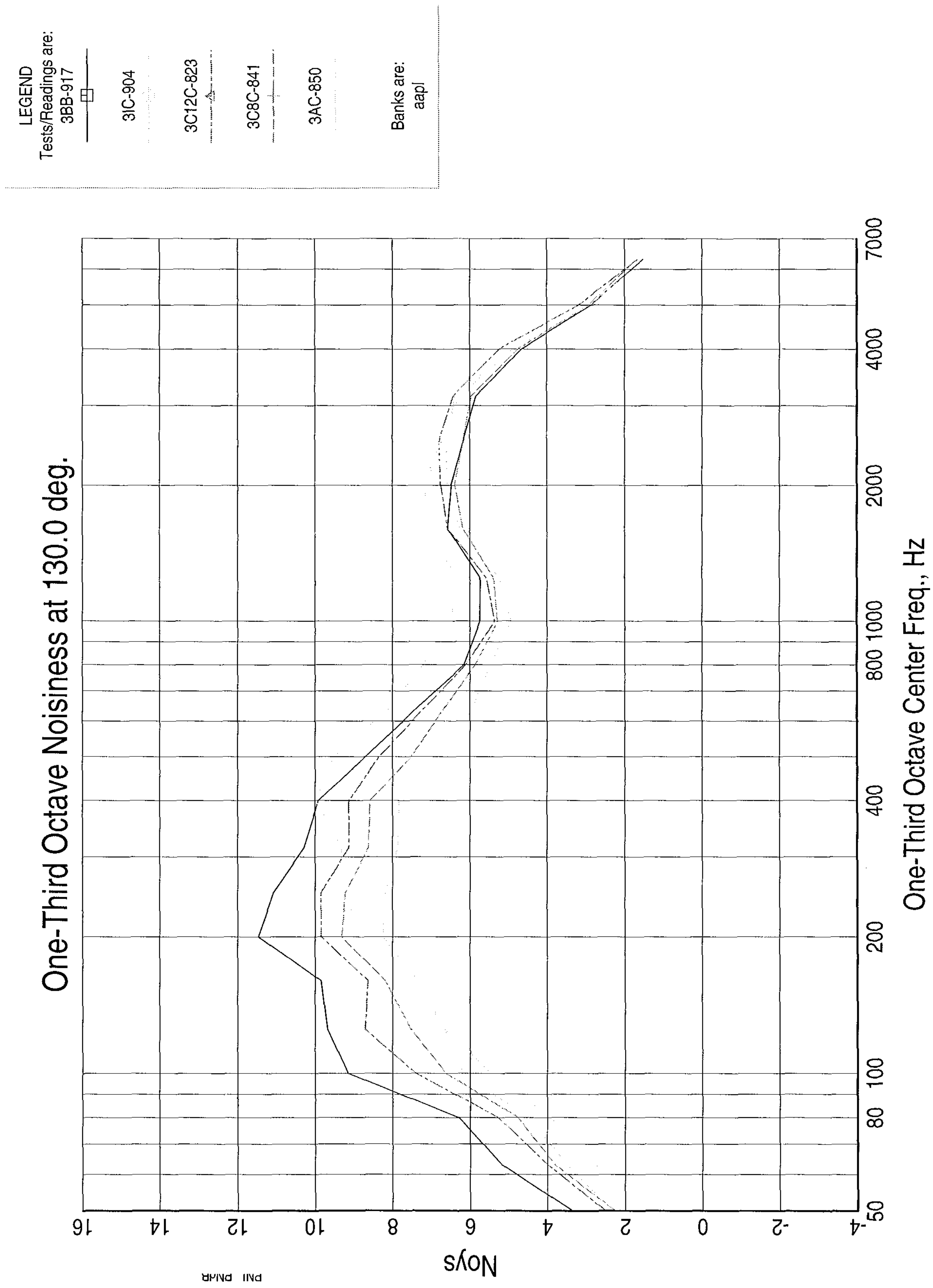
One-Third Octave Noisiness at 130.0 deg.
LEGEND
Tests/Readings are:
3BB-917
3IC-904
3C12C-823
3C8C-841
3AC-850
Banks are:
aapl
Noys
One-Third Octave Center Freq., Hz
50
80
100
200
400
800
1000
2000
4000
7000
-4
-2
0
2
4
6
8
10
12
14
16

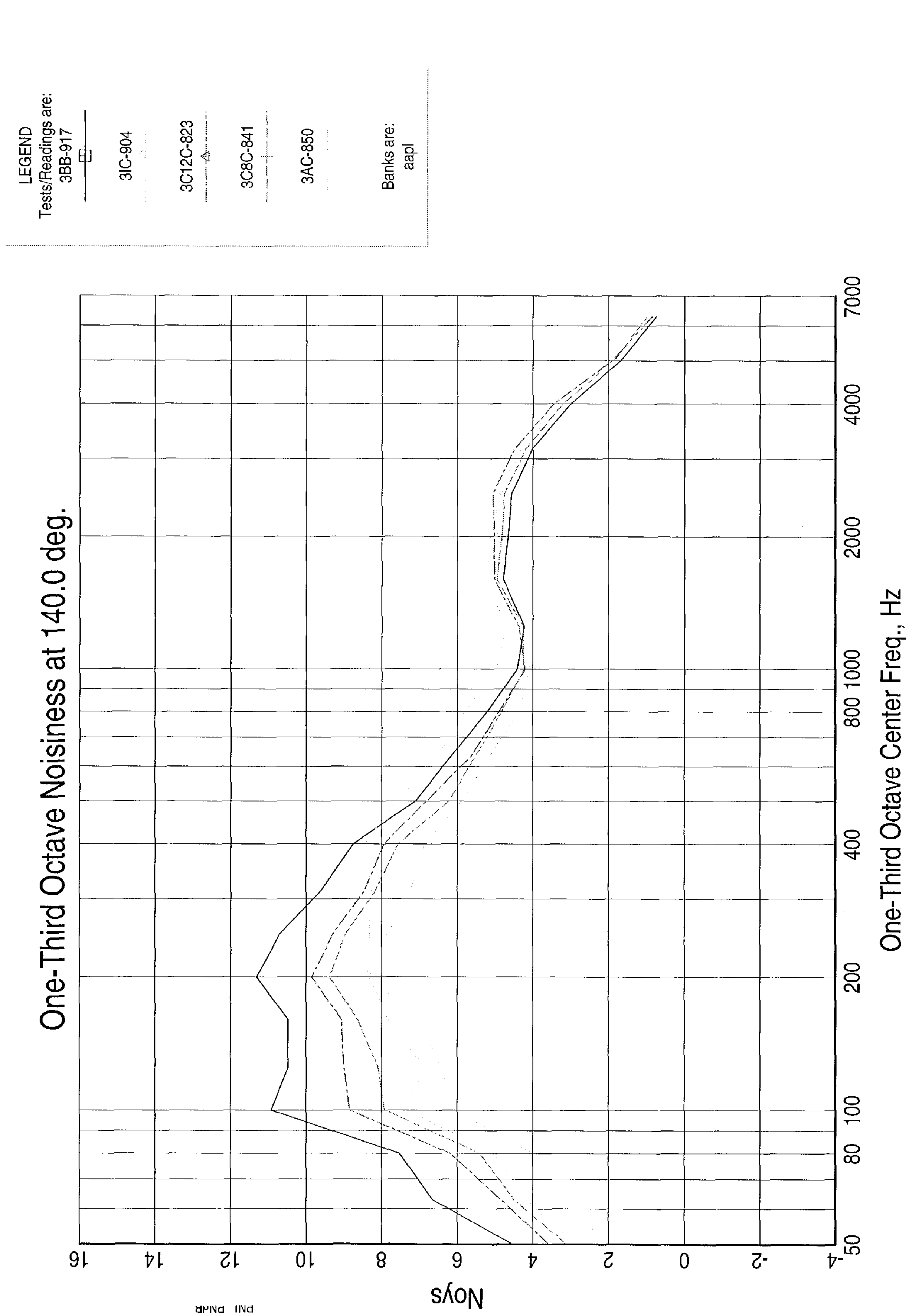
One-Third Octave Noisiness at 140.0 deg.
LEGEND
Tests/Readings are:
3BB-917
3IC-904
3C12C-823
3C8C-841
3AC-850
Banks are:
aapl
Noys
16
14
12
10
8
6
4
2
0
-2
-4
50
80
100
200
400
800
1000
2000
4000
7000
One-Third Octave Center Freq., Hz
PNI PNdB

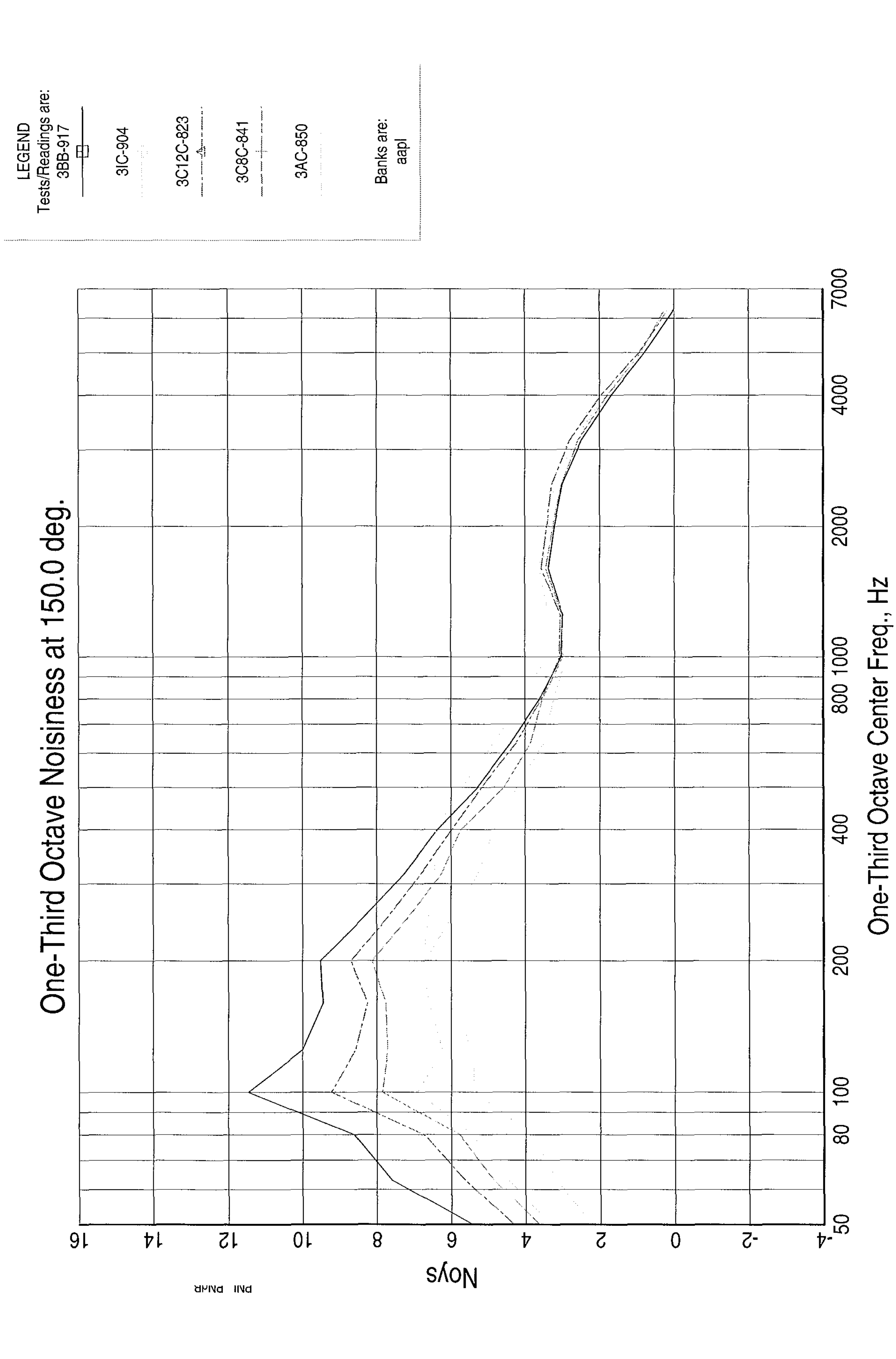
One-Third Octave Noisiness at 150.0 deg.
LEGEND
Tests/Readings are:
3BB-917
3IC-904
3C12C-823
3C8C-841
3AC-850
Banks are:
aapl
Noys
PNL PNdB
-4
-2
0
2
4
6
8
10
12
14
16
50
80
100
200
400
800 1000
2000
4000
7000
One-Third Octave Center Freq., Hz

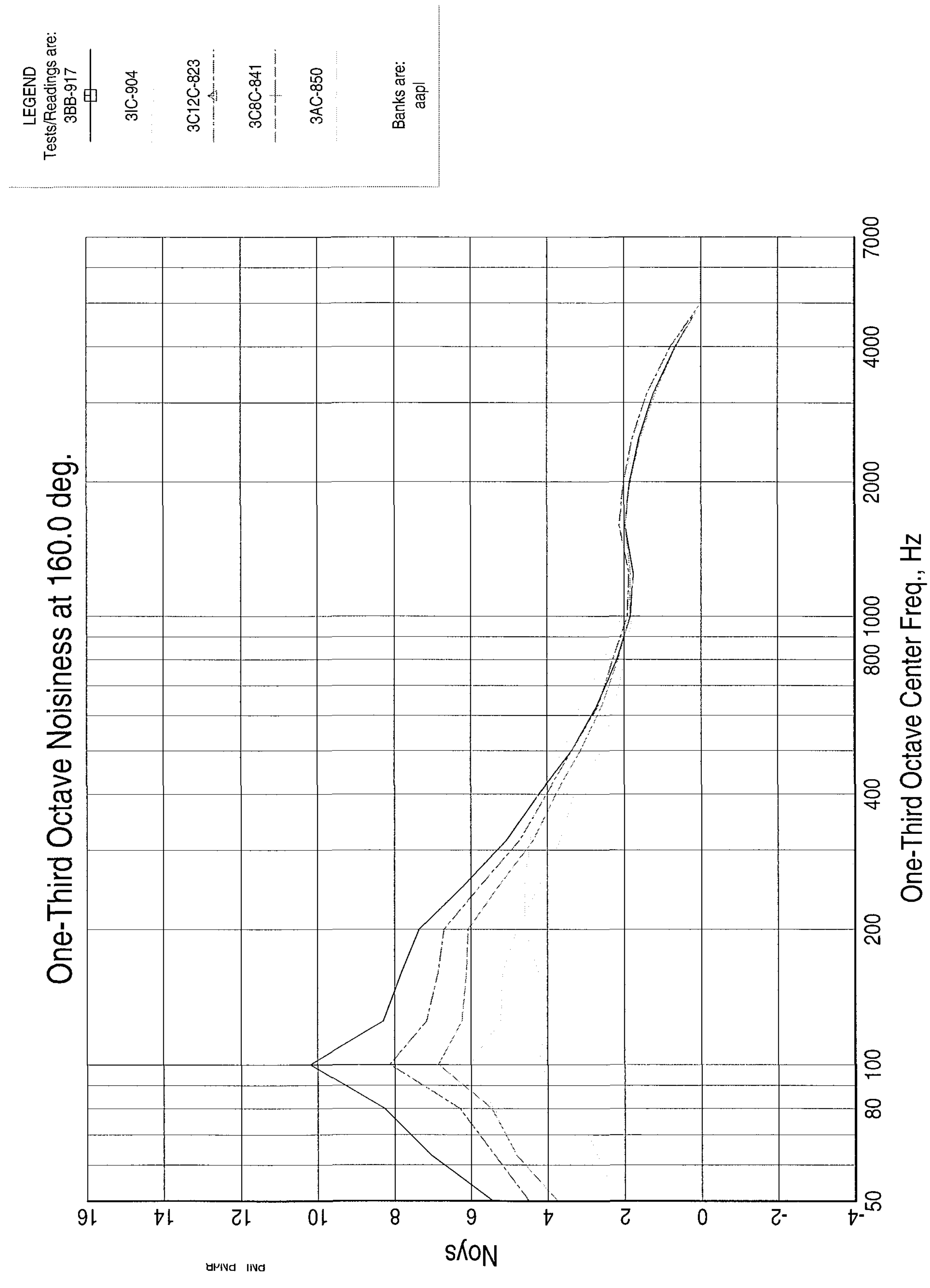
One-Third Octave Noisiness at 160.0 deg.
Noys
One-Third Octave Center Freq., Hz
16
14
12
10
8
6
4
2
0
-2
-4
50
80
100
200
400
800 1000
2000
4000
7000
LEGEND
Tests/Readings are:
3BB-917
3IC-904
3C12C-823
3C8C-841
3AC-850
Banks are:
aapl
PNI PNdB

# REPORT DOCUMENTATION PAGE

*Form Approved*
*OMB No. 0704-0188*



**1. AGENCY USE ONLY** (*Leave blank*)

**2. REPORT DATE**
December 2000

**3. REPORT TYPE AND DATES COVERED**
Final Contractor Report

**4. TITLE AND SUBTITLE**
AST Critical Propulsion and Noise Reduction Technologies for Future Commercial Subsonic Engines
Separate-Flow Exhaust System Noise Reduction Concept Evaluation

**5. FUNDING NUMBERS**
WU–522–81–11–00
NAS3–27720
Area of Interest 14.3

**6. AUTHOR(S)**
B.A. Janardan, G.E. Hoff, J.W. Barter, S. Martens, P.R. Gliebe, V. Mengle, and W.N. Dalton

**7. PERFORMING ORGANIZATION NAME(S) AND ADDRESS(ES)**
General Electric Aircraft Engines
Advanced Engineering Programs Department
One Neumann Way
Cincinnati, Ohio 45215–6301

**8. PERFORMING ORGANIZATION REPORT NUMBER**
E–12237

**9. SPONSORING/MONITORING AGENCY NAME(S) AND ADDRESS(ES)**
National Aeronautics and Space Administration
Washington, DC 20546–0001

**10. SPONSORING/MONITORING AGENCY REPORT NUMBER**
NASA CR—2000-210039
R98AEB152

**11. SUPPLEMENTARY NOTES**
B.A. Janardan, G.E. Hoff, J.W. Barter, S. Martens, and P.R. Gliebe, General Electric Aircraft Engines, Advanced Engineering Programs Department, One Neumann Way, Cincinnati, Ohio 45215–6301; V. Mengle and W.N. Dalton, Allison Engine Company, Indianapolis, Indiana. Project Manager, Naseem Saiyed, Structures and Acoustics Division, NASA Glenn Research Center, organization code 5940, 216–433–6736.

**12a. DISTRIBUTION/AVAILABILITY STATEMENT**
Unclassified - Unlimited
Subject Category: 71 Distribution: Nonstandard
Available electronically at http://gltrs.grc.nasa.gov/GLTRS
This publication is available from the NASA Center for AeroSpace Information, 301–621–0390.

**12b. DISTRIBUTION CODE**

**13. ABSTRACT** ***(Maximum 200 words)***
This report describes the work performed by General Electric Aircraft Engines (GEAE) and Allison Engine Company (AEC) on NASA Contract NAS3–27720 AoI 14.3. The objective of this contract was to generate quality jet noise acoustic data for separate-flow nozzle models and to design and verify new jet-noise-reduction concepts over a range of simulated engine cycles and flight conditions. Five baseline axisymmetric separate-flow nozzle models having bypass ratios of 5 and 8 with internal and external plugs and eleven different mixing-enhancer model nozzles (including chevrons, vortex-generator doublets, and a tongue mixer) were designed and tested in model scale. Using available core and fan nozzle hardware in various combinations, 28 GEAE/AEC separate-flow nozzle/mixing-enhancer configurations were acoustically evaluated in the NASA Glenn Research Center Aeroacoustic and Propulsion Laboratory. This report describes model nozzle features, facility and data acquisition/reduction procedures, the test matrix, and measured acoustic data analyses. A number of tested core and fan mixing enhancer devices and combinations of devices gave significant jet noise reduction relative to separate-flow baseline nozzles. Inward-flip and alternating-flip core chevrons combined with a straight-chevron fan nozzle exceeded the NASA stretch goal of 3 EPNdB jet noise reduction at typical sideline certification conditions.

**14. SUBJECT TERMS**
Acoustic nozzles; Aeroacoustics; Aircraft noise; Engine noise; Exhaust noise; Jet aircraft noise; Jet engines; Mixers; Noise reduction; Noise suppressors; Sonic nozzles; Subsonic jet noise; mixing enhancement; Chevrons

**15. NUMBER OF PAGES**
299

**16. PRICE CODE**
A13

| 17. SECURITY CLASSIFICATION OF REPORT | 18. SECURITY CLASSIFICATION OF THIS PAGE | 19. SECURITY CLASSIFICATION OF ABSTRACT | 20. LIMITATION OF ABSTRACT |
|---|---|---|---|
| Unclassified | Unclassified | Unclassified | |